

**MARINE REMOTE SENSING AND SEABED CHARACTERISATION TECHNIQUES  
FOR INVESTIGATING SUBMERGED LANDSCAPES OFF THE NORTHWEST  
COAST OF QATAR**

by

LUCIE DINGWALL

A thesis submitted to the University of Birmingham for the degree of MASTER OF  
PHILOSOPHY

Department of Classics, Ancient History and Archaeology  
School of History and Cultures  
College of Arts and Law  
University of Birmingham  
June 2014

**UNIVERSITY OF  
BIRMINGHAM**

**University of Birmingham Research Archive**

**e-theses repository**

This unpublished thesis/dissertation is copyright of the author and/or third parties. The intellectual property rights of the author or third parties in respect of this work are as defined by The Copyright Designs and Patents Act 1988 or as modified by any successor legislation.

Any use made of information contained in this thesis/dissertation must be in accordance with that legislation and must be properly acknowledged. Further distribution or reproduction in any format is prohibited without the permission of the copyright holder.

## **ABSTRACT**

The Arabian Gulf is a relatively recent sea that formed as a result of post-glacial sea level rise in the Late Pleistocene and Early Holocene. Prior to this, the former Gulf basin was an open landscape, with a substantial river flowing through it. There is considerable potential within this former landscape for the preservation of drowned archaeological sites and palaeoenvironmental remains from the Early Holocene, and for the preservation of remains of shipwrecks from the Mid-Holocene onwards. Despite the potential, there has been very little research into this submerged landscape, largely due to the difficulty and expense involved. In order to begin to address the gap in knowledge, this research developed and tested new methodologies for the exploration of the submerged landscape within a defined Study Area off the northwest coast of Qatar. The methodology utilised marine remote sensing data, including sidescan sonar and LiDAR bathymetry, and drew on techniques used in terrestrial historic landscape characterisation and acoustic seabed classification, in order to zone the seabed in the Study Area and identify broad zones of archaeological and palaeoenvironmental potential and survival. The seabed characterisation has provided a framework within which to begin more detailed investigations of the submerged landscape, by defining areas of potential to target, and specifying appropriate techniques to use within those areas, in order to maximise the chance of successful exploration of the submerged landscape.

## **Keywords**

Seabed Characterisation; Marine Geophysics; Acoustic Classification; Qatar; Submerged Landscapes; Arabian Gulf

## **ACKNOWLEDGEMENTS**

I would like to thank my supervisors, Professor Vince Gaffney, and especially Dr Richard Cuttler, who provided unstinting support in so many ways, and without whom this research would not have been possible. I would also like to thank H.E Shaykhā al-Mayāssā bint Hamad bin Khalīfah Al-Thānī (Chairperson of the Board of Trustees, Qatar Museums Authority), H.E. Shaykh Ḥasan bin Muhammād Al-Thānī (Vice-Chairman of the Board of Trustees, Qatar Museums Authority) and Faisal Al-Naimī (Director of Antiquities, Qatar Museums Authority), for their support for this research. Many other people provided support and assistance in many different ways, and I would like to extend grateful thanks to the following people:

The University of Birmingham/QNHER marine survey team, and in particular Kate Bain and Robyn Pelling, for undertaking the ground-truthing programme (grab sampling and diving) and high-resolution survey, and generally providing vast amounts of technical, logistical and other support; Ismail Mahmoud Al-Shaikh, Abdul Rahman Al-Obaidly and Abdel Rahman Sorour from the Environmental Studies Centre at Qatar University for kindly carrying out the granulometry analysis on the grab samples and providing a fantastic report; Eoghan Kieran (Geomara) for advice and assistance with the grab sampling and granulometry programme, and for invaluable advice on seabed classification software; Tony Tipple and Chris Elliott from Quester Tangent Software Ltd for providing free access to their software for a trial period, and for providing expert advice on the use of their software; Dr Richard Bates (University of St Andrews) and Brandon Mason (Hampshire and Wight Trust for Maritime Archaeology) for providing advice and assistance with initial processing of the sidescan sonar data; Dr Emma Tetlow (University of Birmingham/QNHER

Project) for providing expert palaeoenvironmental advice and moral support; Tobias Tonner (Coaptics Ltd) and Liam Delaney (University of Birmingham/QNHER Project) for assistance with coordinate system conversions; Dr Simon Fitch (University of Birmingham) for initial assistance with the sidescan sonar data processing; Access to the sidescan sonar data and geotechnical reports was kindly provided by the Qatar — Bahrain Causeway Management and access to the Bathymetric LiDAR data for research purposes was kindly provided by the Hydrographic Office. I would also like to thank Chris Dodds and Isaac Dingwall, who have supported me unwaveringly throughout my research.

## **Contents**

<b>CHAPTER 1: CONTEXT.....</b>	<b>1</b>
1.1 Introduction.....	1
1.2 Overview of The Study Area .....	6
1.2.1 Research Themes .....	6
1.2.2 Geology and Geomorphology .....	10
1.2.3 Sedimentation and Marine Taphonomic Processes.....	14
1.2.4 Climate .....	18
1.2.5 Tides and Salinity .....	18
1.2.6 Sea Levels.....	20
1.2.7 Vegetation History and Palaeo-climate .....	24
<b>CHAPTER 2: REVIEW OF PREVIOUS RESEARCH AND ARCHAEOLOGICAL POTENTIAL .....</b>	<b>27</b>
2.1 An overview of Archaeology in the Arabian Peninsula .....	27
2.1.1 The Palaeolithic.....	27
2.1.2 The Neolithic.....	30
2.1.3 Maritime History.....	35
2.2 Submerged Landscapes Research.....	40
2.2.1 Research Outside the Arabian Gulf .....	40
2.2.2 Research Within the Arabian Gulf .....	43
<b>CHAPTER 3: OVERVIEW OF METHODOLOGY.....</b>	<b>46</b>
3.1 Processes of Seabed Characterisation.....	46
3.2 Primary Characterisation .....	49
3.2.1 Sediment Texture Classification.....	49
3.2.2 Topographic Mapping.....	50
3.2.3 Ground-Truthing .....	52
3.3. Secondary Characterisation .....	53
3.3.1 Identification of Geophysical Anomalies .....	53
3.3.2 Clarification of Geophysical Signatures .....	55
3.4 Defining Character Areas and Assigning Potential .....	55
<b>CHAPTER 4: PRIMARY CHARACTERISATION.....</b>	<b>57</b>
4.1 Sediment Texture Classification.....	57
4.1.1 Methodology .....	57
4.1.1.1 Overview of Sidescan Sonar .....	57
4.1.1.2 Acoustic Techniques for Sediment Texture Classification .....	60

4.1.1.3 Trialling the Classification Methodology .....	62
4.1.1.4 Classification using Swathview .....	65
4.1.2 Results.....	71
4.1.2.1 Area 4 .....	74
4.1.2.2 Area 2/3 .....	78
4.1.2.3 Area 1 .....	82
4.1.2.4 Generating Initial Landscape Units .....	87
4.1.3 Discussion .....	90
4.2 Topographic Mapping.....	97
4.2.1 Methodology .....	97
4.2.1.1 Overview of LiDAR Bathymetry.....	97
4.2.1.2 Generating the Surface Model .....	99
4.2.1.3 Mapping Features.....	103
4.2.2 Results.....	104
4.2.2.1 Topography Within the Study Area .....	105
4.2.2.2 Topography Outside the Study Area .....	120
4.2.2.3 Topography and Sediment Classification.....	123
4.2.3 Discussion .....	127
4.3 Ground Truthing .....	134
4.3.1 Methodology .....	134
4.3.1.1 Direct Sediment Sampling .....	134
4.3.1.2 Video and Photography .....	140
4.3.2 Results.....	141
4.3.2.1 Direct Sediment Sampling .....	141
4.3.2.2 Video Transects.....	148
4.3.3 Discussion .....	151
<b>CHAPTER 5: SECONDARY CHARACTERISATION .....</b>	<b>156</b>
5.1. Identification of Geophysical Anomalies .....	156
5.1.1 Methodology .....	156
5.1.2 Results.....	160
5.1.2.1 Geophysical Anomalies .....	160
5.1.2.2 Geophysical Anomalies and Topography .....	175

5.1.3 Discussion .....	180
5.2 Clarification of Geophysical Signatures .....	184
5.2.1 Methodology .....	184
5.2.1.1 Diver Inspections .....	184
5.2.1.2 High-Resolution Geophysical Survey.....	185
5.2.2 Results.....	185
5.2.2.1 Diver Inspections .....	185
5.2.2.2 High-Resolution Geophysics .....	189
5.2.3 Discussion .....	191
<b>CHAPTER 6: DEFINING CHARACTER AREAS AND ASSIGNING POTENTIAL .....</b>	<b>193</b>
6.1 Refining the Initial Landscape Units into Character Areas.....	193
6.2 Assigning Potential.....	202
<b>CHAPTER 7: DISCUSSION .....</b>	<b>210</b>
7.1 An Evaluation of the effectiveness of the methodologies, and suggestions for further work ....	210
7.2 An evaluation of the archaeological and palaeoenvironmental potential of the submerged landscape within the Study Area .....	225
<b>CHAPTER 8: CONCLUSION: IMPLICATIONS FOR RESEARCH AND MANAGEMENT OF THE MARINE HERITAGE RESOURCE .....</b>	<b>239</b>
<b>APPENDIX 1: PROCESS AND PARAMETERS USED FOR THE ACOUSTIC CLASSIFICATION OF SIDESCAN SONAR DATA.....</b>	<b>243</b>
<b>APPENDIX 2: PROCESS AND PARAMETERS USED FOR PROCESSING THE LIDAR BATHYMETRY DATA .....</b>	<b>247</b>
<b>APPENDIX 3: GRAB SAMPLE GRAIN SIZE ANALYSIS REPORT .....</b>	<b>249</b>
<b>APPENDIX 4: PARAMETERS USED FOR PROCESSING AND MOSAICING SIDESCAN SONAR DATA.....</b>	<b>309</b>
<b>APPENDIX 5: LIST OF ALL ANOMALIES LOGGED FROM THE SIDESCAN SONAR DATA.....</b>	<b>310</b>
<b>APPENDIX 6: DERIVED DATA INCLUDED ON ACCOMPANYING CD .....</b>	<b>352</b>

## Figures

Figure 1 Location of the Study Area (illustration by Nigel Dodds) .....	4
Figure 2 Bathymetry (height data) between Qatar and Bahrain (from Al-Naimi et al., 2012) .....	13
Figure 3 Location of the Bahrain Anticline (from Cuttler, 2014).....	14
Figure 4 Shoreline Reconstructions at 14,000 BP after Lambeck (1996) (from Cuttler et al., 2011b). ....	22
Figure 5 Shoreline reconstructions at 8,200 BP after Lambeck (1996) (from Cuttler and Al-Naimi, 2013). .....	23
Figure 6 Distribution of 'Ubaid and 'Ubaid -Related Sites around the Arabian Gulf (from Cuttler, 2013). ....	33
Figure 7 Sidescan sonar operation (from Al-Naimi et al., 2012).....	58
Figure 8 Coverage of sidescan sonar survey lines in the Study Area. ....	59
Figure 11 Sub-Images (rectangles) generated by Swathview for the purpose of generating image statistics.....	66
Figure 13 Results of the Swathview preliminary seabed classification using catalogues based on the entire dataset, and using catalogues based on trial areas.....	68
Figure 14 Track plot from Swathview showing classified data points (left) and interpolation of data points using Clams (right).....	70
Figure 15 Classified data (left) and mosaic of sidescan sonar data (right) in Area 4. ....	74
Figure 16 Edge of brighter reflectivity demarcating a change in texture in Area 4. ....	75
Figure 17 Trawler scarring in Area 4. ....	76
Figure 18 Pattern of mixed classes south of the reef in Area 4 corresponding with visual patterns in the mosaic data. ....	77
Figure 19 Sand ridges visible in the mosaic data in Area 4 and differentiated as Class 3 in the classified data.....	77
Figure 20 Classified data and mosaic of sidescan sonar data in Area 2/3. ....	78
Figure 21 Mosaic of sidescan sonar data around the reef in Area 3. ....	79
Figure 22 Sand ridges visible in the mosaic data in Area 2 and differentiated as Class 3 in the classified data.....	80
Figure 23 Sand ridges visible in the mosaic data in Area 3 and differentiated as Class 6 in the classified data.....	81
Figure 24 Classified data and mosaic of sidescan sonar data in Area 1. ....	82
Figure 25 Brighter reflective area immediately north of the reef in Area1.....	83

Figure 26 Large band of lower reflectivity in Area 1, differentiated in the classified data mainly as Classes 9 and 4.....	84
Figure 27 Sand ripples in the north of Area 1, visible in the mosaic data.....	85
Figure 28 Sand banks in the southeast of Area 1, visible in the mosaic data and differentiated as Classes 3 (red) and 8 (lime) in the classified data. ....	86
Figure 29 Initial landscape units based on classification of acoustic backscatter. ....	89
Figure 30 Extent of available LiDAR bathymetry. ....	98
Figure 31 3D visualisation of the seabed in the Study Area (created in Erdas Imagine, based on the surface model generated from the bathymetry). ....	102
Figure 32 Surface model of the Study Area created from LiDAR bathymetry. ....	106
Figure 33 Features mapped from the surface model. ....	107
Figure 34 Putative former shorelines in the Study Area. ....	109
Figure 35 Hillshaded surface model with putative former shorelines.....	109
Figure 36 Hillshaded surface model with putative east-west former shoreline. ....	110
Figure 37 Putative east-west former shoreline with sidescan sonar data overlain. ....	110
Figure 38 Putative former shorelines with possible associated mapped features. ....	111
Figure 39 Palaeochannel possibly relating to the former course of Wadi Debayan. ....	112
Figure 40 Cluster of palaeochannels. ....	113
Figure 41 Fishtraps visible in the surface model (top), mapped during the QNHER cultural mapping project (middle) and an example photographed by the QNHER project (bottom). ....	114
Figure 42 Channels and depressions in the north of the Study Area. ....	115
Figure 43 Channels and depressions in the south of the Study Area. ....	115
Figure 44 Megaripples in the north of Area 1.....	116
Figure 45 Possible sand banks between the reef and the bay of Al-Zubārah. ....	117
Figure 46 Possible solution hollow visible in the surface model but not in the sidescan sonar data..	118
Figure 47 Undulations in the seabed to the north of the putative east-west shoreline in Area 1.....	119
Figure 48 The Reef in the west of the Study Area. ....	120
Figure 49 Potential former shorelines to the south of the Study Area. ....	121
Figure 50 Seabed surface in the Gulf of Salwa.....	122
Figure 51 Surface model with the classified data in Area 4. ....	124
Figure 52 Surface model with the classified data in Area 2, West of the Ras Ushayriq Peninsula. ...	125

Figure 53 Surface model with the classified data in Area 3, north of the reef.....	126
Figure 54 Surface model with the classified data in the deep channel in Area 1.....	127
Figure 55 Postulated extent of dry land at 7,000 BP (based on Stanford et al., 2011).....	129
Figure 56 Postulated extent of dry land at 8,000 BP (based on Jameson and Strohmenger, 2012). ..	130
Figure 57 Postulated extent of dry land at 7,000 BP (based on Jameson and Strohmenger, 2012). ..	131
Figure 58 Grab samples overlain on Initial Landscape Units.....	135
Figure 59 Exploratory boreholes drilled in 2008, overlain on Initial Landscape Units.....	137
Figure 60 Vibrocores taken in north of the Study Area in 2009, overlain on Initial Landscape Units.	138
Figure 61 Vibrocores taken in south of the Study Area in 2009, overlain on Initial Landscape Units.	139
Figure 62 Boreholes drilled over the reef in 2009, overlain on Initial Landscape Units.....	139
Figure 63 Grab sample locations overlain on the surface model.....	141
Figure 64 Grab sample locations overlain on the classified data.....	142
Figure 65 Vibrocores and boreholes overlain on the surface model (grab samples are visible in the background).....	144
Figure 66 Vibrocores and boreholes overlain on the classified data (grab samples are visible in the background).....	145
Figure 67 Video transects overlain on surface model.....	148
Figure 68 Video transects overlain on the classified data.....	148
Figure 69 Graph displaying sediment types for each class as derived from ground truthing data (expressed as a percentage of the total number of samples/observations recorded for each class). ..	153
Figure 70 Distribution of all recorded anomalies within the Study Area.....	161
Figure 71 Anomalies interpreted as potential debris, and proven to be debris from ground-truthing. ....	162
Figure 72 Examples of high-confidence anomalies in Area 1: Modern debris relating to artificial reefs (cars, tyres etc).Clockwise starting from the top left corner: QBC_Q10126, QBC_Q10270, QBC_Q10334, QBC_Q10902. (Each image depicts an area measuring 100m x 100m.) .....	163
Figure 73 The same anomaly (QBC_Q10815) visible in different survey lines: Modern debris relating to artificial reefs (each image depicts an area measuring 100m x 100m).....	164
Figure 745 Distribution of anomalies that are possibly depressions.....	166
Figure 75 A selection of anomalies that were logged as possible depressions. From left to right: QBC_Q20071, QBC_Q40064, QBC_Q40119 (each image depicts an area measuring 100m x 100m). ....	166
Figure 76 Anomalies logged as possible debris. From left to right: QBC_Q40089, QBC_Q10001 (each image depicts an area measuring 100m x 100m).....	171

Figure 77 Anomalies logged as areas of possible sediment accumulation. From left to right: QBC_Q40055, QBC_Q20060 (each image depicts an area measuring 100m x 100m). ....	171
Figure 78 Anomalies logged as natural features of potential topographic significance. From left to right: QBC_Q40026, QBC_Q20046, QBC_Q10195 (each image depicts an area measuring 100m x 100m). ....	172
Figure 79 Anomalies logged as potentially partially-buried objects or features. From left to right: QBC_Q10126, QBC_Q10202 (each image depicts an area measuring 100m x 100m). ....	172
Figure 80 A potential seabed crater: QBC_Q20094 (Image depicts an area measuring 100m x 100m). ....	173
Figure 81 Long linear anomaly: QBC_Q10729/Bham0028 (Image depicts an area measuring 100m x 100m). ....	173
Figure 82 Possible debris cluster in Area 1 (the green grid lines represent 500m x 500m squares). ....	174
Figure 83 Long linear anomaly (QBC_Q10729/BHAM0028) visible in the sidescan sonar data, and the surface model of the seabed from the same location (Both images are at same scale and orientation). ....	176
Figure 84 Bright reflective anomalies in Area 2, shown in the surface model to be natural outcrops. ....	177
Figure 85 Seabed crater (QBC_Q20094) visible in the sidescan sonar data (image depicts an area measuring 100m x 100m), and the surface model of the seabed from the same location, showing anomalies QBC_Q20094 and QBC_Q20096.....	177
Figure 86 Bright reflective anomalies in Area 3, shown in the surface model to be natural coral outcrops.....	178
Figure 87 Bright reflective anomalies in the southwest of Area 4, shown in the surface model to be natural outcrops.....	179
Figure 88 Anomaly QBC_Q10051 (modern debris): sidescan sonar, LiDAR points and surface model. ....	181
Figure 89 Anomaly QBC_Q10128 (car reef) visible in the sidescan sonar but not visible in the surface model.....	182
Figure 90 Anomaly QBC_Q10376 (topographic location of potential interest for human settlement) in the sidescan sonar data (image depicts an area measuring 100m x 100m), and in its landscape context in the surface model. ....	183
Figure 91 Anomaly QBC_Q10634 in Area 1: Sediment Basin (Photo by QNHER marine team, 2013). ....	187
Figure 92 Anomaly QBC_Q40118 in Area 4: Linear Ridges (Photo by QNHER marine team, 2013).187	
Figure 93 Anomaly G3/07.05.13/L8/TG1:Car reef in Area 1 (Photo by QNHER marine team, 2013).188	
Figure 94 Long linear anomaly QBC_Q10729/BHAM0028 (Photo by Hampshire and Wight Trust for Maritime Archaeology, 2011). ....	189

Figure 95 Long linear anomaly (QBC_Q10729/BHAM0028) surveyed in high resolution (each image depicts an area measuring 100m x 100m).....	190
Figure 96 Anomaly QBC_Q10815 (car reef) surveyed in low resolution (left) and high resolution (right) (each image depicts an area measuring 100m x 100m).....	191
Figure 97 Cross-correlation of different input datasets with the Initial Landscape Units. ....	194
Figure 98 Final Character Areas (labelled with Character Area numbers). .....	195
Figure 99 Character Areas (labelled with Character Area numbers) showing overall potential. ....	206
Figure 100 Distribution map of major 'Ubaid-related sites in Qatar.....	227
Figure 101 Misfer Cave, Qatar. ....	231
Figure 102 Evidence for archaeological deposits preserved beneath marine deposits at Wadi Debayan (Image by Richard Cuttler/Emma Tetlow). ....	236

## **TABLES**

Table 1: List of acoustic classes generated by Swathview, and their preliminary interpretation	72
Table 2: Initial landscape units - polygon statistics	90
Table 3: Seabed descriptions summarised from the video survey information	149
Table 4: List of terms used for initial categorisation of anomalies	159
Table 5: List of anomalies selected for more detailed examination	168
Table 6: Summary of results of diver inspections on selected anomalies	186
Table 7: Summary of results of diver inspections on anomalies near QBC_Q10729	188
Table 8: Summary description of Final Character Areas	197

## CHAPTER 1: CONTEXT

### 1.1 Introduction

The Arabian Gulf<sup>1</sup> and Peninsula, bordered by Africa, the Levant and the Iranian plateau, are located in a highly significant location in archaeological terms, straddling the African and Eurasian landmasses, and strategically located on an important ancient trade route between the civilisations of Mesopotamia and the Indus Valley (Parker and Goudie, 2008). The sea that currently occupies the Arabian Gulf Basin is relatively recent, having formed as a result of post-glacial sea level rise during the Late Pleistocene and Early Holocene, reaching its highest level just before 6,000 BP (Lambeck, 1996; Bird et al., 2010). Prior to this, the former Gulf basin would have been an open landscape, with a substantial river flowing through it, formed by the confluence of the Tigris and Euphrates Rivers to the north, and containing large, possibly freshwater, lakes (Lambeck, 1996). This resource-rich basin would have been a very attractive habitat for human communities in the region before sea-levels rose, possibly more attractive than the landscape that is now the Arabian Peninsula. The coastal region of the Arabian Peninsula is known to have been a focus for newly-established human settlements in the 7th Millennium BP, just as sea levels were reaching their peak (Parker and Goudie, 2008). Evidence also exists for a very early maritime trade network emerging at that time in the Arabian Gulf (Carter and Crawford, 2010). Research into the archaeology of the submerged continental shelf elsewhere in the world (Faught and Donoghue, 1997; Fitch et al., 2005; Bailey et al.,

---

<sup>1</sup> The Arabian Gulf is also commonly referred to as the Persian Gulf, but as this research focuses on the Arabian side of the Gulf, it is referred to as the Arabian Gulf throughout the thesis.

2007; Gaffney et al., 2007; Westley et al., 2011a) suggests that the former landscape of the Arabian Gulf basin has considerable potential for the survival of drowned archaeological sites and palaeoenvironmental remains from periods pre-dating the marine transgression, and for the presence of shipwrecks dating from the 7th Millennium BP onwards.

Despite this potential, there has been very little research into the submerged landscape of the former Gulf basin. This is due in large part to the difficulty and expense of such exploration and research, and as a result it has often been excluded from archaeological analyses and ignored in the literature. However, the full picture of Prehistoric settlement in the region cannot be adequately understood whilst this highly significant expanse of former landscape remains unexplored. Random survey of such a large area of submerged landscape is unlikely to be either cost-effective, or yield useful results. The need for a research framework within which to begin to explore the marine environment in a meaningful and effective way is therefore required. The continuing development of techniques in marine geophysics, allowing cheaper and more rapid examination of large areas of the seabed than would be possible using diver survey alone, has opened up new possibilities for large-scale exploration of the submerged landscape. Also, the availability of large, remotely-sensed datasets that have been gathered by commercial companies in advance of oil exploration and offshore infrastructure projects makes the costs of undertaking archaeological research of the seabed more feasible.

This research aims to provide a starting point for effective study of the submerged landscape in the Arabian Gulf. It focuses on developing and testing classification and characterisation methodologies for identifying zones of high potential for the survival of archaeological and palaeoenvironmental remains that can subsequently be targeted for more detailed investigations. The approach developed, seabed characterisation, utilises commercially-captured marine geophysics data and LiDAR bathymetry, and draws on techniques used in seabed habitat classification and terrestrial historic landscape characterisation to try and maximise the potential for successful exploration of the submerged landscape.

A large area of the seabed off the northwest coast of Qatar was surveyed by a commercial company using sidescan sonar (a geophysical technique that measures the acoustic reflectivity of the seabed) in 2008, as part of assessments for the proposed Qatar-Bahrain causeway (GEMS, 2008). The part of the survey dataset that lies within Qatari national waters was made available to the Qatar National Historic Environment Record (QNHER) project (Al-Naimi et al., 2012) for the purposes of archaeological assessment. The area surveyed covers 365 square kilometres of the seabed, and now forms the Study Area for this research (Figure 1). Previous research into sea level change indicates that this part of the Gulf between Qatar and Bahrain remained free from marine influence until after 8,000 BP (Lambeck, 1996; Al-Naimi et al., 2012).

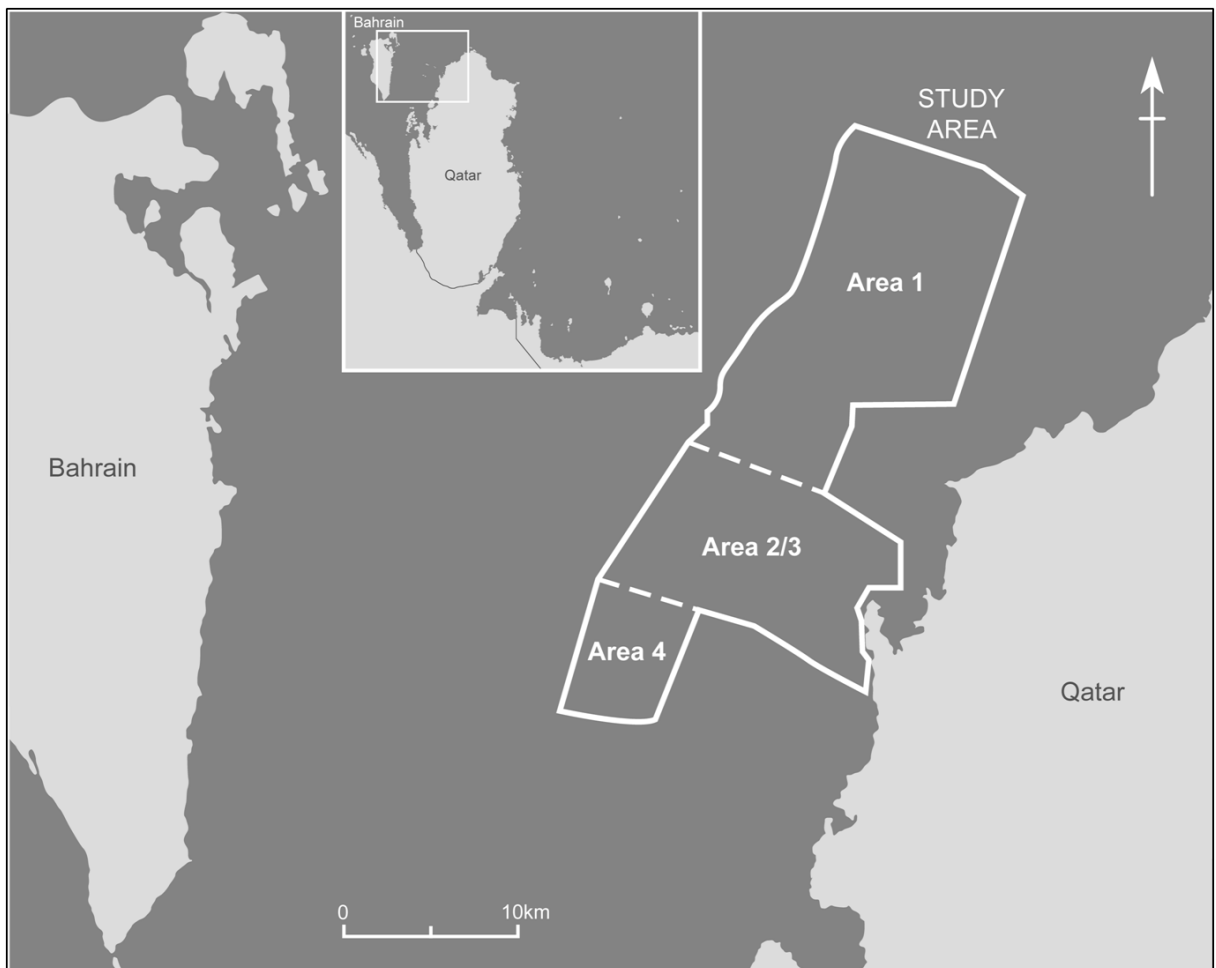


Figure 1 Location of the Study Area (illustration by Nigel Dodds).

The aims and objectives of the research were:

- To develop and test techniques for classifying the submerged landscape in the Study Area into characterisation areas that could be used to target further, more intensive study
- To create the characterisation areas and use them to generate zones of archaeological and palaeo-environmental potential
- To evaluate the effectiveness of the techniques used
- To evaluate the archaeological and palaeoenvironmental potential of the submerged landscape within the Study Area

- To assess the implications for research and management of the marine heritage resource

This was to be achieved by:

- Undertaking acoustic sediment texture classification on the complete sidescan sonar dataset and using the results to classify the seabed in the Study Area into initial landscape units
- Analysing available bathymetry and Holocene sea-level data and integrating the results into the classified data in order to refine the initial landscape units into character zones
- Using ground-truthing data obtained by direct sediment sampling and video footage to validate the character zones
- Analysing the complete sidescan sonar dataset in order to identify and classify geophysical anomalies, set them in a landscape context, and use the results to further inform the character areas
- Targeted diver survey and high-resolution geophysical survey of selected anomalies in order to clarify signature types
- Using the final character areas to generate zones of archaeological and palaeoenvironmental potential

## **1.2 Overview of The Study Area**

The Arabian Gulf is a shallow enclosed sea bounded at the south and west by the Arabian Peninsula, and to the north and east by the Zagros Mountains (Lambeck 1996), with the confluence of the Tigris, Euphrates and Karun rivers forming the Shatt al-Arab and flowing into the northern end of the Gulf. The Study Area itself, an area measuring 365 square kilometres, lies off the northwest coast of Qatar, between the Ras ‘Ushayriq peninsula area, and extends northwest towards the northeast coast of Bahrain. The substantial Qit’at ash Shajarah reef, bordering Bahrain national waters, forms the western edge of the Study Area. The water depths within the Study Area are very shallow, averaging between 1 and 7 m, with the reef lying very close to the surface.

### **1.2.1 Research Themes**

Despite the technical and interpretational difficulties of studying the pre-transgression landscape of the Arabian Gulf, and its consequent marginalisation within research and published literature, it is clear that there are highly significant regional research themes that could be informed by studying it.

There is increasing interest in the dispersal of early humans out of Africa, and the geographical position of the Arabian Peninsula, lying between Africa and Asia, is highly pertinent to this. Recent research into genetics and population movements (Petruglia and Rose, 2009) has suggested that a postulated ‘southern dispersal

'route' would take populations around the southern coast of the Arabian Peninsula and into the Arabian Gulf.

Another major research theme that is relevant to the Study Area is the 'Ubaid phenomenon', that is, the relatively sudden appearance of settlement sites yielding Mesopotamian 'Ubaid pottery around the coastlines of the Arabian Gulf during the second half of the eighth millennium BP. The question as to where these coastal settlers had migrated from is of great significance to the study of Neolithic Arabia. The dating and nature of these sites suggests that they may represent human populations that were displaced from the former Gulf basin by the relatively rapid marine transgression between c.8,000 BP and 7,500 BP (Cuttler, 2013; Rose, 2010). The submerged landscape of the Study Area lies in close proximity to several of these 'Ubaid-related sites, which are considered to be the most significant pre-Islamic sites in Qatar. Linked to the theme of human settlement patterns in the Early and Mid-Holocene is the likelihood that the archaeologically-significant Karst landscape of Northern Qatar extends into the Study Area as a drowned landscape, and also the fact that submarine freshwater springs are known to have existed off Bahrain in recent historical times (Cheesman, 1923).

The nature of potential submerged Prehistoric archaeological remains within the Study Area, and the conditions and locations in which such remains could reasonably be expected to survive marine inundation and sea-level fluctuation, are key issues for this research. In order for settlement remains such as stone walls or cairns to survive marine incursion and remain recognisable, they would have to have been buried

quickly due to the rapid rate of carbonate accretion in the Gulf. The most likely locations for quick burial conditions to occur would be within tranquil areas protected from the full force of wave action whilst sea-levels were rising. Potential marine accretionary locations in the Study Area include sheltered environments on former coastlines such as bays, spits, promontories and drainage channels.

The geographical location of the Arabian Gulf made it a nexus for trade from very early on in maritime history (Al-Naimi et al., 2012, p.255). The Study Area itself lies in close proximity to Bahrain, which is well-documented as a very important maritime trade centre in the Prehistoric period (Killick and Moon, 2005). More recently, principal trade routes to Bahrain and Southern Iraq lie to the north of Qatar, relatively close to the Study Area. There is likely, therefore, to have been a high level of shipping passing near, or through the Study Area. These factors, taken together with the presence of the reef and the shallow water in the Study Area suggest that there is a relatively high probability that shipwrecks could have occurred in the Study Area from the Prehistoric period onwards.

Another important theme is the potential for preservation of palaeoenvironmental remains in the Study Area. The arid climate and wind-deflated landscape of Qatar is not conducive to the preservation of organic remains, and therefore very little palaeoenvironmental evidence survives from terrestrial sites in Qatar. Even sites dating from 2000 years ago are unlikely to contain useful quantities of organic remains (Cuttler, 2014). However, the nature of the Holocene marine transgression may have enabled the preservation of palaeoenvironmental caches dating from the

Late Upper Palaeolithic to Neolithic periods within sediment traps in the submerged landscape (Cuttler, 2010, p.152). This therefore represents our best chance to find palaeoenvironmental remains to inform research into these periods in Qatar , so it is very important that we establish effective methodologies for locating such sediment traps. The potential locations of such sediment traps may well coincide with the potential locations of archaeological remains.

Although the Study Area forms only a small part of the extensive sub-aerial landscape of the former Gulf Basin, it provides a convenient starting point from which to begin to develop methodologies for effective exploration, which may help to provide valuable information on a number of important regional research themes.

### **1.2.2 Geology and Geomorphology**

The Arabian Gulf is a long, shallow, epicontinental sea, covering an area of 210,000 square kilometres, and is connected to the Indian Ocean by the Straits of Hormuz. The Arabian Plate is slowly subducting below the Eurasian Plate, and the Arabian Gulf basin is a direct result of this subduction. The subduction has resulted in a gentle southwest to northeast tilt in the plate, and much of the northern Gulf between Kuwait and Iran is topographically lower than the southern and western Gulf. (Cuttler and Al-Naimi, 2013). Fringing the southern side of the Gulf are coastal islands, coral reefs, tidal channels, tidal flats, raised beaches, and coastal salt flats known as sabkhas (Teller et al., 2000). The Gulf is almost completely surrounded by arid land, and as a result virtually no runoff is received from the Arabian Peninsula, where precipitation is very low (100 mm/yr). The only runoff into the Gulf comes from rivers draining the Zagros Mountains to the northeast and from the confluence of the Tigris, Euphrates and Karun rivers forming the Shatt-al-Arab at the northern end of the Gulf (Teller et al., 2000).

The Qatar peninsula projects from the relatively linear Arabian coastline on the western side of the Gulf (KSEPL, 1973). It consists of an anticlinal dome, with a north-south main axis (Cavalier, 1970), and it has a low-relief landscape with a maximum elevation of about 110m above sea level (Sadiq and Nasir, 2002). The exposed geological sequence on the Qatar peninsula consists of Tertiary limestones and dolomites with interbedded clays, shale, gypsum and marls. This sequence is covered in places by a series of Quaternary and recent deposits. (Leblanc, 2008).

About 70% of the total land surface of the Qatar peninsula is Eocene Dammam formation limestone (Al Saad, 2005). This in turn overlies the Rus formation and the Umm er Radhuma formation (Macumber, 2011). The anticlinal structure of Qatar (the Qatar Arch) controls the outcrop pattern of the Dammam Formation, as do smaller longitudinal folds such as the Dukhan anticline and the Simsima Dome (Al-Saad, 2005). In the south of Qatar, Miocene marls and limestone outcrop in mesas and hills, and significant areas of sand dunes occur in the southeast (Johnstone and Wilkinson, 1960, p.445)

The Fuwayrit Formation is found overlying Eocene sediments at certain locations in Qatar. This formation consists of shallow marine and marine-derived aeolian carbonates, preserved in coastal localities (Williams and Walkden, 2002). A study in 1999 on the Quaternary carbonates along the coastline of Qatar established that the Quaternary Carbonate sequence, which consists almost entirely of detrital limestones, is comprised of three lithostratigraphic units which vary in character along the coastline, and the sequence is considerably more developed along the eastern coast (Abu-Zeid et al., 2001, p.26). The study also established that the great variation in the nature and intensity of freshwater cementation displayed by the Quaternary carbonate sequence was a reflection of very considerable fluctuations in groundwater levels (Abu-Zeid et al., 2001, p.35). The stratigraphy of offshore deposits has not been properly formalised, but studies of sea-floor cores from six localities in the southern Arabian Gulf indicates that the uppermost Pleistocene sequence of marine carbonates and sabkha-derived evaporites represents the offshore equivalent of the Fuwayrit Formation (Williams and Walkden, 2002).

Karst features are a widespread and striking aspect of the landscape of the Qatar peninsula. These consist of more than 9,700 large and small depressions, and several exposed sinkholes and caves , caused by the dissolution of the surface and sub-surface rock. These depressions, which range from 50m to 3km in diameter, overall covering an area of c.33,500 ha, can reach depths of up to 25m (Sadiq and Nasir, 2002, p.132; Macumber, 2011, p.1). They form catchments for surface water runoff, and contain better soils (known as rawdha) than are present in the rest of the peninsula, and are therefore important for agriculture (Macumber, 2011). It is reasonable to assume that these Karst features are also present, albeit in a modified form, in the area that is now submerged around Qatar.

The seabed within the Study Area is relatively flat, with water depths averaging between 1 and 7m between Qatar and Bahrain, dropping to 12m at the northern extent of the Study Area. There are two large drying reefs in the area, the Fasht al Azm reef and the Qit'at ash Shajarah reef (Marin Mätteknik AB, 2002). The former reef extends on a southeast-northwest alignment between the Qatar border and Bahrain, whilst the latter is located along the western edge of the Study Area (Figure 2).

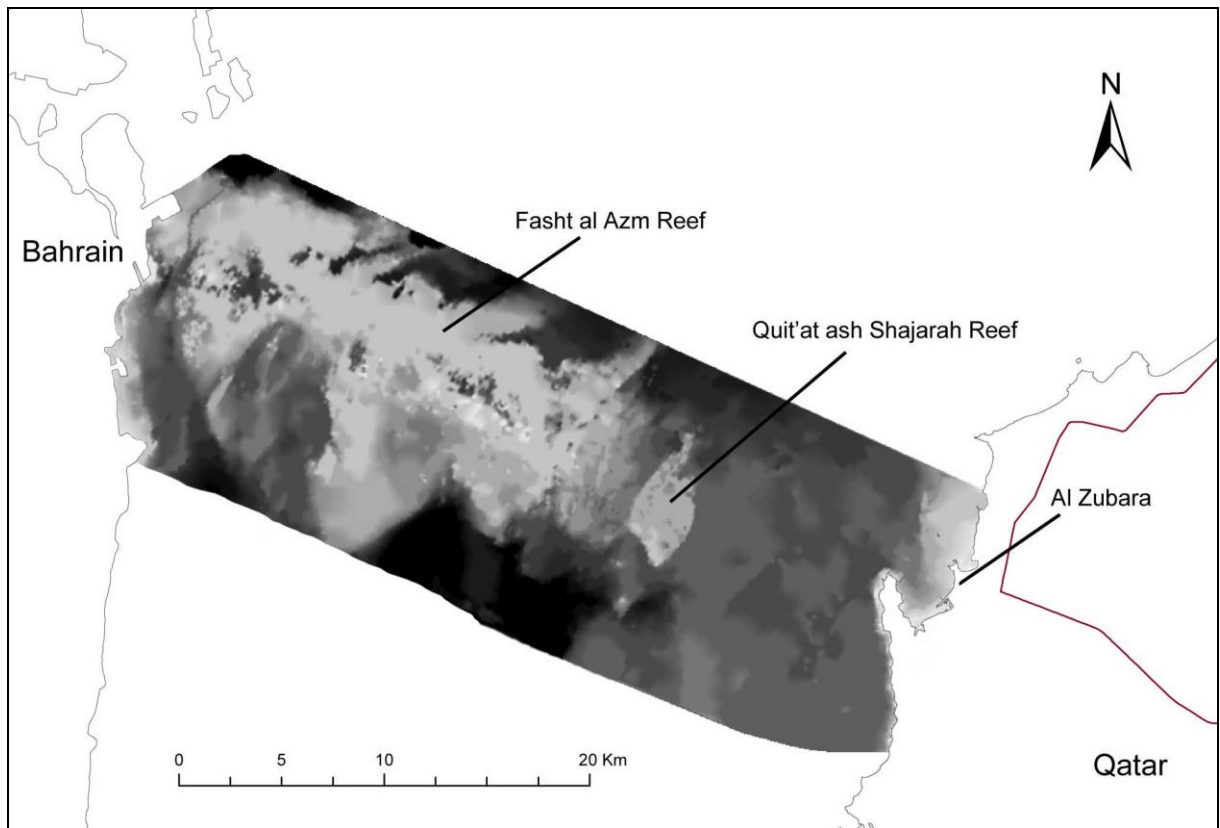


Figure 2 Bathymetry (height data) between Qatar and Bahrain (from Al-Naimi et al., 2012).

The geology and geomorphology of the Study Area itself is influenced by the Bahrain anticline. This consists of an arch or ridge which runs northwest-southeast from Bahrain to Qatar, through the Study Area (Figure 3). This anticline is a significant hazard for shipping and as a result no deep water ports were established along the southwestern coastline during the Late Islamic period (Cuttler, 2014).

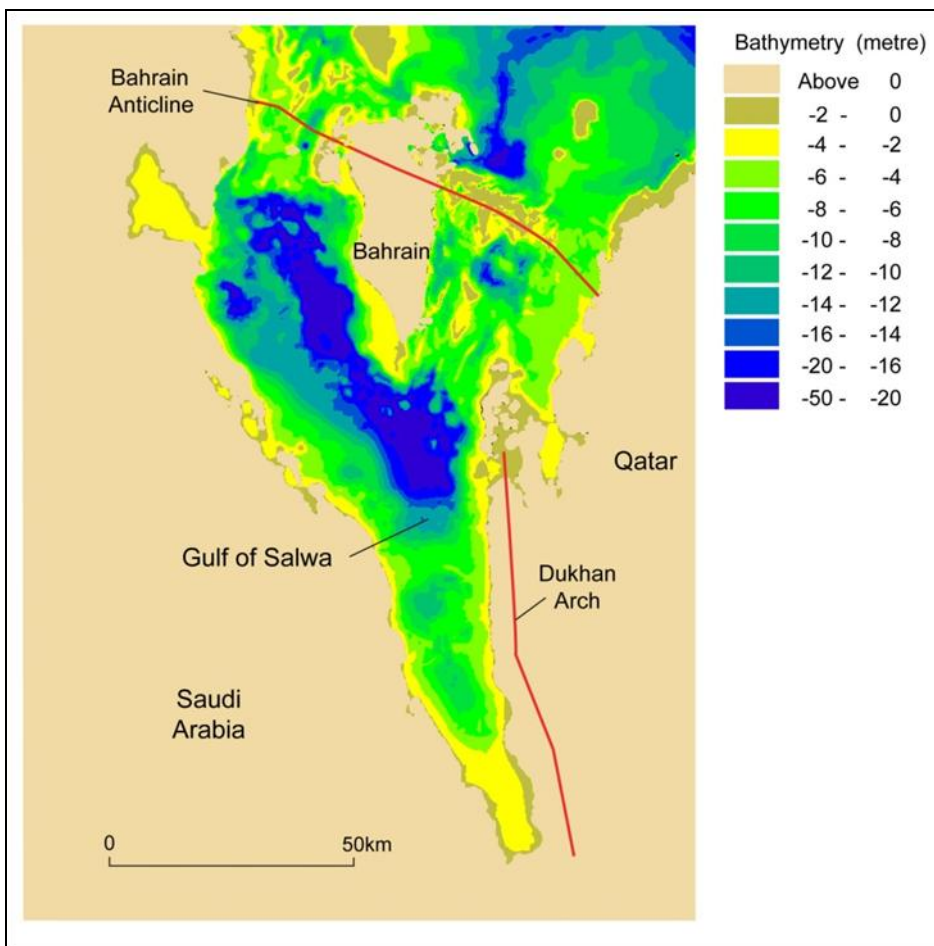


Figure 3 Location of the Bahrain Anticline (from Cuttler, 2014).

Sandbanks that have been tentatively interpreted as drowned sand dunes have been mapped from LANDSAT images in the Gulf of Salwa between Qatar and Bahrain (Al-Hinai et al., 1987, p.254).

### 1.2.3 Sedimentation and Marine Taphonomic Processes

The evidence from sediments in the Gulf, which date from 18,000 B.P. to the present day (Kassler, 1973, cited in Al Ghadban et al., 1998, p.24), indicates that the present sedimentary regime was established soon after 9,000 years B.P. when sea levels

were still considerably lower than present day levels, and a more humid climate developed (Uchupi et al., 1996). On the Arabian Peninsula side of the Gulf, carbonate deposition dominated throughout the Holocene (Uchupi et al., 1999). Impure carbonate sediments tend to occur near the centre of the Gulf, changing to high energy sands and local muddy embayments on the coast (KSEPL, 1973). The present-day seafloor sediments in the Arabian side of the basin are largely wind-borne, as virtually no water-borne sediment reaches the Gulf from the arid Arabian Peninsula (Marin Mätteknik AB, 2002). This lack of water-borne sediment is probably a major factor in the predominance of almost pure carbonate sediments on the Arabian side (Purser, 1973).

There is still insufficient evidence for a detailed picture of sedimentation rates in specific areas of the Gulf. According to Uchupi et al. (1996, p.267), overall sediment patterns in the Gulf are influenced by bottom water leaving the Gulf through the Strait of Hormuz, accretion/deposition and chemical precipitation along the Arabian coast, and also by widespread gas seeps. Although sedimentation rates are generally high throughout the Gulf (Al Ghadban, 1998, p.24), it is clear that there are considerable regional and local differences that are influenced by seabed topography, sediment types, wave energy, the orientation of the coast in relation to the prevailing wind, and the presence or absence of offshore barriers (Alsharhan and Kendall, 2003, p.193). However, in the shallow, Arabian parts of the Gulf, waves and surface currents are almost certainly the strongest influence on sediment transport (KSEPL, 1973). Furthermore, in a small sea like the Gulf, waves are largely created by the wind, so

the prevailing northwest ‘Shamal’ wind is crucial in determining sedimentation patterns (Herman, 1957).

The effects of aeolian deposition by the Shamal are strongest in the northern parts of the Gulf, and along the leeward (east) coast of the Qatar Peninsula (KSEPL, 1973).

Extrapolation from profiles of Holocene sediment accumulation indicates that fine-grained sediments can be up to 10m thick in the low-energy environments of sheltered parts of shallow western coastal areas of the Gulf, such as in the area of Khor and Dakhira to the east of Qatar (Kassler, 1973, cited in Al Ghadban et al. 1998, p.25; KSEPL, 1973). Thick, muddy sediment occurs in sheltered coastal lagoons and depressions, and geophysical survey in the Gulf has indicated that topographic depressions and submerged wadis act as sediment traps for large volumes of mud sediment, which has smoothed out the relief of the seabed. However, this sediment accumulation has not yet completely masked the underlying topography. (Kassler, cited in Purser, 1973, p.31).

Conversely, in the high-energy windward areas along the southwestern coastline of the Gulf, where coarse-grained sediments are laid down, lower sedimentation rates result in sediment thicknesses of less than 2m (Al Ghadban et al., p.25). There are areas off the Saudi Arabian Coast, especially at relatively shallow depths, where marine geophysics data indicates that the sediments are so thin that they barely cover the underlying rock, probably due to the complex topography in that area (Evans, 1966, p.295). In these areas, a thin covering (5 - 20 cm) of sand overlies the

rock, and the hard rock surface tends to be exposed between large mega-ripples (Purser, 1973, p.5).

Ooid build-ups mainly occur in tidally-influenced areas on windward coasts (Williams and Walkden, 2002, p.382). Geological studies carried out around Qatar in the 1960s proved that submarine lithification is in progress in some areas, mainly in areas where there is slower sediment accumulation. (Shinn, 1969, p.139).

The Study Area lies off the northwest coast of Qatar, which directly faces the full force of the northwesterly 'Shamal' wind, a coastal orientation not normally associated with rapid sediment accumulation. However, the picture is more complex, as this area is not fully exposed to strong marine currents due to the protecting barrier of Bahrain and the Saudi Arabian coast. (KSEPL, 1973). An algal coral reef has developed 1-4 km offshore from the northwest tip of the peninsula (Taylor and Illing, 1969, p.72).

The seabed surface, summarised by GEMS (2008), suggests that the northern extent of the Study Area comprises mainly hard coral and rocky substrates interspersed by sands and gravels. The central part appears to consist predominantly of relatively featureless medium to coarse sands, with areas of broad sand ribbons stretching for kilometres in a general north to south direction. East of the reef, the seabed is hard and rocky with numerous coral heads and very complex localised relief. The southern extent of the survey area appears to be characterized by medium to coarse sands and gravels, with evidence of extensive trawler-scars in the west.

#### **1.2.4 Climate**

Most of the southern Arabian Gulf currently falls within the hyper-arid zone in the UNESCO (1979) classification scheme. It falls within the subtropical trade wind belt, and is at present dominated by the Shamal wind (Williams and Walkden, 2002). Qatar itself has an arid to hyper-arid climate, with annual rainfall from winter westerlies averaging 80 mm in the north and less in the south. This small amount of rainfall recharges into the limestone aquifer system, and discharges at the coast, and therefore there is no permanent fresh surface water on the Qatar peninsula (Macumber, 2011). Several substantial wadis, charged seasonally, run from the anticline towards the coast (Cuttler and Al-Naimi, 2013). Although rainfall is low, the country is named ‘Qatar’, the Arabic word for ‘Land of Dews’, due to the frequent occurrence of heavy night dews (Taylor and Illing, 1969, p.71).

#### **1.2.5 Tides and Salinity**

At present, the average tidal range in the Arabian Gulf is small, around 1-2 m (Lambeck, 1996), and in Qatar itself, the normal tidal range changes from one part of the coast to another, for example it is about 1.4m at Doha and only 0.5m in western lagoons. However, in these areas, the movement of water due to the wind is often far more significant than tidal movement (Taylor and Illing, 1969, p.71). A slow circulatory current flows within the Gulf, moving from the Straits of Hormuz anticlockwise along the Persian Coast. This affects the distribution of salinity and temperature in the Arabian Gulf waters as it brings in new oceanic water (KSEPL,

1973). A small amount of freshwater flows into the Gulf, mainly from the Shatt al-Arab, and also from intermittent streams on the Persian Coast (Teller et al., 2000). However, this small amount of freshwater inflow is exceeded by the high rate of evaporation that occurs in this restricted basin with such high temperatures. As a result, the average salinity of the Gulf is relatively high. Water temperature and salinity are closely linked, and both are highest in shallow embayments and lagoons (KSEPL, 1973). The water temperature, although varying throughout the different parts of the Gulf, is generally high, recorded in 1966 (Evans, 1966) to be up to 32°C, and higher in the shallow waters along the coasts, although it should be noted that the temperatures may be quite different nearly 50 years later. This same study recorded salinities ranging from 37 to 38 ‰ in the Straits of Hormuz to 38 to 41 ‰ at the northern end of the Gulf, and reaching higher levels in the coastal areas along the southwestern shore. According to Taylor and Illing (1969, p.71), salinity values of 1.5-1.8 times standard seawater have been logged in some of the more secluded lagoons opening to the west coast of the Gulf, although, as with temperatures, salinity may have changed in the intervening decades. A more recent study was carried out on water temperature and salinity around the coasts of Qatar and Bahrain in 1992 (Abdel-Monim Mubarak and Kubryakov, 2000). This study identified a thin surface layer of water 2m in thickness with a temperature around 26 to 27°C, and relatively low salinity for the Persian Gulf (around 38.1‰). Below this layer, temperature decreased and salinity increased, down to 20.4°C and 39.6‰ at 24m depth. Seasonal variations were observed, due to solar heating and wind circulation.

## 1.2.6 Sea Levels

The Arabian Gulf Basin has been occupied by numerous marine transgressions, of which the Holocene transgression is the most recent. The retreat of glaciers in the northern hemisphere from around 18,000 BP caused a rise in global sea levels from more than 100m below their present levels (Cuttler and Al-Naimi, 2013). The lack of reliable regional sea-level curves, and the considerable debate surrounding the effect of tectonic movement and isostatic loading movements (Lambeck, 1996; Uchupi et al., 1999), means that it is not possible to be exact about the rate and timing of marine transgression within the Arabian Gulf. Lambeck (1996) plotted the marine transgression across the Gulf using seabed bathymetry to create a `glacio-hydro-isostatic model', basing his model on the assumption that the sea-level rise was continuous without still stands or regressions, whilst acknowledging that the rise would not have been spatially uniform (Teller et al., 2000). Sarnthein (1972) estimated that the rising sea levels covered the land laterally at an average rate of 100-120 m per year, with periods of still stands at about 11,300 and 10,500 BP. There must also have been periods of faster transgression, at times greater than 1km per year, during times of rapid eustatic rises, such as are known to have occurred around 12-11.5 BP and 9.5-8.5 BP (Teller et al., 2000).

Models of marine transgression based on bathymetry do not take into account tectonic movement, hydrostatic loading or marine deposition. The evidence suggests that there has not been significant tectonic movement around Qatar during the Holocene, and that deposition levels should not affect results at a landscape scale,

whereas hydrostatic adjustment is likely to have significantly affected models for the Arabian Gulf. The effect of this is that later dates occur than would be expected for the equivalent depth in other parts of the world (Cuttler, 2014, p13-14). This effect is likely to be more pronounced further back in time. Despite these limitations, a good overview of the evidence for the progress of marine transgression in the Arabian Gulf is provided by Cuttler and Al-Naimi (2013), and this overview is summarised here.

It is generally agreed that at the time of the last glacial maximum at about 18,000 BP, the Gulf was entirely free of marine influence. At this time, instead of flowing into the Gulf, it is reasonable to assume that the confluence of the Tigris-Euphrates Rivers (known as the Ur Shatt River) would have flowed through the Gulf basin, discharging into the Gulf of Oman through the Strait of Hormuz (Cuttler and Al-Naimi, 2013). The topography of the former Ur Shatt River valley was relatively flat, and Cuttler (2013) has suggested that the Ur-Shatt would have been a low-energy channel which was more likely to be a corridor of marshland and lakes rather than a high-energy river. Although there are studies that have identified morphological or sedimentological traces of this former watercourse, few details are available (Teller et al. 2000). Lambeck's model (Lambeck, 1996) indicates that during the last glacial maximum, the Ur-Shatt fed three large freshwater lakes on the floor of the basin, along the central part and along the southern side (Figure 4), although the issue of whether they would have been freshwater or saline has not yet been completely resolved. The lake hypothesis is now supported by ETOPO2 data (a combination of satellite altimetry observations, shipboard echo-sounding and data from a Digital Bathymetric Data Base, NOAA), which confirms the presence of a western basin and a central

basin in the Gulf (Cuttler and Al-Naimi, 2013). It is also supported by the analysis of 3D seismic data as part of the QNHER project, which has provided evidence of sediments relating to the eastern lake (Cuttler, 2013). However, these models do not take into account any subsequent tectonic plate movements or extensive marine deposition (Cuttler and Al-Naimi, 2013).

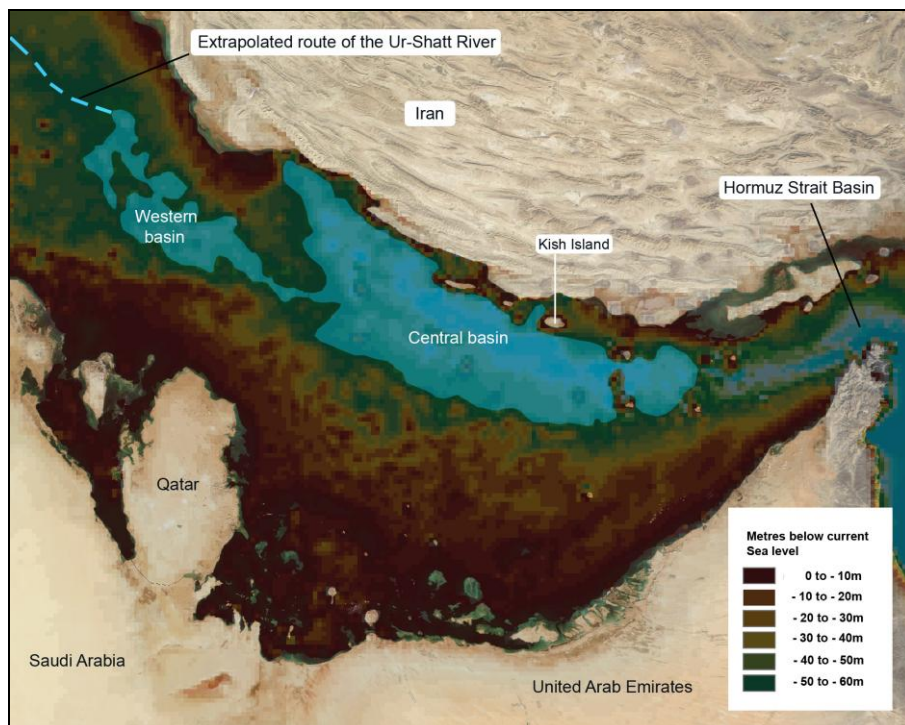


Figure 4 Shoreline Reconstructions at 14,000 BP after Lambeck (1996) (from Cuttler et al., 2011b).

The evidence suggests that the Strait of Hormuz became a narrow waterway at the mouth of the *Ur Shatt* River by 14,000 BP. (Lambeck, 1996). Around 12,500 years ago, the central basin would have been subject to marine incursion, probably causing a change from fresh water to saline lakes (Cuttler and Al-Naimi, 2013). The Western Basin flooded about 1,000 years later (Lambeck, 1996). By 10,000 BP, the marine transgression would have resulted in a long narrow sea, and the Iranian coastline

would already resemble the present-day coastline. However, large areas of the southern and western basin around the Emirates, Qatar and Bahrain would have remained as open landscape at this time (Lambeck, 1996).

After 10,000 BP periods of still-stands were interspersed with periods of more rapid marine transgression. As late as 8,200 BP extensive areas between Qatar, Bahrain and the Emirates remained free from marine influence (Figure 5). The Bahrain anticline would have delayed marine transgression into the Gulf of Salwa until the final stages of sea level rise in the 8th Millennium BP (Cuttler, 2014). The present-day shoreline was reached shortly before 6,000 BP, after which sea levels continued to rise for a further 1-2 m above present-day levels (Lambeck, 1996). During this period, Qatar was almost an island, connected to the remainder of the Arabian Peninsula by a thin strip of land (Cuttler and Al-Naimi, 2013).

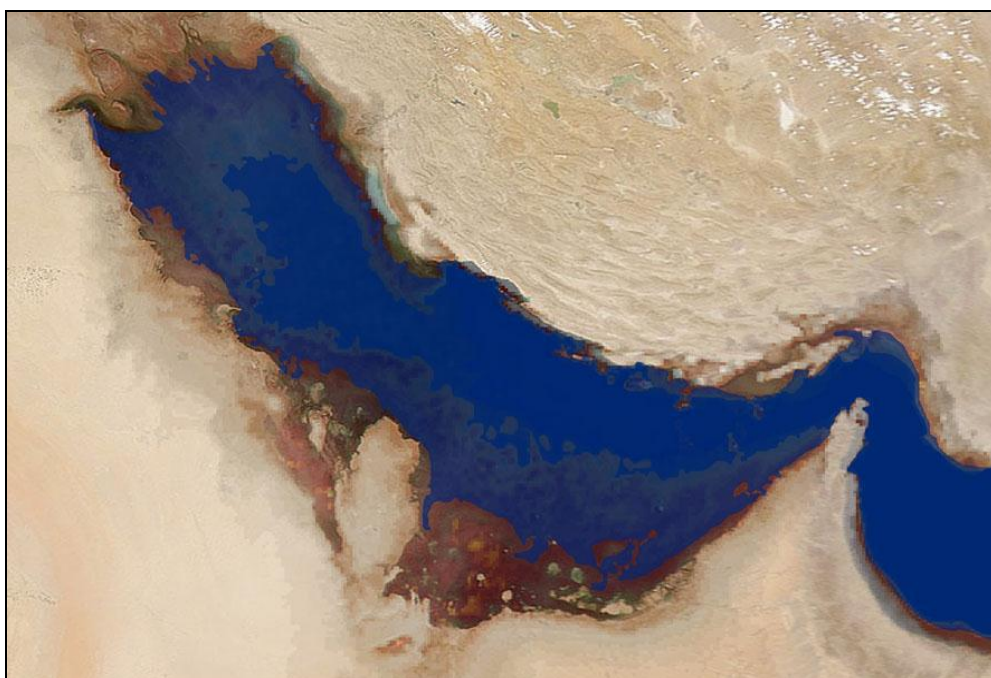


Figure 5 Shoreline reconstructions at 8,200 BP after Lambeck (1996) (from Cuttler and Al-Naimi, 2013).

Evidence for the Mid-Holocene high stand is widespread in the southern Gulf (Williams and Walkden, 2002), and is demonstrated by dated terraces and marine sediments along the southern shore of the Gulf (Uchupi et al., 1999; Lambeck, 1996; Teller et al., 2000). In Qatar, cemented beach sands from the northwestern coast, at locations between 1.5 and 2.5 m above present sea level, were identified and dated by Taylor and Illing (1969) to between  $3930 \pm 130$  and  $4340 \pm 180$  BP. Similarly, Vita-Finzi identified beach rock deposits up to 2m above present sea level from several coastal areas in Qatar, and dated them from between  $4690 \pm 80$  and  $5830 \pm 70$  BP. (Vita-Finzi, 1978, cited in Williams and Walkden, 2002). The evidence indicates that this high stand was due to eustatic change rather than tectonic activity. Both Lambeck (1996) and Williams and Walkden (2002) agree that although the Gulf lies close to an active plate margin, there is no evidence for significant tectonic movement for much of the sea floor or coastline in the southern Gulf during the Holocene, although there are exceptions, such as on the northern side of the Strait of Hormuz (Lambeck, 1996). Recent work at Wadi Debayan, close to the west coast of Qatar, has dated the earliest relic beach terraces there to around 6,000 BP, indicating a sea level high from around 6,000 BP onwards, supporting the sea-level models produced by Lambeck (1996) and Heyvaert and Baeteman (2007).

### **1.2.7 Vegetation History and Palaeo-climate**

The impact of the rise and fall of sea levels on human populations in the Arabian Gulf is also intimately connected with past climate change, which itself had a profound effect on human occupation and exploitation of the area. There is evidence from

sediments in the region that indicate pronounced climate changes, closely linked to global glaciation cycles and prevailing wind systems. Such changes caused phases of increased aridity and humidity relative to the present day climate. (Petruglia, 2005). Most palaeoenvironmental experts recognise widespread evidence for a wetter climate during the Early Holocene period in the region, between around 9,000 and 6,000 BP (Teller et al., 2000). This evidence includes radiocarbon-dated lacustrine sediments that developed during that period in areas that are now in the Arabian Desert regions, including the Rub' al-Khali and Nafud regions (McClure, 1976, p.755; Parker et al., 2006). The wetter phase is linked to the northward migration of the Indian Ocean monsoon into the Gulf region between 8,500–6,000 BP (Parker and Goudie, 2008), bringing higher rainfall, although it is not known exactly how far north this influence reached. Fleitmann et al. (2004, p.20) speculate that the monsoon rainfall activity did not affect areas further north than around 23-24° latitude, whereas most of the Qatar peninsula lies at between 25-26 ° latitude. However, further research is needed to support this hypothesis. After around 6,000 BP, the monsoon migrated southwards, and from 4,500 BP the climate became more arid, with an intense arid period occurring at 4,100 BP. Since then, arid conditions similar to those found in the region today have predominated (Parker and Goudie, 2008).

Faure et al. (2002, p.53-54) proposed a ‘Coastal Oasis’ model, whereby the falling sea levels reduced the sea level pressure on the continental shelf and steepened the water table gradient at the coast, leading to reduced water availability in the interior, but increased freshwater via springs on the newly-emerged coastlines. This model

has considerable significance for research into human settlement patterns in the Gulf Basin both during, and immediately after, the Holocene marine transgression.

## CHAPTER 2: REVIEW OF PREVIOUS RESEARCH AND ARCHAEOLOGICAL POTENTIAL

### 2.1 An overview of Archaeology in the Arabian Peninsula

#### 2.1.1 The Palaeolithic

Very little is known about the Palaeolithic of the Arabian Peninsula as a whole, and it is very difficult to characterise Palaeolithic settlement (Parker et al., 2006) as there are still very few stratified sites, most of the evidence coming from unstratified surface finds, often in deflated landscapes with no geological context (Marks, 2009, p.295). The largest concentrations of Palaeolithic sites are located '*at the margins of modern deserts in the northern and southern portions of the peninsula (Nafud Desert in the north, the Empty Quarter in the south)*' (Petraglia, 2005, p.306). Three stratified sites with lithic assemblages dating to the Middle Palaeolithic period (Jebel Qattar, Jebel Katefah and Jebel Umm Sanman) were recently found along the shores of the Jubbah palaeolake in the Nefud desert in Northern Arabia (Petraglia et al., 2012, p.1).

There has been a considerable amount of debate and uncertainty surrounding the presence, or otherwise, of Palaeolithic remains in the Eastern Arabian Peninsula. Surface finds were reported from Qatar, Bahrain, Oman and Eastern Saudi Arabia from the 1930s onwards (Potts, 1990, p.30-31). An influential Danish survey of the Qatar Peninsula, beginning in the 1950s and continuing into the 1960s (Kapel, 1967)

identified more than 120 Prehistoric sites from surface lithic scatters, which were categorised into 4 groups, A, B, C and D. The A group was initially typologically identified as Palaeolithic ('Mousterian'-related), and the B, C and D groups were typologically classified as following on chronologically from the A group (Rose, 2010). On the basis of Kapel's classifications, a Palaeolithic presence was also identified elsewhere in Eastern Arabia (Kapel, in Bibby, 1973; Masry, 1974; Pullar, 1974), and further attested to in Qatar in the early 1970s (De Cardi, 1978). In the late 1970s, a French research programme investigated a site near Khor in southeastern Qatar and discovered assemblages similar to Kapel's A group present in Middle Holocene layers (Inizan, 1988, p.62; Tixier, 1980, p.197). This research placed Kapel's Qatar A group material in the Neolithic, and not only led to a wholesale reassessment of all Kapel's groups as being Holocene in date, but also led to a general consensus that Palaeolithic material, and by implication, Palaeolithic human activity, was absent from the whole of Eastern Arabia (Potts, 1990, p.31).

However, this position was subsequently revised again in the light of more recent research which has identified several new Palaeolithic sites in Eastern Arabia. Systematic survey in Dhofar, Oman identified evidence of one stratified site, Aybut Al Auwal, and more than 100 surface scatters, containing Middle Palaeolithic lithic assemblages. These assemblages represent technology very similar to that from the late Nubian Complex in northeastern Africa. The sites are all on the Nejd Plateau, and OSL dates obtained from stratified deposits at Aybut Al Auwal produced dates of 106,000 years BP. (Rose et al., 2011, p1; Groucutt and Petraglia, 2012, p.119-120).

Excavations at Jebel Faya in Sharjah Emirate identified stratified Palaeolithic material, providing clear evidence of Upper Pleistocene activity, with the earliest stratified levels dated to c.128,000 years ago (Uerpmann and Uerpmann, 2008; Uerpmann et al., 2009; Marks, 2009; Rose, 2010; Bretzke et al., 2013). Unstratified surface lithic scatters containing material with similarities to the stratified material at Jebel Faya have been identified in Abu Dhabi and Sharjah (Scott-Jackson et al., 2009; Wahida et al. 2009; Rose, 2010).

Although these recent findings can be seen as confirmation of hominin activity in Eastern Arabia in the Upper Pleistocene, the date of the earliest human occupation of the Arabian Peninsula still remains uncertain. Also, there is considerable debate about whether this occupation was continuous or intermittent (Rose, 2010), and whether there was population continuity from the Pleistocene into the Holocene (Uerpmann et al., 2009, p.206). Any evidence for Late Pleistocene human occupation along the former waterway of the Ur-Shatt river corridor will now be submerged (Parker and Goudie, 2008, p.465). Macumber (2011) argues that permanent occupation of the area that now forms the Qatar Peninsula was unlikely in the Upper and Middle Palaeolithic due to the lack of accessible freshwater as a result of low groundwater tables caused by the drop in sea levels. However, it is not currently clear how extensive surface water would have been during ameliorating climatic conditions, or within deep sinkholes which have been subsequently infilled by collapse and/or sediment accumulation. It is also worth noting that Lower Palaeolithic artefacts in Qatar are most likely to have been re-deposited in secondary contexts due to erosion or to re-working by later Neolithic groups (Cuttler, 2010, p.151).

## **2.1.2 The Neolithic**

The marine transgression across the Gulf basin after the last glacial maximum took place between 14,000 and 6,000 years ago, in the Late Pleistocene/Early Holocene, and the environment within the exposed Gulf Basin during this period is likely to have been highly favourable to human settlement (Teller et al., 2000). However, the archaeological and palaeoenvironmental record for the area around the former Gulf basin is scant and incomplete for the Early Holocene, and consists mainly of relatively ephemeral campsites (Rose, 2010). The French investigations of the late 1970s (Tixier, 1980; Inizan, 1988) re-interpreted and re-arranged Kapel's classifications so that Kapel's Qatar B group of lithics, found at a few sites around the Oman peninsula and Qatar (Parker et al., 2006), was classed as the earliest phase of occupation, dating to the beginning of the Holocene. Kapel's A, C and D groups were classed as a single, later group, dating to within the 7th millennium BP (Drechsler, 2009, p.16). Three sites from around the Gulf Basin, Wadi Wutayya in Northern Oman, and Nad al-Thamam and Jebel Faya 1 in Sharjah Emirate, which have been dated by radiometric dates to between 11,000 and 8,500 cal BP, have been used to place the Qatar B sites within the same date range, on the basis of similarities between the lithic technologies (Rose, 2010).

At c.8,000 BP, the Qatar B technology in Qatar was replaced by what was known as the Arabian Bifacial Tradition (ABT), a technology specific to this region of the Peninsula (Cuttler et al., 2011b, p.3). It is worth noting that use of the term ABT is problematic, as it is now considered by flint specialists to be loosely representative of

a range of lithic technologies (Crassard and Dreschler, 2013, p.5-6). The northward migration of the Indian Ocean monsoon in the Early-Mid Holocene led to a significantly wetter period in southern parts of the Gulf region between 8,500-6,000 BP (Parker and Goudie, 2008), making conditions more favourable for human exploitation in areas affected, although Fleitmann et al. (2004, p.20) suggest that the effects of this wetter period reached no further north than 24° latitude. It has been suggested that this improved climate influenced the expansion of settlement in the 8th and 7th millennia BP (Masry, 1997, p.44), a time when larger and more permanent sites appeared in eastern Arabia (Carter, 2010, p.193). However, if we accept Fleitmann's theory, all of the Mid-Holocene sites from the Central Gulf would have been unaffected by the wetter conditions as they lie to the north of 24° latitude (Cuttler, 2013, p.40). Also, there is currently little evidence for an expansion of settlement into the interior of the Arabian Peninsula at this time.

Evidence from the 8th and 7th millennia BP for the presence of domesticated forms of cattle, sheep and goat is increasingly appearing as a result of recent work in the Southern Arabian Peninsula, indicating a change in food procurement. (Drechsler, 2009). However, since the evidence for domesticates is mainly confined to the southern part of the peninsula, there is currently significant debate around their origins (McCorriston and Martin, 2009, p.246-247; McCorriston, 2013). At this period, semi-nomadic herding was predominant in the interior of the Arabian peninsula (Potts, 1990; Uerpmann, 1992, cited in Parker and Goudie, 2008, p.466), and hunting, fishing and the exploitation of marine resources such as shellfish were also important for the coastal settlements at this time (Parker and Goudie, 2008).

It has long been recognised that there was a dramatic increase in settlements appearing around the shoreline of the Gulf in the Mid-Holocene (Rose, 2010). This occurred just after the final phase of marine incursion into the Gulf basin, when sea levels rose to approximately 2-3m higher than present-day levels (Lambeck, 1996). These settlements, predominantly located around the former Mid-Holocene shoreline, are characterised by the presence of ABT lithic artefacts, and display evidence for contact with Mesopotamia during the 8th and 7th millennia BP, in the form of Mesopotamian ‘Ubaid pottery (Carter, 2006, p.58) (Figure 6).

These sites are generally referred to as ‘Ubaid-related sites, as they are clearly not Mesopotamian ‘Ubaid settlements. However, the use of the term ‘Neolithic’ in relation to these sites is the subject of some debate (Crassard and Drechsler, 2013, p.4). The ‘Ubaid-related sites appear to be relatively complex in comparison to the ephemeral campsite-type sites that typify the Early Holocene sites in Eastern Arabia, particularly in relation to the presence of more permanent, stone structures, sophisticated boat-building technology and well-established trade networks (Carter and Crawford, 2010). However, although they do display some evidence for the domestication of plants and animals, they are largely based around hunting, gathering and the exploitation of coastal resources, and with the exception of Arabian Coarse Wares, all of the pottery is imported. Rose (2010) points out that almost all of the stratified ‘Ubaid-related sites in Eastern Arabia appear to have been located in previously unsettled areas. Only Ain Qannas in Saudi Arabia (Masry, 1997) shows evidence of earlier occupation at the site (Rose, 2010). This relatively abrupt change in

settlement patterns is also reflected by unstratified surface sites, where ‘Ubaid pottery and pre-ABT lithics have not so far been found together. (Rose, 2010)

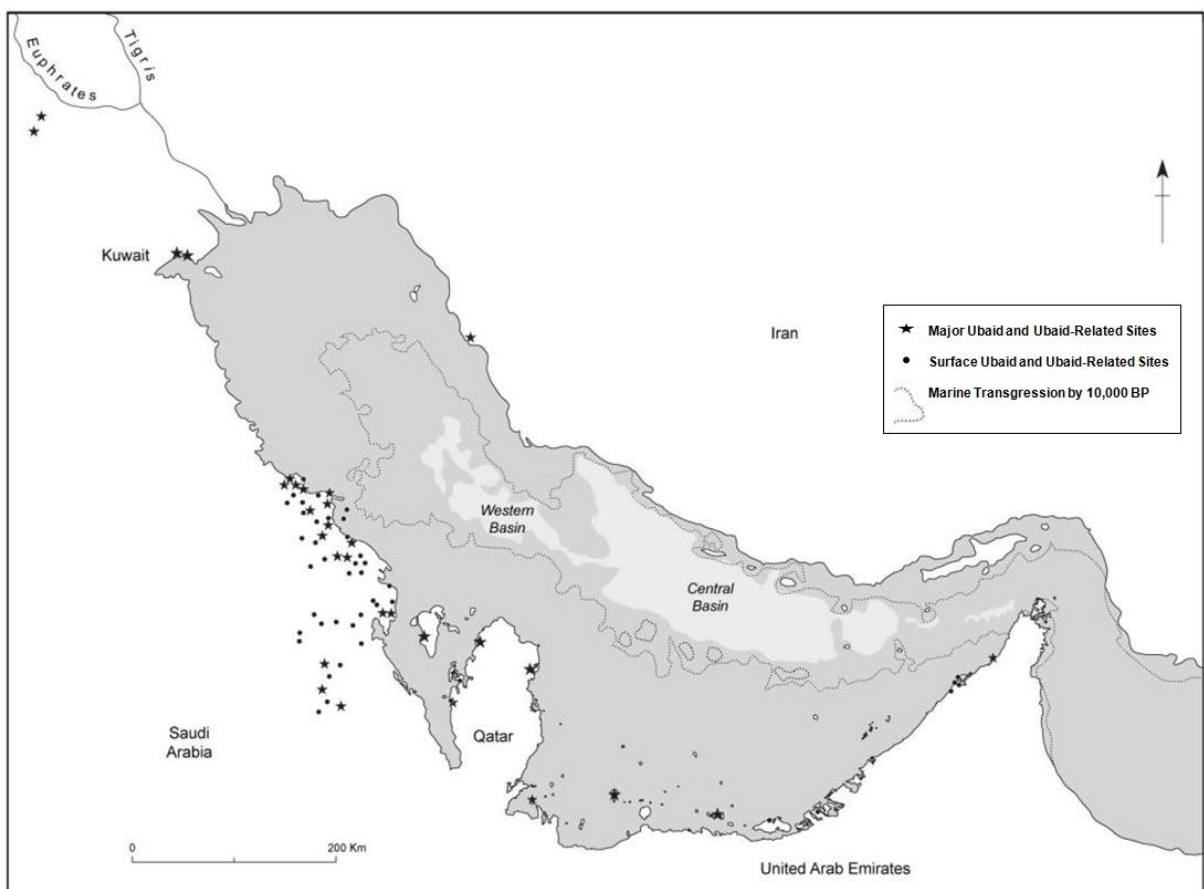


Figure 6 Distribution of ‘Ubaid and ‘Ubaid -Related Sites around the Arabian Gulf (from Cuttler, 2013).

Marine inundation did not occur around the west coast of Qatar until after 8,000 BP (Al Naimi et al., 2012), and occupation of sites along the Qatar coastline begins during the second half of the 8th millennium BP (Carter, 2010). Sites in Qatar include Ras Aburuk/Ra’s Abarāq (De Cardi, 1978, p.82), Bir Zeikrit/Bi’r Zikrīt (De Cardi, 1978, p.115), Site A4 near Dukhan, (Kapel, 1967, p.37), Al-Dasah/al-Da’sah (De Cardi, 1978, p.55), Al-Khor/al-Khawr (Tixier, 1980), and Wadi Debayan/Wādī al-

Ḏaba‘yān (Cuttler et al., 2011b; Tetlow et al., Forthcoming). Outside Qatar, major sites include al-Markh, Bahrain (Roaf, 1976, p.146), Dosariyah/Dawsāriyyah, Saudi Arabia (Drechsler, 2011, p.71), Abu Khamis, Saudi Arabia (Masry, 1997, p.87), Khursaniyah, Saudi Arabia (Masry, 1997, p.84), Ain as-Sayh, Saudi Arabia (McClure and Al-Shaikh, 1993), As-Sabiyah H3, Kuwait (Carter and Crawford, 2010) and Bahra 1, Kuwait (Rutkowski, 2011). There are far fewer ‘Ubaid-related sites in the Lower Gulf than in the Central Gulf, probably as a result of increasing distance from Mesopotamia. (Carter, 2006, p.59).

So far, it has not been possible to firmly establish where these ‘Ubaid-related communities originated from. Whilst the increase in settlement may in part be attributed to the greater archaeological visibility of more permanent settlement, it is also possible that the new settlers migrated into the area as a result of displacement from the Gulf basin by relatively rapid inundation between c. 8,000BP and 7,500BP (Rose, 2010). If this theory is accepted, then Rose proposes that we should not necessarily view the existing, ephemeral Terminal Pleistocene/Early Holocene sites around the Gulf as representative of the population in the region at the time, but rather as ‘more mobile, peripheral elements of a larger core group’ (Rose, 2010, p.850).

The archaeological evidence indicates that there was a break in human settlement in Eastern Arabia in the early 6th Millennium BP. No ABT/‘Ubaid-related sites have been dated to later than 5,800 BP (Parker and Goudie, 2008, p.467), and there is a complete absence of known archaeological sites throughout Eastern Arabia during

the following millennium (Uerpmann, 2003), with the exception of the recently-excavated site at Wadi Debayan in Qatar. The fish midden at this site has been radiocarbon dated to between 5,200 and 4,500 BP (Tetlow et al., Forthcoming). This relatively sudden break in human settlement in Eastern Arabia, and evidence for a major population decline in the Arabian Peninsula as a whole, coincides with the end of the mid-Holocene wet phase, and the onset of arid conditions, following on from the southward migration of the Indian Ocean monsoon (Parker and Goudie, 2008). It has been suggested by Uerpmann (2003) that the break in human settlement is due to this climatic deterioration, but there may also have been other contributory factors, indicated by the evidence from Wadi Debayan of a high energy event affecting the coast of Qatar soon after 4,500 BP (Tetlow et al., Forthcoming).

### **2.1.3 Maritime History**

The potential for archaeological sites within the submerged Gulf is not simply limited to sites from the Late Pleistocene/Early Holocene, but also includes the potential for shipwrecks from the 8th-7th Millennium BP to the present day. The earliest direct evidence for maritime trade in the Gulf consists of boat-related remains found at H3, As-Sabiyah in Kuwait (Carter and Crawford, 2010). These remains took the form of more than 50 fragments of bitumen with reed impressions and barnacles, interpreted as the waterproof coating from sea-going reed bundle boats (Carter, 2006, p.55-56) , and they are the earliest sea-going boat remains yet identified anywhere in the world. Representations of boats were also found at the site, including a ceramic model of a reed bundle boat and a picture of a masted boat painted on a ceramic disc. These

boat-related remains were found in archaeological contexts dating between 7,500 and 7,000 BP (Carter, 2006, p.53-55).

There is also indirect evidence for seafaring and maritime trade in the 8th-7th millennia BP, as represented by quantities of 'Ubaid pottery from Mesopotamia found at more than 60 Arabian Neolithic sites around the coast of the Eastern Arabian Peninsula, including Saudi Arabia, Bahrain and Qatar (Burkholder, 1972; Masry, 1974; De Cardi, 1978). Recent research has led to the general acceptance that this pottery represents an extensive maritime trading network between the Arabian Gulf and Southern Mesopotamia (Carter, 2006; Carter and Crawford, 2010). There is no evidence for boat-building in Qatar at this time, but presence of 'Ubaid pottery at the coastal Neolithic sites in Qatar clearly demonstrates that these settlements were participating in this well-developed maritime trading relationship. The archaeological evidence indicates that the interaction between Mesopotamia and the Gulf petered out during the 7th millennium BP (Carter and Crawford, 2010, p.212).

In the Bronze Age, a complex maritime trade network existed between Southern Mesopotamia, Dilmun/Bahrain, southeastern Arabia and the Indus Valley civilisations (Al-Naimi et al., 2012, p.249) around 5,000-3,500 BP. Of particular relevance to the Study Area, given its location, is Dilmum, which, between 4,500 and 3,500 BP, became a very important international trading nation, channelling trade through the Gulf. This was due in part to its strategic location between the head of the Gulf and the Straits of Hormuz, its safe anchorage and its plentiful freshwater supplies (Killick and Moon, 2005, p.1). There are frequent mentions in cuneiform texts from

Mesopotamia from the 5th Millennium BP onwards of ships sailing from Ur in Southern Mesopotamia to Dilmun, to Magan (Southeastern Arabia) and to Meluhha (thought to be in the Indus Valley) (Roux, p.32). Qatar was clearly a part of this trading network, as Barbar pottery typical of Dilmum has been found at sites in Qatar, including on the Ras Abaruk peninsula (Carter, 2003). A 4th millennium BP dye production site on Khor island in Qatar, which produced quantities of Kassite pottery, is also evidence of significant trade with Mesopotamia (Edens, 1999).

The Arabian Gulf continued in historical times to be a very important trade route linking the West and the East. The Sassanid dynasty, established in Mesopotamia in AD 225, controlled the trade of a wide range of commodities in the Gulf, and by the early Islamic period Arab dhows were trading with India, China, Southeast Asia and East Africa, playing a central role in trade, and in other aspects of society such as exploration, and defence (Al-Naimi et al., 2012). The Arabian Gulf has long been famous for its role in the historic pearl trade, and extensive pearl beds are found all along the Arabian side of the Gulf, with the most productive located to the north and east of Bahrain (Bowen, 1951, p.166). The importance of Bahrain as a pearl-trading centre is apparent from the many references to the pearls of Bahrain by early travellers to the Gulf (Bowen, 1951, p.161). It was estimated in the early 19th Century that there were 1500 pearl fishing boats in Bahrain (Wilson, 1883, p.285), and 900 at the turn of the 20th Century (200 in Qatar) (Bowen, 1951, p.168). The northwest coast of Qatar was well-known to early Arab navigators (Johnson and Wilkinson, 1960, p.444), and the remains of the former pearl-fishing and trading port of Al-Zubārah, in close proximity to the Study Area, are testament to the importance of the

northwest coast of Qatar to maritime trade in the 18th and 19th centuries. Khor Hassan (Khuwayr), further up the coast to the north of Al-Zubārah, became the base of the notorious pirate Rahma bin Jabir, in the early 19th Century (Johnson and Wilkinson, 1960, p.444; Misbahuddin, 1984), again an indication of the role that this stretch of water played in shipping and trade.

However, despite the longevity of this maritime history, there has been very little research into wrecks or other maritime archaeological finds in the Gulf. A relatively recent discovery of an ancient merchant ship and its cargo, lying at a depth of 70m near the port of Siraf in Iran, was reported in 2006 by local fishermen, who discovered it accidentally. More than 40 amphora have been recorded on the seabed, and the wreck is believed to date from the Parthian or Sassanid periods (NOAA, 2006, p.17). There is also an unconfirmed report of a wreck with a cargo of amphora lying at a depth of 10m in a deep-water channel in Bahrain territorial waters. Fragments of amphorae from this site have been retrieved on several occasions by local divers (Al-Naimi et al., 2012, p.249). Elsewhere in the Gulf, twenty-eight stone anchors and ring-stones were discovered from a single submerged site near Qalhat, an important Early Islamic and Medieval port in Oman (Vosmer, 1999, p.250).

Regarding more recent times, there is documentary evidence, in the form of a series of telegrams between various officials, of a major sea battle involving the British navy that took place around the Bay of Al-Zubārah in Qatar in 1895. According to the correspondence, this battle occurred as a result of a potential threat from a fleet of dhows, assembled by the Ottomans and Sheikh Jassim bin Thani, that were

apparently armed and ready for an imminent attack on Bahrain (Wilson, 1895). The British Navy became involved as a result of their relations with, and influence over, the affairs of Bahrain. The battle took place on 6th September 1895, and correspondence from the captain of the British warship H.M.S. Sphinx, records that the warship shelled the fleet of dhows for hours, and then despatched boats, under cover of firing blanks, to set fire to the dhows. The captain states that '*The total number of dhows destroyed as far as can be ascertained from the ship is about 44*' (Pelly, 1895. However, no traces of these boats have ever been found.

An early 18th Century naval cannon was recovered from the sea relatively recently (the exact recovery date is unknown) near Mesaieed/MusayKīd, off the east coast of Qatar, reportedly during the excavation of a new pipeline (QNHER ID 355; Al-Naimi et al., 2102, p.249). There are also documented modern wrecks in Qatari waters, including 17 from the past century recorded within the Qatar National Historic Environment record, which have been recorded from maritime charts. These include wrecks off the northern tip of the Qatar peninsula, to the northeast of the Study Area, which are depicted on an old Admiralty chart, the survey date for which is given as 1925 (UKHO 1925).

## **2.2 Submerged Landscapes Research**

### **2.2.1 Research Outside the Arabian Gulf**

There has been very little work carried out into submerged landscapes in the Arabian Gulf basin, and relatively little has been written about its archaeological significance or potential (Cuttler, 2014). Before detailing the small amount of work that has been done, it is useful to place it into a wider context by providing an overview of investigations into areas of submerged landscape elsewhere in the world.

Research on submerged coastlines has been carried out in the Red Sea, around the Farasan Islands (Bailey et al., 2007), in the context of human occupation in the area of the Bab al-Mandab Straits during periods of lower sea levels. Archaeological survey and underwater exploration recorded archaeological sites, largely shell middens formed in the last 6,000 years, located at characteristic geomorphological locations on land, and then recorded similar locations underwater at submerged former shorelines. Work is continuing to try and identify archaeological sites associated with these shorelines.

In the USA, underwater geoarchaeological studies were carried out in an area of drowned Karst landscape in Apalachee Bay, off Florida in the Gulf of Mexico. The research used seismic profiling, vibrocoring, diver surveys and underwater excavations to reconstruct palaeo-landscape features and to successfully locate and investigate submerged archaeological sites (Faught and Donoghue, 1997).

In Europe, pioneering research was carried out into the palaeo-landscapes of the North Sea, using an extensive 3D seismic dataset that was originally collected for oil exploration purposes, to map Holocene features across a large area of the southern North Sea (Fitch et al., 2005; Gaffney et al., 2007). This work demonstrated how regional-scale studies of submerged landscapes using remotely-sensed data can reveal highly significant information about an archaeological landscape that would have been a major habitation area in the Mesolithic period.

Also in Europe, research has been undertaken into submerged landscapes off the north coast of Ireland using high-resolution multibeam bathymetry to map the palaeo-landscape. The result of this work was the identification of ten areas of high archaeological potential which will be subject to more detailed analysis in subsequent stages of the research (Westley et al., 2011a).

A significant amount of work has been carried out on developing marine classification and characterisation projects around the UK coast. Some of these have been based entirely on environmental attributes, such as the Irish Sea Pilot (Golding et al., 2004), which was not specifically an archaeological or historic classification project. This project was aimed more at ecological aspects of marine conservation, and used geophysical and hydrographical data to map marine landscape types. The Isles of Scilly Rapid Coastal Zone Assessment Survey (Johns et al., 2004), used historical, archaeological, geographical, topographical and environmental data to investigate the submerged heritage around the Isles of Scilly. The survey methodology included extending the existing Historic Landscape Characterisation for the Isles of Scilly

(Land Use Consultants, 1996) to the intertidal and maritime zones. English Heritage undertook an extensive Historic Seascapes Programme in several areas around the English coast for the purposes of resource management (Cornwall County Council, 2008). This programme was guided by the principles of terrestrial historic landscape characterisation, and aimed to map the historic character of the marine environment using maps, charts and other documents together with recent marine data sources such as bathymetry and sediment information. However, none of these projects utilised sidescan sonar data or acoustic classification as part of their methodology.

The research carried out in different parts of the world has shown clearly that random surveys of submerged landscapes are unlikely to yield successful results. All of these studies used landscape-based approaches to a greater or lesser extent as the first stage of investigation, in order to highlight areas of potential that could then be targeted for further, more detailed study, and all of them incorporated topography and geomorphology to some extent. The key to the success of the study in the Gulf of Mexico lay in using knowledge of geological and topographic markers from terrestrial archaeological sites to try and find similar settings on the seabed. In this study, such settings included locations close to fluvial and aquatic features, including karst features, at river estuaries and near lithic resources. This emphasises how important the identification of palaeo-drainage patterns, buried karst features and former coastlines is to the study of the submerged karst landscape off Northern Qatar. The work in the Gulf of Mexico also demonstrated the value of utilising a range of different investigative techniques as the study became more targeted.

## **2.2.2 Research Within the Arabian Gulf**

The lack of research into the archaeological and palaeoenvironmental potential of the Arabian Gulf basin is now beginning to be addressed with the pioneering work that is being carried out by the QNHER project around the Qatar peninsula. A limited amount of assessment work was carried out in 2010/2011 on the sidescan sonar dataset that was collected for the Qatar Bahrain Causeway project. This is the same sidescan sonar dataset that was used for the research outlined in this thesis. This assessment consisted of a rapid review of the sonar contacts originally identified by the survey company, and 83 features of potential archaeological interest were highlighted (Cuttler et al., 2011a). Approximately half of these anomalies were diver-inspected by a team of marine archaeologists in March 2011, but all proved to be of modern or natural origin (Al-Naimi et al., 2012). Despite the lack of significant archaeological finds, this work proved very successful in establishing effective methodologies for ground-truthing seabed anomalies, and in increasing understanding of the interpretation of acoustic signatures from the seabed around Qatar. However, it was apparent from this work that investigating geophysical anomalies in isolation, and using low frequency sidescan sonar data as the sole dataset, was not an effective way of understanding the submerged landscape. It was also equally clear that random surveys would be extremely unlikely to be successful in locating archaeological and palaeoenvironmental remains.

The QNHER project has also been conducting further marine surveys, including a programme of high-resolution sidescan sonar survey using a Klein Hydroscan, which

is capable of collecting very high resolution sidescan data over large areas, and using this to target diver inspections (Cuttler, Forthcoming). In 2012-2013, this work led to the confirmation of the location of seven relatively recent shipwrecks off the north coast of Qatar, which were subsequently inspected by divers. These were all steel-hulled vessels dating to within the last 60 years. Their concentration in the north is probably related to the fact that the principal trade route towards Bahrain and Iraq lies to the north of Qatar (Cuttler, 2014).

Research carried out by Cuttler (2013; 2014), using high-resolution 3D seismic survey data that was collected from the offshore Al Shaheen oil field to the northeast of Qatar for oil exploration purposes, has identified fluvial landscape features. This research has confirmed the presence and character of the Ur-Shatt river (originally postulated by Lambeck, 1996) as a wide, flat valley of marshland, lake and swamps, although it is still not clear if this was a freshwater or saline environment.

Research into human settlement in Arabia in the Palaeolithic period undertaken by Rose (2010) has focused on Prehistoric occupation in and around the Arabian Gulf basin. This research uses hydrological, geoarchaeological and archaeological evidence to support the theory that the former Gulf basin was once an oasis which supported a sizeable human population in the Late Pleistocene and early Holocene.

There has been a significant amount of non-archaeological survey work in the Study Area. Geophysical surveys have been carried out by commercial companies as part of the planning phases of the proposed Qatar-Bahrain Causeway. An acoustic survey

was carried out in 2002 (Marin Mätteknik AB, 2002) which captured bathymetry using a single beam echo sounder (a geophysical technique that captures depth information), shallow seismic data using a sub-bottom profiler (a geophysical technique which provides profiles of the upper layers of the ocean bottom), and sidescan sonar data. However, the acoustic data from this survey was not made available for this research. The survey company logged 107 targets in the sidescan sonar data, and also classified the seabed in the whole of the causeway area in both Qatari and Bahrain waters into 12 types (Marin Mätteknik AB, 2002, p.17), but no information is provided in the report as to how the classification was carried out. Each seabed type is summarised in a short description (two or three sentences) and given a single-sentence description of the area location.

Further acoustic data was captured in the causeway area in 2008 for the purposes of sand-search survey and hydrographic survey (GEMS, 2008). This survey utilised a single beam echo sounder and sidescan sonar, and also a sub-bottom profiler in Qatari waters. The survey company logged a total of 601 contacts in the data from the Qatari side of the causeway project area. The sidescan sonar data collected for this survey is the core dataset that was used for the sediment texture classification and geophysical anomaly identification sections of this research. Geotechnical data, including core sampling (Fugro Peninsular, 2008; QBC Consortium, 2009a, 2009b), and an underwater video survey (Creocean, 2008) were also carried out as part of the causeway planning phase.

## **CHAPTER 3: OVERVIEW OF METHODOLOGY**

This chapter provides an overview of the theory and usage behind historic landscape characterisation methodology, and briefly summarises the stages of the seabed characterisation, and the data sources and techniques to be used. Detailed methodologies for each stage of the characterisation are provided at the beginning of the relevant sections.

### **3.1 Processes of Seabed Characterisation**

A major aim of this research was to test methodologies for investigating the submerged landscape. It was decided, therefore, to explore how concepts and methods used for terrestrial Historic Landscape Characterisation (HLC) could be adapted in novel ways and applied to submerged landscapes in the form of ‘seabed characterisation’. The seabed characterisation aimed to combine principles of HLC, acoustic classification and natural environment mapping, based primarily on a range of environmental attributes, but drawing on human exploitation and interpretational elements wherever possible.

The basic premise of landscape characterisation is to define areas ‘*on the basis of combined shared values of dominant character attributes, with secondary attributes recorded in a consistent and structured manner*’ (Cornwall County Council, 2008: 14). Terrestrial HLC can encompass topography, habitats, natural and semi-natural features and palaeoenvironmental deposits as well as archaeological sites. It can

also encompass intangible and non-visual elements such as cultural and psychological perceptions, and historical associations (Fairclough, 2001). The core principles of landscape characterisation require it to be systematic, comprehensive, repeatable and interpretational.

Many different methodologies have been developed and used for terrestrial landscape characterisation (Aldred and Fairclough, 2003). The methodology used for this seabed characterisation follows the ‘multi-mode’ approach (Aldred and Fairclough, 2003, p.18), a combination of attribute-led description followed by interpretative classification. In this approach, the entire Study Area is divided into initial landscape units on the basis of one or more core attributes. The basic classification can then be built on and supplemented by gathering data on a range of natural environmental and cultural attributes which can then be assigned to each unit. Whilst environmental data can be considered to be more objective and consistent, the human and interpretational dimension is also an important factor in providing a holistic understanding of the landscape. When discussing attributes, it is worth noting that the differentiation between ‘environmental’ attributes and ‘cultural’ attributes is slightly blurred, since environmental attributes can both influence and reflect cultural attributes, and vice versa. It is the ability to accommodate the interplay of these linked factors that is one of the strengths of the seabed characterisation approach.

The characterisation types are defined through analysis and identification of the trends and combinations in which certain attributes occur. Further analysis is then

undertaken to allocate a characterisation type to each unit, according to which type best represents its predominant landscape character. This approach is a very flexible and transparent method, allowing the generation of many different classifications and interpretations, and the creation of intermediate theme mapping which may be used as individual information sources (for example the extents of a particular type of seabed habitat).

The factors influencing the character of the seabed can be classified as primary (or core) attributes, which form the basis for the division of the seabed into initial landscape units, and secondary attributes, which do not necessarily provide seamless, continuous coverage over the landscape, but can be used as supporting data sources to further refine and calibrate the initial landscape units. The procedure is recursive, with the data collection stages and data analysis stages having the potential to inform each other, and the character areas can be gradually refined with each new stage of data input and analysis (Dingwall and Gaffney, 2007). Some patterns will emerge in relation to Prehistoric settlement, and others in relation to maritime exploitation and shipwrecks. This process of calibration and refinement is the essence of the seabed characterisation. The end result of this process is the identification of areas formerly favourable to human occupation, and areas expressing potential for the preservation of palaeoenvironmental and archaeological remains. This latter process takes a step beyond first-stage historic landscape characterisation, as initial landscape characterisation does not normally seek to provide value judgments on the landscape under investigation, the core principle

being that every part of the landscape is classifiable and in need of change-management to some degree.

The core data sources used for the primary characterisation were low-resolution sidescan sonar data and LiDAR bathymetry data. These datasets covered extensive areas of the seabed and were deemed suitable for the primary classification of the seabed. The aim was to undertake the primary classification by carrying out sediment texture classification using the sidescan sonar data, and mapping of seabed topography using the LiDAR bathymetry. This would be further informed by ground-truthing data from direct sediment samples and video footage. The secondary classification would then be undertaken, and would consist of the analysis of individual geophysical anomalies within the sidescan sonar data, and the further targeted investigation of selected anomalies via high-resolution geophysical survey and diver inspection, in order to support the primary classification. The end result of this characterisation process would be a set of contiguous polygons covering the entire Study Area, representing broad character zones, which could be used to assess potential and inform further research.

### **3.2 Primary Characterisation**

#### **3.2.1 Sediment Texture Classification**

The first step of the seabed characterisation process is to establish how the seabed can be divided up into initial landscape units in the most effective and objective way.

Sidescan sonar is an efficient and rapid method of creating images of large areas of seabed based on the acoustic ‘backscatter’ reflected from the sonar beam. It can be used to detect objects that are either raised from, or sunken into, the seabed, and also to identify distinct changes to the material and texture type of the natural seabed (Blondel, 2007). The sidescan sonar data available for the Study Area provides continuous, seamless coverage, and this type of acoustic backscatter data has been successfully used elsewhere in the world for seabed sediment classification, largely for the purposes of natural habitat mapping. Since the seabed sediment usually reflects the character of the underlying substrate, and is therefore a fundamental characteristic of the seabed, sediment classes are a suitable primary attribute that can be used for the division of the seabed into initial landscape units. The acoustic backscatter data captured by the sidescan sonar can be used to aggregate areas (classes) of similar acoustic signature (Penrose et al., 2005), the aim being to reflect the variability in the nature of the seabed sediment, and highlight landscape-scale changes.

### **3.2.2 Topographic Mapping**

The topography of the seabed (bathymetry) is also a major influence on the character of the seabed, although in this characterisation, the aim was not to use bathymetry as the primary dataset for the initial determination of landscape units, but rather to use it to inform and refine the initial units. A surface model can be created from bathymetry that can then be visually inspected for evidence of topographic features that formed when sea-levels were lower. Seabed topography, like sediment

character, is, at least partially, a reflection of the underlying geology, and provides the ability to highlight landscape-scale features that would have been attractive for human settlement, such as former shorelines, and/or features that are conducive to the survival of palaeoenvironmental caches, such as palaeochannels. The shape of the seabed evolves through factors such as erosion, deposition, the energy of the sea and the hardness of the underlying rock. However, the present day seabed is not going to be a direct reflection of the palaeo-land surface, as sedimentary processes associated with marine transgression are likely to have buried the past landscape in some areas and eroded it in others. We need to consider the processes that would have either protected or eroded land surfaces as sea levels rose. Also, any study of seabed mapping and classification has to take into account the mobility of features and sediments, since seabed features such as sand waves and sand ripples are not static features. However, the aim of this part of the research was to define broad areas where conditions are suitable for features of high archaeological and palaeoenvironmental potential to be created and maintained, and use these to inform and refine the character areas.

Sea level changes are critical, since they can be used, together with the topographic data, to locate and define former shorelines. Former shorelines are highly significant, both in relation to patterns of human settlement, and in relation to preservation factors. The marine incursion since the last glacial maximum was not a steady process, with periods of both slow and rapid incursion, and also periods of still-stands. The lack of reliable regional sea-level curves, and the debate surrounding the effect of tectonic movement and isostatic loading movements (Lambeck, 1996;

Uchupi et al., 1999), means that it is not possible to be exact about the timing of marine transgression within the Study Area. However, we have enough detail for the purposes of broad-brush seabed characterisation.

Marine taphonomic processes are also very important in this respect, and it is critical to determine the types of changes which might affect the form and condition of submerged sites prior to, during and after the rise in sea level (Faught and Donoghue, 1997). This is particularly important, since we currently have very little information about how sedimentary regimes and taphonomic processes in the Gulf affect potential archaeological remains. Different depositional environments and preservation factors are likely to apply to Prehistoric sites as opposed to more recent wrecks.

### **3.2.3 Ground-Truthing**

Ground-truthing data is essential for characterisation undertaken via acoustic classification, as it provides validation for the initial classes. The most common ways to ground-truth acoustic classification data are direct sediment sampling and photography. The aim for this characterisation was to undertake a sampling programme over as much of the Study Area as possible, using a Van Veen grab sampler, and then to subject the grab samples to texture analysis (granulometry) in order to test the correlation between the acoustic classes and the sediment characteristics. A further aim was to supplement the ground-truthing element of the seabed characterisation by utilising geotechnical data that was collected for the

planning stages of the Qatar-Bahrain Causeway project (Fugro Peninsular, 2008, QBC Consortium, 2009a; 2009b), together with underwater video survey transects that were taken for benthic habitat assessment purposes, also for the Qatar-Bahrain Causeway project (Creocean, 2008) .

### **3.3. Secondary Characterisation**

#### **3.3.1 Identification of Geophysical Anomalies**

The sidescan sonar data can also be used to identify geophysical anomalies that may represent areas of archaeological significance. The influence of Prehistoric human exploitation of the landscape and the subsequent marine environment, as represented by physical remains on the seabed, is a very important interpretational aspect of the characterisation, and this is where identifying geophysical anomalies from the sidescan sonar data plays a key role. The earliest archaeological remains could consist of relict land surfaces and palaeochannels, as well as buried archaeological sites. Cairns dating from 6,000 years ago, constructed out of rubble, and measuring 1-2 m high and 5m across, are present in the terrestrial Qatari landscape. Building in stone was being undertaken at 'Ubaid-related sites around the Gulf shores 6,500 years ago, as documented by sites such as Ras Abaruk 4b, Qatar (De Cardi 1978, p182), where traces of stone structures were found, As-Sabiyah H3, Kuwait (Carter and Crawford, 2010), where a series of stone structures were excavated, and Marawah Island, Abu Dhabi (Beech et al., 2005), where stone walls up to 0.7m in height survived. It is reasonable to suggest that comparable stone

structures would have been constructed by the populations occupying the former Gulf basin in the period preceding the final phase of marine incursion. Such structures as these would be large enough to be visible on sidescan sonar, but the likelihood of this would depend on subsequent depositional and erosional processes. Features would have to have been buried rapidly in order for them to have been preserved, but would also require some level of subsequent erosion in order to be detected by sidescan sonar.

After the most recent marine transgressions, archaeological remains will consist of shipwrecks, lost cargoes and other marine debris. The aim was to try and reflect these factors through thorough analysis of all geophysical anomalies visible in the sidescan sonar data, and use this analysis to inform the primary characterisation.

### **3.3.2 Clarification of Geophysical Signatures**

As the sidescan sonar data used for the research was low-resolution data, it was expected that selected geophysical anomalies may need further clarification, via a targeted programme of high-resolution geophysical survey and diver inspection, in order to try and further clarify geophysical signature types.

### **3.4 Defining Character Areas and Assigning Potential**

The final stage of the characterisation process is to integrate the analyses from all the different data sources and techniques. Once all the data is collected and integrated, it is possible to analyse and seek consistent patterning in the data, and use this to refine the landscape units into character areas. These character areas should reflect broad environmental trends, which will have had an influence on past human activity in the landscape.

It is essential that part of the interpretational aspect of the seabed characterisation comprises the study of known human settlement patterns in the coastal region of Qatar in the Mid-Holocene, when sea levels were approximately 2-3 m higher than today (Lambeck, 1996, p.50), and the subsequent utilisation of this knowledge to inform pre-transgression settlement patterns in the submerged landscape. The successful discovery of submerged archaeological sites depends on applying our knowledge of geological and topographic markers from terrestrial archaeological sites to find analogous settings on the seabed.

One of the advantages of utilising landscape characterisation approaches is that the recursive nature of the characterisation process allows the integrated data to be manipulated in different ways for different purposes, by combining attributes to derive new information, and using the results to feed back into the characterisation again. In this way, the resulting character areas can be used to generate zones of archaeological and palaeoenvironmental potential. Preservation factors and human settlement patterns are key to this, and certain locations score relatively highly both in terms of being formerly favourable locations for human settlement and for having high preservation potential in terms of the probable presence of extensive sedimentary deposits.

## **CHAPTER 4: PRIMARY CHARACTERISATION**

The following chapter describes the methodology and results of the primary characterisation. This comprises three different strands - the sediment texture classification using the sidescan sonar data, the topographic mapping using the bathymetric LiDAR data, and the ground-truthing data using the direct sampling and visual observation data. Each strand has three sections consisting of the detailed methodology, the results and a discussion.

### **4.1 Sediment Texture Classification**

The sediment texture classification was undertaken by applying acoustic classification techniques to the available sidescan sonar data.

#### **4.1.1 Methodology**

##### **4.1.1.1 Overview of Sidescan Sonar**

The sidescan sonar data collected for the Qatar-Bahrain Causeway project has provided an image of the seabed in the Study Area, which can be used as the basis for landscape-scale investigations. The data consisted of 229 files in xtf format, each representing a single survey line and together covering 365 square kilometres of seabed on the Qatari side of the Causeway Project area. Sidescan sonars are either towed by ships or hull-mounted (Figure 7), and carry sideways-looking transducers

which emit sound pulses, giving an image of sound (sonograph) reflected from the sea floor beneath, and on either side of, the survey vessel (Jones, 1999, p.37).

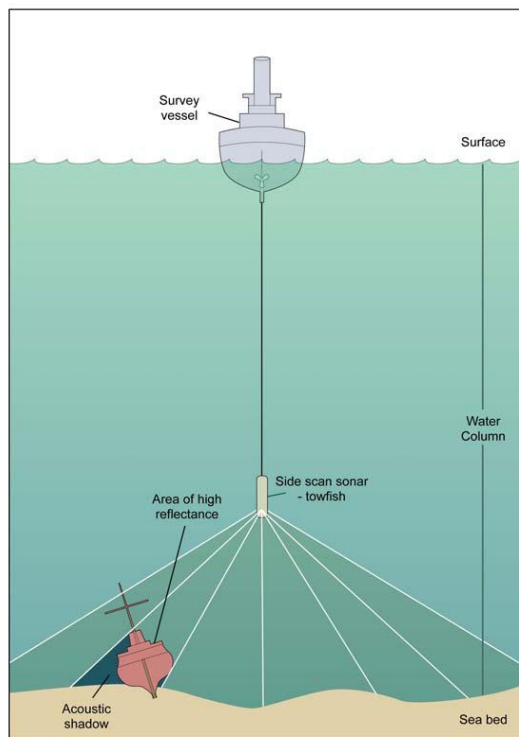


Figure 7 Sidescan sonar operation (from Al-Naimi et al., 2012).

A range of different frequencies can be used to give different resolutions, but as with most geophysics, there is a trade-off between resolution and coverage. Higher frequencies give higher resolution data, but attenuate more quickly with range than lower frequencies, so the widths of the survey lines have to be smaller than with low-resolution surveys. The survey dataset for the Study Area was acquired using single channel sonar at a frequency of 325 Kh in the Qatar-Bahrain Causeway's custom coordinate system (GEMS, 2008). This resolution is relatively low, and the data quality is therefore not as good as could have been obtained with a higher resolution survey, so accurate interpretation of some features could be potentially more difficult.

However, low-resolution surveys enable quicker data capture, thus enabling a larger area of seabed to be surveyed within the time and resources available. In order to ensure comprehensive coverage of the seabed, there should be sufficient overlap between adjacent survey lines, ideally a minimum of 100%. This is because sidescan sonar systems have two side-facing transducers that cannot ensonify the seabed directly beneath the towfish, so an overlapping adjacent swath is necessary to achieve complete seafloor coverage. It is also good practice to overlap survey lines in different directions, as the appearance of certain features can vary considerably when seen from different angles (Blondel, 2007). In the dataset for the Study Area there is very little overlap in the survey lines, they are mainly contiguous, except for the northern part of the Study Area (Area 1) where there are actually gaps between the survey lines (Figure 8).

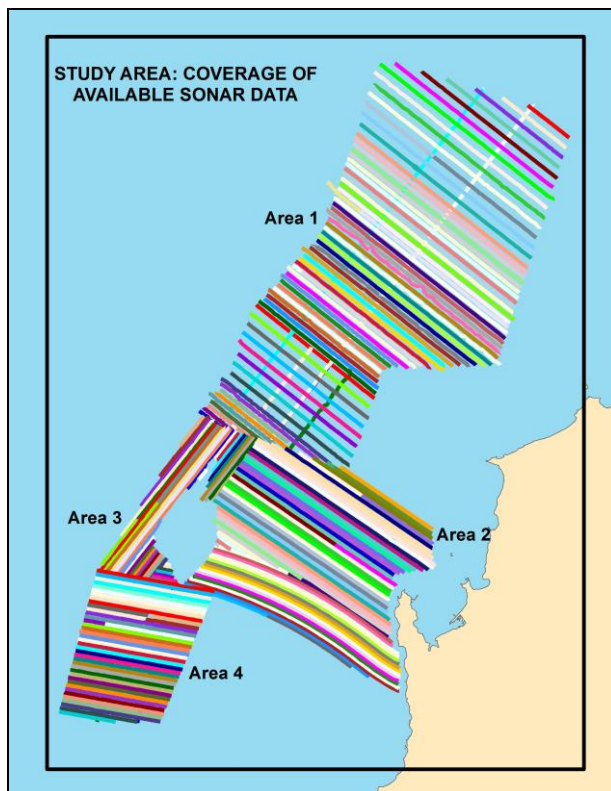


Figure 8 Coverage of sidescan sonar survey lines in the Study Area.

Although the low resolution and the lack of overlap in the survey lines are recognised limitations on the data, a large-scale, low-resolution dataset such as this is suitable for seabed characterisation when used in combination with other datasets, since characterisation is intended as a ‘broad-brush’ study, designed to identify areas of high potential and target them for more detailed investigation, rather than focusing on the detail of individual, small-scale features .

#### **4.1.1.2 Acoustic Techniques for Sediment Texture Classification**

Sediment classification was undertaken using the sidescan sonar data as the base data source. The use of acoustic techniques for large-scale seabed classification and benthic habitat mapping was established in the mid-1990s (Anderson et al., 2008), initially using backscatter data from sidescan sonar, and more recently multibeam echo sounders (MBES), and their use is increasing as the technology evolves to allow larger areas to be surveyed more cheaply at higher resolutions. Multibeam systems produce contoured bathymetry from beneath and to the sides of the survey vessel, and hybrid multibeam systems combine both sidescan sonar and bathymetry (Jones, 1999, p.37).

Acoustic classification consists of classifying the area of surveyed seabed into similar and distinct regions based on the characteristics of the acoustic backscatter. The theory behind it is that classified acoustic data can be used as a proxy for sediment classification, based on the fact that the character of the backscatter is influenced by the roughness of the surface, and therefore the ‘roughness’ of the backscatter is an

indication of the roughness of the physical sediment. The seabed sediment, in turn, usually reflects the character of the underlying substrate. Generally, hard substrate such as exposed rock generates a high backscatter value, whilst soft material such as mud or silt will produce a low backscatter value (Penrose et al., 2005).

The big advantage of this method over photographic and direct sampling methods for mapping seabed sediments is the ability to obtain rapid coverage of large areas of seabed, without the big spatial gaps in the data that photography and discrete sampling inevitably leave. However, the classified acoustic data alone can only provide preliminary baseline mapping, and needs to be analysed in conjunction with ground-truthing data, usually obtained by direct sampling and photography. Although ground-truthing is a necessity for a valid and robust classification, and can be time-consuming to collect, the attributes obtained from well-targeted ground-truthing sites can be potentially applied to large areas of seabed, even to areas which may be remote from the ground-truth sites (Preston, 2009). Depending on the classification methodology, the classified dataset can be used to guide the ground truthing, and also further, more detailed acoustic survey.

In the past, interpretation and classification of the images of the seabed obtained from the acoustic data was usually carried out by skilled, human visual interpreters. Although this is a relatively subjective process, it has been shown to be effective in areas where adjacent seabed types are well-differentiated, or where specific seabed features produce distinctive backscatter. However, in areas of heterogeneous seabed, or where the seabed character changes gradually without clear

differentiation in the backscatter response, visual interpretation becomes more difficult, and other methods have to be investigated (Collier and Brown, 2005). Increasingly, automated processes are being explored, and although generally more objective, these processes can provide new and different challenges. Whilst automated classification can be done more rapidly than visual interpretation, more intensive data cleaning and preparation is required before classification is attempted. This is because the impact of image artefacts such as beam-pattern effects, which are easily detectable and excluded from the classification by human interpreters, needs to be minimised if coherent automated classification results are to be obtained, (Preston, 2009, p.1277).

The classification carried out for the Study Area was ‘unsupervised’ classification. This type of classification is carried out without any foreknowledge of the classes to be created, and can be used in areas where there is little or no ground-truthing data (such as sediment samples or underwater photographs). This is different to ‘supervised’ classification, which can be undertaken where there is sufficient ground-truthing data available from the survey area to create training data that can be used to classify the entire dataset (Ellingsen et al., 2002).

#### **4.1.1.3 Trialling the Classification Methodology**

Trials were carried out using different software to try and establish the best method for classification and interpolation of the data. The first trial used the relatively newly-developed seabed classification module in Chesapeake’s SonarWiz software. The

raw data (xtf format) from the parallel tracks covered by the survey boat were imported into the software, batch processed and used to create a mosaic image of the seabed. The classification module was then run on the mosaic data a number of times using a variety of parameters, including using different gain settings, varying window sizes, trimming the sidescan swaths by varying amounts, using different texturers (statistical processes), setting different window sizes and applying different filters, but no coherent results could be obtained; the classification module was unable to detect enough differentiation in the data (Figure 9). It is not clear why the results were so poor, given the amount of testing that was undertaken with different parameters. It is possible that there may have been issues with the processing of the data, and also at the time of use in 2011, the classification module had only just been released and was still being refined. It was decided that the limited time available could be more usefully spent trialling other software to see if better results could be obtained.

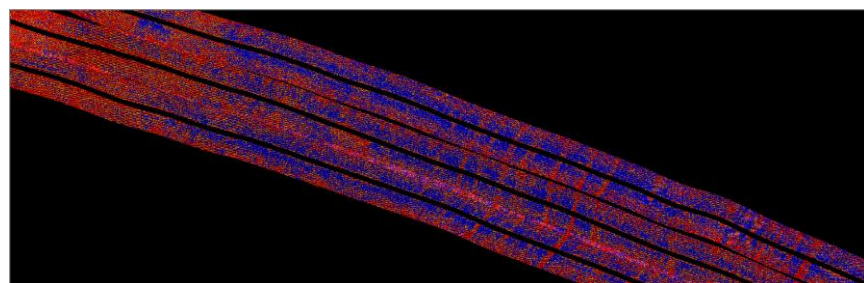


Figure 9 Results of a trial of Sonarwiz's seabed classification module.

The second trial was undertaken using Erdas Imagine image processing software. The mosaic image that was initially created in SonarWiz was exported as a GeoTiff and imported into Erdas Imagine. Unsupervised classification was then carried out on this image, but again no coherent results could be obtained, and the survey lines were all classified as the same complex and unusable mix of pixels (Figure 10).

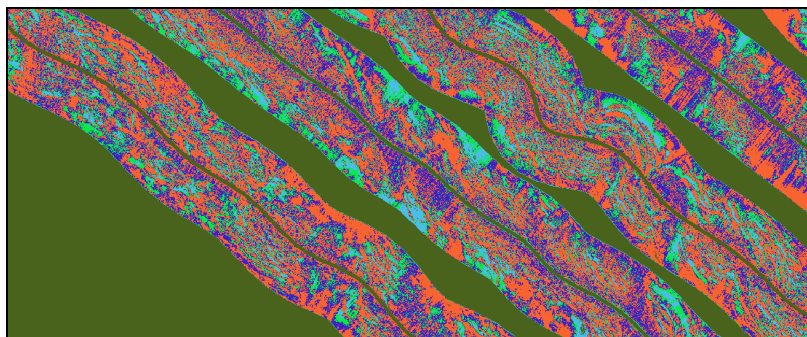


Figure 10 Results of unsupervised image classification in Erdas Imagine.

The third trial was carried out using a specialised seabed classification software called Swathview and a specialised interpolation software called CLAMS, both developed and supplied by Quester Tangent Ltd. These two software packages were very kindly made freely available for a trial period by Quester Tangent, purely for the purposes of this research. The Swathview software classifies the data using the statistical properties of the backscatter images. It allows the selection of an optimal number of classes relating to the composition and diversity of the seabed and assigns records to those classes using principle component analysis and clustering algorithms (Keller, 2011. p.16). Unlike the previous two trials, which used the mosaic data for the classification, Swathview uses the data in image space (Preston, 2009). The advantage of this is that analysis can be carried out with reference to the original geometry with which the data were acquired, such as survey direction and beam angle (Penrose et al., 2005). Fonseca et al. (2009, p.1300) consider that the processing and choices required to create a mosaic image of backscatter data (such as AVG correction methods and normalisation angles) are necessarily subjective, and therefore visual or pixel-based analyses may not be the best approach to seabed classification. They argue that the inherent angular response should be used instead.

The CLAMS interpolation software was specifically designed for the mapping and visualization of seabed classification data. This software differs from other image processing software in that it can perform categorical interpolation of the spatial data. This means that it does not interpolate the data as though it were a continuous variable, and it does not use intermediate class numbers, since the numbering sequence in the seabed classification is arbitrary (Preston, 2009). This categorical interpolation, using the mode rather than the mean of the points for the interpolation, gives much more coherent results than that produced by more general image processing software. After initial trials on subsets of the data, it was clear that the results obtained using Swathview and CLAMS were far better than those obtained in either of the trials that used the mosaic data, so it was decided to use this software for the entire classification.

#### **4.1.1.4 Classification using Swathview**

The basic steps of classification using Swathview consist of importing the raw data, data cleaning, image compensation, generation of image statistics, reducing dimensionality, clustering and mapping (Preston, 2009). The Swathview software performs most of the classification automatically, but as with all image processing, it is necessary for the user to make decisions regarding various parameters that need to be set, and a considerable amount of trial and error is therefore involved in order to establish the optimum settings. It is beyond the scope of this thesis to provide a detailed explanation of the complex statistics behind the processing that is carried out by the software (Quester Tangent, 2012a), but an overview of the processing

steps is necessary in order to demonstrate that sufficient testing was carried out to create a robust classification.

Various parameters can be set for data cleaning, including range masking and angle masking of data. This step is crucial in order to remove along-track artefacts and avoid striping in the classified data. The most significant decision to make is the size of the rectangular sub-images that the software generates during the classification process (Figure 11). The generation of image statistics (called features in Swathview) is carried out within these sub-images or rectangles. Amplitude and texture are analysed within each rectangle, and the centre pixel in the rectangle becomes a data point position for that class. If more rectangles are generated, more data points are created, leading to a higher image resolution, and consequently a longer processing time (Personal Communication, Tony Tipple, Quester Tangent Ltd, 2012).

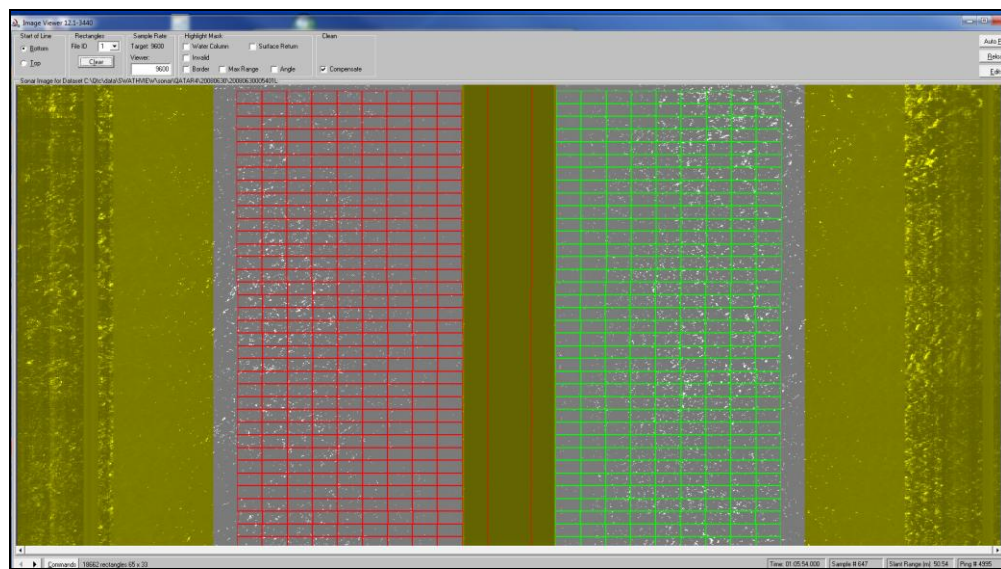


Figure 11 Sub-Images (rectangles) generated by Swathview for the purpose of generating image statistics.

The features generated are merged into a catalogue file and principle component analysis is used to reduce the features to the first three principal components. Once built, the feature catalogue can be applied to whole datasets, or parts of them, to create classified seabed files. Cluster analysis is then performed on a range of classes, chosen by the user, who can select the optimal number of classes once the analysis is complete. The final product is a georeferenced map of the classified data points.

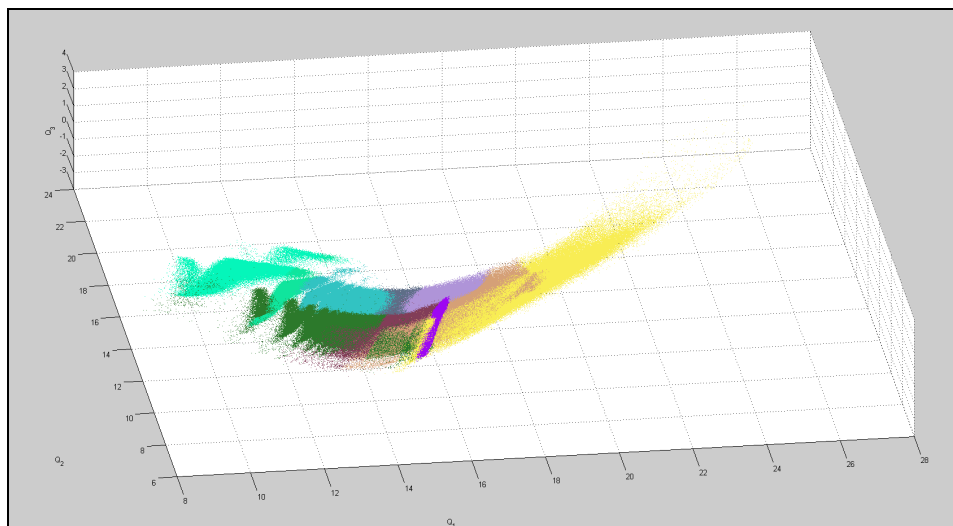


Figure 12 A three-dimensional plot of the clusters generated during the classification process in Swathview.

The resulting georeferenced point data can then be interpolated using the CLAMS software, to create a continuous raster dataset. Again, systematic experimentation has to be carried out using different settings and parameters in order to obtain the best results for the raster dataset. The most significant decision to be made is the grid spacing for the interpolation, as this influences the resolution of the final image.

The raw sonar data, in xtf format, was batch-imported into Swathview. Following initial testing of settings and parameters, a preliminary classification and interpolation was carried out on the entire dataset, and the results analysed. Comparative testing was then carried out on smaller areas in order to test the robustness of the classification results. This was done by running the classification process, using the same parameters as those used for the entire dataset, on two subsets of the data, one from Area 3 and one in Area 4. A catalogue of features was generated from each test area, and each one of these catalogues was used to classify each test area, and also to classify the entire dataset (Figure 13). The settings used for this preliminary classification, the test area files, and the interpolation, are listed in Appendix 1.

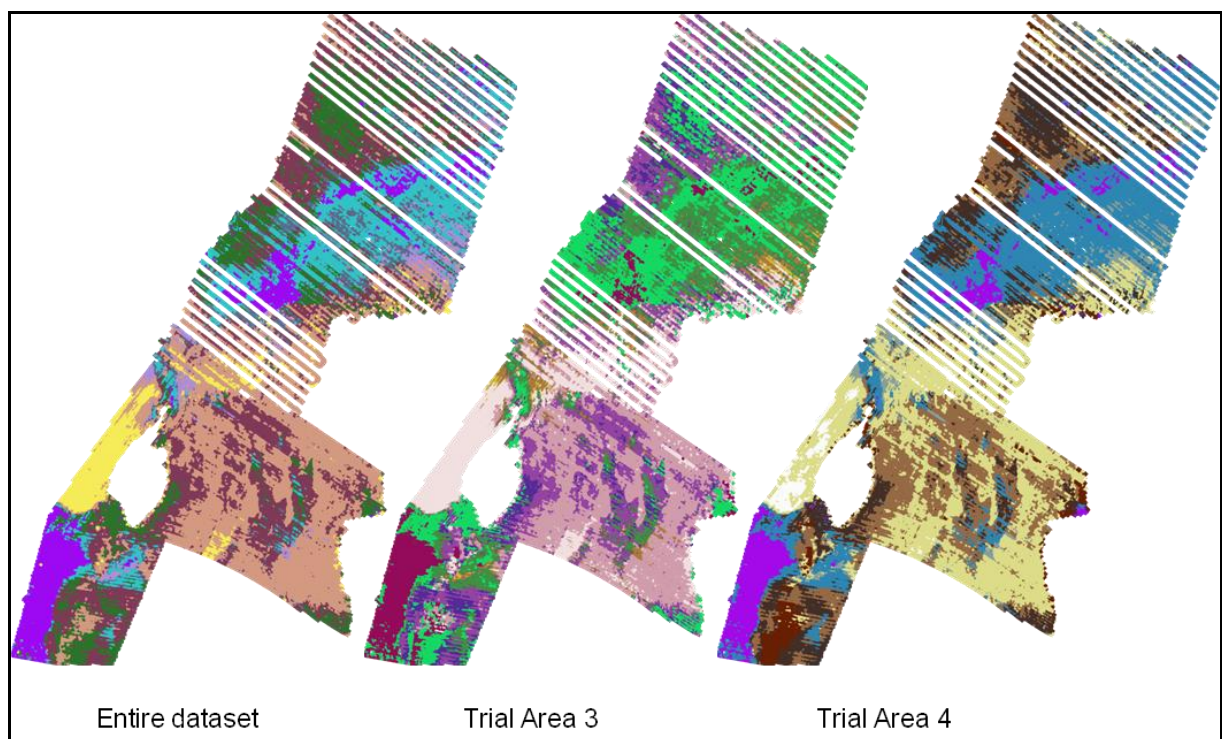


Figure 13 Results of the Swathview preliminary seabed classification using catalogues based on the entire dataset, and using catalogues based on trial areas.

The results of the preliminary classification and the trial areas showed that although there were small discrepancies, the same broad trends were apparent in all of the classifications. Once the general validity of the method had been established by the preliminary classification and the trial areas, further experimentation was undertaken to identify the settings and parameters that gave the best results. Valuable feedback was provided by the expert staff at Quester Tangent during this stage of the process. The preliminary classification indicated that more aggressive angle and range masking needed to be carried out to reduce the along-track striping that was visible in the georeferenced plot. This was always going to be a problem in this particular sidescan sonar dataset as there was no overlap in the survey lines, and in some areas there were gaps between the survey lines. The expert interpolation across data gaps that is provided by the CLAMS software allows for this type of aggressive masking-out of data. Alterations were also made to the rectangle size, so that smaller and more square-shaped sub-images were created.

The settings for the CLAMS interpolation were adjusted, so that the search radius was increased to close up gaps in the interpolated image, and the search size was increased, thus decreasing the amount of fine detail (Quester Tangent, 2012b). The full classification and interpolation process was then run again on the entire dataset, and also on the smaller test areas, using the altered parameters, to obtain the final classification data. The parameters used for the final classification are also included in Appendix 1.

After the final classification was complete, it was necessary to choose the optimal number of classes that would be used for the final classification dataset. On the basis of the statistics generated by Swathview, ten was selected as the optimal class number, so the seabed was ultimately divided into a very large number of data points (more than 2 million), each one of which was allocated to one of ten distinct classes. The resulting track plot displays the geographical position of data associated with each class (Figure 14).

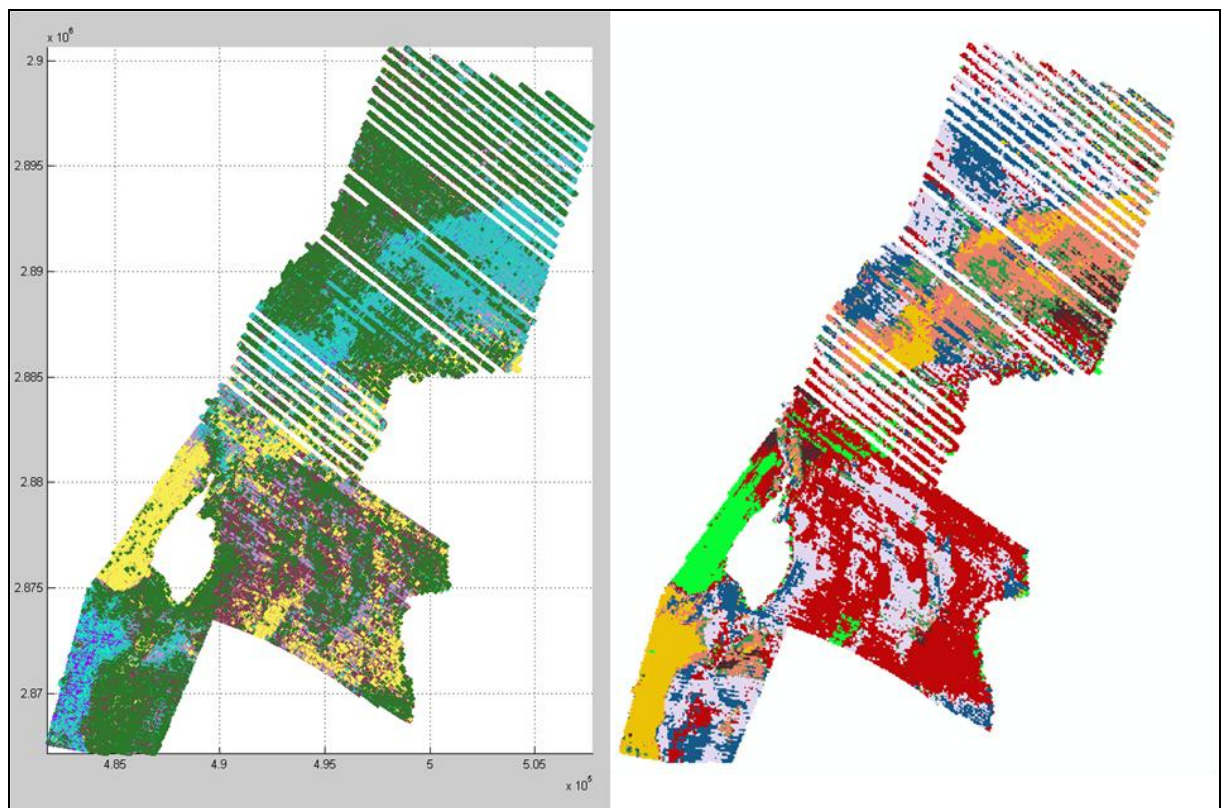


Figure 14 Track plot from Swathview showing classified data points (left) and interpolation of data points using Clams (right).

The software also generates confidence data for each of the classified points, showing the probability that each point belongs to the class to which it has been

assigned. Using this data, it was possible to verify that for the chosen number of classes, the majority of the points had a high level of confidence, and therefore that the classification is robust. Out of a total of 2,033,711 data points, 85% of them had a confidence level of 75% or more, and 51% had a confidence level of 98% or more.

The georeferenced map of the classified data points was converted to a continuous image file using the CLAMS interpolation software (Figure 14), which was then imported into ArcGIS, and analysed. This raster surface was used to create contiguous polygons that formed the initial landscape units for the seabed characterisation.

A considerable amount of testing was carried out using different parts of the dataset and comparing the results in order to ensure that the resulting classification was as robust as possible. Since the classification was unsupervised, the classes needed to be validated by ground-truthing in representative sample areas, in order to more fully understand what type of seabed sediment was represented by each class. However, the classification carried out on the acoustic survey data provided a preliminary dataset which could then be further refined using a range of other data sets.

#### **4.1.2 Results**

As outlined in the methodology section, following extensive trials, the acoustic data from the sidescan sonar survey was eventually classified into ten acoustically distinct classes, and the output of this process was a georeferenced raster image of the

Study Area. The colours allocated to the different classes in the raster image do not have any significance in regard to their interpretation, they have been allocated solely based on the best way to visualise the data. The preliminary interpretation of the classes is summarised in Table 1 below.

Table 1: List of acoustic classes generated by Swathview, and their preliminary interpretation.

<b>Class No.</b>	<b>Colour in Classified Image</b>	<b>Preliminary Interpretation</b>
1	Dark Green	Finer Grained Sediment (Lower Reflectivity)
3	Red	Coarser Grained Sediment (Higher Reflectivity)
4	Yellow	Finer Grained Sediment (Lower Reflectivity)
5	Lilac	Medium Grained Sediment (Medium Reflectivity)
6	Brown	Coarser Sediment (Higher Reflectivity)
8	Lime Green	Coral (High Reflectivity)
9	Salmon	Finer Sediment (Lower Reflectivity)
10	Blue	Medium Grained Sediment (Medium Reflectivity)

The analysis is based on the premise that sandy environments tend to be good reflectors of acoustic energy, while silty/muddy environments tend to be poor reflectors of acoustic energy (Sutherland et al., 2007). However, at this point it is not useful to undertake too much analysis based solely on the classified data, as unless there is more information about what the classes actually represent, then the analysis will have little meaning for archaeological purposes. The real strength of the classification will be demonstrated later in this chapter when integrated analysis of different datasets is undertaken, in order to zone the seabed on the basis of

character and potential. However, before carrying out the integrated analysis it is useful to summarise the general trends displayed by the classified data, and to examine how the classified data compares to the mosaic image of the sidescan data.

The crucial issue when analysing the classification of an extensive area of seabed is to treat it as a broad-brush technique, viewing the image in its entirety, and not to use the classified data for fine detailed analysis, as that is not its purpose. In this respect the classification was successful, in that the overall image appears coherent, and dominant trends in the data can be picked out. There are clearly large, discrete areas where a single class is dominant, especially in the south and centre of the Study Area. The picture is more complex in the north of the Study Area, but this was expected, as there were gaps in the survey lines in this area, making it more difficult to achieve a sensible automated classification. The lack of overlap in the survey lines has led to striping in the classification data that could not be completely removed by pre-classification processing, but it was minimised as far as possible (see methodology section). The different regions of the Study Area are analysed below, starting from the south and moving northwards.

#### 4.1.2.1 Area 4

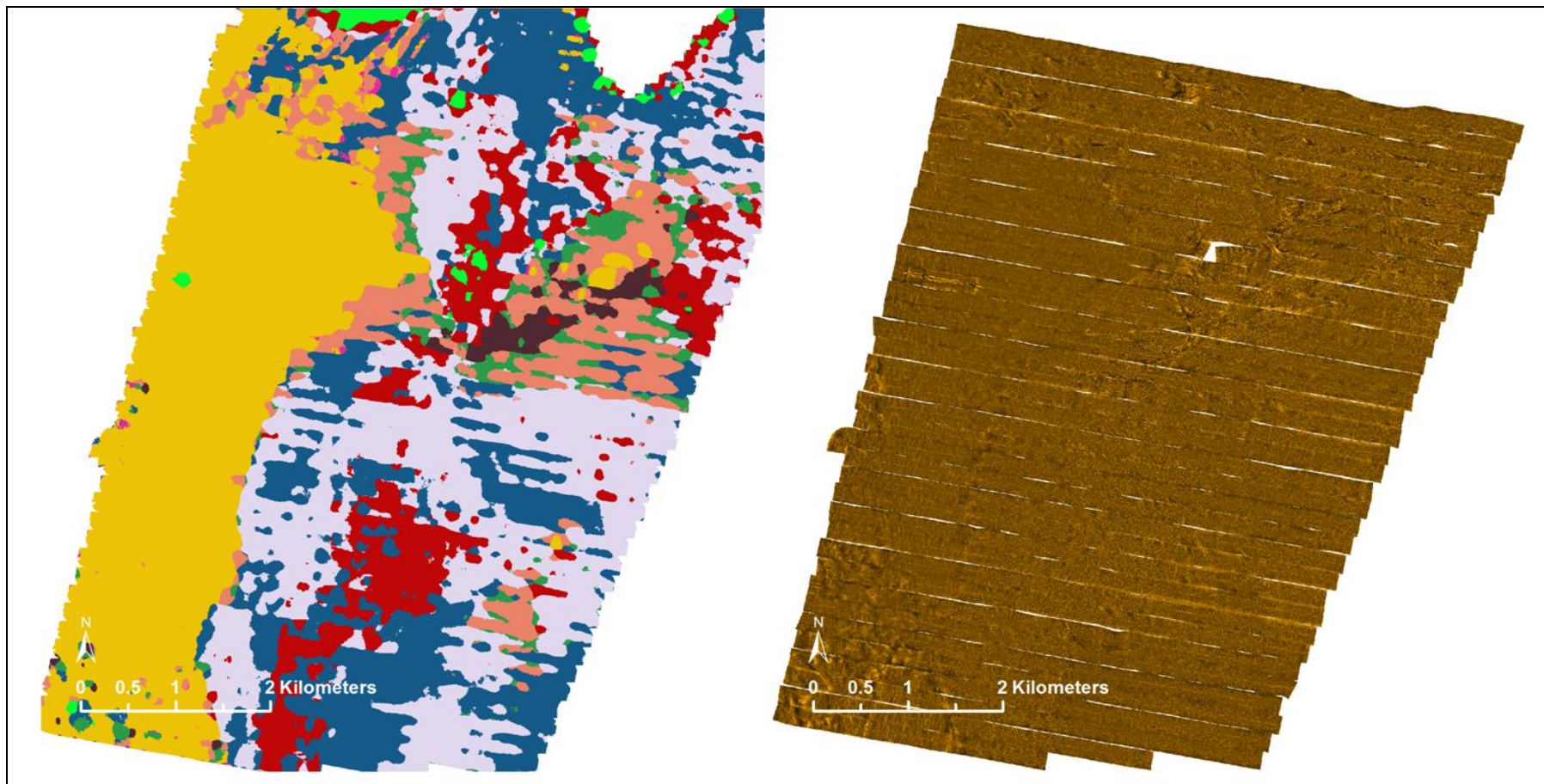


Figure 15 Classified data (left) and mosaic of sidescan sonar data (right) in Area 4.

Classes 4 (yellow) and 5 (lilac) fill the majority of Area 4 (Figure 15). The large yellow area (Class 4) in the southwestern part can be relatively clearly seen in the sonar mosaic, in which it appears as a darker, possibly finer sediment, demarcated from the surrounding area by an edge of brighter reflectivity (Figure 16). Extensive trawler scars are evident all over this area, and the acoustic classification has clearly picked the area out as separate and distinct from the surrounding area.

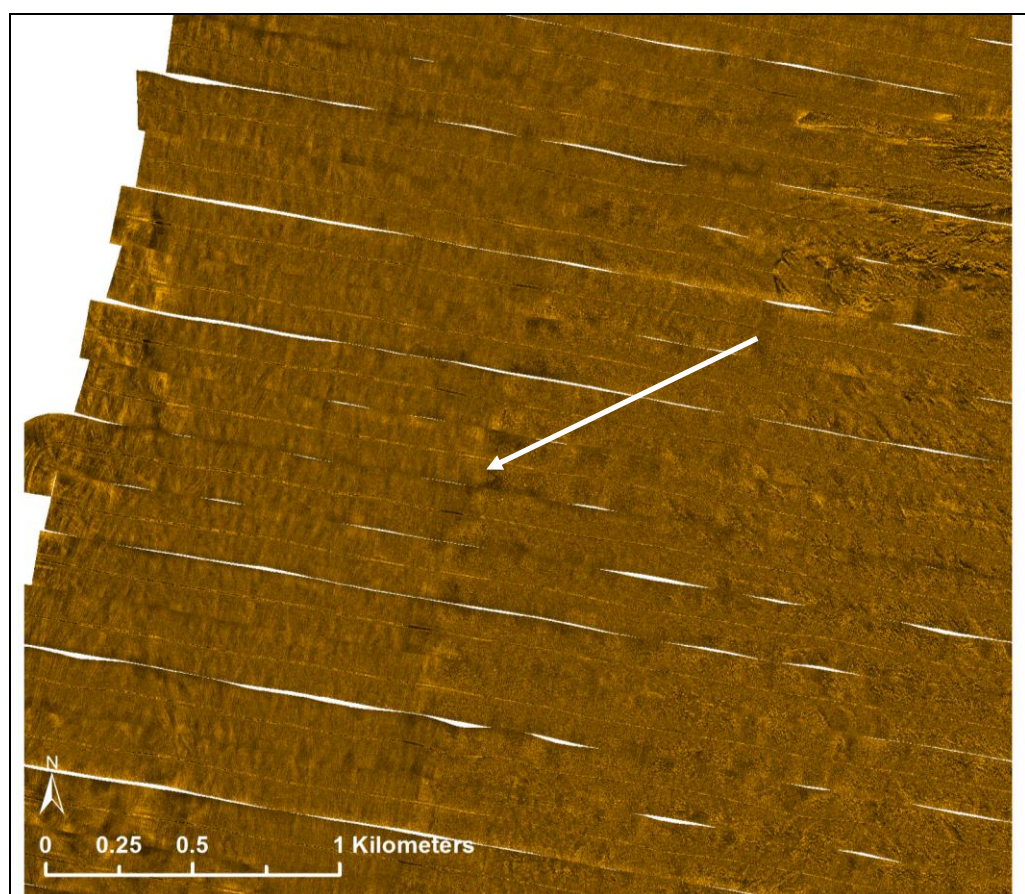


Figure 16 Edge of brighter reflectivity demarcating a change in texture in Area 4.

In the very far southwest corner, brighter patches, possibly indicating coarser sediment and/or hard, rocky substrate, are apparent (Figure 17).

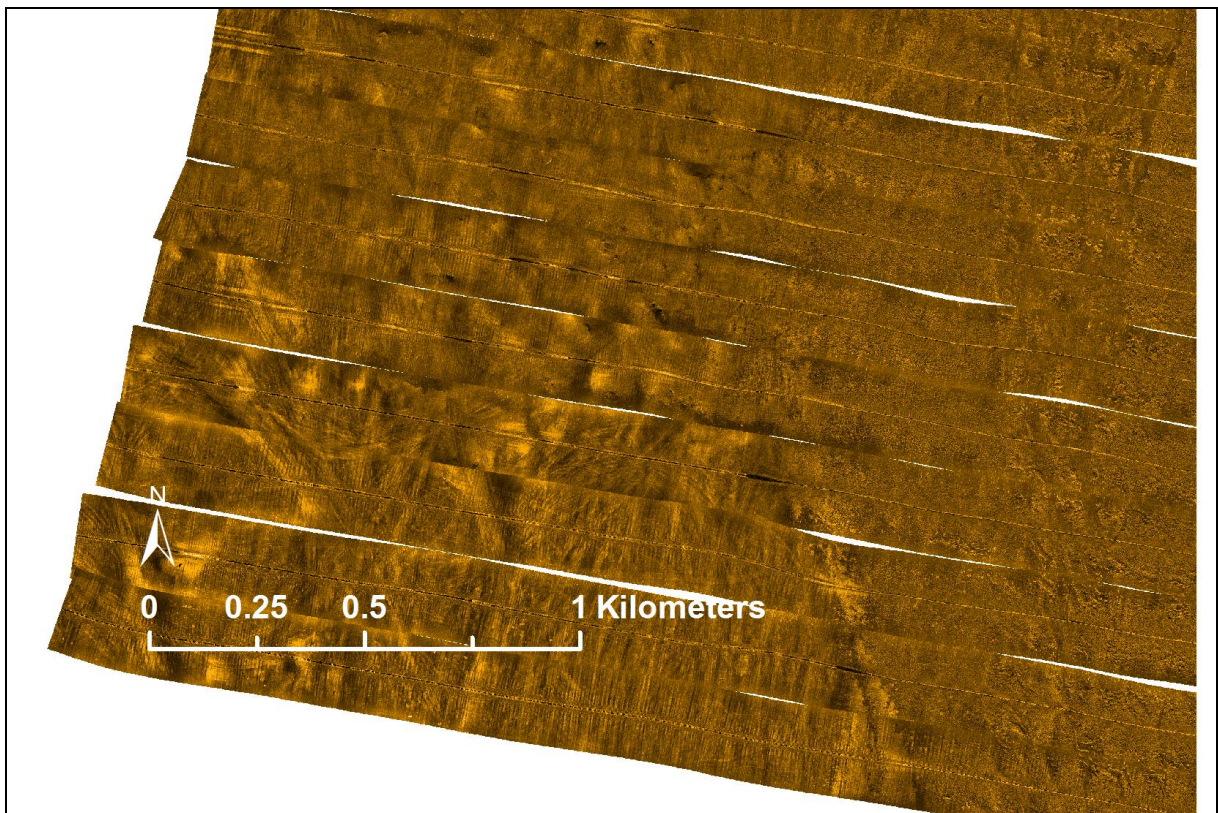


Figure 17 Trawler scarring in Area 4.

Further north in Area 4, closer to the reef, although there is an area of predominantly Class 9 (salmon) in the classified data, it looks very mixed at this point, probably reflecting the complexity of the seabed in the vicinity of a coral reef, where the acoustic classification is able to discern differences that aren't visible to the human eye. The mosaic image here, although it has darker, less reflective areas of possibly finer sediment (represented by Class 9 in the classified data), looks brighter in patches, indicating rougher, harder reflectors such as coral and rocks, in a roughly triangular-shaped area. This triangular shape also emerges as an overall pattern of mixed classes in the classified image (Figure 18).

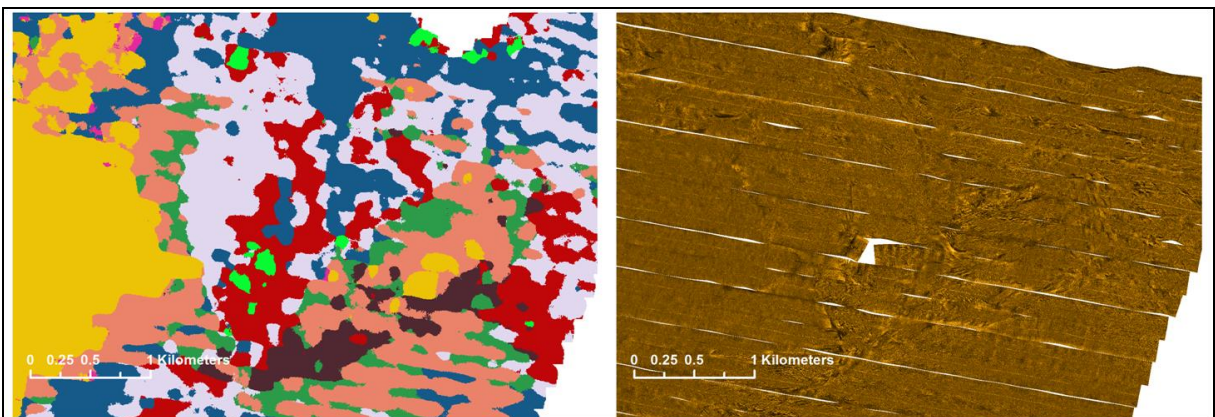


Figure 18 Pattern of mixed classes south of the reef in Area 4 corresponding with visual patterns in the mosaic data.

The area to the south has been classified predominantly as a mix of Class 5 (lilac) and Class 10 (blue), with a band of Class 3 (red), which is an area of brighter reflectivity and therefore possibly coarser sediment, running up the centre. At first view, this area looks relatively homogenous in the mosaic image, but the classification has picked out differences that can also be seen on closer inspection of the mosaic image, which shows an area of northwest-southeast trending sand ridges in the red area (Figure 19).

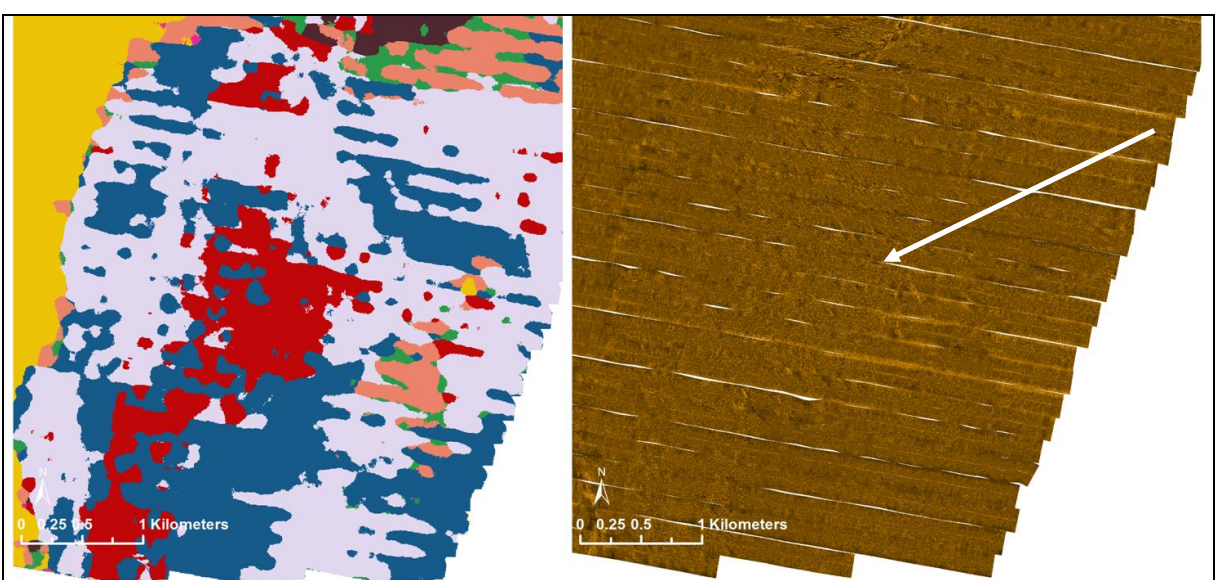


Figure 19 Sand ridges visible in the mosaic data in Area 4 and differentiated as Class 3 in the classified data.

#### 4.1.2.2 Area 2/3

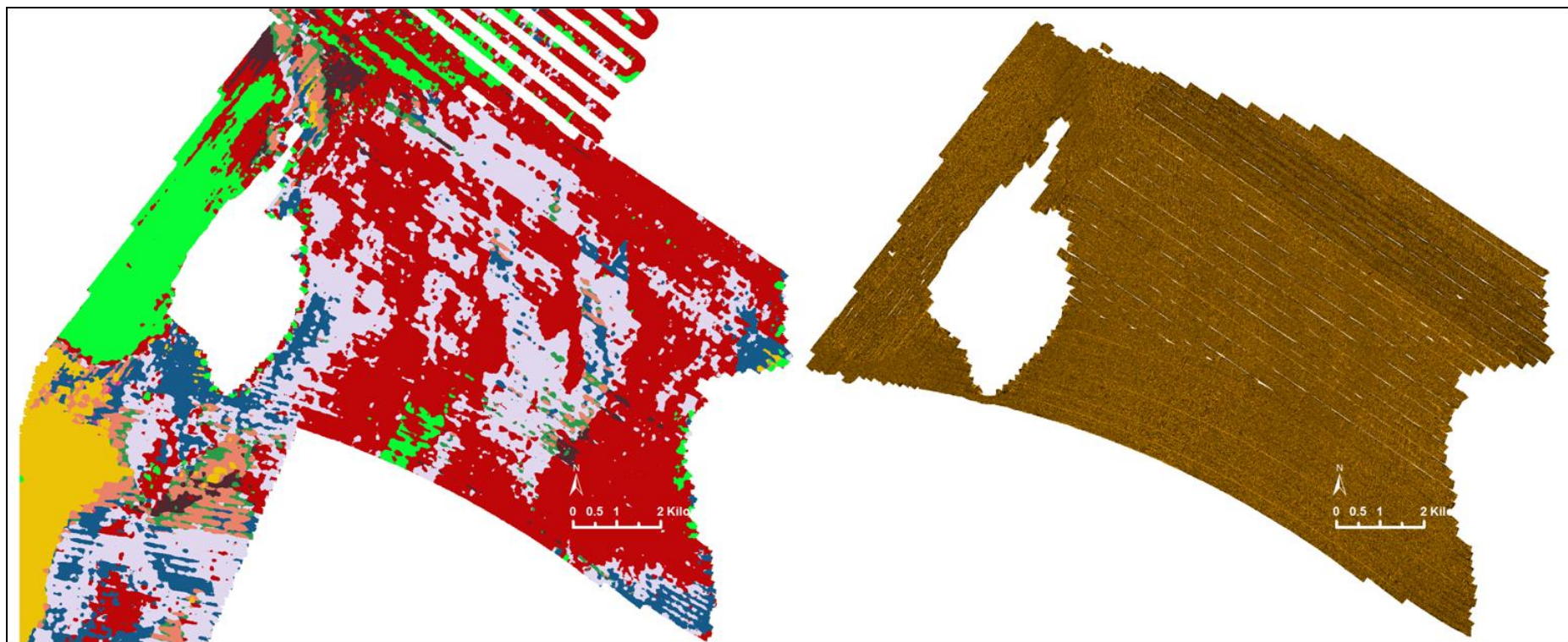


Figure 20 Classified data and mosaic of sidescan sonar data in Area 2/3.

Class 3 (red) dominates Area 2/3, in the centre of the Study Area (Figure 20). There is a gap in the data in the west of Area 2/3 due to the reef, which could not be surveyed with the sidescan sonar as the water was too shallow for the survey vessel. The area immediately to the west of the reef is clearly picked out by the classification as a large area of lime green (Class 8). The same class also appears as small patches ringing the reef, as well as odd outcrops elsewhere, indicating that it is coral. This is where the automated classification really shows its strengths, as the large area of coral does not show up particularly clearly as a separate class in the mosaic image, (Figure 21) although the smaller outcrops do show up as bright reflectors.

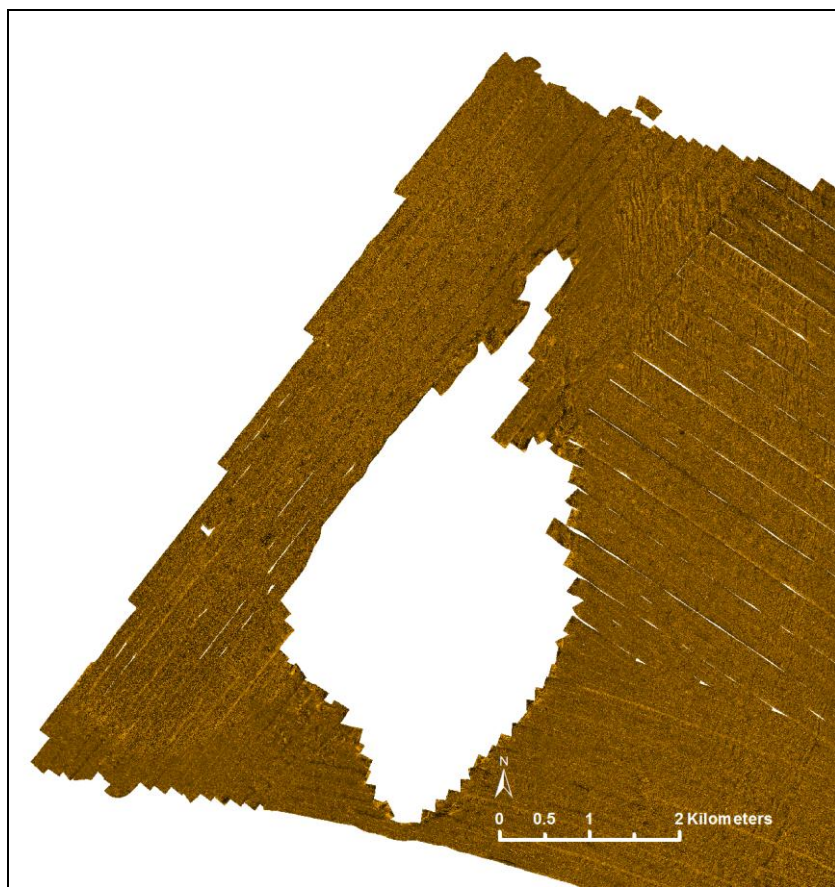


Figure 21 Mosaic of sidescan sonar data around the reef in Area 3.

The area to the east of the reef is predominantly Class 3 (red) and Class 5 (lilac). The red areas in the classified data seem to correspond to brighter reflective areas of north-south trending linear bands in the mosaic data, possibly sand ridges, whereas the lilac areas correspond to less reflective, possibly finer sediment (Figure 22).

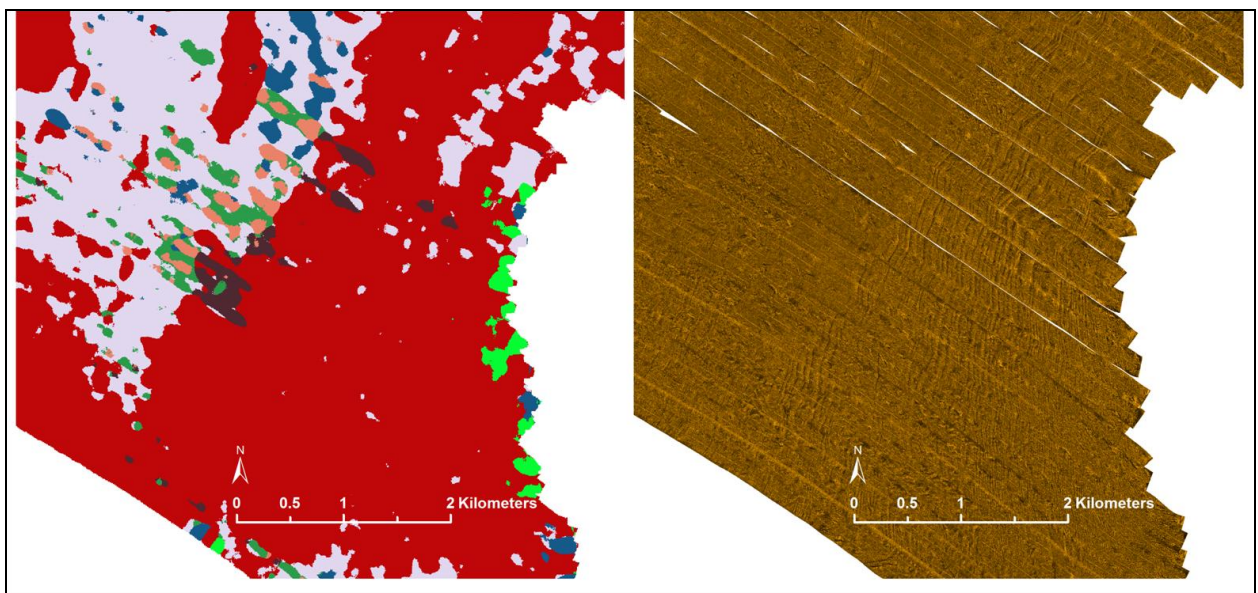


Figure 22 Sand ridges visible in the mosaic data in Area 2 and differentiated as Class 3 in the classified data.

Immediately to the north of the reef, the classified image again shows a rather complex picture. North-south linear bands here have been picked out as Class 6 (brown) (Figure 23) rather than Class 3 (red), as they were further east. The less reflective area to the west has been classed as predominantly Class 9 (salmon), whereas a similar-looking area further to the east was classed as Class 5 (lilac). The automated classification here appears to be picking out differences between classes that actually look quite similar to the human eye.

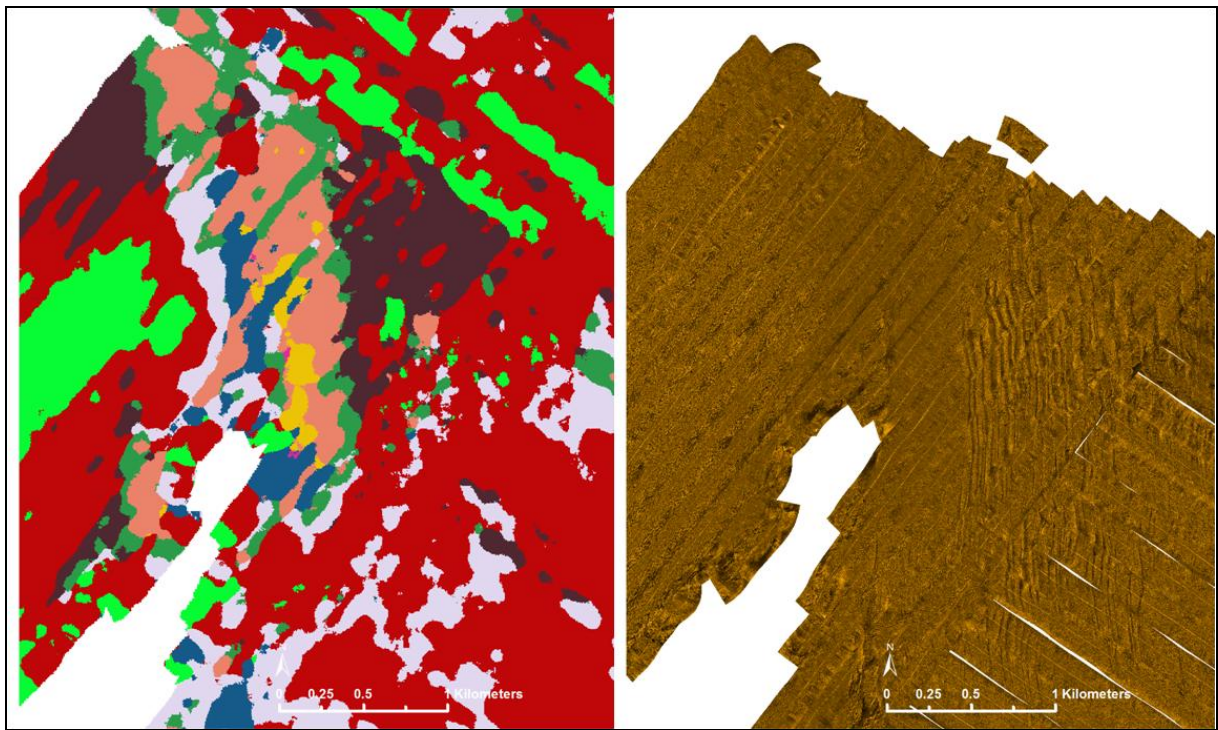


Figure 23 Sand ridges visible in the mosaic data in Area 3 and differentiated as Class 6 in the classified data.

#### 4.1.2.3 Area 1

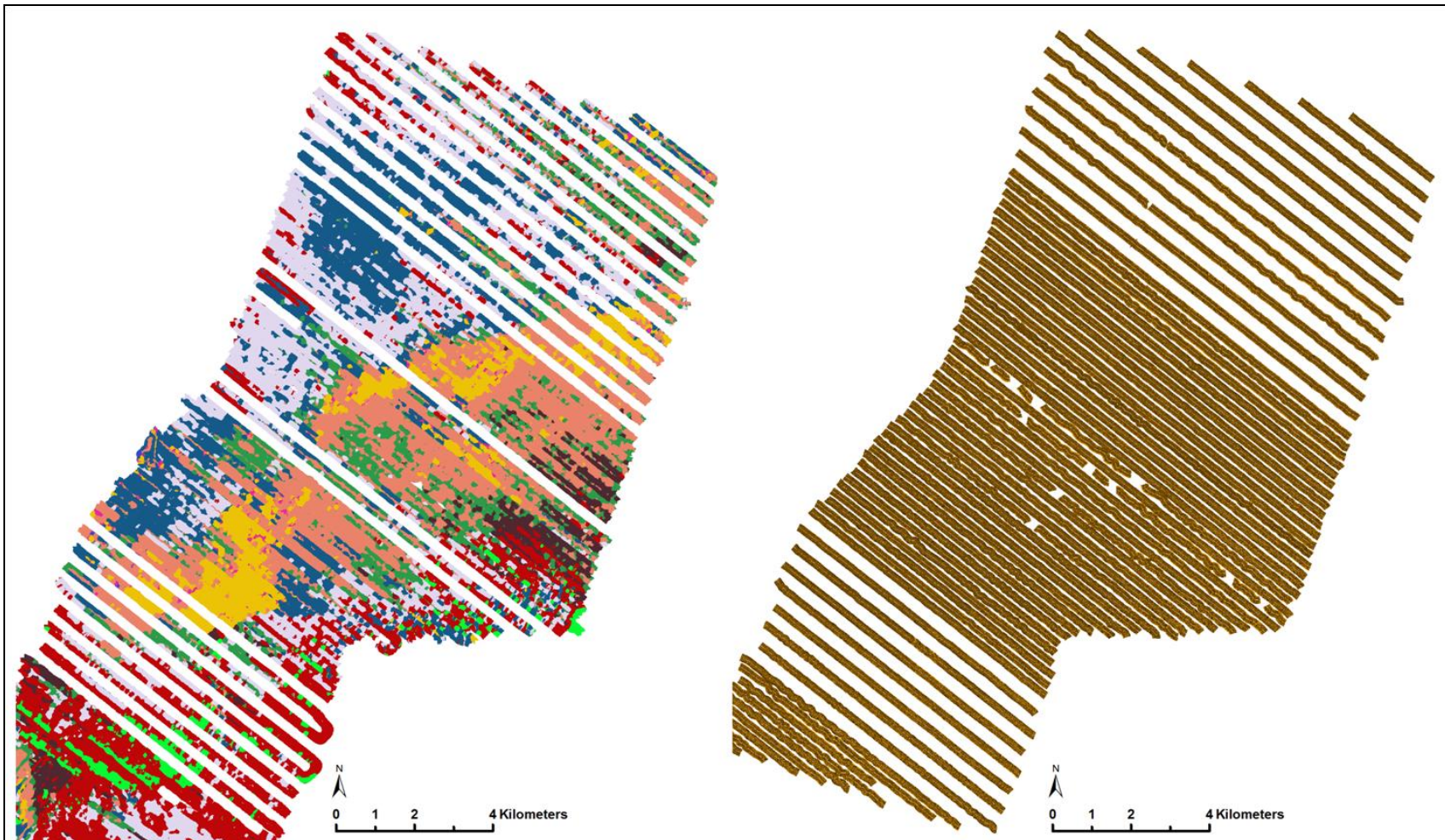


Figure 24 Classified data and mosaic of sidescan sonar data in Area 1.

As previously mentioned, the classification in the north of the Study Area (Area 1 - Figure 24) appears very mixed, particularly the area in the far north, and it is therefore necessary to categorise this area based more on discrete areas of mixed classes rather than areas of single classes.

The area to the north of the reef appears in the classified data as predominantly Class 3 (red) with green patches (Class 8). Although it is quite difficult to see area differentiation in the mosaic image where there are gaps in the survey lines, this area does show up as a more brightly reflective area than the area further to the north, suggesting that it could consist of coarser sediment, and/or rock and coral, which would fit with its location close to the reef (Figure 25).

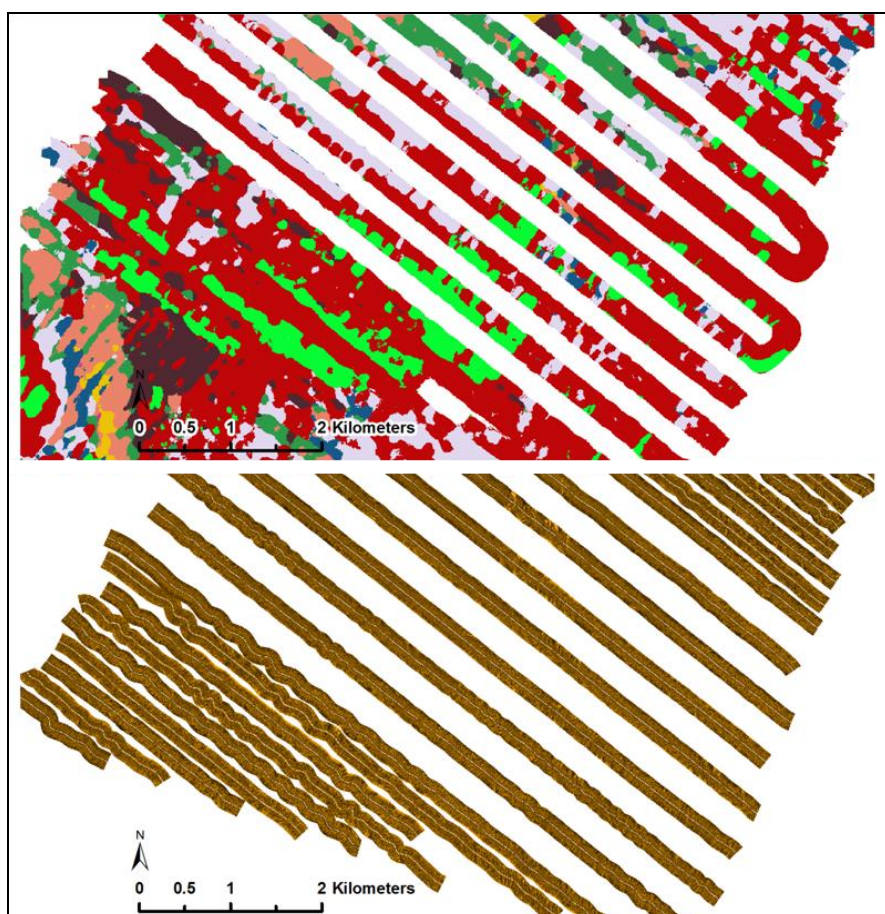


Figure 25 Brighter reflective area immediately north of the reef in Area1.

The most obvious feature in Area 1 is an extensive and relatively cohesive southwest-northeast trending band of classes 4 (yellow) and 9 (salmon), with a few patches of Class 1 (dark green) contained within it (Figure 26). It generally appears in the mosaic image as an area of slightly lower reflectivity than the surrounding areas, possibly because it is finer grained, and contains less rocks and coral.

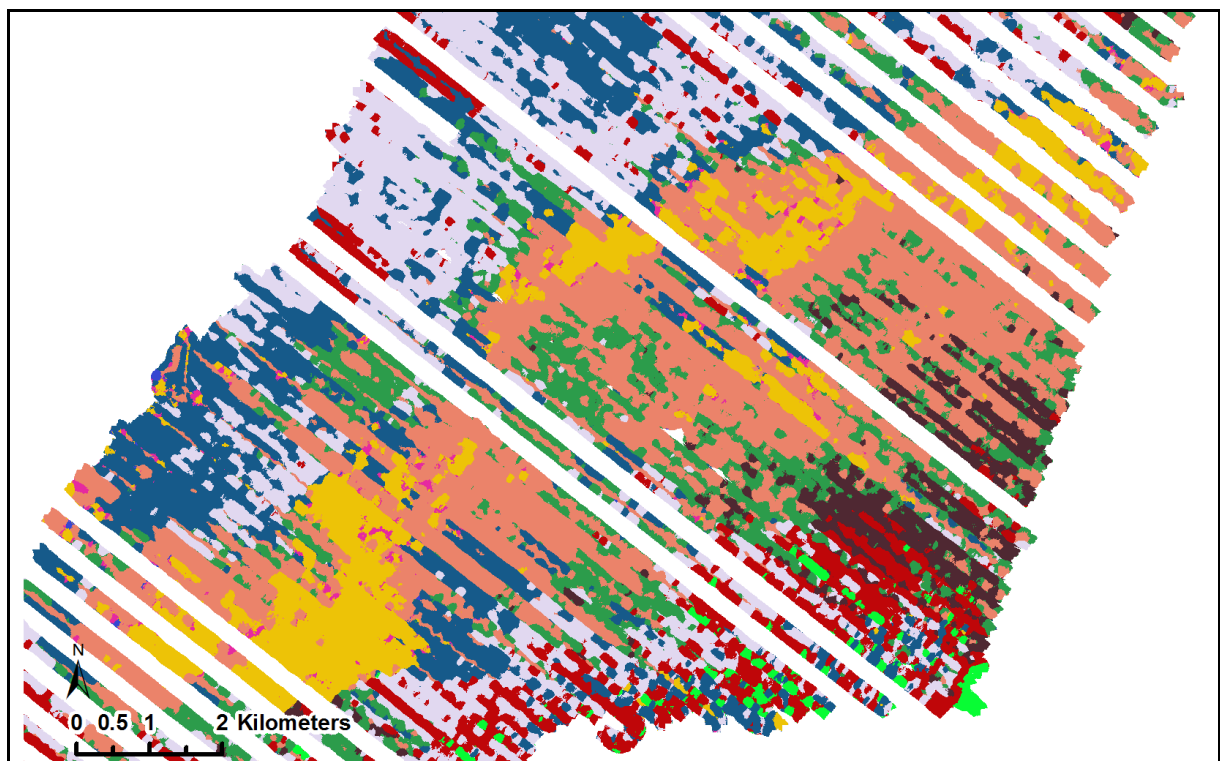


Figure 26 Large band of lower reflectivity in Area 1, differentiated in the classified data mainly as Classes 9 and 4.

This is flanked to the north by another extensive area that, although quite mixed, predominantly consists of classes 5 (lilac) and 10 (blue). This latter area manifests itself in the mosaic image as containing large-scale, north-south aligned linear features (Figure 27), which are probably sand ripples.

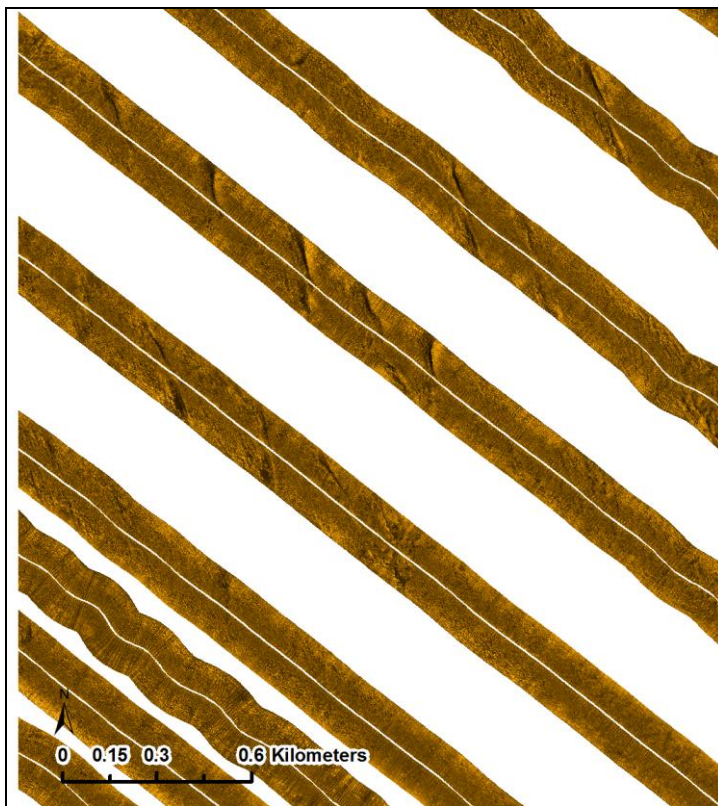


Figure 27 Sand ripples in the north of Area 1, visible in the mosaic data.

In the southeast of Area 1 is another quite mixed area that is largely composed of Class 3 (red), merging into patches of Class 6 (brown) in the north and mixed with patches of Class 8 (lime) in the south. This area can be differentiated in the mosaic image as a concentrated area of bright, reflective curvilinear features which would appear to be sand waves and/or reef structures (Figure 28).

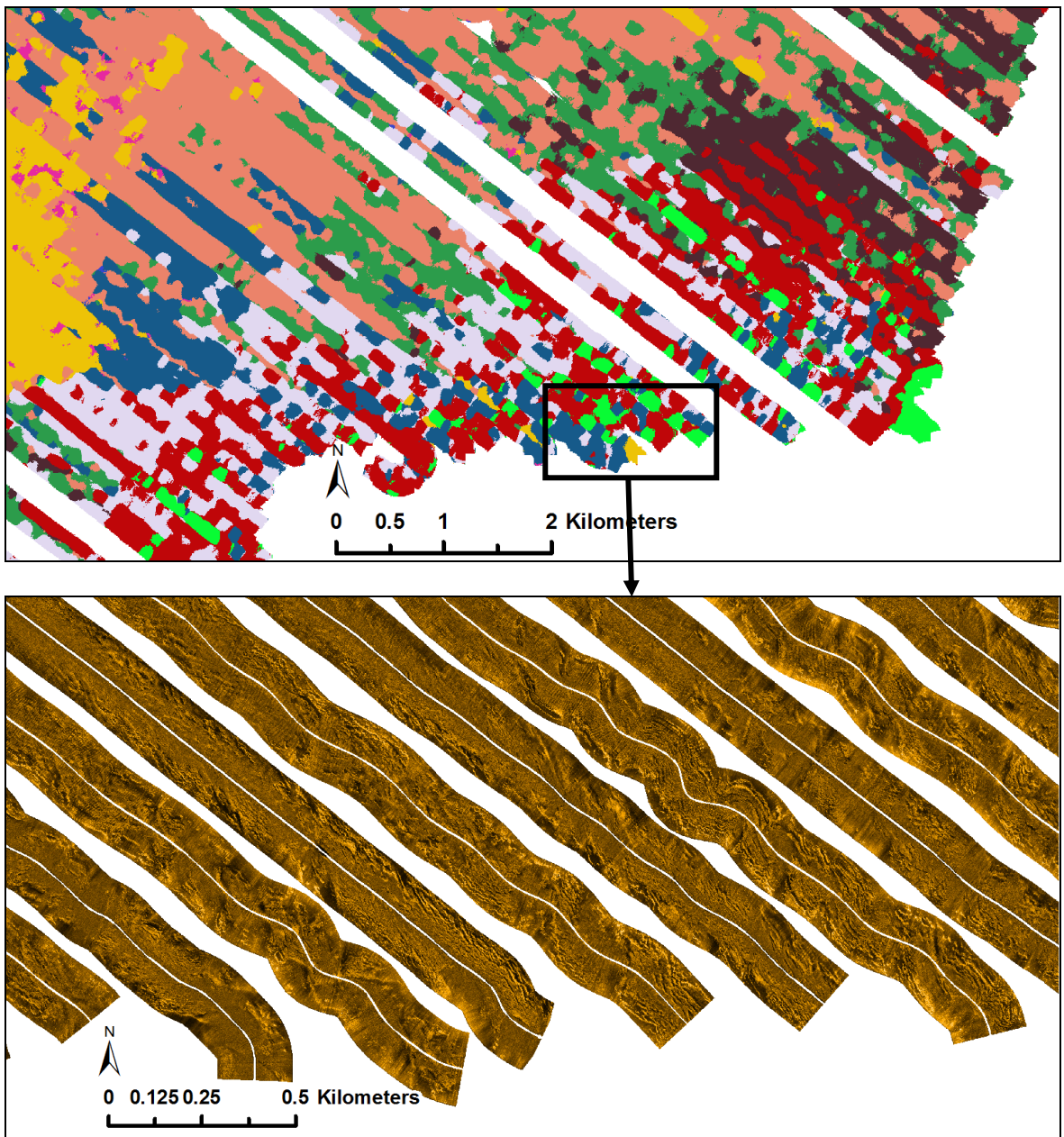


Figure 28 Sand banks in the southeast of Area 1, visible in the mosaic data and differentiated as Classes 3 (red) and 8 (lime) in the classified data.

On initial analysis using solely the mosaic sidescan data, the classes generated by the acoustic classification process largely seem to be coherent and logical. The red (Class 3) and brown (Class 6) areas roughly correlate with areas of brighter reflectivity, suggesting that these areas represent coarser sediments, often

containing areas of sand ripples. The lime green areas (class 8) coincide with the reef, and with other bright reflectors dotted around the mosaic data, suggesting coral reef and coral/rocky outcrops. The salmon (class 9) and yellow (class 4) areas correlate with less reflective areas of seabed, suggesting finer sediments, and no rocky substrate. The lilac (class 5) and blue (class 10) areas indicate finer-grained sediment than that in the red and brown areas, but not as fine as that in the salmon and yellow areas. However, it is not immediately clear, solely on the basis of the mosaic data, as to why the automated classification process has classed the blue and lilac areas separately, since it is difficult to distinguish much difference between these areas in the mosaic data. The dark green areas (Class 1) are harder to interpret as they do not appear as large cohesive areas anywhere, but rather appear mixed in with other classes. However, they occur most frequently with classes that have been interpreted as finer-grained sediments, so it seems logical to assume the green areas also represent a class of finer sediment, albeit with some differences that are not discernible by the human eye in the mosaic data.

#### **4.1.2.4 Generating Initial Landscape Units**

As part of the seabed characterisation process, the classified raster file was polygonised to create initial landscape units, in order to carry out integrated data analysis with other data sets. Initially these polygons were created by automatically converting the raster image to polygon format, which resulted in an enormous and unworkable amount of polygons (more than 39,000), many of which were very small, and not suitable for use as base landscape units. Accordingly, the data was

iteratively processed to merge small polygons into neighbouring polygons. However, although this was an objective and repeatable method that resulted in polygons of a sensible size, it did not always produce a good representation of the dominant class within each merged polygon in areas where the classes were very fragmentary. A different methodology for creating the polygons was then trialled, where the raster image file of the seabed classes was used as the basis for manually digitising polygon boundaries, mostly based on single classes. However, in areas where the classes were very fragmented and mixed, visual judgement was used to define polygons based on the dominant class within a mixed area. This method proved to be the most successful at capturing coherent and useable base landscape units. Although by using this method the initial landscape units were created manually, they were still based on the automated classification undertaken using Swathview, which had picked out differences in the acoustic data that could not be seen by manual visual examination of the unclassified sidescan data. A total of 90 individual polygons were created as a result of this process (Figure 29 and Table 2). Also, as a result of refining the data into polygons of a more useable size at a landscape level, two of the classes, which only covered negligibly small parts of the Study Area, were removed (Classes 2 and 7).

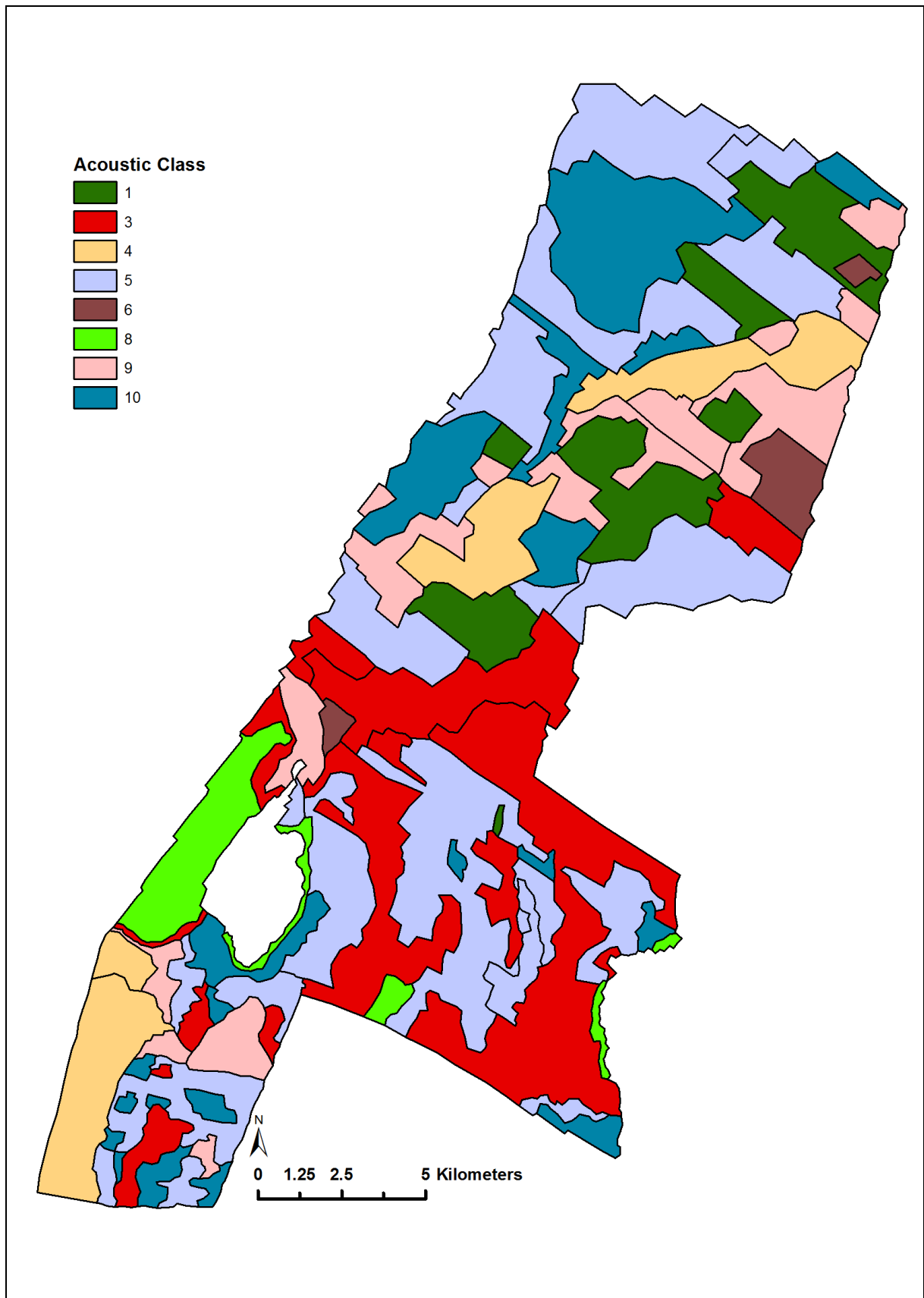


Figure 29 Initial landscape units based on classification of acoustic backscatter.

Table 2: Initial landscape units - polygon statistics.

<b>Class No.</b>	<b>No. Polygons</b>	<b>Total Class Area (Sq Km)</b>	<b>Average Polygon Size (Sq Km)</b>	<b>Max Polygon Size (Sq Km)</b>	<b>Min Polygon Size (Sq Km)</b>
1	7	31.10	4.44	10.44	0.18
3	14	74.97	5.36	30.23	0.19
4	4	32.41	8.10	11.93	1.97
5	22	111.88	5.09	20.86	0.22
6	3	6.45	2.15	4.75	0.71
8	5	13.84	2.78	10.32	1.13
9	15	37.31	2.49	7.76	0.50
10	20	48.26	2.41	18.51	0.19
<b>TOTAL</b>	<b>90</b>	<b>356.22</b>	<b>3.96</b>		

#### 4.1.3 Discussion

Following on from the results of the acoustic classification, it is necessary to critically examine how valid the acoustic classification methodology is in the context of previous work in this field. Sidescan sonar backscatter data has been used for more than 30 years for seabed mapping, and more recently, multibeam backscatter data has also been used. Considerable research has been undertaken in the last decade into assessing different seabed classification methodologies using acoustic backscatter, although almost all of this work has been done for the purposes of geological and/or benthic habitat mapping, rather than for exploring archaeological potential (for example Penrose et al., 2005; Anderson et al., 2008; Brown and

Blondel, 2009; Van Rein et al., 2011). It should also be noted that none of this work has been done in the Arabian Gulf.

Although there are studies that have produced inconclusive results (Kostylev et al. 2001, cited in Orpin and Kostylev, 2006), the published research generally supports the theory that there is a correlation between acoustic backscatter and seabed sediment characteristics (Brown and Blondel, 2009). Collier and Brown (2005) undertook a study to examine the dependence of acoustic backscatter on sediment grain size distribution using sidescan sonar data and sediment grab samples from the Loch Linnhe artificial reef site on the West Coast of Scotland. Overall, the results did support previous studies that have suggested that the highest backscatter tends to correspond with the coarsest sediments, although they also found some issues with coarse sediments having a disproportionate effect on the backscatter response , and stated that '*it would be desirable to improve the correlations obtained between backscatter and sediment grain size properties*' (Collier and Brown, 2005, p.446).

Brown et al. (2011) undertook sediment mapping of a 4,800km<sup>2</sup> area of seabed off Canada by using a semi-automated backscatter classification software (QTC Multiview) on a large multibeam sonar dataset, and obtained promising results for the production of geological maps. However, a study carried out in the Aleutian Islands utilised backscatter response, seafloor rugosity and complexity data to classify the substrate, and did not find a strong correlation between mean sediment grain size and acoustic reflectivity. The researchers emphasised the need for a combination of techniques for ground-truthing, a relatively large number of samples, and ground-

truthing of all potential substrate types represented in the classification (Rooper and Zimmerman, 2007, p.956). Acoustic seabed classification carried out in Western Norway (Ellingsen et al., 2002) using the QTC View system, found that there was generally concordance between the acoustic classification and sediment grain size. However, the study also found that other physical and/or biological factors that could not be detected by grab sampling or coring were influencing the acoustic classes.

When comparing seabed classification from acoustic methods with direct sampling methods or optical methods, it can be seen that each technique has its strengths and weaknesses, for example acoustic survey provides the opportunity to examine large areas more efficiently than direct sampling. It can be difficult to establish the spatial scale of different seabed classes based on discrete sample stations alone, whereas acoustic backscatter provides continuous data. It is likely that this continuous data will result in a more diverse seabed map than would be produced using photography or sampling at discrete locations (Sutherland et al., 2007). Also, research by Orpin and Kostylev (2006) suggests that classification from photography is likely to result in more seabed classes than would be identified from grab samples alone, as photography can show a wider range of textural variability. The researchers attributed this in part to the difficulties in quantifying coarse gravel using grab samplers, which have a tendency to lose the coarsest grains. Rooper and Zimmerman (2007) found that it was not possible to determine sediment grain size from video footage, and Orpin and Kostylev (2006) found that similar backscatter responses could be produced by different mean grain sizes, hence the importance of direct sediment sampling. Also, factors which may affect classification, such as ripple

marks and other micro-topography will not be apparent in grab samples or sediment grain size analysis, but may be detectable in video or backscatter imagery (Ellingsen et al., 2002). The most robust classification, therefore, is likely to result from combining acoustic techniques with photography and grab sampling. The aim of a successful acoustic classification system should be to bring greater powers of analysis into the classification than would be achievable through manual interpretation (Blondel and Sichi, 2009).

A workshop was carried out in 2006 at the University of Ulster in Northern Ireland, which brought together several international research teams involved in developing techniques for interpreting MBES backscatter data. The teams applied a range of acoustic classification approaches to a single common MBES dataset collected from Stanton Banks, in the northeast Atlantic, 120 km west of mainland Scotland, for the purpose of geological and habitat mapping (Brown and Blondel, 2009). The dataset covered a 7.5 x 9 km area, and ground-truthing data was provided by 90 seabed photographs.

Blondel and Sichi (2009) undertook textural analysis via unsupervised classification of the backscatter imagery, using a software called TexAn that was specifically designed for textural analysis of sidescan sonar rather than multibeam data. Although the results were not perfect, the classification worked well in relation to the ground-truthing data, and the translation to multibeam proved to be successful.

Fonseca et al. (2009) used a combination of visual interpretation of the mosaic data and angular response analysis techniques to classify the data, and the approach resulted in a good correlation with the available ground-truthing data.

Marsh and Brown (2009) utilised an artificial neural network model called a self-organising map (SOM) for classifying the data. This approach, based on the beam level angular response and bathymetry rather than just on the mosaic data, does not require any a priori specification of the number or type of classes, and is capable of producing a range of maps with different parameters based on end-user requirements. This work demonstrated that much better results were obtained using the beam-level classification than the directionally-filtered, mosaiced backscatter strength data (Marsh and Brown, 2009, p.1274-1275).

Preston (2009) undertook unsupervised classification of the data based on image amplitudes and texture, followed by assigning attributes based on the available ground-truthing data. Rather than being derived from a geographic mosaic, the classification was done in image space, which means that the axes consist of sample number and ping number, in order to avoid artefacts common in mosaics (Preston, 2009, p.1278). The classification process was carried out using specialised multibeam classification software, (QTC Multiview), and categorical interpolation software (QTC Clams). The resulting acoustic classes correlated well with the ground-truthing data. This is the processing method that is the most similar to that undertaken for the seabed classification off the coast of Qatar, albeit using multibeam data rather than sidescan sonar data.

Simons and Snellen (2009) applied a Bayesian approach, using the averaged backscatter data per beam, so that the MBES calibration was irrelevant, and also, along-swathe seafloor type variations did not affect the classification, since no use was made of the angular dependence of the backscatter data (Simons and Snellen, 2009, p.1267). The results showed a good correlation with the available ground-truthing data.

It has been noted that dense concentrations of seagrass and algae contribute to the acoustic backscatter response, even to the extent where they can mask the acoustic signals from the actual sea floor (Penrose et al., 2005). However, this is less likely to be a concern for low frequency data, where only the dominant return is required, and there are certainly cases where the roughness of rocks, boulders, and bedrock have produced very different backscatter responses, even though the benthic habitat type is the same on all of them (Preston, 2009). Research based on human visual interpretation of high-resolution acoustic backscatter imagery undertaken by Van Rein et al. (2011) in Church Bay, off Rathlin Island near the North of Ireland, found that there was no discernible difference between the imagery taken before and after the removal of 100m<sup>2</sup> of kelp from three sites. The authors also referenced other studies where it was found that it was not possible to easily identify low density seagrass beds from acoustic backscatter data (Van Rein et al., 2011, p.345). Conversely, previous research using acoustic classification has also demonstrated that there is at least some correlation between benthic habitat and substrate type (Brown and Blondel, 2009).

Although the published literature shows varied approaches to, and results from the classification of seabeds using acoustic backscatter data, the two issues that all of the studies emphasise heavily are, firstly, the need for a combination of techniques to be used for classification, as the results from each become far more informative in combination, and secondly, the importance of the amount and quality of the ground-truthing data. It is clear that there is still a lot of work to be done on different methodologies, and that some of the results from trials and experiments seem to conflict with each other. The reality is that the results are probably very specific to the particular seabed type that is being investigated, and it is therefore very important to build up a regional picture and establish which methods work and which don't work for a particular region. Concepts and ideas can be taken from other areas but they need to be refined according to regional variances.

The results presented in section 4.1.2 show that the acoustic classification process in the Study Area has successfully enabled the division of the seabed into a set of initial landscape units based on sediment texture, which is a huge step towards the process of building up knowledge about the archaeological and palaeoenvironmental potential of zones within the submerged landscape. However, these initial polygons are only an interim step in the characterisation process, and need further analysis and refinement. In this form, there are too many landscape units to be useful for landscape-scale study, and not enough is known of their character for them to be meaningful, but they provide the basic building blocks for further characterisation based on bathymetry, ground-truthing data and analysis of geophysical anomalies

(see sections 4.2, 4.3 and Chapter 5). Attributes relating to the character and potential of the seabed in particular zones, derived from the other datasets, can be attached to the base landscape units, and the units refined accordingly.

## **4.2 Topographic Mapping**

### **4.2.1 Methodology**

A surface model of the seabed in the Study Area was generated from the LiDAR bathymetry in order to be able to identify broad zones of high archaeological and palaeoenvironmental potential which could be used to refine the landscape units created from the sediment texture classification.

#### **4.2.1.1 Overview of LiDAR Bathymetry**

The Bathymetry data (seabed topography) was kindly made available by the Hydrographic Section of the Ministry of Municipality and Urban Planning in Qatar. The bathymetry was captured by LiDAR (Light Detection and Ranging) survey, an effective technique for measuring depth in shallow water. The technique consists of an aircraft-mounted laser transmitting light pulses downwards. These pulses reflect from the sea surface and the sea floor, and therefore measure the depth. This type of airborne survey is extremely useful for coastal and shallow-water research. It allows very rapid data collection over large areas in comparison to sonar techniques. Also, it

can cover very shallow areas that cannot be covered by ship-based techniques and therefore allows seamless mapping through the land/sea interface.

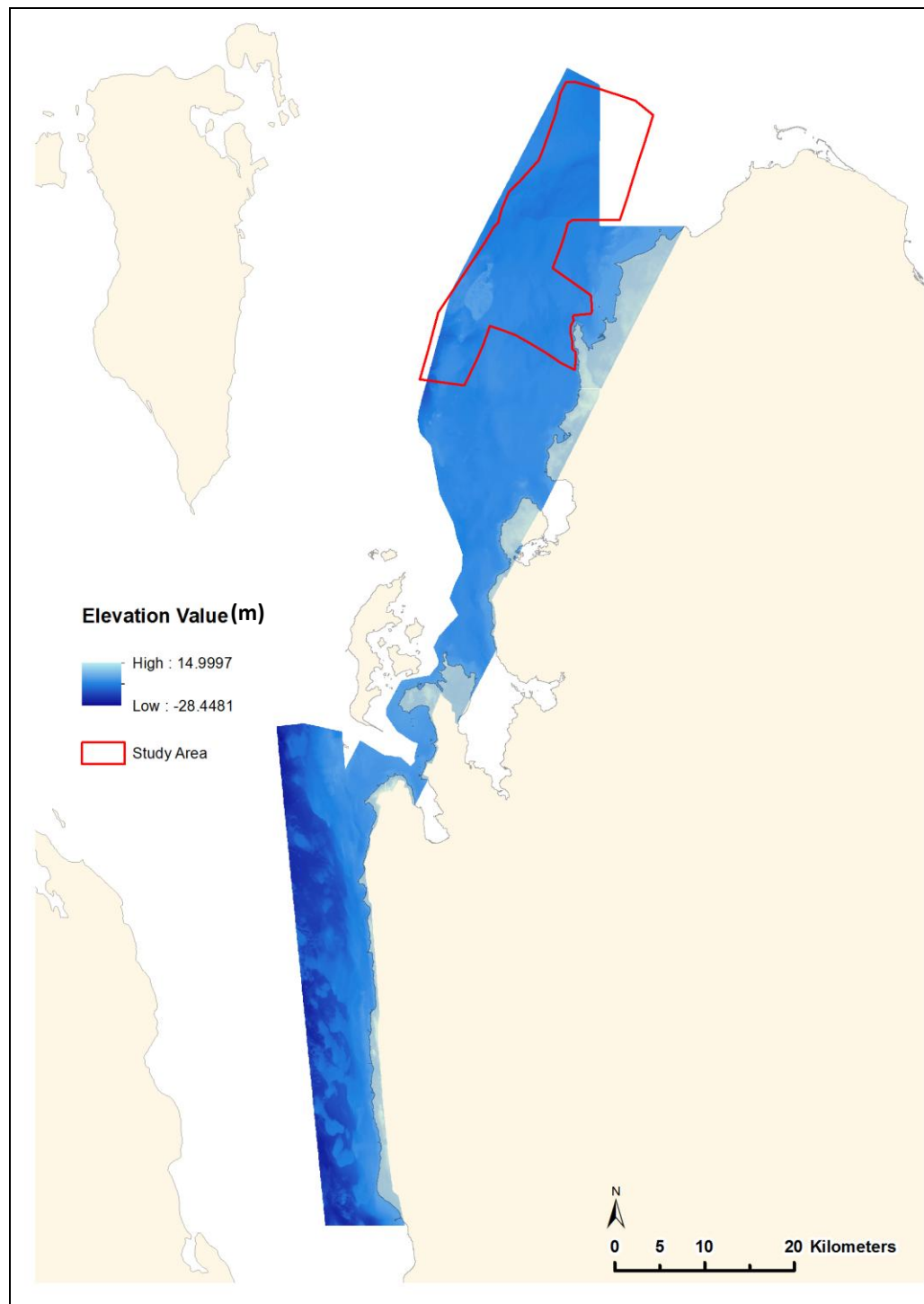


Figure 30 Extent of available LiDAR bathymetry.

The extent of the available bathymetry did not coincide exactly with the extent of the defined Study Area (the extent of the sidescan sonar data), but it did cover a large part of the Study Area, and extended significantly beyond it in the south into the Gulf of Salwa. The survey started approximately 15 km north of Al-Zubārah and continued for some 130 km down the west coast of Qatar to approximately 15km beyond Umm Bab (Figure 30).

#### **4.2.1.2 Generating the Surface Model**

The LiDAR data was provided as ASCII xyz files, containing the three-dimensional coordinates of the points collected by the LiDAR survey, projected in the UTM39N coordinate system. Vertical heights were given in metres based on the Qatar Chart Datum, which lies 0.88m below Qatar Vertical Control Datum (Mean Sea Level at Doha Port). It was processed and analysed using the 3D analyst module in ArcGIS. The first step was to convert the ASCII data to 3D feature data and add the height information (z values). The z values in the data had to be reversed as drying heights were recorded as negative values, and depths below sea level were recorded as positive values. This resulted in a point-based shapefile which could then be used to interpolate a raster elevation model for the seafloor surface. This was done by using the raster interpolation function in ArcGIS, and choosing the ‘natural neighbour’ method of interpolation. It was necessary to experiment with different cell size settings to establish the best balance between resolution of the surface model and feasible processing time and power. As the point data was spaced on average between 5 and 7m apart, it was originally decided to use a cell size of 7m for the

interpolation, as this fitted with the resolution of the original data, and did not use too much processing power, data storage or time. However, this made it difficult to see some of the features when zoomed in, so after further testing, it was decided to use a cell size of 2m for the bathymetry data in the Study Area, and 5m for the data outside the Study Area. It was not possible to use such a high-resolution for the entire dataset due to the processing time and data storage requirements involved. Although the 2m resolution did not add any more detail to the features visible on the surface due to the 7m spacing of the original LiDAR points, it did mean that features were easier to examine when zoomed in. The resulting raster elevation surface was visualised using stretched values along a colour ramp (Figure 30).

It became apparent at this stage, once the coastline was visible in the bathymetry and could be compared to the coastline data that had already been obtained from the Qatar Centre for GIS, that there appeared to be a shift in the bathymetry data to the northwest. All possibilities were examined, including possible coordinate system/projection issues, and the processing of the data was repeated again from scratch. This was done first using the UTM39N projection, which still showed the shift in data, and then using the Qatar National Grid projection in case there was an error in the metadata provided, but the data was still not located correctly. Finally, it was decided to use the coastline data provided by the Centre for GIS to correctly locate the bathymetry data. Two control points were logged with a GPS at known locations on the coast (piers) for ground-truthing purposes, to ensure that the coastline data being used for the correction was actually in the right place itself. Then a series of reference points were logged at identifiable locations over the extent of the

bathymetry and in the coastline data, and the differences in the X and Y coordinates were compared and averaged. It was apparent that in the bathymetry data, the X coordinates were all approximately 80m too far to the west, and the Y coordinates were all approximately 80m too far to the north. This was a constant error noted in all of the reference points, so it was possible to shift the data by adding 80m to the X coordinates and subtracting 80m from the Y coordinates. Once this was done there was a clear fit between the bathymetry and the coastline data. The coordinates of the reference points and the values used for shifting the data are provided in Appendix 2.

The next step was to carry out a hillshade operation on the raster elevation surface in order to create a shaded relief model of the seafloor, and therefore greatly enhance the visualisation of the topography. This was done by using the hillshade tool in 3D analyst, which works by considering the illumination source angle. Shadows can also be considered in the analysis if required, but were not used in this case as a better hillshaded surface was created without the use of shadows. A variety of models were created using different vertical exaggeration factors to further enhance the surface visualisation, and for most of the analysis, a vertical exaggeration factor of 20 was deemed to provide the best results. The elevation surface was then set to be 40% transparent, and layered on top of the hillshaded surface to create an enhanced visualisation of the seafloor topography. The elevation surface draped over the hillshaded surface, with a vertical exaggeration factor of 20, was the final surface model that was used for the analysis. The surface model was also exported into Erdas Imagine software and used to generate a 3D visualisation in order to assist interpretation (Figure 31).

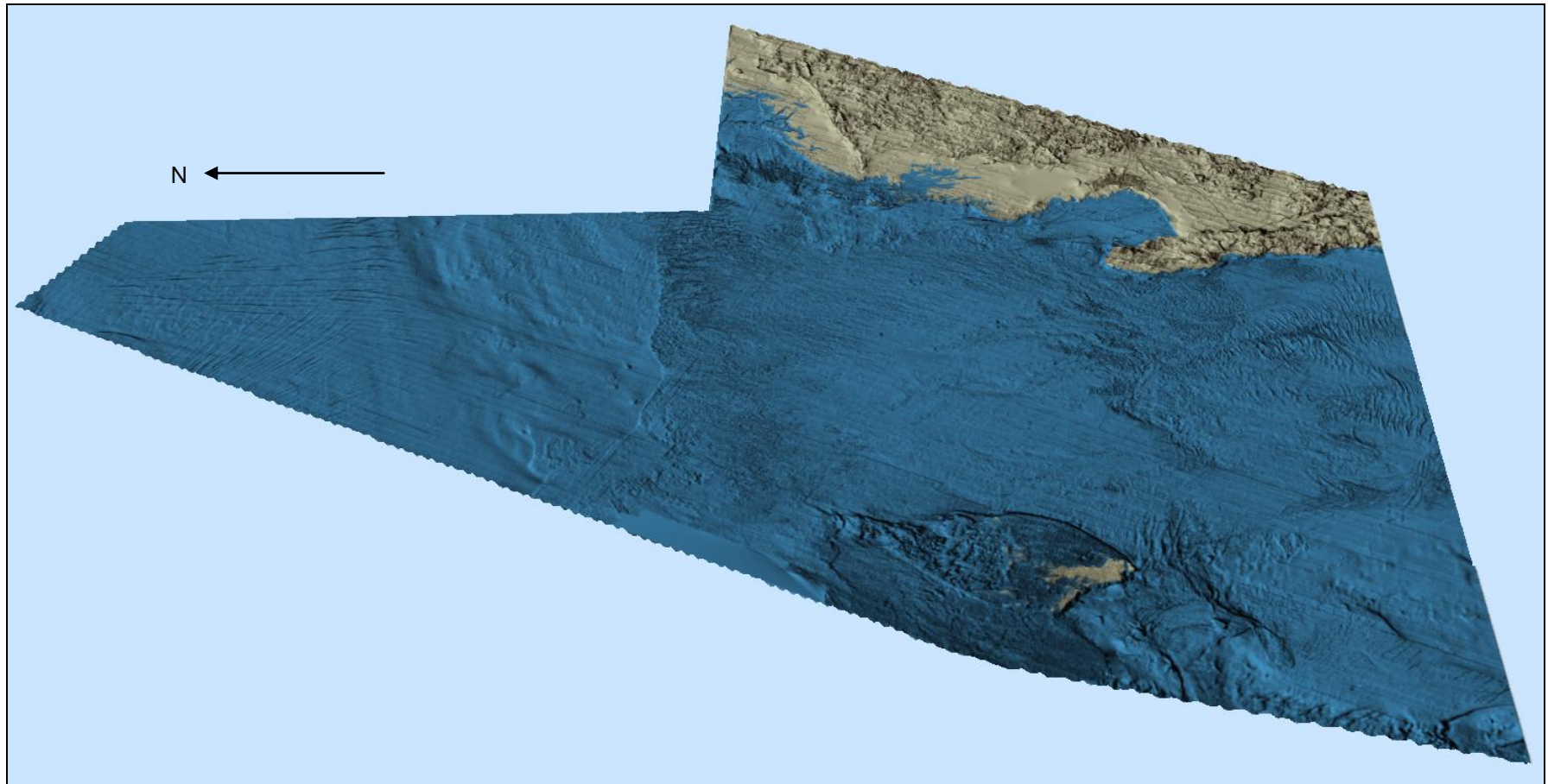


Figure 31 3D visualisation of the seabed in the Study Area (created in Erdas Imagine, based on the surface model generated from the bathymetry).

#### **4.2.1.3 Mapping Features**

The aim was to use the surface model to create a map of significant landscape features by digitising polygons around any significant features or areas of seabed that could be identified. Features or areas were deemed to be significant on the basis of two criteria. The first criteria was whether areas had the potential to be attractive to past humans (Westley et al., 2011a). On the basis of what we know about human settlement in the region in the Early Holocene, attractive areas include former coastlines, which could appear in the surface model as distinct breaks in slope, and sheltered coastal settings such as former bays, estuaries and lagoons. Other features known to be attractive to past humans in terrestrial Qatar in the Mid-Holocene include protective Karst-related settings, for example, former sinkholes. The second criteria was whether areas had the potential for the burial of palaeo-land-surfaces and the presence of palaeoenvironmental caches, that is, areas characterised by sediment deposition rather than erosion. Such areas could include sediment traps, for example, depressions and palaeochannels, as well as smooth areas of seabed with protruding rock outcrops. Other features such as spits and barriers are also indicative of landscape preservation rather than erosion. Key factors in the preservation of wrecks are not exactly the same as those for archaeological sites, but the probable presence of extensive sedimentary deposits is common to both. More features were mapped in the Study Area itself, as the higher resolution of the surface model within the Study Area allowed more detailed analysis. Beyond the Study Area, only larger, landscape-scale features were mapped.

It was also possible to use the surface model generated from the bathymetry in conjunction with information about former sea levels to create models of where shorelines would have been likely to occur in the Early Holocene. This was done by taking minimum and maximum sea level values at specific time periods from the global sea level curve produced by Stanford et al. (2011), and using these values to differentially shade those areas of the surface model that would have been under water and those that would have been dry land within a certain time period. The same was also done with sea level values from the Qatar sea level curve produced by Jameson and Strohmenger (2012), although with this curve there was just a single value for any particular point in time rather than minimum and maximum values. This process was relatively easy to do as the LiDAR bathymetry, unlike bathymetry data generated from sea-based sonar survey, provides seamless coverage from land to sea. The differentially shaded surface models were then compared to the topographic features that had been mapped from the surface model.

#### **4.2.2 Results**

The surface model created from the LiDAR bathymetry has provided a significant amount of detail about the present character and shape of the seabed. However, it is worth noting that there are limitations to the surface model produced by the bathymetry. The resolution of around 7m means that is possible to identify and interpret large, landscape-scale features such as former shorelines and large channels, but smaller, more discrete or ephemeral features will not show up at this resolution. There are also a few small areas within the LiDAR survey area where no

data was collected, and these appear as completely smooth areas in the surface model.

Also, it also has to be borne in mind that the present topography of the seabed will not be an exact reflection of what it would have been in the Early Holocene, as it will have been substantially affected by subsequent processes of erosion and deposition (see Chapter 7). Generally, it is thought that sediment deposition will have had the effect of smoothing out the seabed surface in this area (Marin Mätteknik AB, 2002, p.17) by filling in depressions, hollows and channels.

#### **4.2.2.1 Topography Within the Study Area**

The bathymetry shows that generally the seabed within the Study Area is relatively flat. The two deepest areas are along the southwestern edge of the Study Area, where the seabed averages around 12 to 13m deep (the deepest point here is just under 15m deep), and a southwest-northeast orientated channel in the north of the Study Area, averaging 8 to 9 m deep. Apart from near-shore, the highest areas in the Study Area are on and around the Qit'at ash Shajarah reef in the centre-west of the Study Area, which is only just below the surface of the water at certain points. Apart from the shallower near-shore area to the north of the Ras 'Ushayriq peninsula, the rest of the Study Area averages between 4-6m in depth (Figure 32).

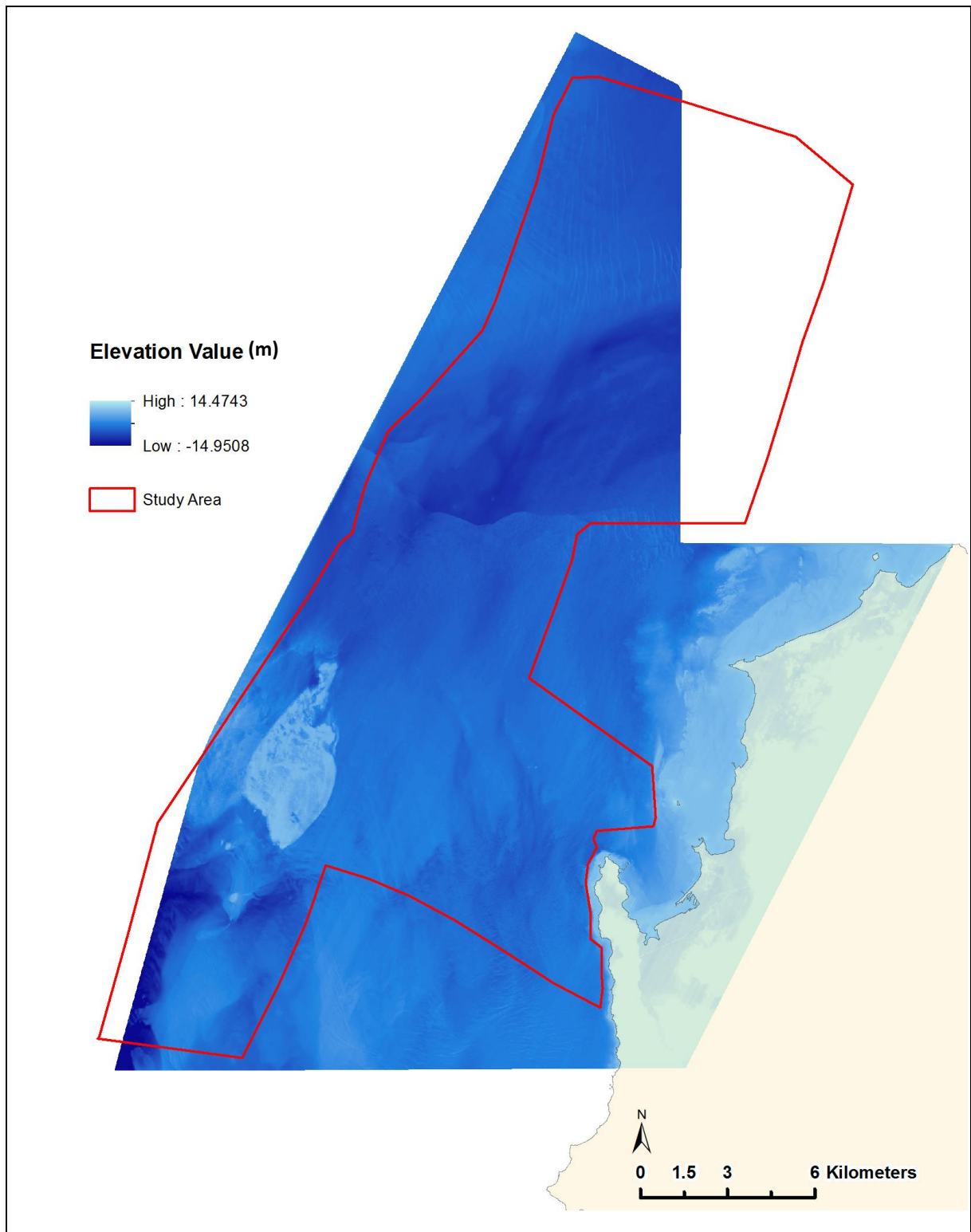


Figure 32 Surface model of the Study Area created from LiDAR bathymetry.

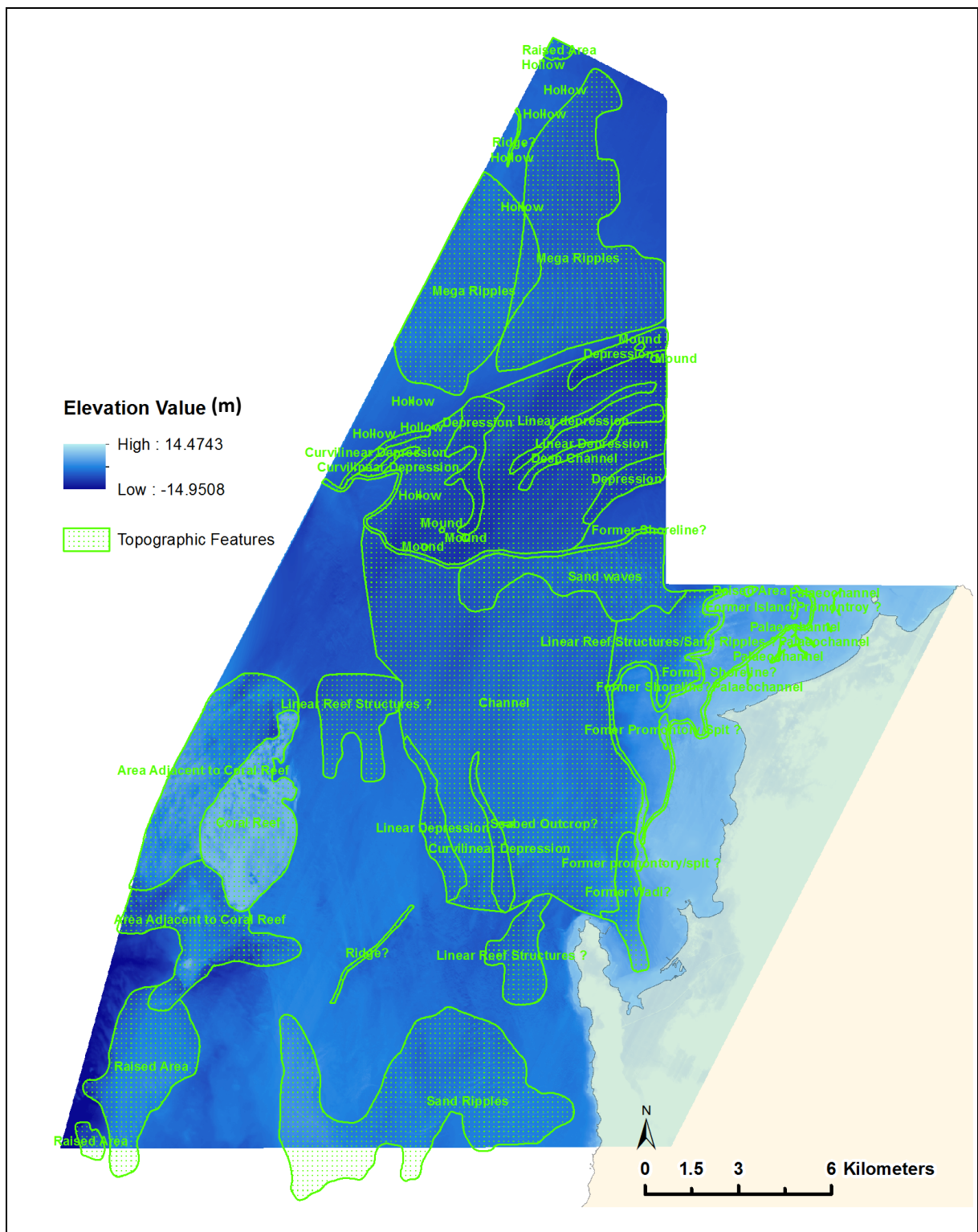


Figure 33 Features mapped from the surface model.

The most prominent seabed feature is the Qit'at ash Shajarah drying reef in the west of the Study Area. The other major feature is a wide, deep, southwest-northeast-trending channel which runs across the north of the Study Area (Figure 33). This channel is more than 5 km wide at its widest point, and it reaches depths of more than 9m in parts.

Most significantly for the purposes of archaeological potential, the surface model shows three coherent linear areas of relatively abrupt change in depth, which have been tentatively interpreted as former shorelines (Figures 34 and 35) that may have formed during periods of still-stands in the marine transgression. These putative former shorelines are extremely significant, as the archaeological evidence from terrestrial sites in Qatar in the Mid-Holocene demonstrates that coastlines were clear foci for human settlement (see Chapter 7).

Two of these potential former shorelines, running roughly north-south, lie close to the present-day coastline to the north of the Ras 'Ushayriq peninsula (Figure 35). The easternmost one roughly follows the -1m contour, possibly on the seaward edge of the intertidal zone. The westernmost one does not closely follow a single contour, instead mirroring the -5m contour in the south and rising to the -2m contour in the north. Both of them appear to lie roughly parallel with each other, looping around a headland and then merging.

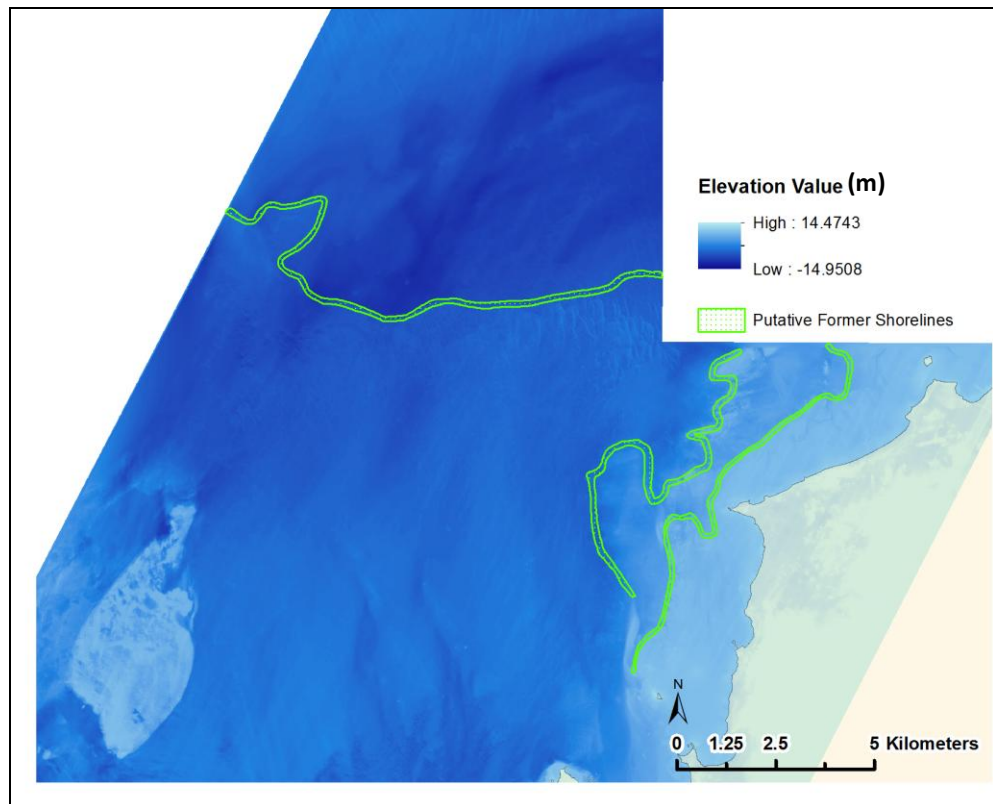


Figure 34 Putative former shorelines in the Study Area.

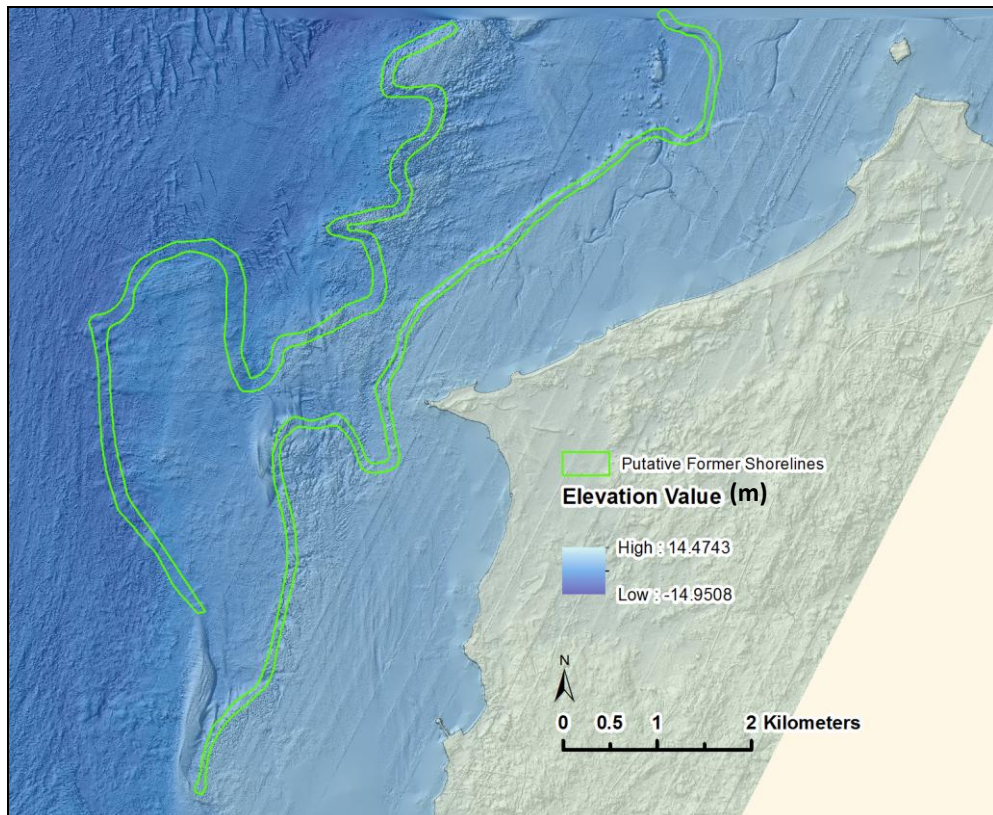


Figure 35 Hillshaded surface model with putative former shorelines.

The third putative shoreline appears as a very abrupt change in depth which runs west-east across the centre of the Study Area (Figure 36), roughly following the -7m contour line. This edge is very clear along most of its length, but it becomes more indistinct towards its western end. The deep, southwest-northeast orientated channel mentioned above lies immediately to the north of this feature.

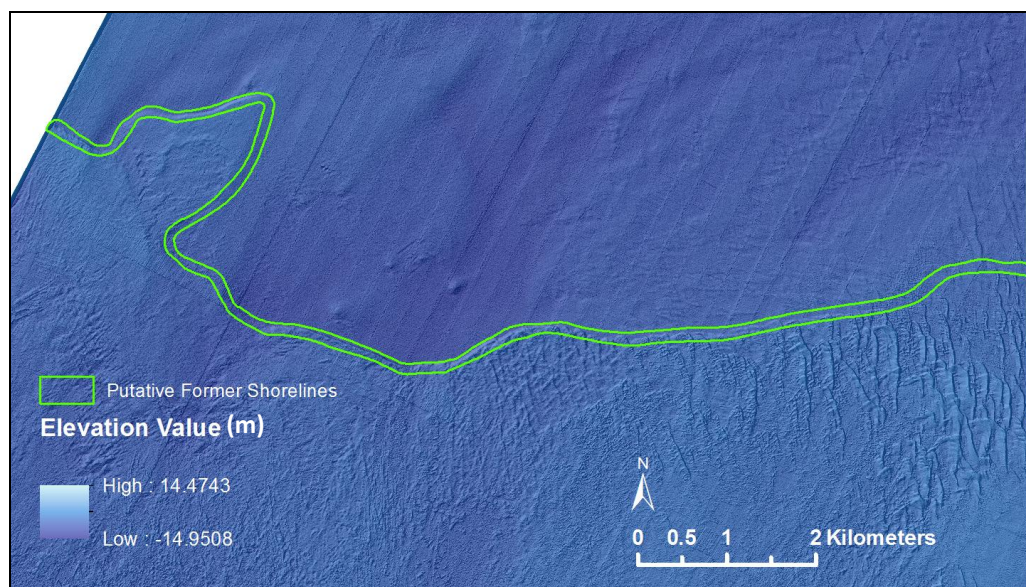


Figure 36 Hillshaded surface model with putative east-west former shoreline.

The edge of this change in depth is also clearly visible in the mosaic image of the sidescan sonar data (Figure 37).

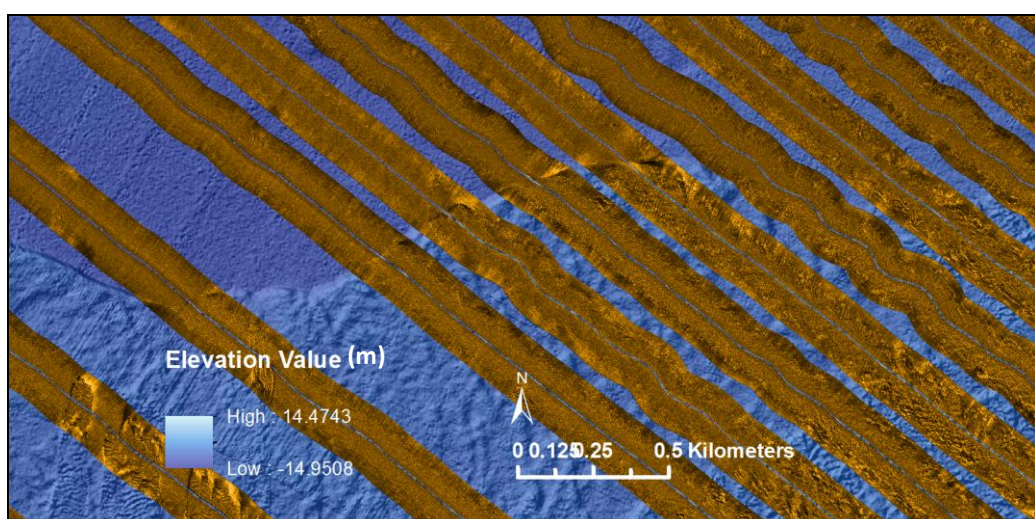


Figure 37 Putative east-west former shoreline with sidescan sonar data overlain.

Several significant topographic features lie in close association with the north-south former shorelines, and are probably related to them (Figure 38). These features consist of raised ridges, likely to be former promontories, spits or islands. These types of feature are highly significant locations for potential human settlement, as are the possible bays and headlands on these shorelines, which may have been both attractive areas for settlement, and protective in terms of deposits.

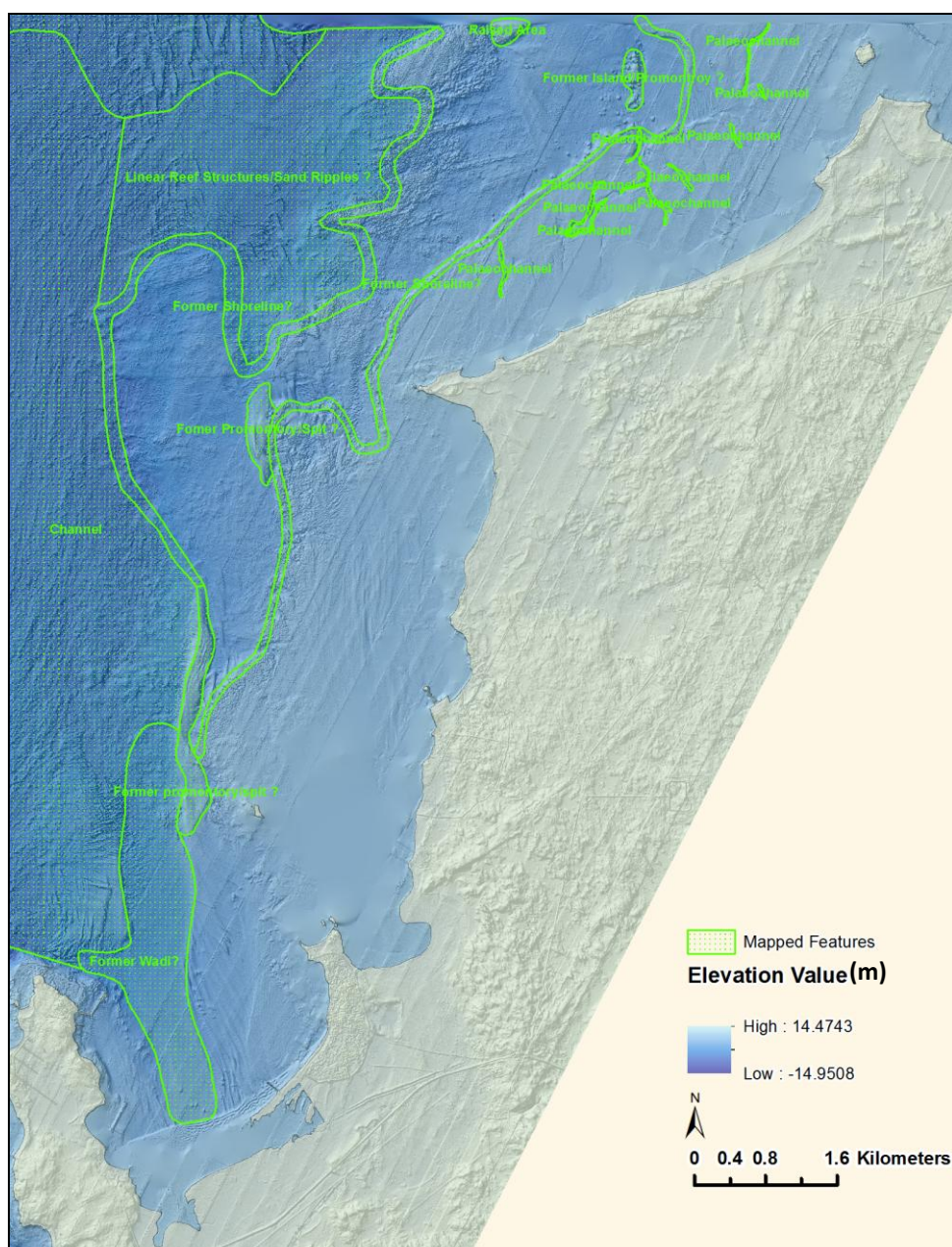


Figure 38 Putative former shorelines with possible associated mapped features.

Another feature in close proximity to the former shorelines is a north-south aligned deeper channel, more than 700m wide, which runs from the east of the Ras 'Ushayriq peninsula northwards (Figure 39). This may represent a former river channel, and its orientation and proximity to a present-day Wadi (Wadi Debayan) suggest that this palaeochannel is actually a continuation of Wadi Debayan.

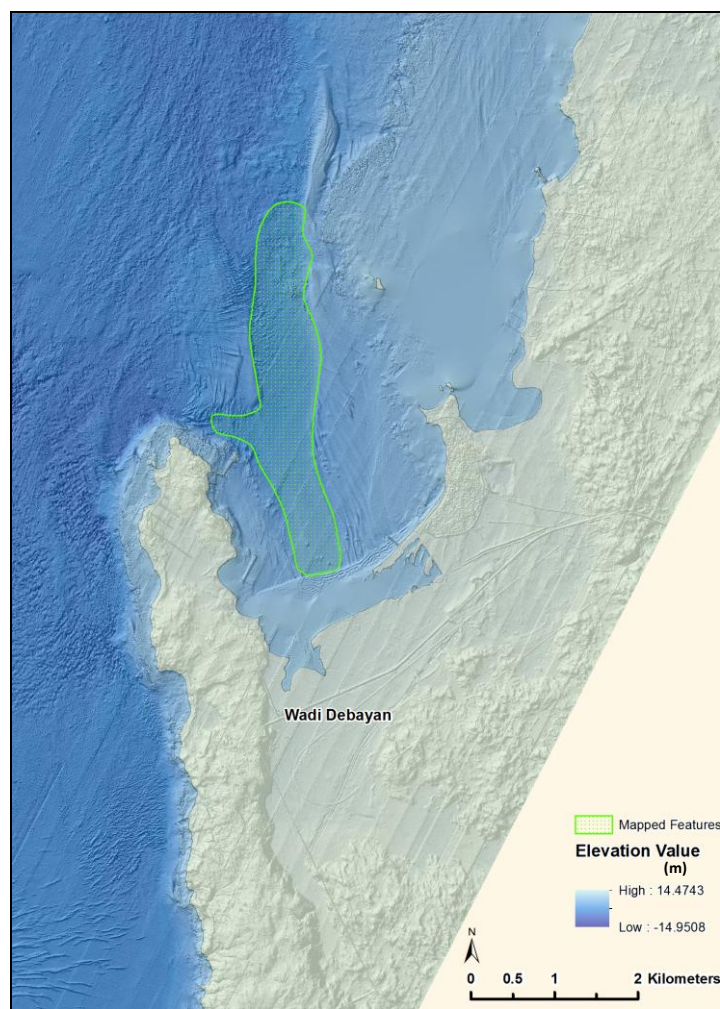


Figure 39 Palaeochannel possibly relating to the former course of Wadi Debayan.

A cluster of small curvilinear depressions, some interconnected, are visible in very shallow depths approximately 1km offshore, in the intertidal zone (Figure 40). These features, interpreted as palaeochannels, are narrow and very shallow, and the most

well-defined channel appears to end at the postulated former shoreline. The location and orientation of this cluster of palaeochannels suggests that they represent a drainage system relating to that shoreline, and are therefore of considerable significance in terms of palaeoenvironmental potential.

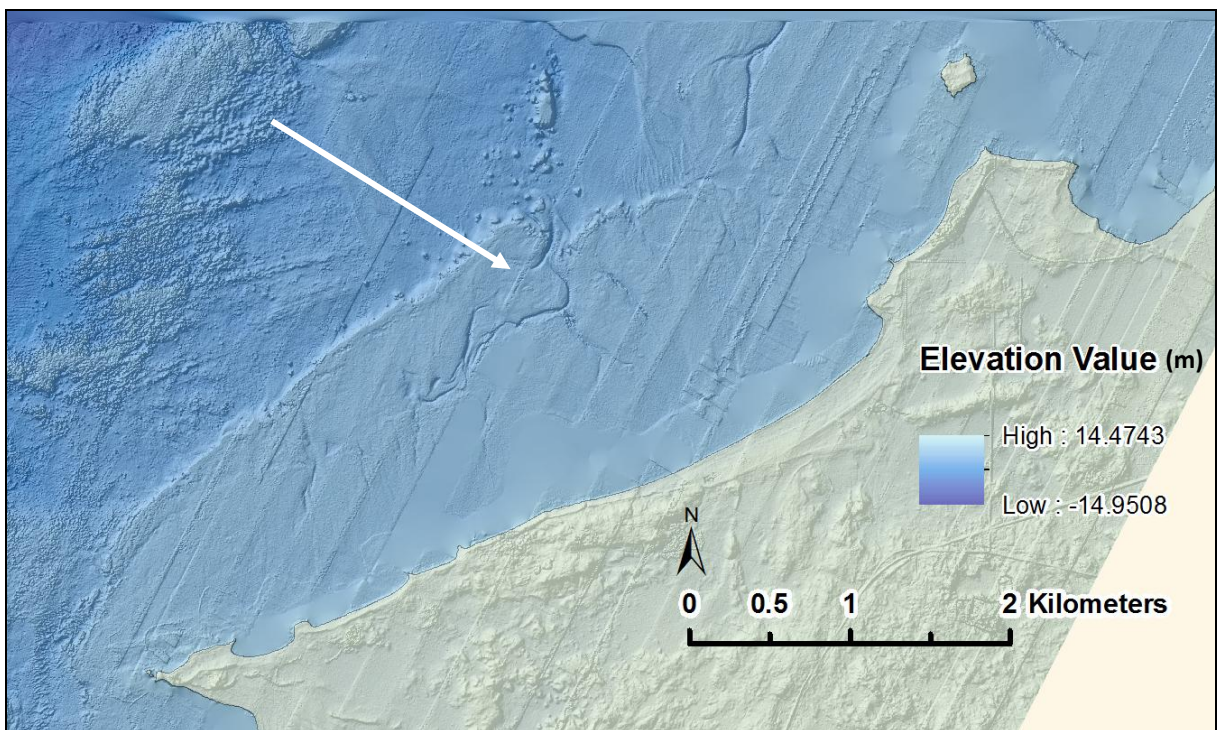


Figure 40 Cluster of palaeochannels.

A few fish traps (currently undated) are just about discernible in the intertidal zone in this area (Figure 41), and these are so ephemeral that it would have been very easy to miss them had their locations not been mapped already as a result of the QNHER cultural mapping project (Breeze et al., 2011). Only a few of the traps mapped by the QNHER can be identified in the surface model, as most of them lie in 'no-data' areas in the bathymetry.

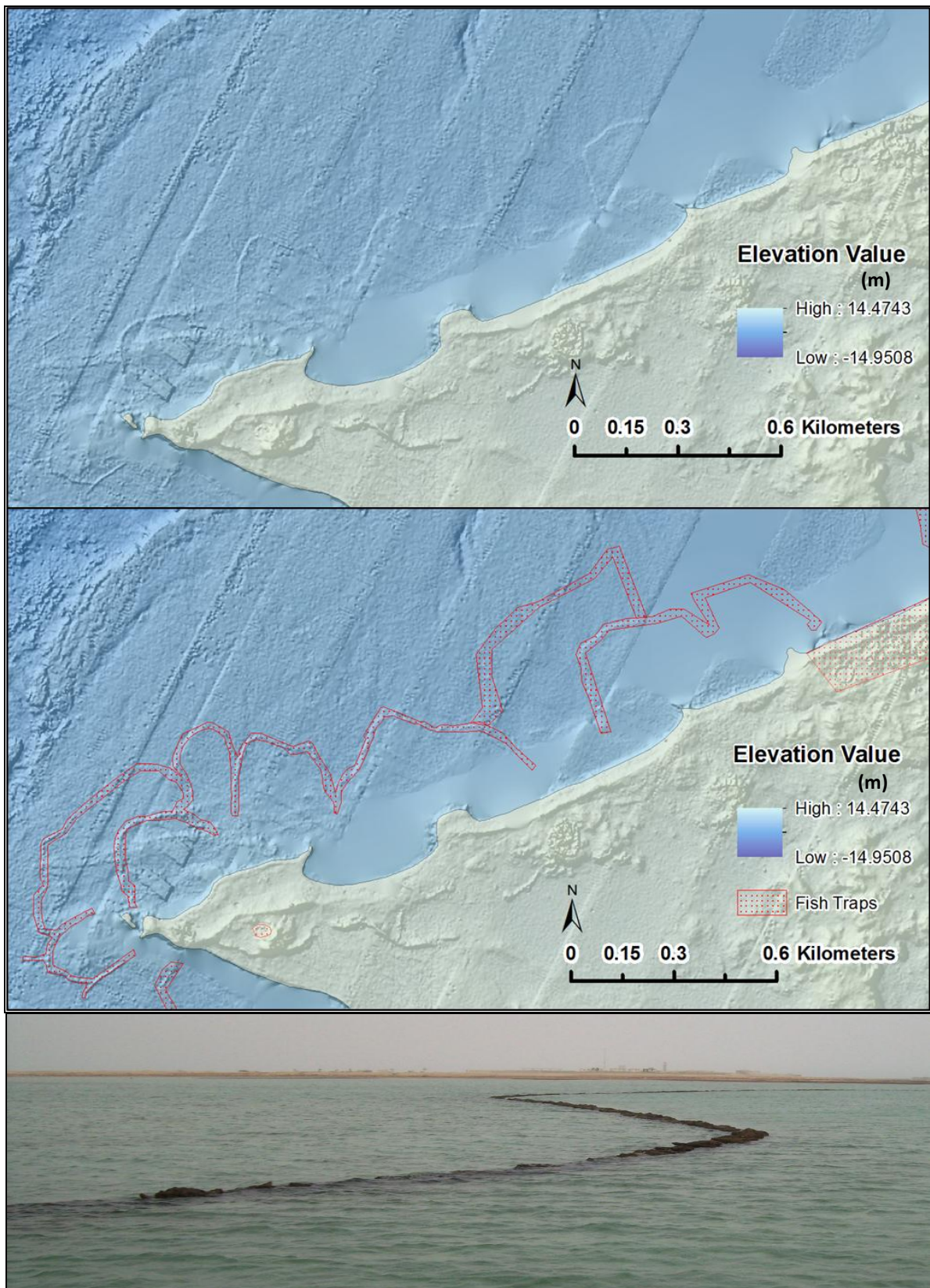


Figure 41 Fishtraps visible in the surface model (top), mapped during the QNHER cultural mapping project (middle) and an example photographed by the QNHER project (bottom).

A number of linear and curvilinear depressions or channels occur in the Study Area. These are concentrated in the deep channel previously mentioned to the north of the west-east shelf (Figure 42), and are almost all on the same southwest-northeast orientation as the channel itself. However, there are also two north-south aligned linear depressions or channels in the south of the Study Area, between the Bay of Al-Zubārah and the reef (Figure 43).

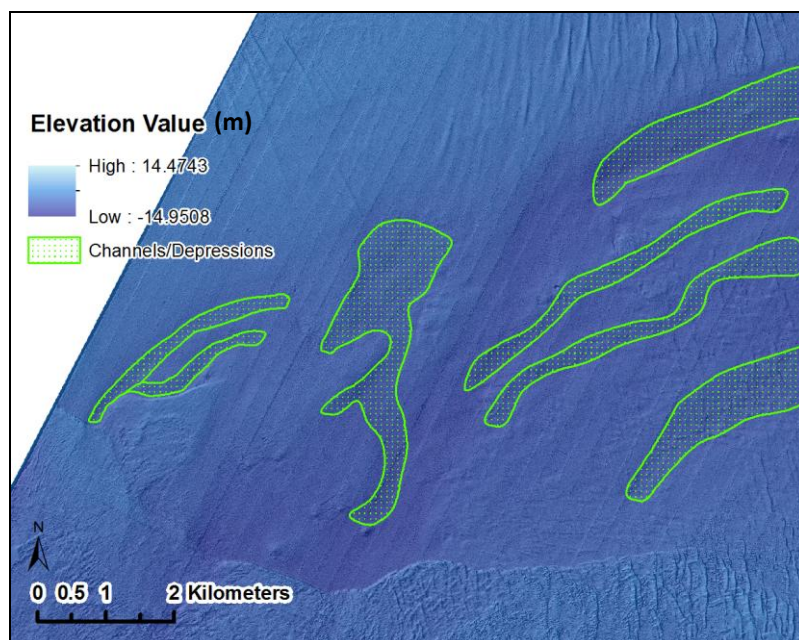


Figure 42 Channels and depressions in the north of the Study Area.

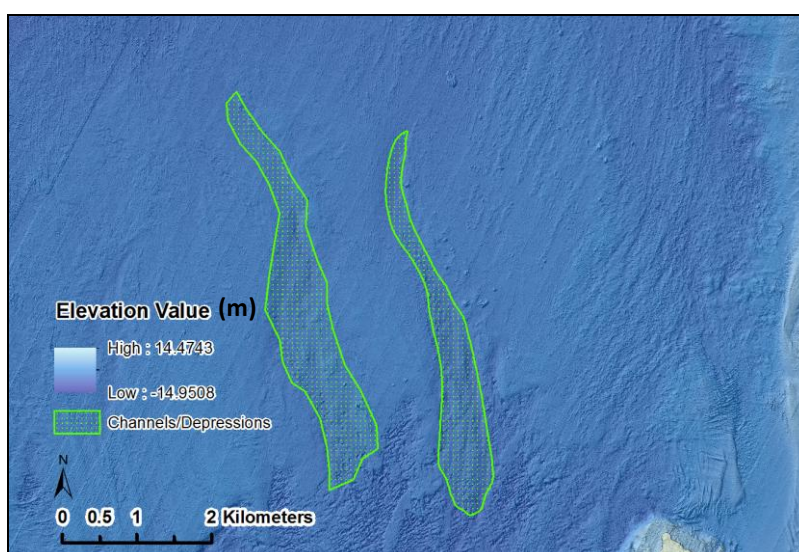


Figure 43 Channels and depressions in the south of the Study Area.

The orientation of these linear and curvilinear depressions are worth highlighting. Those lying in the deep channel in the north (Figure 42), as well as reflecting the orientation of the channel itself, also lie roughly parallel with the southwest-northeast alignment of the present-day and putative former shorelines to the southwest. The linear depressions in the south, to the east of the reef (Figure 43), reflect the north-south orientation of the putative extension of Wadi Debayan, and it is likely that these three features represent palaeochannels that may all be part of a larger drainage system.

Two extensive areas of linear ridges are discernible in the north of the study data, one north-south trending (Figure 44), and one northwest-southeast trending. These are very large, widely-spaced features, between 100m and 200m apart, and are interpreted as sand ripples or 'megaripples'. Another area of smaller, east-west trending sand ripples is visible in the south of the Study Area.

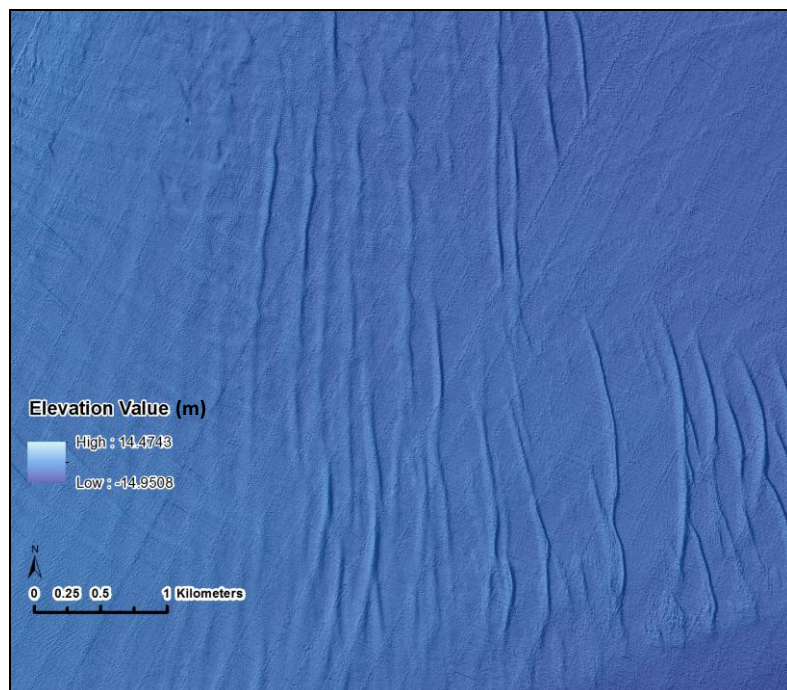


Figure 44 Megaripples in the north of Area 1.

The central area, between the reef and the Bay of Al-Zubārah is dominated by narrower, less prominent north-south trending linear features which are interpreted as either sand banks or linear reef structures (Figure 45).

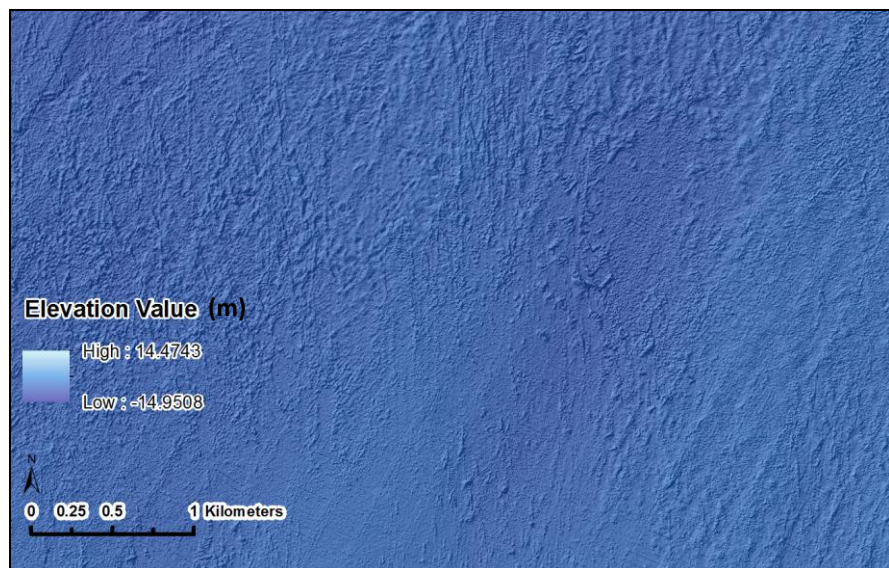


Figure 45 Possible sand banks between the reef and the bay of Al-Zubārah.

Several small hollows can be identified in the surface model, exclusively in the north of the Study Area. These are concentrated into two groups, one in the extreme northwest of the Study Area, and one to the north of the west-east potential former shoreline. The two concentrations are separated by an extensive area of sand ripples where no hollows are present. It seems logical to assume that the sand ripples will have masked any hollows that may have been present in those areas. These features appear as small, but very distinctive circular or sub-circular holes on the sea floor, ranging from 20m to 50m in diameter. They do not appear to be very deep, either because they are filled with sediment, or because the resolution of the LiDAR data may not be sufficient to adequately reflect the morphology of such small

features. These hollows were cross-checked against the sidescan sonar data to see if they could be further clarified, but unfortunately most of them do not lie within the area covered by the sidescan sonar survey. One that did lie within the survey area was not visible in the sidescan sonar data at all, at least in part because it lay at the inner range of the swath, directly below the towfish (Figure 46). It is not clear exactly what these features are, but they have been tentatively interpreted as former solution hollows, as found in the terrestrial Karst landscape of present-day Northern Qatar. It is interesting to note that one of the potential solution hollows lies very close to one of the linear depressions, as it has been noted that sequences of Karst-related depressions in terrestrial Qatar can form linear depressions (Sadiq and Nasir, 2002).

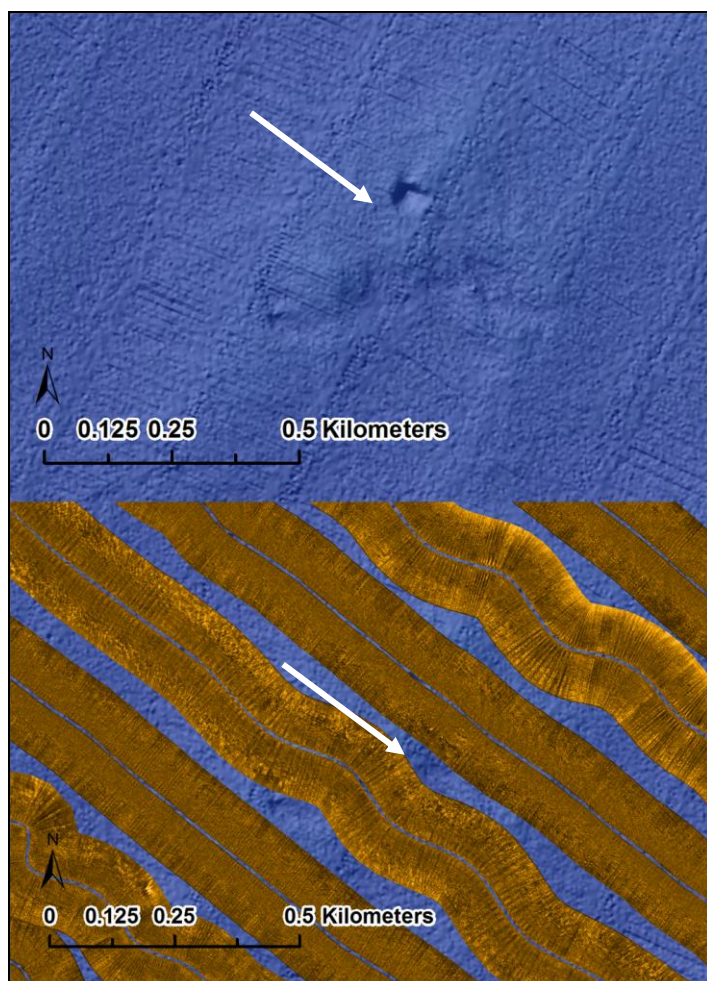


Figure 46 Possible solution hollow visible in the surface model but not in the sidescan sonar data.

There are some very low mound-like features present, mainly to the north of the west-east former shoreline (Figure 47). These are only very slightly elevated, by around 1m, and range in size from 50m to 150m in diameter, so could be better described as undulations. It is possible that these features could represent outcrops in a sediment-covered seabed.

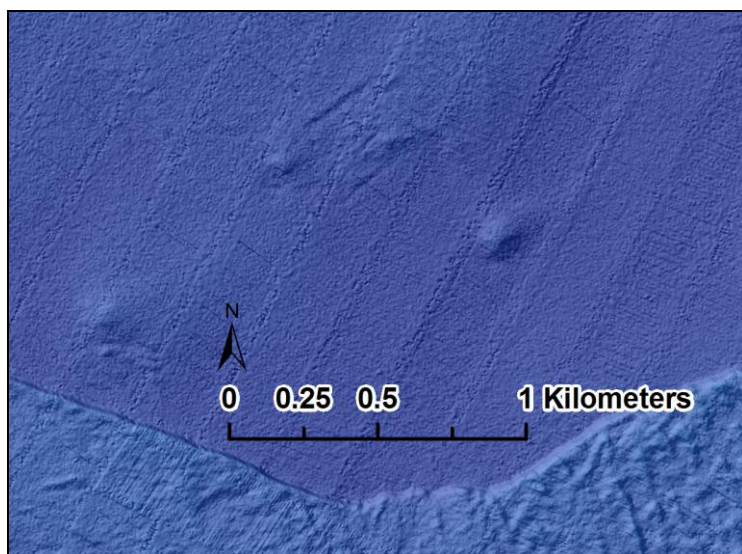


Figure 47 Undulations in the seabed to the north of the putative east-west shoreline in Area 1.

More complex topography exists around the reef (Figure 48), making it difficult to interpret, but it includes a raised area to the west that is likely to be part of the reef formation. There is also an elevated area to the south, which may represent an accumulation of sediment on the leeward side of the reef, and it includes two prominent larger outcrops of either rock or coral. A deeper area in the southwest may represent a basin, but this can only be a tentative interpretation as the feature lies at the edge of the surface model.

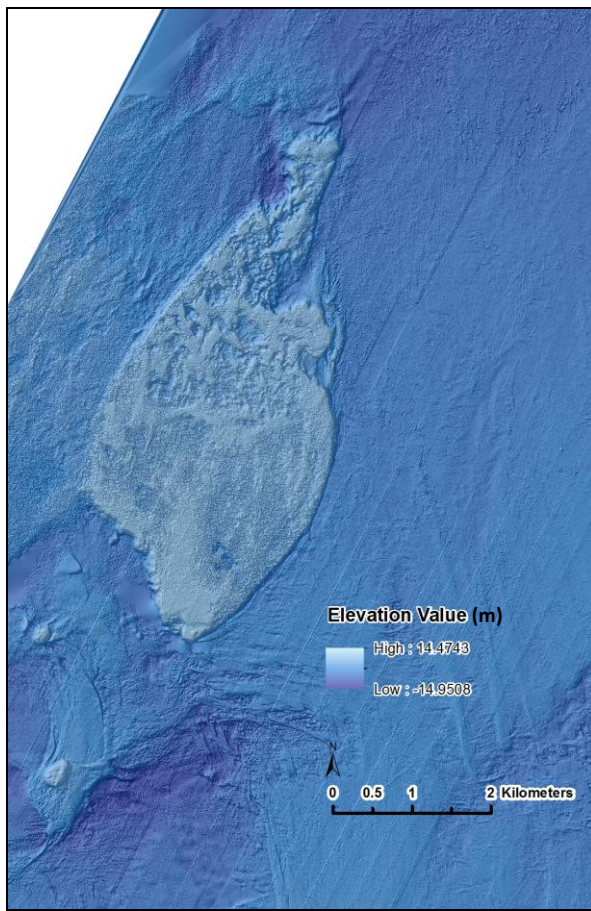


Figure 48 The Reef in the west of the Study Area.

#### **4.2.2.2 Topography Outside the Study Area**

In the area to the south of the Study Area, where topographic features were not mapped in as much detail, greater depths are present, particularly in the far south in the Gulf of Salwa (Figure 49). Here, depths increase to more than 28m in the west, but there are also numerous large areas of significantly higher elevation within this. The predominant features identified were potential former shorelines, which can be traced virtually all the way down the coast, although their occurrence is more sporadic in the area immediately to the south of the Study Area. Due to the narrow width of the data set around the Hawar Islands (which lie in Bahrain territorial waters

and therefore not included in the survey), it is not possible to tell if these putative shorelines in the central area link up to form a continuous feature with those in the south or if they represent different phases of shoreline. However, it is likely that the area around the Hawar Islands may incorporate part of this shoreline.

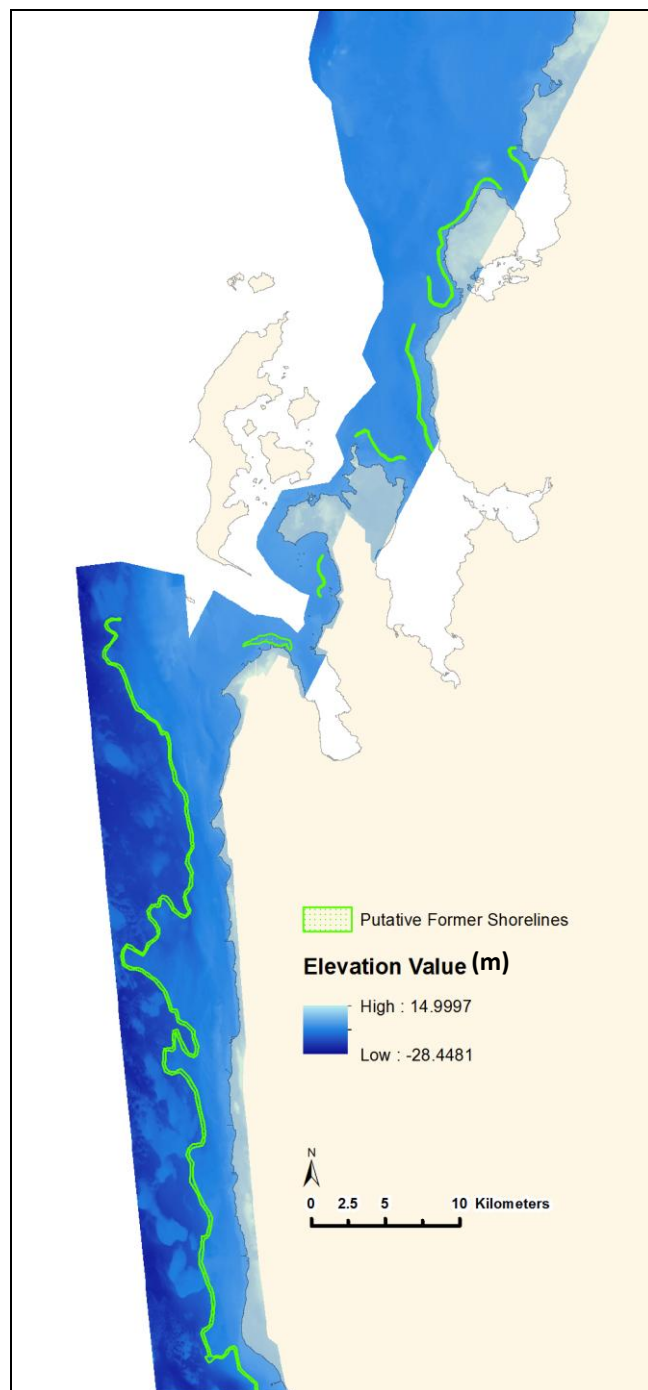


Figure 49 Potential former shorelines to the south of the Study Area.

The areas of higher elevation down in the Gulf of Salwa form quite significant protrusions from the seabed (Figure 50), with elevation changes of 7 or 8 m, and would have been islands at some time in the past, when sea levels were more than 10m lower than present-day levels.

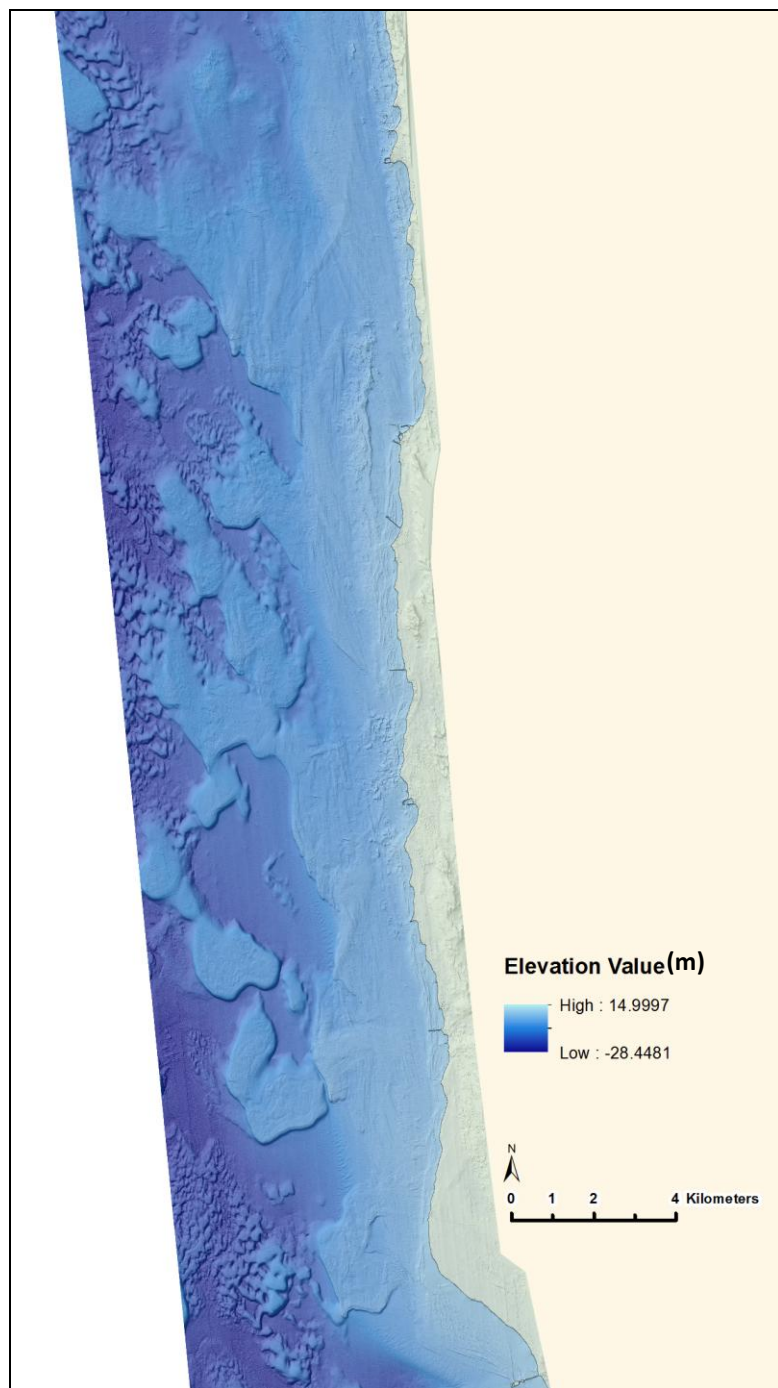


Figure 50 Seabed surface in the Gulf of Salwa.

#### **4.2.2.3 Topography and Sediment Classification**

As part of the integrated analysis of different datasets in order to refine the zoning of the submerged landscape, the results of the acoustic classification and the bathymetry analysis were examined together to see how each could inform and enhance the other. The aim was to highlight those areas where the two datasets were consistent with each other and vice versa, and in particular to see if the surface model could provide useful additional information about the acoustic classes that were generated by the unsupervised acoustic classification process.

The broad patterns of the classified data in the south of Area 4 seems to show a good correlation with the broad patterns that can be discerned in the surface model (Figure 51). The deeper area that is present along the western edge of Area 4 in the surface model is largely reflected by the yellow area (Class 4) in the classification. This coincides with the extensive area of trawler scarring that is visible in the mosaic of the sidescan sonar data. These scars are not visible in the surface model, probably because they are too superficial.

The pattern of raised areas visible in the surface model is also discernible in the classification, including the sub-oval area in the south, and the triangular elevated area immediately south of the reef. There is a complex pattern evident in the topography in the elevated area to the south of the reef, and the classified data in this area is also very complex. The patterns in the two datasets don't reflect each other in detail, but a similar general outline shape can be traced in both datasets.

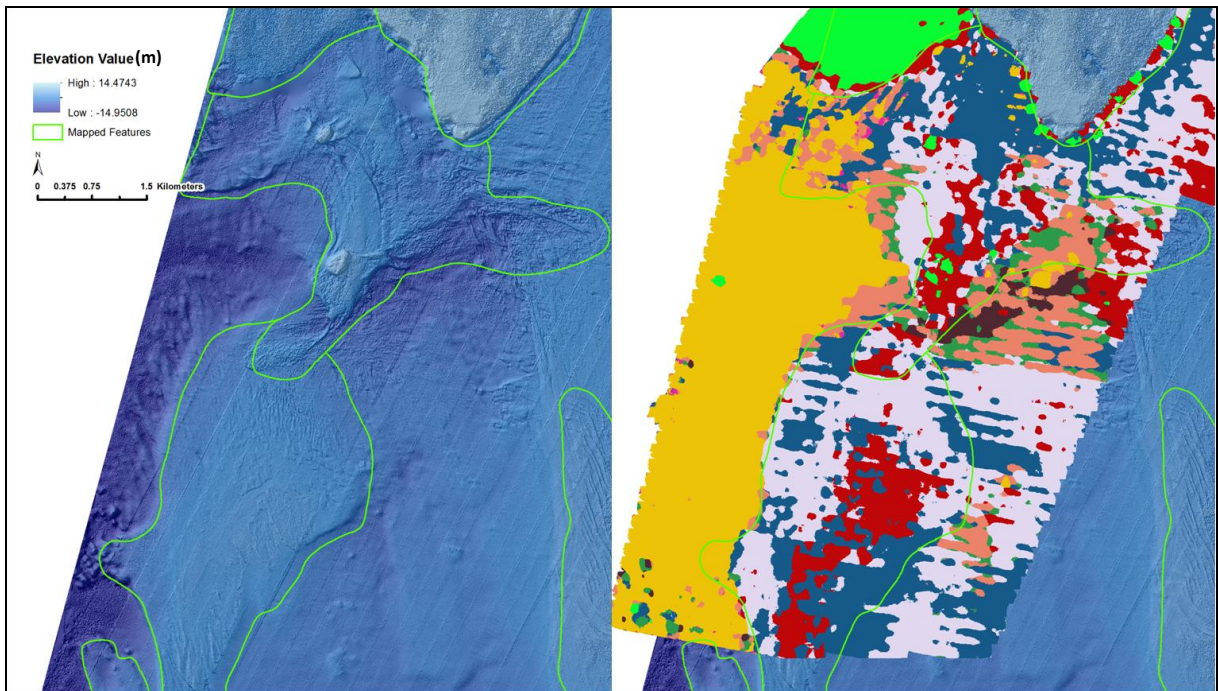


Figure 51 Surface model with the classified data in Area 4.

In Area 2, the deeper north-south trending channels that were identified in the surface model show some coincidence with the lilac north-south-trending areas (Class 5) generated by the acoustic classification (Figure 52), possibly because these channels contain finer sediment than the surrounding area. It is also possible that the northern part of the possible wadi extension that was identified in the surface model to the east of the Ras 'Ushayriq peninsula can start to be discerned in the classified data, but as this is the only part of the channel that lay within the area covered by the sidescan sonar survey, there is not enough data to be more positive about this.

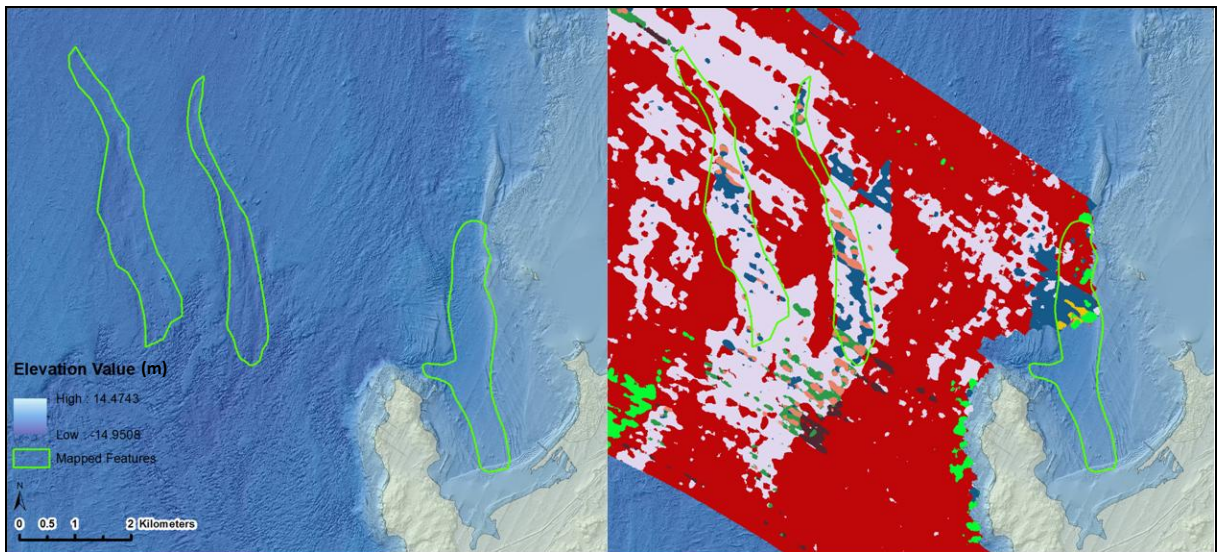


Figure 52 Surface model with the classified data in Area 2, West of the Ras Ushayiq Peninsula.

The raised area to the west of the reef that is clearly visible in the surface model, is equally clearly visible as the lime green area (Class 8) in the classification (Figure 53). The complexity of the classified data immediately to the north of the reef is not really reflected in the topography shown in the surface model, or in the mosaic image of the sidescan data. The automated acoustic classification is obviously detecting changes in the seabed sediment that are not just a factor of depth in this area, but could be influenced by coral formation and differential sediment accumulation around the reef.

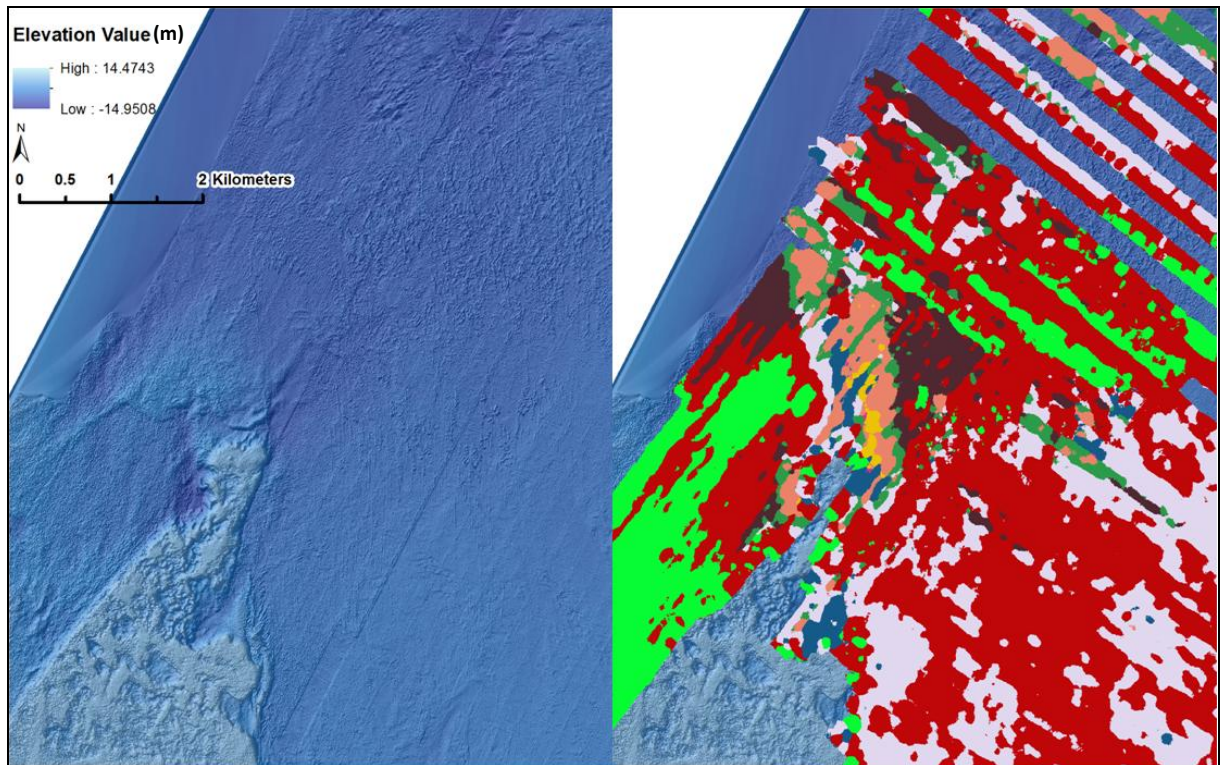


Figure 53 Surface model with the classified data in Area 3, north of the reef.

In Area 1, the large, southwest-northeast trending channel that was identified in the surface model is broadly coincident with the large band of mixed salmon and yellow (Classes 9 and 4) in the classified data (Figure 54). The smaller linear depressions that could be discerned within the bigger channel in the surface model are not readily apparent in the classified data, but the gap between survey lines in this area does not make interpretation of smaller features like this very easy. However, it is clear from this integrated analysis that the yellow and salmon areas correlate closely with the deeper areas within the Study Area.

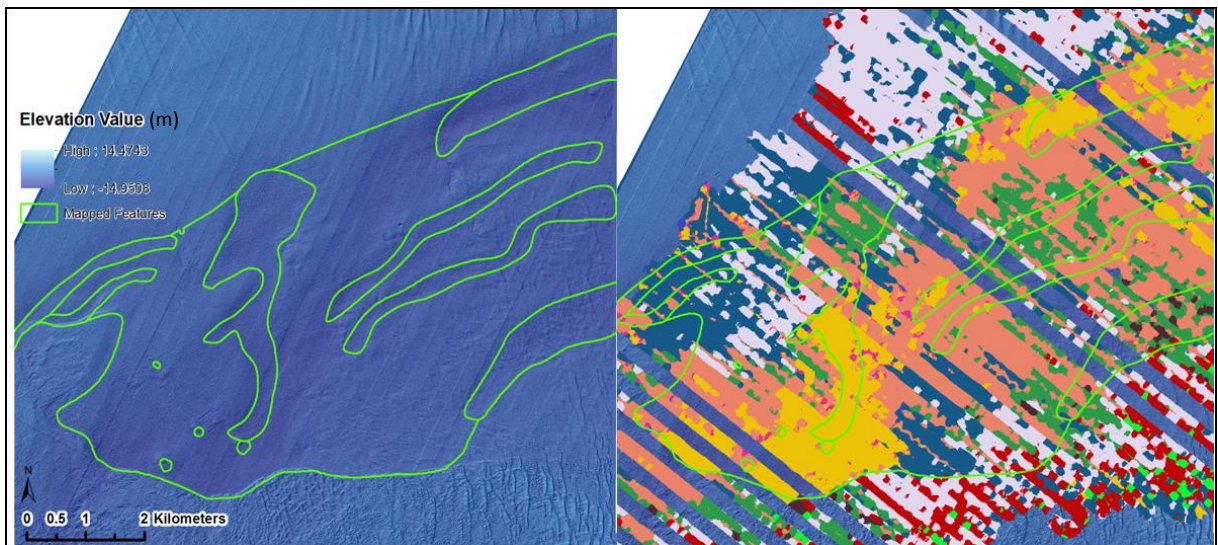


Figure 54 Surface model with the classified data in the deep channel in Area 1.

In the north of Area 1, the classified data consists of a mixed area of blue and lilac (class 10 and class 5 respectively). In the surface model, this area shows a very clearly-defined area of north-south trending, large scale sand ripples. However, the boundary of this area of sand ripples is not clearly-discernible in the classified data.

#### 4.2.3 Discussion

The analysis of the surface model has produced some very promising results through the identification of significant landscape features, that will form the basis of future marine research frameworks and further investigation. Despite the limitations of the data in terms of resolution and coverage, for the purpose of this research, which is to identify areas of archaeological and palaeoenvironmental potential at a landscape scale, the analysis of this dataset has been crucially important as it has enabled the identification of previously unknown landscape features that could be highly significant to locating past human settlement in the Late Pleistocene and Early

Holocene, particularly the putative former shorelines. However, it is necessary to examine these shorelines in association with information about Holocene sea level change. By applying reconstructions of global sea levels to the surface model created from the bathymetry, it is possible to attempt to map the extent of dry land that would have been exposed within certain date ranges and reconstruct shorelines.

Accurate sea level curves have to include elevation data and age dates, and also require the interpretation of palaeo-bathymetry (Jameson and Strohmenger, 2012). However, there are considerable uncertainties and limitations relating both to the application of global sea level curves specifically to Qatar, and to the use of bathymetric models with sea level curves. These issues have been discussed in detail by Lambeck (1996), Rose (2010) and Cuttler (Cuttler and Al-Naimi, 2013; Cuttler, 2013; Cuttler, 2014), and have been summarised in section 1.2.6. As long as these limitations are acknowledged, applying sea level data to the surface model created from the LiDAR bathymetry provides invaluable information about the locations of potential former shorelines. A global sea level reconstruction curve was produced by Stanford et al. (2011), by undertaking statistical analysis on a range of key far-field datasets of relative sea-level change. Even though this model of sea level change has been very carefully and substantially researched, and is applicable for global and macro-scale studies, it is still necessary to accept that there will be limitations in accuracy when applying the model to more detailed studies of sea levels around Qatar. This model gives global sea level ranges (with 99% confidence) between 15m and 11m below present day levels for 8,000 BP, and between 9 and 7.5 m below present day levels for 7,000 BP. Applying these values to the seabed

surface model for the Study Area produces interesting results (Figure 55). On the basis of these values, virtually the entire Study Area apart from the deeper area at the southwest edge, and parts of the deep channel in the north, would still have been dry land at 7,000 BP, regardless of whether the lowest or the highest value in the range is used. The possibility that most of the Study Area remained as dry land as late as 7,000 BP is worth considering, given the theories of Lambeck (1996) and Heyvaert and Baeteman (2007) that the present-day coastline was reached at 6,000 BP, and given the recent evidence dating relic beach terraces at Wadi Debayan to 6,000 BP (Tetlow et al., Forthcoming).

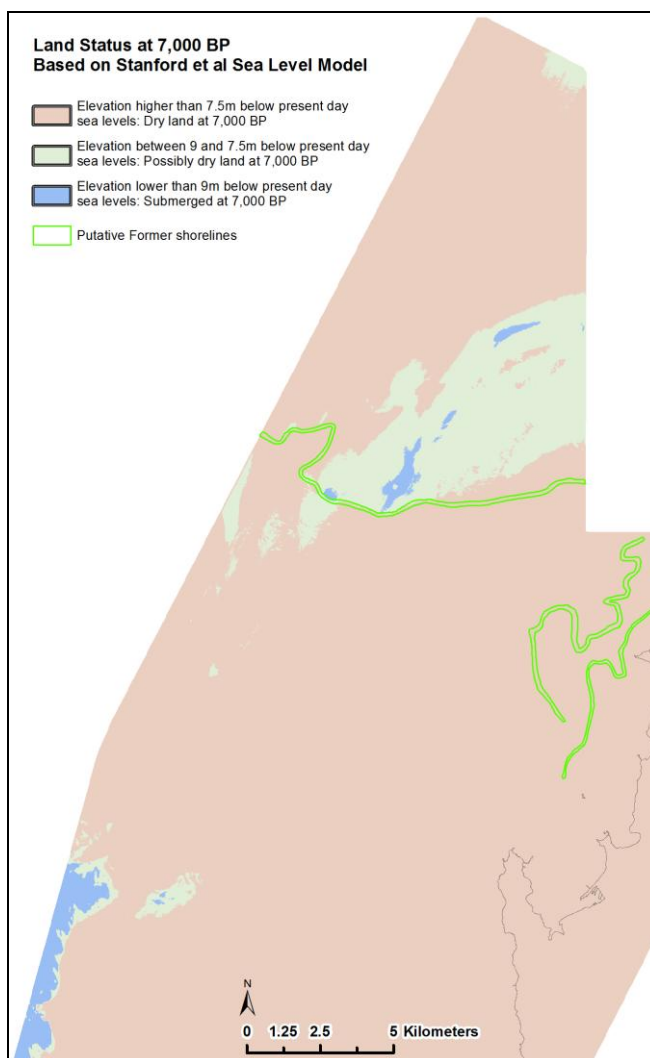


Figure 55 Postulated extent of dry land at 7,000 BP (based on Stanford et al., 2011).

A Qatar-specific sea level curve was published by Jameson and Strohmenger (2012), which was derived from age dating of raised beaches in Qatar. Jameson and Strohmenger propose that the Holocene high stand was initially reached at 7,000 BP in Qatar, which is considerably earlier than the timescale proposed by Lambeck (1996) and Heyvaert and Baeteman (2007). According to Jameson and Strohmenger's curve, the sea level around Qatar at 8,000 BP is placed at 4.3m below present day levels, dropping to 4.7m at around 7,800 BP, before rising to 2m higher than present day levels at 7,000 BP.

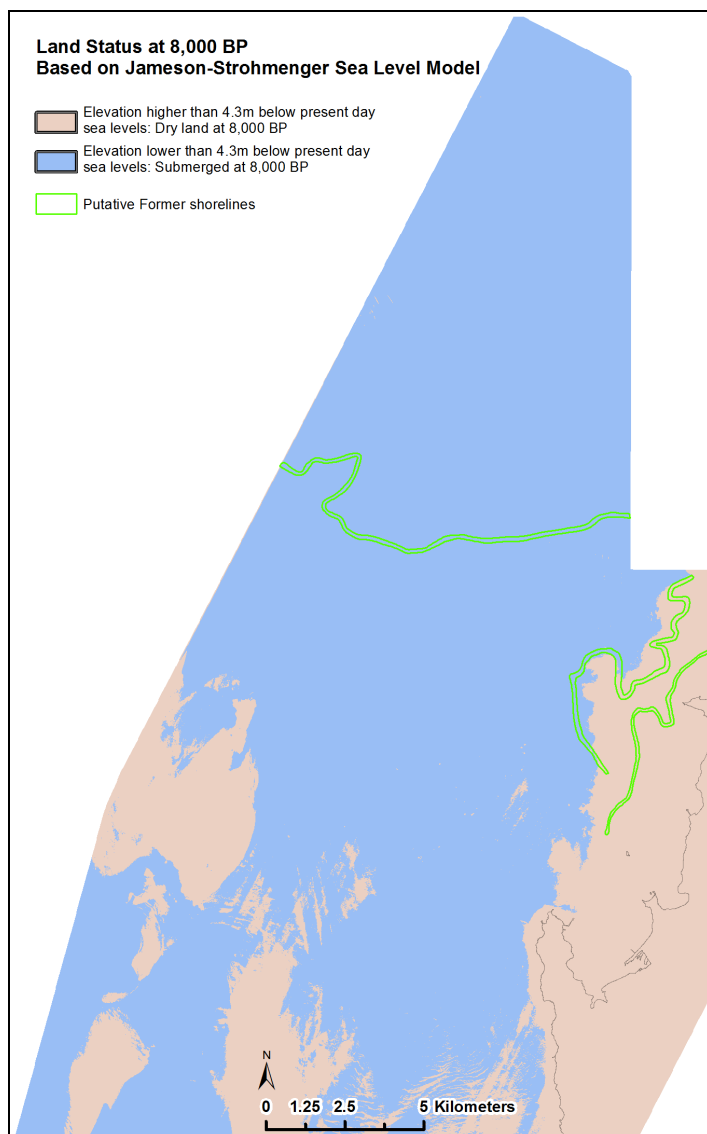


Figure 56 Postulated extent of dry land at 8,000 BP (based on Jameson and Strohmenger, 2012).

Applying these values to the surface model of the Study Area produced quite different results to the Stanford model. On this basis, the model shows that the majority of the Study Area would already have been inundated by 8,000 BP (Figure 56). The western-most potential former shoreline identified to the north of the Ras ‘Ushayriq peninsula fits well with this model, roughly coinciding with the land/sea interface at 8,000 BP. Furthermore, applying these values to the surface model demonstrates that areas of Qatar that are currently dry-land would have been submerged at 7,000 BP (Figure 57).

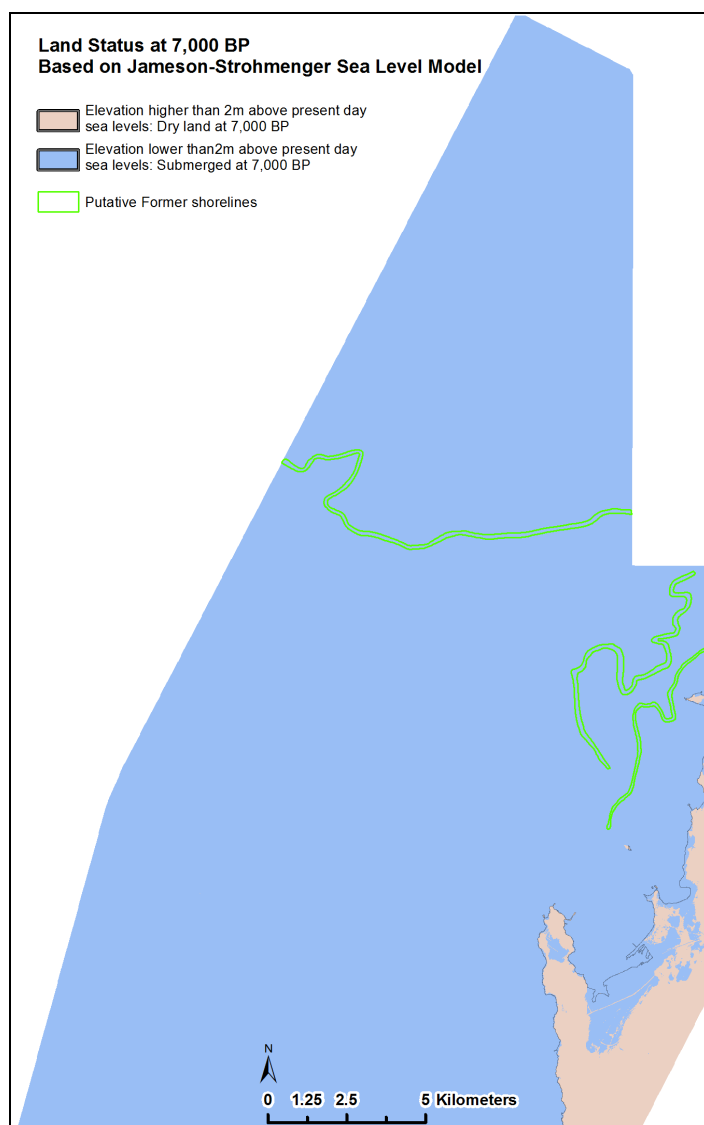


Figure 57 Postulated extent of dry land at 7,000 BP (based on Jameson and Strohmenger, 2012).

The interpretation of the third, west-east orientated potential former shoreline is less clear. When the values from both of the sea level curves discussed above were applied to the surface model, neither model highlighted this feature as a land-sea interface between 8,000 and 7,000 BP. There is no substantial evidence in the literature for a still stand at -7m in the Early Holocene, and this feature may represent a shoreline that had its origins in the previous interglacial period, the Eemian. However, even if this is the case, it would have been a shoreline again at some point during the Early Holocene. This could equally apply to the other two putative shorelines, since there is also no specific evidence for still stands at -2m or -1m either.

The different results obtained for the possible extent of dry land in the Study Area in the Early Holocene outlined above demonstrate that these attempts at shoreline reconstructions cannot be considered to be definitive due to all the problems previously described relating to sea level reconstructions and lack of detailed data. However, they do show that although there is still a lot of work to be done in establishing more detailed and robust models of sea level change around Qatar, there is nothing to conflict with the interpretation of any of these three features as former shorelines.

The wide, deep, southwest-northeast aligned channel in the north of the Study Area could represent a former river bed. The two linear channels to the east of the reef, together with the possible extension of Wadi Debayan to the east, may also be part of a former river channel, which possibly forms a tributary of the deep channel to the

north. This may explain why the west-east orientated putative former shoreline is less distinct at its western end, perhaps displaying estuary-like characteristics where it is bisected by the channel running from the south.

As mentioned previously, the hollows identified in the surface model have been tentatively identified as solution hollows. However, it is also possible that they could be craters that have developed as a result of gas venting from the sea floor. Such features, sometimes termed 'pockmarks', have been noted in the Arabian Gulf, including off Qatar (Uchupi et al., 1996), and also elsewhere in the world, especially in hydrocarbon-bearing areas, such as the North Sea and off Alaska (Ellis and McGuinness, 1986).

The integrated analysis of the surface model and the acoustic classification has proved to be extremely useful in terms of providing context and character to the acoustic classes. One significant result is that in certain parts of the Study Area, there is a clear correlation between depth and the reflectivity of the seabed sediment type, and therefore by extension, there appears to be a clear correlation between depth and sediment texture. The seabed in deeper waters appears to exhibit evidence for finer sediments, although this requires further investigation (see Chapter 7). This is particularly obvious in the case of the deep channel in the north of the Study Area, the broad orientation and shape of which is clearly reflected in the classified image (see Figure 54).

## **4.3 Ground Truthing**

An important component of the seabed characterisation was the validation of the acoustic classes, and the calibration and refining of the defined landscape units by ground-truthing via direct sampling and visual observation.

### **4.3.1 Methodology**

#### **4.3.1.1 Direct Sediment Sampling**

The ground-truthing carried out to validate the sediment classification consisted of direct sampling of the seafloor sediment at locations throughout the Study Area. The locations were selected on the basis of the landscape units defined after the acoustic classification, and 57 sediment samples were collected using a Van Veen grab sampler, collecting on average four grabs at each sample site (Figure 58). It was not possible to get as many samples as ideally would have been desirable from the entire Study Area, especially from the south and east of the Study Area, due to the limited time that the survey team had available to go out on the boat, and the bad weather encountered during the survey. However, as far as possible, at least one sample was taken from every landscape unit that was defined by the acoustic classification.

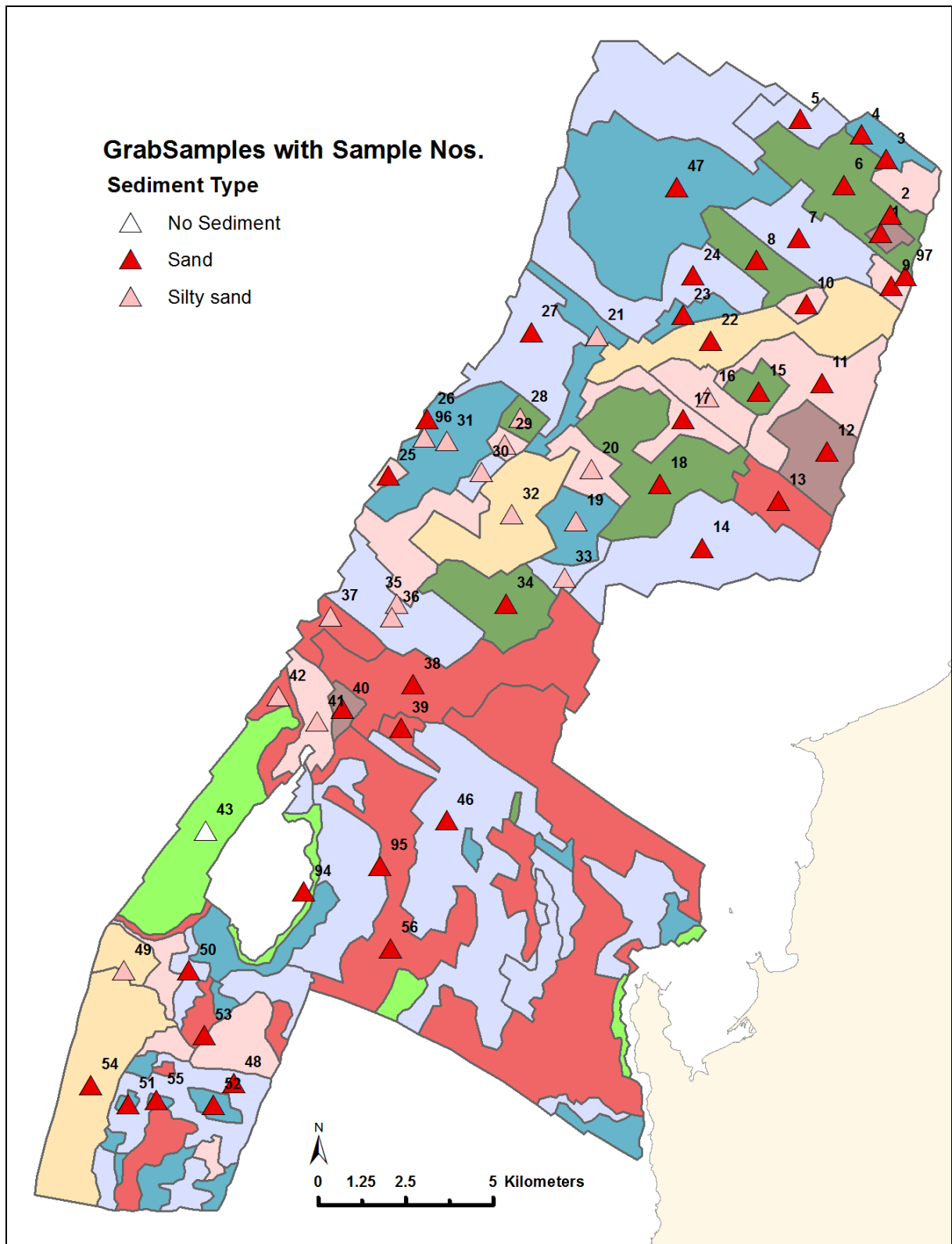


Figure 58 Grab samples overlaid on Initial Landscape Units.

The samples were subject to particle size analysis (granulometry) by specialists from the Environmental Studies Centre (ESC), at Qatar University. The samples were analysed using a laser diffraction particle size analyser (a Malvern Mastersizer). This method requires the samples to be dried, then mixed with distilled water, and passed through a laser beam which hits each particle in the sample. The machine measures the intensity of the light scattered, and uses this data to calculate the size of the particles, and therefore the percentage of each fraction (sand, silt or clay) in the sample (Blott and Pye, 2006). Graphs showing the particle size distribution, and tables showing the percentage volume of particle sizes were produced for each sample, and each sample was then allocated the appropriate sediment type, such as sand or silt, based on the statistics generated by the analysis. The complete granulometry report as provided by the ESC is included as Appendix 3. The results of the granulometry analysis were then used to enhance the acoustic classification analysis, and were integrated into the overall characterisation analysis.

In addition to the targeted grab sampling programme, a significant amount of pre-existing direct sampling data was also available as a result of extensive geotechnical investigations that were undertaken for the Qatar-Bahrain Causeway project. Several coring programmes were carried out in 2008 in order to provide information on the geology and the geotechnical properties of the potential causeway area. 24 exploratory boreholes were drilled along the Qatari side of the causeway route in July 2008 (Figure 59) Fugro Peninsular, 2008).

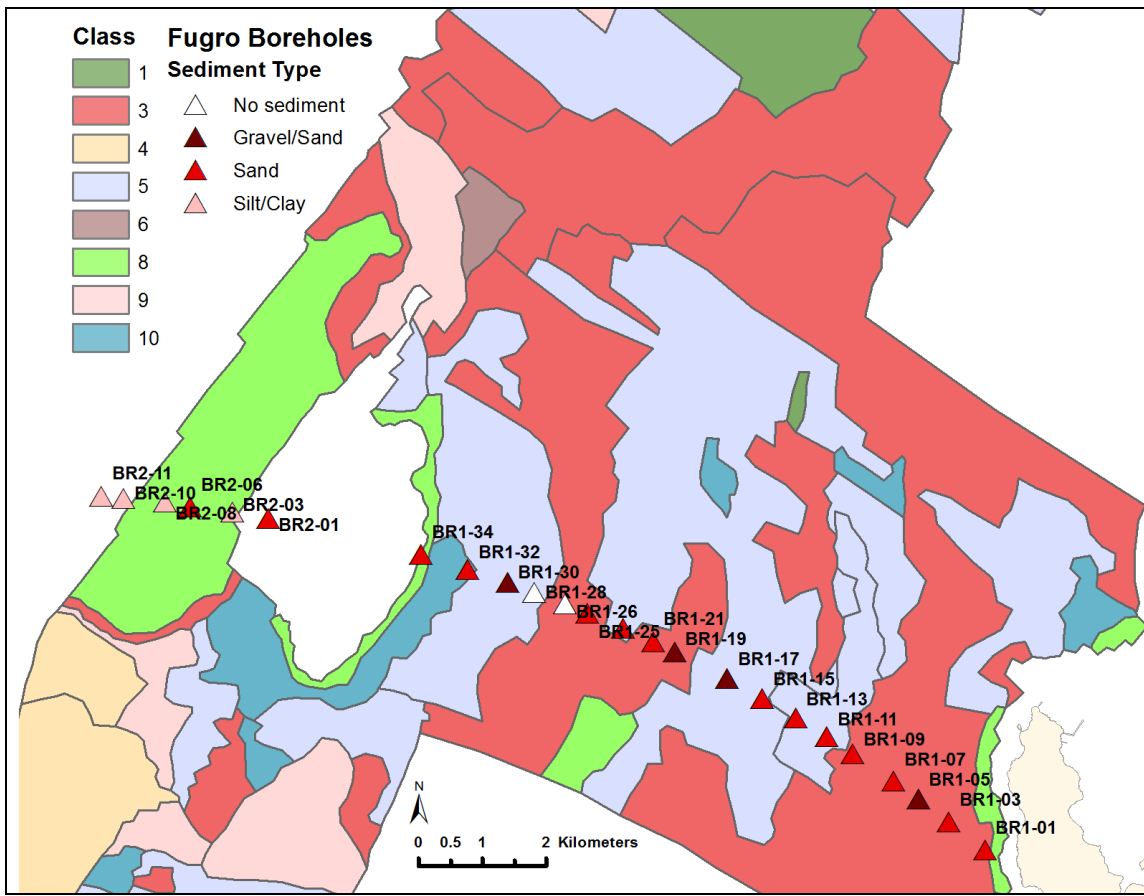


Figure 59 Exploratory boreholes drilled in 2008, overlain on Initial Landscape Units.

A separate coring programme, also carried out in July 2008. This focused on potential sand traps in Qatari waters, located by earlier geophysical survey, that could possibly be suitable for use as borrow areas for the construction of the causeway (Figures 60 and 61), and on areas of natural elevation which had the potential to be used as embankment areas for the causeway (Figure 62) (QBC Consortium, 2009a; 2009b). Two of the potential embankment areas lay in Qatari waters, and 12 boreholes were drilled on one of them, an area of coral heads close to on the Qit'at ash Shajarah reef. A vibrocoring sampling programme was undertaken to confirm (or otherwise) the presence of the sand traps and their suitability as borrow areas. Vibrocoring sampling uses a vibrating motor to liquefy the marine

sediments, which can then be retrieved as a core sample. The two areas in Qatari waters that were targeted for vibrocoring lay in the north and south of the Study Area, with 43 vibrocores taken from the area in the north (Figure 60) and 10 from the area in the south (Figure 61). Laboratory analysis was then carried out on the core samples. This has provided very useful information about the seafloor and sub-bottom sediment type at the coring locations, which can be used to inform the acoustic classification of sediments in those areas covered by the coring programme.

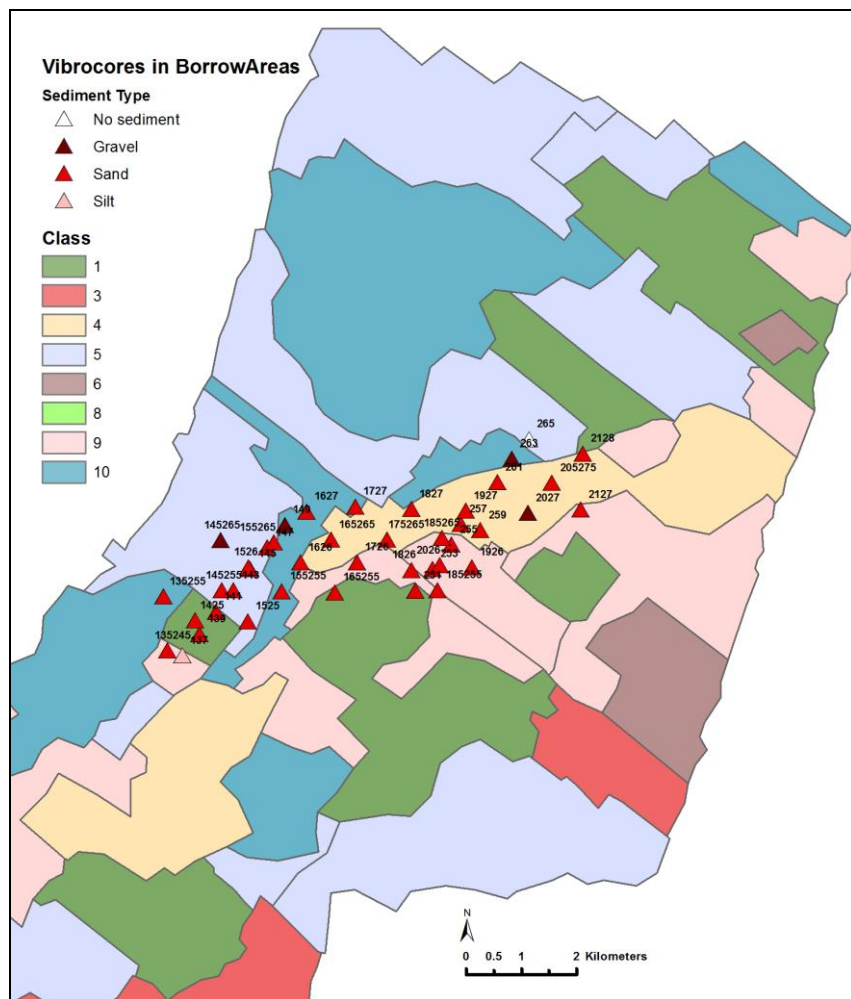


Figure 60 Vibrocores taken in north of the Study Area in 2009, overlaid on Initial Landscape Units.

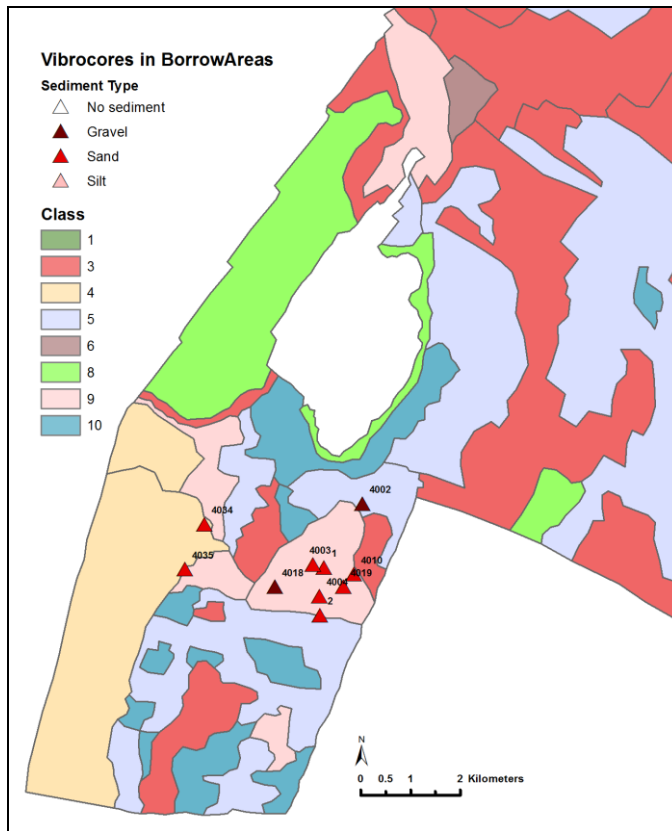


Figure 61 Vibrocores taken in south of the Study Area in 2009, overlaid on Initial Landscape Units.

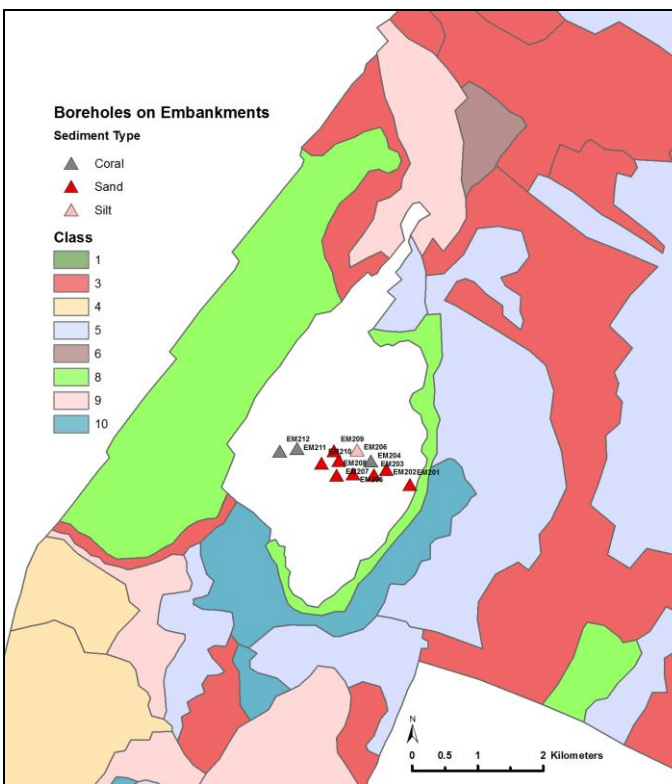


Figure 62 Boreholes drilled over the reef in 2009, overlaid on Initial Landscape Units.

#### **4.3.1.2 Video and Photography**

In addition to the grab samples, video and photographic ground-truthing data was also available for the Study Area. The main video data available was an underwater video-based analysis of the seabed that was carried out by a commercial company for the Qatar-Bahrain Causeway project (Creocean, 2008). This survey was focused on identifying, characterising and assessing the condition of the different biotopes in the area of the proposed causeway. A series of video transects were captured, in shallow areas (under 2m in depth) by divers and in deeper areas (over 2m) by an ROV towed behind a boat (Creocean, 2008, p.1.) The video footage that lay within the Qatar side of the proposed causeway area consisted of 13 transects of approximately 1km each in length, resulting in a total of 5 hours and 12 minutes of footage of the seabed. Although this survey was aimed at recording the seabed habitat, and the video transects only cover the central part of the Study Area, the video footage is very useful for providing a picture of the seabed in known locations that can then be compared with, and used to help clarify, the other data sets in the characterisation, including the sediment classification and the bathymetry.

Some additional photography and video footage was also captured during the grab sampling programme, but the area of seabed covered was very small and the visibility was generally quite poor, so this footage is not very useful either for providing broad-brush landscape information or for providing detailed sediment information for small areas.

## 4.3.2 Results

### 4.3.2.1 Direct Sediment Sampling

The distribution of the grab samples in relation to the different datasets can be seen in Figures 58, 63 and 64. The original aim was to try and cover as much of the Study Area as possible, and to try, within the limited resources available, to get samples from as many of the landscape units as possible. However, as explained previously, for practical reasons some areas were not able to be covered as well as others, for example there is much more limited coverage in Area 2 than any of the other areas.

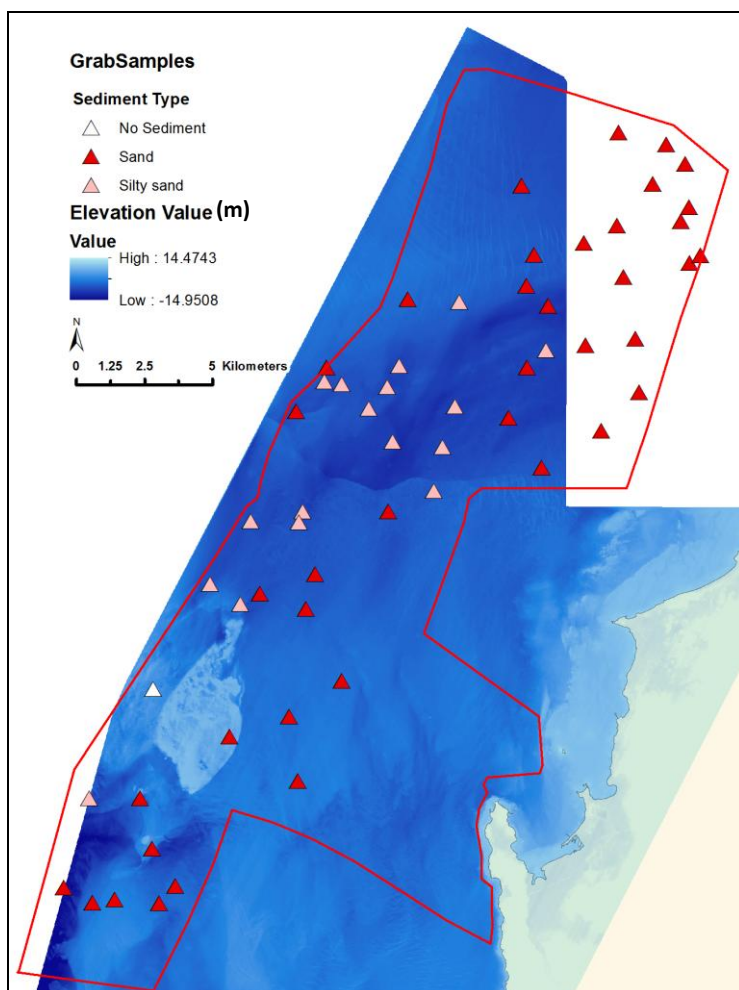


Figure 63 Grab sample locations overlain on the surface model.

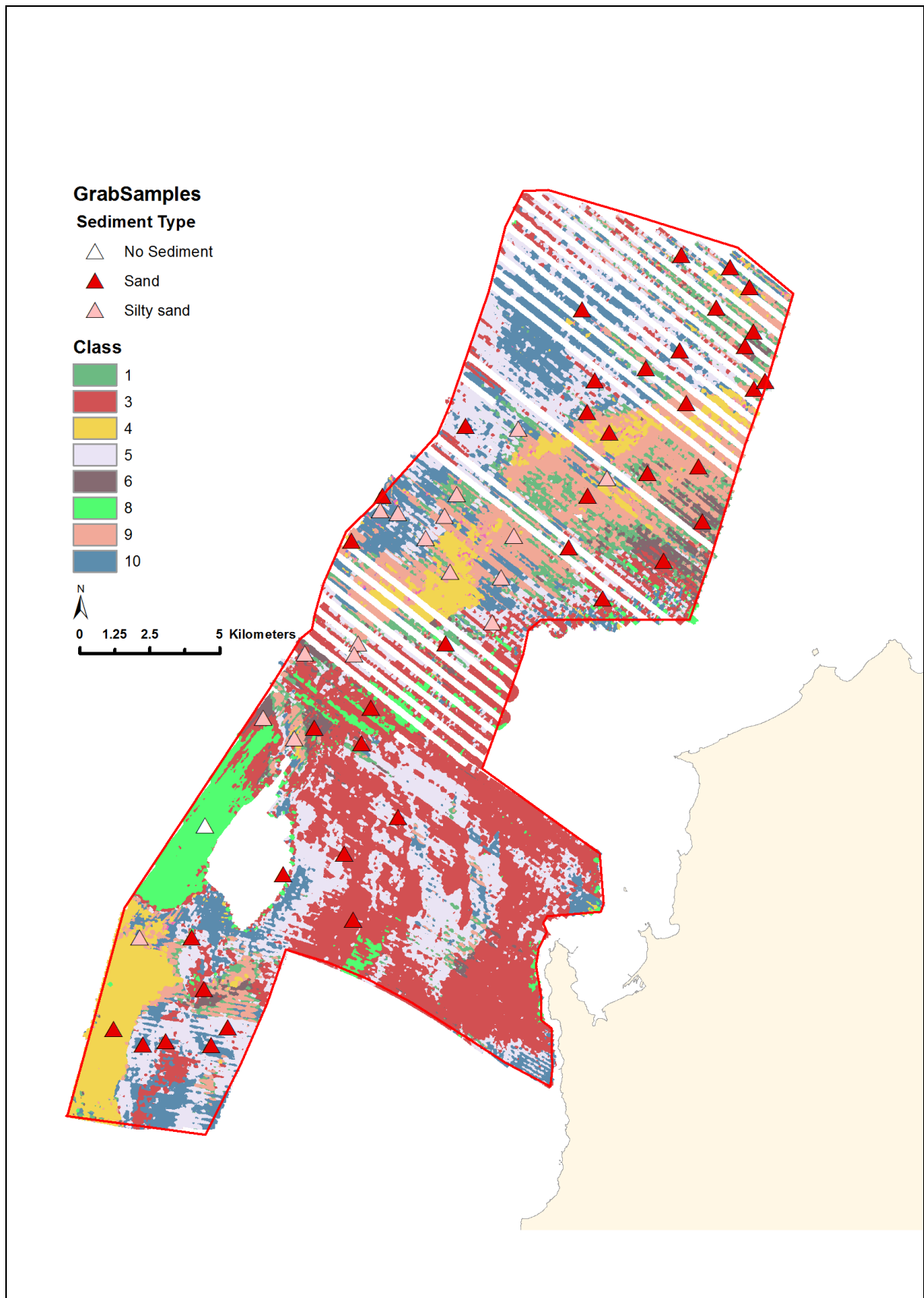


Figure 64 Grab sample locations overlain on the classified data.

Overall, the granulometry analysis appears to indicate that the grab samples were quite homogenous. Out of 57 samples collected, 40 were categorised as sand, and 17 as silty sand.

The samples, symbolised by sediment type (sand or silt) are shown in Figures 63 and 64, overlain over the surface model and the classified data respectively, and it can be seen from this that the distribution of silty sand appears to be concentrated to the northeast of the reef and in the western part of the deep channel in the north of the Study Area. 16 of the 17 samples that were categorised as silty sand are located in this area, with the other one (sample 49) located to the southwest of the reef. One of the samples (43) did not retrieve any sediment at all, as it was located on the coral to the west of the reef. Samples categorised as sand predominate in the northeast corner of the Study Area, and to the east and south of the reef.

The distribution of sediment types as derived from cores and boreholes from the various geotechnical surveys that were undertaken as part of the planning phase for the proposed causeway can be analysed in conjunction with the results of the grab sampling programme (Figures 65 and 66). It has to be borne in mind that the analysis is not a comparison of like with like, as unlike the cores and boreholes, the grab samples were solely surface samples, involving a relatively small amount of material. It is also worth emphasising when analysing the core and borehole results that these surveys were undertaken in targeted locations for specific geotechnical purposes, so the distribution plots will display an inherent bias relating to the purpose of the surveys. Where the marine sediment type changed with depth, the boreholes and

vibrocores have been symbolised in the distribution plots based on the uppermost sediment type.

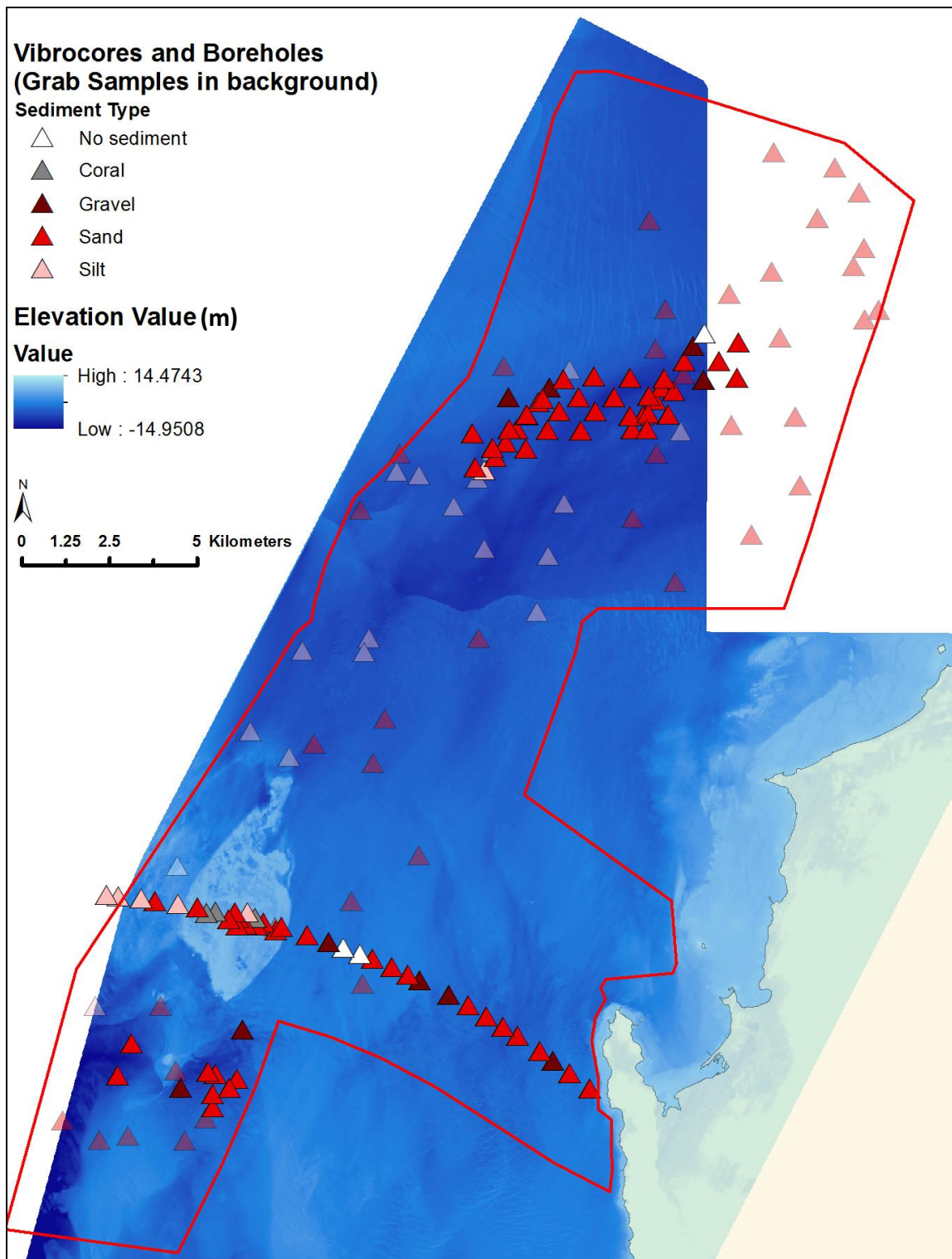


Figure 65 Vibrocores and boreholes overlaid on the surface model (grab samples are visible in the background).

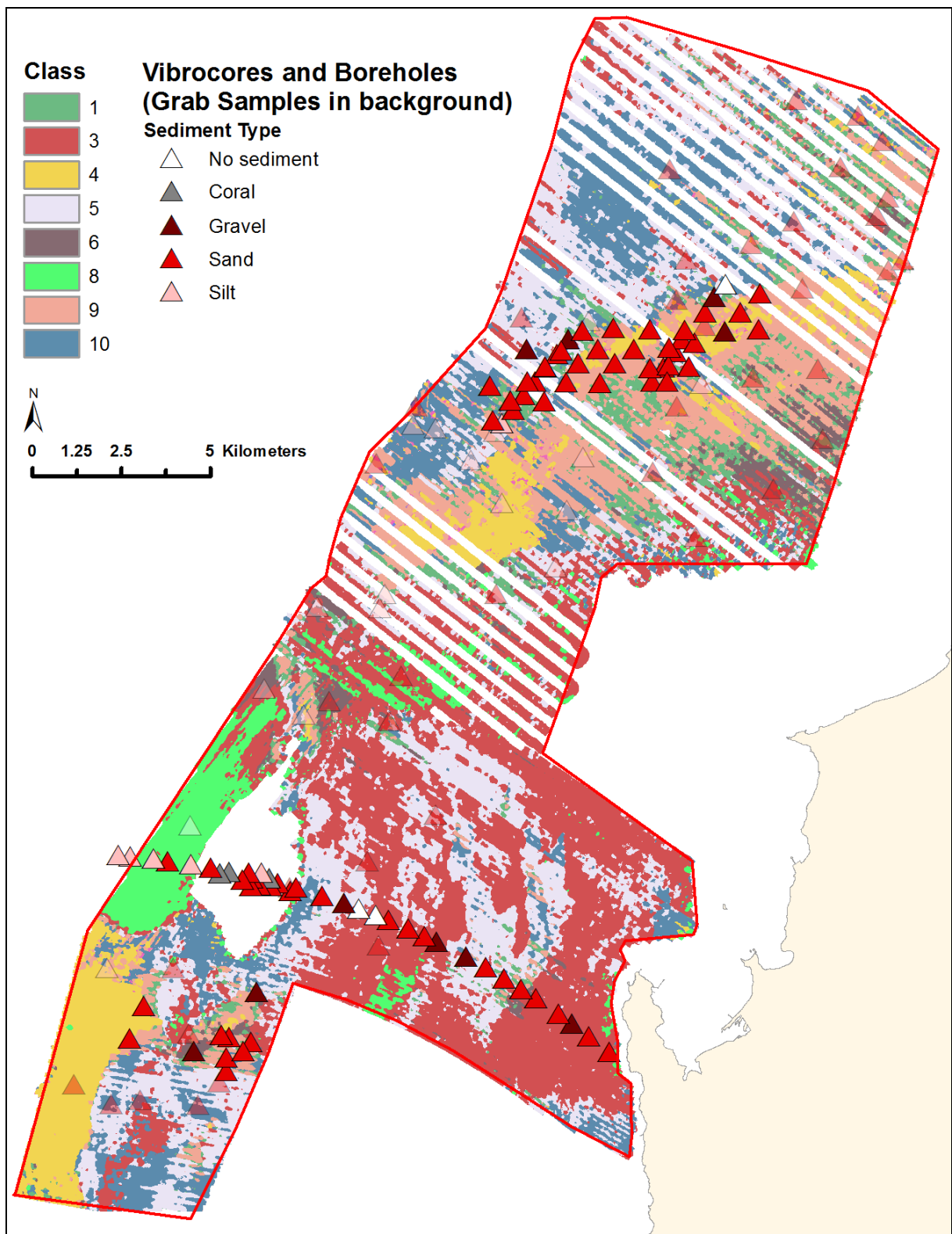


Figure 66 Vibrocores and boreholes overlaid on the classified data (grab samples are visible in the background).

The 43 vibrocores in the north of Area 1 were taken specifically in an area that had been previously identified as having high potential for sand deposits, as the aim of the survey was to confirm locations that could be used as borrow areas for the causeway construction. The distribution plot of these vibrocores, as expected, therefore, shows a heavy concentration of sand in the survey area. The distribution plot shows a band of cores categorised as sand along the north of the deep channel, with a few classed as gravel, whereas the grab samples indicate silty sand in the areas surrounding the vibrocores. This may be a genuine change in the sediment type rather than just a result of the different techniques used, as the grab sample distribution does seem to indicate that the sediments in the area along the north of the channel are coarser. The logs from the vibrocores indicate that the sand deposits in the survey area are thick, mainly over 1m, but extending for more than 3.5 m in some places.

Ten vibrocores were also taken in the area to the south of the reef, for the same purpose of confirming the location of sand deposits for borrow areas. Again, as expected, they show thick sand deposits occurring, which is also consistent with the distribution of the grab samples. The sand survey area coincides with two deeper areas on either side of the submerged reef area that are visible in the surface model. As in the north, the survey areas again correlate with areas that have been classified as yellow and salmon (classes 4 and 9 respectively) in the acoustic classification.

Boreholes from the centre of the Study Area were taken specifically for the purpose of studying proposed embankment areas for the causeway. They are all located on

the reef, as that is the highest land in the Study Area, and therefore they can't provide much useful information about acoustic classes, as there was no sidescan data for the reef area. Apart from one silt sample, the rest are all composed of sand or coral.

The borehole survey carried out along the route line of the proposed causeway in the centre of the Study Area encountered marine sediments from seabed level to a maximum depth of 6m within the Study Area. (Fugro Peninsular, 2008, p.10-11). Marine sediments were generally thicker further westwards, away from the coast and towards the reef. The deposits were characterised by silty fine and medium sand or sandy gravel, locally with thin to thick beds of sandy silt/clay, variably underlain by shelly calcarenite (caprock). The boreholes appear to show a differentiation of sediment texture along the route. The boreholes taken from the area stretching from the coastline west of the Ras 'Ushayriq peninsula to the reef are composed of sand and gravel, whereas most of those taken from the area to the west of the reef are composed of finer, more silty sediments. There were very few grab samples taken from this area so it is difficult to compare them with the borehole data, but the three grab samples that were taken to the east of the reef (46, 56 and 95) were all categorised as sand.

#### 4.3.2.2 Video Transects

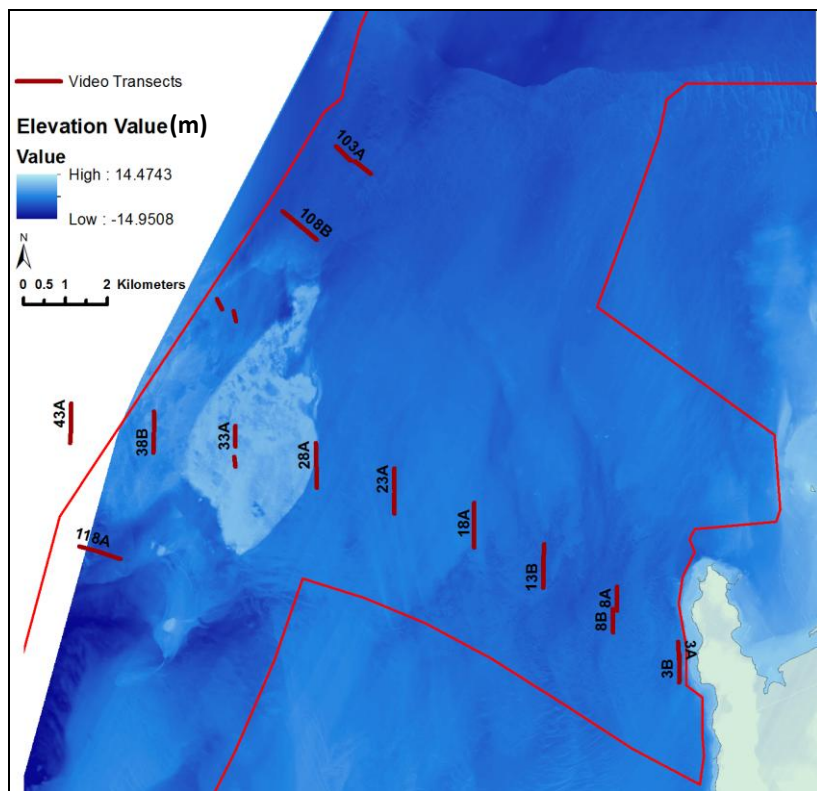


Figure 67 Video transects overlain on surface model.

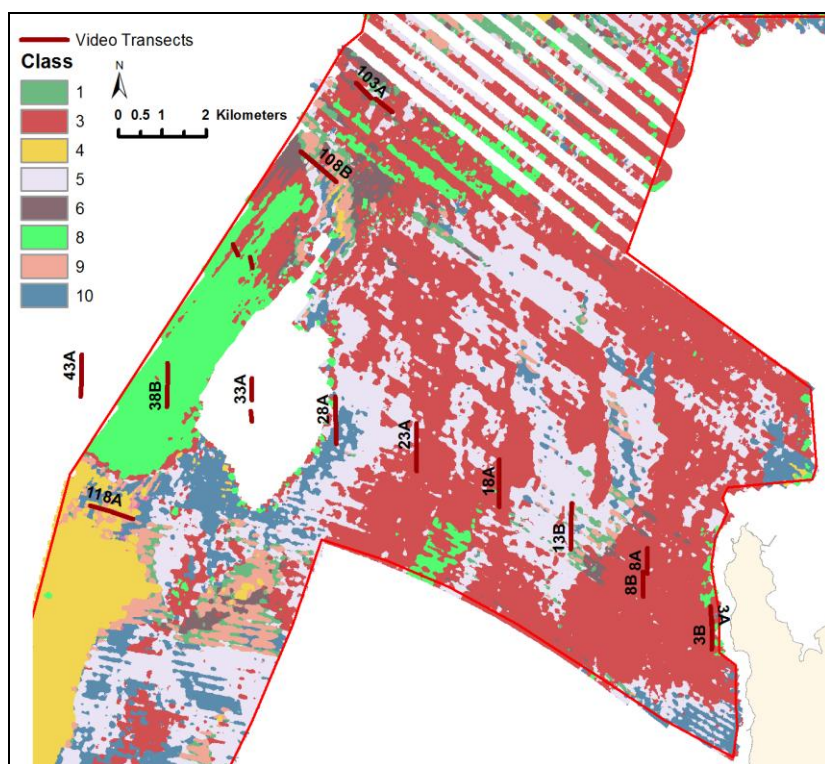


Figure 68 Video transects overlain on the classified data.

The seabed habitat video survey provided additional optical ground-truthing information (Figures 67 and 68). This was concentrated along the route of the causeway, and served as a useful addition to the borehole data that was obtained along the causeway route. A summary of the seabed descriptions from the video transects is provided in Table 3.

Table 3: Seabed descriptions summarised from the video survey information provided by Creocean

<b>Transect No.</b>	<b>Summary of seabed character</b>	<b>Predominant Acoustic Class</b>	<b>Features visible in Surface Model</b>
3a	Flat, sandy bottom, hard substrate visible beneath sand layer	Class 3 (red)	
3b	Sand covering hard substrate, some gravels	Class 3 (red)	
8a	Flat, sandy bottom, ripple marks	Class 3 (red)	Linear features
8b	Flat, sandy bottom, hard substrate visible underneath, some gravels, some sand banks/ripples	Class 3 (red)	Linear features
13a	Sand and gravels, hard substrate visible underneath, sand ripples	Class 5 (lilac)	Ridges
13b	Coral/rock on hard substrate, covered in sand, sand banks	Class 5 (lilac)	Ridges
18a	Sand and gravels	Class 3 (red)	
18b	Sand bank, gravels, some coral	Class 3 (red)	
23a	Sand, rock or coral debris	Class 5 (lilac)	
23b	Sand, calcareous debris	Class 3 (red)	
28a	Sand bank, coral, hard calcareous bottom	Class 8 (lime)	Edge of reef

<b>Transect No.</b>	<b>Summary of seabed character</b>	<b>Predominant Acoustic Class</b>	<b>Features visible in Surface Model</b>
28b	Gravels, sand banks, coral, hard substrate	Class 10 (blue)	Edge of reef
33a	Reef	No data	Reef
33b	Reef	No data	Reef
38a	Reef	Class 8 (lime)	Reef
38b	Reef	Class 8 (lime)	Reef
103a	Sand, seagrass bed	Class 3 (red)	
103b	Sand, seagrass bed	Class 3 (red)	
108a	Sand, coral	Mixed	Edge of reef
108b	Sand, coral, undulating	Mixed	Edge of reef
113a	Coral, some sand	Class 8 (lime)	Reef
113b	Coral, some sand	Class 8 (lime)	Reef
118a	Flat, sandy bottom, featureless	Class 4 (yellow) Class 9 (salmon)	
118b	Flat, sandy bottom, few gravels, featureless	Class 4 (yellow) Class 9 (salmon)	

The video transects indicate that the seabed west of the Ras ‘Ushayriq peninsula largely consists of a flat sandy bottom, with hard substrate often visible, and some ripple marks and sand banks. Moving westwards, coral and rocky debris appear in more and more dense concentrations until the reef itself is reached. Away from the reef to the southwest, the seabed appears to be flat, sandy and featureless, whilst to the north it is sandy with seagrass beds.

### **4.3.3 Discussion**

The homogeneity of the grab samples has meant that the distribution of grab samples alone is not particularly informative in terms of clarifying the classes that were generated by the acoustic classification, as there is not enough differentiation between the samples to define patterns. Also, it is clear that all of the direct sediment samples display a high sand content. However, integrated analysis of all of the ground-truthing information together with the acoustic classification and the surface model has provided considerable illumination on the character of certain parts of the Study Area. Figure 69 shows a percentage breakdown of sediment types for each class, derived from the different types of ground-truthing data obtained - boreholes, vibrocores, grab samples and video transects. The predominant sediment type within each video transect was allocated to the centre point of each transect location, to align the data with the direct sample locations.

In the central part of the Study Area, a comparison of the results from the boreholes across the causeway route to the surface model and the classified acoustic data shows that the area to the east of the reef, appears to be relatively homogenous in terms of depth and topographic features visible in the surface model, and also in terms of acoustic classes. The classified acoustic data in this area is predominantly class 3 (red), which, as mentioned earlier, roughly corresponded in the mosaic data to areas of brighter reflective material forming possible sand ridges. The borehole logs of sand and gravel, and occasionally calcarenite (caprock) in this area, all of which would be likely to be brighter reflectors than silty sand, would seem to support

this interpretation, and the comparison graph (Figure 69) shows that this class has the highest proportion of gravel samples out of all the classes.

The identification of the vibrocoring survey area in the north of the Study Area as a potential sand trap is significant in itself, in that it shows a correlation with the area of the deep channel identified in the surface model. In addition, both of the potential sand trap areas in the north and south of the Study Area also correlate with areas that have been classified as yellow and salmon (classes 4 and 9 respectively), probably representing finer sediment, in the acoustic classification. The comparison graph (Figure 69) shows that Class 4 has the highest proportion of silt samples (apart from the reef), and Class 9 has the smallest proportion of gravel samples apart from Class 1 (the latter of which was also interpreted from the original classification as possibly representing areas of finer sediment). As has already been noted in the integrated analysis of the surface model and the classified data, there seems to be a clear correlation between Classes 4 and 9 and areas of deeper sea. The sediment sampling evidence has shown that these areas can also be correlated with areas of thick sand/silty sand deposits. The single silty sand sample in the southwest of the Study Area, lies in an area of deeper water that is coincident with the large area classified as Class 4 (yellow), suggesting that it could represent a sediment-filled basin. These results show a clear relationship between sonar reflectivity and seabed depth within the Study Area, indicating that finer sediments are occurring in the deeper areas. This is a significant finding as both the surface model and the sediment samples provide independent evidence for the type of sediment and character of the seabed that is represented by classes 4 and 9.

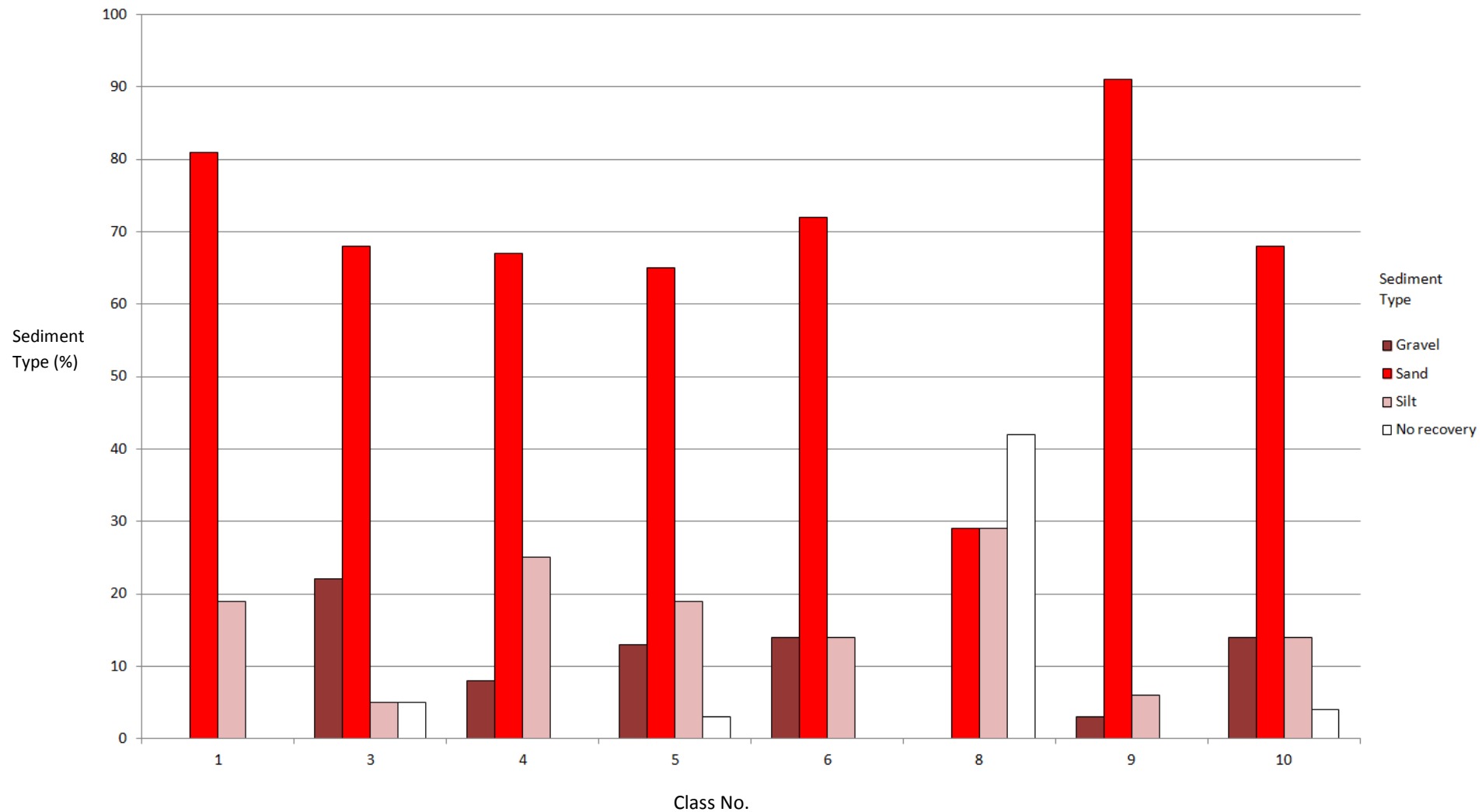


Figure 69 Graph displaying sediment types for each class as derived from ground truthing data (expressed as a percentage of the total number of samples/observations recorded for each class).

The gravels identified in the southwest-northeast aligned deep channel in the north of the Study Area could be related to the coarse-grained sands and gravels identified in the boreholes to the west of the Ras' Ushayriq Peninsula. These may be part of the Hofuf Formation sands and gravels that are found elsewhere around the western side of Qatar, which were continental gravels from Saudi Arabia, laid down during the Miocene (Cavalier, 1970, p.32). Sedimentological evidence from the western region of Abu Dhabi has demonstrated that there was a large river system in the area in the late Miocene (Hill et al., 2012, p.28). The presence of gravels in the Study Area, both in the deep channel in the north, and also in the area to the east of the reef, supports the theory that a former river bed is present in these parts of the Study Area, possibly dating from the Miocene. It is possible that this channel was interrupted by uplift from the Bahrain anticline, which could explain why it is so much more distinct in the north of the Study Area than in the south.

The video footage has confirmed the overall character of the seabed in the area of the causeway, and as far as possible the observations have broadly correlated with the classes generated by the acoustic classification procedure. The interpretation of Class 3 as representing a relatively highly reflective seabed sediment type is supported, in that the seabed character provided by the video transects appears to be mostly sand with visible rock (caprock?) substrate.

However, the video footage has proved to be of limited use for distinguishing fine detail, as the visibility is not very good in some of the transects, and they were filmed relatively quickly, so it is not easy to see the sediment types in detail and establish

whether the seabed sediments are coarse or fine-grained. There is not sufficient scope or detail in the video footage to be able to draw out some of the differences in sediment type that have been identified through the acoustic classification. For example, there appears to be no great difference between the observations in Transects 8A and 8B, which are predominantly Class 3, and the observations in Transects 13A and 13B, which are predominantly Class 5. The comparison graph (Figure 69) shows proportionately more gravel samples from Class 3, and more silt samples from Class 5.

Also, the transects were not as useful as hoped for in clarifying some of the larger-scale landscape features that were visible in the surface model and the mosaic of the sidescan sonar data, as the field of vision is too narrow. However, it has been possible to confirm from the video footage that what had been tentatively interpreted from the bathymetry as possible linear reef structures to the west of the Ras 'Ushayriq peninsula are actually sand ripples. More panoramic views of the seabed, which could be stitched together to create photo mosaics of large areas would be of great benefit for this type of landscape-scale investigation.

## **CHAPTER 5: SECONDARY CHARACTERISATION**

The following chapter describes the methodology and results of the secondary characterisation. This comprises two different strands - the identification of geophysical anomalies within the sidescan sonar data, and the clarification of geophysical signatures through diver inspection and high-resolution geophysical survey. Each strand has three sections consisting of the detailed methodology, the results and a discussion.

### **5.1. Identification of Geophysical Anomalies**

#### **5.1.1 Methodology**

A comprehensive and systematic analysis of the entire sidescan sonar dataset for the Qatar-Bahrain Causeway was undertaken in order to identify all geophysical anomalies that may represent either the remains of shipwrecks, or potential locations for archaeological sites and/or palaeoenvironmental remains. As mentioned previously (see Chapter 2), a limited analysis of selected geophysical anomalies from the dataset was carried out in 2010 (Cuttler et al., 2011a), but the dataset had never been systematically assessed in its entirety for archaeological purposes. The files of data from the parallel tracks covered by the survey boat, obtained from the survey company in xtf format, were batch-imported into a specialist software package called SonarWiz 5, produced by Chesapeake Technology Inc. This is a sidescan and sub-bottom sonar mapping software that is particularly useful for creating mosaic images

of the sonar data, and for the logging of anomalies (contacts) detected in the data. These files were imported, batch processed and stitched together to create a mosaic image of the seabed. Thresholding was set at the import stage, and following import, gain processing was applied to all files. The processing was designed to create the best possible image for aiding visual interpretation of the data. Testing was carried out on a subset of the data in order to ascertain the optimum settings for viewing the data without losing any of the information that the data contained. The testing established that the best results were obtained by using the Empirical Gain Normalization (EGN) function, set to an intensity of 41. The settings and parameters used in the final import and processing are included in Appendix 4.

Bottom tracking had already been carried out on the data, but this was checked individually before commencing the logging of anomalies for each file, and any necessary adjustments were made manually. Every file in the dataset was then examined in the digitizing view in Sonarwiz and any anomalies identified were recorded using the contact manager. Recording consisted of logging the coordinates of each anomaly, recording the measurements (length and width, and also shadow and scour where appropriate), and writing an objective, non-interpretational description. Finally, two attributes were systematically logged for each anomaly, a preliminary interpretation (e.g. debris, buried feature, depression, seabed scar) and a confidence level for likely anthropogenic origin. All of the anomalies were graded with a confidence level of either high, medium or unknown, apart from those that had been ground-truthed during the diver surveys in 2011, which were graded as 'ground-truthed'.

All anomalies were initially recorded without reference to the previous work carried out in 2010 (Cuttler et al., 2011a), or to any other datasets. This was done in order to be as objective and consistent as possible, so that it was possible to test how useful the recording of anomalies was as a technique for deriving meaningful data at a landscape level. The results of the diver inspections carried out in 2011 (Al-Naimi et al., 2012) were subsequently used to refine the interpretation and confidence levels. The criteria for recording anomalies were not the conventional criteria normally used for commercial surveys, where the aim is generally to record potential obstructions on the seabed. In this study, any area that looked slightly different to the surrounding seabed was logged as an anomaly. Anomalies were graded as high confidence where they appeared to be similar in character to those anomalies known from the 2011 work to be anthropogenic. Anomalies were graded as medium confidence where there were reflectors showing in the data, but the signature was less well-defined, presumably because of the nature of the material or feature causing the anomaly, or because the anomaly lay at the far edges of the swath range and was therefore more difficult to resolve. Any other type of anomaly was recorded as unknown confidence, and these included any areas of seabed that looked different from the surrounding area. This grade covered more ephemeral, poorly-defined anomalies.

Specifically, anomalies were logged if they could possibly indicate debris of anthropogenic origin, if they could indicate buried structures or features such as sediment mounds and sand waves, or indicate geological features or other natural locations that may have archaeological or palaeoenvironmental potential, such as

depressions. Sometimes it was not possible to categorise an anomaly other than that it looked different to the surrounding seabed, in which case it was logged as 'unclassified'. The list of terms used to categorise the anomalies is provided in Table 4 below.

Table 4: List of terms used for initial categorisation of anomalies.

Categorisation Term
Buried Features
Debris
Depression
Disturbed Seabed
Hole
Linear Debris
Mound
Natural Location
Partially Buried Object
Seabed Scar
Sediment Accumulation
Unclassified

It should be noted that high confidence does not necessarily mean high archaeological potential, as the diver inspections in 2011 showed that the most obviously anthropogenic anomalies were most likely to be of recent origin, largely caused by dumping of cars, tyres and other objects to create artificial fish reefs (Al-Naimi et al., 2012). In fact, it was considered that the anomalies that were classified as unknown confidence may be of greater archaeological potential. It is these types of more ephemeral anomaly that were perceived to be good candidates for further

research, as so little was currently known about their character or archaeological potential. As a result of this recording policy, a great number of anomalies were identified - 795 in Area 1, 184 in Area 2/3, and 118 in Area 4. All of the recorded anomalies were reviewed, and a representative range was selected to be further clarified and validated via the analysis of other data sets, including bathymetry, and through further survey, including high resolution geophysical survey and diver inspection. The complete register of all recorded anomalies is provided in Appendix 5 and the results of the analysis are presented and discussed below.

## **5.1.2 Results**

### **5.1.2.1 Geophysical Anomalies**

As discussed in the methodology section, the criteria for recording anomalies was to log any areas that looked slightly different to the surrounding area, and accordingly, a complete distribution plot of all recorded anomalies is shown in Figure 70. Most of these anomalies do not have a confirmed interpretation, but this figure shows the initial distribution of where anomalies were visible in the data. It is immediately clear that there is a high concentration in the northwest of the Study Area (the western part of Area 1), and a much sparser distribution in the east of the Study Area (Area 2). The gap in the southwest is due to the presence of the reef, where no sidescan sonar data was available.

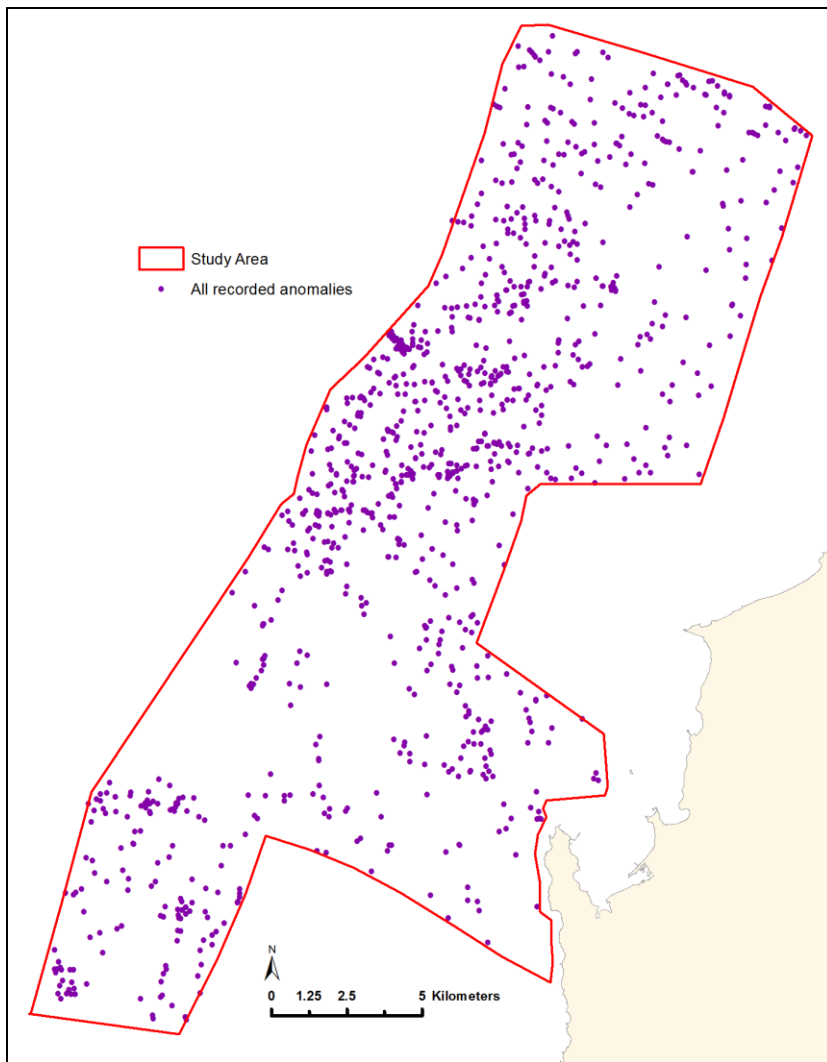


Figure 70 Distribution of all recorded anomalies within the Study Area.

Figure 71 shows the distribution of all anomalies that were categorised as being possible debris (green dots), and therefore of potential anthropogenic origin. The differential distribution of these is quite marked - 196 of these were in Area1, 16 were in Area 2/3 and only 2 in Area 4. Within Area 1, there is a clear concentration in the west of the area. All of the debris anomalies in Areas 2/3 and 4 were classed as medium confidence. In Area 1, 112 were classed as medium confidence and 84 were classed as high confidence. In addition to these, 13 anomalies in Area 1 (the pink crosses) were also logged as debris, and when cross-checked against the work that

was done in 2011 (Cuttler et al., 2011a), were found to have been diver-inspected, and all proved to be dumped cars and/or tyres and old fishing equipment.

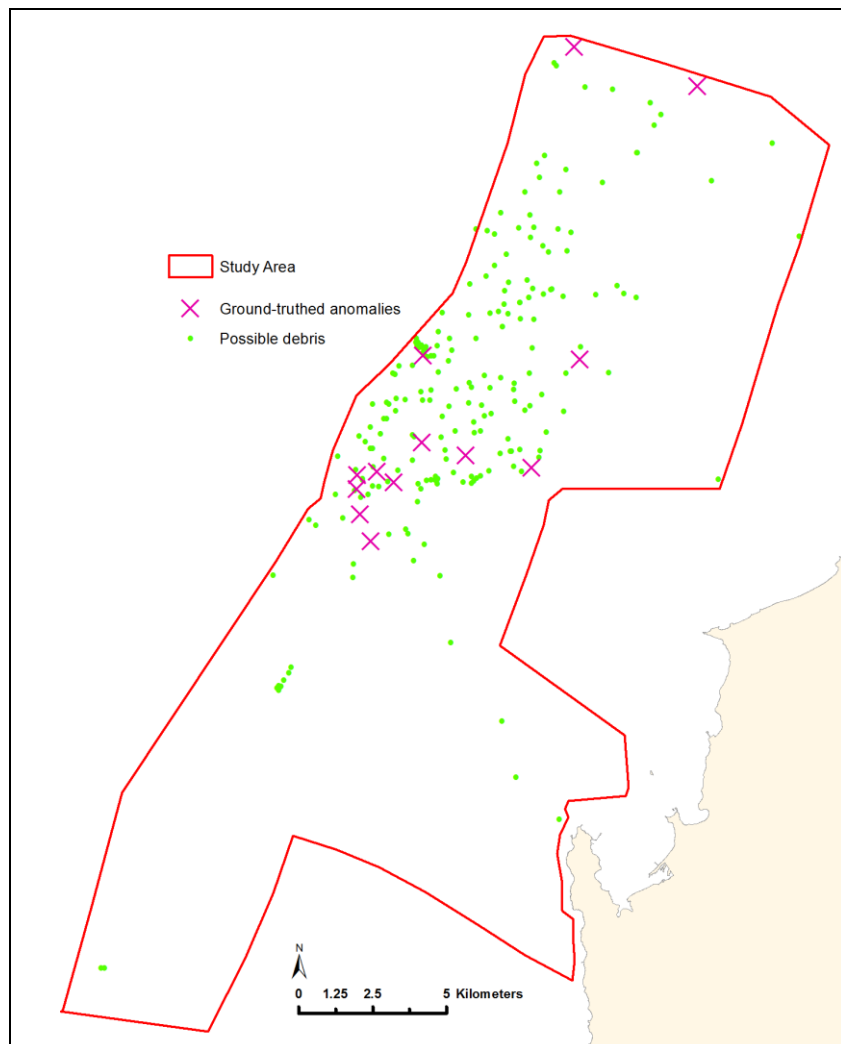


Figure 71 Anomalies interpreted as potential debris, and proven to be debris from ground-truthing.

Most of the high confidence anomalies showed up very clearly as modern debris during the logging of anomalies. When compared to those that had been ground-truthed through diver inspection, the signatures were very characteristic. They consisted of one or more very bright reflectors (the debris), usually quite sharply outlined, with clear acoustic shadows, often lying in a darker area of seabed

representing scouring around the debris, and occasionally including brighter patches indicating areas of coarse sediment build-up around the debris (Figure 72).

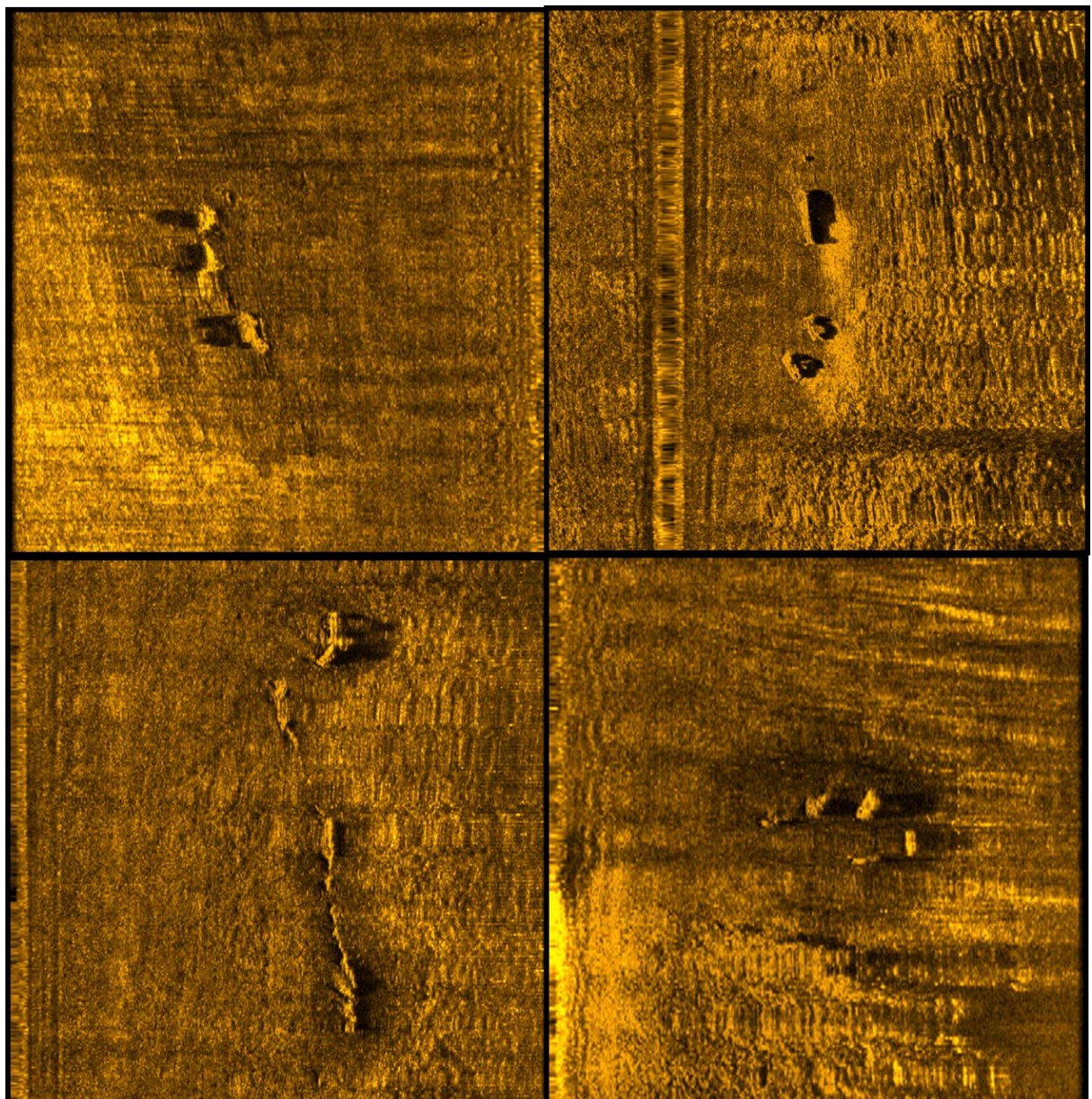


Figure 72 Examples of high-confidence anomalies in Area 1: Modern debris relating to artificial reefs (cars, tyres etc). Clockwise starting from the top left corner: QBC\_Q10126, QBC\_Q10270, QBC\_Q10334, QBC\_Q10902. (Each image depicts an area measuring 100m x 100m.)

This type of anomaly occasionally generated a slightly different signature when located at the outer range of the swath, where the sonar signal was more attenuated. In these cases, the bright reflectors were less sharply defined, did not always display clear shadows, and usually appeared in a dark area of seabed. However, there were a few survey lines running perpendicular to, and overlapping, the main body of survey lines through Area 1, and where anomalies could be cross-referenced with other survey lines in which they didn't lie in the outer range, it was possible to clarify the signature type and apply it to other similar anomalies. Figure 73 shows the same anomaly visible in different survey lines. The image on the right shows the anomaly lying at the outer range of the swath, where it is brighter but less clearly defined than in the image on the left, where the same anomaly lies in the centre of the swath.

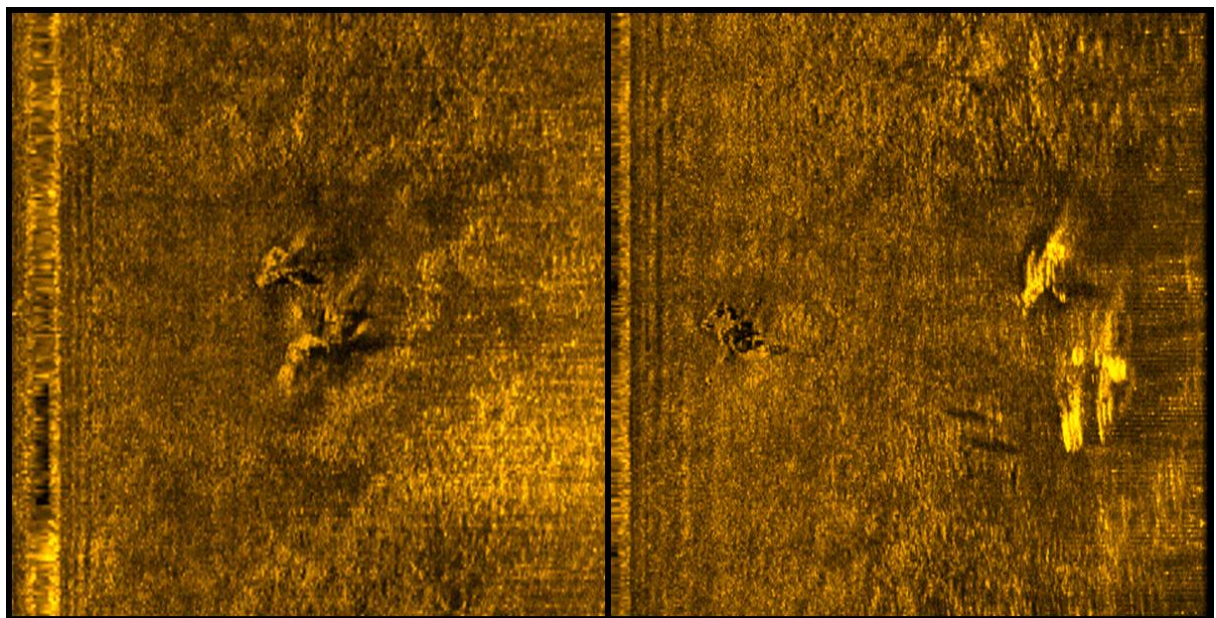


Figure 73 The same anomaly (QBC\_Q10815) visible in different survey lines: Modern debris relating to artificial reefs (each image depicts an area measuring 100m x 100m).

Anomalies like these were not generally selected for further study, as it was clear from the ground-truthing work carried out in 2011 that they represent the dumping of

modern debris, usually cars and tyres, probably for the creation of artificial reefs (Al-Naimi et al., 2012).

Figure 74 shows the distribution of anomalies logged as possible depressions. This was a very tentative classification, as it was not known how depressions may show up in sidescan sonar data in this area, as no one has ever looked for them here before. Features were classed as possible depressions if they displayed what appeared to be finer seabed material within areas of surrounding coarser material, the implication being that this fine material may be sediment that has accumulated in hollows or depressions. It is possible that these features may simply represent differential sediment accumulation, but if they are sediment-filled depressions, they could have the potential to contain palaeoenvironmental remains or buried structures and features, and therefore they were recorded as possible depressions so that they could be easily selected for further investigation. Depressions may also represent locations that were once favourable for human settlement. Some of these anomalies are quite large features, ranging in size from around 20m to over 100m in length (see Figure 75).

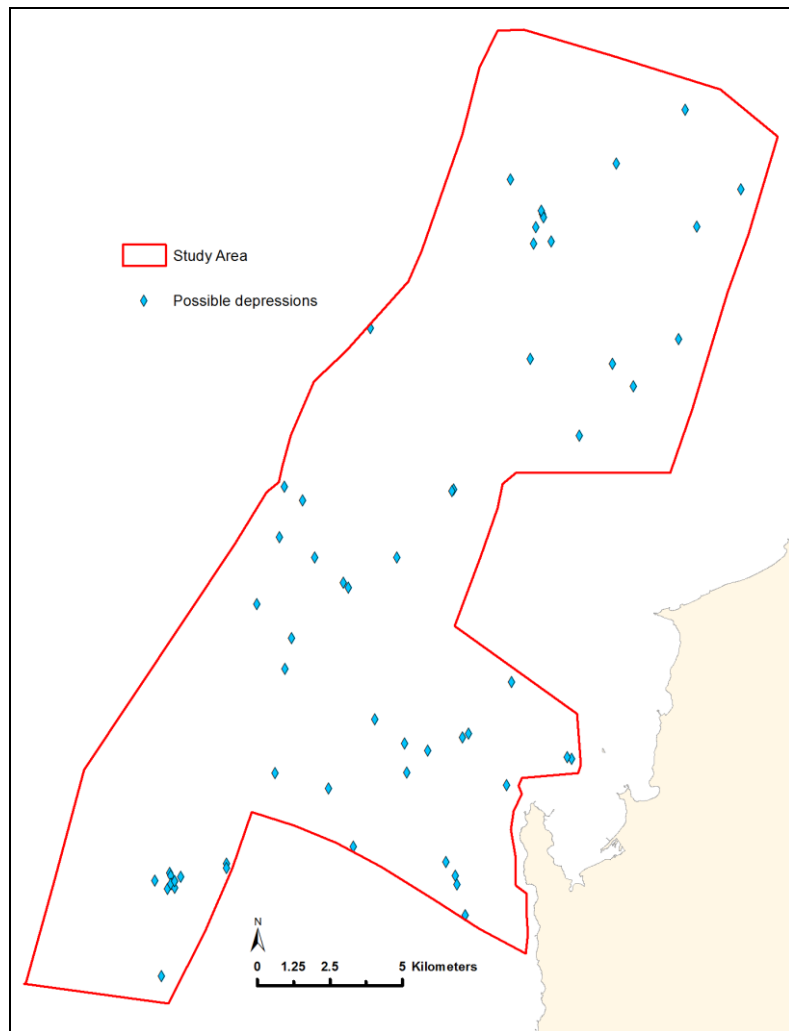


Figure 745 Distribution of anomalies that are possibly depressions.

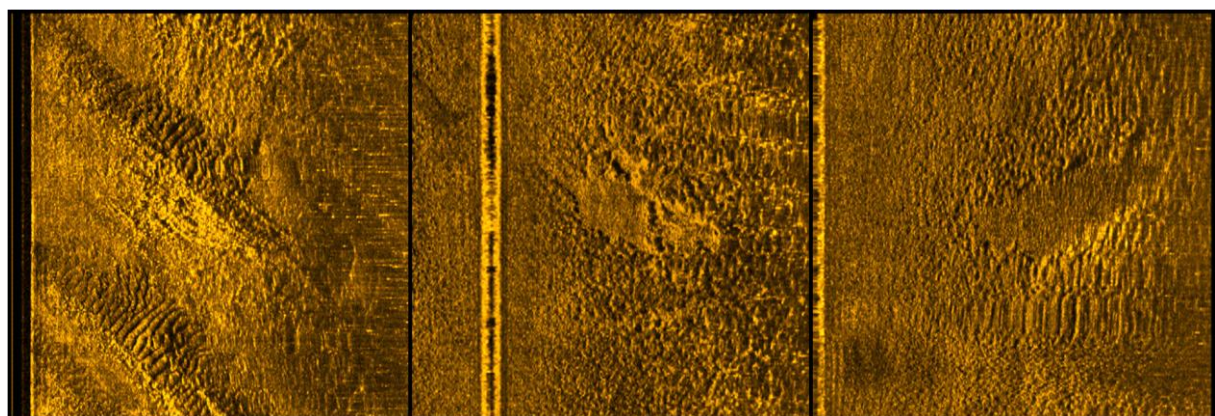


Figure 75 A selection of anomalies that were logged as possible depressions. From left to right: QBC\_Q20071, QBC\_Q40064, QBC\_Q40119 (each image depicts an area measuring 100m x 100m).

A range of different types of anomaly were selected for more detailed examination, either by cross-referencing with other datasets, such as bathymetry, or by higher resolution geophysics survey or diver inspection. The range was selected in order to try and clarify the signatures of types of anomaly that appeared different to those that had been investigated by the work carried out in 2011. As mentioned earlier, anomalies representing obvious modern car-related debris were avoided, but some anomalies classified as possible debris were selected for further study in case they could represent debris from shipwrecks. Other types of anomaly selected included locations of possible buried features/objects, and possible depressions, hollows, mounds, sediment accumulations and other natural features that may represent topographic locations of potential interest for human settlement. Figures 76 to 81 show representative examples of the types of anomaly that were selected for further study, and the full list of selected anomalies is provided in Table 5.

Table 5: List of anomalies selected for more detailed examination.

Contact No.	Latitude	Longitude	Confidence Level	Preliminary Interpretation
QBC_Q10001	26.1641788483	51.0675086975	High Confidence	Debris
QBC_Q10008	26.1921634674	51.0260429382	Medium Confidence	Buried Feature?
QBC_Q10027	26.1201820374	50.9740638733	Unknown Confidence	Buried Feature?
QBC_Q10098	26.1222991943	50.9296150208	High Confidence	Debris
QBC_Q10099	26.1220684052	50.9299507141	High Confidence	Debris
QBC_Q10126	26.1277561188	50.9390869141	Medium Confidence	Buried Feature?
QBC_Q10159	26.0871925354	51.0052795410	Medium Confidence	Buried Feature?
QBC_Q10173	26.0903301239	51.0237998962	Unknown Confidence	Natural Location
QBC_Q10176	26.0943851471	51.0183601379	Medium Confidence	Natural Location
QBC_Q10195	26.0978145599	51.0285263062	Medium Confidence	Buried Feature
QBC_Q10202	26.1259479523	50.9980239868	Medium Confidence	Natural Location
QBC_Q10235	26.0509109497	50.9292297363	Unknown Confidence	Depression?
QBC_Q10345	26.0795593262	50.9499397278	Unknown Confidence	Natural Location
QBC_Q10362	26.0913200378	50.9708328247	High Confidence	Buried Feature?
QBC_Q10376	26.0902423859	50.9799804688	Unknown Confidence	Natural Location
QBC_Q10574	26.1638336182	50.9941406250	Unknown Confidence	Depression?
QBC_Q10582	26.1781387329	50.9776573181	Unknown Confidence	Buried Feature?
QBC_Q10634	26.1872463226	51.0019569397	Medium Confidence	Partially Buried Objects?
QBC_Q10645	26.1772842407	51.0245933533	Medium Confidence	Partially Buried Objects?
QBC_Q10676	26.2013893127	51.0221672058	Unknown Confidence	Buried Feature?
QBC_Q10702	26.2007694244	51.0457038879	Unknown Confidence	Depression?
QBC_Q10726	26.1942138672	51.0716514587	Unknown Confidence	Buried Feature?
QBC_Q10729	26.0780544281	50.9166069031	Unknown Confidence	Buried Feature?
QBC_Q20008	26.0396232605	50.9539299011	Unknown Confidence	Natural Location

Contact No.	Latitude	Longitude	Confidence Level	Preliminary Interpretation
QBC_Q20032	25.9976711273	51.0048599243	Unknown Confidence	Depression?
QBC_Q20045	26.0156154633	50.9666290283	Medium Confidence	Debris
QBC_Q20046	26.0135402679	50.9689636230	Unknown Confidence	Natural Location
QBC_Q20060	26.0014724731	50.9691925049	Unknown Confidence	Mound?
QBC_Q20066	25.9976844788	50.9691009521	Unknown Confidence	Natural Location
QBC_Q20068	26.0000514984	50.9640655518	Unknown Confidence	Debris?
QBC_Q20071	26.0349769592	50.9097480774	Unknown Confidence	Depression?
QBC_Q20080	26.0018577576	50.9552879333	Unknown Confidence	Buried Feature?
QBC_Q20088	26.0020446777	50.9487915039	Unknown Confidence	Depression?
QBC_Q20093	26.0029048920	50.9438056946	Unknown Confidence	Linear Debris?
QBC_Q20094	25.9825687408	50.9758758545	Unknown Confidence	Hole
QBC_Q20098	25.9928531647	50.9495239258	Unknown Confidence	Depression?
QBC_Q30107	25.9956703186	50.9137268066	Unknown Confidence	Unclassified
QBC_Q30113	25.9930953979	50.9116210938	Unknown Confidence	Linear Debris?
QBC_Q30116	25.9878578186	50.9224739075	Unknown Confidence	Depression?
QBC_Q30117	25.9647445679	50.9630203247	Unknown Confidence	Depression?
QBC_Q30121	25.9924755096	50.8957824707	Unknown Confidence	Natural Location
QBC_Q30124	25.9860668182	50.9170112610	Unknown Confidence	Unclassified
QBC_Q30132	25.9577922821	50.9669189453	Unknown Confidence	Depression
QBC_Q30146	25.9918575287	50.8720436096	Unknown Confidence	Linear Debris?
QBC_Q30147	25.9881267548	50.8642044067	Unknown Confidence	Linear Debris?
QBC_Q30149	25.9908180237	50.8585395813	Unknown Confidence	Debris?
QBC_Q30174	26.0338172913	50.8948898315	Unknown Confidence	Buried Feature?
QBC_Q30175	26.0339908600	50.8949546814	Unknown Confidence	Debris?
QBC_Q30176	26.0340347290	50.8953170776	Unknown Confidence	Buried Feature?
QBC_Q30177	26.0348167419	50.8955154419	Unknown Confidence	Linear Debris?

Contact No.	Latitude	Longitude	Confidence Level	Preliminary Interpretation
QBC_Q30178	26.0456485748	50.8976631165	Unknown Confidence	Depression?
QBC_Q30180	26.0327358246	50.8860626221	Unknown Confidence	Debris?
QBC_Q30183	25.9920825958	50.8459053040	Unknown Confidence	Unclassified
QBC_Q30189	26.0602684021	50.8891639709	Medium Confidence	Debris?
QBC_Q40024	25.9772624969	50.8816719055	Unknown Confidence	Natural Location
QBC_Q40026	25.9844532013	50.8379058838	Unknown Confidence	Natural Location
QBC_Q40031	25.9713287354	50.8812484741	Unknown Confidence	Natural Location
QBC_Q40049	25.9601192474	50.8865165710	Unknown Confidence	Natural Location
QBC_Q40055	25.9574604034	50.8707466125	Unknown Confidence	Sediment Accumulation?
QBC_Q40059	25.9588909149	50.8624877930	Unknown Confidence	Depression?
QBC_Q40064	25.9563694000	50.8669052124	Unknown Confidence	Depression?
QBC_Q40071	25.9561614990	50.8610496521	Unknown Confidence	Buried Feature?
QBC_Q40072	25.9574222565	50.8355674744	Unknown Confidence	Unclassified
QBC_Q40075	25.9515342712	50.8676567078	Unknown Confidence	Natural Location
QBC_Q40089	25.9422588348	50.8270797729	Unknown Confidence	Debris?
QBC_Q40097	25.9399833679	50.8259239197	Unknown Confidence	Natural Location
QBC_Q40100	25.9359226227	50.8315277100	Unknown Confidence	Debris?
QBC_Q40102	25.9289989471	50.8649368286	Unknown Confidence	Depression?
QBC_Q40113	25.9325790405	50.8269119263	Unknown Confidence	Unclassified
QBC_Q40118	25.9579067230	50.8681564331	Unknown Confidence	Depression?

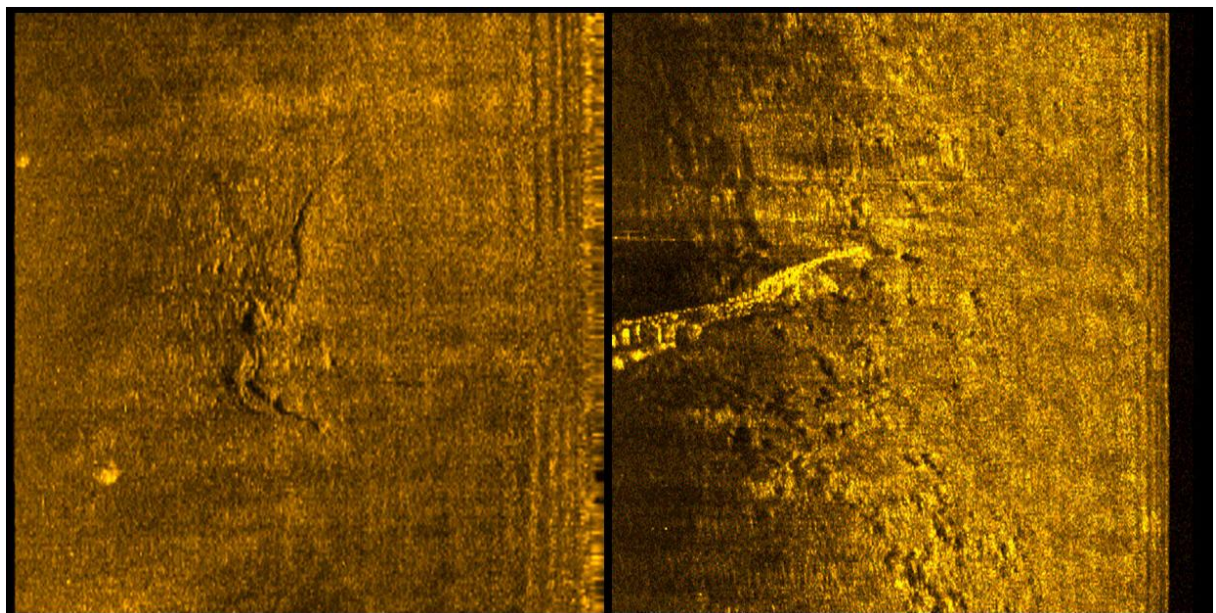


Figure 76 Anomalies logged as possible debris. From left to right: QBC\_Q40089, QBC\_Q10001 (each image depicts an area measuring 100m x 100m).

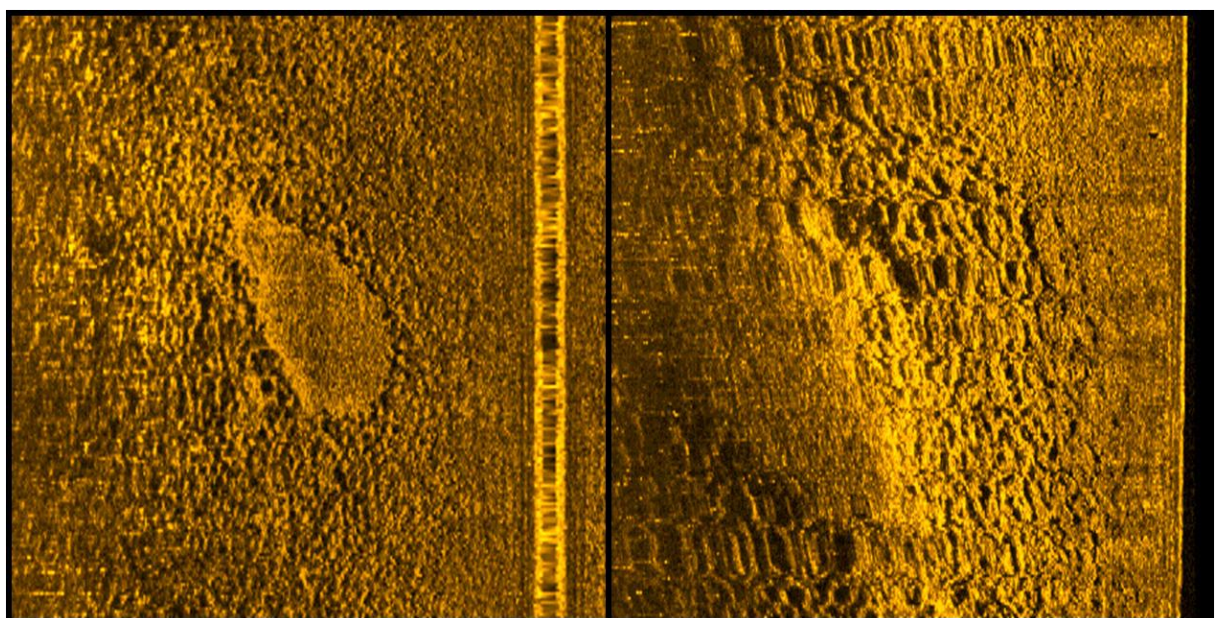


Figure 77 Anomalies logged as areas of possible sediment accumulation. From left to right: QBC\_Q40055, QBC\_Q20060 (each image depicts an area measuring 100m x 100m).

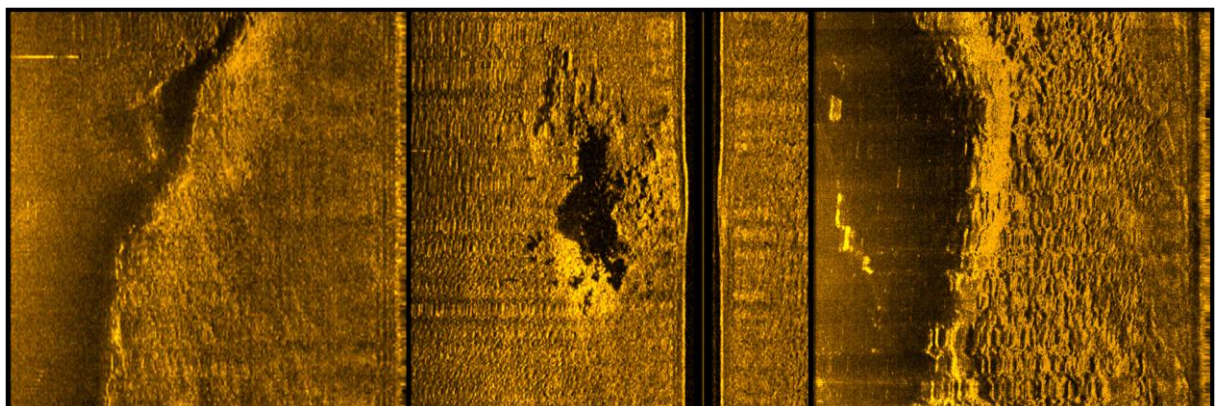


Figure 78 Anomalies logged as natural features of potential topographic significance. From left to right: QBC\_Q40026, QBC\_Q20046, QBC\_Q10195 (each image depicts an area measuring 100m x 100m).

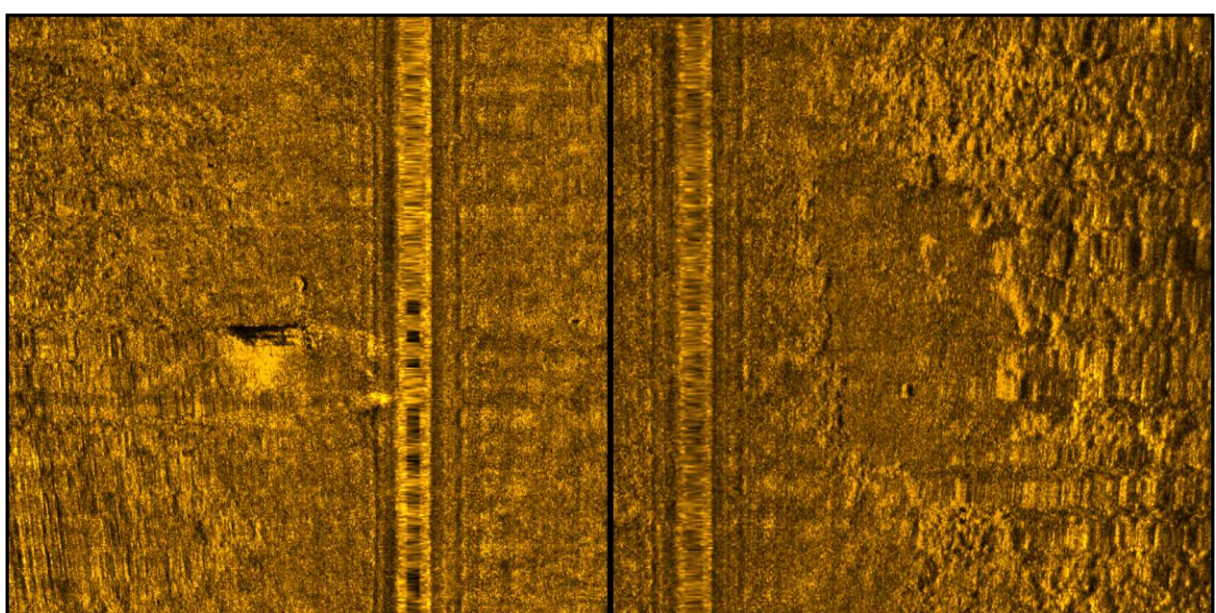


Figure 79 Anomalies logged as potentially partially-buried objects or features. From left to right: QBC\_Q10126, QBC\_Q10202 (each image depicts an area measuring 100m x 100m).

Two anomalies from this selection were of particular interest, a small, but very pronounced hole or crater in the seabed (QBC\_Q20094) and the possible linear feature (QBC\_Q10729). The former looked like it could potentially have been either a small limestone sinkhole, or a hole/crater created as a result of gas venting from the seabed. The character of the linear feature was difficult to determine, but it appeared to be composed of slightly raised, bright linear reflectors lying parallel to, and perpendicular to, each other. This anomaly was investigated by diver inspection in

2011 (Al-Naimi et al., 2012, p.252) but the divers reported nothing visible on the seabed at that location that would explain the anomaly.

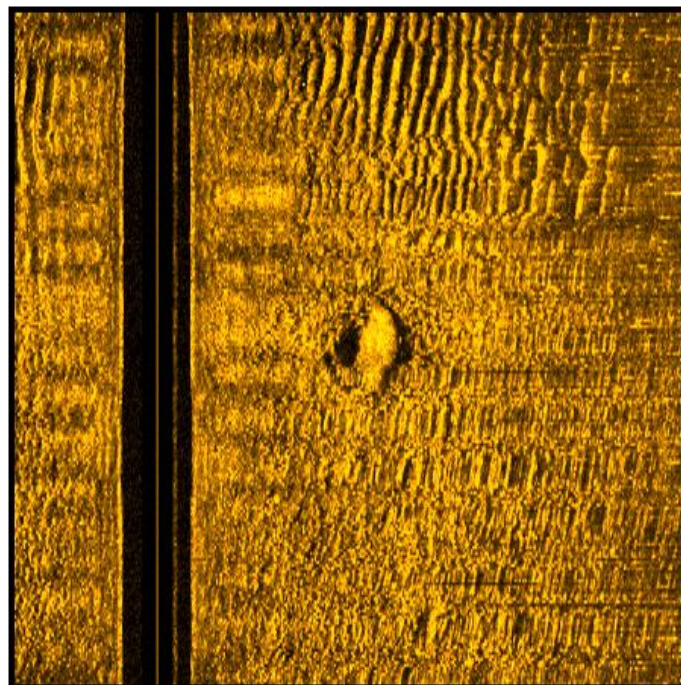


Figure 80 A potential seabed crater: QBC\_Q20094 (Image depicts an area measuring 100m x 100m).

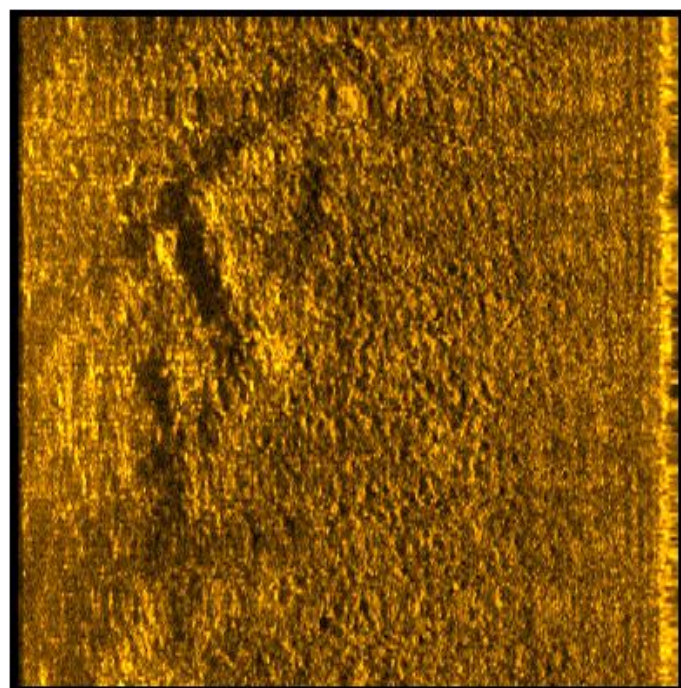


Figure 81 Long linear anomaly: QBC\_Q10729/Bham0028 (Image depicts an area measuring 100m x 100m).

In addition, a high concentration of debris-related anomalies was identified in a cluster in the west of Area 1 (Figure 82). This cluster of debris could be indicative of the way that debris is spread around the seabed after a shipwreck, and so this area was also considered to be of particular interest.

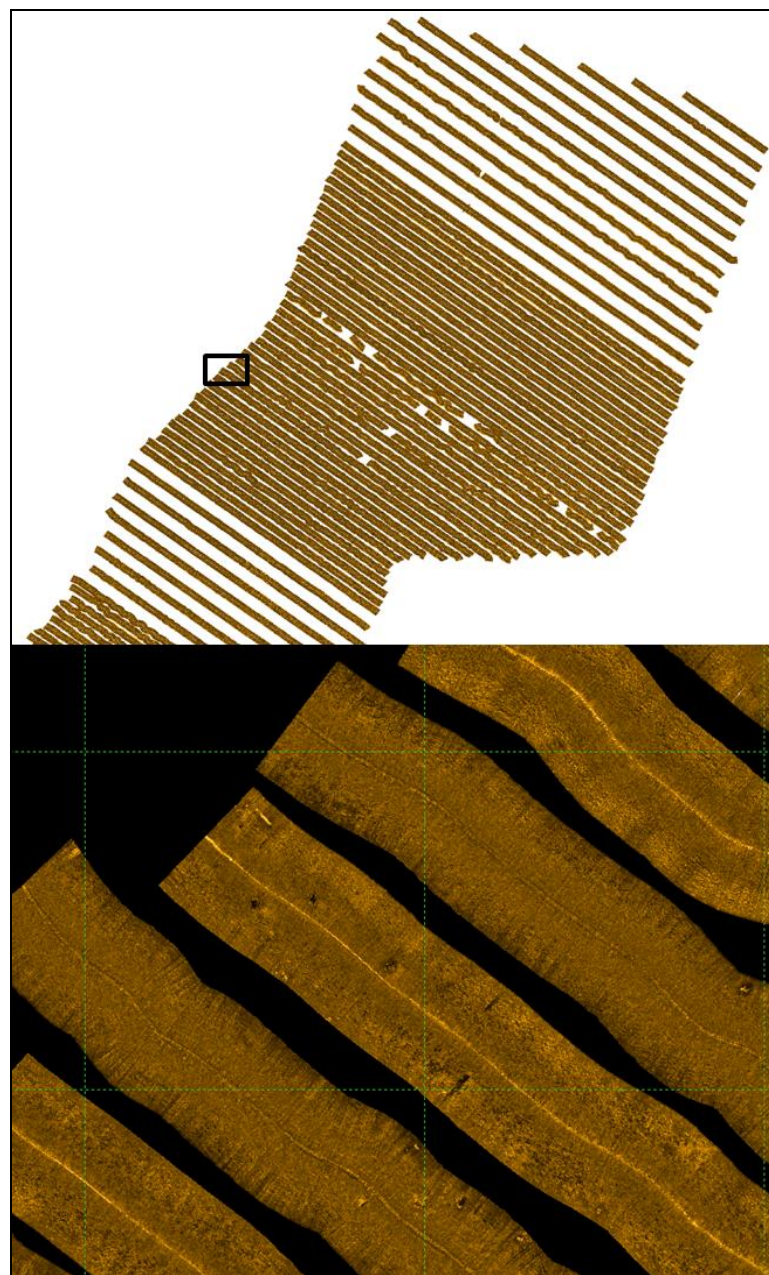


Figure 82 Possible debris cluster in Area 1 (the green grid lines represent 500m x 500m squares).

### **5.1.2.2 Geophysical Anomalies and Topography**

It was not possible within the timescale of this research, or the resources of the QNHER project, to carry out visual observation and/or intensive geophysical survey of all of the anomalies selected for further study. However, as part of the integrated analysis and testing of methodologies, the topographic surface generated from the LiDAR bathymetry was cross-referenced with the selected anomalies to see if they could be further clarified. The location of each one of the anomalies selected for further study was examined in the surface model, and the results analysed.

#### **Area 1**

Out of 23 anomalies selected for further study, nine did not lie within the area covered by the surface model, eight did not show up in the surface model at all, and five were clearly natural features that did not differ significantly from the surrounding seabed. The remaining anomaly from the selected set was the long linear anomaly (QBC\_Q10729) already investigated in 2011. Examination of the surface model in the area of this anomaly does show a feature that could possibly relate to the reflective anomaly (Figure 83), but it is not possible to establish conclusively whether it represents a natural feature or not.

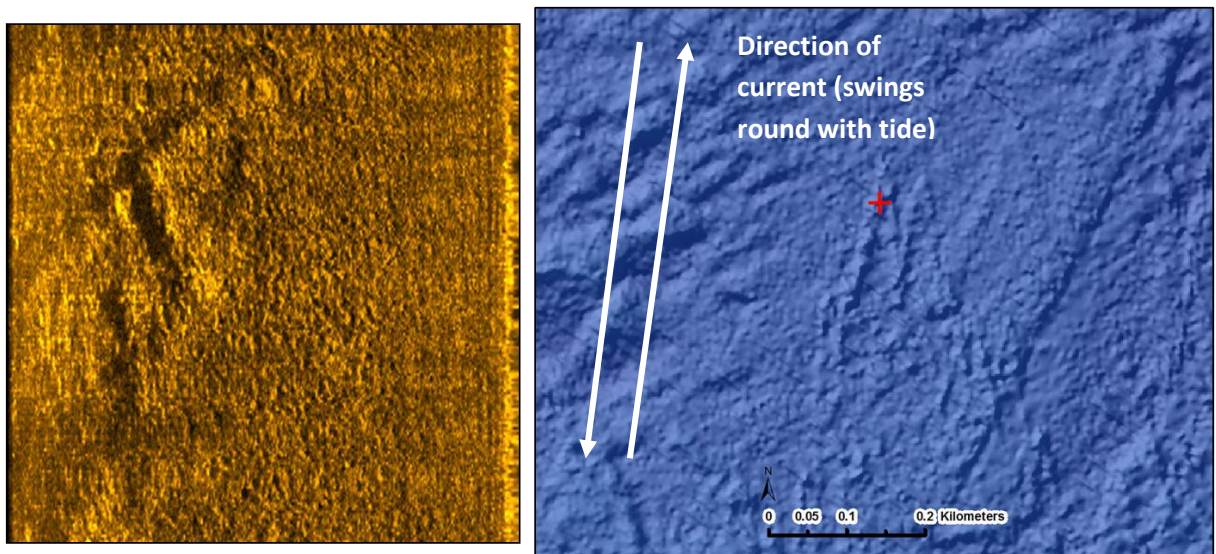


Figure 83 Long linear anomaly (QBC\_Q10729/BHAM0028) visible in the sidescan sonar data, and the surface model of the seabed from the same location (Both images are at same scale and orientation).

## **Area 2**

Out of 13 anomalies selected for further study, three did not show up in the surface model at all, and ten were clearly natural features that did not differ significantly from the surrounding seabed.

None of the anomalies that were recorded as possible debris in Area 2 were visible in the surface model at all (QBC\_Q20012, QBC\_Q20045, QBC\_Q20063 and QBC\_Q20074). One of these, QBC\_Q20045, although not visible itself in the surface model, is surrounded by several other anomalies that were recorded as bright reflectors, and all of these can be seen from the surface model to be rocky/coral outcrops (Figure 84).

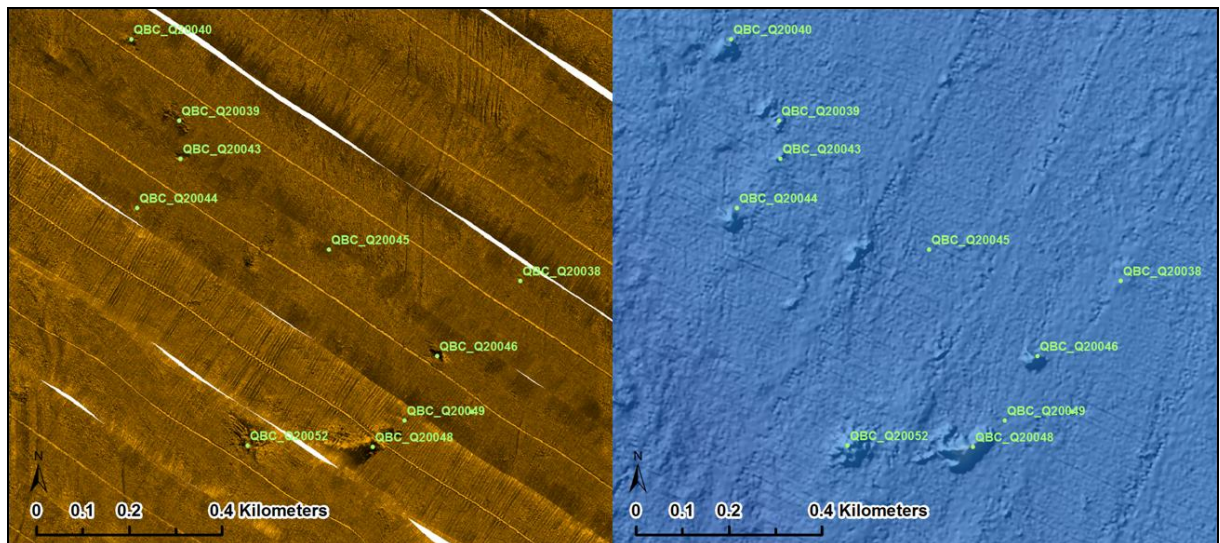


Figure 84 Bright reflective anomalies in Area 2, shown in the surface model to be natural outcrops.

The anomaly that looked like a possible sinkhole or gas vent on the sidescan sonar data (QBC\_Q20094), did not look particularly different to other possible holes in the same area (see QBC\_Q20096 to the southwest on Figure 85). This is probably because the surface model is not of sufficient resolution to clarify features that are this small.

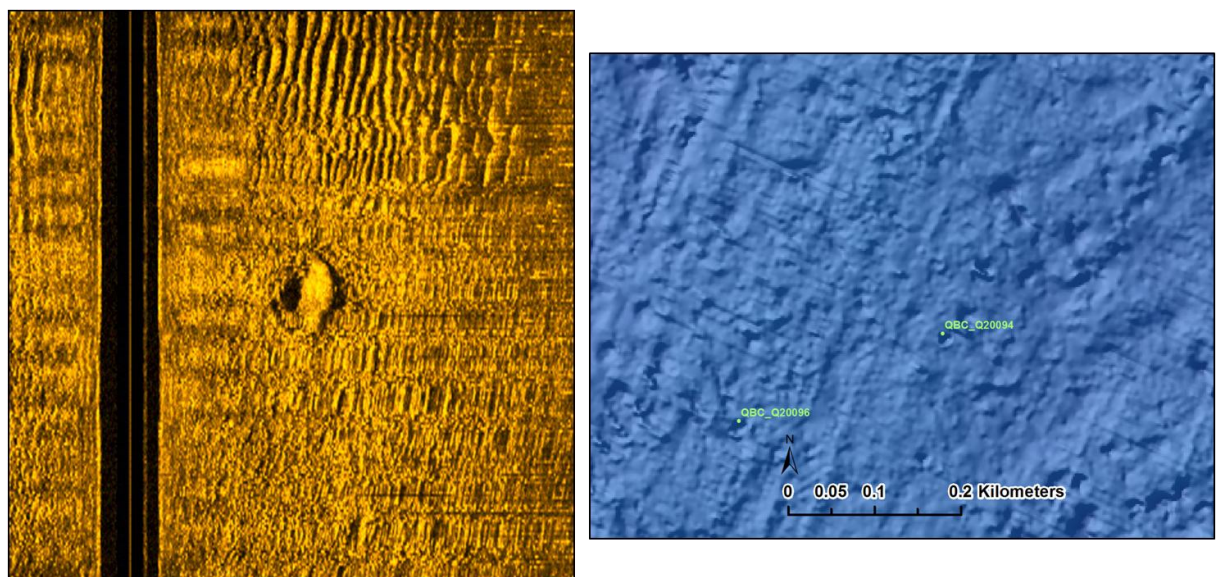


Figure 85 Seabed crater (QBC\_Q20094) visible in the sidescan sonar data (image depicts an area measuring 100m x 100m), and the surface model of the seabed from the same location, showing anomalies QBC\_Q20094 and QBC\_Q20096.

### **Area 3**

Out of 18 anomalies selected for further study, all but two were clearly natural features that did not differ significantly from the surrounding seabed. The other two, which were initially recorded as possible debris from the sidescan data, could not be seen in the surface model.

All of the anomalies that were logged as possible debris in Area 3, including a cluster near the reef (Figure 86), could be seen from the surface model to be natural features, largely coral heads.

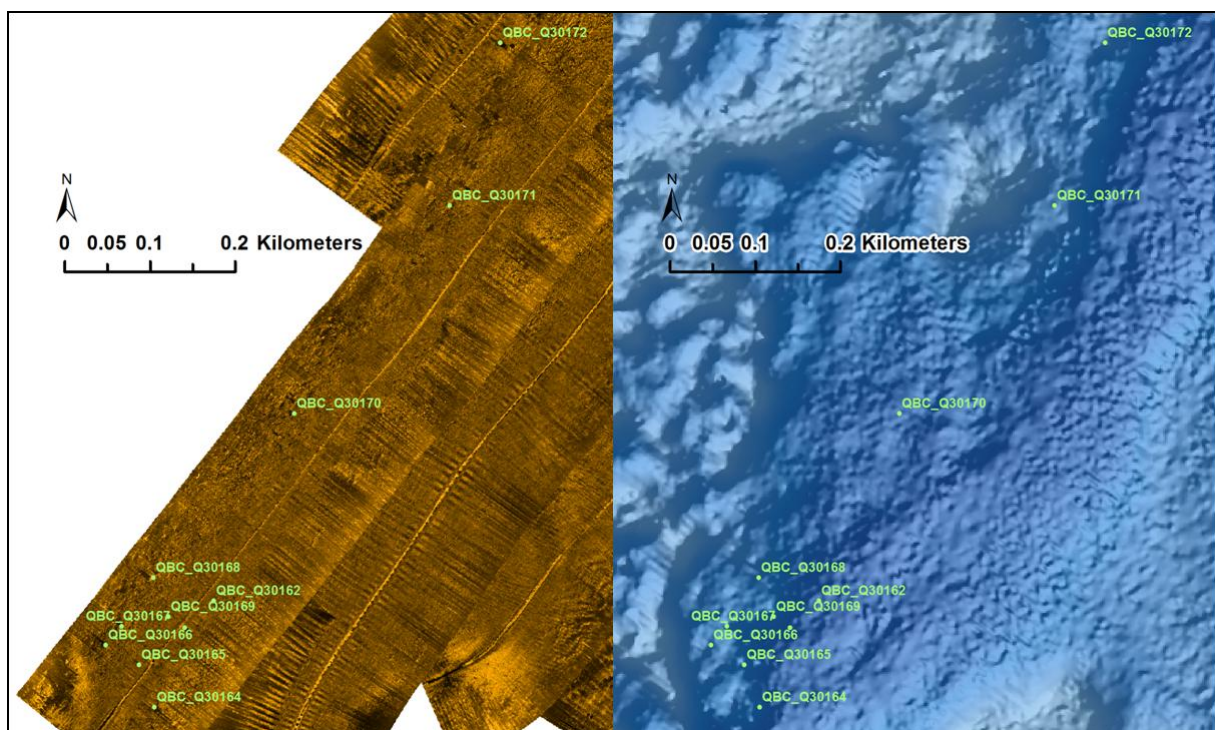


Figure 86 Bright reflective anomalies in Area 3, shown in the surface model to be natural coral outcrops.

## **Area 4**

Out of 16 anomalies selected for further study in Area 4, four did not lie within the area covered by the surface model, six did not show up in the surface model at all, and six were clearly natural features that did not differ significantly from the surrounding seabed.

All of the anomalies that were logged as possible debris in Area 4, mainly in the southwest corner of the area, could be shown from the surface model to be rocky outcrops (Figure 87).

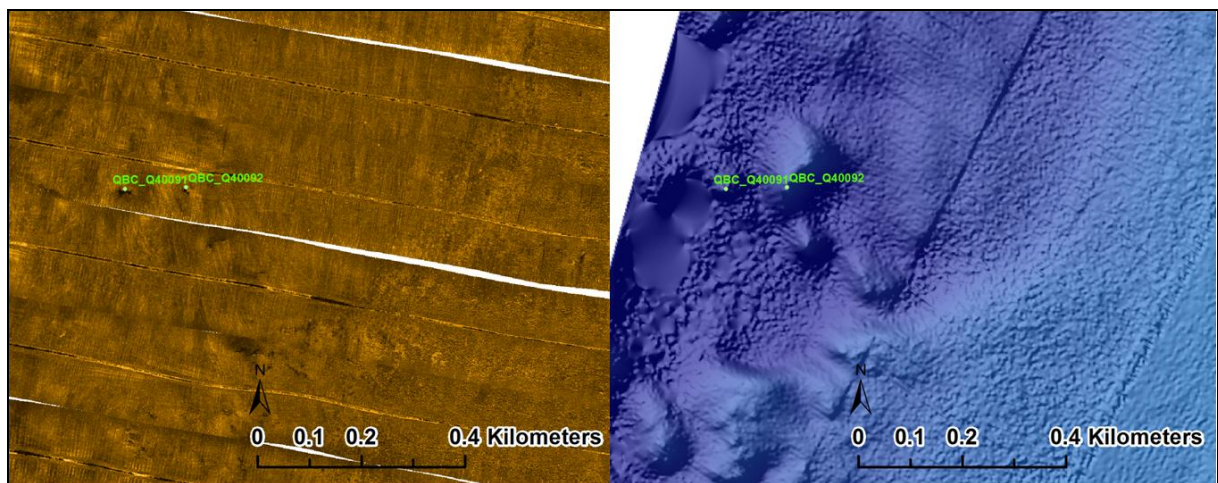


Figure 87 Bright reflective anomalies in the southwest of Area 4, shown in the surface model to be natural outcrops.

Many of the anomalies logged as potential depressions appear to be areas that are in the acoustic shadow of sand banks, rather than actual seafloor depressions. This includes the cluster of potential depressions in Area 4, and that in the north of Area 2.

### **5.1.3 Discussion**

Overall, the identification and analysis of the geophysical anomalies in this low-resolution sidescan sonar dataset has demonstrated that it has limited application as a technique for investigating submerged landscapes. It has not proved a suitable method for locating, identifying and clarifying large-scale features relevant to the use of the former landscape by humans. However, the ability to identify recent debris on the sea floor and produce distribution maps of the anomalies at a landscape level does provide some useful insights into more recent human exploitation of the marine environment, which does have a bearing on seabed characterisation.

It is clear from the distribution of probable debris-related anomalies in Area 1 (Figure 71) that these occur more densely further out from the shore, in the west of the area. This could be due to the increased risks both of causing a shipping hazard, and of being caught dumping material illegally, when closer to the shore. It may also be related to the fact that areas in the south are further away from the main shipping routes around the western Gulf. However, the concentration could also be due to environmental factors, such as the need to create artificial reefs in deeper water, or even the seafloor conditions in certain areas influencing the visibility of seafloor debris in the sidescan sonar data. It may be more difficult, for example, for debris to show up well in areas of seabed where there may be a lot of other bright reflective material such as rocky outcrops or coral heads. It could also be that in these areas the debris gets covered by vegetation and/or sediment more quickly.

It was hoped that integrated analysis of the sonar anomalies with the surface model would be helpful in clarifying the anomalies, but this proved not to be the case with the smaller anomalies. With a few exceptions, the anomalies that were interpreted as debris are either not clearly visible, or not visible at all in the surface model. This could be because the debris was not present when the LiDAR survey was carried out in 2005 (the sidescan sonar data was collected in 2008), or more likely because the debris is too small to show up on a surface model created from data at a resolution of 7m. This is illustrated quite clearly in Figure 88, which shows anomaly QBC\_Q10051 as visible in the sidescan sonar data, the spacing of the LiDAR points in the same area, and the surface model created from those points, which does not show the anomaly at all.

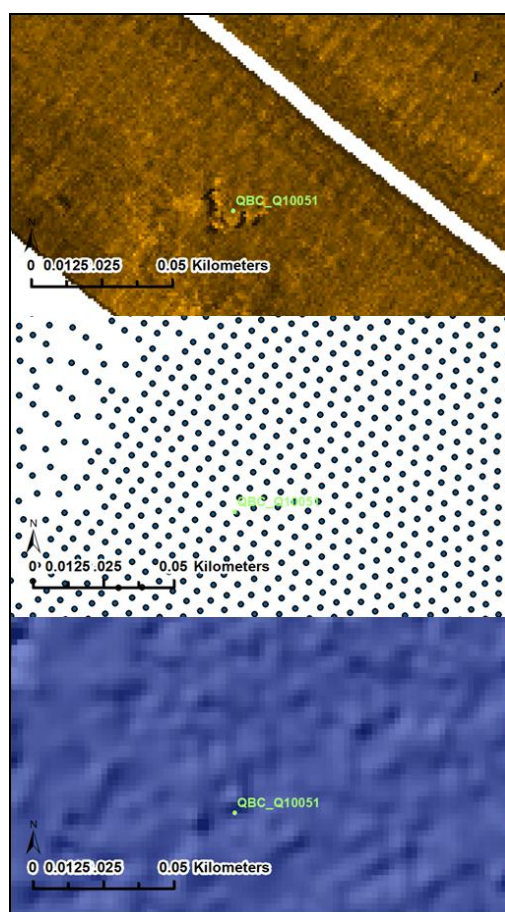


Figure 88 Anomaly QBC\_Q10051 (modern debris): sidescan sonar, LiDAR points and surface model.

Another notable example is QBC\_Q10128, showing very clearly in the sidescan sonar, which diver-inspections in 2011 proved to be a car reef (Bham 0017). This anomaly is not visible in the surface model at all, whereas QBC\_Q10127 to the north (not diver-inspected) is visible in the surface model (Figure 89). The difference in visibility of the two anomalies could be due to the difference in size of the debris, or the distribution of the LiDAR points, or it could simply be that anomaly QBC-Q10128 represents debris that was dumped at a later date, after the LiDAR survey was undertaken.

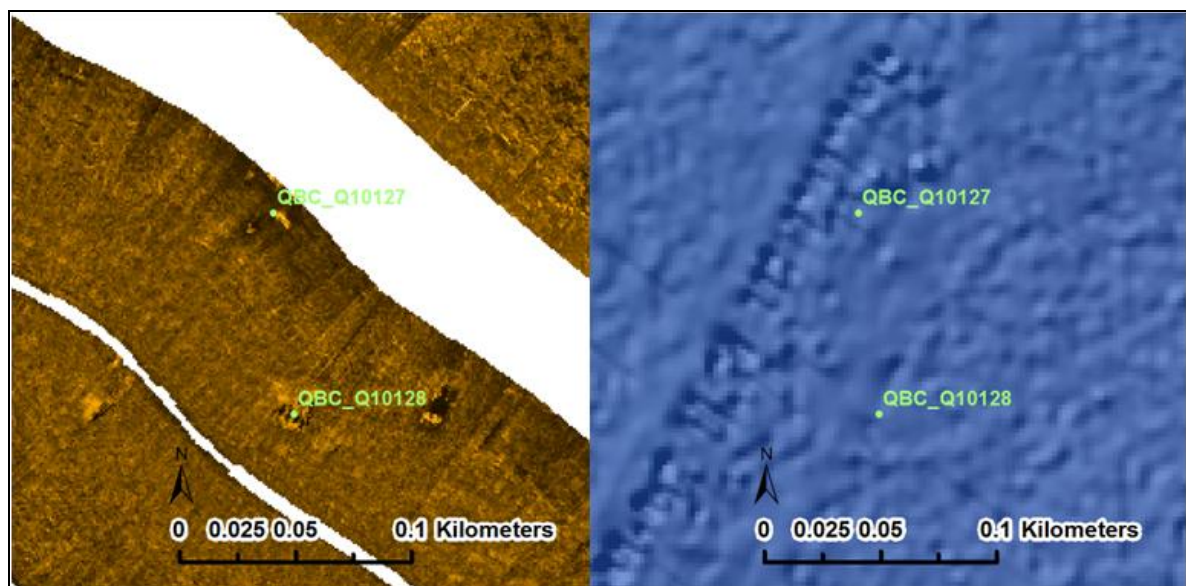


Figure 89 Anomaly QBC\_Q10128 (car reef) visible in the sidescan sonar but not visible in the surface model.

Although, as previously stated, the analysis of the geophysical anomalies has not proved useful for landscape-scale investigations, the surface model used in conjunction with the sidescan sonar data has been extremely useful for clarifying some of the larger and more tentatively-interpreted anomalies, and has largely confirmed that most of these are natural features such as sand ridges, reef

structures, and rock or coral outcrops, that do not hold particular significance for archaeological or palaeoenvironmental potential.

Anomaly QBC\_Q10376 is a good example of why it is not suitable to use geophysical anomalies, and survey data that contains large gaps, as a method for identifying landscape-scale features. When looking at the surface model, it is clear that this anomaly is a part of a larger landscape feature, but that wasn't at all obvious when analysing the survey line in isolation (Figure 90).

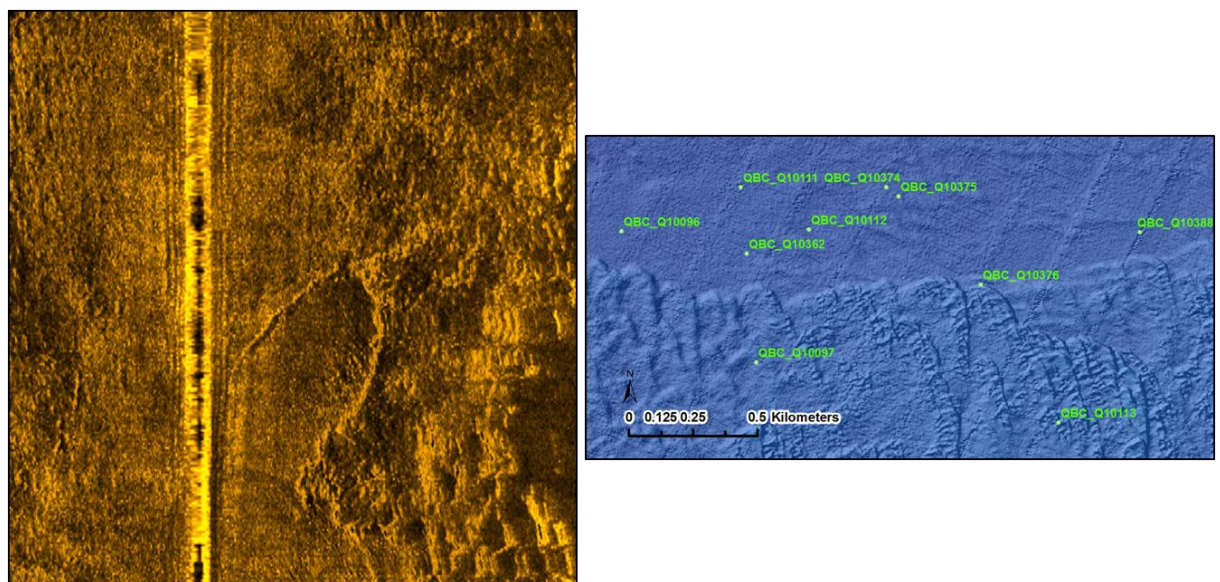


Figure 90 Anomaly QBC\_Q10376 (topographic location of potential interest for human settlement) in the sidescan sonar data (image depicts an area measuring 100m x 100m), and in its landscape context in the surface model.

However, despite the limitations, this analysis has identified two anomalies of potential interest which still merit further investigation, the long linear feature (QBC\_Q10729) and the seabed hole (QBC\_Q20094).

## **5.2 Clarification of Geophysical Signatures**

### **5.2.1 Methodology**

#### **5.2.1.1 Diver Inspections**

The diver inspections carried out on selected geophysical anomalies in 2011 provided very useful ground-truthing data for the clarification of geophysical anomaly signatures in the sidescan sonar data. These diver inspections were targeted on a particular type of anomaly, largely the type with well-defined bright reflectors, often with associated scour. This type of anomaly was targeted because at the time there was no knowledge-base of geophysical signature types for the area, so it was thought that these may represent shipwrecks, or debris from shipwrecks. In the event, they all proved to be the result of modern dumping of cars, tyres and other material in order to create artificial reefs, or fish traps. However, following the systematic assessment and recording of anomalies that was undertaken as part of this characterisation, and in the light of the information gained from the 2011 diver inspections, a different range of anomalies were selected for ground-truthing by diver inspection. The selection did not prioritise the well-defined, clearly anthropogenic anomalies, instead focusing on the more ephemeral anomalies, such as potential depressions, sand waves, areas of differential sediment accumulation and sediment mounds. The reasoning for this was that these types of anomalies may indicate buried objects and features, such as older shipwreck debris, ballast dumps or even, potentially, archaeological sites. Even if these anomalies did not prove to be of

archaeological or palaeoenvironmental interest, the diver inspections would help to build up the knowledge base of geophysical signature types for the area.

### **5.2.1.2 High-Resolution Geophysical Survey**

Further intensive geophysical survey was carried out at a specific, targeted location in order to compare the results with the low-resolution survey, and further clarify selected anomalies. Some testing had already been carried out in the Bay of Al-Zubārah in 2011 using a high-resolution sidescan sonar, and a marine magnetometer, which is designed for the detection of ferromagnetic anomalies (Cuttler, 2011). Further survey in 2013 was carried out using a Klein Hydroscan, which is capable of collecting very high resolution sidescan data over large areas. This data was collected at frequencies of 455KHz and 900KHz. The 900KHZ frequency provided high resolution images up to 75m (total swath of 150m), while the 455KHz simultaneously collected data up to 175m (350m total swath). During the survey the total swath width was limited to 150m to ensure a high-resolution dataset.

## **5.2.2 Results**

### **5.2.2.1 Diver Inspections**

Eight of the selected anomalies were subject to ground-truthing via diver inspection. These eight were chosen for diver inspection partly because they represented good examples of the anomaly signatures that needed to be clarified, and partly because

they were situated in the north of the Study Area and were therefore comparatively accessible for the survey boat, which was based at the port at Al Ruwais. The results can be shown in Table 6 below, and unfortunately, none of the investigated anomalies produced useful information. The anomalies either proved to be natural features of low archaeological and palaeoenvironmental potential, or no features could be observed at the location (Figures 91 and 92). However, those locations where nothing was found should not be dismissed as of no interest on the basis of these diver inspections, since the divers reported that visibility was extremely poor, less than 5m in most cases (see Figure 92), and it is clear that methodologies for ground-truthing these types of anomaly need to be improved.

Table 6: Summary of results of diver inspections on selected anomalies.

Anomaly No.	Longitude	Latitude	Preliminary Interpretation	Interpretation Following Diver Inspection
QBC_Q10702	51.0457038333333	26.2013893	Depression?	No features observed
QBC_Q30183	50.845905304	25.9920825958	Sediment Accumulation	No features observed
QBC_Q40118	50.8681564331	25.957906723	Depression	Linear ridges
QBC_Q10001	51.0675086666667	26.1641788333333	Debris	No features observed
QBC_Q10098	50.929615	26.1222991666667	Debris	Natural undulation
QBC_Q10634	51.0019568333333	26.1872461666667	Partially Buried Objects	Rock outcrop in sediment basin
QBC_Q10645	51.0245933333333	26.1772841666667	Partially Buried Objects	Rock outcrop in sandy hollow
QBC_Q10726	51.0716513333333	26.1942138333333	Buried Feature	Sediment basin



Figure 91 Anomaly QBC\_Q10634 in Area 1: Sediment Basin (Photo by QNHER marine team, 2013).



Figure 92 Anomaly QBC\_Q40118 in Area 4: Linear Ridges (Photo by QNHER marine team, 2013).

A further group of anomalies in the vicinity of the long linear anomaly (QBC\_Q10729) were diver inspected following further intensive geophysical survey, partly to test positional accuracy, and these all proved, as expected, to be car reefs (Figure 93). The results can be shown in Table 7 below.

Table 7: Summary of results of diver inspections on anomalies near QBC\_Q10729.

Anomaly No.	Longitude	Latitude	Prelim Interpretation	Dive Interpretation
QBC_Q10336	50.92655265	26.0960172	Modern Debris	Car reef
G2/03.05.14/L9/TG1	50.9134333333333	26.0759666666667	Bright reflector	Rocks
G2/20.04.13/L4/TG123	50.919195	26.07834	Modern Debris	Car Reef
G3/07.05.13/L8/TG1	50.9146033333333	26.0806816666667	Modern Debris	Car Reef



Figure 93 Anomaly G3/07.05.13/L8/TG1:Car reef in Area 1 (Photo by QNHER marine team, 2013).

### **5.2.2.2 High-Resolution Geophysics**

High-resolution geophysical survey was carried out in the area of the long, linear anomaly (QBC\_Q10729) that was previously identified as meriting further investigation, in order to see if this type of investigation would be more successful at clarifying its nature than the diver inspection in 2011 was (Cuttler, 2014). Although the diver inspection in 2011 did not find anything at the location of the anomaly (Figure 94), it was thought possible that the anomaly was simply too big (greater than 90m long and nearly 30m wide) for divers with limited visibility to gain a wide enough view of the seabed to be able to distinguish the feature from the surrounding seabed, especially as it did not appear to be protruding very high from the seabed.

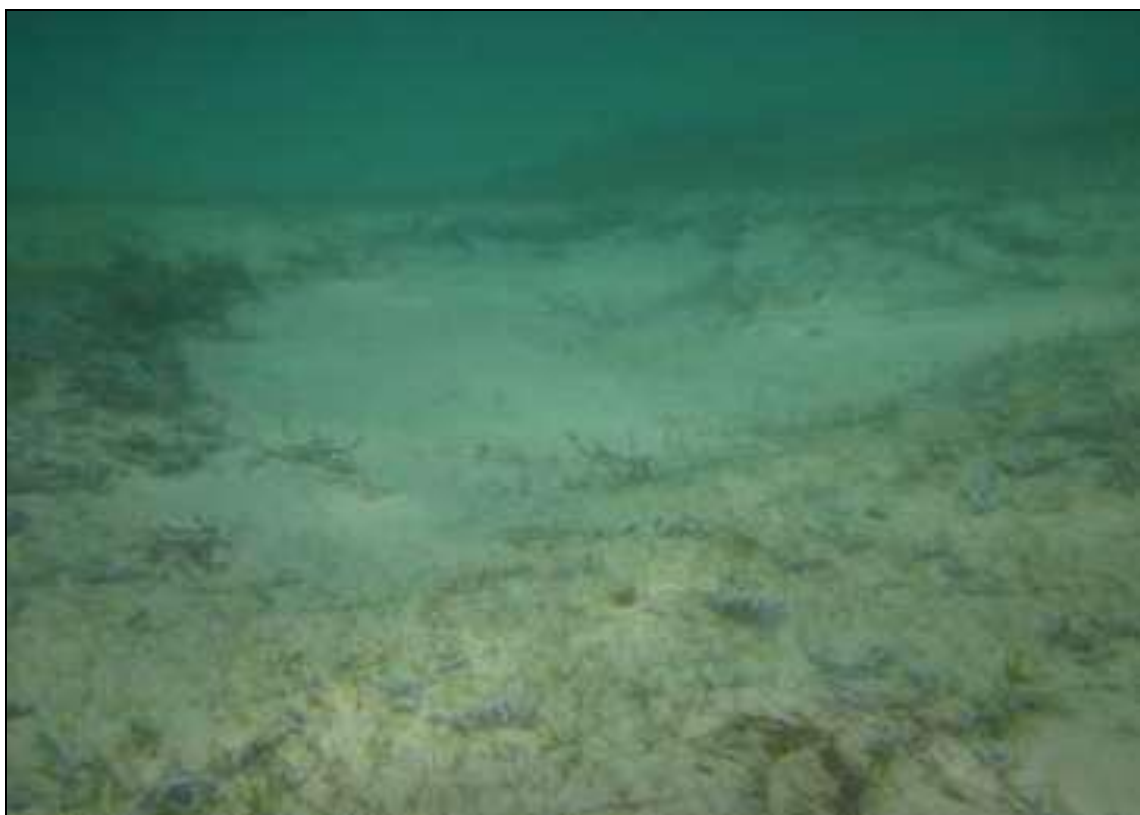


Figure 94 Long linear anomaly QBC\_Q10729/BHAM0028 (Photo by Hampshire and Wight Trust for Maritime Archaeology, 2011).

The high resolution survey was carried out using a Klein hydroscan sidescan sonar at 900KHz. East-west transects were surveyed, at a resolution of 900KHz, in the location of the anomaly, and also covering a significant distance to the north and south. However, nothing relating to the long linear anomaly could be identified in the resulting data. Initially it was thought that there may be a positioning problem, so all coordinates and projections were double-checked, but no error was found. The conclusion was that the anomaly may have been very ephemeral and had disappeared, probably due to the dynamic sedimentation environment of the seabed, in the 5 years since the low-resolution survey was carried out. Finally, it was decided that a southwest-northeast transect would be surveyed along the exact path of the 2008 survey transect in which the anomaly was originally recorded. This time, the anomaly was identified, as shown in Figure 95.

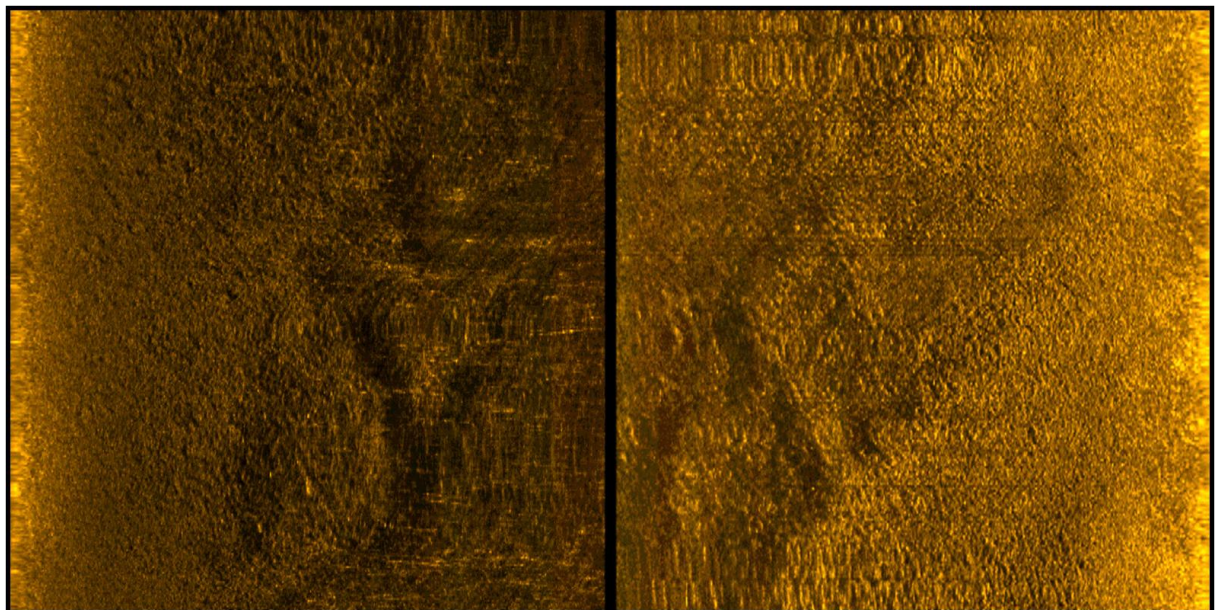


Figure 95 Long linear anomaly (QBC\_Q10729/BHAM0028) surveyed in high resolution (each image depicts an area measuring 100m x 100m).

### 5.2.3 Discussion

The absence of the long linear anomaly in the east-west survey lines, and its presence in the southwest-northeast survey lines, must be due to the effects of the direction of the sonar on the creation of acoustic shadows. This is a significant finding, as it clearly demonstrates how important the direction of survey is, and consequently how important it is to have overlapping survey lines, preferably surveyed from different directions (Cuttler, 2014).

It is also interesting to note that this anomaly did not show up any better in the high-resolution sidescan data than it did in the low-resolution data. It is not clear why this should be the case with this anomaly, as other anomalies were considerably more clear in the high resolution data, for example anomaly QBC\_Q10815 (see Figure 96).

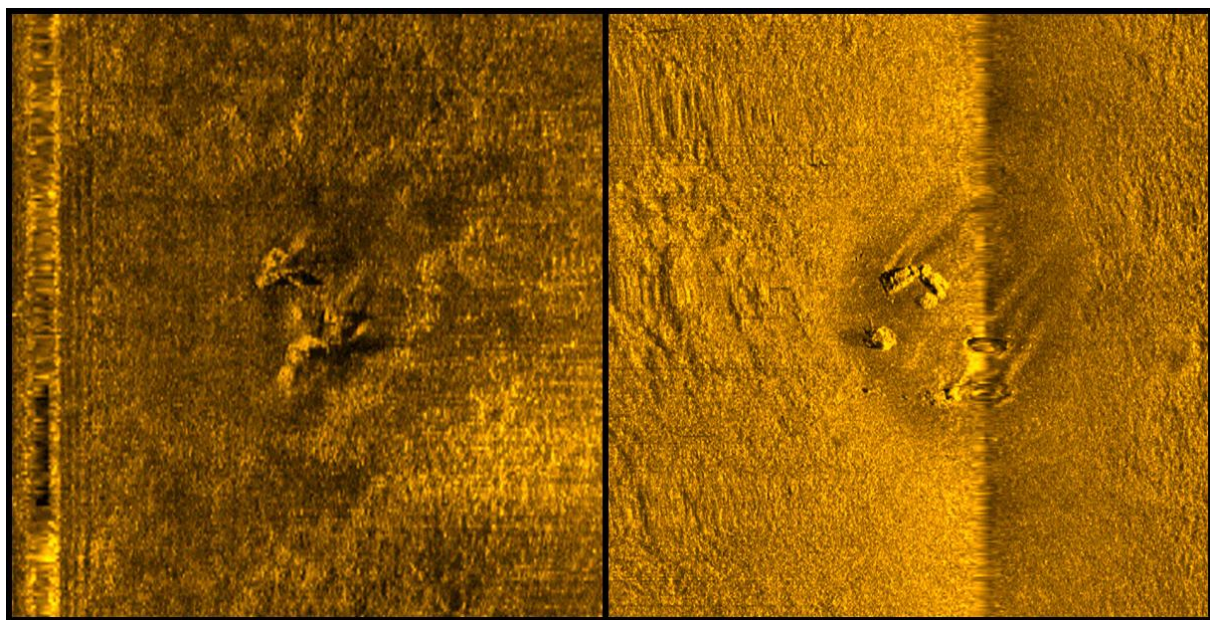


Figure 96 Anomaly QBC\_Q10815 (car reef) surveyed in low resolution (left) and high resolution (right) (each image depicts an area measuring 100m x 100m).

Unfortunately, after surveying the area around the long linear anomaly with low-resolution and high-resolution sidescan sonar, examining the seabed topography in the surface model generated from the bathymetry, and carrying out a diver inspection, we are still no nearer to identifying what the anomaly actually is. The suggested next step would be to use extensive optical techniques, such as an ROV camera, to try and get photographic images of a wide area of the seabed around the anomaly.

Overall, the results of the clarification of geophysical signatures through diver inspection clearly show that diver inspection of selected anomalies has not produced good results, and that this technique is not appropriate for investigating landscape-scale anomalies. This is partly down to poor visibility and the lack of wider vision that is necessary for the interpretation of large topographic features. It is entirely possible, for example, that a diver could actually be in the middle of a feature such as a large depression but not even be aware of it due to the lack of panoramic vision. Diver-inspection is more likely to be successful when targeted at very specific, small-scale locations, as with the artificial car reefs that were successfully identified and recorded in 2011.

However, the comparison of the low and high-resolution data sets has proved very useful for the testing of methodologies, as it demonstrates that the low-resolution sidescan sonar is still sufficient to enable the identification of these more ephemeral anomalies. This, however, does not remove the need or use for targeted high-resolution geophysics once areas of potential have been identified.

## **CHAPTER 6: DEFINING CHARACTER AREAS AND ASSIGNING POTENTIAL**

### **6.1 Refining the Initial Landscape Units into Character Areas**

The end process of the characterisation was to refine the initial landscape units, and designate useable and meaningful Character Areas based on a set of shared attributes, which could subsequently be used to generate zones of archaeological and palaeoenvironmental potential. The refining of the initial landscape units was done by manual cross-correlation of the results of the sediment texture analysis with the topographic mapping and the ground-truthing data, supplemented with information on more recent maritime exploitation from the secondary characterisation process (Figure 97). These factors were used to guide the re-defining of the boundaries of the initial landscape units into character areas, simplifying and interpreting them using the different datasets, thereby creating more cohesive, discrete areas, in order to better represent zones with shared characteristics.

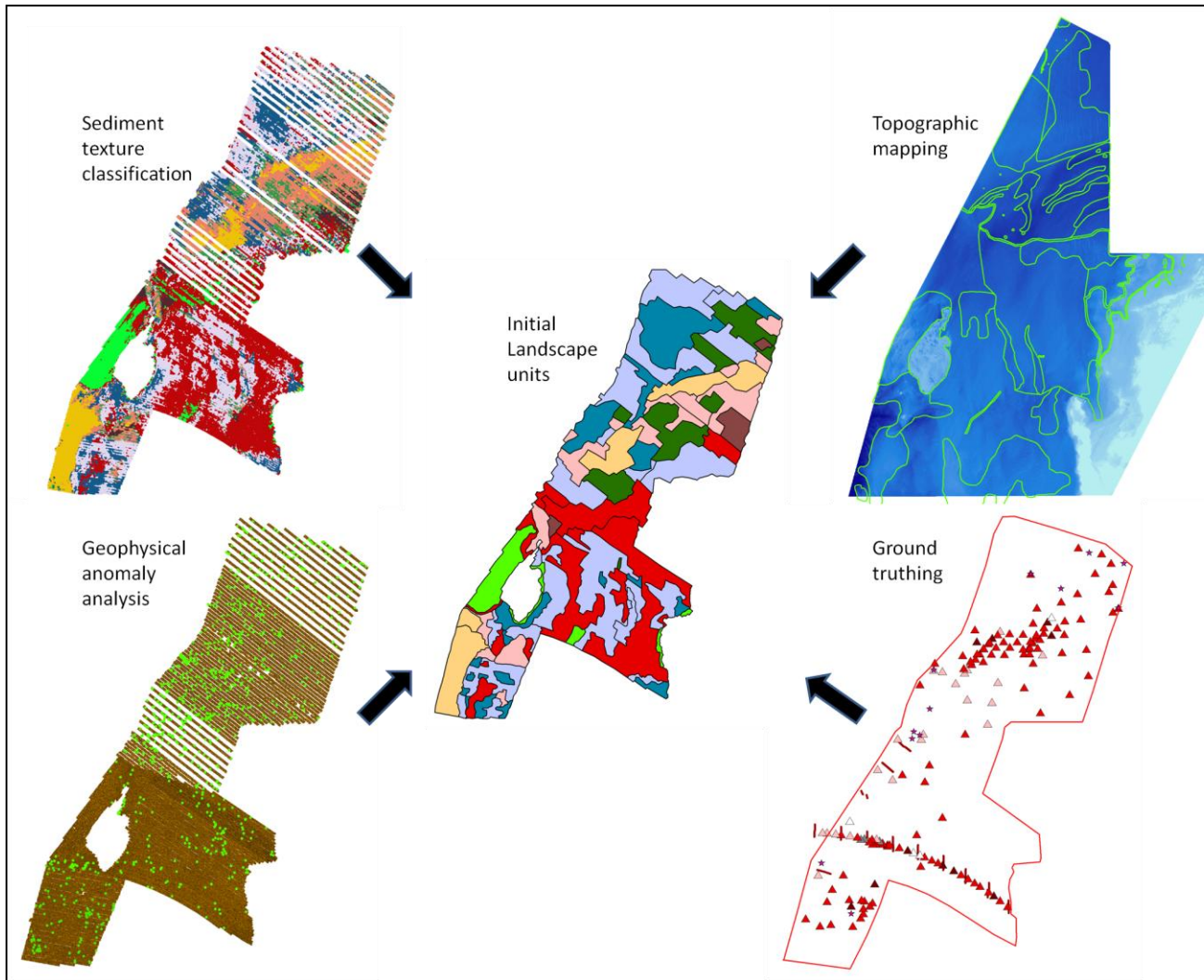


Figure 97 Cross-correlation of different input datasets with the Initial Landscape Units.

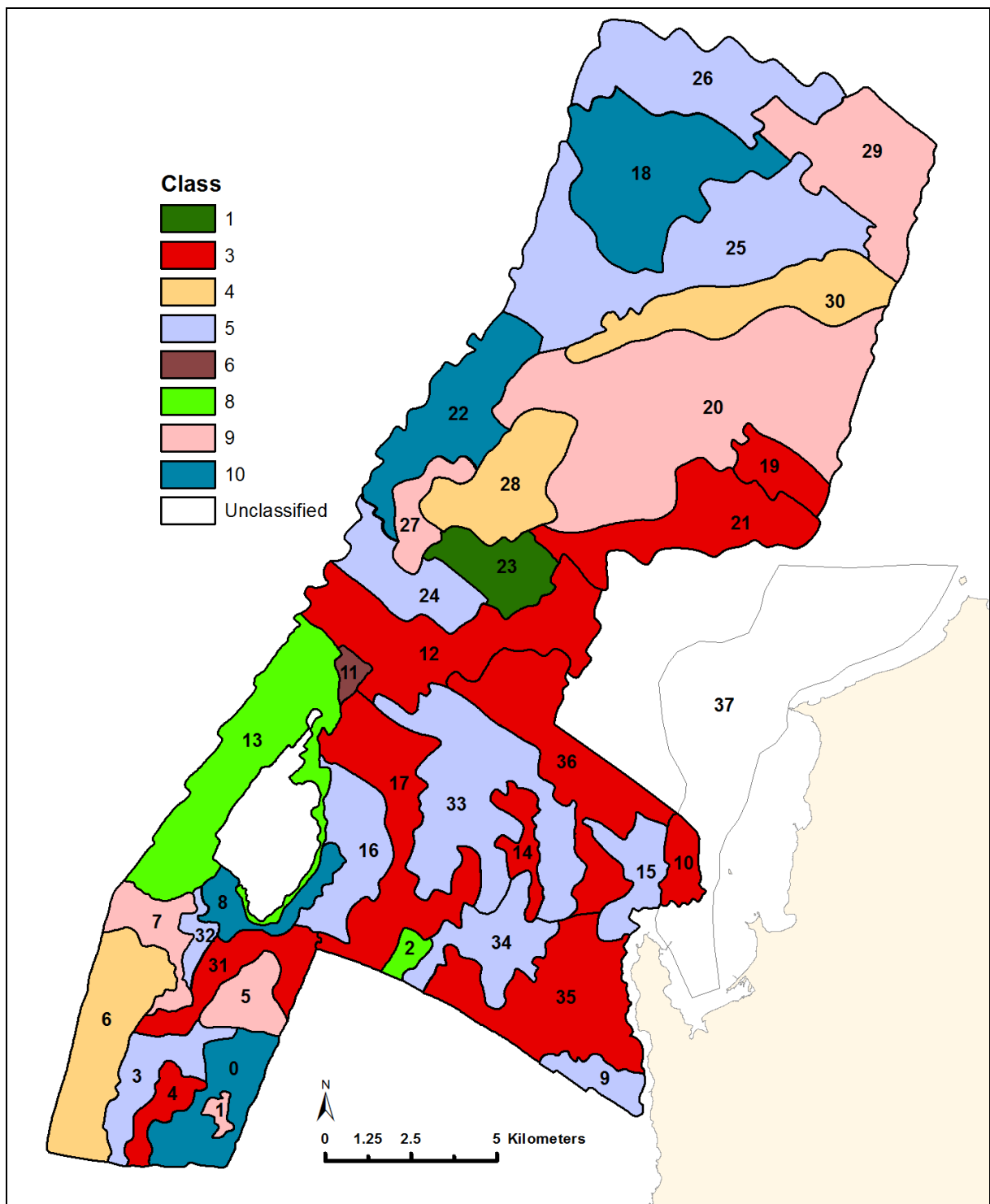


Figure 98 Final Character Areas (labelled with Character Area numbers).

The result of this process was a reduction in the number of landscape units, from the initial 90 (Figures 29 and 97) down to 37 larger character areas (Figure 98). Figure 98 shows the final character areas shaded according to their predominant acoustic class, and Table 8 provides a description of each character area. Figure 98 shows that the overall pattern of the character areas is still heavily based on the acoustic classification, as expected since the acoustic data was the primary dataset. An additional character area that lay outside the main Study Areas was added to the dataset (Character Area 37), based solely on the information gained from the surface model, as there was no sidescan sonar data or ground-truthing data available for these area. This was the near-shore zone northwards of the Ras 'Ushayriq Peninsula, which contained a concentration of highly significant topographic features, such as possible former shorelines and palaeochannels.

Table 8: Summary description of Final Character Areas

Unit ID	Acoustic Class	Sediment Type	Summary	Potential for Extensive Sediment Deposits	Potential for Significant Topographic Features	Overall Archaeological/ Palaeoenvironmental Potential
0	10	Sand	Flat, featureless sandy area	Medium	Low	Low
1	9	Silty Sand	Slight depression containing silty material	Medium	Medium	Medium
2	8	Coral	Ridge, with coral/rocky outcrops	Low	Low	Low
3	5	Sand	Slightly elevated area, with north-south trending sand ripples	Medium	Medium	Medium
4	3	Coarse Sand	Slightly elevated area of coarse sand, with north-south trending sand ripples	Medium	Medium	Medium
5	9	Silty Sand	Slightly lower, silty area adjacent to the reef, containing deep sand deposits	High	Medium	Medium
6	4	Sand	Deep area with extensive trawler scars on the seabed	Medium	Low	Low
7	9	Silty Sand	Silty area adjacent to the reef	Medium	Medium	Medium
8	10	Sand/Coral	Coral area adjacent to the reef	Low	Low	Low

<b>Unit ID</b>	<b>Acoustic Class</b>	<b>Sediment Type</b>	<b>Summary</b>	<b>Potential for Extensive Sediment Deposits</b>	<b>Potential for Significant Topographic Features</b>	<b>Overall Archaeological/Palaeoenvironmental Potential</b>
9	5	Sand	Area of small, east-west trending sand ripples	Medium	Low	Medium
10	3	Sand	Potential former bay/wadi channel, with east-west trending small sand ripples	High	High	High
11	6	Sand	Area of coarse sand with north-south trending large sand ripples	Medium	Low	Low
12	3	Sand	Area of coarse sand with north-south trending large sand ripples	Medium	Medium	Medium
13	8	Coral Reef	Coral reef	Low	Low	Low
14	3	Sand	Area of coarse sand with north-south trending large sand ripples	Medium	Medium	Medium
15	5	Sand	East-west trending and north-south trending sand ripples	Medium	Medium	Medium
16	5	Sand/Gravel	Flat, featureless area of coarse sand and gravel	Medium	Low	Low

<b>Unit ID</b>	<b>Acoustic Class</b>	<b>Sediment Type</b>	<b>Summary</b>	<b>Potential for Extensive Sediment Deposits</b>	<b>Potential for Significant Topographic Features</b>	<b>Overall Archaeological/Palaeoenvironmental Potential</b>
17	3	Sand/Gravel/Coral	Area of coarse sand with north-south trending large sand ripples	Medium	Low	Low
18	10	Sand	North-south trending, very pronounced mega ripples	Medium	Medium	Medium
19	3	Sand	Area of coarse sand, no topographic information available but close to area of potential former shoreline	Medium	No DEM	Medium
20	9	Silty Sand	Deep southwest-northeast trending channel containing depressions, possible solution hollows, and deep sand deposits	High	High	High
21	3	Sand	Edge of potential former shoreline, with pronounced north-south trending sand ripples, coarse sand	Medium	High	High
22	10	Silty Sand	Edge of potential former shoreline, with depressions and potential solution hollows, and a high concentration of debris of recent anthropogenic origin	High	High	High

<b>Unit ID</b>	<b>Acoustic Class</b>	<b>Sediment Type</b>	<b>Summary</b>	<b>Potential for Extensive Sediment Deposits</b>	<b>Potential for Significant Topographic Features</b>	<b>Overall Archaeological/ Palaeoenvironmental Potential</b>
23	1	Sand	Edge of potential former shoreline, with pronounced north-south trending sand ripples	Medium	High	High
24	5	Silty Sand	East-west trending and north-south trending sand ripples. Contains anomaly of potential archaeological interest.	Medium	Medium	Medium
25	5	Sand	North-south trending, very pronounced mega ripples, and a high concentration of debris of recent anthropogenic origin	Medium	Medium	Medium
26	5	Sand	North-south trending, very pronounced mega ripples	Medium	Medium	Medium
27	9	Silty Sand	Edge of potential former shoreline, with potential solution hollows, and a high concentration of debris of recent anthropogenic origin	Medium	High	High
28	4	Sand	Edge of potential former shoreline, with mounds, depressions and a high concentration of debris of recent anthropogenic origin	High	High	High

<b>Unit ID</b>	<b>Acoustic Class</b>	<b>Sediment Type</b>	<b>Summary</b>	<b>Potential for Extensive Sediment Deposits</b>	<b>Potential for Significant Topographic Features</b>	<b>Overall Archaeological/Palaeoenvironmental Potential</b>
29	9	Sand	Area of sand, no Topographic Information	Medium	No DEM	Medium
30	4	Sand	Northern edge of deep southwest-northeast trending channel, with depressions and mounds	High	High	High
31	3	Sand	Area of coarse sand, tail of reef	Medium	Low	Low
32	5	Sand	Tail of reef	Medium	Low	Low
33	5	Sand	Area of finer sand containing linear depressions	Medium	Medium	Medium
34	5	Sand/Gravel	Area of patchy, coarse sand and gravel, with rocky substrate visible in parts, and small sand ripples	Low	Low	Low
35	3	Sand/Gravel	Area of patchy, coarse sand and gravel, with rocky substrate visible in parts, and north-south trending large sand ripples	Low	Low	Low
36	3	Sand	Area of coarse sand with north-south trending large sand ripples	Medium	Medium	Medium

## **6.2 Assigning Potential**

The characterisation of the seabed in the Study Area represents an attempt to zone the seabed based on extensive, continuous data sources, using a systematic methodology. The character zones provide a broad-brush interpretation of the character of the seabed, incorporating every part of the Study Area into the characterisation, in accordance with the principles of historic landscape characterisation. A fundamental principle of terrestrial historic landscape characterisation is that the entire landscape is considered to be significant in its entirety, as the whole of the present-day landscape, to a greater or lesser extent, has been influenced by, and in turn has influenced, human activity. The landscape characterisation data is usually considered to be a means of managing change within the landscape in a non-selective, interpretative manner (Dingwall and Gaffney, 2007, p.17). The characterisation data, therefore, is not in itself a representation of the relative archaeological or historic significance of a particular area of landscape. The same can be said of the character areas created by this seabed characterisation process. However, characterisation data can be used as the basis for assessing the archaeological significance of a landscape. Accordingly, this research aimed to take a step beyond initial characterisation, by using the seabed character zones to provide a coarse-grained assessment of archaeological and palaeoenvironmental potential.

To do this, the attributes of the character zones were further analysed and used to assign levels of potential. The level of potential was assigned on the basis of the probability of extensive sedimentary deposits occurring within the character area, and

on the presence in the area of topographic features known to have been influential in the location of human settlement in the Early-Mid Holocene.

The presence of sedimentary deposits is a fairly rough measure of the potential for preservation of archaeological or palaeoenvironmental deposits, working simply on the basis that the presence of sediment indicates a greater chance of burial and preservation compared to areas of exposed bedrock (Westley et al., 2011b). Similarly, the present-day seabed topography is also a relatively rough measure of potential, as the seabed surface may have changed considerably since the Early Holocene (see Chapter 7 for further discussion on this issue).

The sedimentation rates within the Arabian Gulf as a whole differ markedly depending on morphology and sediment type, and localised relief results in complex sedimentation patterns. Erosion in the Gulf is focused around the shallow coast and the topographic highs, and although the Study Area directly faces the direction of the northwesterly 'Shamal' wind, it is also protected from the full-force of the associated waves and currents by Bahrain and the Saudi Arabian coast (KSEPL, 1973). As a general figure, the averages of the lowest and highest values of sedimentation rates in the different parts of the Gulf are 0.03-2.5 mm per year (Al Ghadban et al., 1998, p.25), but more detailed studies on sedimentation rate are required for localised areas. Geotechnical survey work has shown that sedimentation smooths out the seabed surface, by accumulating in topographic depressions (Marin Mätteknik AB, 2002, p.17), but according to Kassler (cited in Purser, 1973, p.31) this sediment accumulation has not yet completely masked the underlying topography. In order to

obtain a more specific assessment of potential we would need more information about the sedimentation processes, for example how much the deposits are a result of mobile features such as sand ripples. However, despite limitations in our knowledge about sedimentation and erosions rates in specific areas, as a baseline assessment at a landscape-scale, these rough measures are a good starting point from which to base further work.

In their study of submerged landscapes in the North Sea, Gaffney et al. (2007, p.116) used a ranking system to systematically score areas of seabed in their Study Area based on potential for preservation. In this case they created two normalised datasets with different sets of values, one based on landscape feature potential and one based on depth of overlying sediments, and multiplied the two datasets. Areas with both a lack of known features and low levels of sedimentation achieved low scores, and conversely, areas with archaeologically significant features and substantial sediment cover scored highly.

Assigning values for potential to the seabed character areas in Qatar was done on similar principles, except that it was done at the polygon level, and a different ranking system was used. Each character area polygon was assigned two different scores, one for sedimentation potential and one for topographic feature potential. The score values were Low (Value=1), Medium (Value=2) or High (Value=3). Topographic features that led to a designation of high topographic potential for a character area included coastlines, palaeochannels, inlets, spits, promontories and hollows. Other topographic features such as raised areas and slight depressions led to a

designation of medium topographic potential, and character areas which were relatively featureless were assigned a low topographic potential. The combination of values for topographic potential and sediment potential generated the overall potential score for each character zone, either Low (Combined Value of 2 or 3), Medium (Combined Value of 4) or High (Combined Value of 5 or 6). As a result of this process, areas of potential were defined and displayed, as shown in Figure 99.

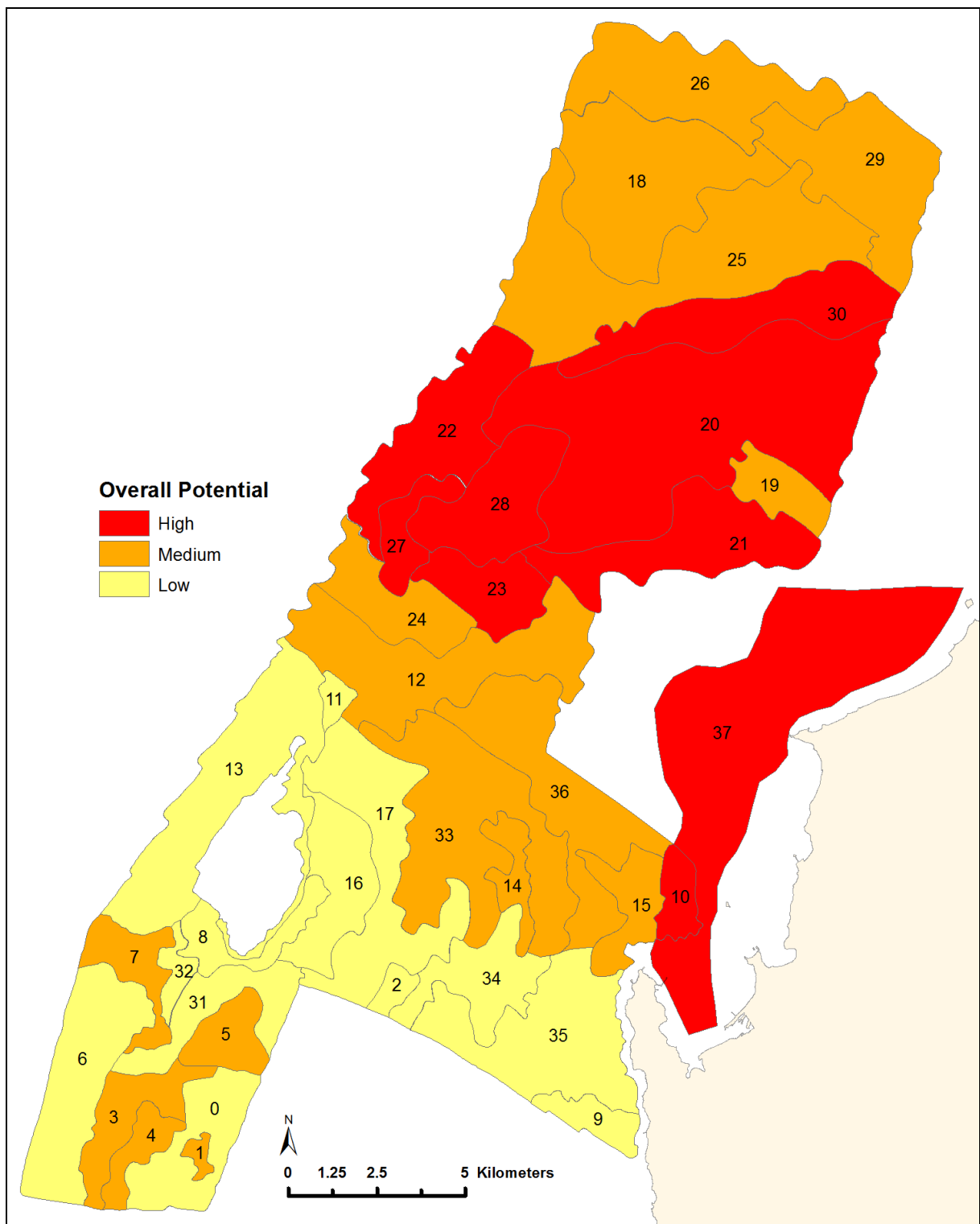


Figure 99 Character Areas (labelled with Character Area numbers) showing overall potential.

The distribution map of the character areas, shaded by potential, clearly shows that the centre of Area 1, and the near-shore zone northwards of the Ras 'Ushayriq Peninsula, are the areas of highest potential, where further investigations should be concentrated. The centre of Area 1, where the deep southwest-northeast channel occurs, clearly shows a cluster of high potential character areas, based on the accumulation of sediment (as evidenced by the vibrocoring logs) together with the occurrence of topographic features that would have been attractive for human settlement, such as channels, hollows and a potential coastline. This combination of possible shoreline combined with the indication of extensive sedimentation could suggest high potential for the preservation of a palaeo-land surface.

The near-shore Character Area (Area 37) north of the Ras 'Ushayriq Peninsula has been assessed as being of high potential without any other primary or secondary characterisation information, apart from Character Area 10 at the north of the potential extension of Wadi Debayan, which was covered by the acoustic sediment classification. The high potential for these areas is due to the presence of two putative former shorelines and a concentration of associated significant topographic features, including the possible wadi extension and a cluster of palaeochannels.

The gentle gradient and generally smooth nature of the seabed in the area to the north of the deep channel supports sedimentation over that area. However, the extensive sand ripples in the north indicate that large quantities of mobile sand overlie the substrate, which may have an effect on the preservation potential of such sediments. It is also possible, however, based on features visible in the surrounding

areas, that these ripples could be infilling and masking other palaeochannels and Karst-related depressions.

The area between the deep channel and the reef has largely been deemed to be of medium potential, on the basis of the north-south linear depressions in the southeast, and the silty material obtained from grab samples in the northwest. However, less ground-truthing data is available from this area than from anywhere else in the Study Area, so to some extent it is a rather unknown quantity, and would benefit from further ground-truthing.

The character areas deemed to be of low potential in the south of Area 2 have been designated as such largely due to the paucity of significant landscape features and the outcrops of rocky substrate identified in the ground-truthing data (boreholes and video footage). The borehole logs interpret this as caprock, formed by submarine lithification of the marine deposits, so it does not exclude the possibility that pre-inundation archaeological and palaeoenvironmental remains could survive beneath this caprock, but palaeoenvironmental remains would be more difficult to access, and it would be impossible to recover archaeological deposits.

The reef area and its immediate surrounding are not close to high-significance landscape features, and there are numerous large coral heads outcropping above the sea floor. These areas were therefore assessed and scored as being of low archaeological and palaeoenvironmental potential. However, south of the reef, there are generally finer-grained silts and muds, and this area of sediment accumulation

(character areas 5 and 7) may have greater potential than the immediate environs of the reef. There may be greater potential for the occurrence of shipwrecks in this area, but any such remains would be likely to be heavily masked by coral growth, and therefore difficult to find and survey.

Character areas 3, 4 and 5 at the south of the Study Area have been assessed as of medium potential, due to the deep sand deposits and the slightly elevated area at the far south. The areas to the east and west are considered to be of low potential due to the overall lack of significant topographic features and the limited information about sedimentation in these areas. However, it may be that further ground-truthing in these areas could change this assessment, since the area to the west (area 6) is one of the deepest parts of the Study Area, and the sediment classification indicates that there may be finer-grained sediments here. Further information would also be needed on the extent of the damage done by the trawler scarring in this character area.

As previously mentioned, there are limitations to the measures used for assigning the potential scores, but on the basis of the evidence that we have, they provide a generalised starting point to begin targeting resources at the areas most likely to yield good results. Within these generalised areas it is already possible to pinpoint specific areas for further investigation, such as possible solution hollows and palaeochannels, and it is expected that as more work is done and the knowledge base grows, then more such localised areas of potential will be identified.

## **CHAPTER 7: DISCUSSION**

### **7.1 An Evaluation of the effectiveness of the methodologies, and suggestions for further work**

It is very important to evaluate how effective this characterisation methodology has been, since using this combination of datasets (sidescan sonar, LiDAR bathymetry, direct sediment sampling, video footage and diver inspection) together with acoustic classification techniques and historic landscape characterisation techniques has never been tried before. Furthermore, apart from the grab samples, the research was undertaken purely using available data that had not been collected specifically for the purposes of archaeological or palaeoenvironmental research. It has clearly raised methodological questions and issues which need further exploration, and it is necessary to examine those aspects that worked well and those that did not, and to assess what datasets should be prioritised for future, research-specific data capture.

Overall, it is important to bear in mind that the value of the seabed characterisation lies in its ability to aid understanding of the submerged prehistoric landscape and delimit areas with archaeological and palaeoenvironmental potential that can be targeted for more intensive investigation, rather than in its ability to identify individual archaeological sites and/or shipwrecks, although discovery of the latter still remain a possibility. Effectively-targeted surveys can provide a wealth of information about the topography, environments and preservation conditions of the submerged landscape even if no archaeological sites are discovered (Bailey, 2011, p.327).

The use of low-resolution sidescan sonar data in the characterisation allowed relatively rapid coverage of large areas of seabed that couldn't easily have been covered using photographic and direct sediment sampling methods. However, this sidescan sonar data was never captured with the intention of using it for archaeological purposes, and one of the aims of the research was to see how effective this low-resolution data could be for landscape-scale studies of the seabed. The results clearly show that for seabed classification and landscape characterisation purposes, which are inherently coarse-grained analyses, low-resolution data is ideal. The data was not so detailed that it provided overly-complex results, and the acoustic classification was able to highlight large-scale trends and changes in the seabed sediment texture, which is exactly what was required for zoning purposes. Ideally, there would have been no gaps between the survey lines in the north of the Study Area, but the acoustic classification methods used allowed satisfactory extrapolation across the gaps for the purposes of broad-brush classification. Now that there are new sonar instruments available that are able to gather high-resolution sidescan sonar data much faster than was previously possible, it may be worth collecting some high-resolution data from a relatively large sample of the seabed within the Study Area - large enough to cover several character areas - and then carrying out acoustic classification trials to compare the difference with the classification results obtained from the low-resolution data. However, the usefulness of this exercise would have to be weighed against the resources required to do it.

The importance of using software specifically designed for acoustic seabed classification cannot be stressed enough. The use of Swathview, and its

accompanying interpolation software, Clams, made the automated unsupervised classification of the sidescan data possible. Without this software, the classification would have had to be done manually, as sensible results could not be obtained from any of the other software packages that were available at the time. The software was very kindly made freely available by the suppliers, Quester Tangent Ltd, for a specific trial period for research purposes. If the software had been purchased and therefore been available for longer, it would have been ideal to have carried out more testing using different parameters. However, even with the amount of testing that was done within the time available, very successful results were obtained, and a coherent and logical division of the seabed was achieved, which was subsequently validated using additional datasets and analysis. There was an element of manual classification in the methodology used, in that the initial landscape unit polygons were manually digitised from the classified image generated by the automated classification. However, the core generation of classes from which the polygons were manually created was automated, unsupervised classification, which picked out acoustic differences in the data that could not be detected manually. One of the outcomes of this research is that successful sediment classification has been carried out using a combination of automated techniques and manual polygonisation, with each method informing the other. This may not be the most objective and repeatable method, but it has certainly been the most practically useful in this context. A possible avenue for further research could be to undertake trials of supervised classification, incorporating what we know about sediments in the Study Area to create training data that can be used to classify the entire dataset, and then comparing this to the results of the unsupervised classification.

The bathymetric surface model has also proved to be incredibly valuable, as it has provided the means to create a seamless surface model of the land/sea interface from the very important shallow zone containing significant coastal structures right out into the deeper parts of the sea in the west of the Study Area. It has therefore, for the first time in this part of the Arabian Gulf, enabled the identification of significant landscape features that could have had considerable influence on the location of human settlement in the Late Pleistocene and Early Holocene. However, there are significant issues still to be considered, a major one of which is how far we can rely on the bathymetry to be representative of the land surface as it was in the Early Holocene. We know from research into submerged landscapes elsewhere in the world, for example in the North Sea (Fitch et al., 2005, p.185), that bathymetric models of the present-day seabed are not necessarily a good reflection of what the palaeo-landscape would have been like, as they will, to some extent, be an expression of current sedimentary processes. It is possible, for example, that some erosional features could have become infilled or buried by sediment, and some landscape features that would have been significant for human settlement in the Early Holocene could have been eroded away. (Fitch et al., 2005, p.194). This is a major part of the reason why significant difficulties have been experienced by researchers when applying historic landscape characterisation techniques in areas where early features are obscured by later sediments (Gaffney et al., 2007, p.111). However, this has been addressed to a limited extent within the characterisation by incorporating information about sedimentation from the acoustic classification and the ground-truthing, and using it as a criteria to assign values for potential. Whilst this

cannot fill the gap in knowledge that exists regarding the palaeo-bathymetry, it can at least provide guidance as to the best areas to target for further research.

One analytical technique based on the bathymetry data that would be worth exploring in the future is Benthic Terrain Modelling. This technique uses bathymetry data to generate models of slope, aspect, rugosity and bathymetric position index (a measure of where a referenced location is relative to the locations surrounding it), which can be used for examining and classifying seabed characteristics. Tools have been developed specifically for undertaking Benthic Terrain Modelling within ArcGIS (NOAA, 2014), and a comparison of such analysis with the acoustic classification of the sidescan data could potentially produce some very useful results.

As far as can be ascertained, this seabed characterisation is the only example of marine historic landscape characterisation that has used acoustic sediment texture classification, bathymetry and ground-truthing to determine character and potential for archaeological purposes. The combined analysis of the topographic surface model with the classified sediment data was pivotal to the success of the research. The level of correlation between the acoustic classification and the topography from the bathymetric surface model was surprisingly high, and, true to the iterative principles of landscape characterisation techniques, each dataset has provided valuable information with which to inform and enhance the other, thus increasing the value of each dataset, and enabling the refining of the initial seabed zoning into character areas.

The ground-truthing data, in the form of direct sampling and video transects, whilst not without its limitations, has largely supported the character zones generated by the combined sediment classification and topographic analysis. However, other than the grab samples, this data was not collected specifically for this research and there would be clear advantages to carrying out coring and optical surveys specifically for archaeological or palaeoenvironmental purposes. This is particularly relevant for finding evidence for buried organic deposits in core samples. There was no evidence for organic remains in any of the vibrocores or boreholes, probably because they were specifically designed to gather information relevant for construction purposes, such as rock strength and compaction. Research in other parts of the world has shown that direct observations and coring become increasingly useful once the scale of the investigation becomes reduced (Faught and Donaghue, 1997). This seabed characterisation could certainly be improved by more intensive ground-truthing, but it would be very resource-intensive to collect grab samples in sufficient densities over the entire Study Area. However, useful results could be obtained by selecting a few smaller areas that include the boundaries of several character zones and collecting a high density of grab samples in these areas. The results could be further improved by extensive photography at each grab sample location.

In terms of optical ground-truthing, rather than narrow video transects or isolated individual photographs, a more useful technique would be to create panoramic views of the seabed, thus enabling a wider view of the character of the seabed in a particular area. This could be done by taking large numbers of photographs in a character zone and stitching them together to create photo-mosaics of larger areas. If

this could be done within the constraints of the visibility conditions that often occur in the Study Area, then it could be of great benefit for this type of landscape-scale investigation, as it may provide more diverse ground-truthing data, and could help to identify some of the larger anomalies and/or landscape features that could not be observed clearly enough during diver inspections. Stereoscopic photography has been used very effectively (albeit in very clear conditions) at the submerged Bronze Age town of Pavlopetri (Henderson et al., 2013). This technique would be too time-consuming to undertake over large areas, but as Autonomous Underwater Vehicles (AUVs) develop and become cheaper, the creation of underwater photo-mosaics is likely to become more cost-effective.

Previous research into classification methods for seabed mapping has suggested that the use of continuous data, such as acoustic data, is likely to result in a more diverse seabed map than would have been the case if direct sampling or photography at discrete locations had been used and extrapolated (Sutherland et al., 2007). This certainly appears to be the case with the seabed classification carried out in the Study Area, since, if direct sediment sampling alone had been used, the result would have been three classes, sand, silty sand and coral, and it would not have been possible to generate meaningful character areas on this basis alone. This clearly shows that the value of the integrated analysis is greater than the sum of its parts, and again validates the use of ideas drawn from historic landscape characterisation techniques.

The secondary characterisation, in the form of systematic analysis of individual geophysical anomalies, was the least successful aspect of the characterisation methodology. However, some useful information about future methodologies to use was obtained from the work that was carried out. The low-resolution sidescan sonar data is clearly perfectly adequate for the initial identification of anomalies caused by more recent debris, as many such anomalies were identified in the low-resolution data and confirmed by diver inspection. The high resolution sidescan sonar data collected using the Klein Hydroscan provided an almost photo-like image of such anomalies, so this would be a useful technique to employ where there is a need to be more certain of what an anomaly may represent before deciding on the allocation of further, possibly expensive, investigative resources. One part of the Study Area where this would be of use is the area of concentrated debris in the west of Area 1 (Figure 82). High resolution sidescan sonar data from this area would probably confirm whether this debris is the result of dumping to create artificial reefs, or whether it represents a spread of debris from a shipwreck.

However, the more ephemeral types of anomaly that were being targeted as part of this landscape-scale analysis did not show up with sufficient clarity in the low resolution sidescan sonar data to be informative, and there is currently no evidence to suggest that high-resolution data would display such anomalies any more clearly. This is evidenced by the fact that the long linear anomaly (QBC\_Q10729) did not show up any better in the high-resolution sidescan data than it did in the low-resolution data. However, it should be noted that this is only a single example, and further testing by gathering high-resolution sidescan sonar data over other anomalies

of a similar ephemeral nature would confirm this. The further high-resolution sidescan sonar survey work undertaken by the QNHER project has shown that the direction of survey is obviously very important for the identification of more ephemeral anomalies (Cuttler, 2014). The results suggest that the most cost-effective and productive methodology for initial rapid prospection of large areas would be a low frequency, wide swath-width sidescan survey with overlapping survey lines surveyed in a minimum of two directions, followed by higher frequency survey in targeted areas based on the results provided by the low frequency survey.

The most useful aspect of the secondary characterisation was the information that it provided about more recent maritime exploitation, mainly fishing activity, in the form of the distribution of modern anthropogenic debris and trawler scarring. A further notable result was how useful the topographic surface model was for clarifying the more ephemeral anomalies, even if it was largely to confirm that they were not of any significance. This enabled the clarification of many of the anomalies that were selected for further study without having to carry out further high-resolution geophysical survey or diver inspection. This is especially significant as diver-inspection is a time-consuming and expensive method for exploring the submerged landscape. A clear outcome of this research, and the work carried out by the QNHER project, is that diver-inspection should be used for very specific, smaller scale inspection of clearly-defined targets, but it is not suitable for ground-truthing landscape-scale geophysical anomalies. It is clear from the experience of the QNHER diving team of diving on known shipwreck locations and not finding anything that there are still problems in ground-truthing small-scale anomalies by diver

inspection, possibly due to currents, wind and GPS accuracy (Personal Communication, Richard Cuttler, 2014). A more robust methodology may be to drop a marker down on an identified anomaly, then carry out a sidescan survey over the marker before diving, to ensure that the anomaly has been correctly located.

Now that we have areas of potential that can be targeted, there is a clear need to collect new data sets in order to improve predictive modelling, and a suite of techniques used in combination - multibeam sonar, sub-bottom profiling and vibrocoring - is likely to produce the most effective results. Of critical importance is the need for sub-bottom profiling in order to try and trace buried and preserved features. Sub-bottom profiling has been successfully used to identify palaeo-features in the North Sea (Gaffney et al., 2007), in the Gulf of Mexico, where it was also used extensively, in combination with bathymetric enhancement methods, for identifying palaeo-drainage patterns, including drowned Karst features such as sinkholes (Faught and Donaghue, 1997), and to identify submarine freshwater springs in the Baltic Sea (Schlüter et al., 2004; Alfred Wegener Institute, 2012). In the Study Area, sub-bottom profiling could be used to confirm, or otherwise, the interpretation of significant features identified from the topographic surface model, and also to try and identify features that do not have a bathymetric expression, such as buried and preserved palaeo-land surfaces, and buried palaeo-drainage features and their sediment fills, including Karst-related depressions and solution hollows. This technique should be prioritised in the areas along, and inland of, the putative former shorelines, and in the areas where the postulated solution hollows are concentrated in the northwest of the Study Area. However, the ability to undertake sub-bottom

profiling inland of the former shorelines may be limited by the shallow water depths in those areas.

In addition to the sub-bottom profiling, targeted core sampling specifically for palaeoenvironmental purposes needs to be undertaken to try and identify organic material, and to provide further information on the sediment in the character areas. As with the sub-bottom profiling, the coring programme should again be concentrated along, and inland of the putative former shorelines. In addition, specific features identified from the topographic surface model should be core-sampled. These include the potential solution hollows in the northwest of the Study Area, the cluster of palaeochannels near the possible former shoreline, the possible continuation of Wadi Debayan, and the deep southwest-northeast channel in the north of the Study Area. If the latter does relate to a large palaeochannel, it would probably be possible to use sub-bottom profiling to map the alignment. This information could then be used to target a vibrocore strategy aimed at the recovery of both former sub-aerial deposits and at deposits associated with marine transgression along the channel.

More detailed bathymetry collected from the areas along and inland of the former shorelines, including extensive multibeam survey in the area of the possible east-west aligned shoreline in the north, integrated with the sub-bottom profiling and the coring from these areas, would provide a better understanding of the changes that have occurred in the submerged landscape since the marine transgression. This work would be improved if more accurate sea level data could be obtained, that takes into account regional hydrostatic adjustments. There are probably enough dates from

terrestrial areas such as Wadi Debayan to begin developing a more secure sea-level curve from around 6,500 BP onwards (Tetlow et al., Forthcoming). The challenge is to obtain information from the submerged areas, and a targeted programme of core sampling based on this research should provide a starting point for this. More detailed bathymetry could also be used to calculate the ‘rugosity’ of the landscape. Rugosity can be defined as a measure of terrain complexity or the ‘bumpiness’ of the terrain. Rugosity is an important influence on the character of the seabed, and this information could be incorporated into the character areas to provide additional information for further targeted work.

It would also be worth exploring the potential for using 2D and 3D seismic data to try and identify significant buried features from the Early Holocene that do not have any bathymetric expression, as was successfully done in the North Sea (Gaffney et al., 2007). Seismic imaging is a geophysics technique that measures the reflectivity of seismic waves, and is used to create sub-surface geological and geomorphological maps. This type of survey is very expensive to undertake, but it is being undertaken extensively in the Arabian Gulf for oil exploration purposes. Future data mining of these datasets may provide a very cost-effective method of interrogating the former landscape and developing research frameworks for targeted, higher-resolution survey. As the information required for archaeological and palaeoenvironmental purposes is limited to relatively shallow depths, it is possible to slice off the top 0.25 sec of data, thus avoiding any commercially sensitive issues such as the location of hydrocarbons.

Whilst the research has demonstrated that the combined analysis of the sidescan sonar data and the bathymetry provided a robust foundation for the initial seabed characterisation, a purpose-designed data capture programme for investigating the submerged landscape would give high priority to volumetric data such as sub-bottom profiling data and/or 3D seismic data. Analysis of such data in combination with high-resolution bathymetry could provide vital comparative information between the palaeo-topography and the present-day seafloor topography in the Study Area. However, as has already been stated, the power of the characterisation approach is the iterative combination of datasets and techniques. Although bathymetry and volumetric data would be primary datasets for a specifically-designed seabed characterisation data-capture programme around Qatar, the results of this research clearly demonstrate that acoustic texture classification of sidescan sonar would still play an important role in characterising and refining landscape units.

There is great potential for much more work to be undertaken using further aspects of terrestrial historic landscape characterisation methodologies, particularly the more cultural elements. Understanding how people worked within the marine environment in more recent centuries can be investigated via the use of both physical and non-physical evidence, in order to provide another layer of interpretational information. Evidence of more recent use of the maritime environment could provide valuable information about the nature of the seabed, preservation potential, tidal and sediment regimes and the location of human activity in the present and the more recent past. The types of information that could be used, in addition to geophysics and survey data, include maritime charts, which can provide evidence of certain types of activity,

such as navigation information, trade routes, shipping routes, anchoring, fishing exclusion zones, hazards, dumping grounds, place names and other cultural information. These information sources can also indicate the absence of certain types of activity, which can be just as significant.

It is also worth exploring further how the characterisation could incorporate local knowledge from people who live and work on or near the sea, or have done in the past. They will have traditions and knowledge drawn from observing the shorelines and working on the sea on a daily basis over extended periods, in all sorts of different conditions. This type of work has been carried out very effectively by the Outer Hebrides Coastal Community Marine Archaeology Pilot Project (Wessex Archaeology, 2012), which involved talking extensively to local fishermen in order to find out about things that people had noticed in the past but had disregarded as unimportant. Interviews with more recent seafarers may well produce anecdotes like that related by Cheesman (1923) of boatmen replenishing drinking water from submarine freshwater springs off Bahrain. This could be of help in locating present day freshwater springs, although extensive pumping since the mid 1920's suggests that groundwater levels have dropped significantly, by as much as 7m, in recent times, which will have affected the output from freshwater springs (Macumber, 2011, p.11).

It would also be worth exploring ways of encompassing some of the more subjective human aspects into the characterisation, in order to consider the less pragmatic aspects of why humans chose certain areas for settlement or other activity. These

principles have been applied successfully in terrestrial characterisation projects, for example the Fort Hood historic landscape characterisation project in Texas (Dingwall and Gaffney, 2007), where aspects such as proximity to significant natural features known to be of importance to hunter-gatherer groups, such as mesa tops and sinkholes, were factored into the classification. Whilst it would be very difficult to include the types of visual attributes and perceptions that terrestrial landscape characterisations involve, it is important to avoid relying too heavily on environmental determinism, and losing the more holistic view of how humans perceived the landscape in which they lived.

This type of landscape-scale contextualisation of the seabed can also provide opportunities for combined management of the historic and natural environment. The ecological character of the seabed can both influence and reflect past and present human exploitation, visibility of features and preservation potential. It is likely that the datasets derived from the seabed characterisation process could be useful for both cultural and natural habitat mapping purposes, thus providing opportunities for interdisciplinary working with natural environment researchers. There are clear crossovers, for example biodiversity levels and species habitats can be closely related to the rugosity of the seabed. Also, integrated analysis of natural habitat data with other datasets could potentially provide valuable information for the location of submarine freshwater springs, since different flora and fauna may occur in areas where there is a higher proportion of fresh water

## **7.2 An evaluation of the archaeological and palaeoenvironmental potential of the submerged landscape within the Study Area**

The submerged Gulf and its former coastlines have the potential to provide valuable new information on a range of important research themes. One of the most obvious outcomes of the seabed characterisation is that it has emphasised the critical importance of former shorelines, which have an influence on virtually every aspect of the significance and potential of the Study Area.

This is particularly pertinent to any study of the Neolithic period in the region, especially in relation to the relatively sudden appearance of 'Ubaid -related sites in previously-unsettled areas around the shoreline of the Gulf in the Mid-Holocene (Rose, 2010). This occurred just after the final phase of marine incursion into the Gulf basin, when sea levels rose to approximately 2-3m higher than present-day levels (Lambeck, 1996). So far, it has not been possible to firmly establish where these communities originated from, but it is possible that they migrated into the area as a result of displacement from the Gulf basin by relatively rapid inundation between c. 8,000BP and 7,500BP (Rose, 2010; Cuttler, 2013).

It is reasonable to propose that there would have been aspects of continuity between the human communities that were established in the former Gulf basin prior to the final phase of marine transgression, and those communities represented by the 'Ubaid-related sites occurring along the eastern coast of the Arabian Peninsula (Cuttler, 2013). It is possible to relate the information on known settlement patterns in

the Mid-Holocene to pre-transgression settlement patterns, and to establish what factors we can draw upon in the submerged landscape that will help to inform this theme.



Figure 100 Distribution map of major 'Ubaid-related sites in Qatar.

It is clear that the sites producing ‘Ubaid pottery in the Arabian Peninsula are found almost exclusively at locations situated on the coast or on the edge of coastal sabkhas, and on islands (Drechsler, 2011). Archaeological evidence shows that occupation of ‘Ubaid -related sites along the Qatar coastline (Figure 100) begins during the second half of the 8th millennium BP (Carter, 2010). Although we lack detailed information on the topographic locations of ‘Ubaid-related sites in Qatar, on the basis of the evidence that we do have, they appear to occur on coastal cliff areas, overlooking the mid-Holocene shoreline, and are generally above the 2m contour (Cuttler and Al-Naimi, 2013). The dating and topographic information for ‘Ubaid-related sites in Qatar is highly significant in relation to the results obtained from the shoreline reconstructions based on Jameson and Strohmenger's sea level curve (Jameson and Strohmenger, 2012). The two putative former shorelines that were identified running northwards of the Ras ‘Ushayriq peninsula coincide with the predicted extent of dry land at 8,000 BP and 7,500 BP respectively. If people were migrating to the higher ground inland of the present-day coastline after 7,500 BP, they may well have migrated from settlements that were on these former shorelines in 8,000 and 7,500 BP.

Ras Aburuk (Ra’s Abarāq) lies on a low plateau to the west of, and overlooking, an oasis depression. It is on a narrow peninsula, which is 1km from the coast on the west (De Cardi, 1978, p.82). Bir Zeikrit (Bi’r Zikrīt) lies on a limestone plateau on the western edge of an oasis depression and within a kilometre of the present coastline. De Cardi (1978, p.115) noted that the site at Bir Zeikrit, unlike modern nomadic encampments in the area, is not located directly adjacent to the water hole. Kapel’s

Site A4, 7km south of Dukhan, lies on a sandy level about 100 yards from the coast (Kapel, 1967, p.37). Al-Dasah (al-Da'sah) lies on the seaward headland of a low terrace, probably an ancient beach, overlooking sabkha (De Cardi, 1978, p.55). De Cardi suggested that the site location was mainly influenced by the availability of fresh water, but also noted that the site overlooks a protected sandy bay (1978, p.72). Al-Khor (al-Khawr) lies on top of fossil cliffs overlooking the sabkha to the north (Tixier, 1980). Wadi Debayan (Wādī al-Ḏabā'yān) lies on the leeward side of a peninsula, above the 3m contour. The wadi mouth may once have been navigable, providing direct access to the sea. This site is of particular relevance to the seabed characterisation since the wadi discharges into the Bay of Al-Zubārah, in close proximity to the Study Area (Cuttler et al., 2011a, Tetlow et al., Forthcoming). A possible extension to the present-day wadi has been tentatively identified in the topographic surface model to the east of the Ras 'Ushayriq peninsula, again emphasising the significance and potential of this area of the submerged landscape.

Outside Qatar, the topographic locations of important 'Ubaid-related sites on the Gulf coast generally follow the pattern observed on the sites in Qatar, although there are exceptions. The site at al-Markh, currently on the west coast of Bahrain, 1km from the present-day coastline and 2m above the current sea level, was an island during the 'Ubaid-related occupation period. There are now extensive areas of sabkha to the north and east (Roaf, 1976, p.146). Dosariyah (Dawsāriyyah), in Saudi Arabia, is located 1.5 km from the present-day coast, within an extensive valley-like trough, and it opens towards the south to the sabkhat al-Şumm (Drechsler, 2011, p.71). According to Masry (1997) the original ground of the site before occupation would

have been an east-facing, gently-sloping hill. As-Sabiyah H3 in Kuwait lies on the inland edge of a peninsula close to the coast, the bay between the peninsula and the mainland now infilled with sabkha. The geomorphological evidence indicates that the sea could be directly accessed from the site during the ‘Ubaid-related occupation period (Carter and Crawford, 2010). The recently-excavated site at Bahra 1 in Kuwait has a less clear relationship with coastal features. It is located in a former active dune field and is 8km from the present coastline, although the distance to the coast would have been much shorter during the Mid-Holocene sea-level high (Rutkowski, 2011).

This brief overview of topographic characteristics of a few selected ‘Ubaid-related sites is far from comprehensive, and needs to be supplemented with detailed, localised site topography in order to establish a comprehensive picture. However, this emphasises how important it is that potential coastal features such as former bays, spits, promontories and drainage channels were identified as part of the characterisation, and the critical importance, therefore, of targeting further investigations in the area of these putative former shorelines.

The close interaction of environmental and cultural factors in seabed characterisation is well demonstrated by the issue of the location of submerged Karst landscapes and their relationship to archaeological potential. The QNHER national cultural mapping program has demonstrated that the distribution of Karst depressions was a significant factor in the location of settlement until very recent times (Breeze et al., 2011). The depressions and holes caused by Karst are an important feature of the present day

terrestrial northern Qatari landscape, tending to occur as sinkholes, simple depressions or compound depressions, some of which can be very large – up to 3km across and more than 25m deep (Sadiq and Nasir, 2002). The Misfer cave (Figure 101), an open cave 40km to the west of Doha, is up to 100m in depth. It is almost certain that the submerged areas between Qatar and Bahrain will have contained Karst features, since drowned Karst is typical along all carbonate coasts except those where there has been rapid tectonic uplift (Ford and Williams, 2007, p.430). Research into submerged Karst landscapes in the Gulf of Mexico has indicated that as well as isolated depressions, many sinkholes occur in linear clusters, forming discontinuous river channel segments (Faught and Donoghue, 1997). Most Karst features in Qatar show northeast-southwest and northwest-southeast orientations, governed by the joints and fractures formed during periods of uplift (Sadiq and Nasir, 2002).



Figure 101 Misfer Cave, Qatar.

The features typical of Karst landscapes, such as springs, sinkholes, depressions and caverns, would have provided very attractive habitats for Prehistoric communities. These features are likely to have had significance for both pragmatic reasons, including access to water and to the more fertile soil (rawdha) that accumulated in the depressions caused by the collapsed Karst features, and for symbolic reasons such as places to bury the dead, or make ritual deposits. On land, these same features tend to preserve and protect evidence for human activity, making them highly significant in archaeological and palaeoenvironmental terms. By analogy, investigating drowned and sediment filled sinkholes on the seabed should substantially increase our chances of finding *in situ* archaeological and palaeoenvironmental deposits (Faught and Donoghue, 1997).

It was considered possible that larger Karst-related features may still be visible on the seabed in the Study Area, possibly appearing as depressions or holes, depending on the sedimentation regime in particular areas. The identification of potential drowned Karst features (the possible solution hollows) in the surface model created from the bathymetry during this research is therefore a particularly exciting development, since finding features of high archaeological and palaeoenvironmental potential such as these was one of the primary aims of the research, and up until now, no such features had been identified in this area of the Arabian Gulf. Whilst further work is required to establish a firm identification of these hollows as a submarine extension of the terrestrial Karst landscape of Northern Qatar, this is certainly a very encouraging baseline from which to start working.

The location of freshwater springs in the submerged landscape is also closely related to cultural factors and archaeological potential. The well-documented occurrence of submarine springs in Karst environments may be associated with springs that developed during times of lower sea levels (Ford and Williams, 2007, p.141). The area around Qatar is the terminus of several aquifers that have a wide catchment area across the Arabian Peninsula, emerging as freshwater springs in the Gulf. Previous research suggests that there is a direct relationship between sea levels and coastal freshwater springs, whereby falling sea levels caused an increase of hydraulic pressure within underground aquifers, causing more fresh water to flow through them and leading to the creation of springs on the exposed coastal shelf, and hence an increase in freshwater at the coast - the 'Coastal Oasis' theory (Faure et al., 2002; Parker and Rose, 2008). These springs can remain active once sea levels rise if there is enough hydraulic pressure from the inland aquifers.

There is plenty of evidence for active submarine freshwater springs in the Mediterranean Sea and the Red Sea (Faure), and in the Arabian Gulf off Bahrain. Church (1996, p.579) reports anecdotal evidence of ancient seafarers restocking their freshwater sources from upwelling plumes that occurred offshore in parts of the world that have limestone terrains, including the Arabian Gulf. Cheesman (1923) visited Bahrain in the 1920s and noted that boats were able to replenish their drinking water from a submarine freshwater spring. As late as the 1950s, a submarine spring located a few miles north of Jubail in Saudi Arabia, from which divers would collect freshwater in skins, was marked by a spar buoy (Bowen, 1951, p.173-174). Submarine freshwater springs are also known from areas of drowned Karst in other

parts of the world, including along the Dinaric Coast of the Adriatic Sea and in New Zealand (Ford and Williams, 2007, p.434).

Research in the Baltic sea has utilised sub-bottom profiling and sediment analysis to understand the formation process of features known as 'Pockmarks', or elongated depressions approximately 1 to 3 m below adjacent seafloor levels, which could potentially be associated with the location of submarine groundwater discharge from sub-seafloor aquifers (Schlüter et al., 2004; Alfred Wegener Institute, 2012). The location of submarine freshwater springs, whether inactive or current, is a highly significant factor when assessing areas of archaeological potential in the submerged landscape off Qatar, since a relatively abundant freshwater supply would have been critical for human settlement during the Early Holocene. This makes the exploration of former shorelines even more significant, given that the evidence suggests that freshwater supplies would have been concentrated at the coast during sea level low-stands. A combination of sub-bottom profiling, and information about water salinity targeted around the putative former shorelines provides a promising methodology for the location of seabed springs off Qatar. A CTD (conductivity, temperature, depth) scanner could provide useful information on water salinity close to the seabed, which may help to identify freshwater discharge from submarine aquifers, and possibly the locations of former sub-aerial springs. However, this would be a very time-consuming method to undertake over large areas, and it may be more useful and cost-effective to examine satellite imagery for evidence of sea surface temperature hotspots (Personal Communication, Richard Bates, 2015).

The levels of potential assigned to most of the character areas relate more to palaeoenvironmental potential than to the potential for finding archaeological sites. This is because the evidence suggests that the sedimentation is so thick in parts, particularly in the deep channel in the north of the Study Area, that there would be no prospect of being able to undertake archaeological excavations in those areas. Also, the borehole data from the central part of the Study Area demonstrated that there are layers of caprock within the marine sediments in this area. Submarine lithification is common around shallow sub-tidal rock around the west coast of Qatar (Marin Mätteknik AB, 2002, p.42), and although archaeological remains could lie preserved underneath this caprock, they could be difficult to locate or investigate further.

Although we don't currently have any evidence for the presence of terrestrial sediments in the submerged landscape, it is clear that more needs to be understood about the sedimentary processes that occurred during marine transgression, in order to ascertain whether these processes would have been likely to have preserved rather than eroded the palaeo-landscape (Westley, 2011a). Recent terrestrial coring work and excavations at Wadi Debayan, lying inland on a palaeo-shoreline to the southeast of the Ras 'Ushayriq Peninsula, revealed evidence of marine deposits that were laid down after 4,500 BP, when sea levels were higher than present day levels, and the site was submerged. These marine deposits were overlying earlier archaeological and palaeoenvironmental deposits, and the nature of the marine deposits, which included a layer of large beach cobbles, was indicative of a high-energy marine event (Figure 102).

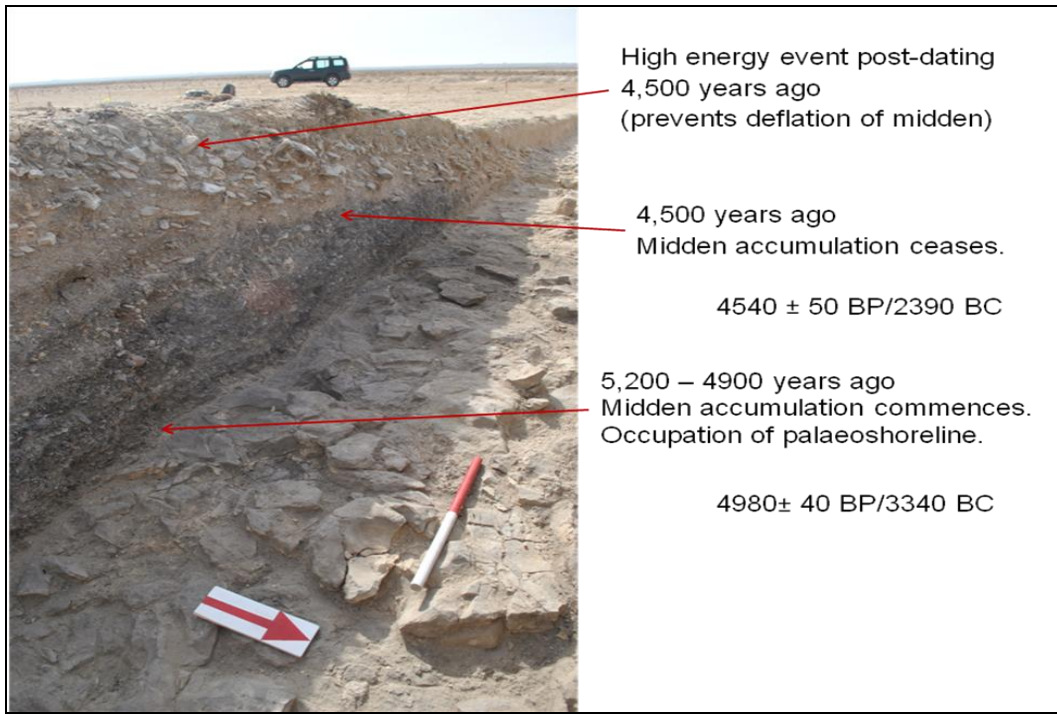


Figure 102 Evidence for archaeological deposits preserved beneath marine deposits at Wadi Debayan  
(Image by Richard Cuttler/Emma Tetlow).

This site clearly demonstrates that there are some environments and conditions where rapid inundation has actively preserved archaeological and palaeoenvironmental deposits under marine sediments (Tetlow et al., Forthcoming). The characterisation has demonstrated that there is significant potential within the currently-submerged landscape for targeting analogous locations, with similar landscape settings that would have been attractive for human settlement, and similar formerly-sheltered situations where protective deposition could have occurred. The general paucity of palaeoenvironmental remains from terrestrial sites in Qatar means that the palaeoenvironmental potential of the submerged landscape is of huge significance for filling the gap in knowledge.

The secondary characterisation has enabled issues of cause and effect to be explored, for example whether certain geophysical anomalies, or the lack of them, are a reflection of the usage of the maritime environment in a particular zone, or whether they are simply more, or less, visible because of the seabed type in that zone, which in turn provides significant information about archaeological potential. The sidescan sonar data shows a very pronounced concentration of geophysical anomalies of likely recent anthropogenic origin, probably cars, tyres etc, in the north of the Study Area, and the reasons for this could shed useful light on the visibility and preservation of certain types of material, and on recent human exploitation of the marine environment.

Parallels can be drawn elsewhere in the world, for example with the Red Bird artificial reef off the coast of Delaware in the USA. This reef is made up of over 900 New York City subway cars, and various other vehicles, decommissioned boats and other objects, covering 1.3 square nautical miles, and creating habitat for fish and other marine creatures (State of Delaware, 2012). This type of exploitation of the seabed has clearly also occurred in the sea off Qatar, although not officially, and not on the organised and extensive scale of the Red Bird Reef. The impact of these structures on the seabed includes changes to the sediment regime around the structures, and, in the case of the Red Bird Reef, increased abundance of marine flora and fauna.

Conversely, an area of extensive trawler-scarring is visible in the mosaic sidescan sonar data in the south of the Study Area, and very few geophysical anomalies are visible in this area. This also coincides with one of the deepest areas of seabed in the

Study Area. It is possible that the depth and character of the seabed in this area has influenced its use as trawler-fishing grounds. However, resolution No. 29 of 1994 of the Council of Ministers in Qatar prohibits fishing through trawling in Qatar waters, so either these scars pre-date 1994, or there has been illicit fishing occurring in this area. These different types of relatively recent marine exploitation have a significant effect on the seabed character, and possibly also on the archaeological potential of the locality.

The seabed characterisation has not really clarified the potential of the Study Area for locating shipwrecks, either historic or more recent. None of the geophysical anomalies identified and selected for further study could be demonstrated to relate to shipwreck debris other than the possibility of the concentration of debris in the west of Area 1 (Figure 82). However, expanding the seabed characterisation to encompass more cultural aspects, as discussed above (section 7.1), may illuminate this aspect of the character of the Study Area.

## **CHAPTER 8: CONCLUSION: IMPLICATIONS FOR RESEARCH AND MANAGEMENT OF THE MARINE HERITAGE RESOURCE**

Given how difficult and expensive it is to investigate submerged landscapes, it is valid to consider whether we should be doing it at all. However, given the significance and potential of the submerged landscape of the former Arabian Gulf basin, and of the Study Area within it, as emphasised in the discussion above, the question really should be *how* we should be doing it, not *whether* we should be doing it. Previous research has already highlighted the environmental and archaeological importance of the submerged landscape around Qatar, as an area that remained free from marine influence until relatively late, that had the potential for freshwater supplies in the form of coastal springs, and that lay in close proximity to known archaeological sites representing new settlements that emerged on the Mid-Holocene coast just after the final inundation. However, this landscape was considered to be unknown and inaccessible territory, and therefore has been largely unconsidered in the archaeological syntheses of the Early Holocene of the region until very recently. This seabed characterisation, together with the research carried out to the east of Qatar using seismic data (Cuttler, 2014), has demonstrated that the situation does not have to remain like this.

The characterisation was undertaken as a response to the need to address the major gap in knowledge about this highly significant landscape, and to address the fact that previous investigation methods clearly weren't working. One of the most significant results of the research is the progress that has been made towards utilising existing

datasets to their maximum potential and developing robust methodologies for the investigation of submerged landscapes in this region. It has successfully drawn on applications of historic landscape characterisation techniques and marine remote sensing techniques that have been used for studying submerged landscapes elsewhere in the world, as well as trialling new combinations of methodologies and datasets. Extensive experimentation and testing was required in order to establish which methods worked and which did not, as this particular combination of techniques and datasets has not been applied to submerged landscapes for the purposes of archaeological research before.

A major outcome from the research is the identification of broad areas of potential containing possible significant landscape features and extensive sedimentary deposits, indicating that there is potential for finding archaeological and palaeoenvironmental remains within the submerged landscape. Another major outcome is the provision of a framework within which to begin more detailed investigations, by highlighting areas of potential to target, and appropriate techniques to use for more detailed, finer-grained investigations. However, it is important to recognise that this research represents a very early stage in the investigation of the submerged landscape, and it is not expected that archaeological sites will be discovered immediately as a result of this research. However, we do know that the possibility exists for sites to be preserved, given the right conditions, and this research has started the process of maximising our chances of finding them. As has been discussed previously, there are limitations to the datasets that have been used, and there is considerable scope for further development of methodologies and

techniques, particularly as technology improves and more data becomes available. The seabed characterisation, like all landscape characterisations, is not a definitive statement of archaeological knowledge or potential of the Study Area. Rather, it should be treated as a way of representing and mapping broad patterns in the landscape based on the best evidence currently available, thus providing a structure to inform and stimulate further research. The characterisation model could, for example, be refined and improved upon with more datasets and further analysis, and used for exploring novel methods of archaeological predictive modelling, such as that undertaken in the North Sea by Fitch (2011). Better knowledge of the topography of the submerged landscape in the Study Area as a result of the seabed characterisation could also be utilised in wider regional studies, such as studies into patterns of human migration (Cuttler et al., 2012).

A sound research basis can facilitate informed decision making relating to the management of the marine historic environment, which can be applied beyond the Study Area. Also, as previously mentioned, landscape characterisation approaches lend themselves very well to combined applications for both the historic and the natural environment. The seabed character areas, and in particular the information about the seafloor topography, could be very useful for studies of the benthic habitat in the Study Area, which could feed into practical conservation strategies for the natural environment. This is very important in the submerged landscape off the coast of Qatar, as there are a range of pressures within this environment, including construction development such as the proposed Qatar-Bahrain Causeway, dredging for new ports, the creation of new land for tourism developments, and oil and gas

exploration. In this respect, the aims and achievements of the seabed characterisation fit within the wider context of the pioneering marine research work being carried out on behalf of the Qatar Museums Authority by the University of Birmingham's QNHER project.

Further research could lead ultimately to a point where it is realistic to search for submerged sites and palaeoenvironmental remains with a reasonable expectation of success. This seabed characterisation represents good progress towards this point, and it is hoped that it proves to be only the beginning of research into a more comprehensive understanding of the submerged landscape of the Arabian Gulf.

## APPENDIX 1: PROCESS AND PARAMETERS USED FOR THE ACOUSTIC CLASSIFICATION OF SIDESCAN SONAR DATA

**Reference system parameters for original survey data (from GEMS Qatar LLC 2008)**  
**Geodetic parameters**

<b>Working Spheroid</b>	<b>Working Projection</b>
Spheroid WGS '84	Grid Projection QBC2001
Datum WGS '84	Projection Type Transverse Mercator
Semi-major Axis (a) 6 378 137.000	Central Meridian 050°49' 00.000" E
Semi-minor Axis (b) 6 356 752.314	Latitude of Origin 25°00' 00.000" N
Inv. Flattening (1/f) 298.257 223 56	False Easting 400000.00
First Eccentricity (e2) 0.0066943800	False Northing 500000.00
	Scale Factor on CM 0.999996

**Datum Transformation Parameters from WGS84 To working spheroid**

<b>WGS84 Spheroid</b>	<b>WGS84 to Working Spheroid</b>
Spheroid WGS84	X shift (dX): N/A
Datum WGS84	Y shift (dY): N/A
Semi-major Axis (a) 6 378 137.000	Z shift (dZ): N/A
Semi-minor Axis (b) 6 356 752.314	X rotation (Rx): N/A
Inv. Flattening (1/f) 298.257 223 56	Y rotation (Ry): N/A
First Eccentricity (e2) 0.006 694 38	Z rotation (Rz): N/A
Second Eccentricity (e'2) 0.006 739 50	Scale correction (ppm): N/A

**Coordinate system used for data analysis**

WGS84 UTM39N

**Software used: Swathview and CLAMS (Quester Tangent Corporation)**

### TRIAL CLASSIFICATION

**Swathview (classification software)**

#### **Batch Processing**

- CLEAN - Sidescan Masking
  - Pick Bottom – None, left as original
  - Mask Water column – offset 5m
  - Angle - Max 90 degrees
  - Range - Relative 80%
  - Preserve Border edits – checked
- GENERATE RECTANGLES
  - Vessel speed - 4.4 knots
  - Ping rate - 5
  - Width \* height (m)
  - Width (samples) - 129

- Height (pings) - 17
- Sample rate - 9600
- GENERATE FEATURES
- Process file id 1

### **Features**

Merge FFV files  
Base FFV channel 1  
Merge channel 1

### **Create Catalogue**

FFV file id 1

### **Auto Cluster**

Select merged .dat.utm file  
Number of classes from 5 to 20  
5 iterations  
15,000 records per iteration  
Saved the relevant number of classes as .dat.utm

### **Clams (Interpolation software)**

#### **Interpolation**

Open the relevant .dat.utm file  
Check the coordinate system  
Node spacing = 5 for X and Y (makes it less pixellated the smaller the value)  
Search radius = 50 (joins up gaps if bigger)  
Search size = 40 (bigger produces less polygons)  
Create  
Save as: surfer  
Xyz  
Geotiff

### **ARGIS**

Open geotiff in ArcGIS (open the \_classes.tif)  
NB transformation problem – image is flipped and shifted on NW point  
Resolved by doing a flip to get it on the right orientation and then a shift on the y axis i.e. deducted values from the y coordinates (used data properties - min and max extents - of geotiff and of sonarwiz coverage files to establish what the shift needed to be. Shifted by -33573.69324 in y axis)  
Go to layer properties, symbology, unique values, build attribute table, alter background colour to clear, use field 'value'

### **FINAL CLASSIFICATION**

### **Swathview (Classification software)**

#### **Batch Processing**

- CLEAN - Sidescan Masking  
Pick Bottom – None, left as original  
Mask Water column – offset 5m

- Angle – 2 degrees min Max 70 degrees
- Range - Relative 60%
- Preserve Border edits – checked
- GENERATE RECTANGLES
  - Vessel speed - 0 knots
  - Ping rate - 0
  - Width \* height (m)
  - Width (samples) - 65
  - Height (pings) - 33
  - Sample rate - 9600
- GENERATE FEATURES
  - Process file id 1

### **Features**

Merge FFV files  
 Base FFV channel 1  
 Merge channel 1

### **Create Catalogue**

FFV file id 1

### **Auto Cluster**

Select merged .dat.utm file  
 Number of classes from 5 to 20  
 5 iterations  
 15,000 records per iteration  
 Saved the relevant number of classes as .dat.utm

### **Clams (interpolation software)**

#### **Interpolation**

Open the relevant .dat.utm file  
 Check the coordinate system  
 Node spacing = 5 for X and Y (makes it less pixelated the smaller the value)  
 Search radius = 100 (joins up gaps if bigger)  
 Search size = 100 (bigger produces less polygons)  
 Create  
 Save as: Geotiff

### **Files used for test areas for both trials**

Area3  
 20080724030952.xtf  
 20080724042616.xtf  
 20080724055140.xtf  
 20080724072234.xtf  
 20080724084848.xtf  
 20080724101218.xtf  
 20080724113257.xtf  
 20080724124624.xtf

**Area4**

20080726100849.xtf  
20080726043129.xtf  
20080726051534.xtf  
20080726055735.xtf  
20080726071558.xtf  
20080726073821.xtf  
20080726082638.xtf  
20080726090147.xtf  
20080726092620.xtf  
20080726105338.xtf  
20080726113249.xtf  
20080726121658.xtf  
20080726130112.xtf  
20080726063909.xtf

**Data Issues**

Files excluded from classification due to problems in loading into Swathview:

20080709064910.xtf

Files excluded from classification due to problems in Swathview processing:

20080703042933.xtf  
20080703121350.xtf  
20080709093527.xtf  
20080709194757.xtf

## APPENDIX 2: PROCESS AND PARAMETERS USED FOR PROCESSING THE LIDAR BATHYMETRY DATA

**Datums used for the LiDAR Survey** (information provided with the data supply)

Horizontal: WGS84

Vertical: QCD which lies 0.88m below QVD (MSL at Doha Port)

### **Coordinate system used for data analysis**

WGS84 UTM39N

### **Software used: ArcGIS (ESRI Inc.)**

#### Step 1: convert ASCII to 3D feature.

3D analyst/Conversion/From file

Output to point

Use -1 to reverse the z values (this is because in xyz data, drying heights are negative and depths below sea level are positive, so both had to be reversed)

Projection set as UTM39N

#### Step 2: append z info

3D analyst/3D features/Add Z information. Check output property Z

#### Step 3: Append Point files together

Data management tools/general/append

#### Step 4: Interpolate surface

3D analyst/Raster interpolation/Natural neighbour

Select z value field and cell size (Both 7m and 2m resolution)

Visualise using Stretch and Invert values

#### Step 5: Hillshade

3D analyst/Raster surface/Hillshade

Leave defaults unchanged (model shadows unchecked, azimuth 315 altitude 45) apart from set z factor to required exaggeration value

**Points Used to Shift Bathymetry Data (based on coast shapefile )**

<b>Area</b>	<b>Bathy X</b>	<b>Coast X</b>	<b>Shift X</b>	<b>Bathy Y</b>	<b>Coast Y</b>	<b>Shift Y</b>
North	499228.175	499307.51	79.335	2873894.052	2873813.575	80.477
North	499788.509	499867.091	78.582	2873443.491	2873364.116	79.375
North	508438.557	508523.245	84.688	2883591.301	2883499.971	91.33
North	503941.48	504021.084	79.604	2880717.915	2880638.314	79.601
<b>Average Shift North Area</b>			<b>+80.55</b>			<b>-82.69</b>
Middle	496773.595	496837.095	63.5	2861453.369	2861381.931	71.438
Middle	495551.764	495635.511	83.747	2857387.52	2857296.296	91.224
Middle	479798.61	479879.044	80.434	2823655.11	2823581.026	74.084
<b>Average Shift Middle Area</b>			<b>+75.89</b>			<b>-78.92</b>
South	476984.466	477062.041	77.575	2822519.302	2822441.727	77.575
South	475589.916	475673.102	83.186	2810301.592	2810223.525	78.067
South	475824.075	475907.737	83.662	2803880.432	2803805.67	74.762
South	478892.997	478981.107	88.11	2774132.514	2774048.409	84.105
<b>Average Shift South Area</b>			<b>+83.06</b>			<b>-78.62</b>

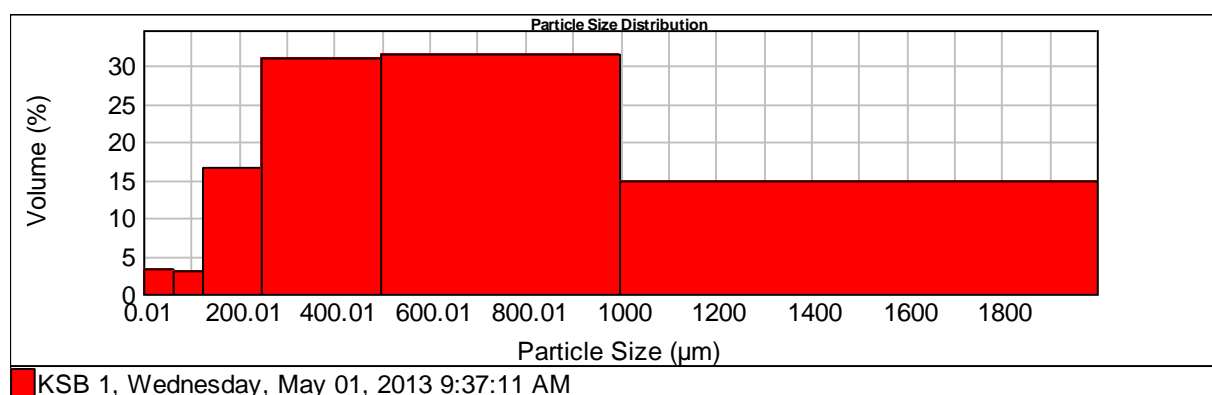
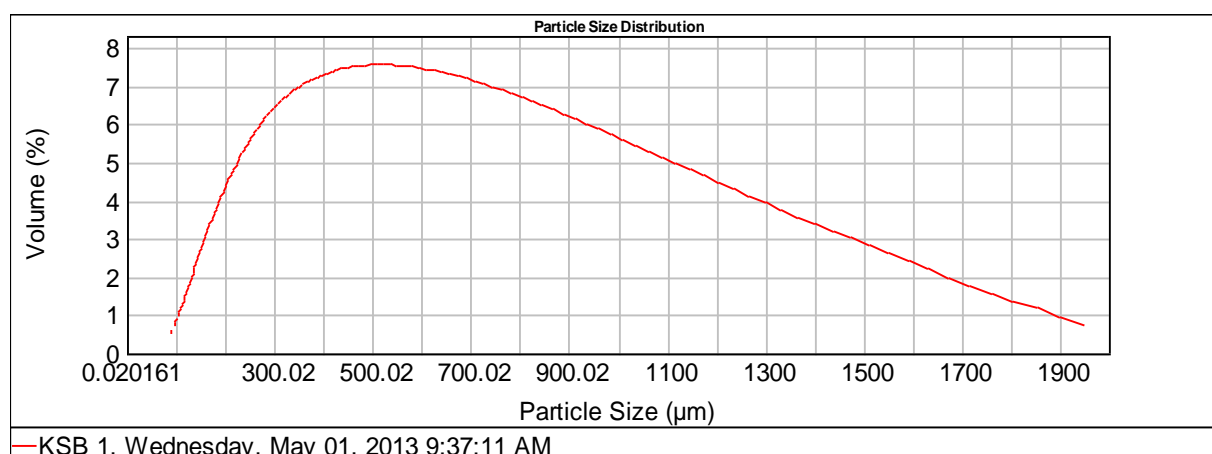
## **APPENDIX 3: GRAB SAMPLE GRAIN SIZE ANALYSIS REPORT**

By Ismail Mahmoud Al-Shaikh, Abdul Rahman Al-Obaidly and Abdel Rahman Sorour, Environmental Studies Centre, Qatar University.

## Particle Size Range and Sediment Type

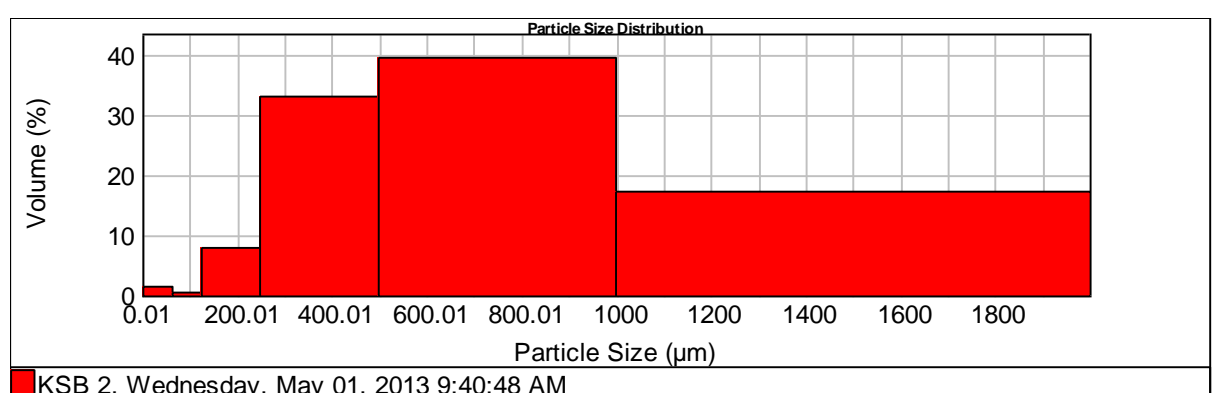
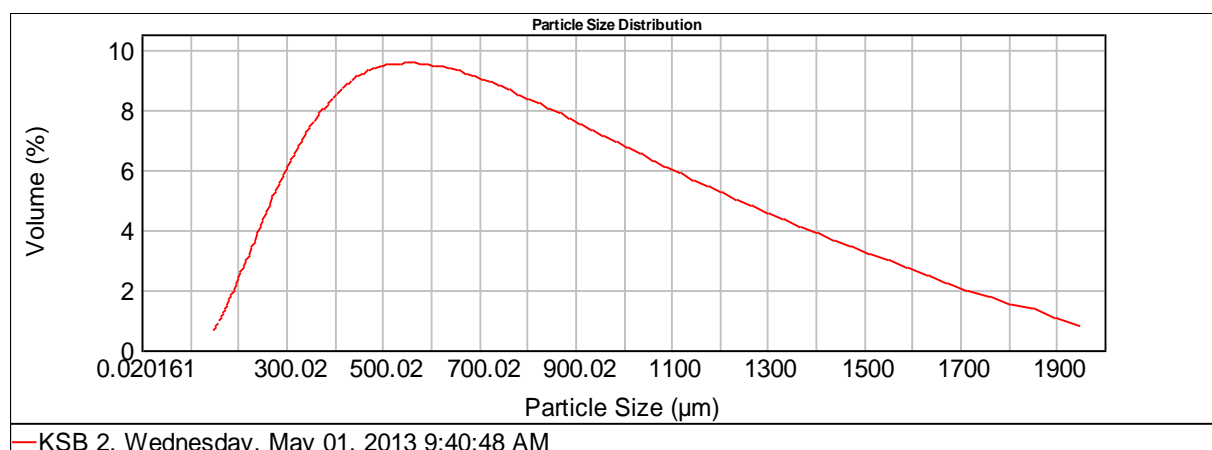
Particle Size Range ( $\mu\text{m}$ )	Sediment Type
0.02 – 4.0	Clay
4.0 – 63.0	Silt
63.0 – 125.0	Very fine sand
125.0 – 250.0	Fine sand
250.0 – 500.0	Medium sand
500.0 – 1000.0	Coarse sand
1000.0 – 2000.0	Very coarse sand

Sample No. 1



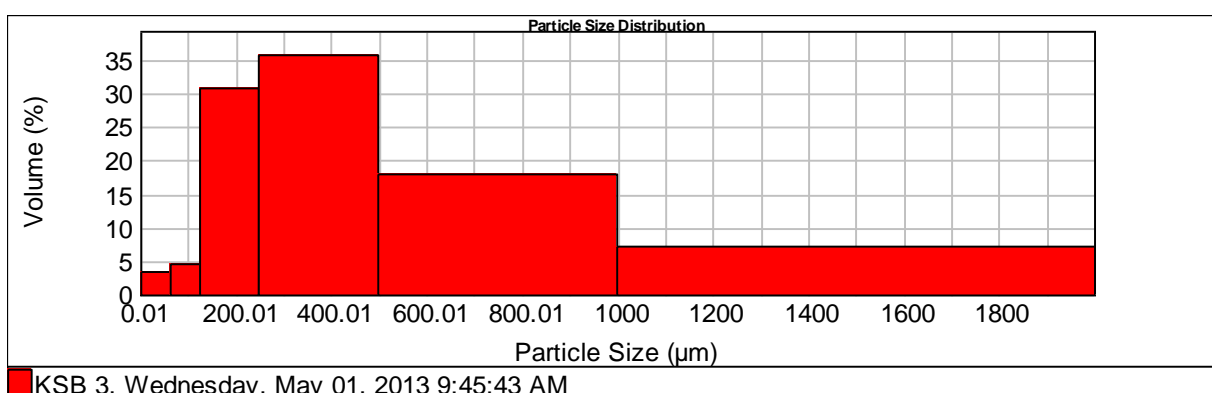
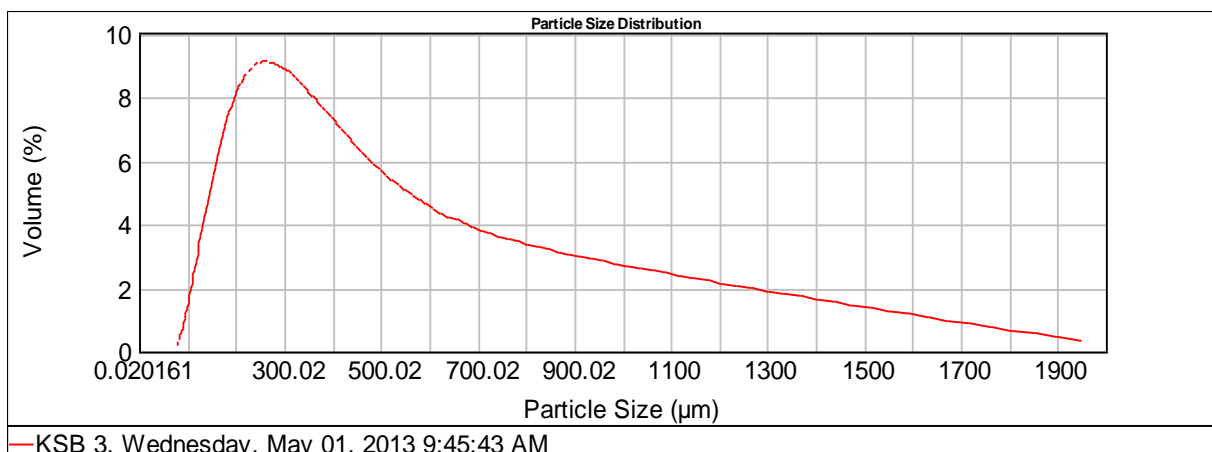
Size ( $\mu\text{m}$ )	Volume In %	Size ( $\mu\text{m}$ )	Volume In %	Size ( $\mu\text{m}$ )	Volume In %	Size ( $\mu\text{m}$ )	Volume In %
0.010	0.00	63.000	2.95	250.000	31.04	1000.000	
4.000	3.10	125.000	16.56	500.000	31.54	2000.000	14.81
63.000		250.000		1000.000			

Sample No. 2



Size ( $\mu\text{m}$ )	Volume ln %	Size ( $\mu\text{m}$ )	Volume ln %	Size ( $\mu\text{m}$ )	Volume ln %	Size ( $\mu\text{m}$ )	Volume ln %
0.010	0.00	63.000	0.36	250.000	33.19	1000.000	17.29
4.000	1.42	125.000	8.01	500.000	39.73	2000.000	
63.000		250.000		1000.000			

Sample No. 3



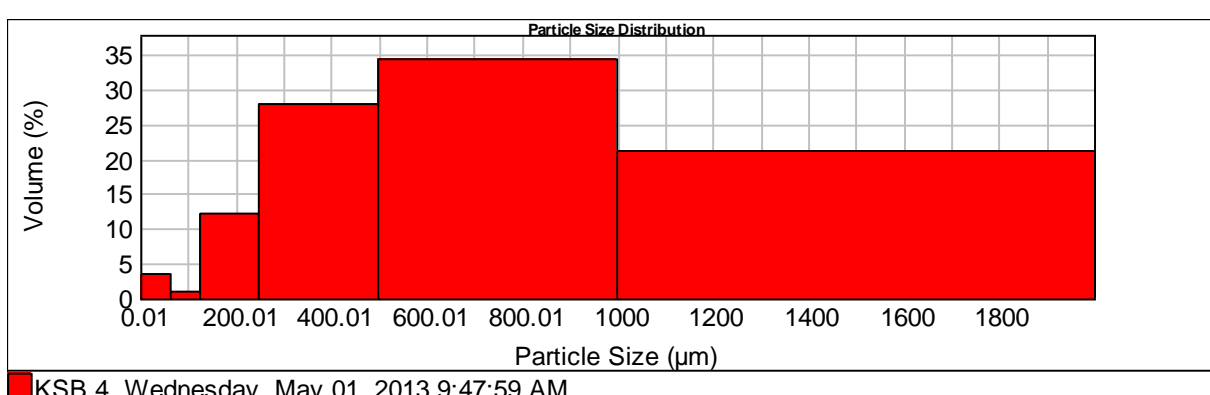
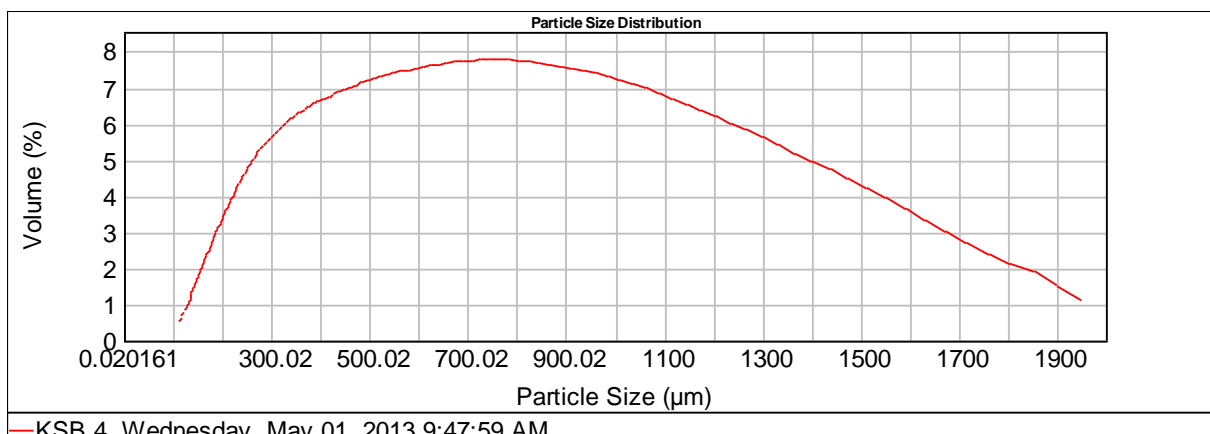
Size ( $\mu\text{m}$ )	Volume In %
0.010	0.07
4.000	3.43
63.000	

Size ( $\mu\text{m}$ )	Volume In %
63.000	4.65
125.000	30.90
250.000	

Size ( $\mu\text{m}$ )	Volume In %
250.000	35.80
500.000	17.96
1000.000	

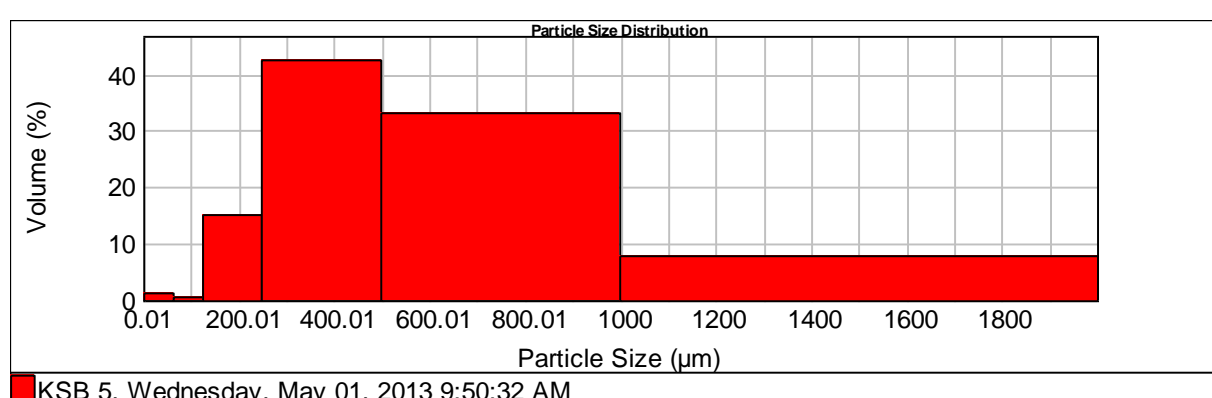
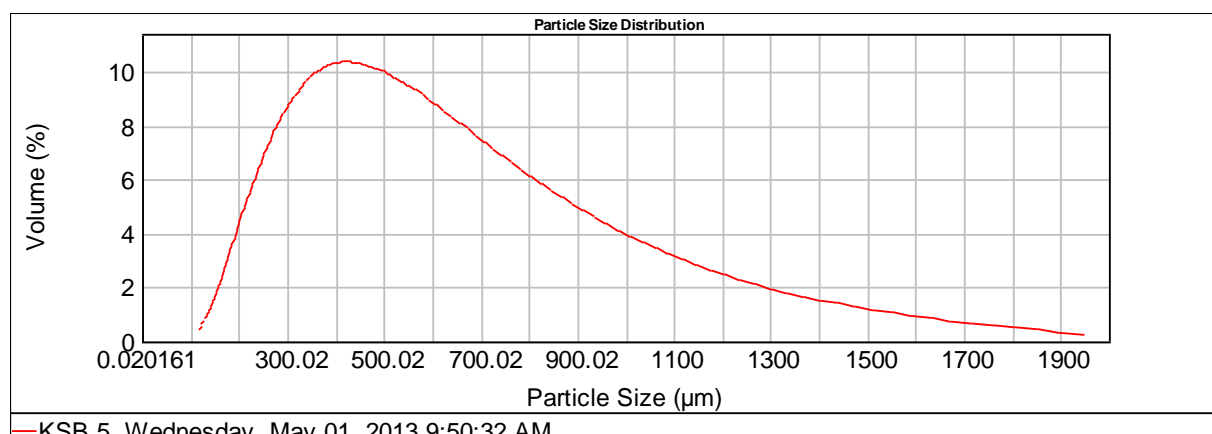
Size ( $\mu\text{m}$ )	Volume In %
1000.000	
2000.000	7.20

Sample No. 4



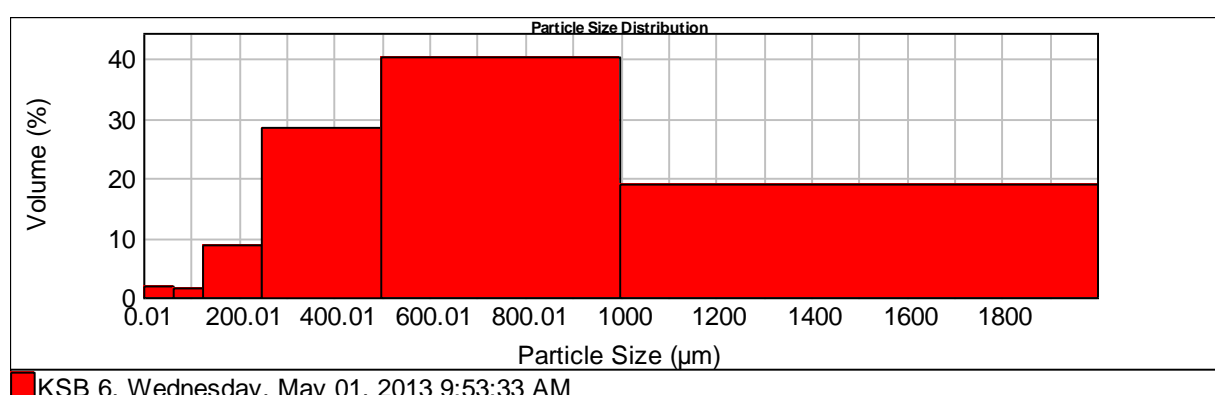
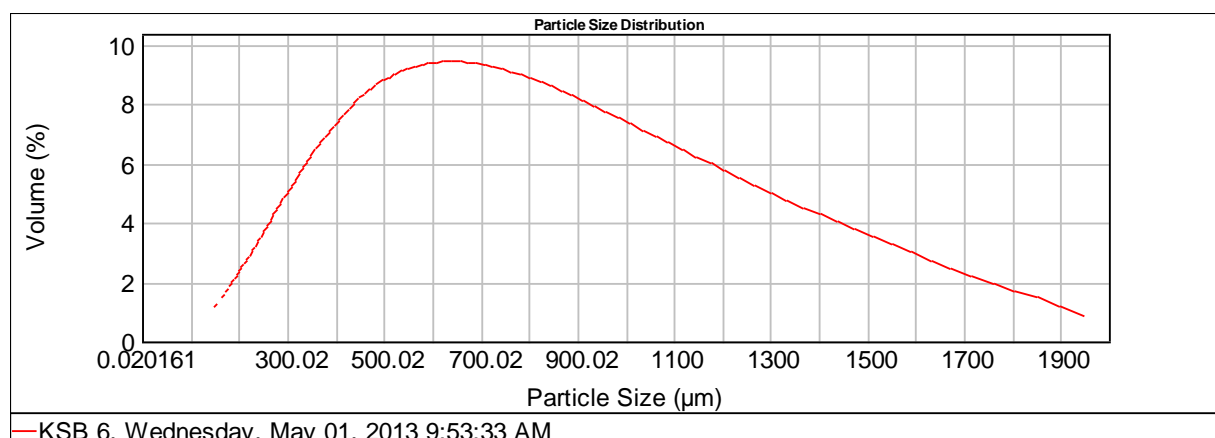
Size ( $\mu\text{m}$ )	Volume In %	Size ( $\mu\text{m}$ )	Volume In %	Size ( $\mu\text{m}$ )	Volume In %	Size ( $\mu\text{m}$ )	Volume In %
0.010	0.00	63.000	1.03	250.000	27.93	1000.000	20.98
4.000	3.45	125.000	12.28	500.000	34.33	2000.000	
63.000		250.000		1000.000			

Sample No. 5



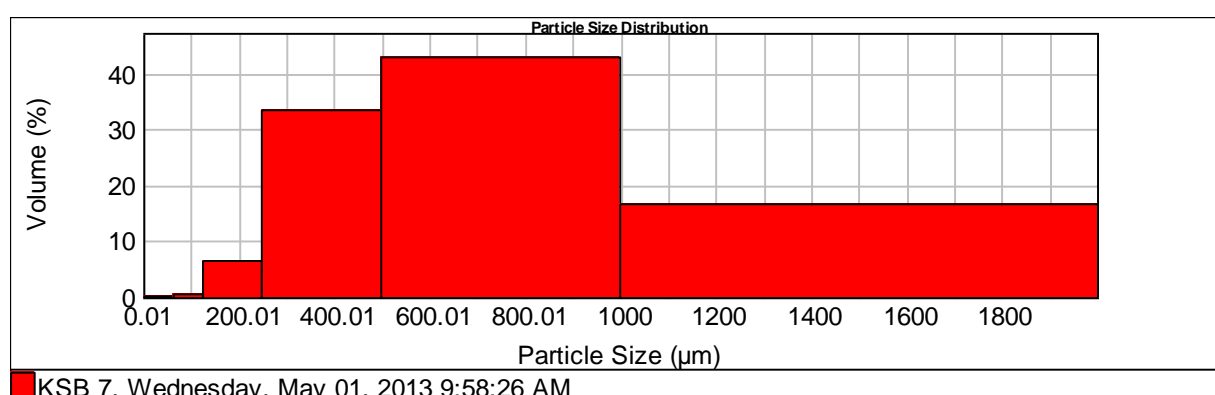
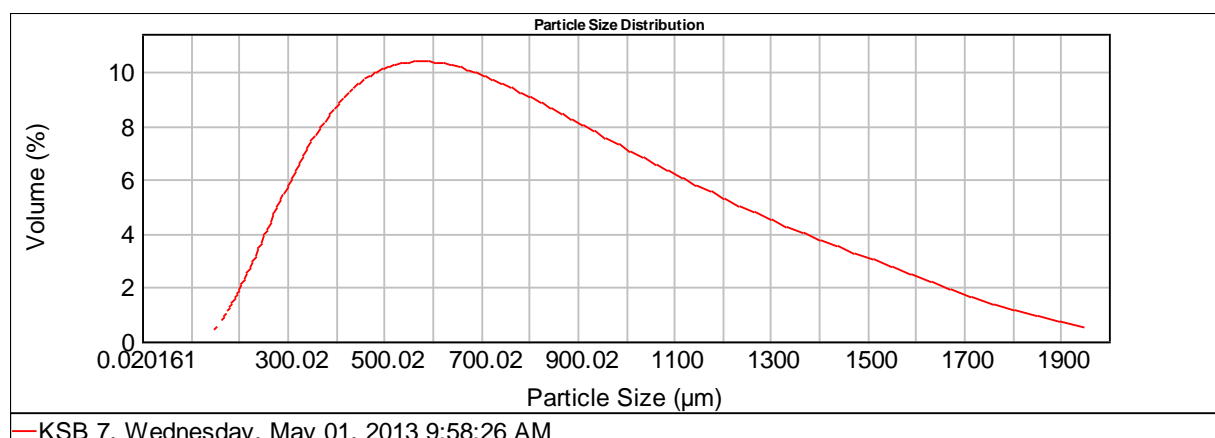
Size (μm)	Volume In %						
0.010	0.00	63.000	0.45	250.000	42.53	1000.000	7.67
4.000	1.32	125.000	15.05	500.000	32.98	2000.000	
63.000		250.000		1000.000			

Sample No. 6



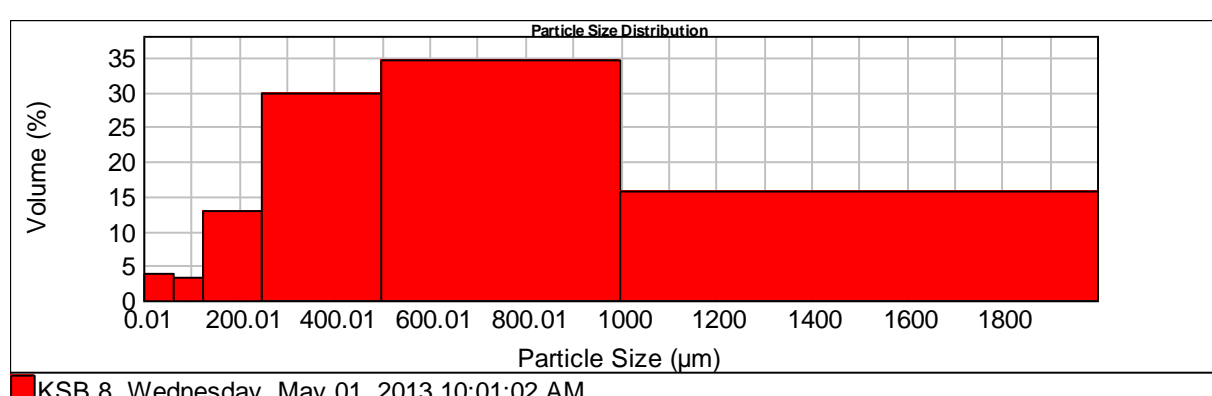
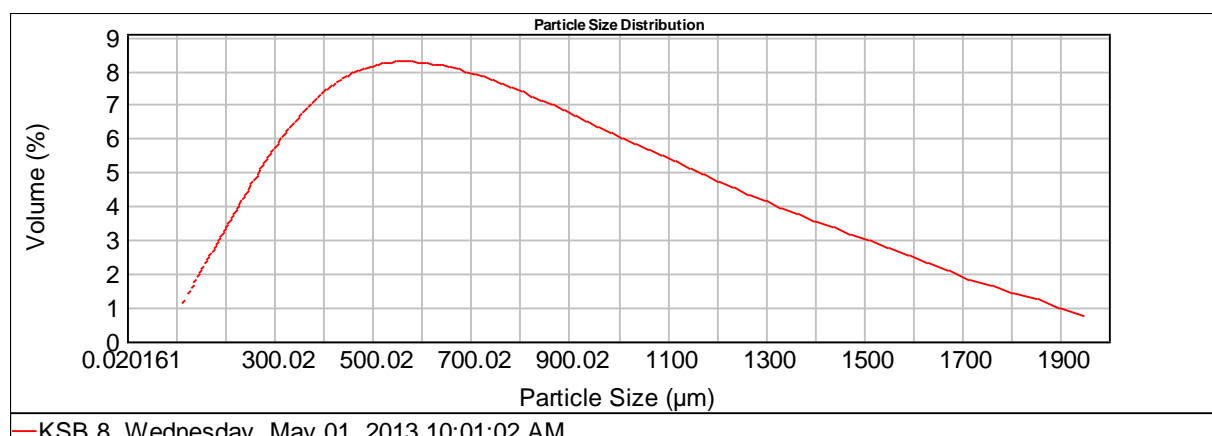
Size ( $\mu\text{m}$ )	Volume In %	Size ( $\mu\text{m}$ )	Volume In %	Size ( $\mu\text{m}$ )	Volume In %	Size ( $\mu\text{m}$ )	Volume In %
0.010	0.00	63.000	1.57	250.000	28.60	1000.000	18.89
4.000	1.85	125.000	8.71	500.000	40.38	2000.000	
63.000		250.000		1000.000			

Sample No. 7



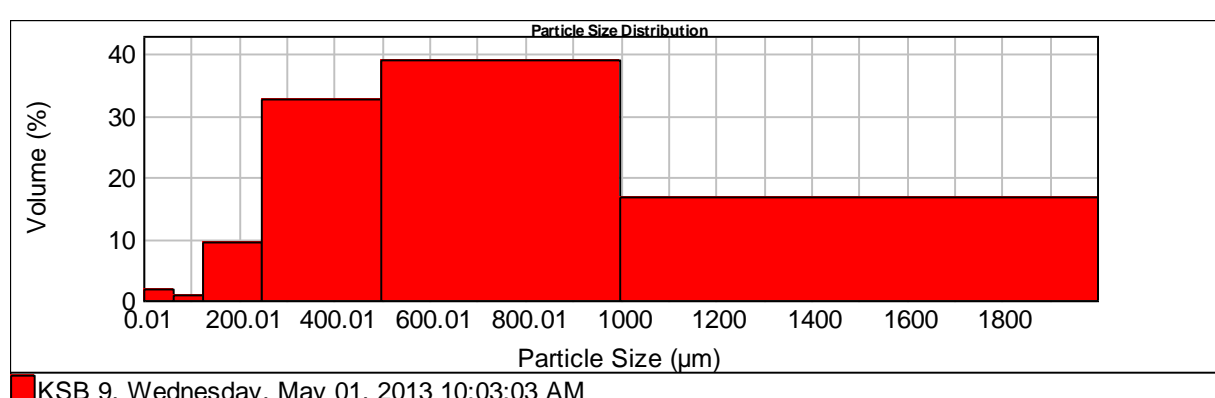
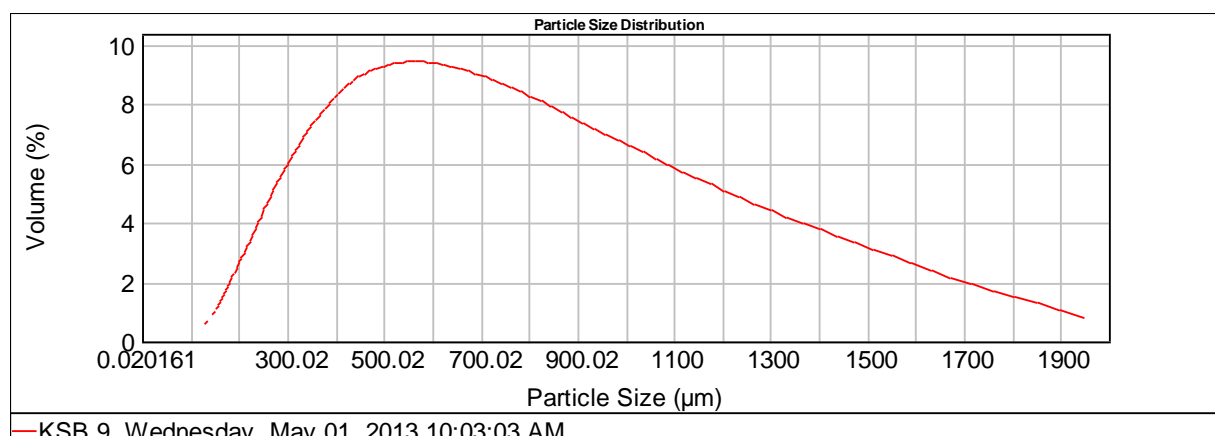
Size ( $\mu\text{m}$ )	Volume In %	Size ( $\mu\text{m}$ )	Volume In %	Size ( $\mu\text{m}$ )	Volume In %	Size ( $\mu\text{m}$ )	Volume In %
0.010	0.00	63.000	0.40	250.000	33.20	1000.000	16.70
4.000	0.31	125.000	6.51	500.000	42.87	2000.000	
63.000		250.000		1000.000			

Sample No. 8



Size ( $\mu\text{m}$ )	Volume In %	Size ( $\mu\text{m}$ )	Volume In %	Size ( $\mu\text{m}$ )	Volume In %	Size ( $\mu\text{m}$ )	Volume In %
0.010	0.06	63.000	3.19	250.000	29.82	1000.000	15.67
4.000	3.80	125.000	12.82	500.000	34.63	2000.000	
63.000		250.000		1000.000			

Sample No. 9



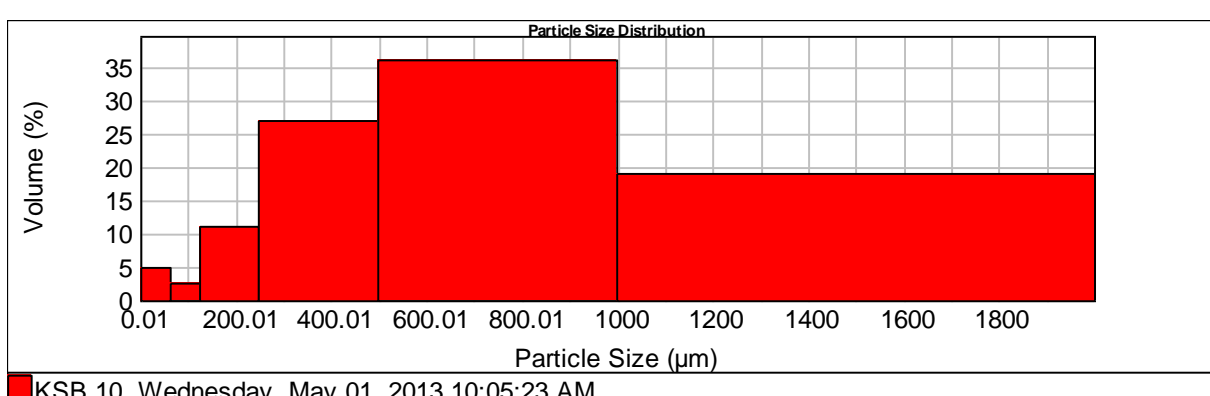
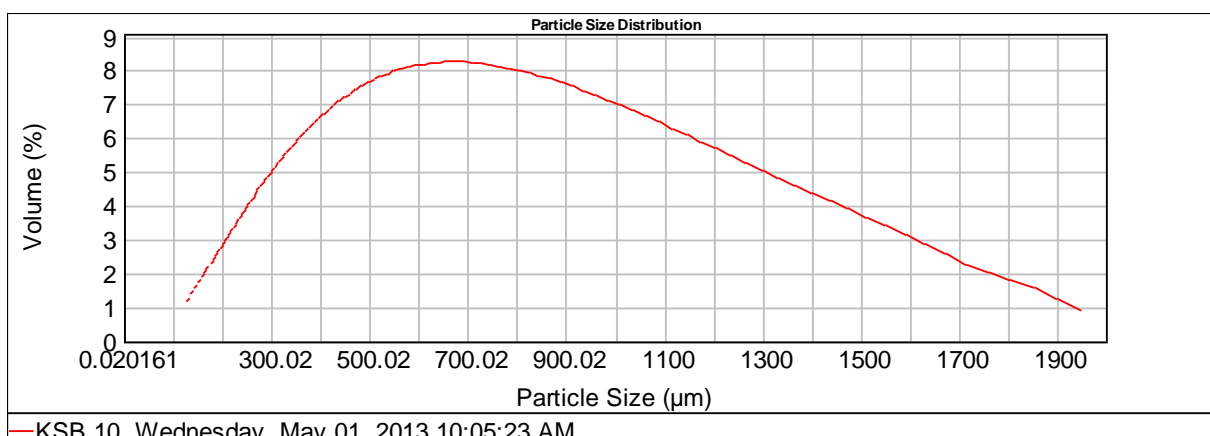
Size ( $\mu\text{m}$ )	Volume In %
0.010	0.00
4.000	1.81
63.000	

Size ( $\mu\text{m}$ )	Volume In %
63.000	0.76
125.000	9.27
250.000	

Size ( $\mu\text{m}$ )	Volume In %
250.000	32.50
500.000	38.99
1000.000	

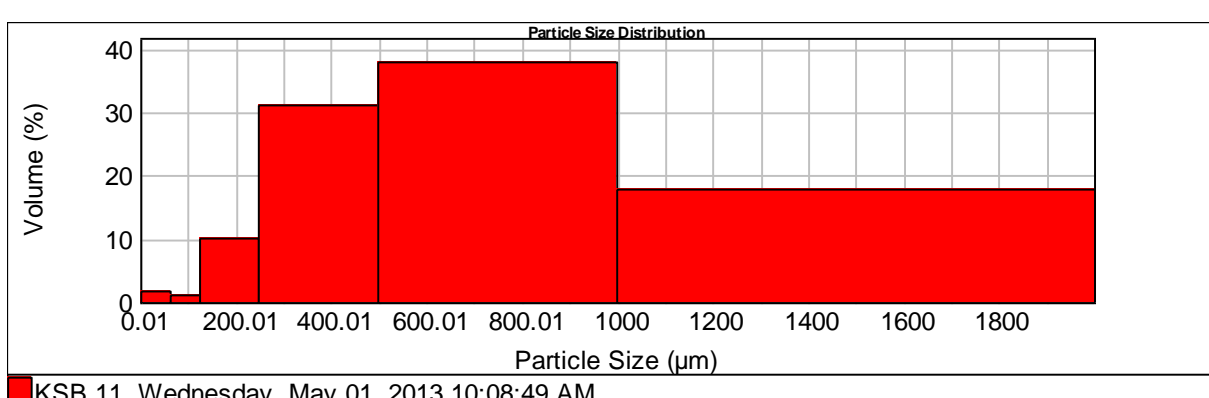
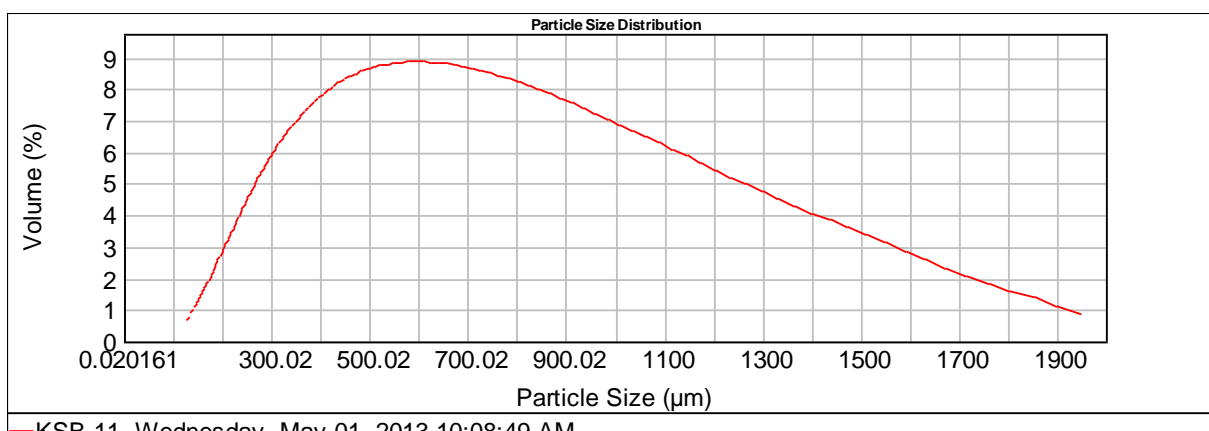
Size ( $\mu\text{m}$ )	Volume In %
1000.000	16.68
2000.000	

Sample No. 10



Size ( $\mu\text{m}$ )	Volume In %	Size ( $\mu\text{m}$ )	Volume In %	Size ( $\mu\text{m}$ )	Volume In %	Size ( $\mu\text{m}$ )	Volume In %
0.010	0.07	63.000	2.64	250.000	26.77	1000.000	18.94
4.000	4.71	125.000	10.86	500.000	36.00	2000.000	
63.000		250.000		1000.000			

Sample No. 11



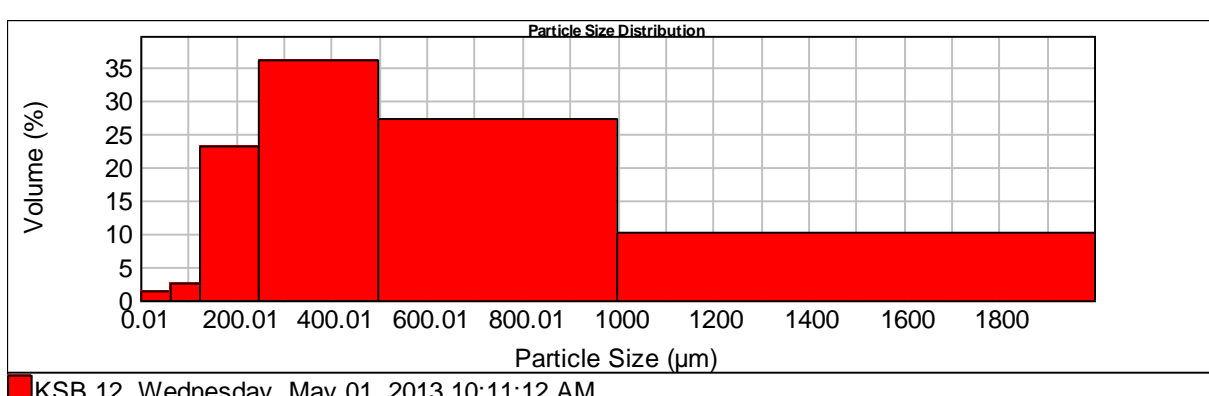
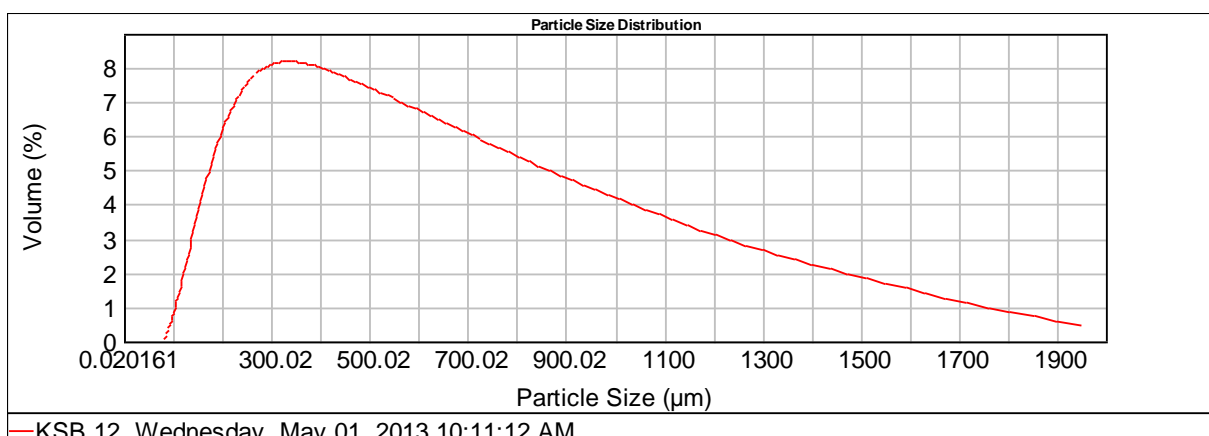
Size ( $\mu\text{m}$ )	Volume In %
0.010	0.00
4.000	1.82
63.000	

Size ( $\mu\text{m}$ )	Volume In %
63.000	0.98
125.000	10.19
250.000	

Size ( $\mu\text{m}$ )	Volume In %
250.000	31.20
500.000	37.94
1000.000	

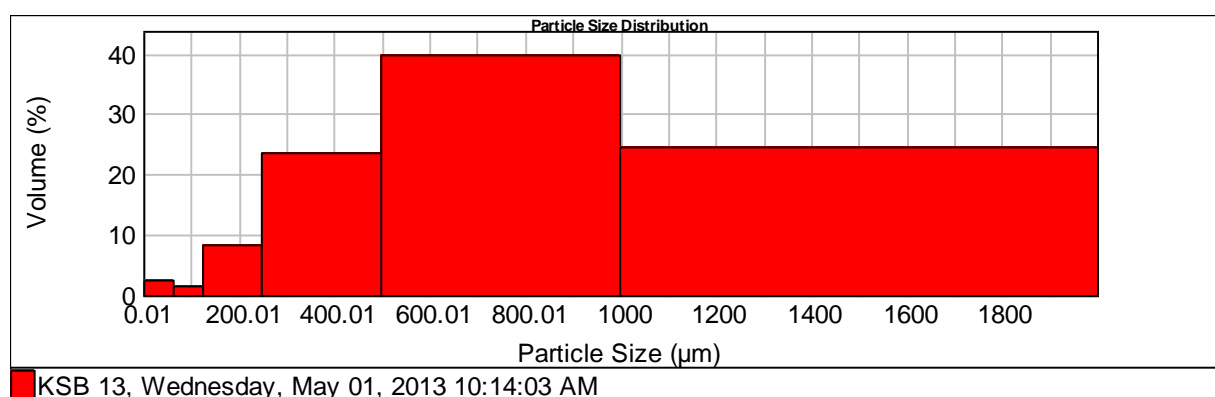
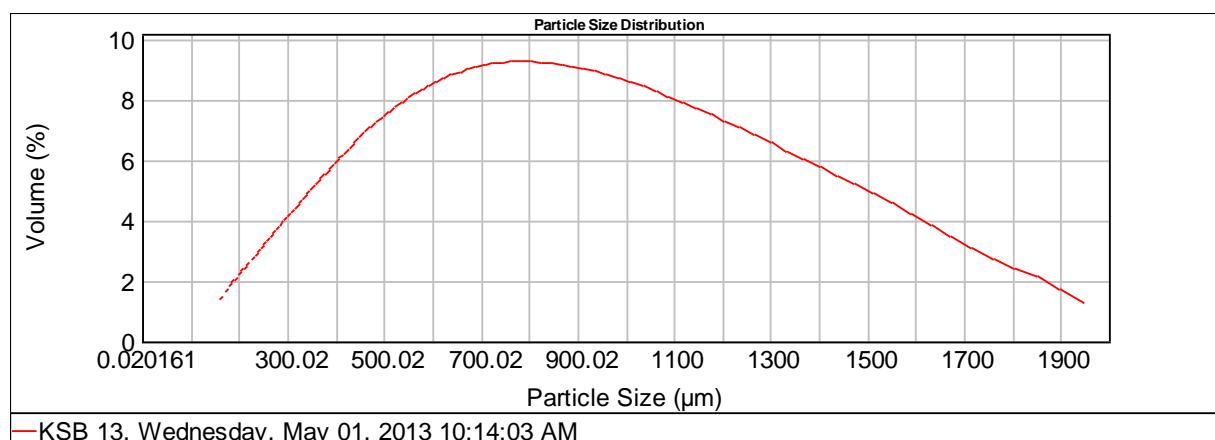
Size ( $\mu\text{m}$ )	Volume In %
1000.000	
2000.000	17.86

Sample No. 12



Size ( $\mu\text{m}$ )	Volume In %	Size ( $\mu\text{m}$ )	Volume In %	Size ( $\mu\text{m}$ )	Volume In %	Size ( $\mu\text{m}$ )	Volume In %
0.010	0.00	63.000	2.57	250.000	35.96	1000.000	
4.000	1.32	125.000	23.00	500.000	27.01	2000.000	10.13
63.000		250.000		1000.000			

Sample No. 13



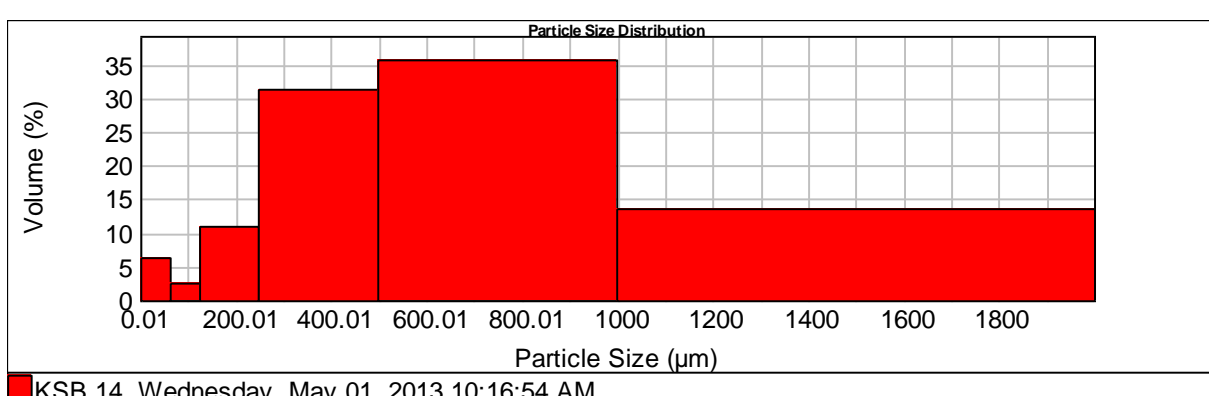
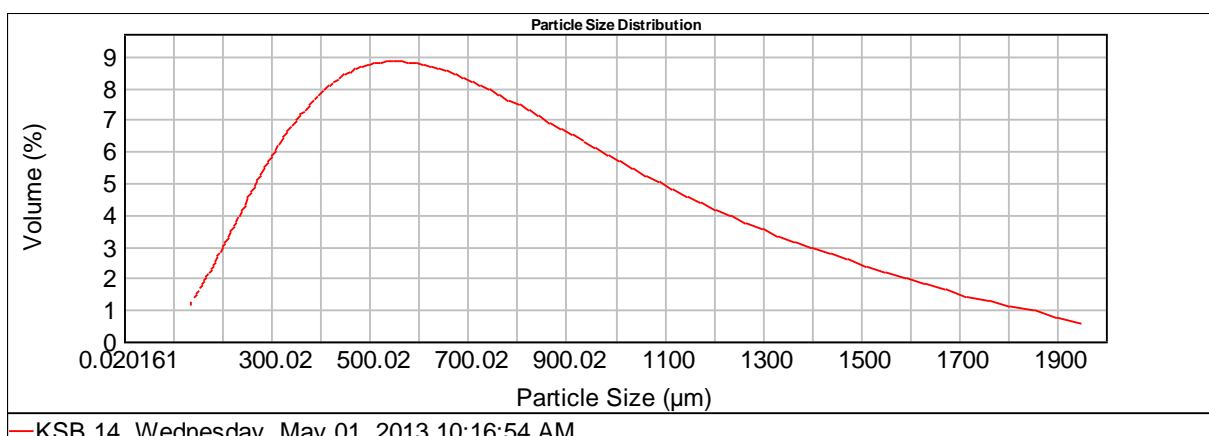
Size ( $\mu\text{m}$ )	Volume In %
0.010	0.00
4.000	2.55
63.000	

Size ( $\mu\text{m}$ )	Volume In %
63.000	1.35
125.000	8.25
250.000	

Size ( $\mu\text{m}$ )	Volume In %
250.000	23.49
500.000	39.80
1000.000	

Size ( $\mu\text{m}$ )	Volume In %
1000.000	24.57
2000.000	

Sample No. 14



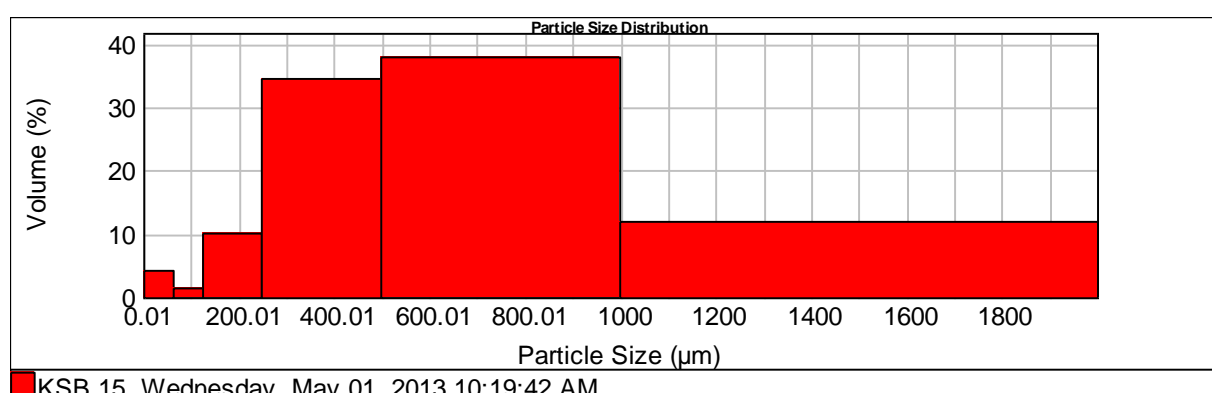
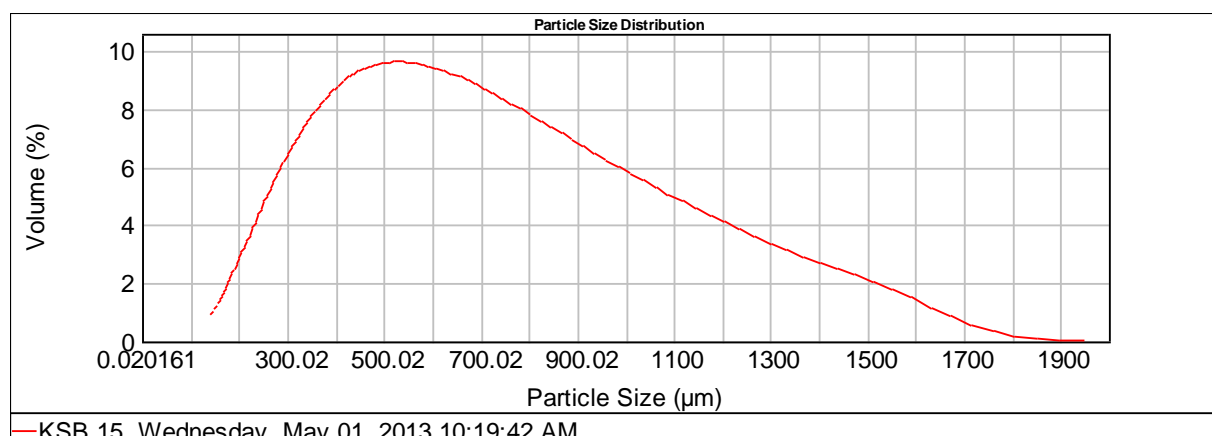
Size ( $\mu\text{m}$ )	Volume In %
0.010	0.06
4.000	6.23
63.000	

Size ( $\mu\text{m}$ )	Volume In %
63.000	2.44
125.000	10.92
250.000	

Size ( $\mu\text{m}$ )	Volume In %
250.000	31.18
500.000	35.74
1000.000	

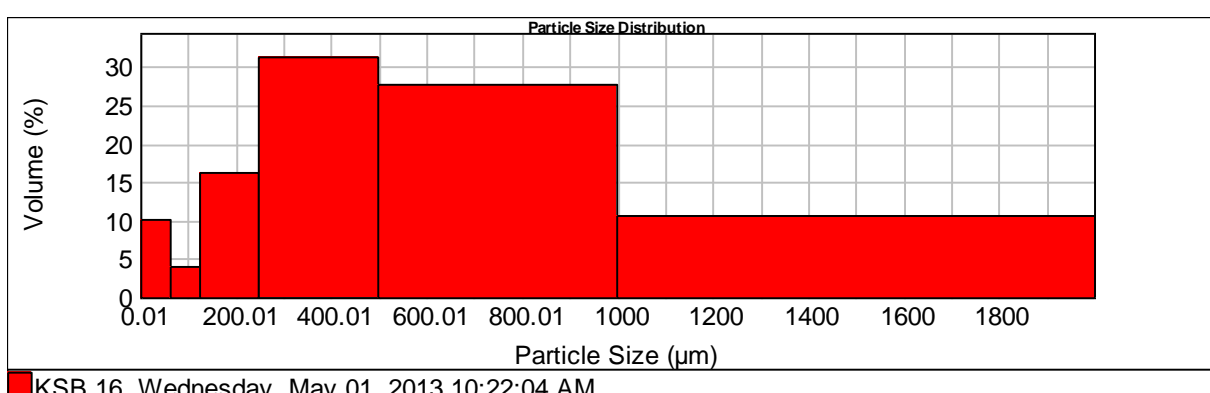
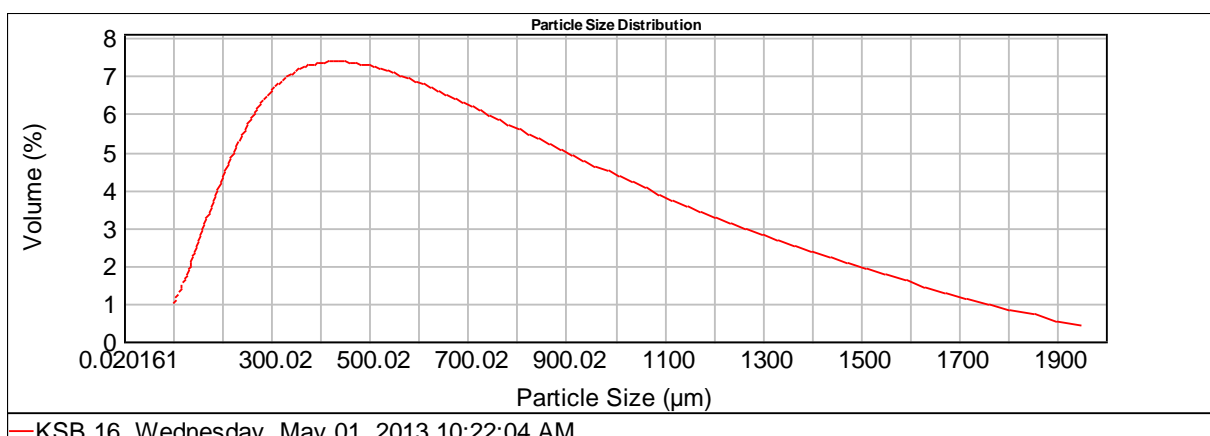
Size ( $\mu\text{m}$ )	Volume In %
1000.000	
2000.000	13.43

Sample No. 15



Size (μm)	Volume In %						
0.010	0.00	63.000	1.49	250.000	34.47	1000.000	11.87
4.000	4.09	125.000	10.07	500.000	38.01	2000.000	
63.000		250.000		1000.000			

Sample No. 16



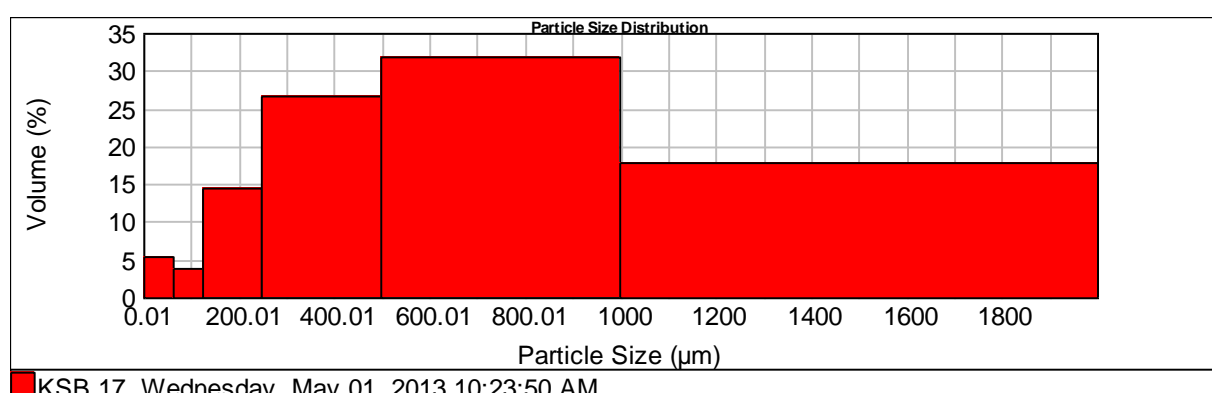
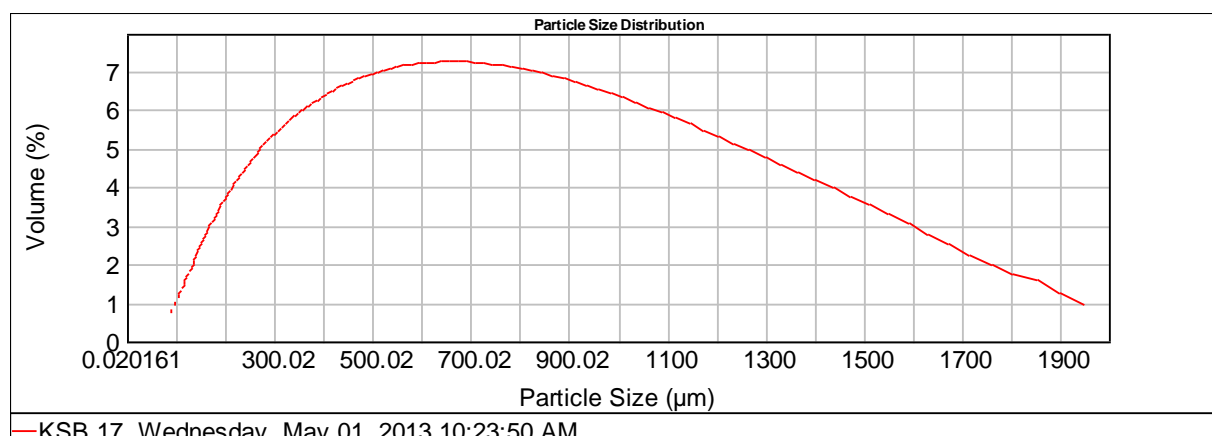
Size ( $\mu\text{m}$ )	Volume In %
0.010	0.29
4.000	9.97
63.000	

Size ( $\mu\text{m}$ )	Volume In %
63.000	4.06
125.000	16.22
250.000	

Size ( $\mu\text{m}$ )	Volume In %
250.000	31.33
500.000	27.58
1000.000	

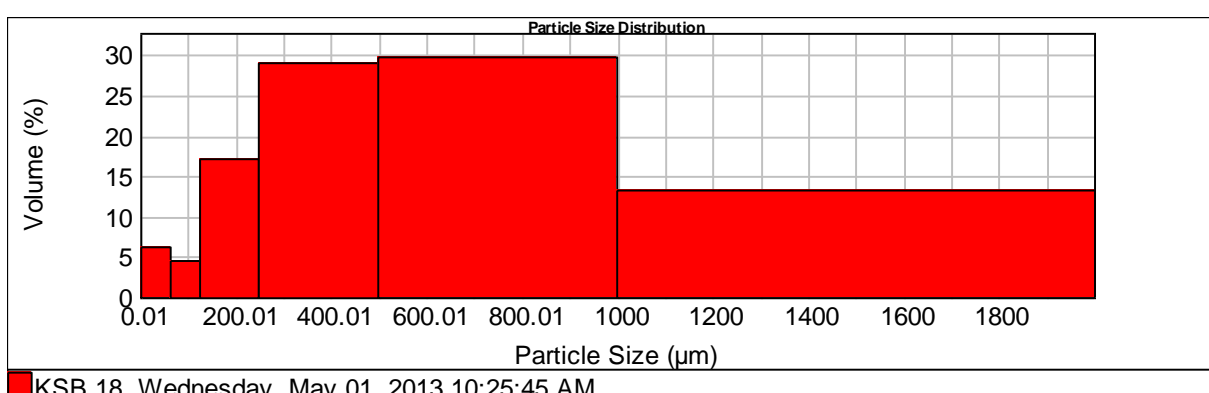
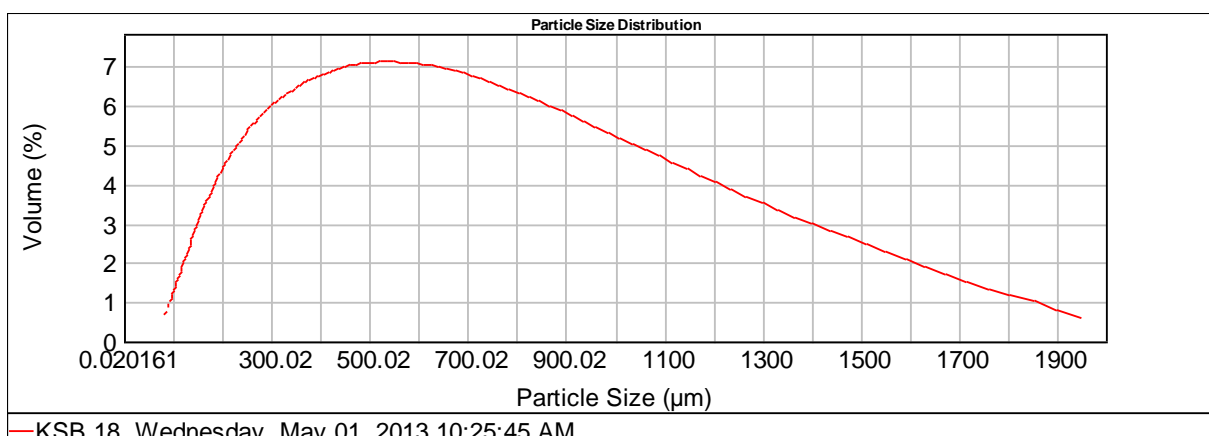
Size ( $\mu\text{m}$ )	Volume In %
1000.000	
2000.000	10.54

Sample No. 17



Size ( $\mu\text{m}$ )	Volume In %	Size ( $\mu\text{m}$ )	Volume In %	Size ( $\mu\text{m}$ )	Volume In %	Size ( $\mu\text{m}$ )	Volume In %
0.010	0.16	63.000	3.79	250.000	26.70	1000.000	17.83
4.000	5.23	125.000	14.44	500.000	31.86	2000.000	
63.000		250.000		1000.000			

Sample No. 18



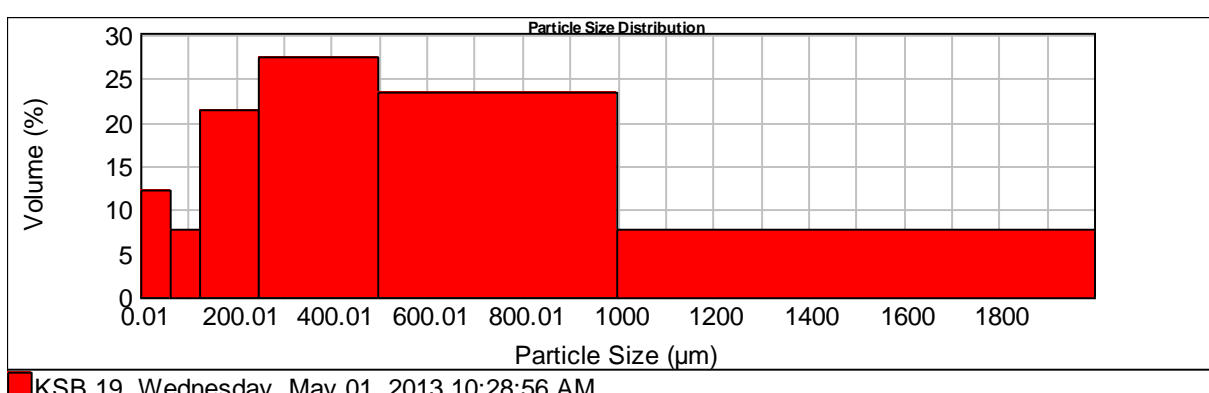
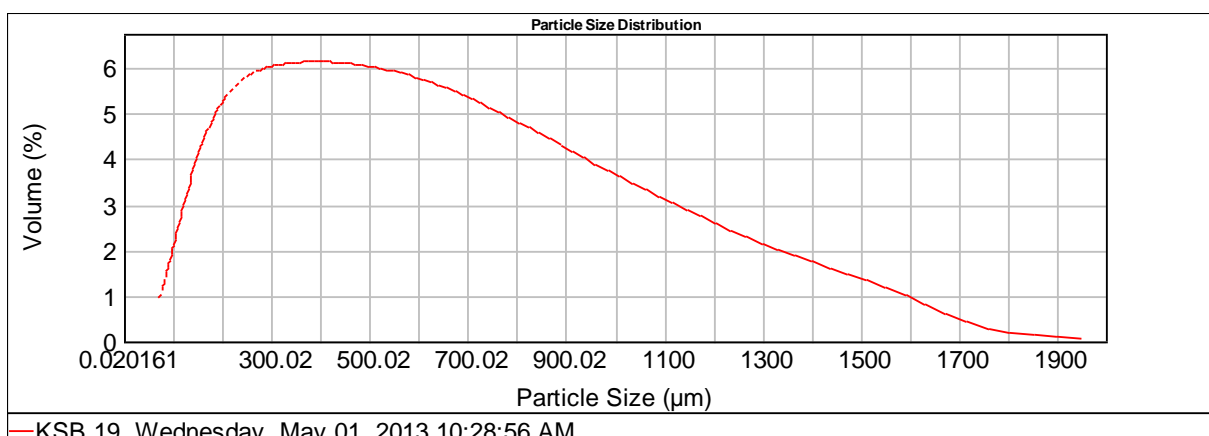
Size ( $\mu\text{m}$ )	Volume In %
0.010	0.16
4.000	6.17
63.000	

Size ( $\mu\text{m}$ )	Volume In %
63.000	4.44
125.000	17.18
250.000	

Size ( $\mu\text{m}$ )	Volume In %
250.000	28.97
500.000	29.79
1000.000	

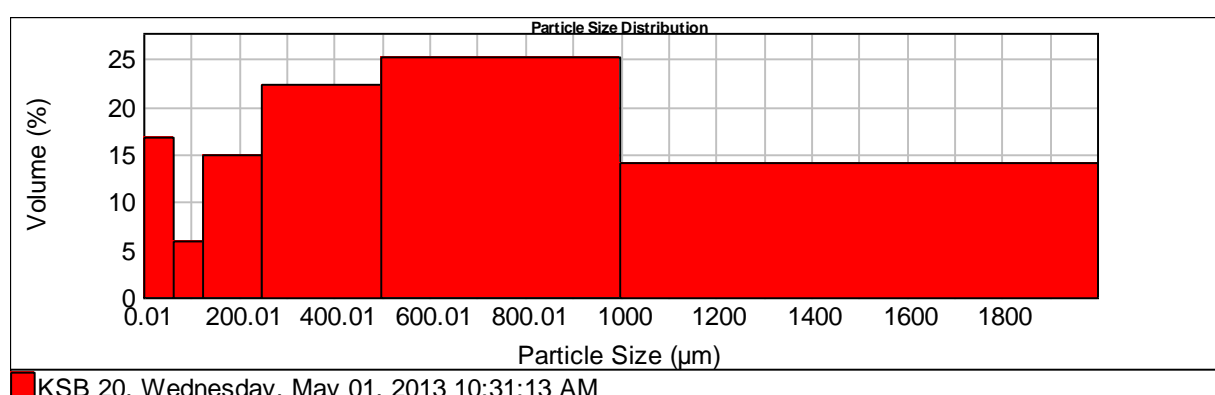
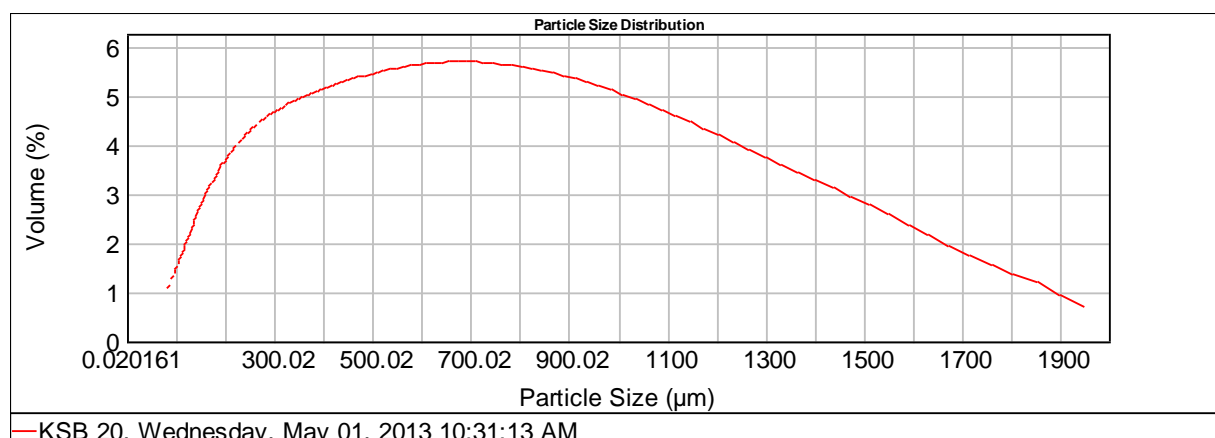
Size ( $\mu\text{m}$ )	Volume In %
1000.000	
2000.000	13.27

Sample No. 19



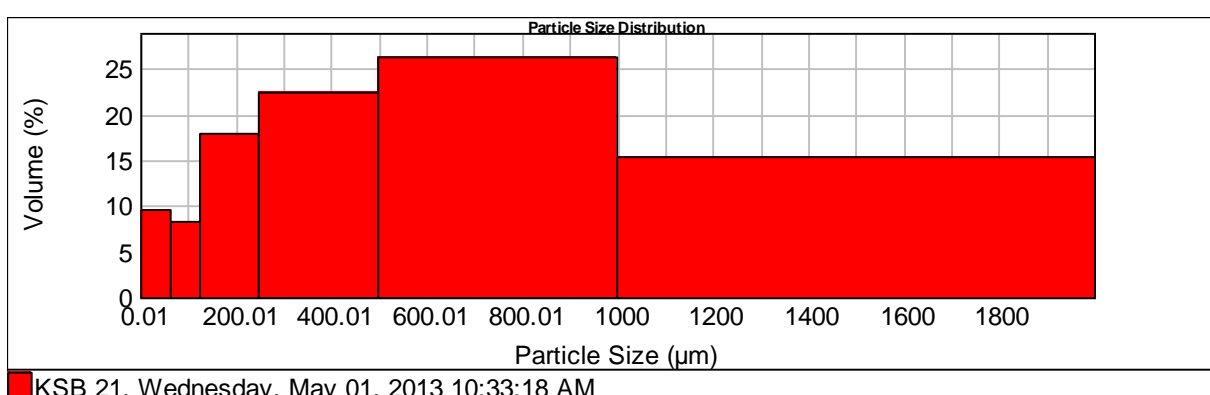
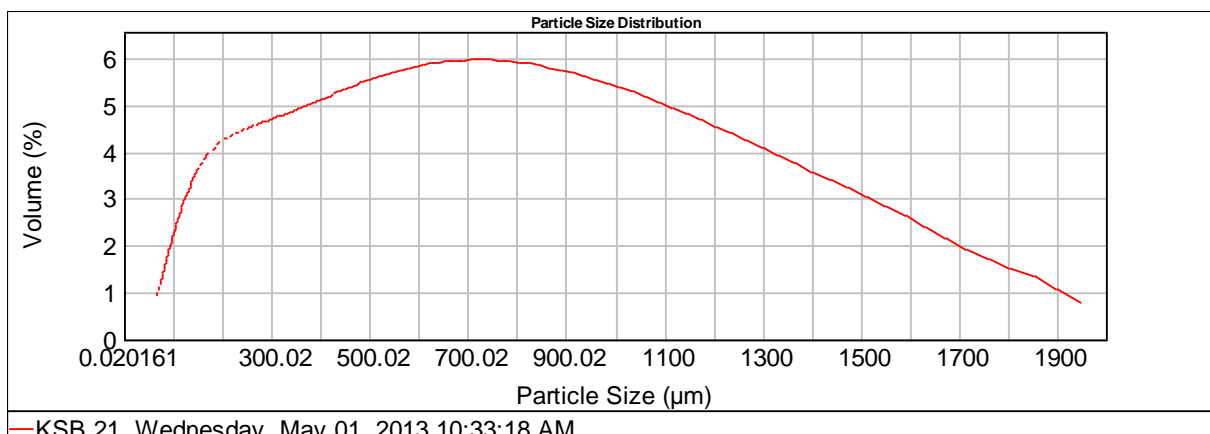
Size ( $\mu\text{m}$ )	Volume In %	Size ( $\mu\text{m}$ )	Volume In %	Size ( $\mu\text{m}$ )	Volume In %	Size ( $\mu\text{m}$ )	Volume In %
0.010	0.45	63.000	7.65	250.000	27.44	1000.000	7.62
4.000	12.17	125.000	21.25	500.000	23.41	2000.000	
63.000		250.000		1000.000			

Sample No. 20



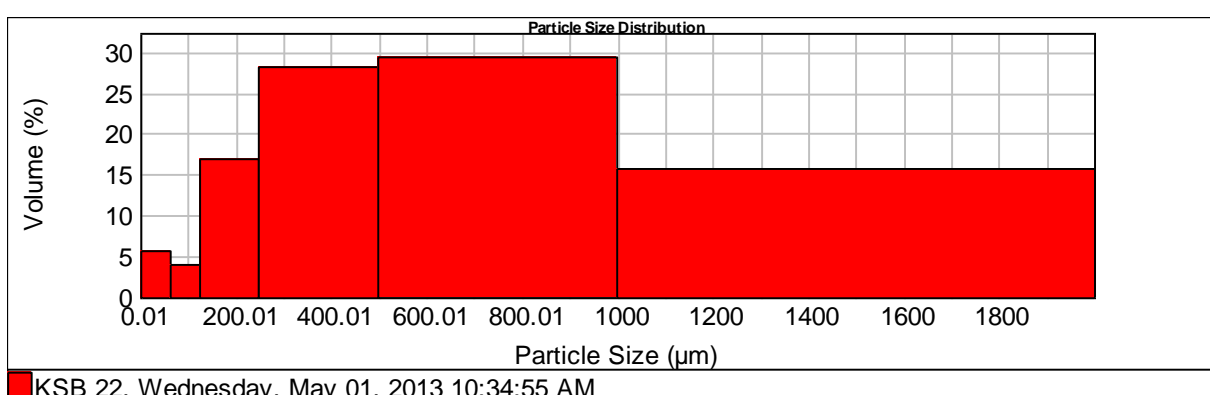
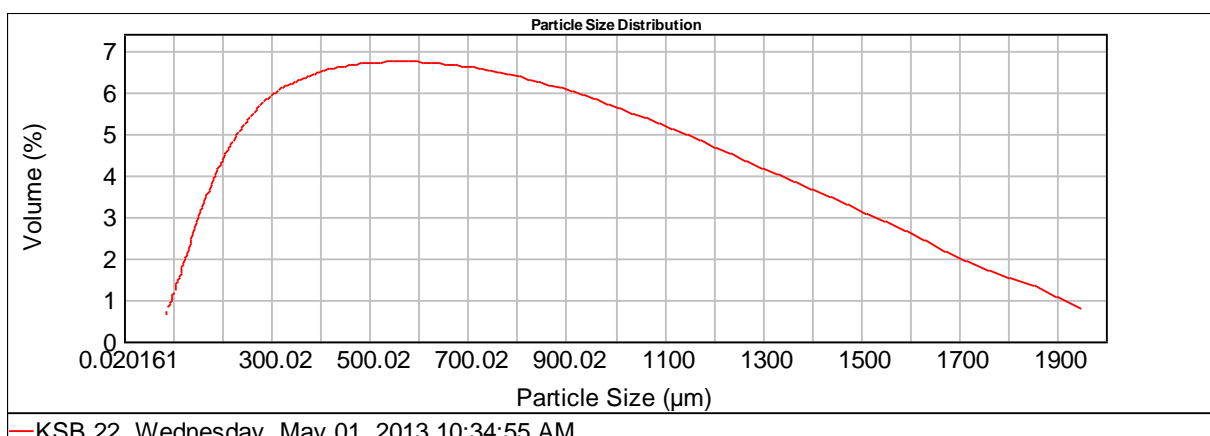
Size ( $\mu\text{m}$ )	Volume ln %	Size ( $\mu\text{m}$ )	Volume ln %	Size ( $\mu\text{m}$ )	Volume ln %	Size ( $\mu\text{m}$ )	Volume ln %
0.010	0.79	63.000	5.92	250.000	22.33	1000.000	
4.000	16.76	125.000	14.92	500.000	25.19	2000.000	14.09
63.000		250.000		1000.000			

Sample No. 21



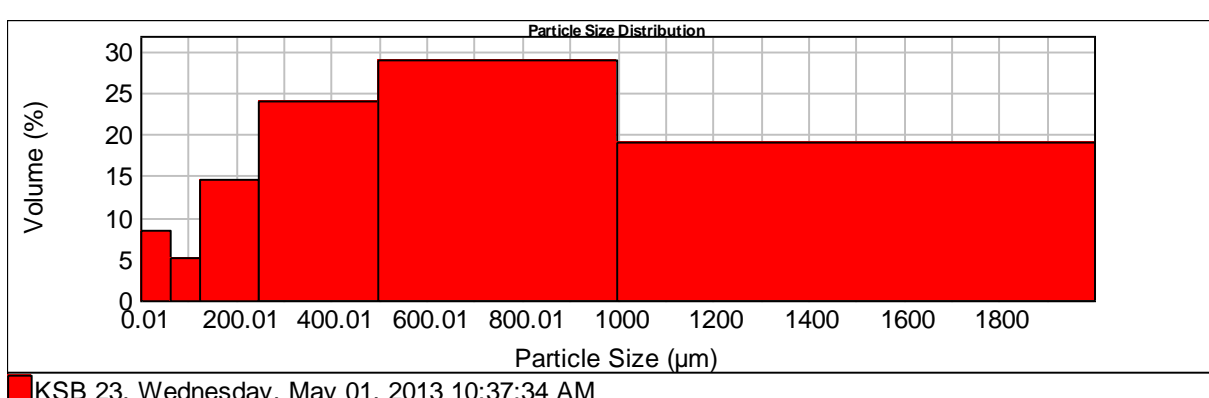
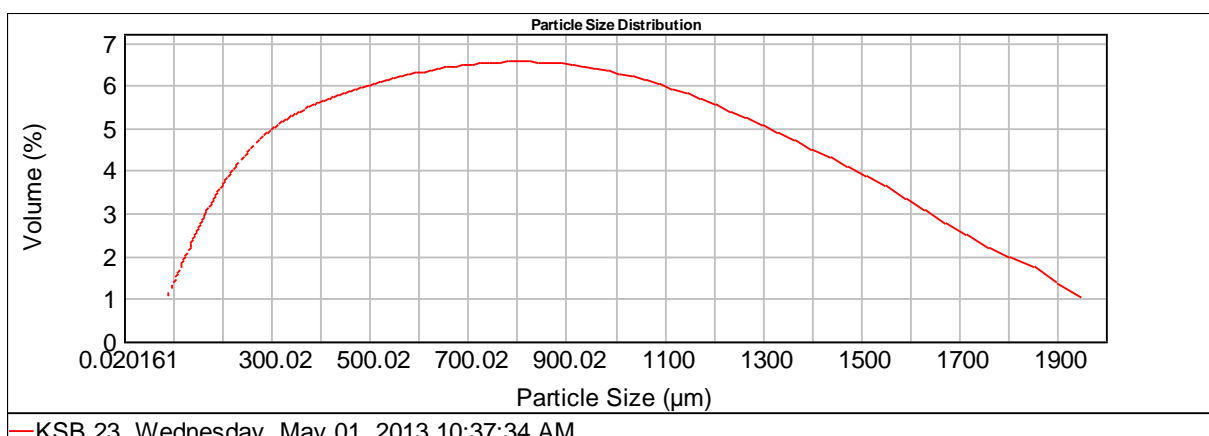
Size ( $\mu\text{m}$ )	Volume In %	Size ( $\mu\text{m}$ )	Volume In %	Size ( $\mu\text{m}$ )	Volume In %	Size ( $\mu\text{m}$ )	Volume In %
0.010	0.42	63.000	8.24	250.000	22.39	1000.000	
4.000	9.60	125.000	17.79	500.000	26.28	2000.000	15.28
63.000		250.000		1000.000			

Sample No. 22



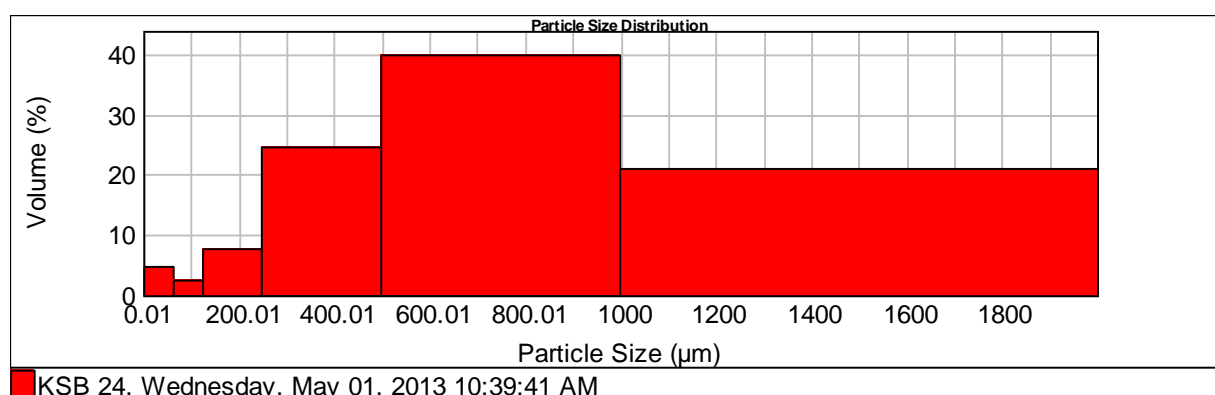
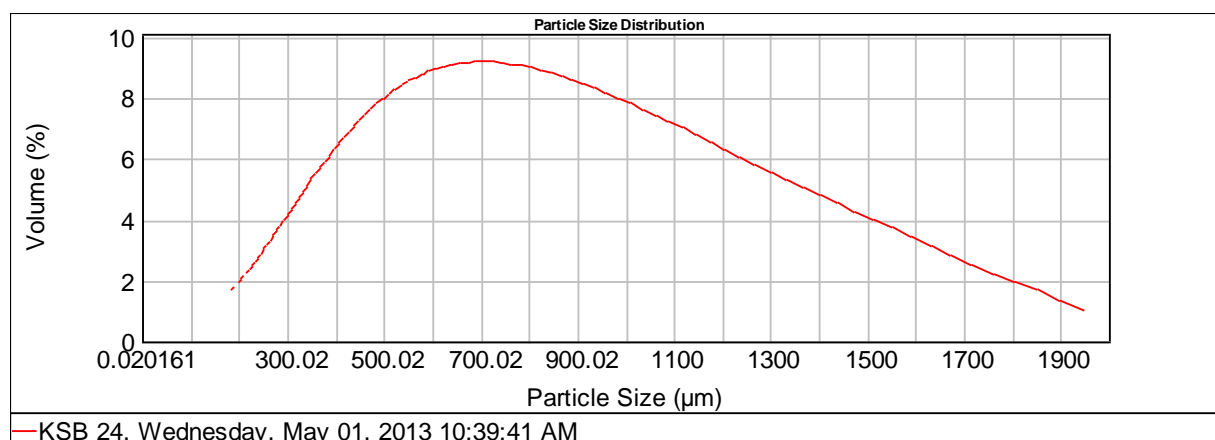
Size ( $\mu\text{m}$ )	Volume In %	Size ( $\mu\text{m}$ )	Volume In %	Size ( $\mu\text{m}$ )	Volume In %	Size ( $\mu\text{m}$ )	Volume In %
0.010		63.000		250.000		1000.000	
4.000	0.16	125.000	3.99	500.000	28.13	2000.000	15.70
63.000	5.69	250.000	16.95	1000.000	29.38		

Sample No. 23



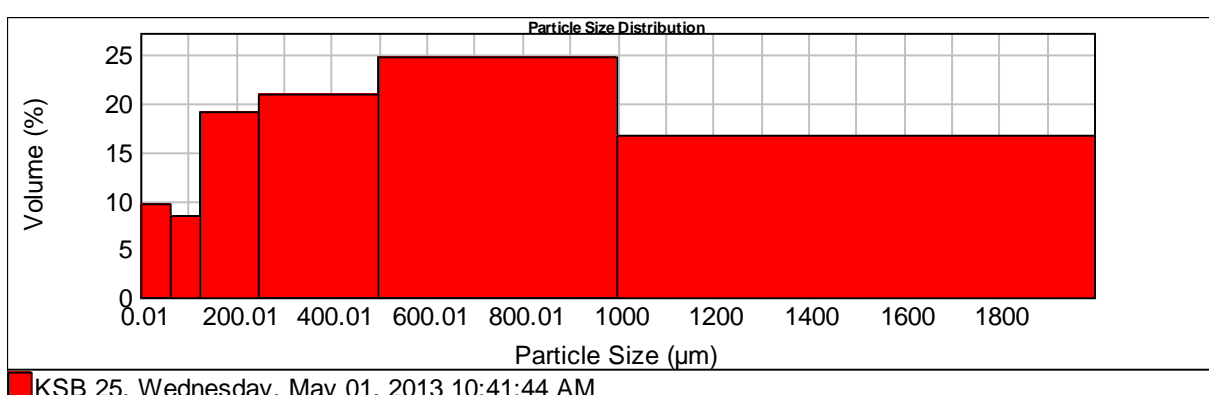
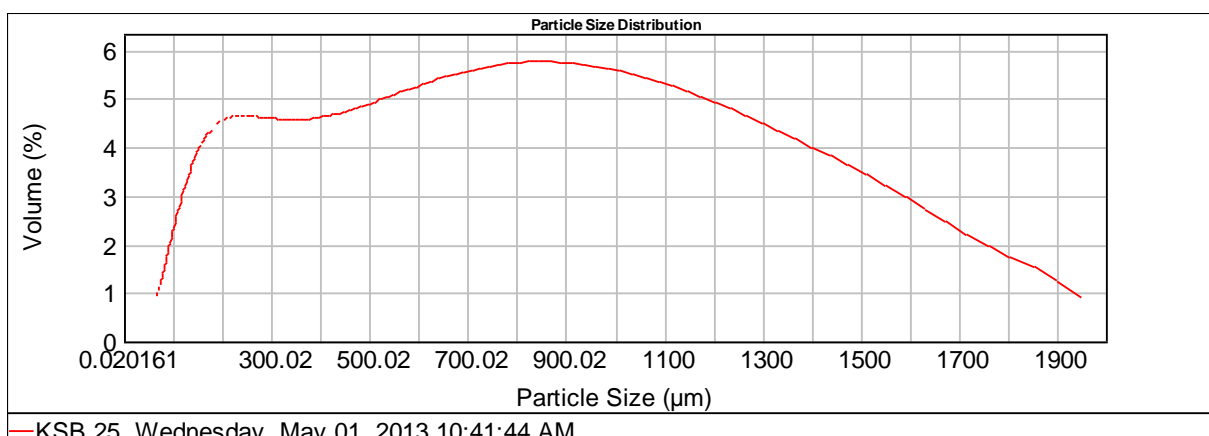
Size ( $\mu\text{m}$ )	Volume In %	Size ( $\mu\text{m}$ )	Volume In %	Size ( $\mu\text{m}$ )	Volume In %	Size ( $\mu\text{m}$ )	Volume In %
0.010	0.29	63.000	5.15	250.000	23.99	1000.000	
4.000	8.28	125.000	14.55	500.000	28.89	2000.000	18.84
63.000		250.000		1000.000			

Sample No. 24



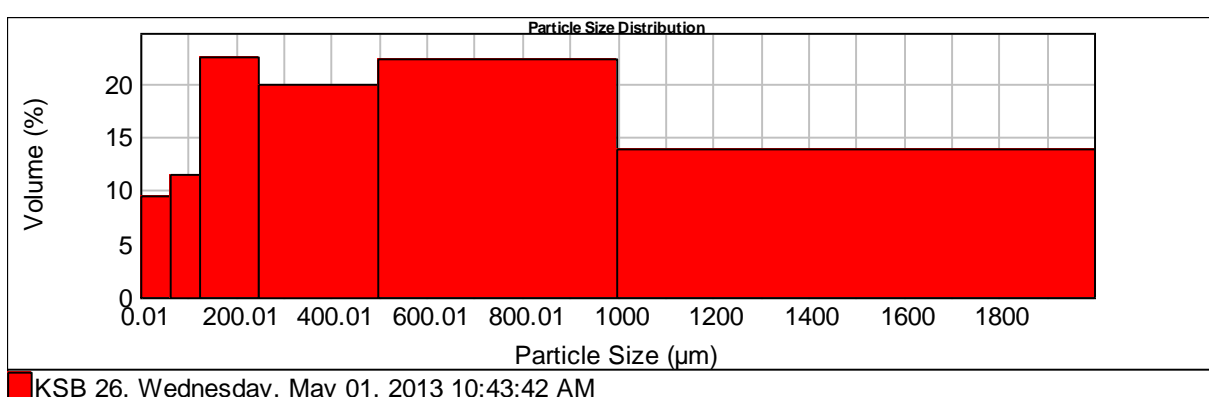
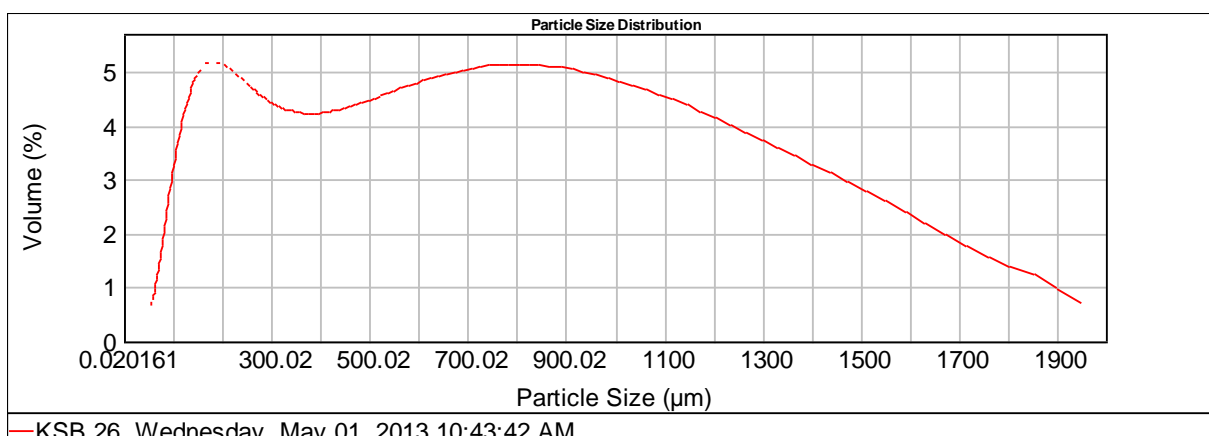
Size ( $\mu\text{m}$ )	Volume In %	Size ( $\mu\text{m}$ )	Volume In %	Size ( $\mu\text{m}$ )	Volume In %	Size ( $\mu\text{m}$ )	Volume In %
0.010	0.07	63.000	2.32	250.000	24.65	1000.000	20.96
4.000	4.55	125.000	7.60	500.000	39.85	2000.000	
63.000		250.000		1000.000			

Sample No. 25



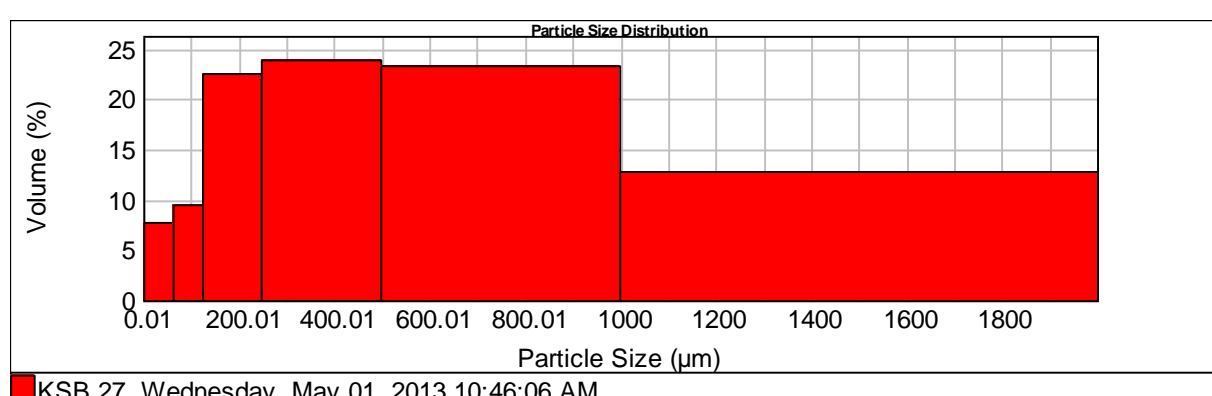
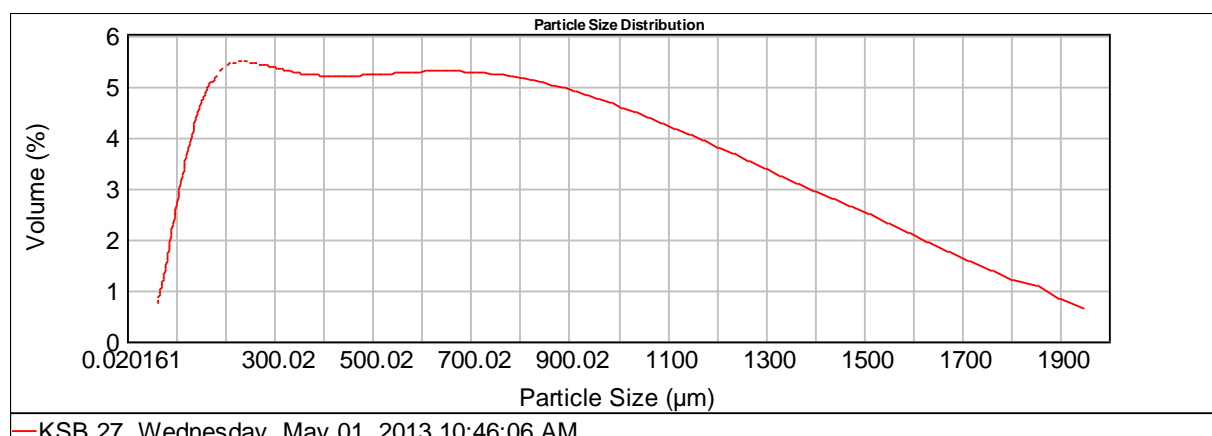
Size ( $\mu\text{m}$ )	Volume In %	Size ( $\mu\text{m}$ )	Volume In %	Size ( $\mu\text{m}$ )	Volume In %	Size ( $\mu\text{m}$ )	Volume In %
0.010	0.40	63.000	8.46	250.000	21.00	1000.000	
4.000	9.54	125.000	19.10	500.000	24.80	2000.000	16.72
63.000		250.000		1000.000			

Sample No. 26



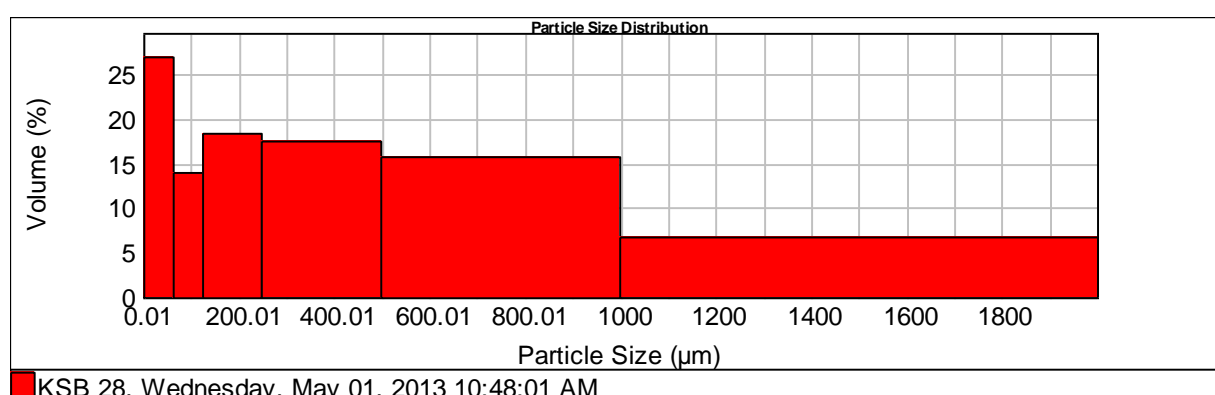
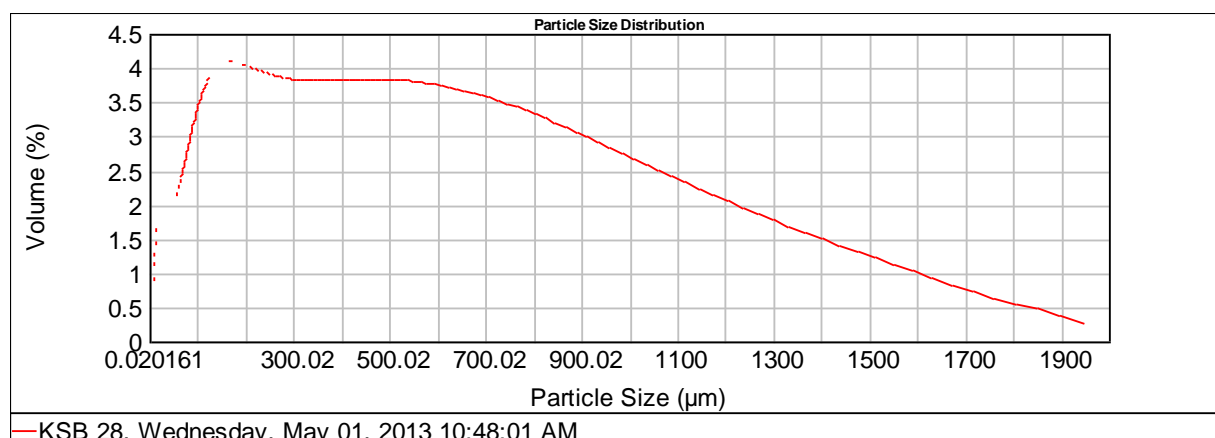
Size ( $\mu\text{m}$ )	Volume In %	Size ( $\mu\text{m}$ )	Volume In %	Size ( $\mu\text{m}$ )	Volume In %	Size ( $\mu\text{m}$ )	Volume In %
0.010	0.46	63.000	11.45	250.000	19.83	1000.000	13.93
4.000	9.51	125.000	22.50	500.000	22.31	2000.000	
63.000		250.000		1000.000			

Sample No. 27



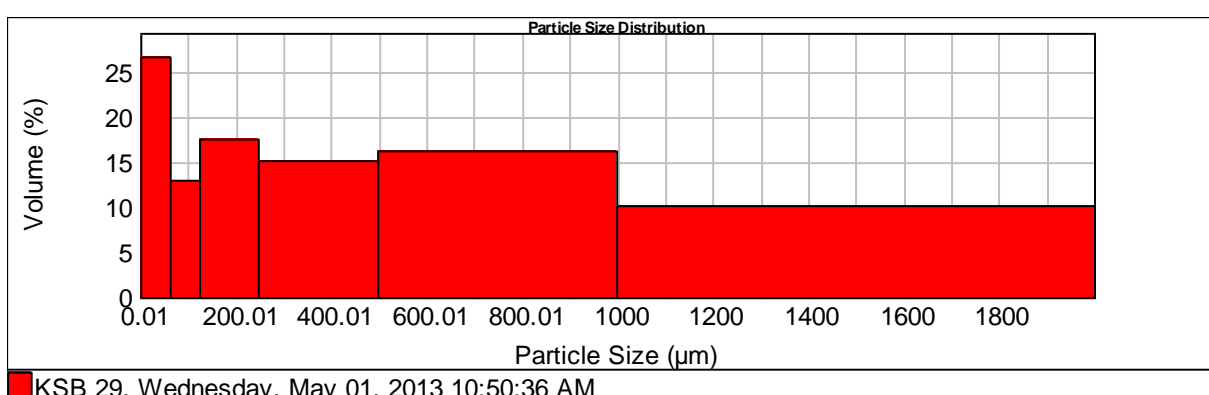
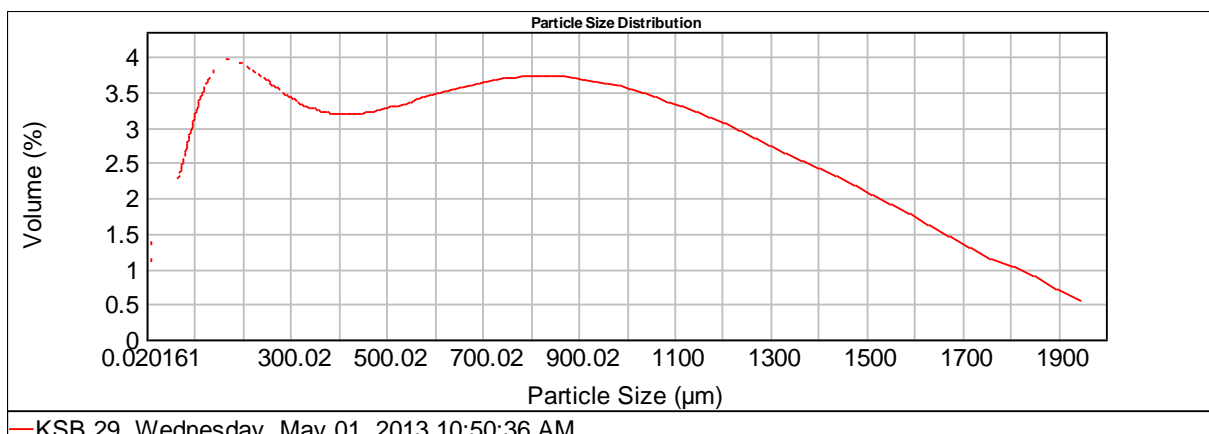
Size ( $\mu\text{m}$ )	Volume In %	Size ( $\mu\text{m}$ )	Volume In %	Size ( $\mu\text{m}$ )	Volume In %	Size ( $\mu\text{m}$ )	Volume In %
0.010	0.27	63.000	9.44	250.000	23.93	1000.000	
4.000	7.78	125.000	22.53	500.000	23.35	2000.000	12.69
63.000		250.000		1000.000			

Sample No. 28



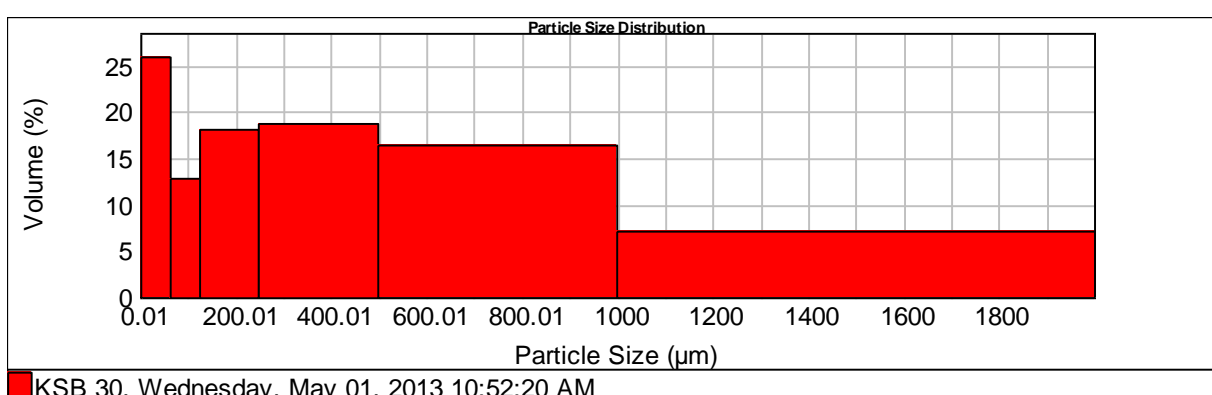
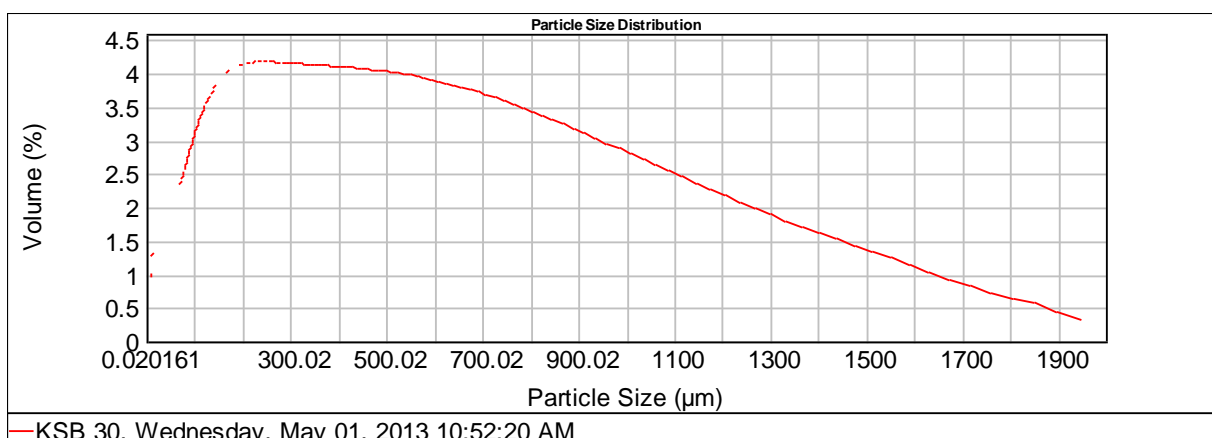
Size ( $\mu\text{m}$ )	Volume In %	Size ( $\mu\text{m}$ )	Volume In %	Size ( $\mu\text{m}$ )	Volume In %	Size ( $\mu\text{m}$ )	Volume In %
0.010	1.08	63.000	13.95	250.000	17.40	1000.000	
4.000	26.94	125.000	18.23	500.000	15.74	2000.000	6.66
63.000		250.000		1000.000			

Sample No. 29



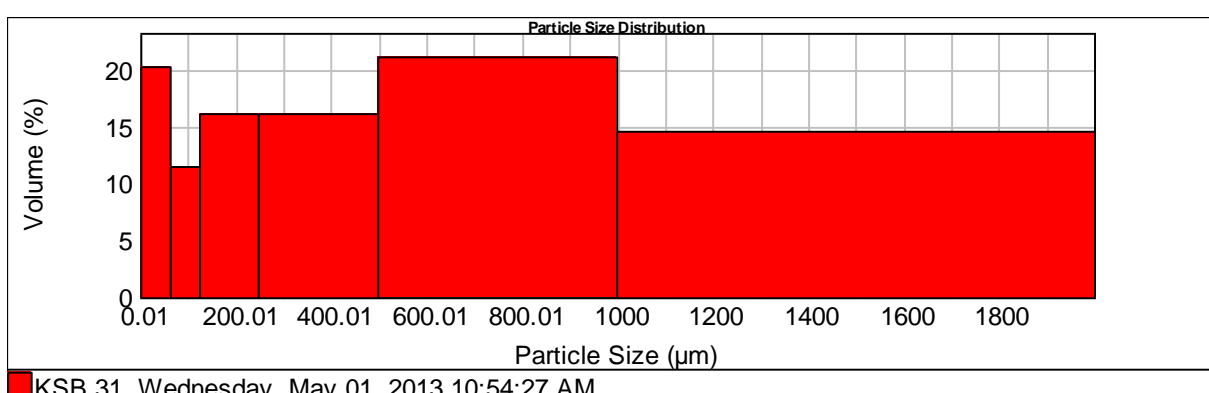
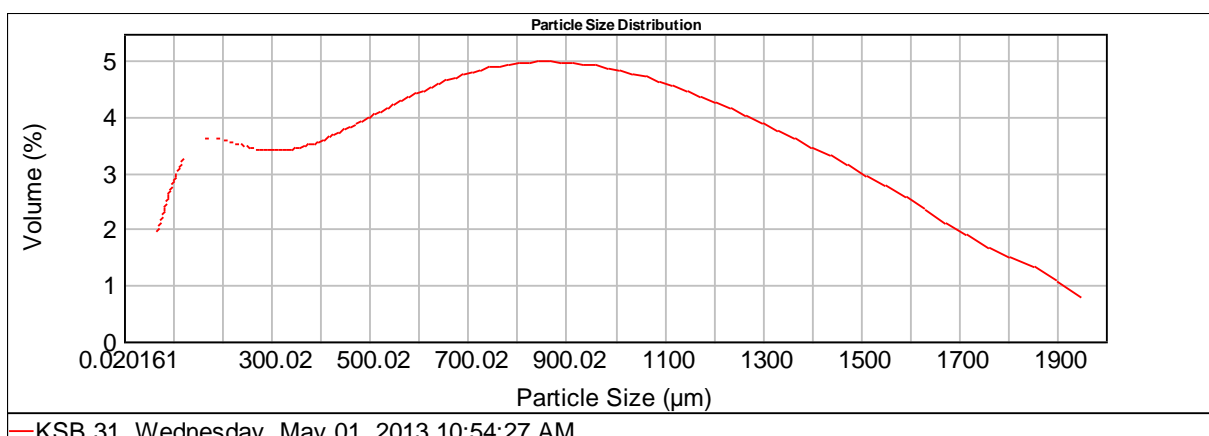
Size ( $\mu\text{m}$ )	Volume In %	Size ( $\mu\text{m}$ )	Volume In %	Size ( $\mu\text{m}$ )	Volume In %	Size ( $\mu\text{m}$ )	Volume In %
0.010	1.26	63.000	12.95	250.000	15.08	1000.000	10.24
4.000	26.79	125.000	17.48	500.000	16.19	2000.000	
63.000		250.000		1000.000			

Sample No. 30



Size ( $\mu\text{m}$ )	Volume In %	Size ( $\mu\text{m}$ )	Volume In %	Size ( $\mu\text{m}$ )	Volume In %	Size ( $\mu\text{m}$ )	Volume In %
0.010	1.02	63.000	12.76	250.000	18.66	1000.000	
4.000	25.96	125.000	18.12	500.000	16.32	2000.000	7.16
63.000		250.000		1000.000			

Sample No. 31



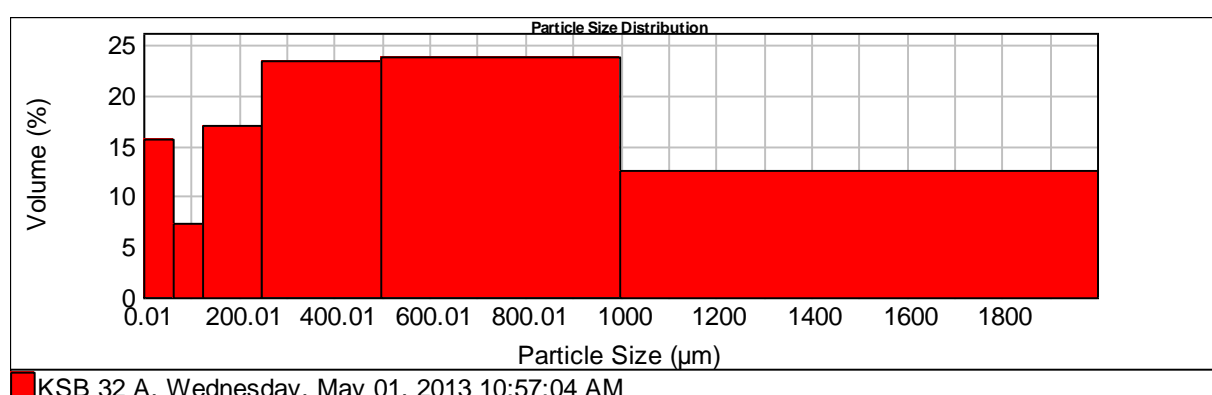
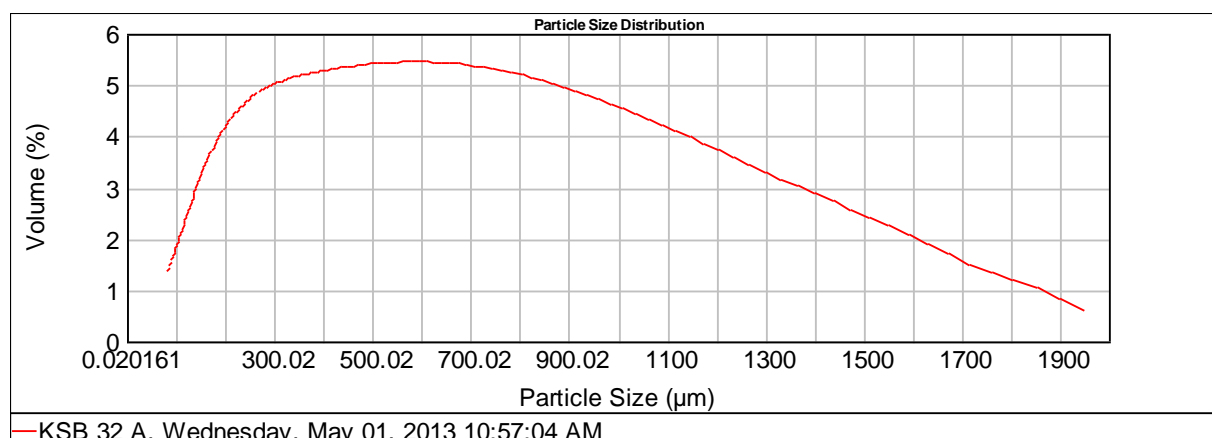
Size ( $\mu\text{m}$ )	Volume In %
0.010	0.72
4.000	20.18
63.000	

Size ( $\mu\text{m}$ )	Volume In %
63.000	11.46
125.000	16.04
250.000	

Size ( $\mu\text{m}$ )	Volume In %
250.000	16.01
500.000	21.12
1000.000	

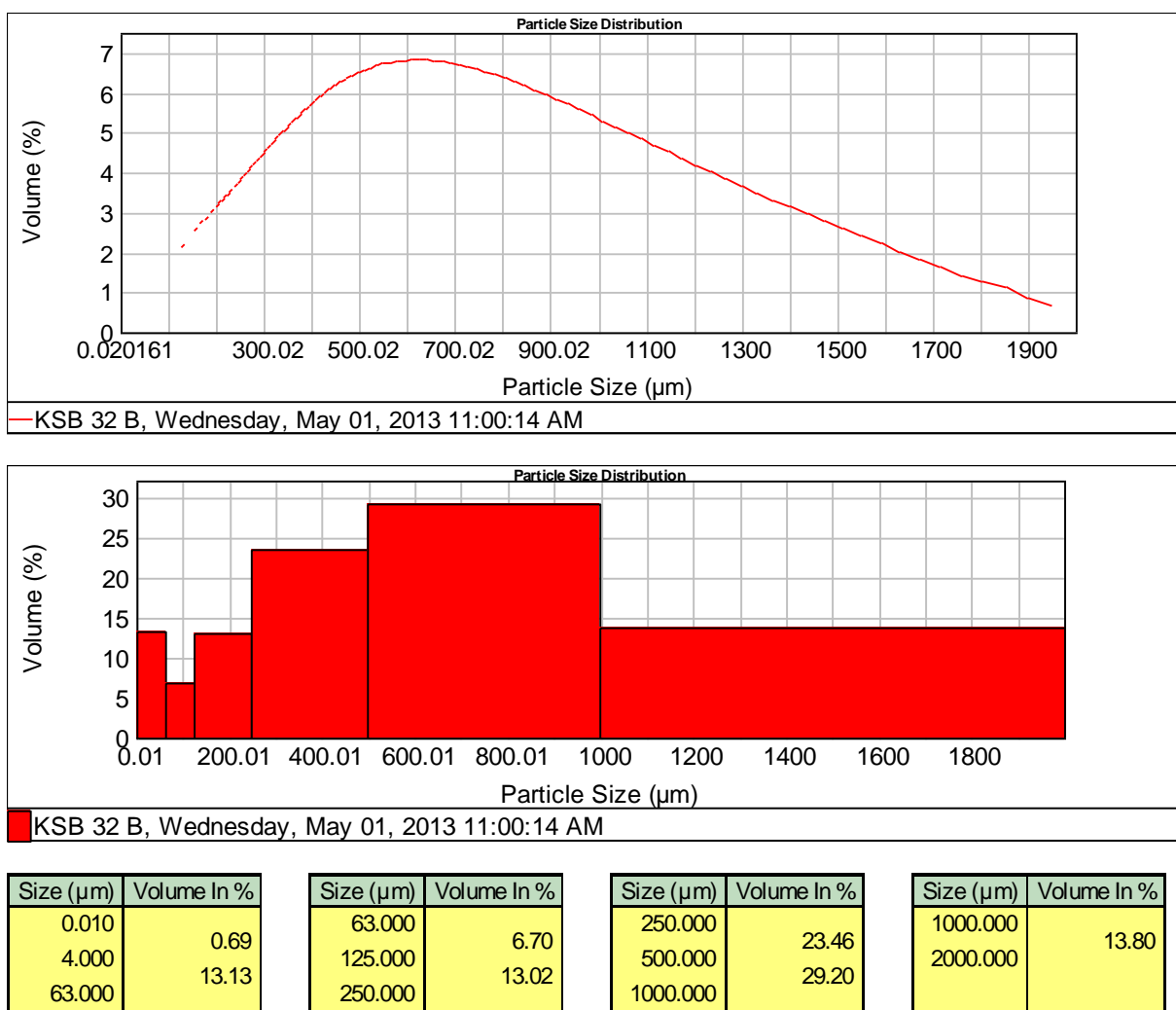
Size ( $\mu\text{m}$ )	Volume In %
1000.000	
2000.000	14.45

Sample No. 32A

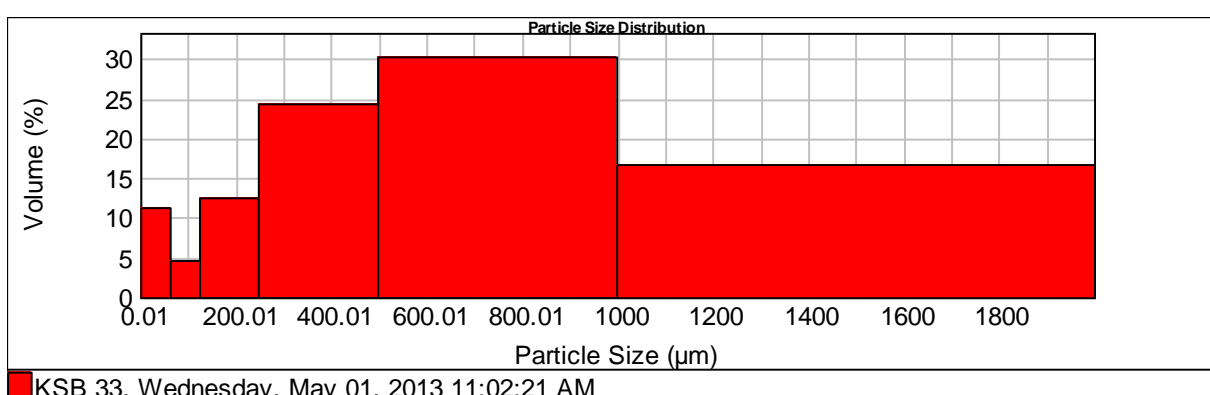
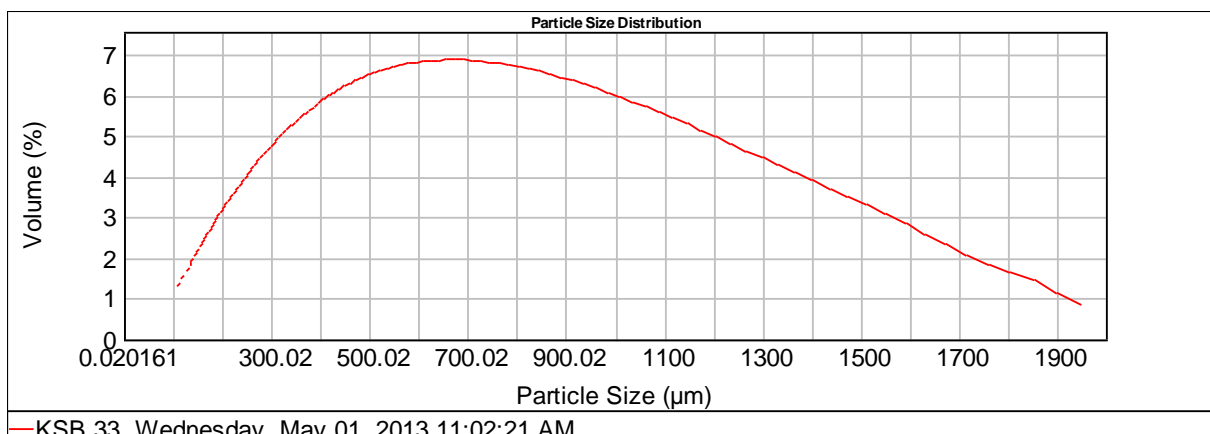


Size ( $\mu\text{m}$ )	Volume In %	Size ( $\mu\text{m}$ )	Volume In %	Size ( $\mu\text{m}$ )	Volume In %	Size ( $\mu\text{m}$ )	Volume In %
0.010	0.65	63.000	7.26	250.000	23.32	1000.000	12.42
4.000	15.56	125.000	17.01	500.000	23.79	2000.000	
63.000		250.000		1000.000			

Sample No. 32B



Sample No. 33



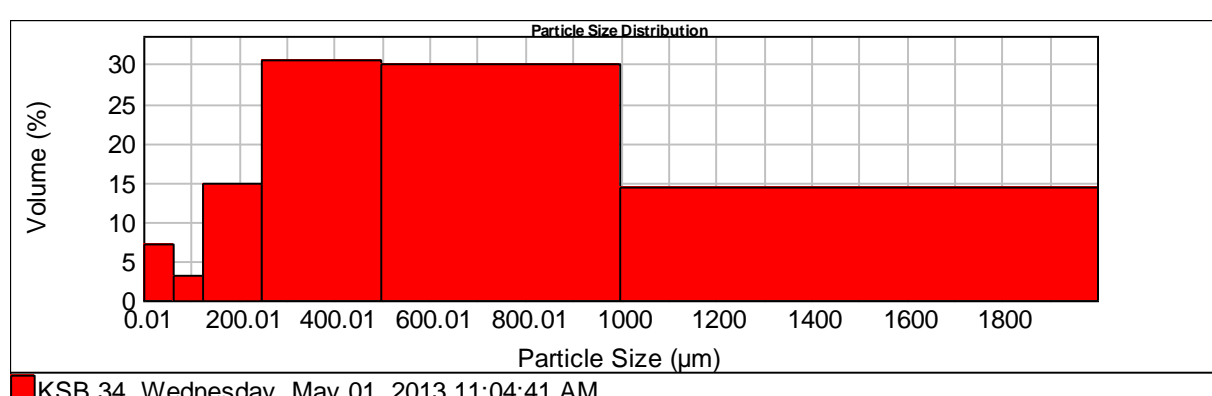
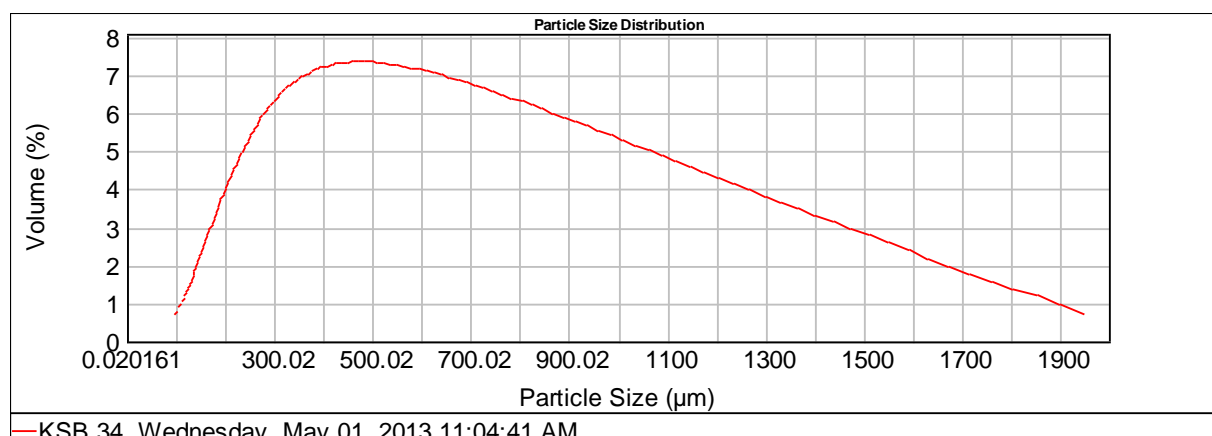
Size ( $\mu\text{m}$ )	Volume In %
0.010	0.38
4.000	11.15
63.000	

Size ( $\mu\text{m}$ )	Volume In %
63.000	4.66
125.000	12.54
250.000	

Size ( $\mu\text{m}$ )	Volume In %
250.000	24.28
500.000	30.23
1000.000	

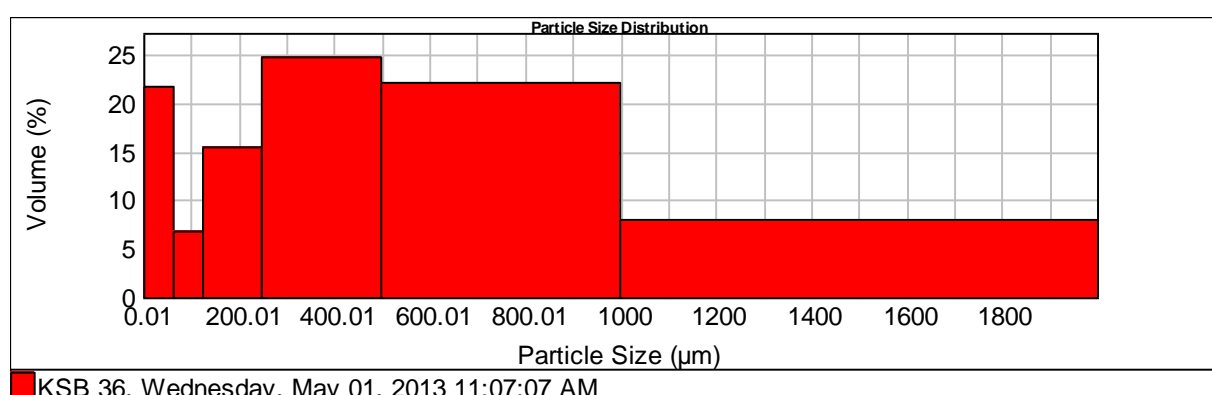
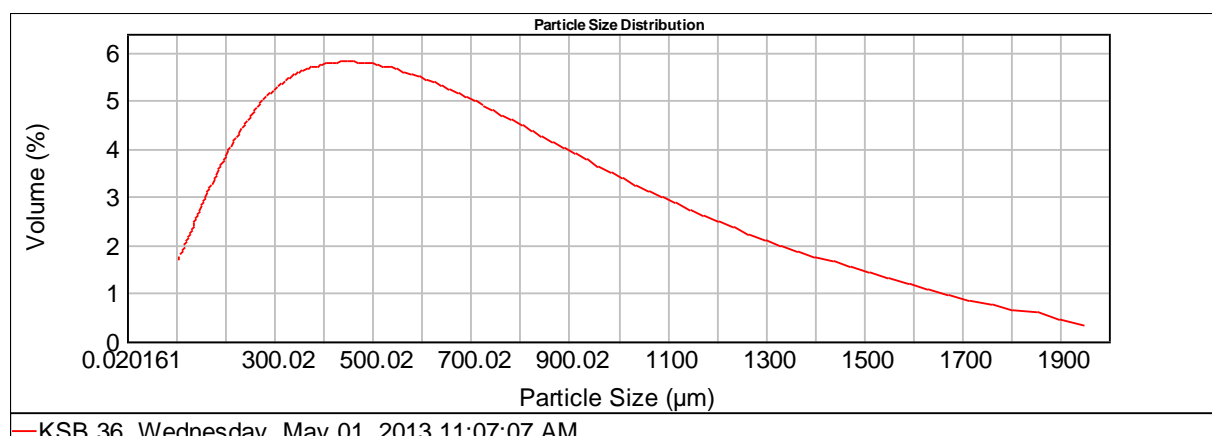
Size ( $\mu\text{m}$ )	Volume In %
1000.000	16.75
2000.000	

Sample No. 34



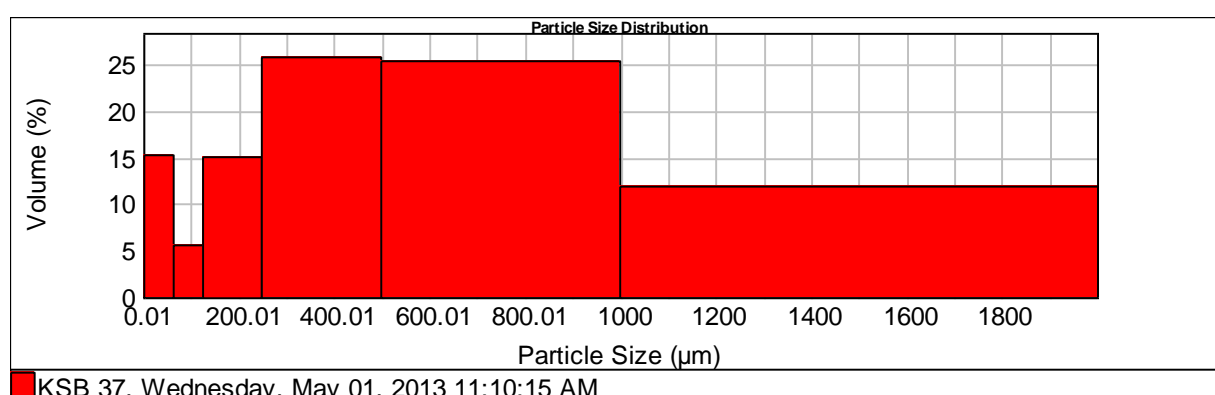
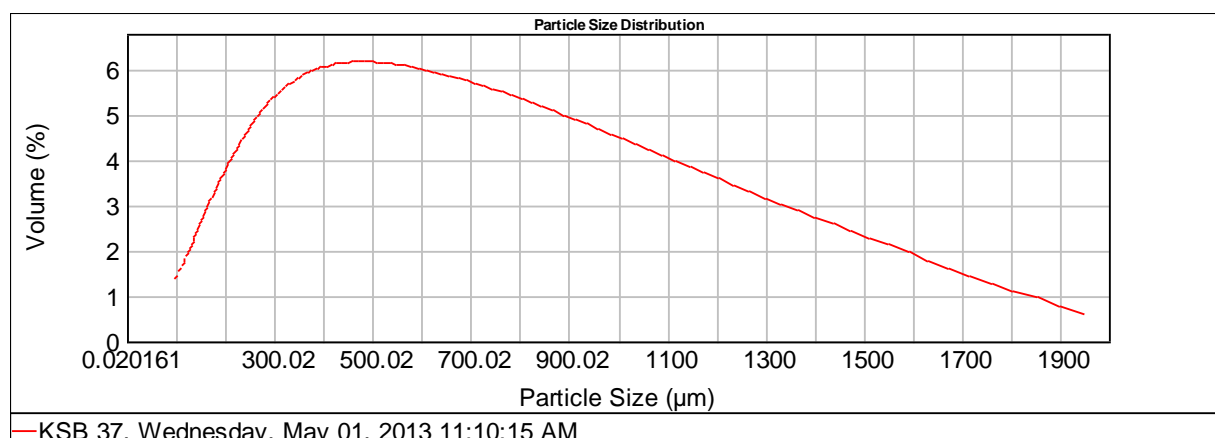
Size ( $\mu\text{m}$ )	Volume In %	Size ( $\mu\text{m}$ )	Volume In %	Size ( $\mu\text{m}$ )	Volume In %	Size ( $\mu\text{m}$ )	Volume In %
0.010	0.15	63.000	3.01	250.000	30.54	1000.000	
4.000	7.05	125.000	14.91	500.000	29.99	2000.000	14.35
63.000		250.000		1000.000			

Sample No. 36



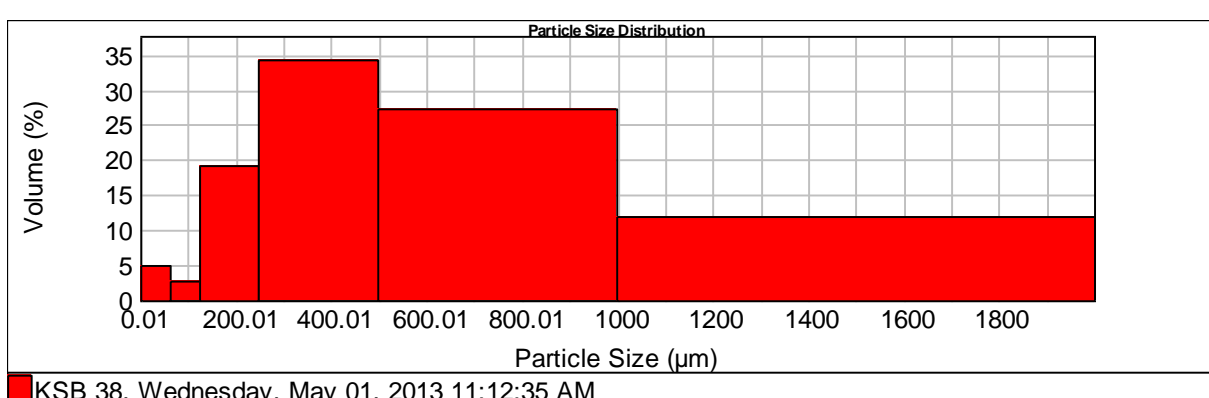
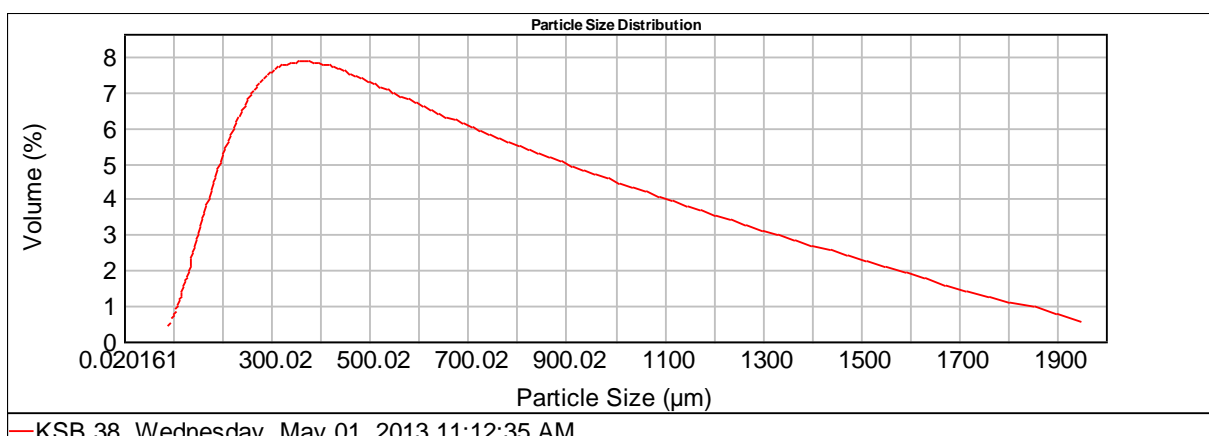
Size ( $\mu\text{m}$ )	Volume In %	Size ( $\mu\text{m}$ )	Volume In %	Size ( $\mu\text{m}$ )	Volume In %	Size ( $\mu\text{m}$ )	Volume In %
0.010	1.33	63.000	6.80	250.000	24.75	1000.000	8.04
4.000	21.69	125.000	15.33	500.000	22.06	2000.000	
63.000		250.000		1000.000			

Sample No. 37



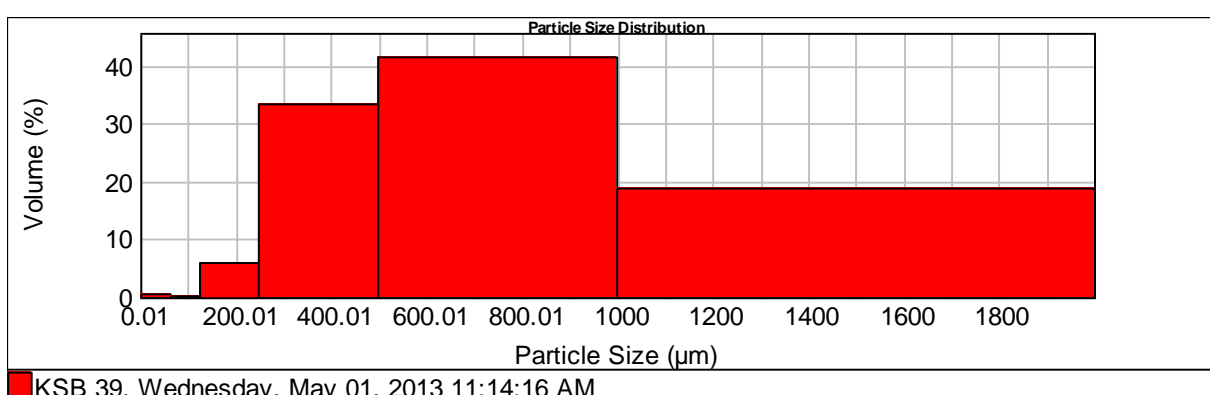
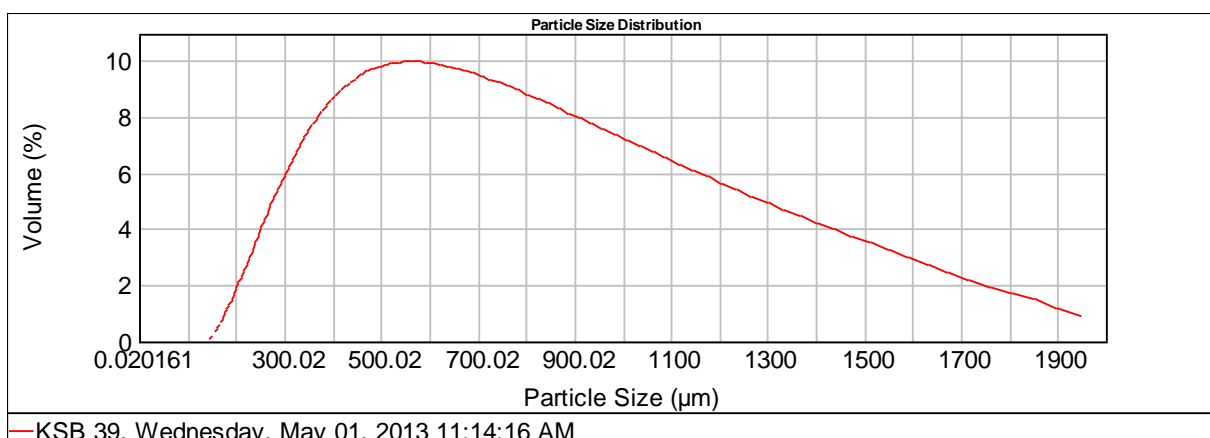
Size ( $\mu\text{m}$ )	Volume In %	Size ( $\mu\text{m}$ )	Volume In %	Size ( $\mu\text{m}$ )	Volume In %	Size ( $\mu\text{m}$ )	Volume In %
0.010	1.04	63.000	5.68	250.000	25.83	1000.000	11.90
4.000	15.30	125.000	14.96	500.000	25.29	2000.000	
63.000		250.000		1000.000			

Sample No. 38



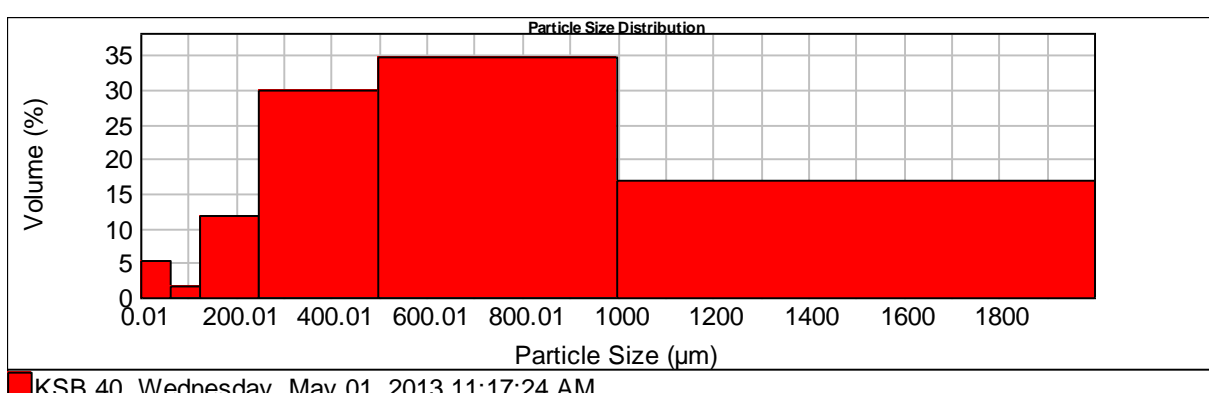
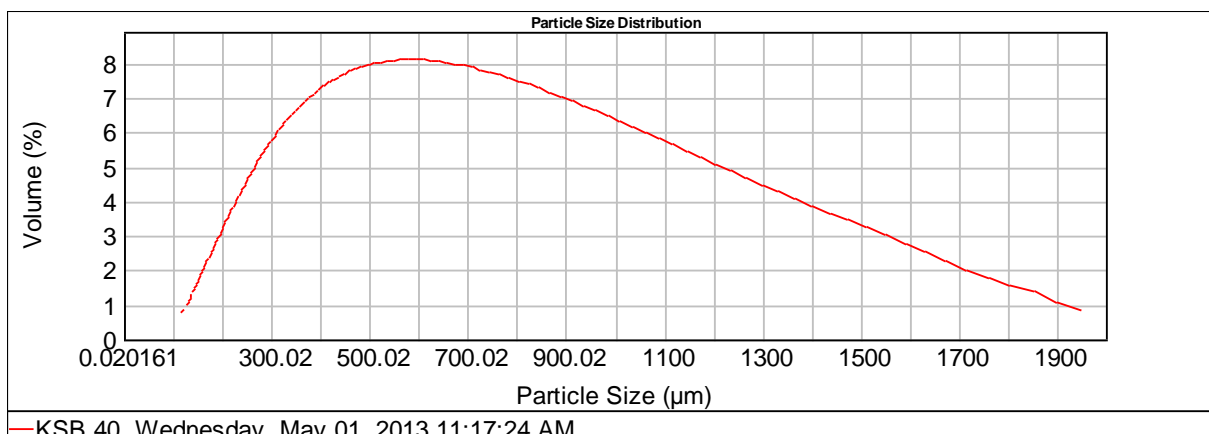
Size ( $\mu\text{m}$ )	Volume In %	Size ( $\mu\text{m}$ )	Volume In %	Size ( $\mu\text{m}$ )	Volume In %	Size ( $\mu\text{m}$ )	Volume In %
0.010	0.13	63.000	2.56	250.000	34.28	1000.000	11.78
4.000	5.02	125.000	19.12	500.000	27.10	2000.000	
63.000		250.000		1000.000			

Sample No. 39



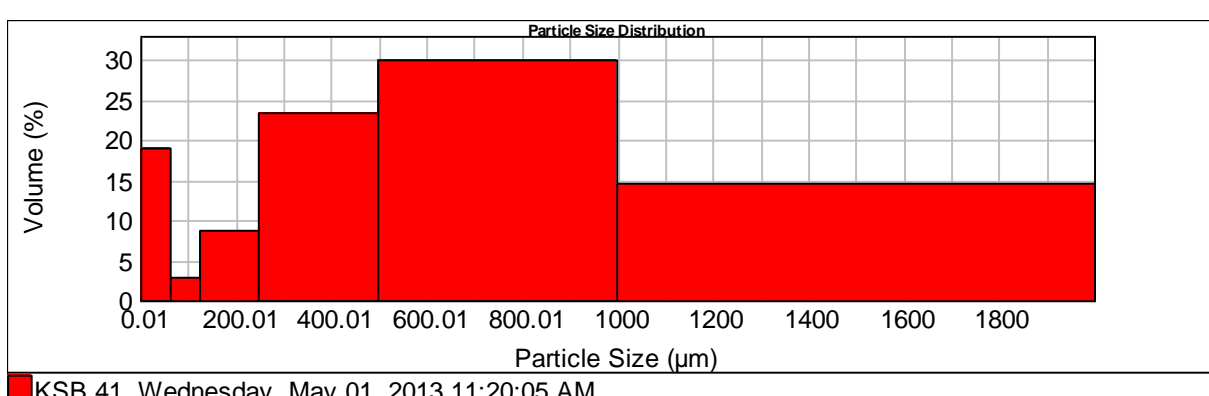
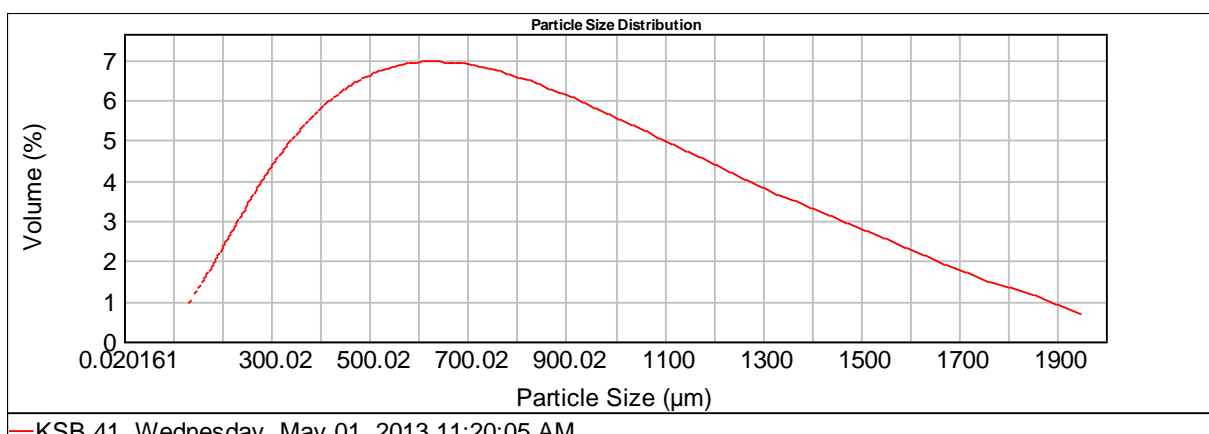
Size ( $\mu\text{m}$ )	Volume In %	Size ( $\mu\text{m}$ )	Volume In %	Size ( $\mu\text{m}$ )	Volume In %	Size ( $\mu\text{m}$ )	Volume In %
0.010	0.00	63.000	0.10	250.000	33.30	1000.000	18.60
4.000	0.62	125.000	5.88	500.000	41.49	2000.000	
63.000		250.000		1000.000			

Sample No. 40



Size ( $\mu\text{m}$ )	Volume In %	Size ( $\mu\text{m}$ )	Volume In %	Size ( $\mu\text{m}$ )	Volume In %	Size ( $\mu\text{m}$ )	Volume In %
0.010	0.16	63.000	1.56	250.000	29.75	1000.000	
4.000	5.12	125.000	11.76	500.000	34.74	2000.000	16.90
63.000		250.000		1000.000			

Sample No. 41



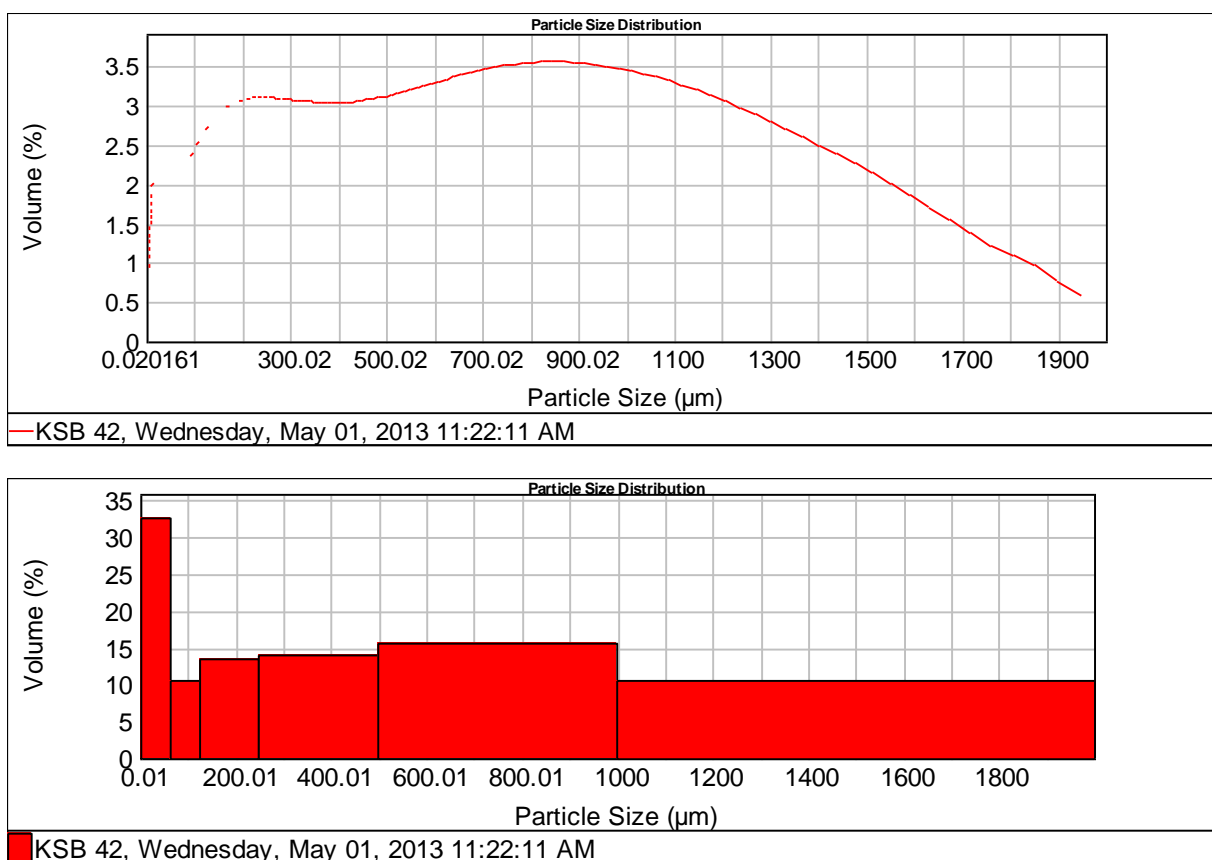
Size ( $\mu\text{m}$ )	Volume In %
0.010	1.89
4.000	18.88
63.000	

Size ( $\mu\text{m}$ )	Volume In %
63.000	2.82
125.000	8.75
250.000	

Size ( $\mu\text{m}$ )	Volume In %
250.000	23.24
500.000	29.96
1000.000	

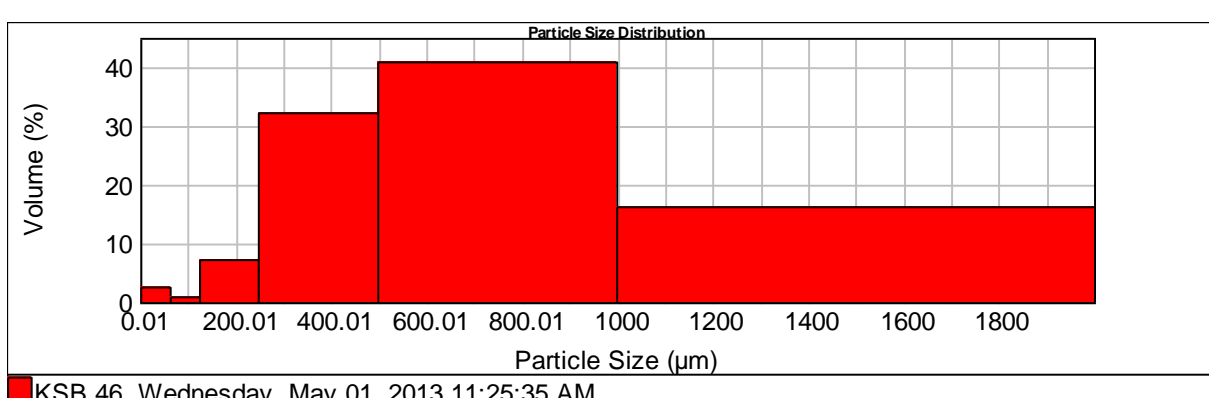
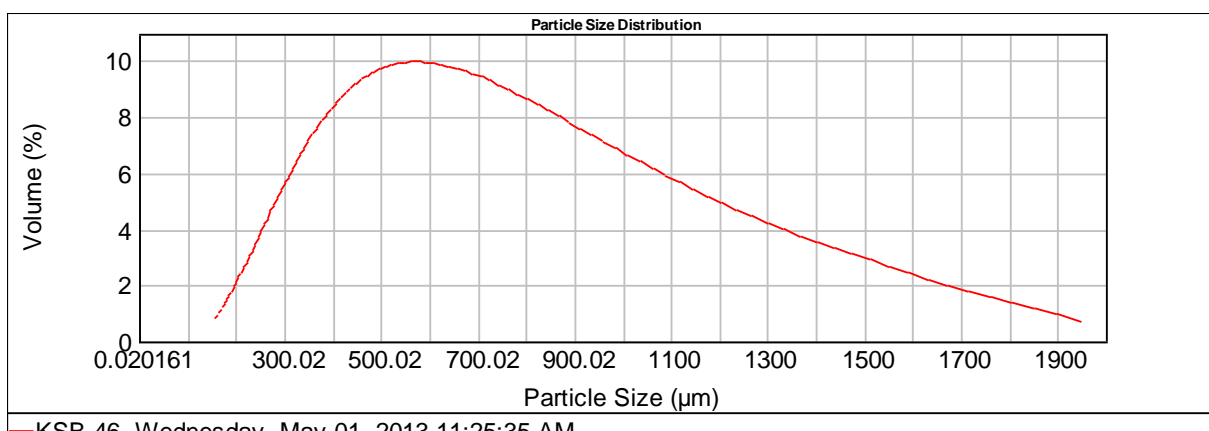
Size ( $\mu\text{m}$ )	Volume In %
1000.000	
2000.000	14.47

Sample No. 42



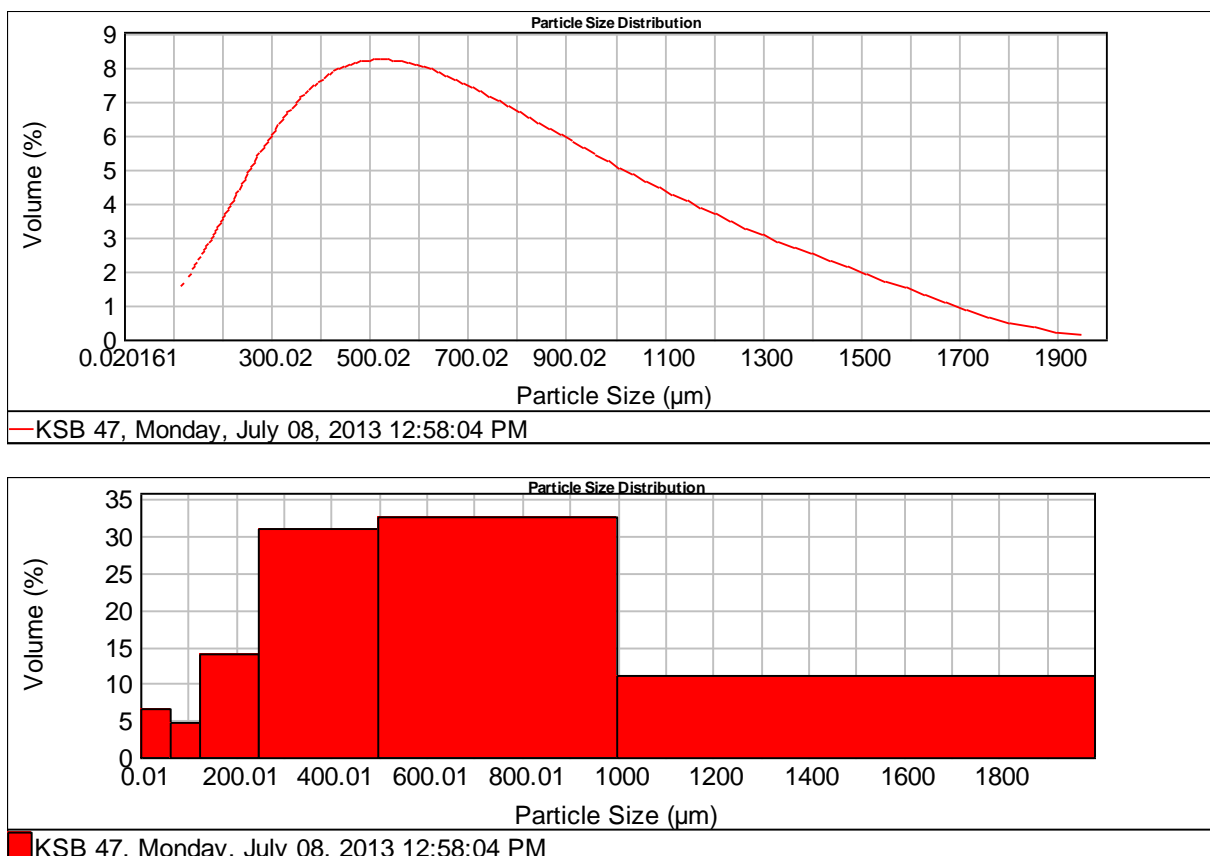
Size ( $\mu\text{m}$ )	Volume In %	Size ( $\mu\text{m}$ )	Volume In %	Size ( $\mu\text{m}$ )	Volume In %	Size ( $\mu\text{m}$ )	Volume In %
0.010	3.54	63.000	10.55	250.000	13.90	1000.000	10.42
4.000	32.64	125.000	13.50	500.000	15.45	2000.000	
63.000		250.000		1000.000			

Sample No. 46



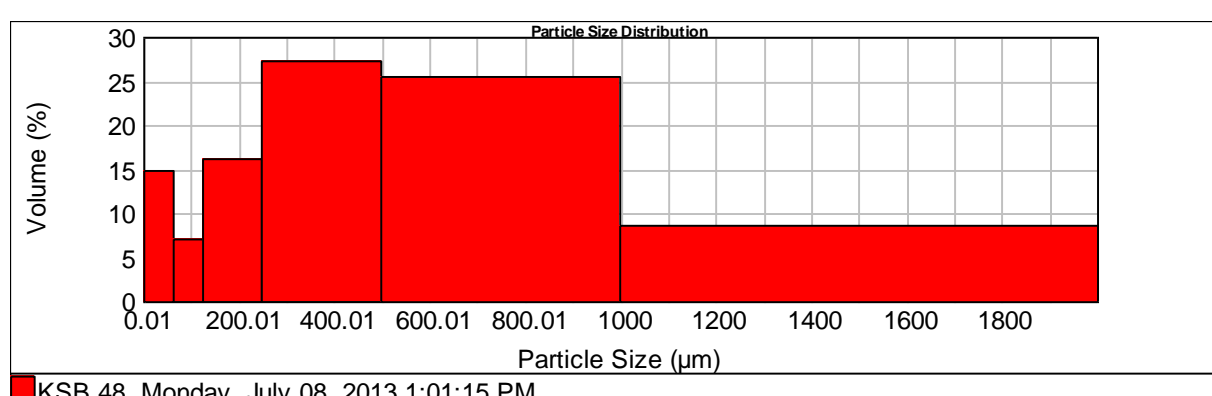
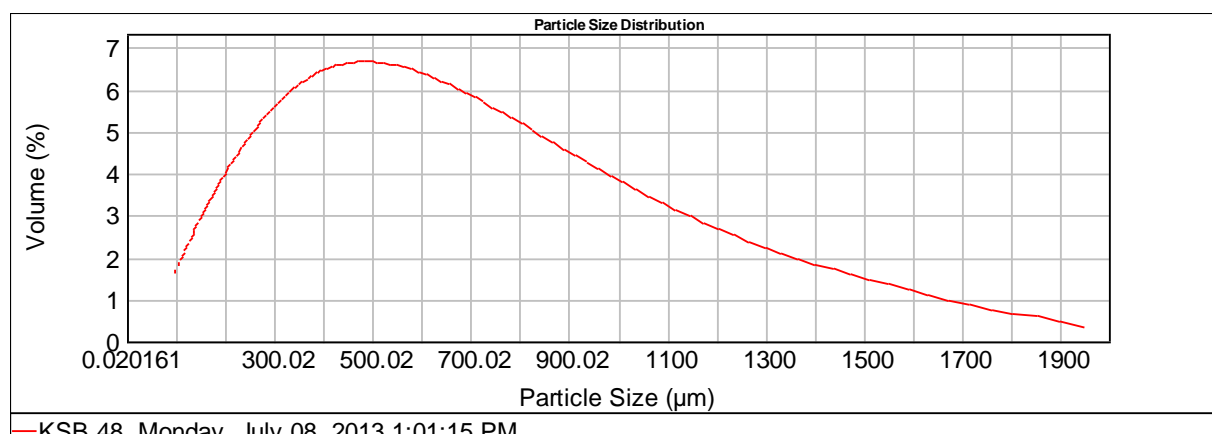
Size ( $\mu\text{m}$ )	Volume In %	Size ( $\mu\text{m}$ )	Volume In %	Size ( $\mu\text{m}$ )	Volume In %	Size ( $\mu\text{m}$ )	Volume In %
0.010	0.00	63.000	0.89	250.000	32.11	1000.000	16.08
4.000	2.66	125.000	7.30	500.000	40.95	2000.000	
63.000		250.000		1000.000			

Sample No. 47



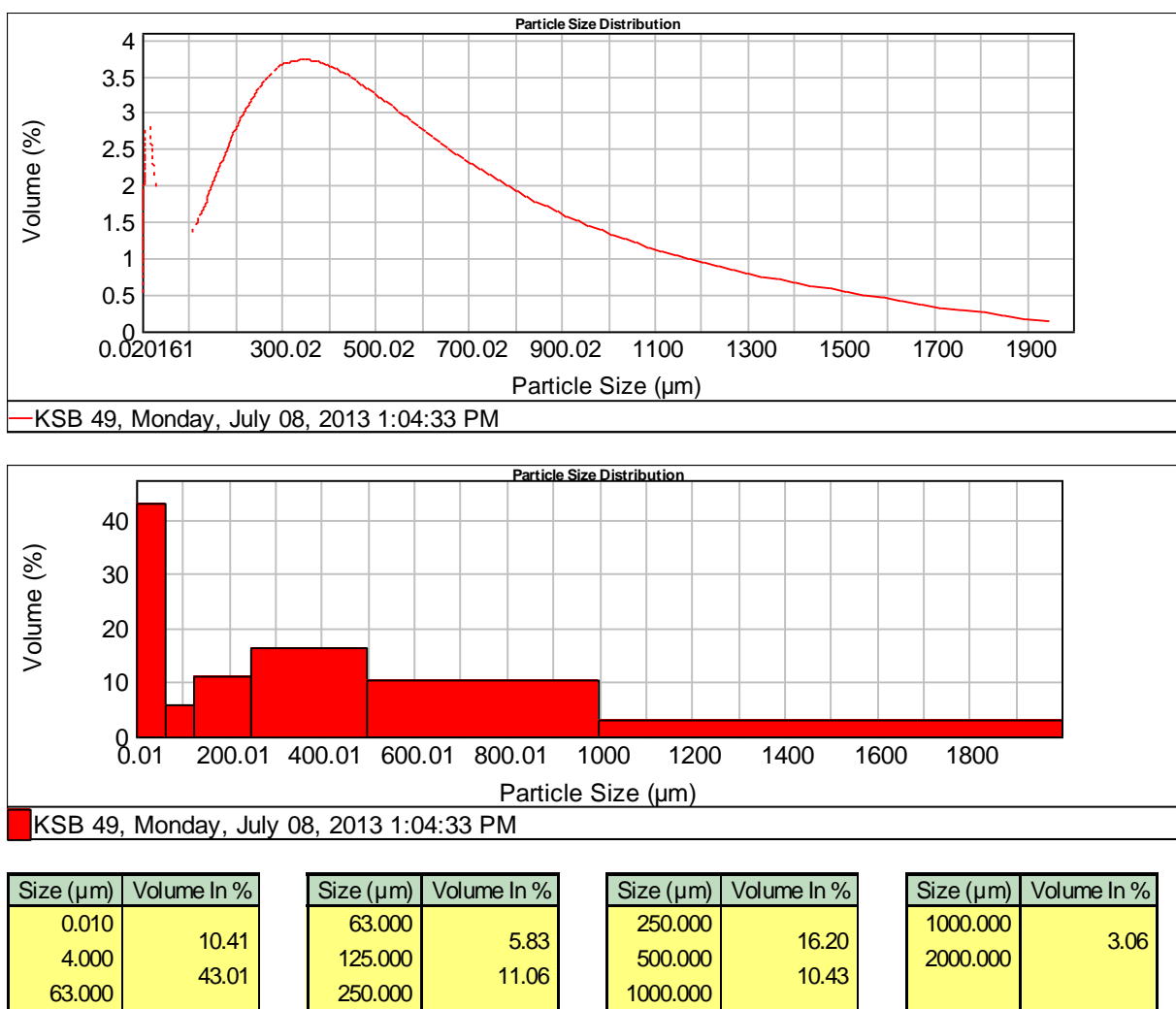
Size ( $\mu\text{m}$ )	Volume In %	Size ( $\mu\text{m}$ )	Volume In %	Size ( $\mu\text{m}$ )	Volume In %	Size ( $\mu\text{m}$ )	Volume In %
0.010	0.26	63.000	4.60	250.000	31.04	1000.000	
4.000	6.57	125.000	13.87	500.000	32.61	2000.000	11.06
63.000		250.000		1000.000			

Sample No. 48

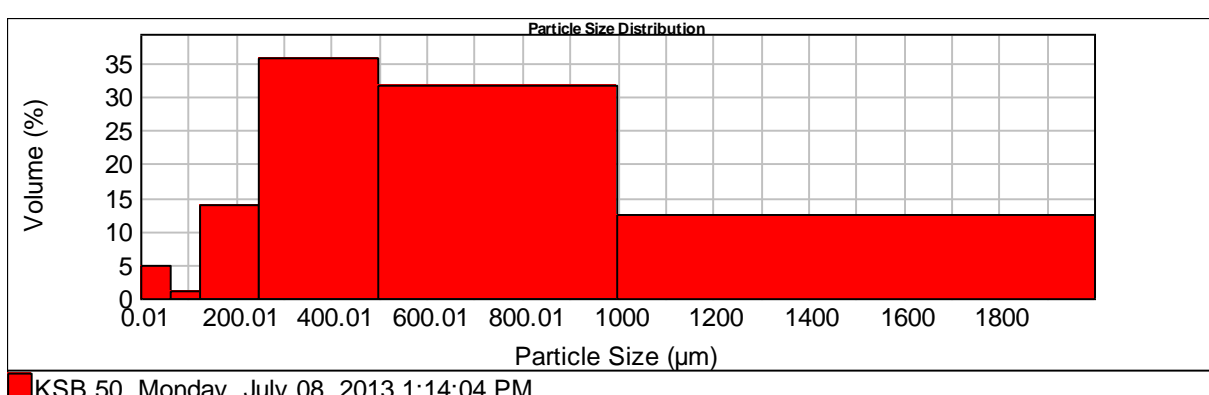
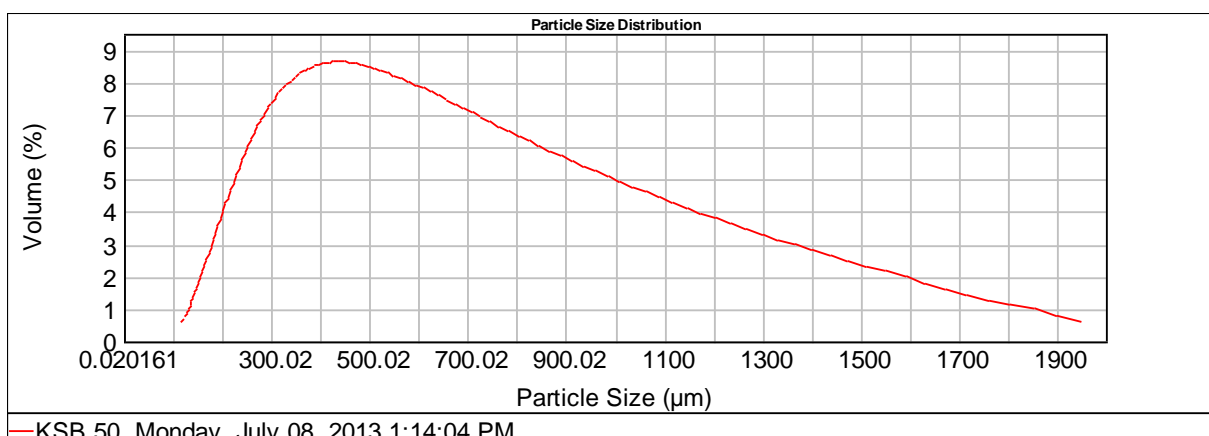


Size ( $\mu\text{m}$ )	Volume ln %	Size ( $\mu\text{m}$ )	Volume ln %	Size ( $\mu\text{m}$ )	Volume ln %	Size ( $\mu\text{m}$ )	Volume ln %
0.010	0.72	63.000	6.94	250.000	27.29	1000.000	8.60
4.000	14.74	125.000	16.16	500.000	25.55	2000.000	
63.000		250.000		1000.000			

Sample No. 49

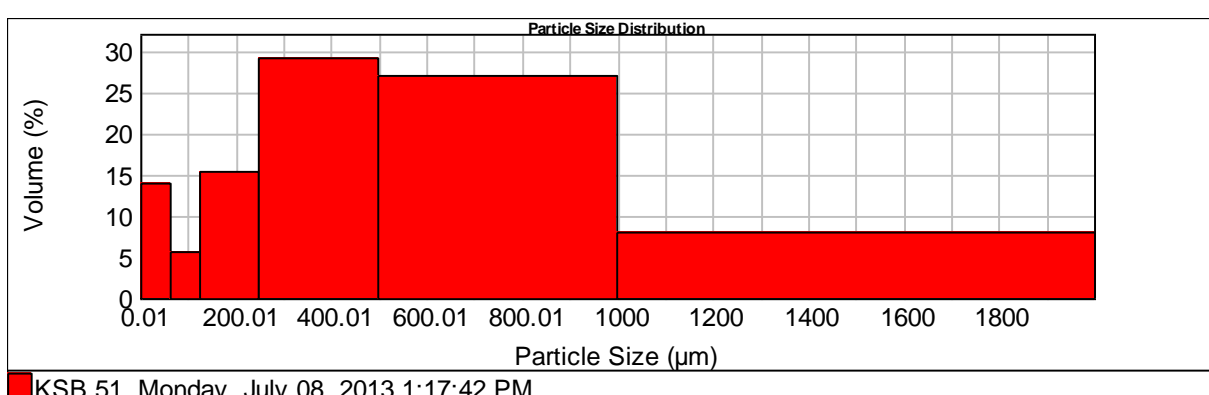
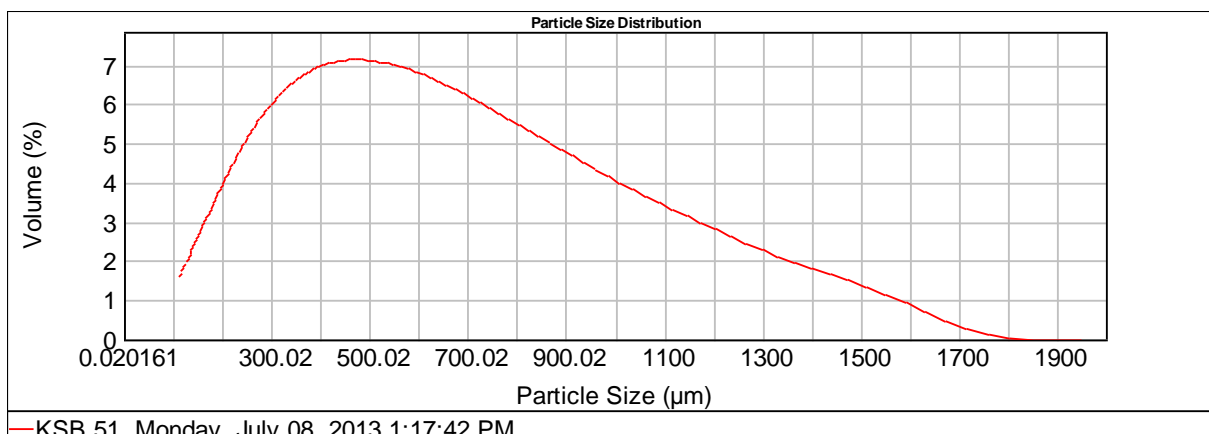


Sample No. 50



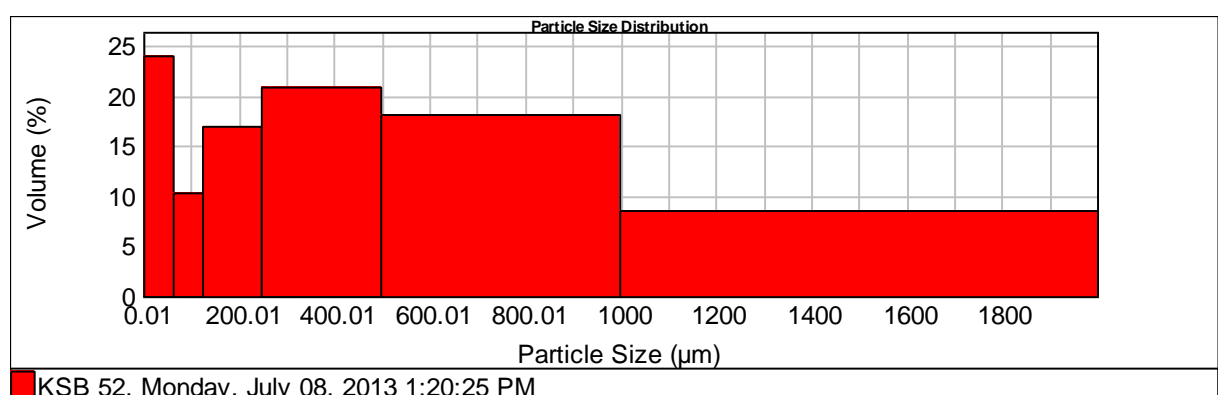
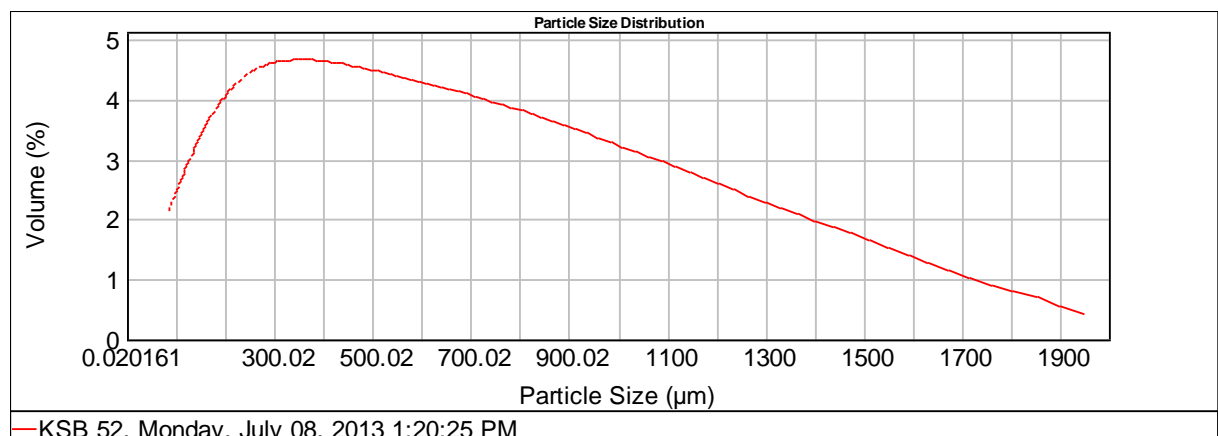
Size ( $\mu\text{m}$ )	Volume ln %	Size ( $\mu\text{m}$ )	Volume ln %	Size ( $\mu\text{m}$ )	Volume ln %	Size ( $\mu\text{m}$ )	Volume ln %
0.010	0.07	63.000	1.12	250.000	35.77	1000.000	12.52
4.000	4.93	125.000	13.96	500.000	31.63	2000.000	
63.000		250.000		1000.000			

Sample No. 51



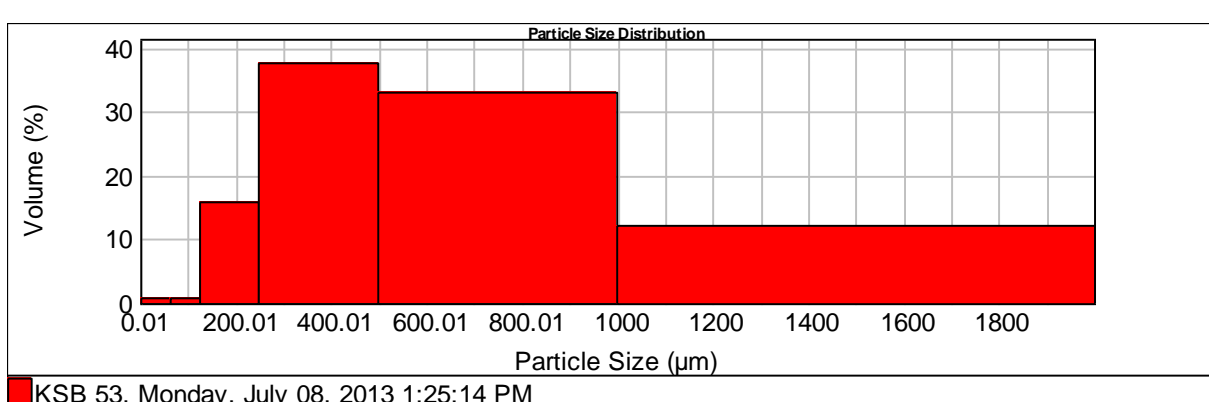
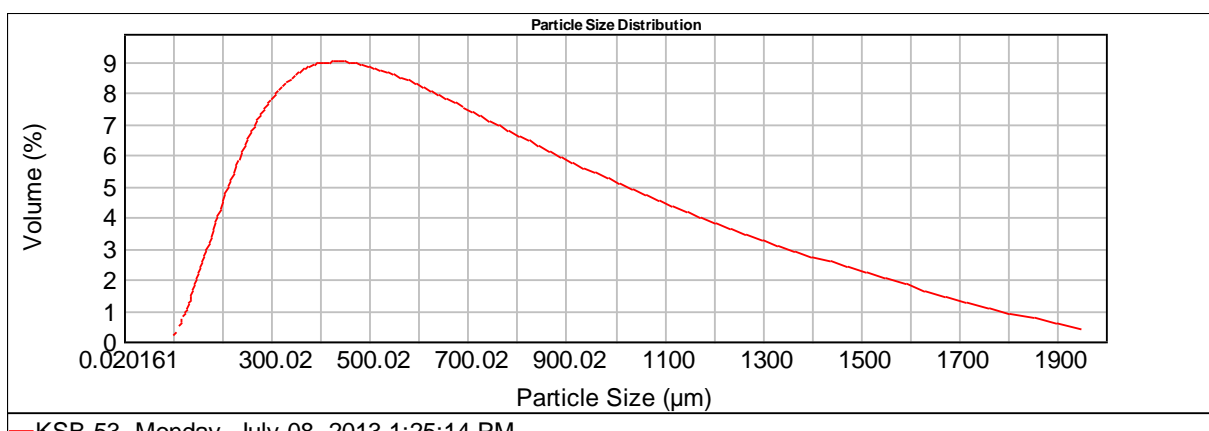
Size ( $\mu\text{m}$ )	Volume ln %	Size ( $\mu\text{m}$ )	Volume ln %	Size ( $\mu\text{m}$ )	Volume ln %	Size ( $\mu\text{m}$ )	Volume ln %
0.010	0.75	63.000	5.57	250.000	29.29	1000.000	7.95
4.000	13.91	125.000	15.41	500.000	27.12	2000.000	
63.000		250.000		1000.000			

## Sample No. 52



Size (µm)	Volume In %						
0.010	1.28	63.000	10.20	250.000	20.78	1000.000	8.59
4.000	24.05	125.000	17.03	500.000	18.08	2000.000	
63.000		250.000		1000.000			

Sample No. 53



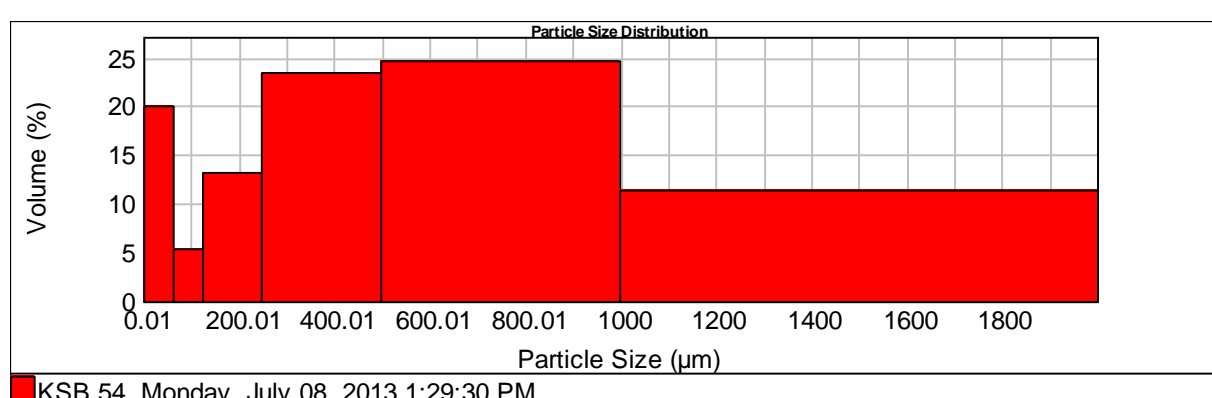
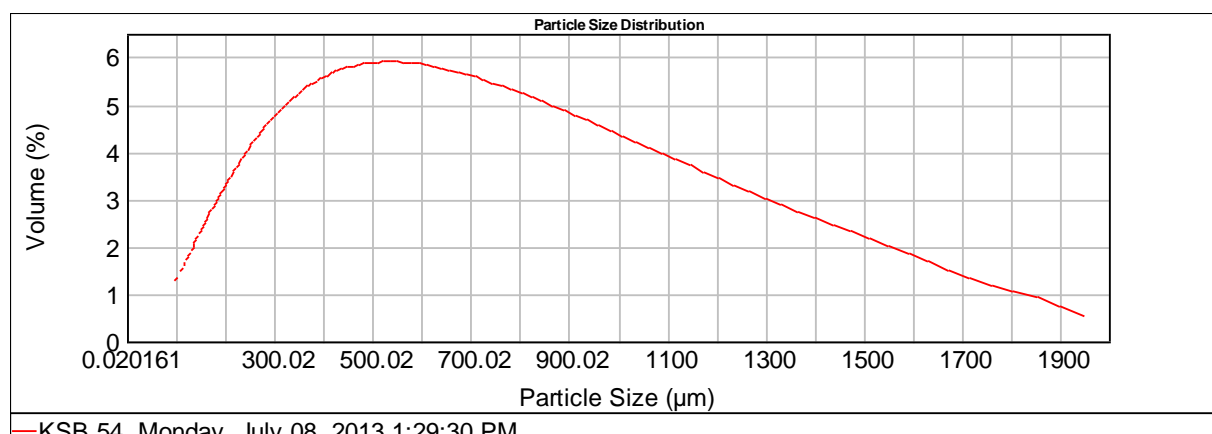
Size ( $\mu\text{m}$ )	Volume In %
0.010	0.00
4.000	0.62
63.000	

Size ( $\mu\text{m}$ )	Volume ln %
63.000	0.80
125.000	15.79
250.000	

Size ( $\mu\text{m}$ )	Volume In %
250.000	37.64
500.000	33.01
1000.000	

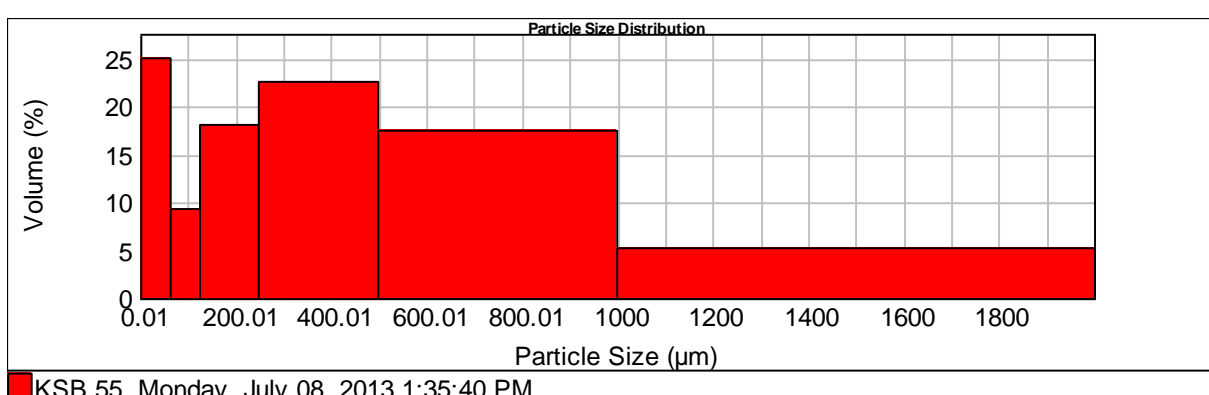
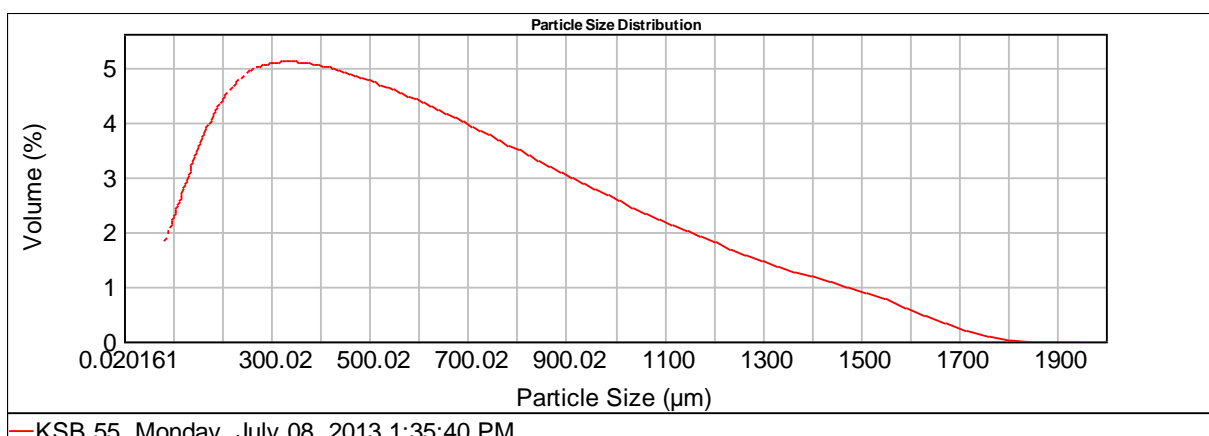
Size ( $\mu\text{m}$ )	Volume ln %
1000.000	
2000.000	12.14

Sample No. 54



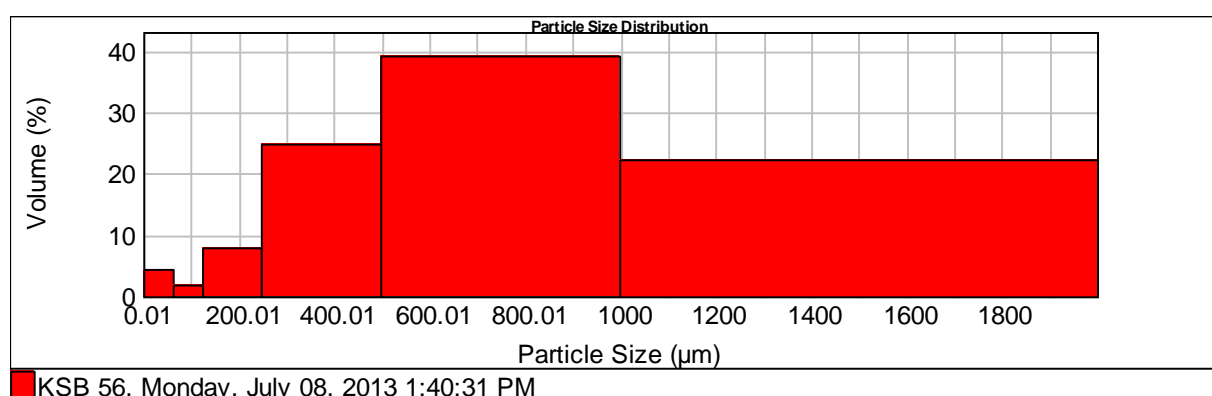
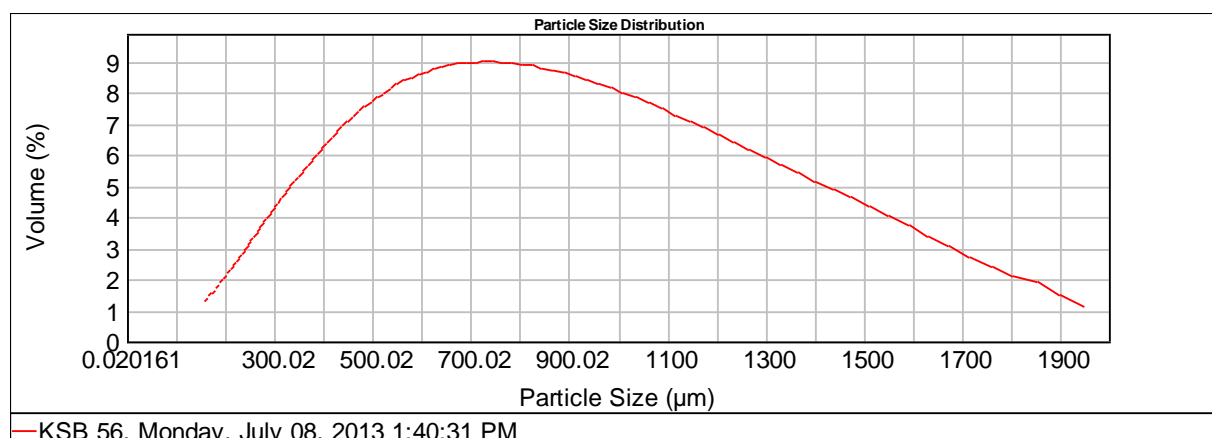
Size ( $\mu\text{m}$ )	Volume ln %	Size ( $\mu\text{m}$ )	Volume ln %	Size ( $\mu\text{m}$ )	Volume ln %	Size ( $\mu\text{m}$ )	Volume ln %
0.010	2.07	63.000	5.35	250.000	23.45	1000.000	11.39
4.000	19.96	125.000	13.12	500.000	24.66	2000.000	
63.000		250.000		1000.000			

Sample No. 55



Size ( $\mu\text{m}$ )	Volume ln %	Size ( $\mu\text{m}$ )	Volume ln %	Size ( $\mu\text{m}$ )	Volume ln %	Size ( $\mu\text{m}$ )	Volume ln %
0.010	2.13	63.000	9.23	250.000	22.73	1000.000	5.14
4.000	25.16	125.000	18.12	500.000	17.49	2000.000	
63.000		250.000		1000.000			

Sample No. 56



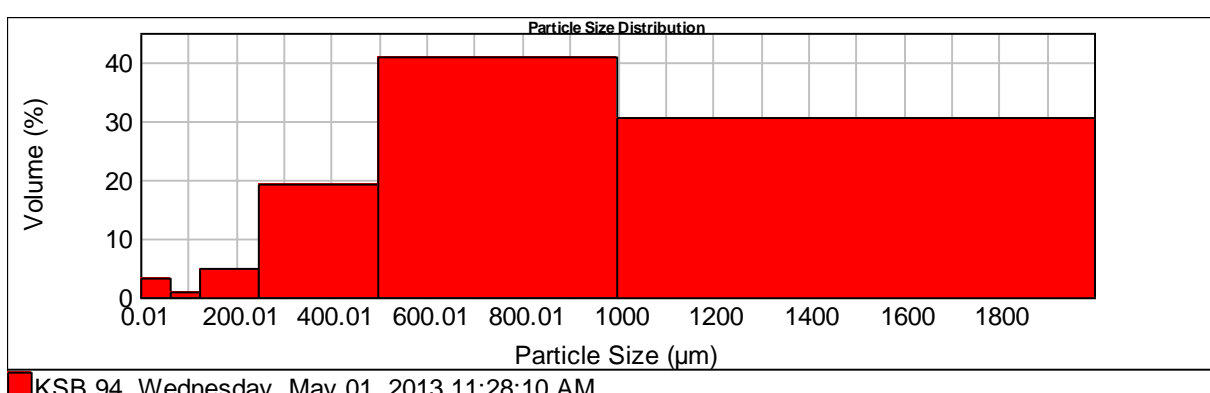
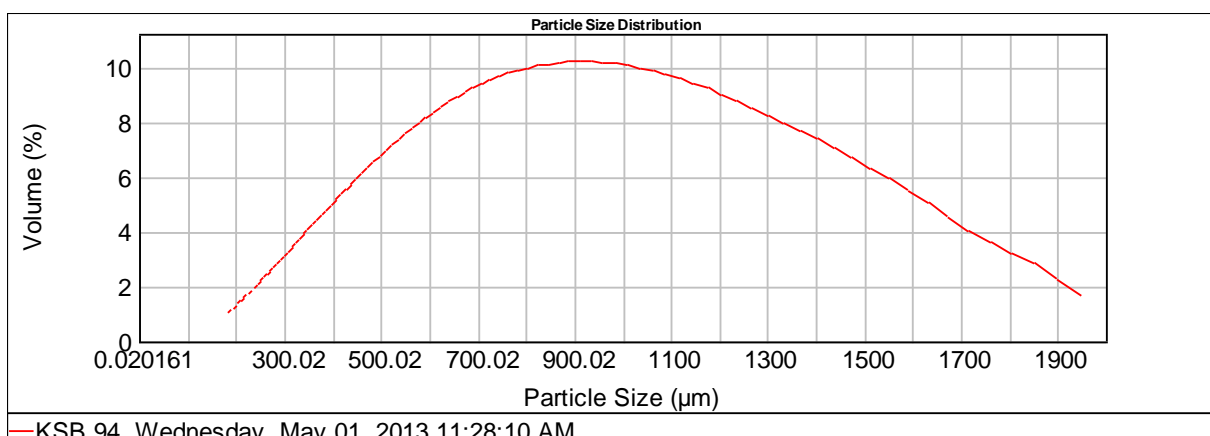
Size ( $\mu\text{m}$ )	Volume In %
0.010	0.06
4.000	4.34
63.000	

Size ( $\mu\text{m}$ )	Volume In %
63.000	1.77
125.000	7.90
250.000	

Size ( $\mu\text{m}$ )	Volume In %
250.000	24.59
500.000	39.15
1000.000	

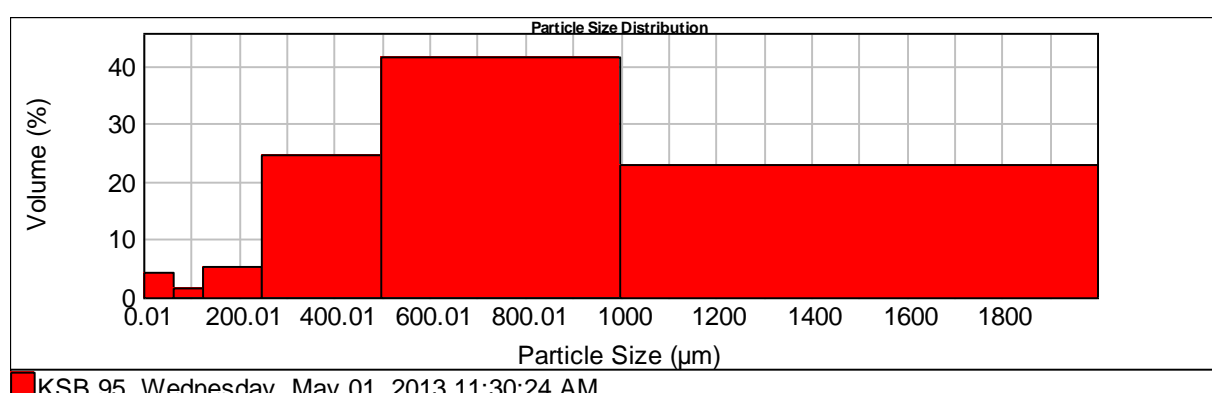
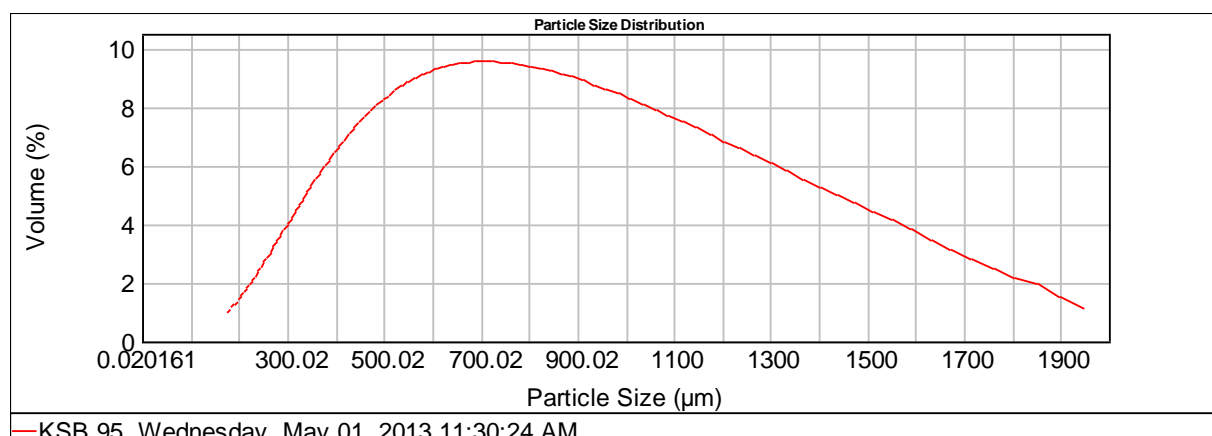
Size ( $\mu\text{m}$ )	Volume In %
1000.000	
2000.000	22.20

Sample No. 94



Size ( $\mu\text{m}$ )	Volume In %	Size ( $\mu\text{m}$ )	Volume In %	Size ( $\mu\text{m}$ )	Volume In %	Size ( $\mu\text{m}$ )	Volume In %
0.010	0.07	63.000	0.96	250.000	19.26	1000.000	30.66
4.000	3.30	125.000	4.73	500.000	41.02	2000.000	
63.000		250.000		1000.000			

Sample No. 95



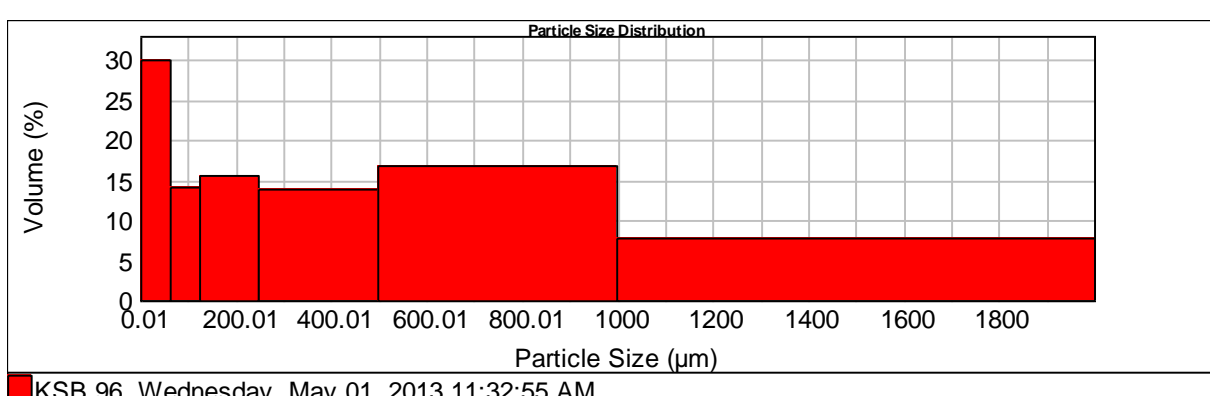
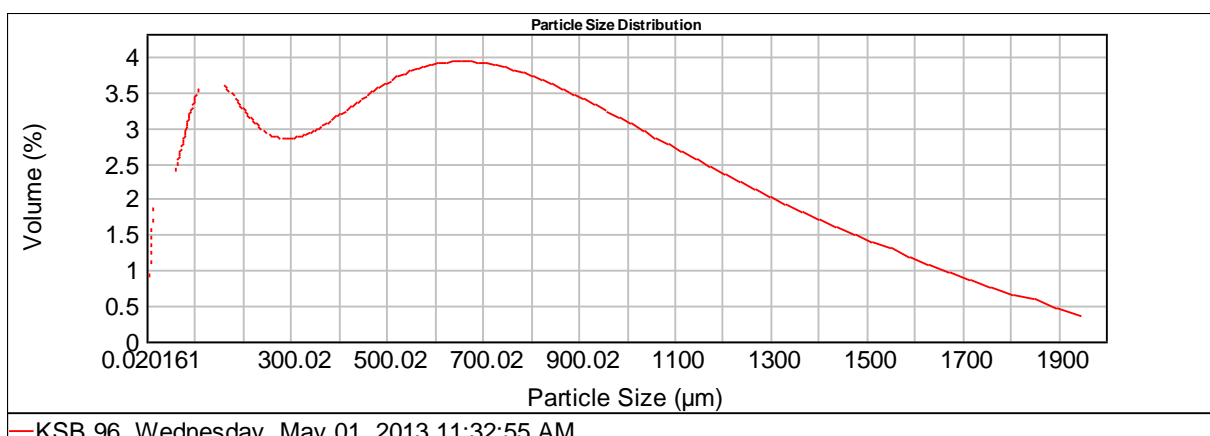
Size (μm)	Volume In %
0.010	0.00
4.000	4.14
63.000	

Size (μm)	Volume In %
63.000	1.43
125.000	5.35
250.000	

Size (μm)	Volume In %
250.000	24.66
500.000	41.56
1000.000	

Size (μm)	Volume In %
1000.000	22.86
2000.000	

Sample No. 96



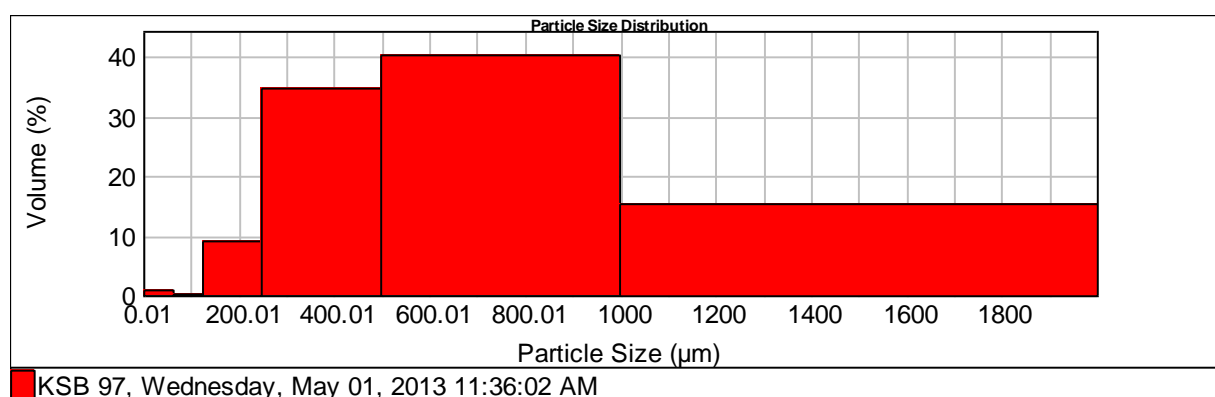
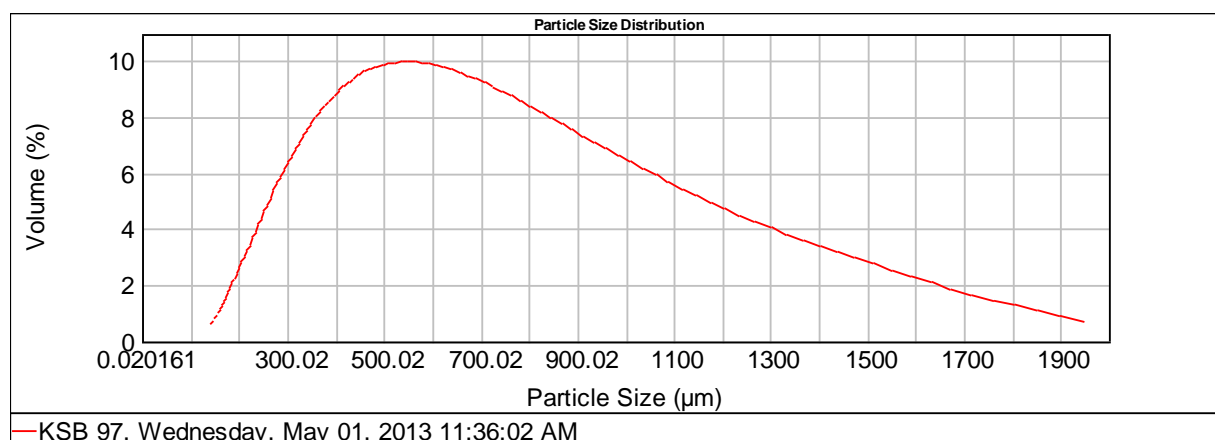
Size ( $\mu\text{m}$ )	Volume In %
0.010	2.15
4.000	30.01
63.000	

Size ( $\mu\text{m}$ )	Volume In %
63.000	14.01
125.000	15.47
250.000	

Size ( $\mu\text{m}$ )	Volume In %
250.000	13.89
500.000	16.82
1000.000	

Size ( $\mu\text{m}$ )	Volume In %
1000.000	
2000.000	7.64

Sample No. 97



Size ( $\mu\text{m}$ )	Volume In %	Size ( $\mu\text{m}$ )	Volume In %	Size ( $\mu\text{m}$ )	Volume In %	Size ( $\mu\text{m}$ )	Volume In %
0.010	0.00	63.000	0.14	250.000	34.60	1000.000	15.37
4.000	0.77	125.000	8.88	500.000	40.24	2000.000	
63.000		250.000		1000.000			

## Grain Size Distribution

Station No.	Sand	Silt	Clay	Sediment type
KSB1	96.9	3.1	0.00	Sand
KSB2	98.58	1.42	0.00	Sand
KSB3	96.5	3.43	0.07	Sand
KSB4	96.55	3.45	0.00	Sand
KSB5	98.68	1.32	0.00	Sand
KSB6	98.15	1.85	0.00	Sand
KSB7	99.69	0.31	0.00	Sand
KSB8	96.14	3.8	0.06	Sand
KSB9	98.19	1.81	0.00	Sand
KSB10	95.22	4.71	0.07	Sand
KSB11	98.18	1.82	0.00	Sand
KSB12	98.68	1.32	0.00	Sand
KSB13	97.45	2.55	0.00	Sand
KSB14	93.71	6.23	0.06	Sand
KSB15	95.91	4.09	0.00	Sand
KSB16	89.74	9.97	0.29	Silty sand
KSB17	94.61	5.23	0.16	Sand
KSB18	93.67	6.17	0.16	Sand
KSB19	87.38	12.17	0.45	Silty sand
KSB20	82.45	16.76	0.79	Silty sand
KSB21	89.98	9.6	0.42	Silty sand
KSB22	94.15	5.69	0.16	Sand
KSB23	91.43	8.28	0.29	Sand
KSB24	95.38	4.55	0.07	Sand
KSB25	90.06	9.54	0.40	Sand
KSB26	90.03	9.51	0.46	Sand
KSB27	91.95	7.78	0.27	Sand
KSB28	71.98	26.94	1.08	Silty sand
KSB29	71.95	26.79	1.26	Silty sand
KSB30	73.02	25.96	1.02	Silty sand

<b>Station No.</b>	<b>Sand</b>	<b>Silt</b>	<b>Clay</b>	<b>Sediment type</b>
KSB31	79.1	20.18	0.72	Silty sand
KSB32-A	83.79	15.56	0.65	Silty sand
KSB32-B	86.18	13.13	0.69	Silty sand
KSB33	88.47	11.15	0.38	Silty sand
KSB34	92.8	7.05	0.15	Sand
KSB36	76.98	21.69	1.33	Silty sand
KSB37	83.66	15.3	1.04	Silty sand
KSB38	94.85	5.02	0.13	Sand
KSB39	99.38	0.62	0.00	Sand
KSB40	94.72	5.12	0.16	Sand
KSB41	79.23	18.88	1.89	Silty sand
KSB42	63.82	32.64	3.54	Silty sand
KSB46	97.34	2.66	0.00	Sand
KSB47	99.74	6.57	0.26	Sand
KSB48	99.28	14.74	0.72	Sand
KSB49	89.59	43.01	10.41	Silty sand
KSB50	99.93	4.93	0.07	Sand
KSB51	99.25	13.91	0.75	Sand
KSB52	98.72	24.05	1.28	Sand
KSB53	100	0.62	0.00	Sand
KSB54	97.93	19.96	2.07	Sand
KSB55	97.87	25.16	2.13	Sand
KSB56	99.94	4.34	0.06	Sand
KSB94	96.63	3.3	0.07	Sand
KSB95	95.86	4.14	0.00	Sand
KSB96	67.84	30.01	2.15	Silty sand
KSB97	99.23	0.77	0.00	Sand

## APPENDIX 4: PARAMETERS USED FOR PROCESSING AND MOSAICING

### SIDESCAN SONAR DATA

**Software used: Sonarwiz (Chesapeake Technology Inc.)**

**Coordinate system used for data analysis**

WGS84 UTM39N

**Logging Anomalies**

***Set up Project***

Coordinate source – auto (use fish if valid, otherwise ship)

Time constant for course smoothing = 300 pings

Coordinate system – UTM84-39N

***Batch import of files***

Course made good - checked

No gain applied

Percentage of sonar range to map - 100%

Channels 3 and 4

Thresholding enabled - sniff carried out on 6 files to establish thresholding value of 2231

***Batch Processing of files***

EGN applied – intensity=41

**Seabed Classification Test**

The same settings were used as for logging anomalies except that the files were trimmed and split where they overlapped, and the nadir transparency was set to 4. Perpendicular survey lines were not included in the mosaic.

## APPENDIX 5: LIST OF ALL ANOMALIES LOGGED FROM THE SIDESCAN SONAR DATA

### Area 1

Contact No	Length(ft)	Width(ft)	Height(ft)	Preliminary Interpretation	Lat(WGS84)	Lon(WGS84)
QBC_Q10001	45.58	7.91	1.89	Debris?	26.164178	51.067508
QBC_Q10002	3.39	3.73	0.21	Debris?	26.172531	51.053955
QBC_Q10003	17.09	1.65	0.17	Seabed Scar?	26.188127	51.033427
QBC_Q10004	0	0	0	Natural?	26.190223	51.030078
QBC_Q10005	13.52	1.9	0.14	Debris?	26.190361	51.028873
QBC_Q10006	10.94	1.54	0.11	Debris?	26.190689	51.028266
QBC_Q10007	11.62	5.98	0.38	Natural?	26.191166	51.02786
QBC_Q10008	22.98	13.1	0.15	Buried Feature?	26.192163	51.026041
QBC_Q10009	4.44	5.14	1.01	Debris? - Modern?	26.198301	51.018376
QBC_Q10010	21.65	17.38	0.94	Buried Feature?	26.198905	51.016678
QBC_Q10011	28.72	2.96	0.07	Natural?	26.202091	51.012029
QBC_Q10012	16.67	3.27	0	Debris?	26.209287	51.004147
QBC_Q10013	14.95	4.82	0.06	Natural?	26.217675	50.989785
QBC_Q10014	24.01	8.2	0.34	Debris?	26.140912	50.946437
QBC_Q10016	53.44	28.49	0.78	Debris? - Modern?	26.132907	50.957824
QBC_Q10018	1.57	1.57	0.28	Debris?	26.124179	50.968431
QBC_Q10020	6.53	2.49	0.12	Natural?	26.121128	50.972238
QBC_Q10021	3.74	4.02	0.29	Unclassified	26.119927	50.973677
QBC_Q10023	52.26	11.04	0.9	Debris?	26.115726	50.980105
QBC_Q10024	14.06	2.11	0.1	Natural?	26.113622	50.983122
QBC_Q10025	11.39	4.22	0.45	Debris - Modern?	26.110508	50.98751

Contact No	Length(ft)	Width(ft)	Height(ft)	Preliminary Interpretation	Lat(WGS84)	Lon(WGS84)
QBC_Q10026	2.43	3.58	1.49	Natural?	26.066991	50.903244
QBC_Q10027	17.9	7.71	0.23	Buried Feature?-	26.120183	50.974065
QBC_Q10030	105.23	5.09	1.2	Seabed Scar?	26.05359	50.922498
QBC_Q10035	44.6	16.38	1.04	Buried Feature?	26.049929	50.927743
QBC_Q10037	5.75	3.8	0.56	Buried Feature?	26.10989	50.915878
QBC_Q10038	20.24	14.35	0.54	Buried Feature?	26.109964	50.916072
QBC_Q10039	4.19	3.48	0.25	Debris?	26.109416	50.916106
QBC_Q10044	7.58	7.63	0.51	Debris?	26.105752	50.922107
QBC_Q10045	4.59	3.04	0.89	Debris?	26.104725	50.923774
QBC_Q10046	9.64	4.98	0.93	Debris?	26.103701	50.925436
QBC_Q10047	7.95	1.67	0	Debris?	26.096653	50.93603
QBC_Q10048	8.47	5.01	0.75	Debris?	26.095658	50.936373
QBC_Q10049	2.92	2.34	0.43	Natural?	26.092541	50.941048
QBC_Q10050	9.96	4.09	0.81	Debris?	26.090631	50.944056
QBC_Q10900	18.32	3.14	0	Duplicate of QBC_Q10050	26.090739	50.944173
QBC_Q10051	21.16	11.32	0.77	Debris? - Modern?	26.089546	50.943997
QBC_Q10052	45.47	1.67	0.9	Debris?	26.089965	50.944877
QBC_Q10053	4.69	3.3	0	Natural?	26.091397	50.943247
QBC_Q10056	0	0	0	Debris?	26.089551	50.943385
QBC_Q10057	3.03	1.08	0.3	Debris?	26.088984	50.944446
QBC_Q10058	8.74	1.92	0	Debris?	26.088443	50.944708
QBC_Q10059	6.5	5.15	3.48	Debris?	26.083818	50.951767
QBC_Q10060	7.27	1.28	0.23	Natural?	26.075834	50.964598
QBC_Q10061	25.94	3.43	0.32	Natural?	26.068163	50.973555
QBC_Q10062	7.32	2.12	1.14	Debris?	26.111185	50.923062
QBC_Q10063	5.59	1.77	1	Debris?	26.108357	50.926696

Contact No	Length(ft)	Width(ft)	Height(ft)	Preliminary Interpretation	Lat(WGS84)	Lon(WGS84)
QBC_Q10064	3.42	1.82	0.2	Natural?	26.107479	50.926505
QBC_Q10065	4.83	2.32	0.48	Debris?	26.108373	50.927508
QBC_Q10066	6.05	2.89	0.51	Buried Feature?	26.107364	50.927361
QBC_Q10067	5.08	4.41	0.09	Buried Feature?	26.107701	50.926639
QBC_Q10068	3.54	1.12	0.09	Buried Feature?	26.100057	50.939206
QBC_Q10069a	2.62	2.55	0.99	Unclassified	26.094479	50.94567
QBC_Q10069b	4.7	2.72	0.41	Buried Feature?	26.094703	50.945614
QBC_Q10071	3.44	1.99	0.43	Debris?	26.091898	50.948385
QBC_Q10072	9.34	2.37	0.76	Debris?	26.091842	50.950222
QBC_Q10073	2.77	0.74	0.49	Debris?	26.089504	50.953108
QBC_Q10074	2.41	0.74	0.16	Debris?	26.08955	50.953583
QBC_Q10075	26.41	12.41	0.97	Debris?	26.08889	50.953501
QBC_Q10076	5.51	2.39	0.76	Buried Feature?	26.082374	50.962397
QBC_Q10077	15.57	1.55	0	Natural?	26.080693	50.965024
QBC_Q10078	13.09	21.76	0.41	Natural?	26.084755	50.959102
QBC_Q10079	4.28	2.2	0.36	Natural?	26.113025	50.927079
QBC_Q10080	4.21	1.84	0.81	Debris?	26.113302	50.927475
QBC_Q10081	7.17	5.55	0.72	Debris?	26.112738	50.92822
QBC_Q10082	23.98	10.99	0	Location?	26.11209	50.928692
QBC_Q10083	7.52	3.61	1.01	Debris?	26.110706	50.930578
QBC_Q10084	19.52	2.98	0	Location?	26.104293	50.93928
QBC_Q10085	17.58	13.28	0.92	Debris?	26.098616	50.947458
QBC_Q10086	10.05	7.91	0.09	Buried Feature?	26.09642	50.952379
QBC_Q10087	3.33	0.73	0.13	Debris?	26.095703	50.95399
QBC_Q10088	1.66	0.94	0.64	Natural?	26.092932	50.956692
QBC_Q10089	22.08	12.26	0	Unclassified	26.092969	50.957561

Contact No	Length(ft)	Width(ft)	Height(ft)	Preliminary Interpretation	Lat(WGS84)	Lon(WGS84)
QBC_Q10090	19.63	19.47	0	Natural?	26.083392	50.969561
QBC_Q10091	34.48	12.42	0.52	Buried Feature?	26.077678	50.977986
QBC_Q10092	6.84	6.32	0	Buried Feature?	26.115737	50.931746
QBC_Q10093	8.57	1.95	0.31	Debris?	26.114192	50.93375
QBC_Q10094	6.77	4.35	0.41	Debris?	26.108821	50.941569
QBC_Q10095	6.01	2.99	0	Debris?	26.092568	50.962845
QBC_Q10096	22.95	4.17	0.11	Buried Feature?	26.092101	50.965949
QBC_Q10097	98.26	2.28	0	Linear Debris?	26.087507	50.971216
QBC_Q10098	23.27	6.76	0	Debris?	26.122298	50.929615
QBC_Q10099	14.99	6.1	0	Debris?	26.122068	50.929949
QBC_Q10100	3.84	2.77	0	Debris?	26.121916	50.930422
QBC_Q10101	1.26	0.5	0.16	Debris?	26.120506	50.933141
QBC_Q10102	1.62	0.75	0.25	Debris?	26.12021	50.933567
QBC_Q10103	4.42	2.17	0.44	Buried Feature?	26.117515	50.936816
QBC_Q10104	11.6	5.15	0.69	Debris?	26.116663	50.939105
QBC_Q10105	4.66	1.89	1.02	Debris?	26.114032	50.942135
QBC_Q10107	6.12	6.17	1.33	Buried Feature? - Duplicate	26.111764	50.945494
QBC_Q10106	0	0	0	Duplicate of QBC_Q10107	26.111778	50.945571
QBC_Q10108	9.08	6.57	0.8	Debris?	26.10403	50.95733
QBC_Q10109	1.56	1.25	0.37	Debris?	26.103142	50.95729
QBC_Q10110	16.81	8.48	0.87	Debris?	26.097583	50.9661
QBC_Q10111	10.64	3.62	0.47	Debris?	26.093648	50.970599
QBC_Q10112	15.62	10.02	0.73	Debris?	26.092174	50.973257
QBC_Q10113	16.51	0.85	0	Natural?	26.085384	50.983023
QBC_Q10114	3.49	1.68	0.27	Natural?	26.125137	50.934866
QBC_Q10115	6.9	0.68	0.37	Debris?	26.124633	50.936281

Contact No	Length(ft)	Width(ft)	Height(ft)	Preliminary Interpretation	Lat(WGS84)	Lon(WGS84)
QBC_Q10116	11.24	1.57	0	Buried Feature?	26.12002	50.941669
QBC_Q10117	34.54	1.34	0	Natural?	26.11693	50.94535
QBC_Q10118	1.54	1.27	1.18	Natural?	26.111446	50.953896
QBC_Q10119	26.06	8.07	0	Buried Feature?	26.109767	50.956038
QBC_Q10120	12.25	3.84	0.58	Buried Feature?	26.102049	50.968652
QBC_Q10121	1.6	1.02	0.35	Natural?	26.09922	50.971846
QBC_Q10122	1.22	1.13	0.34	Natural?	26.099352	50.971723
QBC_Q10123	0.71	0.95	0.43	Natural?	26.099284	50.971785
QBC_Q10124	7.98	2.54	1.11	Debris?	26.09884	50.972745
QBC_Q10125	34.3	5.02	0.74	Buried feature?	26.098345	50.974332
QBC_Q10126	3.98	2.74	1.28	Buried Feature?	26.127756	50.939085
QBC_Q10127	6	2.75	0.25	Debris?	26.128502	50.939809
QBC_Q10128	16.21	4.9	0.66	Bham0074 - Cars	26.127721	50.9399
QBC_Q10129	0	0	0	Debris?	26.127713	50.940492
QBC_Q10130	6.55	5.48	0	Debris?	26.127253	50.941361
QBC_Q10131	23.06	1.42	0	Seabed Scar?	26.127141	50.941242
QBC_Q10132	6.64	5.41	0.89	Debris?	26.126667	50.941273
QBC_Q10133	0	0	0	Hole?	26.126209	50.94185
QBC_Q10134	19.17	2.89	0	Debris?	26.1226	50.945164
QBC_Q10135	24.74	4.12	0	Debris?	26.112494	50.959673
QBC_Q10136	6.64	4.07	0	Debris?	26.109849	50.962975
QBC_Q10137	5.22	3.97	0	Debris?	26.109132	50.967272
QBC_Q10138	7.46	1.37	0.69	Debris?	26.098517	50.979507
QBC_Q10139	50.05	1.78	0	Natural?	26.095911	50.983161
QBC_Q10140	1.41	1.08	0.58	Natural?	26.096149	50.983603
QBC_Q10141	16.18	7.11	0	Debris?	26.130633	50.944689

Contact No	Length(ft)	Width(ft)	Height(ft)	Preliminary Interpretation	Lat(WGS84)	Lon(WGS84)
QBC_Q10142	3.55	1.79	0.61	Debris?	26.12952	50.944773
QBC_Q10143	2.54	2.54	0.53	Debris?	26.128734	50.944708
QBC_Q10144	0	0	0	Debris?	26.128266	50.94669
QBC_Q10145	3.38	2.34	0.45	Buried Feature?	26.128192	50.947362
QBC_Q10146	16.76	7.05	0	Debris?	26.126096	50.948485
QBC_Q10147	2.92	1.71	0	Natural?	26.126761	50.949553
QBC_Q10148	1.76	0.58	0.23	Natural?	26.12299	50.954576
QBC_Q10149	3.11	1.8	0	Debris?	26.119636	50.960689
QBC_Q10150	33.33	3.41	0	Natural?	26.11807	50.961883
QBC_Q10151	10.15	2.76	0.5	Debris?	26.117805	50.962641
QBC_Q10152	2.25	1.14	0.62	Debris?	26.116527	50.963562
QBC_Q10153	31.79	4.59	0	Debris?	26.109352	50.974734
QBC_Q10155	8.78	3.94	0.52	Debris?	26.104284	50.981682
QBC_Q10156	3.69	2.14	0	Buried feature?	26.09757	50.989577
QBC_Q10157	12.02	1.49	0	Natural?	26.091728	50.999054
QBC_Q10158	3.01	2.77	0.1	Natural?	26.090182	51.000899
QBC_Q10159	12.43	18.1	0.15	Buried Feature?	26.087193	51.005279
QBC_Q10160	6.06	1.62	0.99	Debris? - Modern?	26.135037	50.945099
QBC_Q10161	44.17	13.51	0.88	Debris? - Modern?	26.132914	50.948831
QBC_Q10162	67.45	2.03	0	Natural?	26.122775	50.961895
QBC_Q10163	10.03	0.65	0.16	Natural?	26.121548	50.963778
QBC_Q10164	5.83	2.51	0.91	Debris?	26.12081	50.96621
QBC_Q10165	1.76	1.47	0	Debris?	26.117534	50.968357
QBC_Q10166	19.26	11.17	0.67	Debris?	26.117197	50.97072
QBC_Q10167	0	0	0	Object in Water Column?	26.116877	50.970623
QBC_Q10168	8.94	2.9	0.79	Debris? - Modern?	26.112267	50.976146

Contact No	Length(ft)	Width(ft)	Height(ft)	Preliminary Interpretation	Lat(WGS84)	Lon(WGS84)
QBC_Q10169	49.67	1.59	0	Seabed Scar?	26.112176	50.978016
QBC_Q10170	14.58	2.96	0.78	Buried Feature?	26.105195	50.986914
QBC_Q10172	58.46	4.21	0	Location?	26.098402	50.996512
QBC_Q10173	5.4	2.08	0.18	Location?	26.090331	51.023801
QBC_Q10175	4.92	3.52	0.38	Natural?	26.092546	51.022249
QBC_Q10176	0	0	0	Location?	26.094385	51.018362
QBC_Q10177	2.28	2.27	0	Hole?	26.115219	50.989037
QBC_Q10178	9.81	4.7	0.5	Debris?	26.116643	50.986132
QBC_Q10179	1.17	1.57	0.44	Debris?	26.116962	50.986285
QBC_Q10180	30.6	10.05	0	Location?	26.119999	50.983597
QBC_Q10181	5.11	1.51	0.19	Natural?	26.137381	50.957887
QBC_Q10182	9.83	3.37	0.52	Debris? - Modern?	26.140096	50.95542
QBC_Q10184	8.07	4.68	0.82	Debris?	26.122287	50.988372
QBC_Q10185	7.22	4.84	0.71	Debris?	26.125707	50.981833
QBC_Q10186	0	0	0	Debris? - Modern?	26.130007	50.976833
QBC_Q10187	5.59	3.6	0.73	Debris?	26.136482	50.966842
QBC_Q10188	20.52	6.76	0.3	Debris? - Modern?	26.140766	50.96262
QBC_Q10189	3.75	2.95	0	Hole?	26.147616	50.952451
QBC_Q10190	5.1	2.14	0	Debris? - Modern?	26.149583	50.955742
QBC_Q10191	10.91	7.98	0	Debris?	26.143373	50.967286
QBC_Q10192	6.99	2.63	0.27	Debris? - Modern?	26.140544	50.968642
QBC_Q10193	6.85	4.42	0.62	Debris?	26.138977	50.972897
QBC_Q10194	35.86	2.36	0	Seabed Scar?	26.103934	51.022202
QBC_Q10195	6.94	3.15	0	Buried Feature?	26.097815	51.028528
QBC_Q10196	11.03	3.42	0.73	Debris? - Modern?	26.089698	51.039936
QBC_Q10197	39.71	10.8	0	Natural?	26.098603	51.035768

Contact No	Length(ft)	Width(ft)	Height(ft)	Preliminary Interpretation	Lat(WGS84)	Lon(WGS84)
QBC_Q10198	87.39	28.38	0	Location?	26.116708	51.012945
QBC_Q10199	7.28	5.99	1.01	Debris? - Modern?	26.122426	51.002891
QBC_Q10200	23.65	2.32	0	Natural?	26.123063	51.003561
QBC_Q10201	0	0	0.8	Unclassified	26.124505	50.999772
QBC_Q10202	51.84	30.17	0	Location?	26.125948	50.998024
QBC_Q10203	5.2	2.44	0.68	Debris - Modern?	26.130334	50.993269
QBC_Q10204	1.69	0.7	0.27	Debris?	26.129516	50.993047
QBC_Q10205	10.56	5.94	0.13	Buried Feature?	26.140785	50.978639
QBC_Q10206	2.79	2.37	0.72	Debris?	26.140742	50.978097
QBC_Q10207	6.04	2.23	0.53	Debris? - Modern?	26.143998	50.972776
QBC_Q10208	11.67	8.95	0.53	Debris?	26.14765	50.967655
QBC_Q10209	16.49	6.85	0.81	Debris?	26.15206	50.961337
QBC_Q10210	11.33	3.38	0	Debris?	26.11286	50.922721
QBC_Q10211	0	0	0	Location?	26.112947	50.924671
QBC_Q10213	4.9	5.04	0.53	Debris?	26.103412	50.936359
QBC_Q10214	5.67	2.52	0.42	Debris?	26.102886	50.936858
QBC_Q10215	6.05	1.4	0.46	Debris?	26.102337	50.938217
QBC_Q10216	8.58	4.45	0.75	Bham0073 - Cars	26.101064	50.939624
QBC_Q10217	15.94	1.05	0	Natural?	26.097927	50.944155
QBC_Q10218	4.06	2.44	1.25	Debris?	26.095919	50.947739
QBC_Q10219	0	0	0	Unclassified	26.092693	50.950983
QBC_Q10220	14.13	8.38	0.95	Debris?	26.090578	50.956323
QBC_Q10221	0	0	0	Location?	26.089928	50.957252
QBC_Q10222	2.44	0.83	0.35	Buried Feature?	26.089615	50.956595
QBC_Q10223	2.86	1.79	0	Debris?	26.088618	50.959718
QBC_Q10224	52.84	7.75	0	Natural?	26.062097	50.906542

Contact No	Length(ft)	Width(ft)	Height(ft)	Preliminary Interpretation	Lat(WGS84)	Lon(WGS84)
QBC_Q10225	101.93	12.77	0	Natural?	26.059907	50.909682
QBC_Q10226	24.58	12.78	0	Natural?	26.068826	50.905008
QBC_Q10227	30.58	18.43	0	Location?	26.066123	50.909461
QBC_Q10228	9.65	4.97	1.4	Debris?	26.065381	50.909654
QBC_Q10229	97.17	4.84	0	Seabed Scar?	26.061457	50.914405
QBC_Q10230	92.29	6.12	0	Data problem?	26.060353	50.916225
QBC_Q10231	83.7	2.17	0	Linear Debris?	26.060518	50.91724
QBC_Q10232	28.89	8.22	0	Depression?	26.060296	50.917675
QBC_Q10233	84.05	3.61	0	Seabed Scar?	26.055883	50.922871
QBC_Q10234	0	12.3	0	Depression?	26.052369	50.927506
QBC_Q10235	0	0	0	Depression?	26.050911	50.929229
QBC_Q10236	2.87	1.68	0.98	Debris? - Modern?	26.077354	50.901243
QBC_Q10237	10.11	5.08	1.27	Debris? - Modern?	26.075569	50.903497
QBC_Q10238	9.08	2.32	0.76	Debris?	26.074429	50.90462
QBC_Q10239	38.06	21.79	0	Location?	26.070272	50.911597
QBC_Q10240	10.03	1.9	0.41	Natural?	26.062519	50.922783
QBC_Q10241	0	0	0.47	Debris?	26.043976	50.948712
QBC_Q10242	3.83	2.9	1.35	Debris?	26.043286	50.949088
QBC_Q10243	0	0	0.3	Debris?	26.043442	50.949323
QBC_Q10244	7.06	5.38	0.96	Natural?	26.054666	50.901281
QBC_Q10245	2.75	1.86	0.64	Natural?	26.051646	50.899967
QBC_Q10246	4.23	2.36	0.96	Natural?	26.067749	50.895292
QBC_Q10247	23.56	15.17	0	Location?	26.066965	50.896625
QBC_Q10248	55.37	1.44	0	Natural?	26.05887	50.907371
QBC_Q10249	4.92	2.04	0.71	Debris?	26.063726	50.916268
QBC_Q10250	2.07	2.07	1.04	Debris?	26.063292	50.917283

Contact No	Length(ft)	Width(ft)	Height(ft)	Preliminary Interpretation	Lat(WGS84)	Lon(WGS84)
QBC_Q10251	31.51	1.85	0	Natural?	26.06366	50.915651
QBC_Q10252	16	6.06	0	Location?	26.078566	50.903123
QBC_Q10253	34.11	30.74	0	Location?	26.069383	50.916591
QBC_Q10254	23.94	2.24	0	Seabed Scar?	26.068958	50.918444
QBC_Q10255	99.32	3.45	0	Data problem?	26.06761	50.917947
QBC_Q10256	5.93	1.84	0	Natural?	26.067568	50.919924
QBC_Q10257	4.8	1.48	0.71	Natural?	26.045402	50.950653
QBC_Q10258	8.12	6.24	0	Natural?	26.042201	50.95442
QBC_Q10259	21.93	12.4	0	Location?	26.069299	50.915386
QBC_Q10260	49.4	14.2	0	Depression?	26.082551	50.907172
QBC_Q10261	21.12	4.05	0	Debris?	26.07874	50.912878
QBC_Q10262	4.65	1.75	0.54	Debris? - Modern?	26.077936	50.912727
QBC_Q10263	38.51	10.29	0	Depression?	26.078133	50.913414
QBC_Q10264	12.09	11.9	0	Location?	26.073948	50.917897
QBC_Q10265	10.44	3.6	0.91	Bham0020 - cars	26.07089	50.922166
QBC_Q10266	7.75	3.46	0.38	Natural?	26.046325	50.956833
QBC_Q10267	4.6	2.06	0.26	Natural?	26.042798	50.962266
QBC_Q10268	7.43	4.27	0.33	Natural?	26.041907	50.96437
QBC_Q10269	4.65	1.6	0	Natural?	26.044931	50.960365
QBC_Q10270	10.63	3.41	0.74	Debris? - Modern?	26.085082	50.910245
QBC_Q10271	37.77	1.79	0	Natural?	26.083989	50.91146
QBC_Q10272	3.71	0.91	0.57	Natural?	26.08364	50.912842
QBC_Q10273	10.08	14.29	0.49	Bham0019 - Cars	26.078984	50.918596
QBC_Q10274	37.24	12.83	0	Location?	26.075106	50.923526
QBC_Q10275	55.93	45.92	0	Location?	26.064642	50.939217
QBC_Q10276	5.96	2.28	0.89	Debris?	26.060076	50.94573

Contact No	Length(ft)	Width(ft)	Height(ft)	Preliminary Interpretation	Lat(WGS84)	Lon(WGS84)
QBC_Q10277	63.21	3.6	0	Depression?	26.060305	50.945978
QBC_Q10278	7.28	4.72	0.23	Natural?	26.057685	50.950464
QBC_Q10279	7.35	1.92	0.74	Buried Feature?	26.055975	50.952156
QBC_Q10280	31.94	1.71	0	Natural?	26.053293	50.955595
QBC_Q10281	8.35	2.95	0.23	Natural?	26.047329	50.96471
QBC_Q10282	9.36	0.93	0.2	Natural?	26.046697	50.964255
QBC_Q10283	35.11	5.12	0.42	Buried Feature?	26.044793	50.966205
QBC_Q10284	44.75	2.26	0	Natural?	26.08994	50.911351
QBC_Q10285	4.79	1.94	0.4	Debris? - Modern?	26.086224	50.916698
QBC_Q10286	12.15	3.36	0.54	Bham0017 - Cars	26.086726	50.917386
QBC_Q10287	8.29	3.39	0.71	Debris? - Modern?	26.084214	50.918716
QBC_Q10288	2.61	0.87	0.43	Debris?	26.082951	50.922121
QBC_Q10289	6.82	1.58	0.11	Natural?	26.080507	50.924306
QBC_Q10290	8.33	4.56	0	Natural?	26.078858	50.92888
QBC_Q10291	0	0	0	Location?	26.07881	50.928273
QBC_Q10292	54.39	32.54	0.74	Natural?	26.076672	50.931454
QBC_Q10293	3.9	2.29	0.69	Debris? - Modern?	26.074413	50.933972
QBC_Q10294	12.72	1.97	0.55	Debris?	26.072967	50.934841
QBC_Q10295	19.62	9.98	0	Buried Feature?	26.070205	50.939847
QBC_Q10297	0	0	0	Duplicate of QBC_Q10295	26.070232	50.939827
QBC_Q10298	4.2	2.34	0.79	Debris? - Modern?	26.06983	50.940326
QBC_Q10299	48.04	1.62	0	Natural?	26.068463	50.941823
QBC_Q10300	10.49	8.3	0	Location?	26.0641	50.947909
QBC_Q10301	14.73	10.39	0.36	Natural ?	26.055367	50.959361
QBC_Q10302	3.02	2.42	0.7	Debris? - Modern?	26.096733	50.910892
QBC_Q10303	6.4	2.68	0	Debris?	26.092732	50.917014

Contact No	Length(ft)	Width(ft)	Height(ft)	Preliminary Interpretation	Lat(WGS84)	Lon(WGS84)
QBC_Q10304	23.89	2.62	0.81	Bham0016 - Tyres	26.091109	50.917744
QBC_Q10305	6.69	3.08	0.53	Debris?	26.089936	50.919292
QBC_Q10306	4.64	3.57	0	Debris?	26.089514	50.919463
QBC_Q10307	5.24	1.82	0.72	Debris? - Modern?	26.087683	50.922878
QBC_Q10308	11.56	3.47	0	Debris? - Modern?	26.087451	50.92484
QBC_Q10309	4.01	2.67	0.46	Natural?	26.080841	50.933292
QBC_Q10310	35.32	2.38	0	Natural?	26.076909	50.937072
QBC_Q10311	4.56	3.65	0.69	Debris?	26.076836	50.938696
QBC_Q10312	5.59	2.57	0	Natural?	26.071291	50.947673
QBC_Q10313	41.42	14.3	0.47	Natural?	26.067197	50.951187
QBC_Q10314	74.78	2.91	0	Seabed Scar?	26.065338	50.954863
QBC_Q10315	18.32	1.11	0	Natural?	26.062645	50.958109
QBC_Q10316	4.89	3.06	0.35	Natural?	26.057918	50.964623
QBC_Q10317	27.29	6.41	0	Buried Feature?	26.056922	50.965199
QBC_Q10318	3.53	1.13	0	Natural ?	26.101537	50.912217
QBC_Q10319	3.58	2.22	0	Natural?	26.097268	50.916536
QBC_Q10320	24.95	10.81	0	Seabed Scar?	26.097572	50.917563
QBC_Q10321	4.99	2.1	1.1	Debris?	26.093511	50.923065
QBC_Q10322	13.95	4.36	0.66	Bham0013 - Tyres	26.092083	50.924327
QBC_Q10323	4.08	1.3	0.58	Debris?	26.091531	50.925976
QBC_Q10324	23.37	10.23	0	Natural?	26.09102	50.925282
QBC_Q10325	5.73	3.24	0	Debris?	26.088973	50.927951
QBC_Q10326	13.12	4.8	0.89	Bham0012 - Cars	26.088844	50.929978
QBC_Q10327	57.44	19.08	0.63	Buried Feature?	26.083173	50.936775
QBC_Q10328	6.32	1.71	0	Debris?	26.083721	50.93771
QBC_Q10329	7.8	2.18	0.87	Debris? - Modern?	26.082836	50.93811

Contact No	Length(ft)	Width(ft)	Height(ft)	Preliminary Interpretation	Lat(WGS84)	Lon(WGS84)
QBC_Q10330	6.15	3.01	0	Natural?	26.080197	50.940258
QBC_Q10331	6.44	2.71	0.98	Debris?	26.103053	50.918189
QBC_Q10332	4.45	2.62	0.83	Debris? - Modern?	26.101257	50.92039
QBC_Q10333	11.7	8.91	0.17	Natural ?	26.100566	50.920102
QBC_Q10334	78.8	4.18	0.68	Debris? - Modern?	26.099281	50.921995
QBC_Q10335	4.09	2.19	0.94	Debris?	26.099227	50.92284
QBC_Q10336	57.23	34.68	0.62	Debris? - Modern?	26.096039	50.926544
QBC_Q10337	6.41	2.16	0.94	Debris?	26.095839	50.927719
QBC_Q10338	17.77	3.66	1.42	Debris? - Modern?	26.092555	50.931337
QBC_Q10339	5.27	2.1	0.7	Debris?	26.090511	50.93551
QBC_Q10340	0	0	0	Data problem?	26.090887	50.935667
QBC_Q10341	5.06	1.86	1.02	Debris? - Modern?	26.088323	50.938225
QBC_Q10342	7.62	2.53	0.71	Debris? - Modern?	26.086813	50.939104
QBC_Q10343	0	0	0	Duplicate of QBC_Q10342	26.086859	50.939092
QBC_Q10344	5.45	1.71	0.47	Debris?	26.087336	50.940866
QBC_Q10345	51.55	15.54	0	Location?	26.079559	50.949938
QBC_Q10346	15.94	15.63	0	Natural?	26.075275	50.955642
QBC_Q10347	15.43	6.64	0	Natural?	26.072676	50.959533
QBC_Q10349	10.28	1.71	0	Natural ?	26.062442	50.975204
QBC_Q10350	3.78	3.33	0.65	Debris?	26.114509	50.930767
QBC_Q10352	66.08	1.53	0	Natural?	26.10597	50.940842
QBC_Q10353	12.94	3.21	0.37	Debris?	26.10262	50.945964
QBC_Q10354	34.81	3.58	0	Data problem?	26.10227	50.94849
QBC_Q10355	5.32	2.3	0.68	Bham0040 - Cars	26.097135	50.954447
QBC_Q10356	4.62	2.1	0	Natural?	26.092559	50.959382
QBC_Q10357	12.56	2.52	0.85	Debris?	26.092271	50.962169

Contact No	Length(ft)	Width(ft)	Height(ft)	Preliminary Interpretation	Lat(WGS84)	Lon(WGS84)
QBC_Q10358	18.5	8.3	0	Buried feature?	26.091498	50.960999
QBC_Q10359	6.33	3.28	0	Debris? - Modern?	26.114074	50.939762
QBC_Q10360	6.94	4.88	0.86	Debris?	26.109001	50.946489
QBC_Q10361	7.83	3.63	0	Debris?	26.104551	50.950737
QBC_Q10362	14.54	2.91	0.84	Buried Feature?	26.091321	50.970833
QBC_Q10363	3.44	3.19	1.16	Debris?	26.124418	50.931742
QBC_Q10364	29.94	1.5	0	Net?	26.118995	50.938643
QBC_Q10365	1.51	2.23	0.49	Debris?	26.119324	50.93896
QBC_Q10366	4.2	3.33	1.17	Debris?	26.117135	50.94257
QBC_Q10367	7.03	3.33	0.95	Debris - Modern?	26.112085	50.948764
QBC_Q10368	5.47	1.91	0.96	Debris? - Modern?	26.107309	50.957101
QBC_Q10369	17.69	3.41	0.91	Debris? - Modern?	26.104606	50.959414
QBC_Q10370	3.53	1.23	0.61	Debris?	26.099705	50.96755
QBC_Q10371	16.69	3.95	0.96	Debris? - Modern?	26.0983	50.969533
QBC_Q10372	8.04	4.55	0	Debris?	26.098361	50.969887
QBC_Q10373	8.61	6.31	0.38	Buried Feature?	26.095926	50.971923
QBC_Q10374	100.7	1.13	0	Seabed Scar?	26.093658	50.97629
QBC_Q10375	4.46	2.17	0	Bham0038 - Cars	26.093331	50.976766
QBC_Q10376	29.13	1.52	0	Location?	26.090243	50.979979
QBC_Q10377	2.83	3.04	0	Buried Feature?	26.12209	50.944676
QBC_Q10378	15.37	12.25	0.51	Buried Feature?	26.117737	50.948732
QBC_Q10379	11.26	4.67	0.31	Natural?	26.115013	50.952333
QBC_Q10380	12.77	9.72	0.59	Buried Feature?	26.114713	50.952828
QBC_Q10381	6.54	3.28	0.7	Debris? - Modern?	26.113137	50.955331
QBC_Q10382	6.61	2.24	0.79	Debris? - Modern?	26.109259	50.960807
QBC_Q10383	3.51	1.9	0.96	Buried Feature?	26.108103	50.962087

Contact No	Length(ft)	Width(ft)	Height(ft)	Preliminary Interpretation	Lat(WGS84)	Lon(WGS84)
QBC_Q10384	7.4	2.97	0	Debris?	26.099536	50.973515
QBC_Q10385	80.89	2.34	0	Natural ?	26.099046	50.976504
QBC_Q10386	10.38	2.83	0.82	Buried feature?	26.098194	50.977084
QBC_Q10387	5.4	2.33	0.74	Debris? - Modern?	26.096483	50.979281
QBC_Q10388	48.43	1.69	0	Natural?	26.092071	50.986189
QBC_Q10389	29.51	10.77	0	Location?	26.090276	50.989229
QBC_Q10390	5.75	1.07	0.24	Location?	26.088617	50.990707
QBC_Q10391	7.26	4.01	0.13	Natural ?	26.088166	50.992154
QBC_Q10392	38.71	17.8	0	Depression?	26.081654	50.965677
QBC_Q10393	16.84	7.15	0.42	Debris?	26.082116	50.964915
QBC_Q10394	25.28	11.11	0	Depression?	26.081151	50.965134
QBC_Q10395	3.49	1.75	0.48	Natural ?	26.074486	50.959364
QBC_Q10396	29.57	4.91	0.54	Duplicate of QBC_Q10313	26.067142	50.951194
QBC_Q10397	7.75	3.57	0.96	Duplicate of QBC_Q10276	26.060116	50.945687
QBC_Q10398	21.23	3.96	0.28	Debris?	26.132888	50.937619
QBC_Q10399	8.99	6.81	0	Depression?	26.132258	50.936895
QBC_Q10400	16.74	3.35	1.11	Debris?	26.131783	50.937512
QBC_Q10401	10.8	5.03	1.18	Debris?	26.13177	50.938311
QBC_Q10402	17.03	3.44	0	Debris?	26.130814	50.937899
QBC_Q10403	6.42	2.2	1.05	Debris?	26.130915	50.939438
QBC_Q10407	8.55	5.93	0	Debris?	26.130206	50.938566
QBC_Q10408	24.87	3.09	0.93	Debris?	26.129648	50.9402
QBC_Q10409	10.53	3.08	1.85	Debris?	26.129444	50.940623
QBC_Q10410	6.53	3.49	0	Debris?	26.129233	50.940292
QBC_Q10411	6.08	4.32	1.17	Debris?	26.130272	50.940832
QBC_Q10412	3.22	3.27	0	Natural?	26.130334	50.939137

Contact No	Length(ft)	Width(ft)	Height(ft)	Preliminary Interpretation	Lat(WGS84)	Lon(WGS84)
QBC_Q10413	3.28	2.06	0.51	Debris?	26.129181	50.941226
QBC_Q10414	74.61	2.1	0	Seabed Scar?	26.128383	50.941777
QBC_Q10415	29.82	1.47	0	Natural?	26.128076	50.942728
QBC_Q10416	0	0	0	Debris?	26.12765	50.942574
QBC_Q10417	4.71	1.85	0	Natural?	26.131683	50.936887
QBC_Q10418	3.61	1.82	0.84	Debris?	26.127657	50.943502
QBC_Q10419	12.05	7.85	0.94	Debris?	26.119333	50.955536
QBC_Q10420	66.94	11.25	0.74	Debris?	26.118021	50.956311
QBC_Q10421	5.94	2.77	0	Natural?	26.112134	50.966925
QBC_Q10422	4.73	1.94	0.45	Natural?	26.10829	50.971582
QBC_Q10423	7.27	2.59	0	Natural?	26.097671	50.984475
QBC_Q10424	7.85	2.53	0.65	Natural?	26.096792	50.987606
QBC_Q10425	9.63	4.64	0	Natural?	26.08853	50.997432
QBC_Q10426	2.2	1.47	0.67	Natural?	26.132898	50.944483
QBC_Q10427	11.02	2.02	0.62	Buried Feature?	26.130293	50.94753
QBC_Q10428	15.59	5.21	0.57	Debris?	26.129287	50.94973
QBC_Q10429	12.98	1.83	0	Debris?	26.12179	50.959458
QBC_Q10430	6.82	6.23	0.8	Debris?	26.121587	50.960683
QBC_Q10431	12.99	3.59	0	Natural?	26.121122	50.959972
QBC_Q10432	6.19	2.77	0.77	Natural?	26.120058	50.96336
QBC_Q10433	8.74	5.66	0	Natural?	26.117114	50.967657
QBC_Q10434	4.89	3.38	0.83	Debris?	26.113673	50.971041
QBC_Q10435	5.08	2.5	0.86	Debris - Modern?	26.110855	50.974373
QBC_Q10436	15.4	8.21	0.34	Natural?	26.088292	51.015315
QBC_Q10437	49	2.38	0	Natural?	26.093642	51.00693
QBC_Q10438	13.33	7.38	0	Object in Water Column?	26.107673	50.987568

Contact No	Length(ft)	Width(ft)	Height(ft)	Preliminary Interpretation	Lat(WGS84)	Lon(WGS84)
QBC_Q10439	14.11	4.58	0	Object in Water Column?	26.109215	50.98577
QBC_Q10440	10.65	2.94	0	Natural?	26.112253	50.982443
QBC_Q10441	6.15	2.29	0	Natural?	26.115561	50.9784
QBC_Q10442	3.85	2.26	0	Debris?	26.119473	50.973045
QBC_Q10443	37.07	19.91	0	Natural?	26.118104	50.972227
QBC_Q10444	12.03	9.41	0	Object in Water Column?	26.119496	50.971046
QBC_Q10445	11.19	3.23	0.94	Debris?	26.119187	50.970769
QBC_Q10446	7.53	5.78	0.7	Natural?	26.120371	50.96879
QBC_Q10447	15.25	9	0	Object in Water Column?	26.122053	50.967423
QBC_Q10448	4.4	1.87	0.24	Natural?	26.133035	50.953097
QBC_Q10449	8.92	2.97	0	Debris?	26.134125	50.957602
QBC_Q10450	5.17	1.89	0.23	Natural?	26.128833	50.965904
QBC_Q10451	13.78	5.18	0.76	Debris?	26.127867	50.96907
QBC_Q10452	43.53	3.92	0	Natural?	26.122308	50.974889
QBC_Q10453	11.89	1.8	1.23	Debris?	26.122296	50.975878
QBC_Q10454	13.81	7.03	0	Debris?	26.120713	50.976605
QBC_Q10455	27.69	15.84	0	Unclassified	26.12092	50.97602
QBC_Q10456	21.23	11.37	0	Mound?	26.101249	51.006154
QBC_Q10457	0	0	0	Depression?	26.0986	51.009047
QBC_Q10458	25.54	3.82	0	Unclassified	26.090337	51.019905
QBC_Q10459	11.72	7.85	0.63	Unclassified	26.140022	50.957661
QBC_Q10460	13.45	15.23	0	Unclassified	26.140349	50.959474
QBC_Q10461	5.79	1.6	0.9	Buried Feature?	26.137013	50.963788
QBC_Q10462	1.17	0.57	0	Buried Feature?	26.137314	50.963271
QBC_Q10463	9.03	2.7	0	Debris?	26.124795	50.978596
QBC_Q10464	8.43	5.9	0.33	Debris?	26.116303	50.990638

Contact No	Length(ft)	Width(ft)	Height(ft)	Preliminary Interpretation	Lat(WGS84)	Lon(WGS84)
QBC_Q10465	116.46	35.15	0	Location?	26.098932	51.016057
QBC_Q10466	14.57	5.64	0.67	Debris?	26.141276	50.965515
QBC_Q10467	19.38	8.29	0	Depression?	26.122558	50.992131
QBC_Q10468	16.43	5.65	0.25	Natural?	26.117767	50.997205
QBC_Q10469	17.16	5.24	0.58	Natural?	26.116921	50.998238
QBC_Q10470	37.55	1.46	0.27	Natural?	26.095451	51.02946
QBC_Q10471	30.07	9.78	0	Data problem?	26.142646	50.972823
QBC_Q10472	54.31	26.26	0	Data problem?	26.142073	50.973382
QBC_Q10473	2.98	2.1	0.78	Debris?	26.1388	50.977506
QBC_Q10474	4.25	2.58	0	Debris?	26.138399	50.976924
QBC_Q10475	8.35	1.52	0.4	Natural?	26.13651	50.980969
QBC_Q10476	54.89	2.44	0.66	Bham0032 - Cars	26.126558	50.993165
QBC_Q10477	3.09	1.45	0.15	Natural?	26.12219	51.001116
QBC_Q10478	8.42	1.85	1.27	Duplicate	26.122387	51.002858
QBC_Q10479	109.15	31.53	0	Location?	26.100921	51.030072
QBC_Q10480	7.38	3.77	0.88	Debris - Modern?	26.150078	50.968992
QBC_Q10481	15.49	5.94	0.55	Debris?	26.145429	50.975783
QBC_Q10482	9.61	9.62	0	Data problem?	26.141467	50.981648
QBC_Q10483	6.62	2.9	0	Natural?	26.141977	50.981637
QBC_Q10484	17.52	6.99	0	Debris?	26.141425	50.982197
QBC_Q10485	8.03	2.52	0.14	Debris?	26.140669	50.982893
QBC_Q10486	0	0	0	Location?	26.129037	50.998825
QBC_Q10487	5.08	4.15	0.62	Debris - Modern?	26.155279	50.964161
QBC_Q10488	8.02	2.38	0.24	Natural?	26.146583	50.978489
QBC_Q10489	3.87	3.11	0	Object in Water Column?	26.144162	50.98089
QBC_Q10490	50.58	1.71	0	Natural?	26.144382	50.981644

Contact No	Length(ft)	Width(ft)	Height(ft)	Preliminary Interpretation	Lat(WGS84)	Lon(WGS84)
QBC_Q10491	24.74	12.95	0.22	Buried Feature?	26.142245	50.982567
QBC_Q10492	40.21	2.9	0	Natural?	26.129952	51.000018
QBC_Q10493	4.99	2.17	0.24	Debris?	26.155025	50.970307
QBC_Q10494	8.34	4.94	0	Natural?	26.152498	50.974397
QBC_Q10495	5.29	2.12	0.64	Debris - Modern?	26.150855	50.975168
QBC_Q10496	11.65	11.06	0	Debris?	26.146534	50.980692
QBC_Q10497	0.32	1.35	0.75	Natural?	26.146553	50.982844
QBC_Q10498	39.75	1.78	0	Natural?	26.136876	50.996083
QBC_Q10499	6.16	6.16	0	Natural?	26.124703	51.013823
QBC_Q10500	36.82	19.71	0	Depression?	26.114017	51.027796
QBC_Q10501	2.5	1.5	0	Buried Feature?	26.111836	51.030317
QBC_Q10502	8.16	3.6	0.59	Debris?	26.166536	50.957756
QBC_Q10503	9.45	3.69	0	Debris?	26.166218	50.959665
QBC_Q10504	2.81	2.1	0.65	Debris - Modern?	26.158738	50.968206
QBC_Q10505	6	4.86	0.39	Debris?	26.147941	50.983211
QBC_Q10506	22.79	12.87	0.31	Debris?	26.14809	50.983509
QBC_Q10507	17.52	2.46	0.78	Debris?	26.145884	50.987333
QBC_Q10508	47.22	2.16	0	Natural?	26.132228	51.005321
QBC_Q10509	38.78	2.62	0	Depression?	26.121144	51.020555
QBC_Q10510	8	7.81	0.85	Debris - Modern?	26.166047	50.961688
QBC_Q10511	5.02	2.36	0.97	Debris?	26.16495	50.964133
QBC_Q10512	16.62	1.71	0	Natural?	26.159574	50.972543
QBC_Q10513	64.28	26.03	0	Data problem?	26.11668	51.031117
QBC_Q10514	1.17	1.03	1.1	Linear Debris?	26.167868	50.964272
QBC_Q10515	4.13	1.79	0.34	Debris?	26.152482	50.985184
QBC_Q10516	23.66	15.91	0	Location?	26.150527	50.988769

Contact No	Length(ft)	Width(ft)	Height(ft)	Preliminary Interpretation	Lat(WGS84)	Lon(WGS84)
QBC_Q10517	11.15	7.75	0.18	Buried Feature?	26.149864	50.988512
QBC_Q10518	12.56	2.76	0	Natural?	26.148256	50.992184
QBC_Q10519	37.03	19.75	0	Natural?	26.147807	50.991207
QBC_Q10520	2.42	2.46	0.5	Debris?	26.140752	51.001409
QBC_Q10521	72.52	35.64	0	Location?	26.129018	51.019557
QBC_Q10522	9.98	8.04	0.48	Buried Feature?	26.113749	51.039725
QBC_Q10523	4.6	3	0	Debris?	26.162758	50.976398
QBC_Q10524	3.97	1.32	0	Natural?	26.155817	50.985357
QBC_Q10525	8.06	2.12	0.2	Natural?	26.152347	50.990761
QBC_Q10526	18.11	8.04	0	Natural?	26.146921	50.996365
QBC_Q10527	13.65	4.49	0.77	Debris?	26.146352	50.998449
QBC_Q10528	31.79	3.78	0	Data problem?	26.140886	51.007253
QBC_Q10529	4.39	1.97	0.25	Debris?	26.131362	51.020367
QBC_Q10530	15.03	6.97	0.45	Mound?	26.116336	51.043928
QBC_Q10531	55.84	4	0	Seabed Scar?	26.120435	51.039476
QBC_Q10532	21.15	7.12	0.31	Mound?	26.123701	51.034668
QBC_Q10533	0	0	0	Location?	26.1307	51.023848
QBC_Q10534	41.5	2.24	0	Seabed Scar?	26.132132	51.022748
QBC_Q10536	5.5	3.92	0	Natural?	26.148023	50.999444
QBC_Q10537	5.97	3.66	0	Debris?	26.159526	50.982383
QBC_Q10538	32.13	3.73	0.4	Debris?	26.161349	50.980513
QBC_Q10539	10.28	4.22	0.32	Debris?	26.162772	50.978272
QBC_Q10540	9.45	2.46	0	Debris?	26.163896	50.976284
QBC_Q10541	0	0	0	Seabed Scar?	26.16652	50.975039
QBC_Q10542	7.74	5.14	0.38	Debris?	26.166842	50.972396
QBC_Q10543	12.58	3.1	0.46	Debris?	26.171508	50.966158

Contact No	Length(ft)	Width(ft)	Height(ft)	Preliminary Interpretation	Lat(WGS84)	Lon(WGS84)
QBC_Q10544	28.58	4.57	0	Data problem?	26.174761	50.967491
QBC_Q10545	7.08	2.15	0.79	Debris? - Modern?	26.166958	50.977564
QBC_Q10546	2.65	2.51	1.03	Debris?	26.163965	50.981973
QBC_Q10547	16.97	3.77	0	Debris?	26.159758	50.98872
QBC_Q10548	6.61	2.02	0.88	Debris? - Modern?	26.170851	50.976167
QBC_Q10549	15.57	16.41	0	Natural?	26.168964	50.979454
QBC_Q10550	9.34	4.68	0.52	Debris?	26.167225	50.981809
QBC_Q10551	10.53	2.82	0.3	Debris?	26.165512	50.981963
QBC_Q10553	13.34	5.71	0	Depression?	26.1587	50.993389
QBC_Q10554	27.51	10.63	0	Natural?	26.156295	50.997212
QBC_Q10555	13.63	3.58	0.23	Natural?	26.154688	50.999428
QBC_Q10556	20.02	4.54	0.85	Debris?	26.149203	51.005646
QBC_Q10557	12.46	5.48	0.53	Natural?	26.146558	51.010588
QBC_Q10558	6.52	3.68	0	Natural?	26.14617	51.011798
QBC_Q10559	11.92	6.12	0.67	Debris?	26.145515	51.012185
QBC_Q10560	6.33	4.85	0	Natural?	26.145584	51.010885
QBC_Q10561	15.57	12.1	0.78	Natural?	26.145229	51.012155
QBC_Q10562	23.42	4.12	0	Natural?	26.135378	51.024372
QBC_Q10563	46.61	2.49	0	Location?	26.13448	51.027722
QBC_Q10564	5.63	3.31	0.42	Natural?	26.170553	50.981335
QBC_Q10565	8.23	5.33	0	Debris?	26.167984	50.985344
QBC_Q10566	6.01	1.76	0.89	Debris?	26.166546	50.985764
QBC_Q10567	114.51	59.16	0	Location?	26.160261	50.995137
QBC_Q10568	6.24	3.23	0.83	Debris?	26.159135	50.99692
QBC_Q10569	8.33	4.06	0.51	Debris?	26.147722	51.011473
QBC_Q10570	1.34	1.04	0.7	Debris?	26.178741	50.972303

Contact No	Length(ft)	Width(ft)	Height(ft)	Preliminary Interpretation	Lat(WGS84)	Lon(WGS84)
QBC_Q10571	6.01	2.63	0.63	Debris? - Modern?	26.177788	50.974457
QBC_Q10572	11.51	4.71	0.76	Buried Feature?	26.16657	50.990345
QBC_Q10573	7.1	5.57	0	Debris?	26.165421	50.990076
QBC_Q10574	10.28	8.97	0	Depressions?	26.163834	50.994139
QBC_Q10575	56.51	23.73	0	Location?	26.160125	50.998018
QBC_Q10576	13.72	7.52	0	Depression?	26.159465	50.999357
QBC_Q10577	8.7	6.93	1.73	Debris?	26.149734	51.012472
QBC_Q10578	2.55	0.75	0.31	Debris?	26.141918	51.025165
QBC_Q10579	11.53	7.56	0	Natural?	26.137986	51.028675
QBC_Q10580	30.78	11.58	0	Depression?	26.128764	51.043474
QBC_Q10581	13.38	12.62	0	Hole?	26.184715	50.967615
QBC_Q10582	0.7	0.7	0.28	Buried Feature?	26.178139	50.977658
QBC_Q10583	5.85	3.21	0.88	Buried Feature?	26.163234	50.998661
QBC_Q10584	87.5	37.91	0	Location?	26.137295	51.035618
QBC_Q10585	6.22	2.84	0.44	Buried Feature?	26.170374	50.991912
QBC_Q10586	24.98	10.32	0	Depression?	26.168026	50.996343
QBC_Q10587	23.34	10.27	0	Depression?	26.167003	50.996646
QBC_Q10588	35.91	28.56	0	Location?	26.159944	51.007962
QBC_Q10590	5.77	3.69	1.07	Debris? - Modern?	26.182407	50.979411
QBC_Q10591	25.01	19.16	0	Depression?	26.178901	50.985306
QBC_Q10592	4.78	2.57	0.58	Debris? - Modern?	26.17788	50.986311
QBC_Q10593	10.19	2.68	0	Natural?	26.165607	51.002126
QBC_Q10594	7.85	3.8	0	Natural?	26.131552	51.050247
QBC_Q10595	5.54	4.69	0.4	Buried Feature?	26.189683	50.974796
QBC_Q10596	4.98	2.99	1.16	Debris?	26.186551	50.978421
QBC_Q10597	74.85	16.43	0	Location?	26.186509	50.977432

Contact No	Length(ft)	Width(ft)	Height(ft)	Preliminary Interpretation	Lat(WGS84)	Lon(WGS84)
QBC_Q10598	5.58	1.58	0	Buried Feature?	26.184185	50.980576
QBC_Q10599	10.78	3.86	0.87	Buried Feature?	26.17903	50.988005
QBC_Q10600	6.86	1.59	0.2	Natural?	26.176783	50.990843
QBC_Q10601	1.64	1.02	0.62	Debris?	26.175218	50.993276
QBC_Q10602	9.09	5.43	0.22	Natural?	26.152577	51.026579
QBC_Q10603	12.85	9.62	0.45	Partially Buried Objects?	26.190087	50.979844
QBC_Q10604	6.61	1.6	0	Debris?	26.18898	50.981179
QBC_Q10605	3.38	3.14	1	Debris?	26.18466	50.988254
QBC_Q10607	6.08	5.84	1.01	Buried Feature?	26.183321	50.991329
QBC_Q10608	9.41	5.47	0	Natural?	26.141162	51.051057
QBC_Q10609	40.17	3.46	0	Buried Feature?	26.140807	51.050964
QBC_Q10610	102.16	9.88	0	Location?	26.13782	51.05379
QBC_Q10611	5.16	2.11	0	Natural?	26.201705	50.971514
QBC_Q10612	6.91	2.24	0.77	Partially Buried Objects?	26.20069	50.97364
QBC_Q10613	18.72	1.57	0	Natural?	26.201114	50.972691
QBC_Q10614	8	2.46	0	Natural?	26.19561	50.982688
QBC_Q10616	79.28	1.22	0	Seabed Scar?	26.190535	50.989366
QBC_Q10617	9.95	5.72	0	Buried Feature?	26.186639	50.993278
QBC_Q10618	4.22	1.05	0.39	Debris?	26.186522	50.995093
QBC_Q10619	4.24	2.58	0	Debris?	26.180739	51.00083
QBC_Q10620	8.92	3.44	0	Debris?	26.177484	51.005494
QBC_Q10621	3.72	1.62	0	Partially Buried Objects?	26.176614	51.007299
QBC_Q10622	6.26	0.61	0.45	Partially Buried Objects?	26.170585	51.016889
QBC_Q10623	6.77	1.75	0	Natural?	26.151562	51.042322
QBC_Q10624	61.39	23.74	0	Data problem?	26.174451	51.019493
QBC_Q10625	33.99	15.43	0	Natural?	26.161599	51.036097

Contact No	Length(ft)	Width(ft)	Height(ft)	Preliminary Interpretation	Lat(WGS84)	Lon(WGS84)
QBC_Q10626	3.45	1.13	0.29	Natural?	26.149057	51.05548
QBC_Q10627	4.87	1.19	0.38	Natural?	26.20637	50.975389
QBC_Q10628	79.21	2.7	0	Natural?	26.200845	50.983092
QBC_Q10629	74.16	2.33	0	Seabed Scar?	26.196759	50.988643
QBC_Q10630	1.99	0.92	0.41	Partially Buried Objects?	26.196139	50.989419
QBC_Q10631	1.27	0.63	0.4	Debris?	26.190244	50.996395
QBC_Q10632	4.52	3.91	0	Debris?	26.188869	50.998967
QBC_Q10633	82.51	13.26	0	Location?	26.186787	51.001022
QBC_Q10634	11.1	5.94	1.24	Partially Buried Objects?	26.187246	51.001958
QBC_Q10635	11.01	1.21	0	Natural?	26.184534	51.00623
QBC_Q10636	5.51	3.26	0.96	Partially Buried Objects?	26.200751	50.990649
QBC_Q10637	9.59	4.37	0.8	Debris?	26.20047	50.99143
QBC_Q10638	11.62	9.5	0	Natural?	26.199125	50.9938
QBC_Q10639	6.57	3.86	0.46	Partially Buried Objects?	26.195732	50.99836
QBC_Q10640	16.82	9.4	0	Debris?	26.196356	50.997651
QBC_Q10641	9.02	4.2	0.97	Debris?	26.189589	51.005185
QBC_Q10642	7.9	2.42	0.56	Debris?	26.185853	51.010229
QBC_Q10643	7.68	4.57	0.72	BHAM0022 - coral head	26.183558	51.015647
QBC_Q10644	15.42	4.65	2.44	Debris?	26.177719	51.023168
QBC_Q10645	7.3	2.66	0	Partially Buried Objects?	26.177284	51.024593
QBC_Q10646	6.78	4.53	0	Mound?	26.157792	51.050043
QBC_Q10647	3.09	2.55	0	Natural?	26.153292	51.055598
QBC_Q10648	16.28	7.55	0	Natural?	26.212976	50.980034
QBC_Q10649	5.97	2.49	0.57	Natural?	26.213094	50.98174
QBC_Q10650	6.39	2.66	0.94	Partially Buried Objects? - Asses	26.196144	51.005155
QBC_Q10651	33.44	7.24	0	Debris?	26.189869	51.012283

Contact No	Length(ft)	Width(ft)	Height(ft)	Preliminary Interpretation	Lat(WGS84)	Lon(WGS84)
QBC_Q10652	11.53	9.4	0	Debris?	26.18925	51.013595
QBC_Q10653	7.02	6.09	0	Natural?	26.186561	51.017296
QBC_Q10654	15.42	10.51	0	Depression?	26.183959	51.021857
QBC_Q10655	13.32	8.76	0	Depression?	26.16408	51.049672
QBC_Q10656	5.68	3.03	0	Debris?	26.161197	51.055817
QBC_Q10657	36.08	2.78	0	Unclassified	26.154432	51.064211
QBC_Q10658	6.43	4.17	0.59	Natural?	26.219383	50.979669
QBC_Q10659	9.22	3.21	0	Natural?	26.218145	50.983593
QBC_Q10660	4.14	2.26	0.79	Debris?	26.21736	50.984428
QBC_Q10661	7.19	3.27	0.84	Debris?	26.216642	50.98503
QBC_Q10662	77.74	2.2	0	Seabed Scar?	26.216053	50.985567
QBC_Q10663	2.01	2.45	0.78	Debris?	26.214963	50.986993
QBC_Q10664	7.59	3.14	0	Debris?	26.210859	50.990777
QBC_Q10665	34.55	12.87	0	Debris?	26.210029	50.994777
QBC_Q10666	5.1	1.47	0.96	Partially Buried Objects? - Asses	26.20775	50.997027
QBC_Q10667	48.7	2.84	0	Seabed Scar?	26.203179	51.00384
QBC_Q10668	10.47	7.75	0	Object in Water Column?	26.170889	51.047996
QBC_Q10669	3.77	3.31	0.27	Partially Buried Objects?	26.171655	51.04787
QBC_Q10670	88.05	2.73	0	Linear Debris?	26.200506	51.014543
QBC_Q10671	7.1	8.35	0.73	Bham0003 - 2 cars	26.222486	50.991231
QBC_Q10672	6.98	4.33	1.08	Partially Buried Objects?	26.217146	50.998854
QBC_Q10673	4.5	3.06	0.47	Partially Buried Objects?	26.217635	50.999494
QBC_Q10674	2.65	2.42	1.04	Debris? - Modern?	26.205136	51.017049
QBC_Q10675	1.81	1.19	0.76	Debris?	26.201617	51.020594
QBC_Q10676	23.03	17.08	0	Buried Feature?	26.20139	51.022168
QBC_Q10677	2.33	1.84	0.81	Debris?	26.199145	51.024446

Contact No	Length(ft)	Width(ft)	Height(ft)	Preliminary Interpretation	Lat(WGS84)	Lon(WGS84)
QBC_Q10678	5.98	2.3	0.85	Partially Buried Objects?	26.196575	51.0279
QBC_Q10679	1.66	0.67	0.45	Debris?	26.187724	51.040428
QBC_Q10680	1.8	1.07	0	Debris?	26.18188	51.049147
QBC_Q10681	4.82	1.92	0.16	Natural?	26.172046	51.062369
QBC_Q10682	1.18	0.88	0.5	Debris?	26.217385	51.007933
QBC_Q10683	0.91	0.62	0.34	Debris?	26.215904	51.009766
QBC_Q10684	0	0	0	Unclassified	26.206748	51.02219
QBC_Q10685	78.19	1.17	0	Seabed Scar?	26.203884	51.027346
QBC_Q10686	30.87	4.86	0	Natural?	26.184855	51.05447
QBC_Q10687	13.34	9.84	0	Depression?	26.175814	51.064984
QBC_Q10688	0.77	0.78	0.3	Natural?	26.211105	51.024764
QBC_Q10689	5.69	2.32	1.22	Partially Buried Objects? - Duplicate	26.207801	51.029506
QBC_Q10690	6.51	4.41	0.52	Natural?	26.204605	51.03247
QBC_Q10691	0	0	0	Unclassified	26.19526	51.046282
QBC_Q10692	7.49	5.08	0	Debris?	26.181437	51.067004
QBC_Q10693	9.18	6.63	0	Location?	26.178017	51.071213
QBC_Q10694	6.53	2.04	0.57	BHAM0001 - metal angle iron	26.210442	51.032916
QBC_Q10695	1.38	0.8	0.35	Natural?	26.21056	51.033607
QBC_Q10696	60.47	14.24	0	Location?	26.20892	51.034508
QBC_Q10697	62.84	7.46	0	Location?	26.208273	51.035456
QBC_Q10698	2.79	1.19	0.45	Natural?	26.207628	51.035773
QBC_Q10699	1.58	0.58	0.25	Natural?	26.206796	51.038223
QBC_Q10700	24.85	5.03	0	Natural?	26.204538	51.042405
QBC_Q10701	25.62	1.72	0	Location?	26.204608	51.041937
QBC_Q10702	101.59	13.77	0	Depression?	26.20077	51.045704
QBC_Q10703	49.74	2.6	0	Natural?	26.19924	51.048303

Contact No	Length(ft)	Width(ft)	Height(ft)	Preliminary Interpretation	Lat(WGS84)	Lon(WGS84)
QBC_Q10704	1.28	1.56	0.64	Debris?	26.1932	51.056634
QBC_Q10705	75.29	3.97	0	Buried Feature?	26.193103	51.057825
QBC_Q10706	0.84	0.28	0.69	Debris?	26.192831	51.05833
QBC_Q10707	13.27	1.98	0.25	Natural?	26.192357	51.059489
QBC_Q10708	1.32	0.64	0.63	Natural?	26.182613	51.072906
QBC_Q10709	1.12	0.93	0.66	Natural?	26.20862	51.043284
QBC_Q10710	2.6	1.12	0.53	Natural?	26.208763	51.044473
QBC_Q10711	1.59	0.85	0.24	Natural?	26.207304	51.046158
QBC_Q10712	2.26	0.79	0.4	Natural?	26.205436	51.048515
QBC_Q10713	1.72	1.25	0.47	Natural?	26.204865	51.048351
QBC_Q10714	0.35	0.35	0.27	Natural?	26.205088	51.048356
QBC_Q10715	1.29	0.97	0.59	Natural?	26.204389	51.050096
QBC_Q10716	10.63	8.12	0	Unclassified	26.204007	51.050221
QBC_Q10717	0	0	0.79	Debris?	26.19546	51.062176
QBC_Q10718	1.29	1.08	0.29	Natural?	26.19307	51.066298
QBC_Q10719	6.34	3.35	0	Mound?	26.19078	51.068742
QBC_Q10720	30.67	24.82	0	Location?	26.201079	51.062081
QBC_Q10721	0.63	0.38	0.48	Natural?	26.200876	51.063127
QBC_Q10722	0.88	0.38	0.28	Natural?	26.200962	51.063092
QBC_Q10723	1.38	0.75	0.39	Natural?	26.200706	51.063513
QBC_Q10724	1.13	0.92	0.21	Natural?	26.200986	51.06344
QBC_Q10725	43.15	5.26	0	Buried Feature?	26.194527	51.071913
QBC_Q10726	19.88	11.89	0	Buried Feature?	26.194214	51.071651
QBC_Q10727	29.49	2.04	0	Seabed Scar?	26.193718	51.073781
QBC_Q10728	7.94	3.98	0.21	Buried Feature?	26.192236	51.075747
QBC_Q10729	86.3	32.31	0	BHAM0028 - NOT PROPERLY LOCATED ?	26.078054	50.916605

Contact No	Length(ft)	Width(ft)	Height(ft)	Preliminary Interpretation	Lat(WGS84)	Lon(WGS84)
QBC_Q10800	0	0	0	Partially Buried Objects? - Duplicate of QBC_Q100689	26.207795	51.029454
QBC_Q10801	4.97	2.37	0	Debris?	26.198023	51.021605
QBC_Q10802	26.77	4.03	0	Debris? - Duplicate of QBC_Q10651	26.189848	51.012473
QBC_Q10803	10.41	3.4	0	Debris? - Duplicate	26.145484	50.975717
QBC_Q10804	5.63	2.63	0.68	Debris - Modern? - Duplicate of QBC_Q10207	26.143949	50.972733
QBC_Q10805	22.25	6.6	0	Debris?	26.140839	50.971974
QBC_Q10806	16.93	7.01	0	Duplicate of QBC_Q10187	26.136399	50.966768
QBC_Q10807	19.95	2.69	0	Debris?	26.117499	50.951097
QBC_Q10809	10.5	6.32	0	Debris?	26.102439	50.938059
QBC_Q10810	18.23	3.56	0		26.102819	50.936521
QBC_Q10812	21.17	14.72	1.05	Partially Buried Objects?	26.100444	50.934951
QBC_Q10813	5.82	2.29	0.51	Partially Buried Objects?	26.089422	50.925223
QBC_Q10814	8.24	3.33	0.9	Debris - Modern? - duplicate of QBC_Q10308	26.087427	50.924932
QBC_Q10815	26.34	14.15	0.91	Debris - Modern?	26.085005	50.92127
QBC_Q10816	0	0	0	Disturbed seabed ?	26.073977	50.913471
QBC_Q10817	57.5	9.44	0		26.074453	50.91239
QBC_Q10818	12.8	5.17	0	Unclassified	26.073308	50.910517
QBC_Q10819	15.65	6.53	0	Unclassified	26.07261	50.909795
QBC_Q10820	30.8	16.32	0	Depression?	26.066651	50.905448
QBC_Q10821	0	0	0	Duplicate of QBC_Q10729	26.077841	50.916601
QBC_Q10822	11.24	6.24	0.96	Partially Buried Objects?	26.084648	50.921714
QBC_Q10824	7.42	2.78	0.85	Duplicate of QBC_Q1807	26.117655	50.951166
QBC_Q10825	0	0	0	Debris - Modern? Duplicate of QBC_Q10806 and QBC_Q10187	26.136519	50.966809
QBC_Q10826	0	0	0	Debris - Modern? Duplicate of QBC_Q10804	26.143991	50.972805
QBC_Q10827	0	0	0	Duplicate of QBC_Q10803	26.145584	50.975927
QBC_Q10829	6.76	2.48	0.7	Debris - Modern?	26.148292	50.977067

Contact No	Length(ft)	Width(ft)	Height(ft)	Preliminary Interpretation	Lat(WGS84)	Lon(WGS84)
QBC_Q10830	19.74	4.38	0	Depression?	26.169129	50.996058
QBC_Q10831	0	0	0	Duplicate of QBC_Q10651	26.189858	51.012523
QBC_Q10832	6.52	5.22	0	Debris?	26.19204	51.0143
QBC_Q10833	0	0	0	Duplicate of QBC_Q100689	26.207859	51.029534
QBC_Q10834	0	0	0	Duplicate of QBC_Q10816	26.07404	50.913514
QBC_Q10835	0	0	0	Duplicate of QBC_Q10815	26.08498	50.921268
QBC_Q10836	0	0	0	duplicate of QBC_Q10308	26.087481	50.925022
QBC_Q10837	0	0	0	Duplicate of QBC_Q10813	26.089259	50.925087
QBC_Q10838	0	0	0	Duplicate of QBC_Q10812	26.100483	50.934926
QBC_Q10839	0	0	0	Duplicate of QBC_Q10107	26.111848	50.945664
QBC_Q10840	3.89	2.8	0.86	Debris - Modern?	26.064826	50.936662
QBC_Q10841	2.47	1.05	0.38	Partially Buried Objects?	26.068584	50.940235
QBC_Q10842	0	0	0	Duplicate of QBC_Q10298	26.069907	50.940324
QBC_Q10843	6.83	2.52	0.43	Debris - Modern?	26.088594	50.956422
QBC_Q10844	1.01	0.6	0.45	Debris?	26.089272	50.95716
QBC_Q10845	6.21	2.36	1.01	Debris - Modern?	26.090141	50.958149
QBC_Q10846	1.43	0.41	0.54	Debris?	26.090735	50.959415
QBC_Q10847	0	0	0	Duplicate of QBC_Q10110	26.097505	50.96587
QBC_Q10848	3.63	1.17	0.53	Debris?	26.181361	51.037826
QBC_Q10849	5.33	1.66	0.56	Debris?	26.146677	51.00794
QBC_Q10850	0	0	0	Duplicate of QBC_Q10203	26.130408	50.993318
QBC_Q10851	0	0	0	Duplicate of QBC_Q10023	26.115736	50.979872
QBC_Q10852	0	0	0	Duplicate of QBC_Q10168	26.112219	50.976101
QBC_Q10853	0	0	0	Duplicate of QBC_Q10120	26.102052	50.968747
QBC_Q10854	10.85	1.42	0.76	Duplicate of QBC_Q10840	26.064851	50.936623
QBC_Q10855	4.41	2.3	0.76	Duplicate of QBC_Q10298	26.069825	50.940309

Contact No	Length(ft)	Width(ft)	Height(ft)	Preliminary Interpretation	Lat(WGS84)	Lon(WGS84)
QBC_Q10856	11.42	3.45	0.68	Duplicate of QBC_Q10843	26.088514	50.956385
QBC_Q10857	4.73	2.02	0	Duplicate of QBC_Q10221	26.089954	50.957033
QBC_Q10858	9.3	5.48	0.69	Duplicate of QBC_Q10845	26.09017	50.958092
QBC_Q10859	0.37	0.18	0	Debris?	26.090517	50.958006
QBC_Q10860	3.81	1.44	0.41	Duplicate of QBC_Q10846	26.0908	50.959455
QBC_Q10861	39.99	1.31	0	Linear Debris?	26.099693	50.966635
QBC_Q10862	4.42	2.36	0.55	Debris - Modern?	26.102055	50.968746
QBC_Q10863	4.93	3.01	0.49	Duplicate of QBC_Q10023	26.115733	50.979878
QBC_Q10864	0	0	0	Duplicate of QBC_Q10203	26.130369	50.993332
QBC_Q10865	0	0	0		26.097435	50.964845
QBC_Q10866	0	0	0	Duplicate of QBC_Q10849	26.146739	51.007851
QBC_Q10867	0	0	0	Duplicate of QBC_Q10848	26.181363	51.037869
QBC_Q10869	6.04	5.96	1.28	Natural?	26.049892	50.892192
QBC_Q10901	6.6	3.55	0.72	Debris - Modern?	26.089642	50.942611
QBC_Q10902	5.96	3.54	1.05	Debris - Modern?	26.089445	50.941131
QBC_Q10903	0	0	0	Duplicate of QBC_Q10344	26.087449	50.940918
QBC_Q10904	7.42	4.05	0	Debris?	26.08548	50.939336
QBC_Q10905	0	0	0	Duplicate of QBC_Q10327	26.083135	50.936817
QBC_Q10906	27.85	15.69	0	Disturbed seabed ?	26.077989	50.931212
QBC_Q10907	8.85	5.52	0.48	Debris?	26.072828	50.928273
QBC_Q10908	0	0	0	Duplicate of QBC_Q10231	26.060548	50.917317
QBC_Q10909	3.98	1.87	0.98	Debris?	26.059662	50.916193

## Area 2 and 3

Contact No	Length(ft)	Width(ft)	Height(ft)	Preliminary Interpretation	Lat(WGS84)	Lon(WGS84)
QBC_Q20001	17.45	7.88	0.35	Natural?	26.034871	50.969744
QBC_Q20002	3.78	2.09	0.26	Natural?	26.022824	50.989369
QBC_Q20003	28.81	14.45	0	Location?	26.015682	51.00121
QBC_Q20004	11.15	4.29	0	Natural?	26.029393	50.975943
QBC_Q20005	18.62	1.64	0	Debris?	26.021609	50.985721
QBC_Q20006	5.74	1.49	0.38	Natural?	26.037301	50.961285
QBC_Q20007	5.41	2.96	1.32	Debris?	26.043259	50.949102
QBC_Q20008	32.26	5.33	0	Location?	26.039622	50.953929
QBC_Q20009	7.58	4.17	0	Natural?	26.031682	50.966108
QBC_Q20010	15.52	5.42	0.59	Location?	26.023692	50.980616
QBC_Q20011	30.22	20.9	0	Depression?	26.021348	50.985627
QBC_Q20012	3.79	2.23	0.61	Debris?	26.039721	50.949273
QBC_Q20013	10.91	6.17	0	Hole?	26.028365	50.969804
QBC_Q20014	10.83	3.15	0.74	Natural?	26.038261	50.95344
QBC_Q20015	89.29	1.93	0	Linear Debris?	26.035609	50.953278
QBC_Q20016	3.41	1.81	0.62	Natural?	26.028178	50.966301
QBC_Q20017	0.79	19.91	0	Location?	26.018519	50.982515
QBC_Q20018	16.84	2.11	0.53	Natural?	26.012999	50.991011
QBC_Q20019	3.25	0.96	0.32	Natural?	26.037128	50.946973
QBC_Q20020	47.18	7.05	0	Natural?	26.031579	50.957676
QBC_Q20021	2.87	1.73	0.64	Debris?	26.03056	50.958093
QBC_Q20022	47.36	4.22	0.37	Unclassified	26.01596	50.983347
QBC_Q20023	13.55	3.34	0.88	Natural?	26.014797	50.983851
QBC_Q20024	49.06	33.56	0	Location?	26.047384	50.92857

Contact No	Length(ft)	Width(ft)	Height(ft)	Preliminary Interpretation	Lat(WGS84)	Lon(WGS84)
QBC_Q20025	13.9	2.44	0	Debris?	26.040639	50.937346
QBC_Q20027	6.8	4.71	0	Natural?	26.032283	50.950897
QBC_Q20028	35.31	1.64	0	Natural?	26.012014	50.98432
QBC_Q20029	27.21	5.3	0	Unclassified	26.008609	50.989855
QBC_Q20030	0	0	0	Unclassified	25.999482	51.005706
QBC_Q20031	27.53	7.47	0	Depression?	25.997185	51.006401
QBC_Q20032	30.63	22.52	0	Depression?	25.997672	51.004862
QBC_Q20033	16.23	11.15	0	Hole?	26.025869	50.960361
QBC_Q20034	96.04	52.54	0	Location?	26.026234	50.957138
QBC_Q20035	8.44	1.56	0.3	Natural?	26.030321	50.94946
QBC_Q20036	12.37	2.67	0.61	Debris?	26.023908	50.95936
QBC_Q20037	41.82	4.7	0	Seabed scar?	26.008555	50.983086
QBC_Q20038	18.73	0.9	0	Natural?	26.015007	50.970753
QBC_Q20039	74.1	41.85	0	natural	26.018131	50.963395
QBC_Q20040	52.45	34.27	0	natural	26.019713	50.962363
QBC_Q20041	8.53	5.19	1.3	Debris?	26.032559	50.938596
QBC_Q20043	37.41	15.23	0.58	location	26.017383	50.963429
QBC_Q20044	12.12	1.04	0	hole?	26.016424	50.962491
QBC_Q20045	16.75	2.18	0	Debris?	26.015616	50.966629
QBC_Q20046	65.8	20.3	0	location	26.013541	50.968965
QBC_Q20047	25.21	4.29	0	Seabed scar?	26.012459	50.969711
QBC_Q20048	113.87	53.67	0	location	26.011772	50.967575
QBC_Q20049	14.69	3.27	0.34	Natural?	26.012287	50.968259
QBC_Q20050	17.63	4.01	0.49	Natural?	26.024893	50.943524
QBC_Q20051	13.86	8.25	0	Hole?	26.023127	50.945239
QBC_Q20052	96.86	71.72	0	Natural?	26.011805	50.964874

Contact No	Length(ft)	Width(ft)	Height(ft)	Preliminary Interpretation	Lat(WGS84)	Lon(WGS84)
QBC_Q20053	33.67	12.93	0	Depression?	26.005168	50.970761
QBC_Q20054	23.18	3.95	1.56	Natural?	26.006324	50.970422
QBC_Q20055	12.64	4.84	0.74	Natural?	26.00827	50.967464
QBC_Q20056	9.27	5.01	0.61	Natural?	26.008231	50.96518
QBC_Q20057	29.83	4.27	0	Natural?	26.008954	50.963154
QBC_Q20058	18.91	5.53	0	Depression?	26.003936	50.968802
QBC_Q20059	3.18	1.41	0.73	Debris?	25.993794	50.985838
QBC_Q20060	61.18	37.13	0	Mound?	26.001472	50.969192
QBC_Q20061	15.49	7.51	0	Hole?	26.007525	50.961633
QBC_Q20062	48.69	21.63	0	Sediment accumulation?	26.000014	50.970078
QBC_Q20063	8.69	7.28	2.16	Debris?	25.998462	50.971358
QBC_Q20064	5.64	3.33	1.31	Debris?	25.987718	50.986676
QBC_Q20065	40.74	12.06	0	Depression?	25.98895	50.983912
QBC_Q20066	8.35	3.79	1.35	Natural?	25.997685	50.969099
QBC_Q20067	31.05	6.36	1.03	Natural?	25.998971	50.968183
QBC_Q20068	19.12	4.65	0.59	Debris?	26.000052	50.964064
QBC_Q20069	32.09	3.03	0	Natural?	26.003802	50.960695
QBC_Q20070	2.73	2.49	0.64	Debris?	26.010633	50.949374
QBC_Q20071	38.32	12.2	0	Depression?	26.034977	50.909748
QBC_Q20072	25.21	2.98	0	Natural?	26.036274	50.907219
QBC_Q20073	11.59	3.98	0.31	Debris?	25.99973	50.963871
QBC_Q20074	4.68	2.29	1.19	Debris?	25.985496	50.986134
QBC_Q20075	0	0	0	Debris?	25.985699	50.986791
QBC_Q20076	11.24	4.75	0	Debris?	25.98548	50.987437
QBC_Q20077	8.89	2.96	1.24	Debris?	25.990019	50.974952
QBC_Q20078	8.85	2.56	0.37	Debris?	25.998364	50.959999

Contact No	Length(ft)	Width(ft)	Height(ft)	Preliminary Interpretation	Lat(WGS84)	Lon(WGS84)
QBC_Q20079	10.35	3.01	0.58	Debris?	26.000616	50.957843
QBC_Q20080	25.93	31.87	1.21	Buried features?	26.001858	50.955288
QBC_Q20081	5.82	1.45	0.34	Debris?	26.026197	50.916223
QBC_Q20082	7.22	3.47	1.5	Debris?	26.032657	50.906264
QBC_Q20083	57.88	9.44	0	Depression?	26.009534	50.938401
QBC_Q20084	11.87	2.69	0.55	Debris?	26.007582	50.941897
QBC_Q20085	12.36	6.1	0.29	Debris?	26.008765	50.942045
QBC_Q20086	82.15	25.16	0	Depression?	25.999753	50.956708
QBC_Q20087	10.92	9	0.65	Debris?	25.985574	50.977561
QBC_Q20088	24.61	12.44	0	Depression ?	26.002045	50.94879
QBC_Q20089	3.01	2.26	1.16	Buried features?	26.005229	50.943802
QBC_Q20090	21.7	6.03	0	hole?	26.026321	50.903746
QBC_Q20091	20.52	7.04	0	Depression?	26.025408	50.9074
QBC_Q20092	29.71	1.61	0	Hole?	26.005373	50.940511
QBC_Q20093	43.41	3.94	0.5	Linear Debris?	26.002905	50.943807
QBC_Q20094	7.71	4.32	0	Hole?	25.982569	50.975877
QBC_Q20096	14.9	12.33	1.22	Debris?	25.981652	50.973519
QBC_Q20097	4.06	2.65	0.66	Debris?	25.974627	50.978978
QBC_Q20098	31.37	17.29	0	Depression?	25.992853	50.949522
QBC_Q20099	19.87	3.64	0	Natural?	26.01989	50.904247
QBC_Q20100	68.85	2.53	0	Natural?	26.010368	50.913935
QBC_Q20101	31.91	3.37	0	Location?	26.007956	50.912479
QBC_Q20102	17.88	5.05	0.56	Debris?	25.993403	50.932861
QBC_Q20103	6.38	3.6	1.1	Debris?	26.003767	50.913513
QBC_Q20104	24.32	1.36	0	Seabed scar?	26.003197	50.913515
QBC_Q30105	11.35	4.4	0	Debris?	25.977768	50.960233

Contact No	Length(ft)	Width(ft)	Height(ft)	Preliminary Interpretation	Lat(WGS84)	Lon(WGS84)
QBC_Q30106	11.83	10.31	0.87	Debris?	25.977577	50.960399
QBC_Q30107	29.3	4.84	0	Unclassified	25.995671	50.913725
QBC_Q30108	3.88	1.51	1.15	Debris?	25.958976	50.986071
QBC_Q30109	10.7	6.9	0	Natural?	25.986144	50.934308
QBC_Q30110	55.23	4.81	0.98	Natural?	25.975427	50.955838
QBC_Q30111	34.99	3.32	0	Seabed scar?	25.988777	50.923005
QBC_Q30112	8.24	3.96	0.46	Debris?	25.992048	50.91507
QBC_Q30113	47.15	3.1	0	Linear Debris?	25.993095	50.911622
QBC_Q30114	15.49	4.05	0.46	Natural?	25.998981	50.897624
QBC_Q30115	20.51	8.26	0	Hole?	25.988612	50.917231
QBC_Q30116	33.68	12.91	0	Depression?	25.987858	50.922473
QBC_Q30117	46.89	23.3	0	Depression?	25.964744	50.963022
QBC_Q30118	23.42	9.08	0	Depression?	25.992698	50.904102
QBC_Q30120	19.72	2.98	0	Linear Debris?	25.992489	50.902197
QBC_Q30121	103.01	3	0	Natural?	25.992475	50.895784
QBC_Q30122	5.1	3.82	0	Hole?	25.990982	50.902169
QBC_Q30123	88.19	7.71	0	Unclassified	25.987257	50.915365
QBC_Q30124	96.05	4.07	0	Unclassified	25.986066	50.917011
QBC_Q30125	11.56	3.37	0	Debris?	25.977564	50.93689
QBC_Q30126	33.12	3.09	0	Seabed scar?	25.977464	50.937645
QBC_Q30127	17.39	3.98	0	Depression?	25.960588	50.966248
QBC_Q30128	93.87	4.71	0	Natural?	25.99261	50.890159
QBC_Q30129	98.22	2.98	0	Seabed scar?	25.979662	50.927369
QBC_Q30130	12.46	4.36	0.46	Debris?	25.975852	50.936445
QBC_Q30131	34.51	1.81	0	Natural?	25.960882	50.96314
QBC_Q30132	33.38	8.95	0	Depression?	25.957793	50.96692

Contact No	Length(ft)	Width(ft)	Height(ft)	Preliminary Interpretation	Lat(WGS84)	Lon(WGS84)
QBC_Q30133	63.54	2.97	0	Seabed scar?	25.978715	50.926276
QBC_Q30134	5.47	1.47	0.22	Debris?	25.986519	50.892238
QBC_Q30135	8.73	2.17	0.57	Debris?	25.962336	50.950633
QBC_Q30136	96.79	1.7	0	Natural?	25.985557	50.893222
QBC_Q30137	20.36	3.14	0	Depression?	25.948145	50.969633
QBC_Q30138	37.3	7.62	0	Depression?	25.969652	50.930996
QBC_Q30139	80.15	26.76	0	Location?	25.955473	50.956545
QBC_Q30140	34.58	27.58	0	Natural?	25.975749	50.91299
QBC_Q30141	95.65	6.02	0.86	Natural?	25.975314	50.916018
QBC_Q30142	6.77	3.28	0.4	Debris?	25.990113	50.866632
QBC_Q30143	3.48	3.01	0	Debris?	25.990316	50.866171
QBC_Q30144	14.79	3.79	0	Unclassified	25.989013	50.86602
QBC_Q30145	36.85	8.08	0	Natural?	25.991626	50.867082
QBC_Q30146	24.46	1.22	0	Linear Debris?	25.991857	50.872043
QBC_Q30147	31.23	1.05	0	Linear Debris?	25.988126	50.864203
QBC_Q30148	30.6	3.16	0	Natural?	25.991997	50.86839
QBC_Q30149	6.09	3.72	0.6	Debris?	25.990818	50.858539
QBC_Q30150	5.3	3.32	1.37	Debris?	25.990016	50.860044
QBC_Q30151	7.02	4.33	0	Natural?	25.995585	50.863937
QBC_Q30152	9.04	3.89	0	Unclassified	25.991102	50.856636
QBC_Q30153	5.16	5	0	Unclassified	25.989567	50.856227
QBC_Q30154	9.38	2.91	0	Unclassified	25.990474	50.856215
QBC_Q30155	7.88	2.85	0	Unclassified	25.990071	50.857458
QBC_Q30156	6.12	4.87	1.1	Unclassified	25.988864	50.856032
QBC_Q30157	5.05	2.64	0	Unclassified	25.99027	50.855844
QBC_Q30158	10.77	3.02	0	Natural?	25.993669	50.856892

Contact No	Length(ft)	Width(ft)	Height(ft)	Preliminary Interpretation	Lat(WGS84)	Lon(WGS84)
QBC_Q30159	18.33	5.78	1.16	Debris?	25.997508	50.860406
QBC_Q30160	11.21	1.55	0	Linear Debris?	25.992489	50.850839
QBC_Q30161	20.77	10.97	0.93	Debris?	25.993421	50.851087
QBC_Q30162	4.4	3.46	1.67	Debris?	26.026144	50.891788
QBC_Q30163	5.67	2.27	2.22	Debris?	26.025856	50.89145
QBC_Q30164	6.33	3.85	0.59	Debris?	26.025013	50.891097
QBC_Q30165	5.21	5.2	1.13	Debris?	26.025462	50.890914
QBC_Q30166	5.18	3.5	0.88	Debris?	26.025673	50.890524
QBC_Q30167	4.16	3.35	0.71	Debris?	26.025872	50.890714
QBC_Q30168	6	5.38	0.88	Debris?	26.026389	50.891085
QBC_Q30169	3.24	1.36	0.37	Debris?	26.025976	50.891257
QBC_Q30170	6.81	2.48	0.53	Debris?	26.028128	50.89273
QBC_Q30171	5.31	4.04	0.47	Debris?	26.030331	50.894548
QBC_Q30172	5.17	2.79	0.91	Debris?	26.032058	50.895138
QBC_Q30174	38.24	3.32	0.44	Buried features?	26.033817	50.894891
QBC_Q30175	5.59	2.57	0.55	Debris?	26.033991	50.894954
QBC_Q30176	33.97	3.82	0.21	Buried features?	26.034035	50.895316
QBC_Q30177	47.63	1.4	0.49	Linear Debris?	26.034817	50.895515
QBC_Q30178	42.05	10.3	0	Depression?	26.045648	50.897662
QBC_Q30179	7.8	4.83	2.18	Debris?	26.044424	50.895195
QBC_Q30180	6.12	1.43	1.02	Debris?	26.032736	50.886064
QBC_Q30181	8.29	7.15	1.49	Debris?	26.044475	50.895084
QBC_Q30182	7.69	2.49	0	Debris?	26.04388	50.894803
QBC_Q30183	45.21	40.42	0	Unclassified	25.992082	50.845904
QBC_Q30184	41.06	19.18	0	Unclassified	25.992179	50.845926
QBC_Q30185	8.07	7.23	0	Unclassified	25.993254	50.843139

Contact No	Length(ft)	Width(ft)	Height(ft)	Preliminary Interpretation	Lat(WGS84)	Lon(WGS84)
QBC_Q30186	5.97	2.61	0	Natural?	25.996373	50.843966
QBC_Q30187	28.63	2.77	0	Linear Debris?	25.992991	50.841089
QBC_Q30188	23.14	7.49	2.36	Natural?	26.053965	50.884765
QBC_Q30189	7.86	3.06	1.89	Debris?	26.060268	50.889165

#### Area 4

Contact No	Length(ft)	Width(ft)	Height(ft)	Preliminary Interpretation	Lat(WGS84)	Lon(WGS84)
QBC_Q40001	9.17	6.3	0.32	Buried feature?	25.932107	50.861681
QBC_Q40002	94.47	1.96	0	Seabed scar?	25.924947	50.858498
QBC_Q40003	8.64	6.75	0	Natural?	25.926054	50.858424
QBC_Q40004	99.51	2.43	0	Seabed scar?	25.931503	50.861094
QBC_Q40005	33.62	2.36	0	Seabed scar?	25.938567	50.862092
QBC_Q40006	22.84	5.17	0	Disturbed Seabed	25.940958	50.862832
QBC_Q40008	13.98	5.53	0.3	Natural?	25.986061	50.873693
QBC_Q40009	66.13	2.08	0	Seabed scar?	25.987743	50.869673
QBC_Q40010	3.58	1.53	1.53	Debris?	25.988274	50.8648
QBC_Q40011	2.66	1.92	0.64	Debris?	25.987836	50.86551
QBC_Q40012	4.28	1.54	0.22	Natural?	25.989284	50.85452
QBC_Q40013	23.67	1.01	0	Natural?	25.991374	50.839758
QBC_Q40014	2.77	1.67	0.91	Buried feature?	25.990097	50.837026
QBC_Q40015	7.69	2.02	0	Natural?	25.990882	50.840948
QBC_Q40016	8.94	3.36	0	Natural?	25.987067	50.857546
QBC_Q40017	71.48	1.94	0.29	Linear Debris?	25.980771	50.88926
QBC_Q40018	74.73	3.13	0	Seabed scar?	25.986048	50.849994

Contact No	Length(ft)	Width(ft)	Height(ft)	Preliminary Interpretation	Lat(WGS84)	Lon(WGS84)
QBC_Q40019	61.72	1.26	0	Seabed scar?	25.987655	50.846209
QBC_Q40020	70.44	0.55	0	Unclassified	25.987127	50.842702
QBC_Q40021	31.21	1.23	0	Seabed scar?	25.988522	50.841997
QBC_Q40022	3.95	1.99	0	Natural?	25.987938	50.838971
QBC_Q40023	49.01	26.34	0	Location?	25.977381	50.884258
QBC_Q40024	97.43	0	0	Location?	25.977262	50.88167
QBC_Q40025	4.47	3.12	0	Unclassified	25.981833	50.854398
QBC_Q40026	104.92	0	0	Location?	25.984453	50.837905
QBC_Q40027	99.93	0	0	Location?	25.981649	50.85249
QBC_Q40028	67.49	2.02	0	Seabed scar?	25.977321	50.865097
QBC_Q40029	6.26	4.05	0	Natural?	25.978028	50.851914
QBC_Q40030	4.76	3.8	0	Natural?	25.977766	50.852149
QBC_Q40031	77.92	7.31	0.84	Location?	25.971329	50.88125
QBC_Q40032	9.23	5.44	1.07	Natural?	25.973929	50.863919
QBC_Q40033	0	0.74	0	Linear Debris?	25.97656	50.847923
QBC_Q40034	8.29	5.27	1.2	Debris - modern?	25.972184	50.860145
QBC_Q40035	0	0.76	0	Linear Debris?	25.973636	50.83635
QBC_Q40036	9.03	3.45	0	Unclassified	25.972746	50.838404
QBC_Q40037	7.31	2.76	0	Unclassified	25.969904	50.848385
QBC_Q40038	126.85	17.28	0	Depression?	25.964237	50.887264
QBC_Q40039	48.53	12.33	0	Depression?	25.962862	50.887205
QBC_Q40040	0	0	0	Unclassified	25.961924	50.887342
QBC_Q40041	7.92	3.96	0	Natural?	25.963152	50.880036
QBC_Q40042	6.94	4.41	0	Unclassified	25.964352	50.875995
QBC_Q40044	92.28	0.73	0	Seabed scar?	25.966476	50.85934
QBC_Q40045	4.48	1.59	0	Debris?	25.969016	50.839139

Contact No	Length(ft)	Width(ft)	Height(ft)	Preliminary Interpretation	Lat(WGS84)	Lon(WGS84)
QBC_Q40046	7.15	1.12	0.1	Natural?	25.967363	50.850407
QBC_Q40047	4.65	2.85	0	Unclassified	25.965044	50.857902
QBC_Q40048	32.07	1.21	0	Seabed scar?	25.960408	50.886675
QBC_Q40049	49.03	12.43	0	Natural?	25.960118	50.886517
QBC_Q40050	19.89	16.94	0	Depression?	25.961303	50.867656
QBC_Q40051	4	2	0	Unclassified	25.966443	50.843104
QBC_Q40052	23.52	6.94	0	Depression?	25.960415	50.868114
QBC_Q40053	32.63	13.84	0	Depression?	25.960072	50.871546
QBC_Q40054	8.62	5.25	0	Hole?	25.957434	50.875804
QBC_Q40055	40.62	19.22	0	Sediment accumulation?	25.957461	50.870748
QBC_Q40056	44.65	13.59	0	Depression? - Duplicate	25.958747	50.869402
QBC_Q40057	45.78	15.97	0	Depression? - Duplicate	25.957867	50.86819
QBC_Q40058	5.99	3.25	0.32	Debris?	25.958019	50.866742
QBC_Q40059	97.61	20.33	0	Depression?	25.95889	50.862487
QBC_Q40060	4.52	3.19	0.85	Debris?	25.964182	50.834745
QBC_Q40061	11.63	3.42	0	Unclassified	25.963187	50.832818
QBC_Q40062	30.29	1.39	0	Seabed scar?	25.963085	50.829337
QBC_Q40063	7.75	2.89	0	Unclassified	25.96245	50.832142
QBC_Q40064	47.34	13.77	0	Depression?	25.956369	50.866906
QBC_Q40065	32.36	10.82	0	Depression?	25.956751	50.869363
QBC_Q40066	20.95	12.78	0	Sediment accumulation?	25.955581	50.876598
QBC_Q40067	64.96	1.67	0	Seabed scar?	25.953895	50.882226
QBC_Q40068	30.47	2.92	0	Hole?	25.955256	50.867615
QBC_Q40069	22.05	6.03	0	Hole?	25.955473	50.867196
QBC_Q40070	4.2	2.42	0	Unclassified	25.95574	50.861931
QBC_Q40071	79.69	20.53	0	Buried features?	25.956161	50.86105

Contact No	Length(ft)	Width(ft)	Height(ft)	Preliminary Interpretation	Lat(WGS84)	Lon(WGS84)
QBC_Q40072	9.8	6.67	0.42	Unclassified	25.957421	50.835568
QBC_Q40073	11.25	8.02	0	Debris?	25.950385	50.878201
QBC_Q40074	19.91	15.89	0	Sediment accumulation?	25.951354	50.879572
QBC_Q40075	23.81	6.86	0	Natural?	25.951534	50.867655
QBC_Q40076	19.47	3.33	0	Natural?	25.951729	50.86673
QBC_Q40077	78.28	1.86	0	Seabed scar?	25.953003	50.848071
QBC_Q40078	50.42	3.32	0	Seabed scar?	25.948526	50.866514
QBC_Q40079	11.63	12.86	0	Unclassified	25.948783	50.87525
QBC_Q40080	0	0	0	Location?	25.947379	50.878228
QBC_Q40081	11.1	7.62	0	Unclassified	25.945731	50.874101
QBC_Q40082	98.21	1.23	0	Seabed scar?	25.950966	50.840941
QBC_Q40083	10.14	5.53	0	Buried features?	25.949666	50.837692
QBC_Q40084	9.75	5.07	0	Debris?	25.941409	50.874538
QBC_Q40085	71.09	1.34	0	Seabed scar?	25.94	50.863017
QBC_Q40086	8.37	4.83	0	Debris?	25.944913	50.841861
QBC_Q40087	6.43	4.66	0	Debris?	25.945882	50.825839
QBC_Q40088	7.21	2.61	0	Debris?	25.937896	50.87336
QBC_Q40089	44.6	6.21	0	Debris?	25.942259	50.82708
QBC_Q40090	37.83	3.31	0	Seabed scar?	25.94043	50.827707
QBC_Q40091	10.14	9.68	1.35	Debris?	25.93982	50.830971
QBC_Q40092	6.63	2.66	1.37	Debris?	25.939852	50.832139
QBC_Q40093	46.63	1.72	0	Seabed scar?	25.936133	50.861157
QBC_Q40094	7.19	3.42	0	Natural?	25.932808	50.874257
QBC_Q40095	5.18	2.73	0	Debris?	25.939733	50.82807
QBC_Q40096	5.71	3.23	0	Debris?	25.94	50.826521
QBC_Q40097	29.24	8.5	0	Natural?	25.939984	50.825925

Contact No	Length(ft)	Width(ft)	Height(ft)	Preliminary Interpretation	Lat(WGS84)	Lon(WGS84)
QBC_Q40098	88.18	2.99	0	Unclassified	25.938848	50.826256
QBC_Q40099	38.71	24.66	0	Unclassified	25.936521	50.828418
QBC_Q40100	14.26	7.67	0	Debris?	25.935923	50.831528
QBC_Q40101	92.46	1.46	0	Seabed scar?	25.935402	50.836563
QBC_Q40102	104.76	17.6	0	Depression?	25.928998	50.864938
QBC_Q40103	116.89	0.71	0	Seabed scar?	25.93095	50.85438
QBC_Q40104	8.05	4.27	0.9	Natural?	25.934183	50.83233
QBC_Q40105	16.52	5.05	1.35	Natural?	25.934876	50.827527
QBC_Q40106	5.72	4.98	0.38	Natural?	25.932611	50.829857
QBC_Q40107	6.86	2.26	0.75	Natural?	25.933705	50.830691
QBC_Q40108	26.86	3.4	0	Natural?	25.932396	50.831335
QBC_Q40109	10.55	3.43	0.45	Natural?	25.932459	50.832626
QBC_Q40110	62.63	2.12	0	Seabed scar?	25.924592	50.869542
QBC_Q40111	107.23	1.55	0	Seabed scar?	25.925479	50.869238
QBC_Q40112	14.75	10.57	1.02	Natural?	25.930967	50.827903
QBC_Q40113	99.32	26.23	0	Unclassified	25.93258	50.826912
QBC_Q40114	6.68	3.82	0.21	Natural?	25.98773	50.857431
QBC_Q40116	12.88	7.83	0	Unclassified	25.963887	50.850258
QBC_Q40117	40.44	8.35	0	Sediment accumulation?	25.952159	50.846663
QBC_Q40118	59.29	15.25	0	Depression? - Duplicate	25.957907	50.868155
QBC_Q40119	44.47	14.35	0	Depression? - Duplicate	25.958824	50.869361
QBC_Q40120	3.8	1.79	0.26	Natural?	25.967127	50.871502
QBC_Q40121	28.05	4.68	0.32	Natural?	25.985138	50.875706

## **APPENDIX 6: DERIVED DATA INCLUDED ON ACCOMPANYING CD**

The data created during the research is included on an accompanying data CD. The data included is purely derived data, and no original survey data has been included due to data ownership/copyright reasons. The exception to this is the grab sample locations and granulometry report, which was undertaken specifically for this research.

The data can either be opened as a map package or a map document in ArcGIS, or the data files can be imported into other compatible GIS packages.

### **ArcGIS Map Package**

DataCD.mpk

### **ArcGIS Project**

DataCD.mxd

### **Shapefiles (In folder called DataForCD)**

(NB layer files (.lyr) for each shapefile/grid are also included)

#### **Background Mapping:**

Coast\_UTM39N.shp

SurveyArea.shp

Qatar\_UbaidSites.shp

#### **Acoustic Classification**

Classes (Raster grid File)

#### **Topographic Mapping**

TopographicFeatures.shp

#### **Ground Truthing**

GrabSamples.shp (shapefile contains hyperlinks to granulometry report:  
..../hyperlinks/GranulometryReport.pdf)

#### **Geophysical Anomalies:**

Area1AllContacts.shp

Area3AllContacts.shp

Area4AllContacts.shp

Area1Debris.shp

Area3Debris.shp

Area4Debris.shp

Area1Depressions.shp

Area3Depressions.shp

Area4Depressions.shp

Area1GroundTruthed.shp

Area1LongLinearFeature.shp

**Seabed Characterisation**

InitialLandscapeUnits.shp

FinalCharacterAreas.shp (by acoustic class)

FinalCharacterAreas.shp (by overall potential)

## BIBLIOGRAPHY

- Abdel Monim-Mubarak, W. and Kubryakov, A.I. 2000 Hydrological Structure of Waters of the Persian Gulf According to the Data of Observations in 1992. **Physical Oceanography**, 11 (5): 459-471.
- Abu-Zeid, M.M., Abd El Hameed, A.E.T., Al Kuwari , A.J. (2001) Diagenesis in the Coastal Quaternary Carbonates in Qatar, Arabian Gulf. **Carbonates and Evaporites**, 16 (1): 26-36.
- Al-Ghadban, A.N., Abdali, F. and Massoud, M.S. (1998) Sedimentation Rate and Bioturbation in the Arabian Gulf. **Environment International**, 24 (1/2): 23-31.
- Al-Hinai, K.G., Moore, J.M. and Bush, P.R. (1987) LANDSAT Image Enhancement Study of Possible Submerged Sand-Dunes in the Arabian Gulf. **International Journal of Remote Sensing**, 8 (2): 251-258.
- Al-Naimi, F., Cuttler, R., Alhaidous, I.I., Dingwall, L., Momber, G., Al-Naimi, S., Breeze, P. and Al-Kawari, A.A. (2012) Landscape Signatures and Seabed Characterisation in the Marine Environment of North-west Qatar. **Proceedings of the Seminar for Arabian Studies**, 42: 245-260.
- Al-Saad, H. (2005) Lithostratigraphy of the Middle Eocene Dammam Formation in Qatar, Arabian Gulf: Effects of Sea-Level Fluctuations Along a Tidal Environment. **Journal of Asian Earth Sciences**, 25: 781–789.
- Aldred, O. and Fairclough, G. (2003) **Historic Landscape Characterisation: Taking Stock of the Method**. London: English Heritage/Somerset County Council.
- Alfred Wegener Institute (2012) **Case Study “Eckernfoerde Bay” – The SubGate Project** [online]. Available from : [www.awi.de/en/research/research\\_divisions/geosciences/marine\\_geochemistry/sub\\_marine\\_groundwater\\_discharge\\_in\\_the\\_coastal\\_zone/eckernfoerde\\_bay\\_the\\_subgate\\_project/](http://www.awi.de/en/research/research_divisions/geosciences/marine_geochemistry/sub_marine_groundwater_discharge_in_the_coastal_zone/eckernfoerde_bay_the_subgate_project/) [Accessed 31 August 2013].
- Alsharhan, A.S. and Kendall, C.G.St.C. (2003) Holocene Coastal Carbonates and Evaporites of the Southern Arabian Gulf and their Ancient Analogues. **Earth-Science Reviews**, 61: 191–243
- Anderson, J.T., Holliday, D.V., Kloster, R., Reid, D.G., and Simard, Y. (2008) Acoustic Seabed Classification: Current Practice and Future Directions. **ICES Journal of Marine Science**, 65: 1004–1011.
- Bailey, G., Al Sharekh, A., Flemming, N., Lambeck, K., Momber, G., Sinclair, A. and Vita-Finzi, C. (2007) Coastal Prehistory in the Southern Red Sea Basin, Underwater Archaeology and the Farasan Islands. **Proceedings of the Seminar for Arabian Studies**, 37: 1-16.

Bailey, G.N. (2009) "The Red Sea, Coastal Landscapes, and Hominin Dispersals." In Petraglia, M.D. and Rose, J.I. (eds.) **The Evolution of Human Populations in Arabia: Paleoenvironments, Prehistory and Genetics**. Dordrecht: Springer. pp.15-37.

Bailey, G.N. (2011) "Continental Shelf Archaeology: Where Next ?" In Benjamin, J., Bonsall, C., Pickard, C. and Fischer, A. (eds.) **Submerged Prehistory**. Oxford: Oxbow Books.

Beech, M., Cuttler, R., Moscrop, D., Kallweit, H. and Martin, J. (2005) New Evidence for the Neolithic Settlement of Marawah Island, Abu Dhabi, United Arab Emirates. **Proceedings of the Seminar for Arabian Studies**, 35: 37-56.

Bibby, T.G. (1973) **Preliminary Survey in East Arabia, 1968**. Copenhagen: Gyldendal.

Bird, M.I., Austin, W.E.N., Wurster, C.M., Fifield, L.K., Mojtabahid, M. and Sargeant, C. (2010) Punctuated Eustatic Sea-Level Rise in the Early Mid-Holocene. **Geology**, 38 (9): 803-806.

Blondel, P. (2007) **The Handbook of Sidescan Sonar**. Chichester: Springer-Praxis.

Blondel, P. and Sichi, O.G. (2009) Textural Analyses of Multibeam Sonar Imagery from Stanton Banks, Northern Ireland Continental Shelf. **Applied Acoustics**, 70: 1288–1297.

Blott, S.J. and Pye, K. (2006) Particle Size Distribution Analysis of Sand-Sized Particles by Laser Diffraction: an Experimental Investigation of Instrument Sensitivity and the Effects of Particle Shape. **Sedimentology**, 53: 671–685.

Bowen, R.L. (1951) The Pearl Fisheries of the Persian Gulf. **Middle East Journal**, 5, (2): 161-180.

Breeze, P., Cuttler, R. and Collins, P. (2011) Archaeological Landscape Characterisation in Qatar through Satellite and Aerial Photographic Analysis, 2009 to 2010. **Proceedings of the Seminar for Arabian Studies**, 41: 13-26.

Bretzke, K., Armitage, S.J., Parker, A.G., Walkington, H. and Uerpmann, H-P. (2013) The Environmental Context of Palaeolithic Settlement at Jebel Faya, Emirate Sharjah, UAE. **Quaternary International**, 300: 83–93.

Brown, C.J. and Blondel, P. (2009) Developments in the Application of Multibeam Sonar Backscatter for Seafloor Habitat Mapping. **Applied Acoustics**, 70: 1242–1247.

Brown, C.J., Todd, B.J., Kostylev, V.E. and Pickrill, R.A. (2011) Image-Based Classification of Multibeam Sonar Backscatter Data for Objective Surficial Sediment Mapping of Georges Bank, Canada. **Continental Shelf Research**, 31: S110–S119.

Burkholder, G. (1972) 'Ubaid Sites and Pottery in Saudi Arabia. **Archaeology**, 25: 264-269.

Carter, R. (2003) "Tracing Bronze Age Trade in the Arabian Gulf. Evidence for Way-Stations of the Merchants of Dilmun between Bahrain and the Northern Emirates." In Potts, D., Al-Naboodah, H. and Hellyer, P. (eds.) **Archaeology of the United Arab Emirates. Proceedings of the First International Conference on the Archaeology of the U.A.E (Abu Dhabi, 15-18 April 2001)**. London: Trident Press. pp.124–131.

Carter, R. (2006) Boat Remains and Maritime Trade in the Persian Gulf During the Sixth and Fifth Millennia BC. **Antiquity**, 80: 52–63.

Carter, R. (2010) "The Social and Environmental Context of Neolithic Seafaring in the Persian Gulf." In Anderson, A., Barrett, J.H. and Boyle, K.V. (eds.) **The Global Origins and Development of Seafaring. Cambridge**: McDonald Institute for Archaeological Research, University of Cambridge.

Carter, R. and Crawford, H. (eds.) (2010) **Maritime Interactions in the Arabian Neolithic: Evidence from H3, As-Sabiayah, an 'Ubaid-Related Site in Kuwait**. American School of Prehistoric Research Monograph Series. Leiden: Brill.

Cavelier, C. 1970 **Geological Description of the Qatar Peninsula (Arabian Gulf)**. Government of Qatar Department of Petroleum Affairs Unpublished Report

Cheesman, R.E. (1923) From Oqair to the Ruins of Salwa. **The Geographical Journal** 62 (5): 321-335.

Church, T.M. (1996) An Underground Route for the Water Cycle. **Nature**, 380: 579-580.

Collier, J.S. and Brown, C.J. (2005) Correlation of Sidescan Backscatter with Grain Size Distribution of Surficial Seabed Sediments. **Marine Geology**, 214: 431–449.

Cornwall County Council (2008) **England's Historic Seascapes: Historic Seascapes Characterisation (HSC), National HSC Method Statement**. Report No. 2008R024. Cornwall: County Council

Crassard, R. and Drechsler (2013) Towards New Paradigms: Multiple Pathways for the Arabian Neolithic. **Arabian Archaeology and Epigraphy**, 24: 3-8.

Creocean (2008) **Qatar Bahrain Causeway Project. Underwater Video Survey: Causeway Layout and Shipping Channels. Final Report**. Report No. 1080055. Unpublished.

Cuttler R.T.H. (ed.) (2011) **Reconstruction of the Late Pleistocene and Holocene Depositional Systems and Palaeogeography of Qatar. Stage 2 Data Analysis**,

**Assessment and Potential.** Qatar National Historic Environment Record Project. Doha: Qatar Museums Authority/University of Birmingham.

Cuttler, R.T.H. (2013) Considering Marine Transgression as a Mechanism for Enforced Migration and the Coastal Gulf 'Ubaid Phenomenon. The Neolithic of Arabia: New Paradigms and Future Perspectives, Lyon (France). **Arabian Archaeology and Epigraphy**, 24: 37-43.

Cuttler, R.T.H. (2014) **Human Populations and Former Sub-aerial Landscapes of the Arabian Gulf: Research and conservation.** PhD Thesis, University of Birmingham, UK.

Cuttler R.T.H. (ed.) (Forthcoming) **Qatar National Historic Environment Record Project. Historic Landscapes and Palaeoenvironments: Terrestrial and Marine Analysis.** Unpublished. Doha: Qatar Museums Authority/University of Birmingham.

Cuttler, R.T.H., Fitch, S. and Breeze, P. (2011a) **An Archaeological Impact Assessment of Sidescan Sonar Data from the Qatar Areas of the Qatar-Bahrain Causeway.** IBM VISTA Centre, University of Birmingham for the Qatar Museums Authority. Unpublished report.

Cuttler, R.T.H., Tetlow, E. and Al-Naimi, F. (2011b) Assessing the Value of Palaeoenvironmental Data and Geomorphological Processes for Understanding Late Quaternary Population Dynamics in Qatar. **Proceedings of the Seminar for Arabian Studies**, 41: 47-60.

Cuttler, R.T.H., Fitch, S., and Al-Naimi, F.A. (2012) "Considering the 'Terra Incognita' and the Implications for the Cultural Resource Management of the Arabian Gulf Palaeolandscape." In Hellyer, P., Al Naboodah, H. and Potts, D. (eds.) **Archaeology of the United Arab Emirates: Proceedings of the Second International Conference on the Archaeology of the U.A.E.** London: Trident Press. pp.235-245.

Cuttler, R.T.H. and Al-Naimi, F.A. (2013). From Land-Locked Desert to Maritime Nation: Understanding Taphonomic Processes and Landscape Evolution in Qatar and the Arabian Peninsula from 14,000BP. **Adumatu**, 28

De Cardi, B. (ed.) (1978) **Qatar Archaeological Report: Excavations 1973.** Oxford: Oxford University Press.

Dingwall, L. and Gaffney, V. (eds.) (2007) **Heritage Management at Fort Hood, Texas: Experiments in Historic Landscape Characterisation.** Oxford: Archaeopress.

Drechsler, P. (2009) **The Dispersal of the Neolithic Over the Arabian Peninsula.** BAR International Series 1969. Oxford: Archaeopress.

Drechsler, P. (2011) Places of Contact, Spheres of Interaction. The 'Ubaid Phenomenon in the Central Gulf Area as Seen from a First Season of

Reinvestigations at Dosariyah (Dawsāriyyah), Eastern Province, Saudi Arabia. **Proceedings of the Seminar for Arabian Studies**, 41: 69-82.

Edens, C. (1999) Khor Ile-Sud, Qatar: The Archaeology of Late Bronze Age Purple-Dye Production in the Arabian Gulf. **Iraq**, 61: 71-88

Ellingsen, K.E., Gray, J.S., and Bjørnbom, E. (2002) Acoustic Classification of Seabed Habitats Using the QTC VIEW™ System. **ICES Journal of Marine Science**, 59: 825–835.

Ellis, J.P. and McGuinness, W.T. (1986) Pockmarks of the Northwestern Arabian Gulf. **Advances in Underwater Technology, Ocean Science and Offshore Engineering**, 6: 353-367.

Evans, G. 1966 The Recent Sedimentary Facies of the Persian Gulf Region. **Philosophical Transactions of the Royal Society of London. Series A, Mathematical and Physical Sciences**, 259 (1099): 291-298.

Fairclough, G.J. (2001) Boundless Horizons – Historic Landscape Characterisation. **English Heritage Conservation Bulletin**, 40: 21-26.

Faught, M.K. and Donoghue, J.F. (1997) Marine Inundated Archaeological Sites and Palaeofluvial Systems: Examples from a Karst-Controlled Continental Shelf Setting in Apalachee Bay, Northeastern Gulf of Mexico. **Geoarchaeology**, 12 (5): 417–458.

Faure, H., Walter, R.C. and Grant, D.R. (2002) The Coastal Oasis: Ice Age Springs on Emerged Continental Shelves. **Global and Planetary Change**, 33: 47–56.

Fleitmann, D., Matter, A., Pint, J.J. and Al-Shanti, M.A. (2004) **The Speleothem Record of Climate Change in Saudi Arabia**. Saudi Geological Survey Open-File Report SGS-OF-2004-8. Unpublished.

Fitch, S., Thomson, K. and Gaffney, V. (2005) Late Pleistocene and Holocene Depositional Systems and the Palaeogeography of the Dogger Bank, North Sea. **Quaternary Research**, 64: 185-196.

Fitch, S. (2011) **The Mesolithic Landscape of the Southern North Sea**. PhD Thesis, University of Birmingham, UK.

Fonseca, L., Brown, C., Calder, B., Mayer, L. and Rzhanov, Y. (2009) Angular Range Analysis of Acoustic Themes from Stanton Banks Ireland: A Link Between Visual Interpretation and Multibeam Echosounder Angular Signatures. **Applied Acoustics**, 70: 1298–1304.

Ford, D. And Williams, P. (2007) **Karst Hydrogeology and Geomorphology**. England: Wiley.

Fugro Peninsular (2008) **Qatar Bahrain Causeway Project Offshore Geotechnical Investigation. Qatar-Bahrain Volume 1.** Report No. PQ/3145/08/01. Unpublished.

Gaffney, V., Thomson, K. and Fitch, S. (eds.) (2007) **Mapping Doggerland: The Mesolithic Landscapes of the Southern North Sea.** Oxford: Archaeopress.

GEMS (2008) **Geophysical Survey Report, Qatar Site, Qatar-Bahrain Causeway.** Report No. GME08030-GPH-001. Unpublished.

Golding, N., Vincent, M.A. and Connor, D.W. (2004) **The Irish Sea Pilot. Report on the Development of a Marine Landscape classification for the Irish Sea.** JNCC Report No. 346. Unpublished.

Groucutt, H.S. and Petraglia, M.D. (2012) The Prehistory of the Arabian Peninsula: Deserts, Dispersals, and Demography. **Evolutionary Anthropology**, 21: 113–125.

Henderson, J., Pizarro, O., Johnson-Roberson, M. and Mahon, I. (2013) Mapping Submerged Archaeological Sites using Stereo-Vision Photogrammetry. **International Journal of Nautical Archaeology**, 42 (2): 243–256.

Herman, J.J.H.C. (1957) **Surface Sediments of the Persian Gulf Near the Qatar Peninsula.** PhD Thesis, University of Utrecht, Netherlands.

Heyvaert , V.M.A. and Baeteman , C. (2007) Holocene Sedimentary Evolution and Palaeocoastlines of the Lower Khuzestan Plain (Southwest Iran). **Marine Geology**, 242: 83–108.

Hill, A., Bibi, F., Beech, M. and Yasin Al-Tikriti, W. (2012) “Before Archaeology: Life and Environments in the Miocene of Abu Dhabi.” In Potts, D.T. and Hellyer, P. (eds.) **Fifty Years of Emirates Archaeology.** Abu Dhabi/Dubai: Motivate Publishing. pp21-33.

Inizan, M-L. (1988) **Préhistoire à Qatar: Mission Archéologique Française à Qatar:** Volume. 2. Paris: CNRS.

Jameson, J. and Strohmenger, C.J. (2012) Relative Sea-Level Changes During the Late Pleistocene to Holocene of Qatar: Implications for Eustasy and Tectonics. **Adapted from Oral Presentation at AAPG Annual Convention and Exhibition, Long Beach, California, April 22-25, 2012** [online]. Available from: [http://www.searchanddiscovery.com/pdfz/documents/2012/50704jameson/ndx\\_jameson.pdf.html](http://www.searchanddiscovery.com/pdfz/documents/2012/50704jameson/ndx_jameson.pdf.html) [Accessed 25 March 2014]

Jones, E.J.W. (1999) **Marine Geophysics.** Chichester: Wiley.

Johns, C., Larn, R. and Tapper, B. (2004) **Rapid Coastal Zone Assessment for the Isles of Scilly.** Cornwall County Council Report No. 2004R030. Cornwall: Cornwall: County Council

- Johnstone, T.M. and Wilkinson, J.C. (1960) Some Geographical Aspects of Qatar. **The Geographical Journal**, 126 (4): 442-450.
- Kapel, H. (1967) **Atlas of the Stone-Age Cultures of Qatar. Reports of the Danish Archaeological Expedition to the Arabian Gulf**. Aarhus: Aarhus University Press.
- Keller, B.M. (2011) **Imaging the Twilight Zone: The Morphology and Distribution of Mesophotic Zone Features, A Case Study from Bonaire, Dutch Caribbean**. Master of Science Thesis, University of Delaware, USA.
- Killick, R. and Moon, J. (eds.) (2005) **The Early Dilmun Settlement at Saar**. Saar Excavation Report Volume 3. Ludlow: Archaeology International Ltd.
- KSEPL Carbonate Group of 1965-1969 (1973) **Holocene Carbonate Sediments of the Southern Arabian Gulf, Parts I-VIII**. Netherlands: Koninklijke/Shell.
- Lambeck, K. (1996) Shoreline Reconstructions for the Persian Gulf Since the Last Glacial Maximum. **Earth and Planetary Science Letters**, 142: 43-57.
- Land Use Consultants (1996) **Isles of Scilly Historic Landscape Assessment and Management Strategy**. Unpublished.
- LeBlanc, J. (2008) **A Fossil Hunting Guide To the Tertiary Formations of Qatar, Middle East**. First Edition [online]. Available from: [https://drive.google.com/folderview?id=0B\\_FRE6vSR2MeMGwyaXdsNDVsdnM&usp=sharing](https://drive.google.com/folderview?id=0B_FRE6vSR2MeMGwyaXdsNDVsdnM&usp=sharing) [accessed December 2013].
- Macumber, P.G. (2011) A Geomorphological and Hydrological Underpinning for Archaeological Research in Northern Qatar. **Proceedings of the Seminar for Arabian Studies**, 41: 1-14.
- Marin Mätteknik AB (2002) **Qatar-Bahrain Causeway. Acoustic Survey Report. Preliminary Environmental and Engineering Studies. Phase 1 – Studies and Surveys**. Report No. 54085-PR-009 Issue No. 1. Unpublished.
- Marks, A.E. (2009) "The Palaeolithic of Arabia in an Inter-Regional Context." In Petraglia, M.D. and Rose, J.I. (eds.) **The Evolution of Human Populations in Arabia: Paleoenvironments, Prehistory and Genetics**. Dordrecht: Springer. pp.295-308.
- Marsh, I and Brown, C. (2009) Neural Network Classification of Multibeam Backscatter and Bathymetry Data from Stanton Bank (Area IV). **Applied Acoustics**, 70: 1269–1276.
- Masry, A.H. (1997) **Prehistory in Northeastern Arabia: The Problem of Interregional Interaction**. London: Kegan Paul International.

McClure, H.A. (1976) Radiocarbon Chronology of Late Quaternary Lakes in the Arabian Desert. **Nature**, 263: 755-756.

McClure, H.A. and Al-Shaikh, N.Y. (1993) Palaeogeography of an 'Ubaid Archaeological Site, Saudi Arabia. **Arabian Archaeology and Epigraphy**, 4: 107–125.

McCorriston, J. and Martin, L. (2009) "Southern Arabia's Early Pastoral Population History: Some Recent Evidence." In Petraglia, M.D. and Rose, J.I. (eds.) **The Evolution of Human Populations in Arabia: Paleoenvironments, Prehistory and Genetics**. Dordrecht: Springer. pp.237-250.

McCorriston, J. (2013) The Neolithic in Arabia: a View from the South. **Arabian Archaeology and Epigraphy**, 24: 68–72.

McCorriston, J. and Martin, L. (2009) "Southern Arabia's Early Pastoral Population History: Some Recent Evidence." In Petraglia, M.D. and Rose, J.I. (eds.) **The Evolution of Human Populations in Arabia: Paleoenvironments, Prehistory and Genetics**. Dordrecht: Springer. pp.237-250.

Misbahuddin, K. (1984) **The Role of Raḥmah bin Jabīr bin 'Adhbī in the History of Eastern Arabia (1783-1826)**. Master of Arts Thesis, Institute of Islamic Studies, McGill University, Canada.

NOAA (2006) **National Marine Protected Areas Center Marine Cultural and Historic Newsletter**. Volume 3 (12), 1st December 2006.

NOAA (2014) **Digital Coast. Benthic Terrain Modeler** [online]. Available from: <http://coast.noaa.gov/digitalcoast/tools/btm> [accessed 3rd February 2015].

Orpin, A.R. and Kostylev, V.E. (2006) Towards a Statistically Valid Method of Textural Sea Floor Characterization of Benthic Habitats. **Marine Geology**, 225: 209–222.

Parker, A.G., Goudie, A.S., Stokes, S., White, K., Hodson, M.J., Manning, M. and Kennet, D. (2006) A Record of Holocene Climate Change from Lake Geochemical Analyses in Southeastern Arabia. **Quaternary Research**, 66: 465–476.

Parker, A.G. and Goudie, A.S. (2008) Geomorphological and Palaeoenvironmental Investigations in the Southeastern Arabian Gulf Region and the Implication for the Archaeology of the Region. **Geomorphology**, 101: 458-470

Parker, A.G. and Rose, J.I. (2008) Climate Change and Human Origins in Southern Arabia. **Proceedings of the Seminar for Arabian Studies**, 38: 25-42.

Pelly, J.H. (1895) Telegram No. 360. H.M.S. "Sphinx" at Zobara, the 7th September 1895. From Captain J. H. Pelly, Commander and Senior Naval Officer to Colonel F.

A. Wilson, Political Resident, Persian Gulf. **British Library Indian Office Reports Collections**, IOR R/15/1/314.

Penrose, J.D., Siwabessy, P.J.W., Gavrilov, A., Parnum, I., Hamilton, L.J., Bickers, A., Brooke, B., Ryan, D.A. and Kennedy, P. (2005) **Acoustic Techniques for Seabed Classification**. Cooperative Research Centre for Coastal Zone Estuary and Waterway Management. Technical Report 32, September 2005.

Petraglia, M.D. (2005) Hominin Responses to Pleistocene Environmental Change in Arabia and South Asia. **Geological Society, London, Special Publications**, January 1, 2005, 247: 305-319

Petraglia, M.D. and Rose, J.I. (eds.) (2009) **The Evolution of Human Populations in Arabia: Paleoenvironments, Prehistory and Genetics**. Dordrecht: Springer.

Petraglia, M.D., Alsharekh, A., Breeze, P., Clarkson, C., Crassard, R., Drake, N.A., Groucott, H.S., Jennings, R., Parker, A.G., Parton, A., Roberts, R.G., Shipton, C., Matheson, C., Al-Omari, A. and Veall, M.A. (2012) Hominin Dispersal into the Nefud Desert and Middle Palaeolithic Settlement along the Jubbah Palaeolake, Northern Arabia. **PLoS ONE** [online], 7 (11): e49840. doi:10.1371/journal.pone.0049840.

Potts, D.W. (1990) **The Arabian Gulf in Antiquity. Volume I. From Prehistory to the Fall of the Achaemenid Empire**. Oxford: Clarendon Press.

Preston, J. (2009) Automated Acoustic Seabed Classification of Multibeam Images of Stanton Banks. **Applied Acoustics**, 70: 1277–1287.

Pullar, J. (1974) Harvard Archaeological Survey in Oman, 1973: Flint Sites in Oman. **Proceedings of the Seminar for Arabian Studies**, 4: 33-48.

Purser, B.H. (ed.) (1973) **The Persian Gulf. Holocene Carbonate Sedimentation and Diagenesis in a Shallow Epicontinental Sea**.

QBC Consortium (2009a) **Geotechnical Factual Report. Qatar-Bahrain Causeway Project Embankment Data**. Report No. QBC-ME-P2GT-ALL-GEN-TRP-001 Rev. 0.1. Unpublished.

QBC Consortium (2009b) **Geotechnical Factual Report. Qatar-Bahrain Causeway Project Borrow Areas Data**. Report No. QBC-ME-P2GT-ALL-GEN-TRP-002 Rev. 1.0. Unpublished.

Quester Tangent (2012a) **QTC SWATHVIEW 12.1 User Manual and Reference**: DMNSWVW-0000-R06. Unpublished. Canada: Quester Tangent.

Quester Tangent (2012b) **QTC CLAMS™ 12.1 User Guide and Reference**: DMN-CLAM-0000-R03. Unpublished. Canada: Quester Tangent.

Roaf, M. (1976) Excavations at Al Markh, Bahrain. **Proceedings of the Seminar for Arabian Studies**, 6: 144-160.

Rooper, C.N. and Zimmermann, M. (2007) A Bottom-Up Methodology for Integrating Underwater Video and Acoustic Mapping for Seafloor Substrate Classification. **Continental Shelf Research**, 27: 947–957.

Rose, J.I. (2010) New Light on Human Prehistory in the Arabo-Persian Gulf Oasis. **Current Anthropology**, 51 (6): 849-883.

Rose, J.I., Usik, V.I., Marks, A.E., Hilbert, Y.H., Galletti, S.C., Parton, A., Geiling, J.M., Černý, V., Morley, M.W & Roberts, R.G. (2011) The Nubian Complex of Dhofar, Oman: An African Middle Stone Age Industry in Southern Arabia. **PLoS ONE** [online], 6(11): e28239. doi:10.1371/journal.pone.0028239

Roux, G. (1964) **Ancient Iraq**. UK: Penguin.

Rutkowski, L. (ed.) (2011) **Kuwaiti-Polish Investigations in Northern Kuwait. As-Sabbiya 2007-2010**. Unpublished. Al-Jahra/Warsaw: National Council for Culture, Arts and Letters, Kuwait, and Polish Centre of Mediterranean Archaeology, University of Warsaw.

Sadiq, A.M. and Nasir, S.J. (2002) Middle Pleistocene Karst Evolution in the State of Qatar, Arabian Gulf. **Journal of Cave and Karst Studies**, 64 (2): 132-139.

Sarnthein, M. (1972) Sediments and History of the Postglacial Transgression in the Persian Gulf and Northwest Gulf of Oman. **Marine Geology**, 12: 245-266.

Schlüter, M.J., Sauter, E.J., Andersen, C.E., Dahlgaard, H. and Dando, P. (2004) Spatial Distribution and Budget for Submarine Groundwater Discharge in Eckernförde Bay (Western Baltic Sea). **Limnology and Oceanography**, 49 (1): 157–167

Scott-Jackson, J.E., Scott-Jackson, W.B. and Rose, J.I. (2009) “Palaeolithic Stone Tool Assemblages from Sharjah and Ras al Khaimah in the United Arab Emirates.” In Petraglia, M.D. and Rose, J.I. (eds.) **The Evolution of Human Populations in Arabia: Paleoenvironments, Prehistory and Genetics**. Dordrecht: Springer. pp.125-238.

Shinn, E.A. (1969) Submarine Lithification of Holocene Carbonate Sediments in the Persian Gulf. **Sedimentology**, 12: 109-144.

Simons, D.G. and Snellen, M. (2009) A Bayesian Approach to Seafloor Classification Using Multi-Beam Echo-Sounder Backscatter Data. **Applied Acoustics**, 70: 1258–1268.

Spoor, R.H. (1997) Human Population Groups and the Distribution of Lithic Arrowheads in the Arabian Gulf. **Arabian Archaeology and Epigraphy**, 8: 143-160.

Stanford, J.D., Hemmingway, R., Rohling, E.J., Challenor, P.G., Medina-Elizalde, M. and Lester, A.J. (2011) Sea-level Probability for the Last Deglaciation: A Statistical Analysis of Far-Field Records. **Global and Planetary Change**, 79: 193-203.

State of Delaware (2012) **Division of Fish and Wildlife. Red Bird Reef Sinkings** [online]. Available from: [www.dnrec.delaware.gov/fw/Fisheries/Pages/Red%20Bird%20Reef%20sinkings.aspx](http://www.dnrec.delaware.gov/fw/Fisheries/Pages/Red%20Bird%20Reef%20sinkings.aspx) [accessed 27th August 2013].

Stoffers, P. and Ross, D.A. (1979) Late Pleistocene and Holocene Sedimentation in the Persian Gulf/Gulf of Oman. **Geology**, 23: 181-208.

Sutherland, T.F., Galloway, J., Loschiavo, R., Levings, C.D. and Hare, R. (2007) Calibration Techniques and Sampling Resolution Requirements for Groundtruthing Multibeam Acoustic Backscatter (EM3000) and QTC VIEW™ Classification Technology. **Estuarine, Coastal and Shelf Science**, 75: 447-458.

Taylor, J.C.M. and Illing, L.V. (1969) Holocene Intertidal Calcium Carbonate Cementation, Qatar, Persian Gulf. **Sedimentology**, 12: 69-107.

Teller, J.T., Glennie, K.W., Lancaster, N. and Singhvi, A.K. (2000) Calcareous Dunes of the United Arab Emirates and Noah's Flood: the Postglacial Reflooding of the Persian (Arabian) Gulf. **Quaternary International**, 68-71: 297-308.

Tetlow, E.A., Cuttler, R.T.H and Al Naimi, F.A (Forthcoming) **Wadi Debayan: A Neolithic Landscape**.

Tixier, J. (1980) **Mission Archéologique Française à Qatar: 1976-77, 1977-78**. Paris: CNRS Recherches Anthropologiques.

Uchupi, E., Swift S.A. and Ross D.A. (1996) Gas Venting and Late Quaternary Sedimentation in the Persian (Arabian) Gulf. **Marine Geology**, 129: 237-269.

Uchupi, E., Swift S.A. and Ross D.A. (1999) Late Quaternary Stratigraphy, Palaeoclimate and Neotectonism of the Persian (Arabian) Gulf Region. **Marine Geology**, 160: 1–23.

Uerpmann, M. (2003) “The Dark Millennium — Remarks on the Final Stone Age in the Emirates and Oman.” In Potts, D., Al-Naboodah, H. and Hellyer, P. (eds.) **Archaeology of the United Arab Emirates. Proceedings of the First International Conference on the Archaeology of the U.A.E (Abu Dhabi, 15-18 April 2001)**. London: Trident Press. pp.74–81.

Uerpmann, M. and Uerpmann, H-P. (2008) “Neolithic Faunal Remains from al-Buhais 18 (Sharjah, UAE).” In Uerpmann, H-P., Uerpmann, M. and Jasim, S.A. (eds.) **The Natural Environment of Jebel al-Buhais: Past and Present, The Archaeology of Jebel al-Buhais, Volume 2**. Tübingen: Kerns Verlag. pp.97-132.

Uerpmann, H-P., Potts, D.T. and Uerpmann, M. (2009) "Holocene (Re-)Occupation of Eastern Arabia." In Petraglia, M.D. and Rose, J.I. (eds.) **The Evolution of Human Populations in Arabia: Paleoenvironments, Prehistory and Genetics**. Dordrecht: Springer. pp.205-214.

**UKHO 1925 Maritime Chart, Persian Gulf.**

Van Rein, H., Brown, C.J., Quinn, R., Breen, J. and Schoeman, D. (2011) An Evaluation of Acoustic Seabed Classification Techniques for Marine Biotope Monitoring Over Broad-Scales ( $>1 \text{ km}^2$ ) and Meso-Scales ( $10 \text{ m}^2 - 1 \text{ km}^2$ ). **Estuarine, Coastal and Shelf Science**, 93: 336-349.

Vosmer, T. (1999) Indo-Arabian Stone Anchors in the Western Indian Ocean and Arabian Sea. **Arabian Archaeology and Epigraphy**, 10: 248-263.

Wahida, G., Al-Tikriti, W.Y., Beech, M. and Al Meqbali, A. (2009) "A Middle Palaeolithic Assemblage from Jebel Barakah, Coastal Abu Dhabi Emirate." In Petraglia, M.D. and Rose, J.I. (eds.) **The Evolution of Human Populations in Arabia: Paleoenvironments, Prehistory and Genetics**. Dordrecht: Springer. pp.117-124.

Wessex Archaeology (2012) **Outer Hebrides Coastal Community Marine Archaeology Pilot Project** [online]. Available from: <http://blogs.wessexarch.co.uk/ohccmapp/> [accessed 31st August 2013].

Westley, K., Quinn, R., Forsythe, W., Plets, R., Bell, T., Benetti, S., McGrath, F. And Robinson, R. (2011a) Mapping Submerged Landscapes Using Multibeam Bathymetric Data: a Case Study from the North Coast of Ireland. **The International Journal of Nautical Archaeology**, 40 (1): 99–112.

Westley, K., Bell, T., Plets, R. and Quinn, R. (2011b) "Investigating Submerged Archaeological Landscapes: a Research Strategy Illustrated with Case Studies from Ireland and Newfoundland, Canada." In Benjamin, J., Bonsall, C., Pickard, C. and Fischer, A. (eds.) **Submerged Prehistory**. Oxford: Oxbow Books.

Williams, A.H. and Walkden, G.M. (2002) "Late Quaternary Highstand Deposits of the Southern Arabian Gulf: a Record of Sea-Level and Climate Change." In Clift, P.D., Kroon, D., Gaedicke, C. and Craig, J. (eds.) **The Tectonic and Climatic Evolution of the Arabian Sea Region**. London: Geological Society. pp371-386.

Wilson, D. (1833) Memorandum Respecting the Pearl Fisheries in the Persian Gulf. **Journal of the Royal Geographical Society of London**, (3): 283-286.

Wilson, Col. F.A. (1895) Telegram No. 98, Dated Bushire, the 15th September 1895. From Colonel F. A. Wilson, Political Resident, Persian Gulf To The Secretary to the Government of India, Foreign Department. **British Library Indian Office Reports Collections**, IOR R/15/1/314.